ICRP ref 4838-4528-4881
20 September 2012

Annals of the ICRP

ICRP PUBLICATION XXX

Occupational Intakes of Radionuclides Part 3

DRAFT DOCUMENT

Occupational Intakes of Radionuclides Part 3

ICRP Publication XXX

Approved by the Commission in XXX

Abstract- The 2007 Recommendations (*Publication 103*, ICRP, 2007) introduced changes to the radiation and tissue weighting factors used in calculation of effective dose. In addition, *Publication 103* clarified the need for separate calculation of equivalent dose to males and females and sex-averaging in the calculation of effective dose (ICRP, 2007) and adopted the use of reference anatomical computational phantoms, in place of the composite mathematical models that have been used previously.

These substantial changes implied a revision of the dose coefficients for internal exposure, published previously in the *Publication 30* series (ICRP, 1979, 1980, 1981, 1988b). This work was performed by Committee 2 and its Task Groups INDOS and DOCAL.

This report is the third in a series of documents replacing the *Publication 30* series and *Publication 68* (ICRP, 1994b) and providing revised dose coefficients for occupational intakes of radionuclides (OIR) by inhalation and ingestion. It provides data on individual elements and their radioisotopes, including biokinetic data and models, dose coefficients and data for bioassay interpretation. Electronic disks accompanying this series give extensive additional information.

This third report in the series provides the above data for the following elements : Ruthenium (Ru), Antimony (Sb), Tellurium (Te), Iodine (I), Caesium (Cs), Barium (Ba), Iridium (Ir), Lead (Pb), Bismuth (Bi), Polonium (Po), Radon (Rn), Radium (Ra), Thorium (Th) and Uranium (U).

The current version, posted for public consultation, contains only the biokinetic data and the models. An exception is made for Radon, where some preliminary dose coeffcients are provided for information only.

The total set of dose coefficients and data for bioassay interpretation will be included in the final version.

Keywords: Occupational exposure, Internal Dose Assessment, Biokinetic and Dosimetric models, Bioassays interpretation.

CONTENTS

PREFACE

The 2007 Recommendations (*Publication 103*, ICRP, 2007) introduced changes to the radiation weighting factors used in the calculation of equivalent dose to organs and tissues and also changes to the tissue weighting factors used in the calculation of effective dose. In addition, an important development was the adoption of reference anatomical computational phantoms, in place of the composite mathematical models that have been used for all previous calculations of organ doses. *Publication 103* also clarified the need for separate calculation of equivalent dose to males and females and sex-averaging in the calculation of effective dose (ICRP, 2007).

These changes implied a revision of the dose coefficients initially provided in the *Publication 30* series (ICRP, 1979, 1980, 1981, 1988b). This work was performed by Committee 2 and its Task Groups INDOS and DOCAL.

This report is the third in a series of documents replacing the *Publication 30* series and *Publication 68* (ICRP, 1994b) and providing revised dose coefficients for occupational intakes of radionuclides (OIR) by inhalation and ingestion. It provides also radionuclide-specific information for the design and planning of monitoring programmes and retrospective assessment of occupational internal doses, replacing *Publications 54* and *78* (ICRP, 1988a, 1997b).

The first report of this OIR series included chapters describing the control of occupational exposures, biokinetic and dosimetric models, monitoring methods, monitoring programmes and retrospective dose assessment.

The following reports provide data on individual elements and their radioisotopes, including biokinetic data and models, dose coefficients and data for bioassay interpretation. Electronic disks accompanying this series give extensive additional information.

The second report in the series provided data for the following elements : Hydrogen (H), Carbon (C), Phosphorus (P), Sulphur (S), Calcium (Ca), Iron (Fe), Cobalt (Co), Zinc (Zn), Strontium (Sr), Yttrium (Y), Zirconium (Zr), Niobium (Nb), Molybdenum (Mo) and Technetium (Tc).

This third report provides the data for the following elements: Ruthenium (Ru), Antimony (Sb), Tellurium (Te), Iodine (I), Caesium (Cs), Barium (Ba), Iridium (Ir), Lead (Pb), Bismuth (Bi), Polonium (Po), Radon (Rn), Radium (Ra), Thorium (Th) and Uranium (U).

Subsequent reports will provide data for the other elements.

The current version, posted for public consultation, contains only the biokinetic data and the models. An exception is made for Radon, where some preliminary dose coeffcients are provided for information only.

The total set of dose coefficients and data for bioassay interpretation will be included in the final version.

The membership of the Task Group on Internal Dosimetry (INDOS) at the time of the completion of this report was:

Members:

F Paquet (Chair)	G Etherington	J L Lipsztein
E Ansoborlo	A Giussani	D Melo
M R Bailey	R A Guilmette	

E J A Blanchardon	J D Harrison	
H Doerfel	R W Leggett	

Corresponding Members:

A Bouville	A Luciani	D Whillans
C-M Castellani	D Newton	
R Cruz-Suarez	D Nosske	
C Hurtgen	D M Taylor	

The membership of the Task Group on Dose Calculations (DOCAL) at the time of the completion of this report was:

Members:

W E Bolch (Chair)	A Endo	N Ishigure
M Zankl	V Berkovski	T P Fell
D Nosske	L Bertelli	N E Hertel
N Petoussi-Henss	K F Eckerman	J G S Hunt
M Pelliccioni		

Corresponding Members:

A Birchall	H Schlattl
G Gualdrini	M Stabin
D Jokisch	R Tanner
C Lee	X G Xu

The membership of Committee 2 was:

(2009-2013)

H-G Menzel (Chair)	W E Bolch	J D Harrison
F Paquet	M R Bailey	R Cox
N Ishigure	N Petoussi-Henss	M Balonov
G Dietze	R W Leggett	A S Pradhan
D Bartlett	K F Eckerman	J L Lipsztein
V Berkovski	A Endo	J Ma

1. INTRODUCTION

(1) The present report is Part 3 of a report series aimed at providing revised dose coefficients for occupational intakes of radionuclides (OIR) by inhalation and ingestion. It also presents radionuclide-specific information for the design and planning of monitoring programmes and retrospective assessment of occupational internal doses.

(2) This report series replaces the *Publication 30* series (ICRP, 1979, 1980, 1981, 1988b), *Publications 54*, *68* and *78* (ICRP, 1988a, 1994b, 1997). The revised dose coefficients, dose per unit content values and reference bioassay functions have been calculated using the *Publication 100* (ICRP, 2006) Human Alimentary Tract Model (HATM) and a revision of the *Publication 66* (ICRP, 1994a) Human Respiratory Tract Model (HRTM) which takes account of more recent data. The revisions made to the HRTM are described in Part 1 of this report series. In addition, information is provided in this report series on absorption to blood following inhalation and ingestion of different chemical forms of elements and their radioisotopes, in those cases for which it is currently judged that the data are sufficient to make specific recommendations. Revisions have been made to many models for the systemic biokinetics of radionuclides, making them more physiologically realistic representations of uptake and retention in organs and tissues and of excretion.

(3) The dose coefficients and dose per unit content values presented in this report series 1 are given for a Reference Worker with an average breathing rate of 1.2 m^3 h^{-1} during an 8 h working day. These data are provided for a range of physico-chemical forms for each radionuclide and for a range of aerosol particle size distributions. Data for ingestion and injection (i.e. direct entry to the blood) are provided to allow the interpretation of bioassay data for cases of inadvertent ingestion (e.g. of material on contaminated skin) or rapid absorption through intact or damaged skin (injection).

(4) Data are presented in a standard format for each element and its radioisotopes. Each element section provides information on chemical forms encountered in the workplace; principal radioisotopes, their physical half-lives and decay modes; reviews of data on inhalation, ingestion and systemic biokinetics; the structure and parameter values for the systemic biokinetic model; and information on the interpretation of individual monitoring data. Each section in the printed documents also includes tables of:

- Dose coefficients (committed effective dose, Sv, per Bq intake) for inhalation of 5 µm AMAD aerosols with the default absorption Types appropriate for the element, for all relevant radioisotopes;
- Principal emissions of selected radioisotopes;
- Measurement techniques, detection limits typically achieved in a practical monitoring programme, and improved detection limits that could be achieved by suitable choice of measurement parameter values, for selected radioisotopes;
- Committed effective dose (Sv) per unit measurement (Bq) for an acute intake by inhalation of a 5 µm AMAD aerosol with the default absorption Types appropriate

[1] The current version, posted for public consultation, contains only the biokinetic data and the models. An exception is made for Radon, where some preliminary dose coeffcients are provided for information only. The total set of dose coefficients and data for bioassay interpretation will be included in the final version

for the element, for selected radioisotopes;

- Bioassay data (i.e. whole body and/or organ retention, and daily urinary and faecal excretion, Bq per Bq intake), at various times after an acute intake by inhalation of a 5 μm AMAD aerosol with the default absorption Types appropriate for the element;

(5) Bioassay data are also presented graphically.

(6) In cases for which sufficient information is available (principally for actinide elements), lung absorption is specified for different chemical forms and dose coefficients and bioassay data are calculated accordingly.

(7) The full data set of this report is provided on electronic disk. This disk contains in addition to the printed document:

Dose coefficients

- Committed equivalent dose coefficients for organs and tissues, for males and females;
- Dose coefficients for all chemical forms considered;
- Dose coefficients for an inhaled aerosol with particle sizes ranging from an AMTD of 0.001 μm to an AMAD of 20 μm;
- Dose coefficients for intake by ingestion, with the default f_A values appropriate for the element, for all relevant radioisotopes;
- Dose coefficients for radioisotopes not given in the printed reports in this series.

Bioassay data

- Committed effective dose (Sv) per unit measurement (Bq) for an acute intake by inhalation of an aerosol with particle sizes ranging from an AMTD of 0.001 μm to an AMAD of 20 μm;
- Committed effective dose (Sv) per unit measurement (Bq) for an acute intake by ingestion, with default f_A values appropriate for the element;
- Bioassay data (i.e. whole body and/or organ retention, and daily urinary and faecal excretion, Bq per Bq intake), for an acute intake by inhalation of an aerosol with particle sizes ranging from an AMTD of 0.001 μm to an AMAD of 20 μm;
- Similar bioassay data for an acute intake by ingestion
- Figures giving measured activity content per unit dose (Bq Sv^{-1}) in selected body tissues, urine (daily excretion) or faeces (daily excretion), at various times after intake by inhalation or ingestion. These data can also be used to facilitate decisions about the design of monitoring programmes and the extent of the assessment required, as described in Chapter 5 of OIR Part 1.

(8) The list of elements included in Part 3 is: Ruthenium (Ru), Antimony (Sb), Tellurium (Te), Iodine (I), Caesium (Cs), Barium (Ba), Iridium (Ir), Lead (Pb), Bismuth (Bi),

Polonium (Po), Radon (Rn), Radium (Ra), Thorium (Th) and Uranium (U).

References

ICRP, 1979. Limits for intake of radionuclides by workers. ICRP Publication 30, Part 1. Ann. ICRP 2(3/4).

ICRP, 1980. Limits for intakes of radionuclides by workers. ICRP Publication 30, Part 2. Ann. ICRP 4(3/4).

ICRP, 1981. Limits for intakes of radionuclides by workers. ICRP Publication 30, Part 3. Ann. ICRP 6 (2/3).

ICRP, 1988a. Individual monitoring for intakes of radionuclides by workers: design and interpretation. ICRP Publication 54, Ann. ICRP 19 (1-3).

ICRP, 1988b. Limits for intakes of radionuclides by workers: An Addendum. ICRP Publication 30, Part 4. Ann. ICRP 19 (4).

ICRP, 1994a. Human respiratory tract model for radiological protection. ICRP Publication 66. Ann. ICRP 24 (1-3).

ICRP, 1994b. Dose coefficients for intake of radionuclides by workers. ICRP Publication 68. Ann. ICRP 24 (4).

ICRP, 1997. Individual monitoring for internal exposure of workers – Replacement of ICRP Publication 54. ICRP Publication 78. Ann. ICRP 27 (3/4).

ICRP, 2006. Human alimentary tract model for radiological protection. ICRP Publication 100. Ann. ICRP 36 (1-2).

ICRP, 2007. The 2007 Recommendations of the International Commission on Radiological Protection. ICRP Publication 103. Ann. ICRP 37 (2-4).

2. RUTHENIUM (Z = 44)

2.1. Chemical forms in the workplace

(9) Ruthenium is a transition metal which may exist in various oxidation states from II to VIII. It is assumed that oxidation states (III) and (IV) are the most stable, while in strongly oxidation conditions the oxo-anion RuO_4^{2-} is very stable. Ruthenium may be encountered in industry in a variety of chemical and physical forms, such as oxides (RuO_2 and RuO_4 (vapour state)), halides, sulphides and different cyanides.

(10) Ruthenium-103 is produced in the nuclear industry as a fission product. At the Chernobyl accident, ruthenium became volatile during the fire and was found in metallic form, hundreds of kilometres away from the plant (Pollanen, 1997).

Table 2-1. Isotopes of ruthenium addressed in this report

Isotope	Physical half-life	Decay mode
Ru-94	51.8 m	EC, B+
Ru-95	1.643 h	EC, B+
Ru-97	2.9 d	EC
Ru-103	39.26 d	B-
Ru-105	4.44 h	B-
Ru-106[a]	373.59 d	B-

[a] Data for these radionuclides are given in the printed copy of this report. Data for other radionuclides are given on accompanying electronic disk.

2.2. Routes of Intake

2.2.1. Inhalation

Absorption Types and parameter values

(11) Some information is available on the behaviour of inhaled ruthenium in man following accidental intakes as an oxide or in irradiated fuel fragments. Information is available from experimental studies of ruthenium as tetroxide, chloride, citrate, dioxide, and irradiated uranium dioxide.

(12) Absorption parameter values and Types, and associated f_A values for gas and vapour forms of ruthenium are given in Table 2-2 and for particulate forms in Table 2-3. Exposures to gas and vapour forms of ruthenium are relatively unusual compared to exposures to particulate forms, and therefore it is proposed here that particulate form is assumed in the absence of information (ICRP, 2002).

Gases and vapours

Ruthenium tetroxide (RuO_4)

(13) Ruthenium tetroxide (melting point 26°C, boiling point 40°C) has a high vapour pressure at room temperature and is thought to have been involved in several human inhalation incidents (Snipes and Kanapilly, 1983). It is very reactive, and converts to ruthenium dioxide in contact with organic or other reactive surfaces.

(14) Snipes et al. (1977) carried out pilot experiments in which the biokinetics of ^{103}Ru

were followed for ~2 weeks after inhalation of $^{103}RuO_4$ by dogs and rats. In both species initial deposition was primarily in the nasopharyngeal region (NP, broadly equivalent to the extrathoracic airways) and tracheobronchial region (TB, equivalent to the bronchial and bronchiolar regions). Clearance was rapid and mainly fecal: ~85% of the initial body burden (IBB) was retained with a half-time of ~1 day, and the rest with a half-time of ~1 week. At the end of the study most of the ^{103}Ru retained in the body in dogs was in the lungs, but in rats was associated with the nasal turbinates.

(15) Runkle et al. (1980) followed the biokinetics of ^{106}Ru for 112 days after inhalation of $^{106}RuO_4$ by rats. Complementary experiments were conducted to measure absorption of ^{106}Ru following gavage of $^{106}RuO_4$ or $^{106}RuO_2$: fractional absorption was estimated to be ~0.01 for both. The overall pattern following inhalation was similar to that observed by Snipes et al. (1977): 85%, 13.8% and 1.2% IBB were retained with biological half-times of 0.6, 4 and 69 days, respectively. Initial deposition was mainly in the NP and TB regions. After the first week most of the ^{106}Ru retained was associated with the nasal turbinates and head skin, with little systemic uptake. Although most of the ^{106}Ru deposited in the turbinates cleared within a few days, ~2% was retained with a half-time of ~70 days. As discussed below, bound state parameter values for ruthenium of $f_b = 0.05$ and $s_b = 0.1\ d^{-1}$ were chosen here. Assuming these values, dissolution parameter values fitted here for $^{106}RuO_4$ inhaled by rats (with regional deposition of 99.8% ET and 0.2% AI) were: $f_r = 0.92$, $s_r = 0.35\ d^{-1}$ and $s_s = 0.01\ d^{-1}$.

(16) Snipes (1981) followed the biokinetics of ^{106}Ru for 512 days after inhalation of $^{106}RuO_4$ by dogs. In a complementary experiment the biokinetics of ^{106}Ru were followed for 5 days after ingestion of $^{106}RuO_2$ by dogs: fractional absorption was estimated to be ~0.005. The overall pattern after inhalation was similar to that observed by Snipes et al. (1977), but clearance was even faster: 90%, 0.7% and 0.3% IBB were retained with effective half-times of 1.2, 14 and 170 days, respectively. Again, initial deposition was primarily in the NP and TB regions. The respiratory tract and pelt contained the highest levels of ^{106}Ru with relatively little systemic uptake. The NP region contained a high proportion of the body content of ^{106}Ru at all times. The trachea, larynx and lung contained similar amounts of ^{106}Ru at 512 days after exposure, reflecting long-term retention of some of the initial deposit in all regions of the respiratory tract. Autoradiographs showed that the ^{106}Ru dispersion in the turbinates and lymph nodes was relatively uniform: only single tracks were observed with no indications of focal accumulation. The long-term retention of a fraction of the ^{106}Ru in the conducting airways, from which most particles are cleared rapidly, and the uniform dispersion shown in the autoradiographs, provide strong evidence for a bound fraction for ruthenium. Based on the results of this study, bound state parameter values for ruthenium of $f_b = 0.05$ and $s_b = 0.1\ d^{-1}$ were chosen here. Assuming these values, dissolution parameter values fitted here for $^{106}RuO_4$ inhaled by dogs (with regional deposition of 35% ET_1; 35% ET_2; 17% BB and 0.02% AI) were: $f_r = 0.4$, $s_r = 10\ d^{-1}$ and $s_s = 0.001\ d^{-1}$.

(17) Snipes and Kanapilly (1983) pointed out that incidents involving a release of RuO_4 into room air might produce complex exposure atmospheres, with components including RuO_4 vapour, ultrafine particles formed by self-nucleation of RuO_2, molecular RuO_4 or RuO_2 adsorbed on or attached to particles in the air. Such complex mixtures of vapour and particles could yield deposition and dose patterns different from those of RuO_4 vapour or of a simple particulate aerosol. To provide data to assist in assessing doses from such exposures, Snipes and Kanapilly (1983) followed the biokinetics of ^{106}Ru for 112 days after inhalation by rats of $^{106}RuO_4$ mixed with an aerosol of fused aluminosilicate particles (FAP, 0.69 µm diameter.) Particle size analysis and the initial deposition pattern indicated that most of the ^{106}Ru in the exposure chamber was in the form of molecular RuO_4, with ~25% associated with particles

~0.1 µm diameter, and <5% associated with the FAP. It was estimated that 60% IBB deposited in the upper respiratory tract, 10% in the TB region, 12% in the AI region and 18% was external contamination, mainly on the nares and head skin. Clearance was rapid and mainly via the alimentary tract to faeces: 92% and 8% IBB were retained with effective half-times of 0.7 and 30 days, respectively. Clearance of ^{106}Ru from the AI region had an effective half-time of ~30 days and was predominantly by dissolution. As discussed below, bound state parameter values for ruthenium of f_b = 0.05 and s_b = 0.1 d^{-1} were chosen here. Assuming these values, dissolution parameter values fitted here (with regional deposition of 87% ET_2 and 13% AI) were: f_r = 0.9, s_r = 0.5 d^{-1} and s_s = 0.001 d^{-1}. These are similar to those assessed for RuO_4 alone. The main difference is in the higher lung deposition.

(18) A worker accidentally inhaled $^{103}RuO_4$ vapour while performing experiments in which ^{103}Ru was distilled from a neutron-irradiated ^{235}U sample (Webber and Harvey, 1976). External measurements made from 8 to 36 days after the incident indicated that inhaled activity was retained primarily in the region of the nose and mouth. Activity was also detected in the lower abdominal area. There was no evidence of concentration of activity in other tissues. The half-time for biological removal from the body was ~15 d. There is insufficient information available to assess parameter values from the reported measurements, but the observations are consistent with parameter values f_r = 0.4 and s_s = 0.001 d^{-1} derived above from experimental studies.

(19) In two other human exposure incidents (Pusch 1968; Howells et al., 1977) it was suspected that the released activity was RuO_4, but that it was converted at least in part to particulate forms of ruthenium, notably RuO_2, during mixing and interacting with room air (Snipes and Kanapilly, 1983). In both cases the ruthenium was only detected in the chest. Details are given below in the ruthenium dioxide section.

(20) Based on the experimental studies, dissolution parameter values used here for RuO_4 are: f_r = 0.5, s_r = 1 d^{-1} and s_s = 0.001 d^{-1}, with bound state parameter values for ruthenium of f_b = 0.05 and s_b = 0.1 d^{-1} (consistent with assignment to default Type M) and f_A = 0.01. Regional deposition of 40% ET_1; 40% ET_2; 12% BB; 7% bb and 1% AI is assumed here, based on $^{106}RuO_4$ inhaled by dogs.

(21) However, the study by Snipes and Kanapilly (1983) and the accidental exposures suggest that mixing with the ambient aerosol could lead to greater lung deposition of RuO_4 and conversion to RuO_2 before intake. For prospective assessments of potential releases of RuO_4 it is therefore proposed that the exposure is to 50% RuO_4 vapour and 50% RuO_2 particulate (5 µm AMAD aerosol). For retrospective assessment it should be recognised that a wide range of mixtures is possible.

Particulate aerosols

Ruthenium chloride

(22) Thompson et al. (1958) measured excretion of ^{106}Ru for 60 days after administration of ruthenium chloride to rats by intratracheal instillation, and the tissue distribution at the end of the experiment. They estimated that cumulative urinary excretion accounted for ~29% of the initial lung deposit (ILD), cumulative faecal excretion ~66%, activity in the respiratory tract ~2%, and activity in systemic tissues ~3% of the administered amount. Excretion in faeces exceeded that in urine for about 15 days, and was much higher than following intravenous or intraperitoneal injection. This suggests that much of the activity deposited in the lung was cleared by particle transport to the alimentary tract before it could be absorbed, i.e. that s_r <100 d^{-1}. However, ~10% ILD was excreted in urine in the first few days,

suggesting that s_r >1 d^{-1}.

(23) Burykina (1969) followed the lung retention of ^{106}Ru for 75 days after administration of ruthenium chloride to rats by intratracheal instillation. Although there was some rapid clearance from the lungs ~10% ILD remained in the lungs at 75 d. As discussed below, bound state parameter values for ruthenium of f_b = 0.05 and s_b = 0.1 d^{-1} are used here. Assuming these values, dissolution parameter values fitted here were: f_r = 0.8, s_r = 4 d^{-1} and s_s = 0.007 d^{-1}, consistent with assignment to Type M.

(24) Dobryakova (1970) followed the biokinetics of ^{106}Ru for 14 days after administration of ruthenium chloride to rats by intratracheal instillation. There was rapid absorption from the lungs: ~50% of the ILD was absorbed at 30 minutes and ~70% ILD at 1 day. Subsequent clearance was slower and excretion mainly faecal, with ~6% ILD remaining in the lungs at 14 d. As discussed below, bound state parameter values for ruthenium of f_b = 0.05 and s_b = 0.1 d^{-1} are used here. Assuming these values, dissolution parameter values fitted here were: f_r = 0.8, s_r = 10 d^{-1} and s_s = 0.1 d^{-1}, consistent with assignment to Type F.

(25) Although specific parameter values for ruthenium chloride based on *in vivo* data are available, they are not adopted here, because inhalation exposure to it is unlikely. Instead, ruthenium chloride is assigned to Type F.

Ruthenium oxalate

(26) Newton and Latven (1971) followed the biokinetics of ^{106}Ru for 16 days after inhalation by a dog of ^{106}Ru oxalate, heat-treated at 100°C. (Other dogs inhaled ^{106}Ru oxalate aerosols heat-treated at 500°C or 1000°C, which was thought to convert most of the ^{106}Ru to $^{106}RuO_2$: see below). In a complementary experiment fractional absorption of ^{106}Ru from the alimentary tract after administration of the same material by gavage to a dog was estimated to be ~0.2. Following inhalation, clearance was rapid: 73% IBB was excreted in the first 4 days, and the rest with a half-time of 14 days. At 16 days, 40% of the retained ^{103}Ru was in the lungs, (~10% ILD) suggesting either Type F or Type M behaviour. The rest was widely distributed. However, 4% was associated with the nasal turbinates: a much larger fraction than after inhalation of particles treated at higher temperatures (~0.1%), and suggesting retention of a bound fraction.

(27) Newton et al. (1975, 1976) followed the biokinetics of ^{106}Ru for 365 days after inhalation by hamsters of ^{106}Ru oxalate aerosols heat-treated at 27°C, 300°C, 600°C or 1100°C. It was considered that at 27°C and 300°C mixed aerosols were formed which contained ruthenium oxalate and degradation products, but at 600°C or 1100°C most of the ^{106}Ru was converted to $^{106}RuO_2$: see below. In dissolution tests *in vitro* (synthetic serum ultrafiltrate at 37°C) ~38% and ~33% dissolved from aerosol samples formed at 27°C and 300°C, respectively, mainly in the first day, suggesting f_r ~0.3, and s_r >10 d^{-1}. At 8 days after inhalation of aerosol formed at 27°C, ~30% of the retained ^{106}Ru was in the lungs, with ~5% in the skeleton and ~20% in soft tissues. For the particles formed at 300°C, lung retention was somewhat higher and systemic uptake lower. For both aerosols, ~7% was in the skull, and was attributed to retention of ^{106}Ru in the NP region. As discussed below, bound state parameter values for ruthenium of f_b = 0.05 and s_b = 0.1 d^{-1} are used here. Assuming these values, dissolution parameter values fitted here for the aerosol formed at 27°C were: f_r = 0.36, s_r = 37 d^{-1} and s_s = 0.1 d^{-1}, consistent with assignment to Type F; and for the aerosol formed at 300°C, f_r = 0.28, s_r = 34 d^{-1} and s_s = 0.008 d^{-1}, consistent with assignment to Type M.

(28) Although specific parameter values for ruthenium oxalate based on *in vivo* data are available, they are not adopted here, because inhalation exposure to it is unlikely. Instead, ruthenium oxalate is assigned to Type F.

Ruthenium citrate

(29) Boecker and Harris (1969) followed the biokinetics of ^{106}Ru for 512 days after inhalation of ^{106}Ru citrate by dogs. Whole-body retention was represented by a four-component exponential function: 80%, 13%, 4% and 3% IBB were retained with effective half-times of 0.6, 11, 53 and 280 days, respectively. The large amounts excreted in the first few days, in both urine and faeces, suggest that much of the activity deposited in the respiratory tract was absorbed rapidly, at a rate similar to particle transport from the upper airways to the alimentary tract. Subsequent excretion was mainly to urine. Soon after exposure, the lungs contained about 40% IBB, and this decreased to ~4% IBB after 16 days. There was wide distribution of the ^{106}Ru retained in the body, but the concentration in lungs remained higher than in other tissues. The authors suggested that hydrolysis of the polyvalent ruthenium might have caused the long-term lung retention. As discussed below, bound state parameter values for ruthenium of $f_b = 0.05$ and $s_b = 0.1$ d^{-1} are used here. Assuming these values, dissolution parameter values fitted here were: $f_r = 0.8$, $s_r = 0.3$ d^{-1} and $s_s = 0.005$ d^{-1}, consistent with assignment to Type M. Although specific parameter values for ruthenium citrate based on *in vivo* data are available, they are not adopted here, because inhalation exposure to it is unlikely. Instead, ruthenium citrate is assigned to Type M.

Ruthenium dioxide (RuO_2)

(30) Bair et al. (1961) followed the biokinetics of ^{106}Ru for 490 days after inhalation of $^{106}RuO_2$ aerosols by mice. Clearance was initially rapid: ~95% IBB cleared within a few days. After the first day the lungs contained more ^{106}Ru than any other tissue. Lung retention was fit by a 3-component exponential function with 83%, 15% and 2% ILD retained with biological half-times of 7, 28 and 230 days. It was estimated that the ILD was ~25% IBB. Systemic uptake (bone and muscle) accounted for ~1% IBB at 1 day, and decreased slowly thereafter. As discussed below, bound state parameter values for ruthenium of $f_b = 0.05$ and $s_b = 0.1$ d^{-1} are used here. Assuming these values, dissolution parameter values fitted here were: f_r ~0.3, s_r ~10 d^{-1} and s_s ~0.001 d^{-1}, consistent with assignment to Type M.

(31) Burykina (1962) measured the tissue distribution of ^{103}Ru at times up 11 days after administration of $^{103}RuO_2$ to rats by intratracheal instillation. There were very low activities measured in systemic tissues, <0.01% ILD in total, indicating Type S behaviour.

(32) Stuart and Gaven (1970) followed the biokinetics of ^{106}Ru for 39 months after inhalation of $^{106}RuO_2$ by dogs. The $^{106}RuO_2$ was avidly retained in the lungs. After the early clearance phases, whole body retention was fit by a single exponential function with biological half-times in the range 5 - 9 years. From 7 to 39 months >98% of retained ^{106}Ru was in the lungs or associated lymph nodes. As discussed below, bound state parameter values for ruthenium of $f_b = 0.05$ and $s_b = 0.1$ d^{-1} are used here. Assuming these values, dissolution parameter values fitted here were: $f_r = 0.0005$, $s_r = 100$ d^{-1} and $s_s = 0.0004$ d^{-1}, consistent with assignment to Type S.

(33) As outlined above, Newton and Latven (1971) followed the biokinetics of ^{106}Ru for 16 days after inhalation by a dog of ^{106}Ru oxalate aerosols heat-treated at 500°C or 1000°C, which was thought to convert most of the ^{106}Ru to $^{106}RuO_2$. In complementary experiments fractional absorption of ^{106}Ru from the alimentary tract after administration of the same materials by gavage to dogs were estimated to be ~0.02 and 0.003. Following inhalation, ~50% IBB was excreted in the first few days, and the rest with a half-time of ~40 and ~300 days, respectively. At 16 days after inhalation of aerosol formed at 1000°C, 97% of the retained ^{103}Ru was in the lungs, with ~2% in the skeleton and soft tissues combined,

suggesting either Type M or Type S behaviour. For the particles formed at 500°C, lung retention was somewhat lower and systemic uptake higher.

(34) As outlined above, Newton et al. (1975, 1976) followed the biokinetics of ^{106}Ru for 365 days after inhalation by hamsters of ^{106}Ru oxalate aerosols heat-treated at 600°C or 1100°C. In dissolution tests *in vitro* (synthetic serum ultrafiltrate at 37°C for 20 days) dissolution was negligible. At 365 days after inhalation of aerosol formed at 1100°C, ~84% of the retained ^{106}Ru was in the lungs, with ~1% in the skeleton and ~1% in soft tissues. For the particles formed at 600°C, lung retention was somewhat lower and systemic uptake higher. As discussed below, bound state parameter values for ruthenium of f_b = 0.05 and s_b = 0.1 d^{-1} are used here. Assuming these values, dissolution parameter values fitted here were: f_r = 0.001, s_r = 100 d^{-1} and s_s = 0.003 d^{-1}, for the aerosol formed at 1100°C; and f_r = 0.001, s_r = 100 d^{-1} and s_s = 0.0045 d^{-1}, for the aerosol formed at 600°C, consistent with assignment to Type M.

(35) Five workers were monitored for several months following acute inhalation of ^{106}Ru, thought to be in the form of RuO_2 (Hesp and Coote, 1970). *In vivo* chest counts were started 3–13 days after intake and continued up to 377 days. Measurements of urinary ^{106}Ru were started 15–22 days after intake and continued up to 354 days after intake. Long-term retention of $^{106}RuO_2$ occurred in the chest, presumably in lungs and lymph nodes. The biological half-time for chest retention averaged 206 days (range 174–428 days). A similar average half-time was indicated by urinary data. On average, daily loss in urine was equivalent to about 44% of daily biological removal from the chest. The other 56% presumably was lost in faeces or retained in systemic tissues. As discussed below, bound state parameter values for ruthenium of f_b = 0.05 and s_b = 0.1 d^{-1} are used here. Assuming these values, dissolution parameter values fitted here were: f_r = 0.001, s_r = 100 d^{-1} and s_s = 0.002 d^{-1}, consistent with assignment to Type M.

(36) As noted in the section on ruthenium tetroxide above, in two reported incidents it was suspected that RuO_4 was released into the environment but converted to RuO_2 by interaction with the ambient aerosol.

(37) Seven persons were monitored by external counting following accidental inhalation of ^{103}Ru (Pusch 1968). Drops of water containing fission products of ^{235}U had been accidentally spread on a laboratory floor, and ^{103}Ru in the droplets apparently became airborne and spread throughout the building. The chemical form of airborne ^{103}Ru was not determined but may have been a mixture of $^{103}RuO_4$ vapour and particulate ^{103}Ru, possibly RuO_2 formed by interaction of $^{103}RuO_4$ with the ambient aerosol through processes described by Snipes and Kanapilly (1983). Ruthenium was not detected in any organ other than the lungs. Measurements of retention in the chest were started 3 days after exposure and continued for 1-4 months. The biological half-time averaged ~80 days (range 64 to 93 days). Urinary excretion accounted for ~20% of urinary plus faecal losses in the early days after exposure, suggesting Type M behaviour.

(38) Thirty-five workers were exposed for 10-15 minutes to airborne ^{106}Ru while working in a building where nuclear fuel was reprocessed (Howells et al., 1977). The released activity appeared to have been $^{106}RuO_4$, but this presumably was converted in part to particulate forms of ^{106}Ru during mixing and interacting with room air (Snipes and Kanapilly, 1983). Later analysis of samples from the contaminated building indicated that the ruthenium was in an oxide form (Howells et al., 1977). Immediately after the incident, individuals were monitored by external counting. Localization (longitudinal and lateral scanning) began within 8 days and indicated that the observed ^{106}Ru was retained in the lungs, with no significant translocation to other body organs. Measurements of chest activities were made on 11 workers for 3 years.

Biological half-times estimated for seven workers were in the range 625-3500 days. They were not determined for the other three, because their fitted effective half-times equalled or exceeded the physical half-life of ^{106}Ru. The apparent increase in lung content was attributed to redistribution of activity to sites with higher counting efficiency. The long biological half-times are consistent with the hypothesis that the deposited ^{106}Ru had been converted to $^{106}RuO_2$, and suggest Type S behaviour.

(39) Based on these studies ruthenium dioxide is assigned to default Type S.

Irradiated fuel fragments

(40) Rundo (1965) measured mixed fission products *in vivo* from 6 to 864 days after suspected accidental inhalation of irradiated uranium by a worker. Measurements indicated that the activity was mainly located in the lungs. Biological clearance of ^{103}Ru could not be measured, suggesting a half-time >230 days, and Type M or S behaviour of the ruthenium present.

(41) Mirell and Blahd (1989) made whole-body measurements of activity on seven people from about two weeks to several months after exposure to the initial Chernobyl reactor accident plume in Kiev, Ukraine. Biological retention half-times were similar for different radionuclides (45 days for ^{103}Ru) and different from those expected for systemic retention, indicating that they were trapped in particles and metabolically inert, thus indicating Type M rather than Type F behaviour.

(42) The *in vitro* dissolution of samples of particles released from the Chernobyl accident was measured for up to 60 d (Cuddihy et al., 1989). For all radionuclides, including ^{103}Ru and ^{106}Ru, 10% dissolved in a few hours, and the rest with a half-time of 160 d. Hence $f_r = 0.1$, s_r ~10 d^{-1}, and $s_s = 0.004$ d^{-1}, consistent with assignment to Type M.

(43) Lang et al, (1994) followed the biokinetics of ^{95}Zr, ^{95}Nb, ^{103}Ru, and ^{141}Ce for 3 months after intratracheal instillation of neutron-irradiated UO_2 particles into rats. For the ^{103}Ru the amounts in kidney and bone were <1% ILD. It was assessed here that f_r ~0.01, and s_s ~ 0.005 d^{-1}, suggesting Type M or S behaviour.

(44) Based on these studies ruthenium associated with irradiated fuel fragments is assigned to default Type M.

Rapid dissolution rate for ruthenium

(45) Following deposition in the respiratory tract of the most soluble forms studied (chloride, oxalate and citrate), a rapid phase of dissolution was observed. Analysis here suggested values of s_r of the order of 10-100 d^{-1}, but it was considered that there was insufficient information to select a rapid dissolution rate, s_r, for ruthenium different from the general default value of 100 d^{-1}, which is applied here to all Type F forms of ruthenium.

Extent of binding of ruthenium to the respiratory tract

(46) Following deposition in the respiratory tract of the most soluble forms studied (citrate, chloride and oxalate), a rapid phase of dissolution was observed, but was incomplete. The strongest evidence that the retention was at least partly due to binding to respiratory tract tissues, rather than transformation to relatively insoluble particles, comes from studies of inhaled RuO_4. Long-term retention of a fraction of the ruthenium was observed throughout the respiratory tract, but notably in the ET and conducting airways, from which most particles are cleared rapidly. Autoradiographs showed that the ruthenium dispersion in the turbinates and lymph nodes was relatively uniform: only single tracks were observed with no indications of focal accumulation, supporting the view that the ruthenium was in a bound rather than

particulate form. Based on the results of a study of $^{106}RuO_4$ inhaled by dogs (Snipes, 1981), bound state parameter values for ruthenium of $f_b = 0.05$ and $s_b = 0.1$ d^{-1} were chosen here.

(47) There is experimental evidence that ruthenium in soluble form deposited in the conducting airways is retained in a bound state. It is therefore assumed here that these bound state parameter values apply throughout the respiratory tract (ET_2, BB, bb and AI regions).

Table 2-2. Deposition and absorption for gas and vapour compounds of ruthenium

	Percentage deposited (%)[a]						Absorption[b]			
Chemical form/origin	Total	ET_1	ET_2	BB	bb	AI	f_r	s_r (d^{-1})	s_s (d^{-1})	Absorption from the alimentary tract, f_A
Ruthenium tetroxide	100[b]	40	40	12	7	1	0.5	1	0.001	0.01

[a] *Percentage deposited* refers to how much of the material in the inhaled air remains in the body after exhalation. Almost all inhaled gas molecules contact airway surfaces, but usually return to the air unless they dissolve in, or react with, the surface lining.

[b] It is assumed that for ruthenium the bound fraction f_b is 0.05 with an uptake rate $s_b = 0.1$ d^{-1}.

Table 2-3. Absorption parameter values for inhaled particulate forms of ruthenium and for ingested ruthenium

		Absorption parameter values[a]			
Inhaled particulate materials		f_r	s_r (d^{-1})	s_s (d^{-1})	Absorption from the alimentary tract, f_A
Default parameter values[b,c]					
Absorption Type	Assigned forms				
F	Chloride, oxalate	1	30	–	0.05
M	Citrate, all unspecified forms[d]	0.2	3	0.005	0.01
S	Dioxide	0.01	3	$1x10^{-4}$	$5x10^{-4}$
Ingested material					
All chemical forms					0.05

[a] It is assumed that for ruthenium the bound fraction f_b is 0.05 with an uptake rate $s_b = 0.1$ d^{-1}, and that this applies throughout the respiratory tract (ET_2, BB, bb and AI regions). The values of s_r for Type F, M and S forms of ruthenium (30, 3 and 3 d^{-1}, respectively) are the general default values.

[b] Materials (e.g. ruthenium chloride) are listed here where there is sufficient information to assign to a default absorption Type, but not to give specific parameter values (see text).

[c] For inhaled material deposited in the respiratory tract and subsequent cleared by particle transport to the alimentary tract, the default f_A values for inhaled materials are applied: i.e. the product of f_r for the absorption Type and the f_A value for ingested soluble forms of ruthenium (0.05).

[d] Default Type M is recommended for use in the absence of specific information, i.e. if the form is unknown, or if the form is known but there is no information available on the absorption of that form from the respiratory tract.

2.2.2. Ingestion

(48) Measurements of the urinary and faecal excretion of ruthenium by a male volunteer after ingestion of chloro-complexes of Ru(III) and Ru(IV), Ru-contaminated clams or nitrosyl Ru(III) suggested that absorption was about 0.01 and perhaps somewhat greater for nitrosyl Ru(III) (Yamagata et al, 1969). Studies by Veronese et al. (2003) and Giussani et al. (2008) used stable isotopes for the determination of the absorption and retention of ruthenium in five

human subjects. They obtained absorption values of $(7.5\pm1.2)\cdot10^{-3}$ for inorganic ruthenium (poorly complexed ruthenium), 0.039±0.005 for Ru-citrate, and <0.04 for Ru-ascorbate.

(49) Results from a number of studies of the absorption of ^{106}Ru administered as the chloride to mice, rats, rabbits, guinea pigs, chickens, cats, dogs and monkeys, including values for fasted animals, were in the range of 0.02 - 0.06 (Burykina, 1962; Thompson et al, 1958; Furchner et al, 1971; Bruce and Carr, 1961; Stara et al, 1971). Values for ^{106}Ru administered as the oxide to rats and rabbits were in the range of 0.003 - 0.03. Bruce and Carr (1961), Bruce (1963) measured the absorption of Ru administered in the form of nitrosyl derivatives. Both nitrato and nitro- complexes of nitrosyl Ru are formed during dissolution in nitric acid in the reprocessing or U fuels. The nitro-complexes are probably more important because they are more resistant to hydrolysis in neutral and alkaline conditions. Results obtained for the nitrato-nitrosyl complex in rats and rabbits were 0.06 and 0.13, respectively. A value of 0.04 was reported for the absorption of Ru administered to rats as a nitro-nitrosyl (Bruce, 1963). Stara et al. (1971) estimated absorption of Ru in cats given nitrosyl Ru compounds as between 0.1 and 0.15. Cantone et al. (1994) used stable isotopes to estimate absorption in a rabbit as 0.06.

(50) In *Publication 30* (ICRP, 1980), an absorption value of 0.05 was recommended for all chemical forms of Ru. This value was adopted in *Publication 56* (ICRP, 1989) for dietary intakes. In this report, the default assumption is an f_A of 0.05.

2.2.3. Systemic Distribution, Retention and Excretion

2.2.3.1. Summary of the database

Data for human subjects

(51) Whole-body retention of ruthenium was measured in a healthy adult male who ingested different chemical forms of ^{103}Ru ($T_{1/2}$ = 39.3 d) or ^{106}Ru ($T_{1/2}$ = 373.6 d) on different occasions (Yamagata et al., 1969, 1971). Data for ^{103}Ru indicated two retention components with biological half-times of 2.3 d and 30 d. The early component may have reflected unabsorbed activity, including activity bound in the intestinal mucosa as observed in laboratory animals after oral administration of ruthenium (Nelson et al., 1962; Bruce et al., 1962; Stara et al., 1971). The longer-term behavior of ^{103}Ru in the subject could not be determined due to the short radiological half-life. Results from a later study on the same subject using ^{106}Ru suggested a retention component with half-time of about 9 d and a second component with half-life 32 d. At longer times, the estimated biological half-time lengthened with the period of observation: 81 d based on observations in the period 40-80 d after intake, 122 d at 80-150 d after intake, 158 d at 150-350 d after intake, and 385 d at 350-660 d after intake.

(52) Veronese, Giussani, and coworkers measured the rate of disappearance of the stable isotope ^{101}Ru from blood plasma and its rate of urinary excretion following intravenous injection into healthy volunteers (Veronese et al., 2001, 2003, 2004; Giussani et al., 2008). Solutions with different degrees of complexation of ruthenium with citrate were injected in different experiments. In all cases there was an initial rapid distribution of ruthenium between plasma and the interstitial fluids. The subsequent pattern of disappearance from plasma depended on the form administered. A relatively fast component of clearance was followed by a relatively slow phase, but the ratio of the size of the fast and slow components varied with the degree of complexation of ruthenium in the injected solution. The investigators concluded that the fast and slow components represented ruthenium complexed

with citrate and inorganic ruthenium, respectively. The half-times of the fast and slow components of clearance were estimated as 17 +/- 2 min (mean +/- standard deviation) and 23 +/- 2 h, respectively. The fast component represented an estimated 82 +/- 2% of the total for solutions with highly complexed ruthenium and 17 +/- 2% for solutions with the lowest degree of complexation. Urinary excretion of ruthenium was rapid following injection of highly complexed ruthenium, with more than 40% of the injected amount excreted in urine during the first 12 h and up to 70% over the first 2 d. Total excretion amounted to less than 25% of the injected amount over the first 48 h after administration of the solution with the lowest degree of complexation.

Data for laboratory animals

(53) Furchner et al. (1964, 1971) investigated the systemic biokinetics of ^{106}Ru in mice, rats, monkeys, and dogs receiving $^{106}RuCl_3$ orally or by intraperitoneal or intravenous injection. For each species, whole-body retention data from injection studies were fit by a sum of four exponential terms. Short- and intermediate-term retention as represented by the first three terms was broadly similar in the four species. Long-term retention represented about 17% (14.7-18.7%) of the injected amount in all four species, but corresponding biological half-times were more variable: about 750 d in mice, 500 d in rats, 200 d in monkeys, and 1500 days in dogs. The large differences in derived long-term half-times may have been due in part to the different lengths of observation periods, e.g. 276 d for monkeys and 970 d for dogs, but this does not fully explain the differences.

(54) Boecker and Harris (1969) investigated the behavior of ^{106}Ru in beagles after acute inhalation of ^{106}Ru citrate. By a few days after intake the systemic burden represented the preponderance of total-body activity although the concentration of ^{106}Ru in the lungs exceeded that in other tissues throughout the 512-day study. A sum of four exponential terms fit to whole-body retention data paralleled a retention curve determined earlier by Furchner et al. (1964) for dogs receiving $^{106}RuCl_3$ by intravenous injection. As determined in one of the dogs in the inhalation study, losses by urinary and faecal excretion were roughly the same over the first three days, but thereafter daily urinary excretion generally was 3-7 times greater than daily faecal excretion.

(55) Cumulative urinary excretion over the first 3 d after intravenous or intraperitoneal injection of $^{106}RuCl_3$ into monkeys, dogs, rats, and mice was 21.6-29.0% of the injected amount (Furchner et al., 1971). Cumulative faecal excretion was more variable, ranging from 4.1% in dogs to 18.7% in mice. The urinary to faecal excretion ratio over the first three days was 2.6 in monkeys, 5.5 in dogs, 2.2 in rats, and 1.6 in mice.

(56) In guinea pigs receiving $^{106}RuCl_3$ by subcutaneous injection, about two-thirds of the injected ruthenium was excreted in urine and faeces over the first 47 d (Burykina, 1962). The urinary to faecal excretion ratio during that period was 2.7.

(57) In rats, cumulative urinary excretion over the first 60 d accounted for 53.8% of the administered amount after intravenous injection and 51.8% after intraperitoneal injection of ^{106}Ru as chlorides (Thompson et al., 1958). The urinary to faecal excretion ratio during the same period was 2.8 for intravenous injection and 2.4 for intraperitoneal injection.

(58) Compared with intravenous or intraperitoneal injection data for ruthenium chlorides, higher rates of urinary and faecal excretion have been estimated for activity absorbed to blood after inhalation of ^{106}Ru as ruthenium tetroxide vapor (RuO_4) by rats (Runkle et al. (1980) or dogs (Snipes, 1981). The systemic distribution of retained ^{106}Ru was broadly similar to that determined in injection studies involving other forms of ruthenium.

(59) The time-dependent distribution of ruthenium in systemic tissues and fluids has been

studied in several animal species including mice, rats, rabbits, hamsters, guinea pigs, and dogs (Durbin et al., 1957; Thompson et al., 1958; Durbin, 1960; Bair et al., 1961; Bruce and Carr, 1961; Nelson et al., 1962; Burykina, 1962; Bruce, 1963; Seidel et al., 1963; Boecker and Harris, 1969; Furchner et al., 1971; Newton et al., 1976; Runkle and Snipes, 1978; Runkle et al., 1980; Snipes, 1981). A relatively high concentration of ruthenium in blood is indicated in some studies (Burykina, 1962; Newton and Latven, 1971; Snipes, 1981). Liver and kidneys are important repositories for ruthenium in the early days and weeks following its absorption to blood. Bone has been identified as an important long-term repository for ruthenium in some studies (Thompson et al., 1958; Bair et al., 1961; Burykina, 1962; Boecker and Harris, 1969). Reported fractions of systemic activity in liver, kidneys, and bone at any given time after intake are variable. For example, the liver contained roughly 6% of the administered activity at 2 d after intraperitoneal injection of ^{106}Ru as chloride into rats (Furchner et al., 1971) but about 19-26% of the absorbed activity at 1-3 days after subcutaneous injection of ^{106}Ru as chloride into guinea pigs (Burykina, 1962). Muscle and skin generally show much lower concentrations than liver and kidneys, particularly at early times after uptake to blood, but usually contain much or most of the systemic activity due to their large mass (Burykina, 1962; Boecker and Harris, 1969; Furchner et al., 1971). Nelson et al. (1962) concluded from an autoradiographic study of mice given ^{103}Ru chloride by intravenous injection that the distribution pattern of ruthenium is determined to a large extent by its elevated uptake and retention in connective tissues.

(60) Thompson et al. (1958) concluded from studies of rats administered ^{106}Ru chlorides by different modes that activity was retained more tenaciously in bone tissue than in visceral organs of rats and that deposition was greater in bone of young growing rats than in older animals. After oral administration of ruthenium as nitrosyl-trinitrate to rabbits, the concentration of ruthenium in bone was not uniform but highest in the ends of bones, apparently associated with higher deposition in areas of better blood supply and possibly bone growth (Bruce and Carr, 1961). Nelson et al. (1962) found in an autoradiographic study on mice given ^{103}Ru chloride by intravenous injection that the concentration of ^{103}Ru was low in cortical bone but that the epiphyseal plates had significant early uptake and the periosteal layer had marked activity throughout the 32-day period of observation. In relatively long-term studies, activity in bone usually has represented a substantial portion of the systemic content of ruthenium at times remote from intake (Thompson et al., 1958; Bair et al., 1961; Burykina, 1962; Boecker and Harris, 1969), but there are exceptions. For example, in a study on rats, activity in bone was estimated to represent at most 8.4% of systemic activity during the first 283 d after intraperitoneal injection of ^{106}Ru as chloride (Furchner et al., 1971). By contrast, in guinea pigs receiving ^{106}Ru as chloride by subcutaneous injection, activity in bone was estimated to represent about 40% of the systemic activity at 50 d after administration. At 128-512 d after inhalation of ^{106}Ru as citrate by dogs, activity in the skeleton represented nearly 30% of the systemic activity as estimated from data for muscle, pelt, liver, kidneys, and gastrointestinal tract.

2.2.3.2. Biokinetic model for systemic ruthenium

(61) The biokinetic model for systemic ruthenium is taken from a paper by Leggett (2012). The model structure is shown in Figure 2-1. Transfer coefficients are listed in Table 2-4.

(62) The model for blood is based on data of Veronese et al. (2003, 2004) on the rate of disappearance of ruthenium from blood plasma following intravenous injection of different

forms of ruthenium. Model parameter values are based on data for the form removed most slowly from plasma (a solution with a low degree of complexation of ruthenium with citrate), in view of the prolonged retention of ruthenium in blood indicated by some inhalation or injection studies on laboratory animals (Burykina, 1962; Newton and Latven, 1971; Snipes, 1981). Retention components determined for blood plasma in the human study are assumed to apply to whole blood.

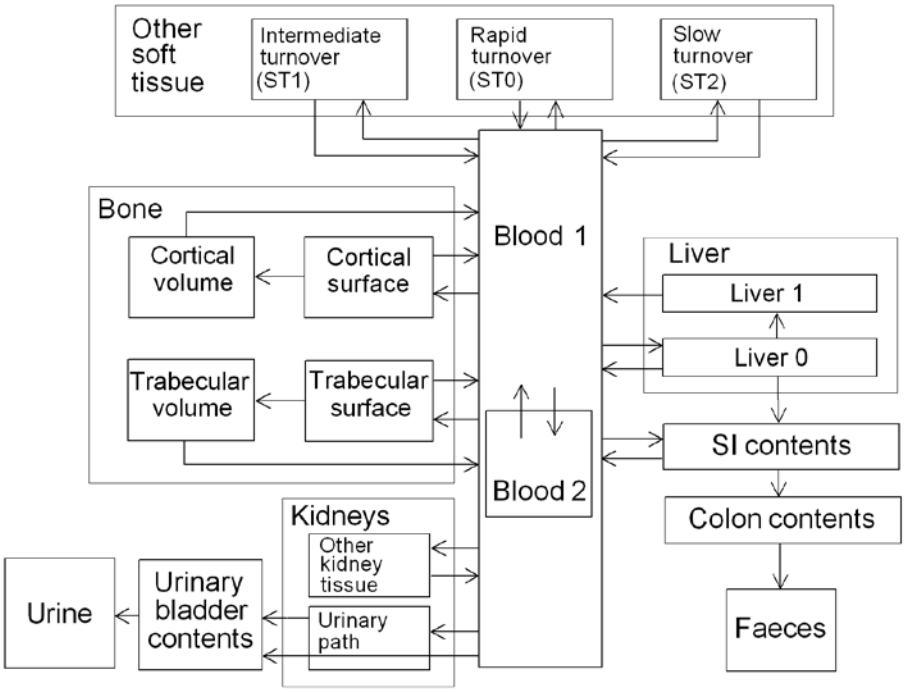

Figure 2-1. Structure of the biokinetic model for systemic ruthenium.

947

Table 2-4. Transfer coefficients for systemic ruthenium

From	To	Transfer coefficient (d^{-1})
Blood 1	Small intestine contents	3.0
Blood 1	Urinary bladder contents	17
Blood 1	Liver 0	12
Blood 1	Kidney urinary path	7.76
Blood 1	Other kidney tissue	0.24
Blood 1	Blood 2	27
Blood 1	ST0	15
Blood 1	ST1	5.0
Blood 1	ST2	5.0
Blood 1	Cortical bone surface	2
Blood 1	Trabecular bone surface	6
Blood 2	Blood 1	0.6931
Liver 0	Blood 1	0.09704
Liver 0	Small intestine contents	0.03466
Liver 0	Liver 1	0.006931
Liver 1	Blood 1	0.003798
Urinary path	Urinary bladder contents	0.1386
Other kidney tissue	Blood 1	0.003798
ST0	Blood 1	0.09902
ST1	Blood 1	0.0231
ST2	Blood 1	0.0009495
Cortical bone surface	Blood 1	0.07922
Trabecular bone surface	Blood 1	0.07922
Cortical bone surface	Cortical bone volume	0.0198
Trabecular bone surface	Trabecular bone volume	0.0198
Cortical bone volume	Blood 1	0.0000821
Trabecular bone volume	Blood 1	0.000493

948

949 (63) In the model, blood is divided into two compartments called Blood 1 and Blood 2.
950 Ruthenium entering blood is assigned to Blood 1, which is a rapid-turnover pool. Blood 2 is
951 a more slowly exchanging pool that contains most of the activity in blood except for a short
952 period soon after acute uptake of ruthenium. Activity leaves Blood 1 at the rate 100 d^{-1},
953 corresponding to a half-time of ~10 min, with 27% of outflow going to Blood 2 and the
954 remaining 73% divided among tissue compartments, urinary bladder contents, and
955 gastrointestinal contents. Activity moves from Blood 2 back to Blood 1 with a half-time of 1
956 d.

957 (64) Urinary excretion is assumed to arise from transfer of activity from blood into the
958 urinary bladder contents and transfer from blood to the kidneys (Urinary path) and subsequent
959 release to the urinary bladder contents over a period of days. Faecal excretion is assumed to
960 arise in part from biliary secretion of ruthenium into the small intestine contents after uptake
961 by the liver and in part from secretion from Blood 1 into the small intestine contents.
962 Parameter values for urinary and faecal excretion are set so that: model predictions are in
963 reasonable agreement with early urinary data for a human subject injected with low-
964 complexed Ru and for monkeys, dogs, rats, and mice injected with ^{106}Ru; urinary excretion
965 represents about 80% of total excretion based on data for different animal species but with
966 data for dogs and monkeys given relatively high weight; and the two sources of faecal

967 excretion contribute equally to endogenous faecal excretion of ruthenium, in the absence of
968 specific data on relative contributions of these sources.
969 (65) The distribution of ruthenium leaving blood is based to a large extent on the time-
970 dependent distribution of ruthenium determined in laboratory animals, particularly dogs
971 because of the availability of relatively long-term data for dogs. In addition to the 27% of
972 outflow from Blood 1 assigned to Blood 2, outflow from Blood 1 is distributed as follows:
973 12% to Liver, 8% to Kidneys, 8% to Bone, 17% to the Urinary bladder contents, 3% to Small
974 intestine contents, and 25% to Other. Activity entering Liver is assigned to the rapid-turnover
975 liver compartment called Liver 0. Fractions 0.97 and 0.03 of activity entering Kidneys are
976 assigned to Urinary path and Other kidney tissue, respectively. Three-fourths of activity
977 entering bone is assigned to Trabecular bone surface and one-fourth to Cortical bone surface.
978 Activity entering Other (25% of outflow from Blood 1) is divided as follows: 15% to the
979 short-term retention compartment ST0; 5% to the intermediate-term compartment ST1, and
980 5% to the long-term retention compartment ST2.
981 (66) Biological half-times for compartments are set to reproduce different phases of loss
982 of ruthenium from the total body observed in laboratory animals and a human subject, and the
983 time-dependent distribution of systemic activity in dogs. Activity is removed from Liver 0
984 with a biological half-time of 5 d, with 25% going to the Small intestine contents (biliary
985 secretion), 5% to Liver 1, and 70% to Blood 1. Activity transfers from Liver 1 to Blood 1
986 with a half-time of 0.5 y. Activity transfers from Urinary path to Urinary bladder contents
987 with a half-time of 5 d and from Other kidney tissues to Blood 1 with a half-time of 0.5 y.
988 Activity in soft-tissue compartments ST0, ST1, and ST2 returns to Blood 1 with half-times of
989 7 d, 30 d, and 2 y, respectively. Activity leaves Cortical bone surface or Trabecular bone
990 surface with a half-time of 7 d, with 80% transferring to Blood 1 and 20% to the
991 corresponding bone volume compartment. Activity transfers from Cortical bone volume or
992 Trabecular bone volume to Blood 1 at the rate of bone turnover.
993
994 **2.2.3.3. Treatment of radioactive progeny**
995
996 (67) The radioactive progeny addressed in the derivation of dose coefficients for
997 ruthenium isotopes are all isotopes of rhodium or technetium. Rhodium and ruthenium have
998 similar chemical properties and appear from limited comparative data to have broadly similar
999 biokinetics in rats. Therefore, rhodium produced in systemic compartments by decay of
1000 ruthenium is assigned the biokinetic model for ruthenium. Technetium atoms produced in a
1001 systemic compartment of the ruthenium model that is identifiable with a compartment of the
1002 characteristic model for technetium (i.e. the model applied in this report to technetium as a
1003 parent radionuclide) are assigned the characteristic model for technetium from their time of
1004 production. Technetium atoms produced in compartments of the ruthenium model that are
1005 ambiguous with regard to the characteristic model for technetium are assigned a transfer
1006 coefficient to the blood compartment of the technetium model, named Blood, and upon
1007 reaching Blood are assigned the characteristic model for technetium. For modeling
1008 convenience, the blood compartment of the technetium model is identified with the central
1009 blood compartment of the ruthenium model, named Blood 1. Technetium atoms produced in
1010 compartments of the liver, kidneys, or other soft tissues of the ruthenium model are assumed
1011 to transfer to Blood with a half-time of 1.6 d, the shortest removal half-time from other soft
1012 tissue in the technetium model. Technetium atoms produced in Blood 2 of the ruthenium
1013 model are assumed to transfer to Blood at the rate 1000 d^{-1}, a default value used in this report
1014 to represent rapid biological removal.

2.3. Individual monitoring

^{106}Ru

(68) ^{106}Ru is a beta emitter but it is by measured using the 0.512 and 0.622 MeV gamma rays from its short-lived daughter, ^{106}Rh. Urine bioassay and/or Whole Body counting may be used to estimate the content of ^{106}Ru internally deposited in the body.

Isotope	Monitoring Technique	Method of Measurement	Typical Detection Limit	Achievable detection limit
^{106}Ru	Urine Bioassay	γ-ray spectrometry of ^{106}Rh	10 Bq/L	3 Bq/L
^{106}Ru	Whole Body Counting	γ-ray spectrometry of ^{106}Rh	200 Bq	130 Bq
^{106}Ru	Lung Counting	γ-ray spectrometry of ^{106}Rh	42 Bq*	

* Lung monitoring of ^{106}Ru is not generally used in routine monitoring of workers. Monte Carlo program Visual Monte Carlo was used to simulate the photon emission, to calculate the calibration factor for the geometry and radionuclide, and to calculate the minimum detectable activity (MDA) in the lung. (Hunt et al, 2012)

References

Bair, W.J., Willard, D.H., Temple, L.A., 1961. The behavior of inhaled $^{106}RuO_2$ particles. Health Phys. 5:90-98.

Boecker, B.B., Harris, A.M., 1969. Tissue distribution, excretion and dosimetry of inhaled ^{106}Ru citrate in the beagle dog. In: Fission Product Inhalation Program Annual Report, 1968-1969. LF-41. pp. 111-116. Lovelace Foundation for Medical Education and Research, Albuquerque, New Mexico. Available from National Technical Information Service, Springfield, Virginia.

Bruce, R.S., 1963. Some factors influencing the absorption, retention and elimination of ruthenium. In: Diagnosis and treatment of radioactive poisoning. Vienna:IAEA, pp. 207-244.

Bruce, R.S., Carr, T.E.F., 1961. Studies in the metabolism of carrier-free radioruthenium - II. The uptake of nitrosyl-ruthenium complexes from the gastrointestinal tract. Reactor Science and Technology 14, 145-154.

Bruce, R.S., Carr, T.E.F., Collins, M.E., 1962. Studies in the metabolism of carrier-free radioruthenium - III. The behavior of nitrosyl-ruthenium in the gastrointestinal tract. Health Phys. 8, 397-406.

Burykina, L.N., 1969. On the problem of the toxicity of ruthenium-106 under repeated intratracheal administration to rats. In: Radioactive isotopes and the body, Moskalev, Yu. I., ed. Izdatel'stvo Medisina, Moscow. AEC-tr-7195, United States Atomic Energy Commission Division of Technical Information, pp. 388-396.

Burykina, L.N., 1962. The metabolism of radioactive ruthenium in the organism of experimental animals. In: The Toxicology of Radioactive Substances, Vol. 1 (A.A. Letavel and E.P. Kurlyandsicaya, Eds.) pp 60-76. Pergamon Press, Oxford.

Cantone, M.C., de Bartolo, D., Gambarini, G., Giussani, A., Ottolenghi, A., Pirola, L., Hansen, Ch., Roth, P., Werner, E., 1994. Proton nuclear activation in stable tracer technique for ruthenium metabolism studies. Nucl. Instrum. Methods Phys. Res., Sect. A. 353 (1-3), 440-443.

Cuddihy, R.G., Finch, G.L., Newton, G.J., Hahn, F.F., Mewhinney, J.A., Rothenberg, S.J., Powers, D.A., 1989. Characteristics of radioactive particles released from the Chernobyl nuclear reactor. Environ. Sci. Technol. 23 (1), 89-95.

Dobryakova, G.V., 1970. Dynamics of the removal of Te-127 and Ru-106 from rat lungs. In: Moskalev, Yu. I., Editor. Radioaktiv. Izotopy Vnesh. Srede Organizme. pp. 57-63. Moscow: Atomizdat.

Durbin, P.W., 1960. Metabolic characteristics within a chemical family. Health Phys. 2:225-238.

Durbin, P.W., Scott, K.G., Hamilton, J.G., 1957. Distribution of radioisotopes of some heavy metals in the rat. University of California (Berkely) Publ. Pharmocol. 3, 1-34.

Furchner, J.E., Richmond, C.R., Drake, G.A., 1964. Ruthenium-106 in mice, rats, and dogs: Interspecies comparisons. LA-3132-MS, Los Alamos Scientific Laboratory, Los Alamos, NM, pp. 19-24.

Furchner, J.E., Richmond, C.R., Drake, G.A., 1971. Comparative metabolism of radionuclides in mammal-VII. Retention of 106-Ru in the mouse, rat, monkey and dog. Health Phys. 21, 355-365.

Giussani, A., Cantone, M.C., Gerstmann, U., Greiter, M., Hertenberger, R., Höllriegl, V., Leopold, K., Veronese, I., Oeh, U., 2008. Biokinetics of ruthenium isotopes in humans and its dependence on chemical speciation. 12th International Congress of the International Radiation Protection Association, IRPA 12, Buenos Aires, Argentina, 19-24 October 2008 (Proceedings on CD).

Hesp, R., Coote, J., 1970. Body radioactivity studies on a series of cases in which ruthenium-106 oxide was inhaled. Health Safety Dep., U. K. At. Energy Auth., Sellafield/Seascale/Cumberland, Engl. U. K. At. Energy Auth., Prod. Group, PG Rep. No. 979 W.

Howells, H., Ward, F.A., Coulston, D.J., Woodhouse, J.A., 1977. In-vivo measurement and dosimetry of ruthenium-106 oxide in the lung. In: Proceedings of a symposium on the handling of radiation accidents. Vienna: International Atomic Energy Agency. IAEA-SM-215/54, pp. 83-102.

ICRP, 1980. International Commission on Radiological Protection. Limits on Intakes of Radionuclides for Workers. ICRP Publication 30, Pt.2. Pergamon Press, Oxford. Ann. ICRP 4, (3/4).

ICRP, 1989. International Commission on Radiological Protection. Age-dependent Doses to Members of the Public from Intake of Radionuclides. Pt.1. ICRP Publication 56. Pergamon Press, Oxford. Ann. ICRP 20, (2).

ICRP, 2002. Guide for the Practical Application of the ICRP Human Respiratory Tract Model. ICRP Supporting Guidance 3 Ann. ICRP, 32(1-2).

Lang, S., Kosma, V.M., Kumlin, T., Halinen, A., Salonen, R.O., Servomaa, K., Rytomaa, T., Ruuskanen, J., 1994. Distribution and short-term effects of intratracheally instilled neutron-irradiated UO_2 particles in the rat. Environ. Res. 65 (1), 119-31.

Mirell, S.G., Blahd, W.H., 1989. Biological retention of fission products from the Chernobyl plume. Health Phys. 57 (4), 649-52.

Nelson, A., Ullberg, S., Kristoffersson, H., Ronnback, C., 1962. Distribution of radioruthenium in mice. Acta Radiol. 58, 53-360.

Newton, G.J., Latven, R.K., 1971. Distribution and excretion in the beagle dog of ^{106}Ru-Rh aerosols subjected to thermal degradation. In: Fission Product Inhalation Program Annual Report, 1970-1971. LF-144. Albuquerque, NM: Lovelace Foundation, pp. 81-85.

Newton, G.J., Servilla, P., Wagner, J., Boecker, B.B., 1975. Radiation dose patterns from ^{106}Ru aerosols inhaled by Syrian hamsters. I. In: Inhalation Toxicology Research Institute Annual Report 1974-1975. LF-52. Albuquerque, NM: Lovelace Biomedical and Environmental Research Institute, pp. 75-78.

Newton, G.J., Snipes, M.B., Boecker, B.B., Wagner, J.A., 1976. Radiation dose patterns from ^{106}Ru aerosols inhaled by Syrian hamsters. II. Retention and distribution. In: Inhalation Toxicology Research Institute Annual Report 1975-1976. LF-56. Albuquerque, NM: Lovelace Biomedical and Environmental Research Institute, pp. 79-83.

Pollanen, R., 1997. Highly radioactive ruthenium particles released from the Chernobyl accident:

particle characteristics and radiological hazard. Radiat. Prot. Dosim. 71(1), 23-32

Pusch, W.M., 1968. Determination of effective half-life of ruthenium-103 in man after inhalation. Health Phys. 15 (6), 515-17.

Rundo, J., 1965. A case of accidental inhalation of irradiated uranium. Brit. J. Radiol. 38, 39–50.

Runkle, G.E., Snipes, M.B., 1978. Dose patterns for $^{106}RuO_4$ inhaled by Fischer-344 rats and beagle dogs. In: Inhalation Toxicology Research Institute Annual Report. LF-60. Albuquerque, NM: Lovelace Biomedical and Environmental Research Institute, pp. 55-60.

Runkle, G.E., Snipes, M.B., McClellan, R.O., Cuddihy, R.G., 1980. Metabolism and dosimetry of inhaled $^{106}RuO_4$ in Fischer-344 rats. Health Phys. 39, 543-553.

Seidel, D., Catsch, A., Schweer, K.H., 1963. [Decorporation of radionuclides (studies on radioruthenium)] Strahlentherapie 122, 595-610.

Snipes, M.B., 1981. Metabolism and dosimetry of ruthenium-106 inhaled as ruthenium-106 tetraoxide by beagle dogs. Health Phys. 41 (2), 303-317.

Snipes, M.B., Kanapilly, G.M., 1983. Retention and dosimetry of ruthenium-106 inhaled along with inert particles by Fischer-344 rats. Health Phys. 44 (4), 335-348.

Snipes, M.B. Runkle, G.E., Sproul, S.M., 1977. Deposition, retention and dosimetry of inhaled ruthenium aerosols. In: Inhalation Toxicology Research Institute Annual Report, 1976-1977. LF-58, UC-48. Albuquerque, NM: Lovelace Biomedical and Environmental Research Institute, pp. 22-26.

Stara, J.F., Nelson, N.S., Krieger, H.L., Kahn, B., 1971. Gastrointestinal absorption and tissue retention of radioruthenium. In: Skoryna, S. C., Waldron-Edward, D. Intestinal absorption of metal ions, trace elements and radionuclides. Oxford and New York: Pergamon Press, pp. 307-318.

Stuart, B.O., Gavin J.C., 1970. Long-term retention and translocation of inhaled ^{106}Ru-$^{106}RhO_2$ in beagles. Pacific Northwest Lab. Report, BNWL-1050, 3.43-3.45.

Thompson, R.C., Weeks, M.H., Hollis, L., Ballou, J.F., Oakley, W.D., 1958. Metabolism of radioruthenium in the rat. Am. J. Roentgen. 79, 1026-1044.

Veronese, I., Cantone, M.C., Giussani, A., Maggioni, T., Birattari, C., Bonardi, M., Groppi, F., Garlaschelli, L., Werner, E., Roth, P., Höllriegl, V., Louvat, P., Felgenhauer, N., Zilker, Th., 2003. Stable tracer investigations in humans for assessing the biokinetics of ruthenium and zirconium radionuclides. Rad. Prot. Dosim. 105, 209–212.

Veronese, I., Giussani, A., Cantone, M.C., Birattari C., Bonardi M., Groppi, F., Höllriegl V., Roth, P., Werner, E., 2004. Influence of the chemical form on the plasma clearance of ruthenium in humans. App. Radiat. Isot. 60, 7-13.

Veronese, I., Giussani, A., Cantone, M.C., De Bartolo, D., Roth, P., Werner, E., 2001. Kinetics of systemic ruthenium in human blood using a stable tracer. J. Radiol. Prot. 21:31-38.

Webber, C. E., Harvey, J.W., 1976. Accidental human inhalation of ruthenium tetroxide. Health Phys. 30, 352-355.

Yamagata, N., Iwashima, K., Iinuma, T.N., Watari, K., Nagai, T., 1969. Uptake and retention experiments of radioruthenium in man -I. Health Phys. 16, 159-166.

Yamagata, N., Iwashima, K., Iinuma, T. A., Ishihara, T., Watari, K., 1971. Long-term retention of radioruthenium in man. Health Phys. 21:63.

3. Antimony (Z = 51)

3.1. Chemical Forms in the Workplace

(69) Antimony is a semi-metal or metalloid which mainly occurs in oxidation states III, IV and V. Antimony may be encountered in industry in a variety of chemical and physical forms, such as oxides, sulphides, chlorides, fluorides, tartrate and trihydride. It may also be encountered in two anionic forms which are (SbO_2^-) and (SbO_3^-). ^{124}Sb and ^{125}Sb are fission products which may be associated with irradiated fuel or corrosion products. ^{125}Sb also occurs as a neutron activation product of tin which may be present in reactor components containing zirconium.

Table 3-1. Isotopes of antimony addressed in this report

Isotope	Physical half-life	Decay mode
Sb-115	32.1 m	EC, B+
Sb-116	15.8 m	EC, B+
Sb-116m	60.3 m	EC, B+
Sb-117	2.80 h	EC, B+
Sb-118m	5.00 h	EC, B+
Sb-119	38.19 h	EC
Sb-120	15.89 m	EC, B+
Sb-120m	5.76 d	EC
Sb-122	2.724 d	B-, EC, B+
Sb-124[a]	60.20 d	B-
Sb-124n	20.2 m	IT
Sb-125[a]	2.759 y	B-
Sb-126	12.35 d	B-
Sb-126m	19.15 m	B-, IT
Sb-127	3.85 d	B-
Sb-128	9.01 h	B-
Sb-128m	10.4 m	B-, IT
Sb-129	4.40 h	B-
Sb-130	39.5 m	B-
Sb-131	23.03 m	B-

[a] Data for these radionuclides are given in the printed copy of this report. Data for other radionuclides are given on accompanying electronic disk.

3.2. Routes of Intake

3.2.1. Inhalation

Absorption Types and parameter values

(70) Information is available from experimental studies of antimony inhaled by laboratory animals as chloride, tartrate or oxide. Studies of workers occupationally exposed to stable antimony have been summarised by IARC (1989). Some information is also available on the behaviour of inhaled ^{125}Sb in man.

(71) Absorption parameter values and Types, and associated f_A values for particulate

forms of antimony are given in Table 3-2.

Antimony chloride

(72) Djurić et al. (1962) followed the biokinetics of ^{124}Sb after inhalation by rats of antimony chloride for 140 days. From the results, absorption parameter values calculated by the task group were $f_r \sim 1$, and $s_r \sim 0.5$ d^{-1}. About 1% of the initial lung deposit (ILD) was retained in the lungs with a half-time of about 70 days, giving assignment to Type F. However, from about 2 weeks after intake the concentration of ^{124}Sb in the blood was higher than that in the lungs, and hence the long-term lung retention observed may have been largely due to ^{124}Sb in the blood.

Antimony tartrate

(73) Felicetti et al. (1974b) followed the biokinetics of ^{124}Sb after inhalation by hamsters of trivalent and pentavalent antimony tartrate aerosols (heat-treated at 100°C) for 32 days. In complementary experiments with the same materials, absorption in the GI tract was found to be only about 1%. In contrast, both forms showed similar, rapid absorption from the lungs: the authors noted that by 2 hours post exposure less than 1% of the initial body burden (IBB) remained in the lungs, indicating $f_r \sim 1$, and $s_r > 10$ d^{-1}. It was also noted that there was considerable faecal excretion and hence limited absorption in the upper respiratory tract, indicating $s_r < 100$ d^{-1}. A central value for s_r of 30 d^{-1} is adopted here. It was estimated here that about 1% of the of the ILD was retained in the lungs at 2 days and 0.1% ILD at 32 days, and calculated that $f_r \sim 0.99$, and $s_s \sim 0.1$ d^{-1}, giving assignment to Type F. Although similar lung clearance was observed for the two forms, some differences in the systemic tissue distribution, e.g. between liver and skeleton, were noted.

(74) Thomas et al. (1973) and Felicetti et al. (1974a) followed the biokinetics of ^{124}Sb after inhalation, by mice and dogs respectively, of aerosols formed by heat-treating antimony tartrate droplets at various temperatures. For each aerosol, groups of mice were killed at intervals to 52 d, and one dog was killed at 32, 64 and 128 d. The chemical form of the antimony after heat treatment was not determined, but the aerosol treated at the lowest temperature (100°C) was referred to as tartrate. From the results in mice, it was estimated here that about 1% ILD was retained in the lungs at 2 days and 0.03% ILD at 32 days, and calculated that that $f_r \sim 0.99$, and $s_s \sim 0.1$ d^{-1} (as for the hamster study above). Insufficient information was given to estimate absorption parameter values in dogs, but at 32 d, 0.23% ILD was retained, giving assignment to Type F.

(75) Although specific parameter values for antimony tartrate based on *in vivo* data are available, they are not adopted here, because inhalation exposure to it is unlikely. Instead, antimony tartrate is assigned to Type F.

Antimony oxides

(76) Newton et al. (1994) measured the accumulation and retention of stable antimony trioxide (Sb_2O_3) in the lungs of rats during 13 weeks inhalation exposure and for 28 weeks after exposure. It was estimated here, from measurements in the group exposed to the lowest concentration (0.25 mg m^{-3}), that the lung retention half-time was about 50 d, indicating Type M or S behaviour.

(77) Groth et al. (1986) measured the accumulation of antimony in the lungs of rats after 9 months of chronic inhalation exposure to stable Sb_2O_3. Concentrations in lungs were considerable higher than in any other tissue. It was estimated here that the lung retention half-time was about 50 d, indicating Type M or S behaviour.

(78) Rose and Jacobs (1969) followed whole-body retention of ^{124}Sb for 300 d in one worker exposed to an aerosol, said to be oxide, resulting from activation of antimony contamination on a ^{60}Co source. The authors assessed that during the period 10 d to 6 weeks, there was significant absorption and excretion in urine, but that subsequently the non-transportable activity was retained in the lungs where it decreased only with the physical half-life. This indicates that the overall behaviour might be Type M or S, but there is insufficient information to determine which.

(79) Smelter workers exposed by inhalation to stable antimony trioxide and pentoxide showed a positive relationship between measured antimony lung content and period of employment such that there was about a tenfold increase for 40 y of employment (McCallum et al., 1971). This indicates that at least some of the material was retained in the lungs on a time-scale of years. Other workers with pulmonary changes related to exposure to antimony trioxide had measured urinary excretion of antimony in hundreds of μg/l both during and after employment (McCallum, 1963). This indicates that there is also significant absorption of antimony from the material in the lungs. Although the human data suggest possible Type M and S behaviour, the paucity of results do not provide a basis for firmer classification.

Antimony sulphide

(80) Groth et al. (1986) measured the accumulation of antimony in the lungs of rats after 9 months of chronic inhalation exposure to stable antimony ore concentrate, which is principally antimony trisulphide (stibnite) Sb_2S_3. Concentrations in lungs were considerable higher than in any other tissue. It was estimated here that the lung retention half-time was about 20 d, indicating Type M behaviour. Compared to rats exposed to oxide in a similar study (see above), the lung concentrations were lower, but concentrations in other tissues were similar, suggesting that the sulphide dissolved faster in the lungs than the oxide.

Other compounds

(81) As noted above, Thomas et al. (1973) and Felicetti et al. (1974a) followed the biokinetics of ^{124}Sb following inhalation, by mice and dogs respectively, of aerosols formed by heat-treating droplets of antimony tartrate aerosols at various temperatures. The chemical form of the antimony after heat treatment was not determined, but the higher temperatures, 500°C and ~1,000°C, were expected to result in an oxide form (Felicetti et al, 1974a). From the results in mice, it was estimated here that for aerosols formed at both the higher temperatures (500°C and 1,100°C) ~5% ILD was retained in the lungs at 2 days and ~1% ILD at 32 days, and it was calculated that f_r ~0.95, s_r ~3 d^{-1}, and s_s ~0.03 d^{-1}. Absorption was thus considerably slower than for the tartrate aerosols formed at 100°C, but still gave assignment to Type F. Insufficient information was given to estimate absorption parameter values in dogs, but at 32 d after inhalation of the aerosols formed at the higher temperatures (500°C and 1,000°C), 25% and 5% ILD was retained in the lungs, giving assignment to Types M and F respectively.

(82) Garg et al. (2003) followed whole-body retention of ^{125}Sb for 200–2400 d in seven workers exposed to an aerosol (probably oxide) produced by saw-cutting of an irradiated zirconium alloy pressure tube. Detailed measurements indicated that most of the retained activity was in the lungs, even at a year after intake. The authors assessed that lung retention at 180 days after intake was 58-91% of the initial alveolar deposit (estimated from the lung content at 7 d after intake), giving assignment to Type S in each person. However, as the ^{125}Sb and parent tin were presumably minor constituents of the zirconium alloy, the particle matrix might well have been predominantly oxides of other metals (and/or the metals

themselves), notably zirconium, which has a highly insoluble oxide (see zirconium section).

Rapid dissolution rate for antimony

(83) Evidence from the antimony tartrate studies outlined above suggests a rapid dissolution rate of the order of 30 d^{-1}, which is applied here to all Type F forms of antimony.

Extent of binding of antimony to the respiratory tract

(84) Evidence from the antimony tartrate studies outlined above suggests that following the rapid phase of absorption only about 1% of the ILD clears relatively slowly from the lungs. There is no evidence available that clearance of this material is mainly by absorption to blood, as assumed for material in the 'bound state'. It is therefore assumed that for antimony the bound state can be neglected, i.e. $f_b = 0.0$.

Table 3-2. Absorption parameter values for inhaled and ingested antimony

Inhaled particulate materials		Absorption parameter values[a] f_r	s_r (d^{-1})	s_s (d^{-1})	Absorption from the alimentary tract, f_A
Default parameter values[b,c]					
Absorption Type					
F	Chloride, tartrate	1	30	–	0.05
M	Trioxide, all unspecified forms[d]	0.2	3	0.005	0.01
S	—	0.01	3	$1x10^{-4}$	$5x10^{-4}$
Ingested materials					
All forms					0.05

[a] It is assumed that for antimony the bound state can be neglected, i.e. $f_b = 0.0$. The values of s_r for Type F, M and S forms of antimony (30, 3 and 3 d^{-1}, respectively) are the general default values.

[b] Materials (e.g. antimony chloride) are generally listed here where there is sufficient information to assign to a default absorption Type, but not to give specific parameter values (see text).

[c] For inhaled material deposited in the respiratory tract and subsequent cleared by particle transport to the alimentary tract, the default f_A values for inhaled materials are applied: i.e. the product of f_r for the absorption Type and the f_A value for ingested soluble forms of antimony (0.05).

[d] Default Type M is recommended for use in the absence of specific information, i.e. if the form is unknown, or if the form is known but there is no information available on the absorption of that form from the respiratory tract.

3.2.2. Ingestion

(85) No controlled studies on antimony absorption in humans have been carried out, though an accidental exposure to antimony-containing dust (Rose and Jacobs, 1969) demonstrated absorption to be less than 0.05. Results from experiments using female rhesus monkeys suggest that the absorption of Sb administered as tartar emetic (antimony potassium tartrate) was about 0.3 (Waitz et al, 1965) while comparable studies with rats gave lower values of about 0.05 for this compound (Moskalev, 1964). Most studies performed on different chemical forms of Sb(III) and Sb(V) indicated that intestinal absorption was not usually greater than 0.01 (Rose and Jacobs, 1969; Thomas et al, 1973; Felicetti et al, 1974b), whereas Gerber et al. (1982) found a value of 0.07 for Sb(III) in pregnant mice. Chertok and

Lake (1970) reported that, for dogs fed with ^{122}Sb in debris from a sub-surface nuclear test site, absorption was at least 0.04. Results obtained by Van Bruwaene et al. (1982) for the excretion of ^{124}Sb after oral administration as the chloride, compared with data for intravenous injection, suggested absorption greater than 0.02. Inaba et al. (1984) administered ^{125}Sb to rats, either mixed with blood or biologically incorporated into blood cells and reported absorption of about 0.01 and 0.5, respectively.

(86) In *Publication 30* (ICRP, 1981), the recommended absorption values were 0.1 for antimony in tartar emetic and 0.01 for all other forms. In *Publication 69* (ICRP, 1995), a value of 0.1 was applied to dietary intakes. Because of the variability of the data, a single f_A value of 0.05 is recommended here for all situations where specific information is not available.

3.2.3. Systemic Distribution, Retention and Excretion

3.2.3.1. Summary of the database

(87) The biokinetics of antimony in the human body is not well characterized despite a long history of therapeutic use of stable antimony and a number of bioassay studies on workers exposed to known levels of stable antimony in air. Subjects administered antimony compounds for therapeutic purposes generally have received large masses of antimony compared with the estimated normal body content. It is uncertain whether the biokinetic data for these subjects reflect normal biokinetics of antimony, but comparative data for different masses of administered antimony do not reveal a mass effect on the excretion rate.

(88) Antimony occurs in nature either in the trivalent or pentavalent state, with the trivalent state being the more common and more stable. Trivalent and pentavalent antimony initially show different biokinetics after entering the systemic circulation. For example, Sb(III) is excreted in urine at a lower rate and accumulated by red blood cells at a higher rate than Sb(V) in the first day or two after intravenous or intramuscular injection. There is evidence of some reduction of Sb(V) to Sb(III) *in vivo* and convergence of the systemic biokinetics of these two initial forms over time, but data on the rate and extent of conversion of Sb(V) to Sb(III) are inconsistent.

(89) Information on the time dependent distribution of systemic antimony comes mainly from animal studies. Some species dependence in the behavior of antimony is indicated. For example, rats have shown much higher accumulation of antimony in red blood cells (RBC) than mice, dogs, or human subjects. The collective animal data indicate rapid early loss of absorbed or injected antimony in urine and concentration of much of the retained antimony in the liver, skeleton, and skin or pelt. The longest observed biological half-times for systemic antimony have varied from several days to a few months. Study periods generally have been too short to detect any small long-term component of retention.

Human subjects

(90) Boyd and Roy (1929) compared the rate of excretion of antimony by patients following intravenous administration of Sb(III) as antimony sodium tartrate and Sb(V) as ethylstibamine. Following injection of Sb(III) about 2.5% of the antimony was excreted from 0-24 h, 2% from 24-48 h, and 1% or less from 48-72 h. Following injection of Sb(V) about 19% of the antimony was excreted in urine from 0-2.5 h, 41% from 0-24 h, 6% from 24-48 h, and 1.25% from 48-72 h. Thereafter, daily excretion remained at 1% or less through day 13 following injection. Intramuscular injection of the Sb(V) compound produced a slightly

lower excretion rate over the first two days than intravenous injection of the same compound.

(91) Khalil (1931) examined urine, faeces, sweat, milk, and sputum as routes of excretion of antimony in subjects undergoing treatment with Sb(III) as antimony potassium tartrate or stibophen. Urine and faeces appeared to be the only significant routes of excretion. During the 45-d observation period about 45-50% of administered antimony was excreted in urine and about 3.5% was excreted in faeces.

(92) Goodwin and Page (1943) measured urinary excretion of stable antimony by human subjects from 1-48 h after intravenous or intramuscular injection of Sb(III) as stibophen or intravenous injection of Sb(V) as sodium stibogluconate. Cumulative urinary excretion at 24 and 48 h after injection of Sb(III) was 20.4 +/- 2.2% (mean +/- standard deviation) and 23.9 +/- 3.6%, respectively, after intravenous injection and 24.0 +/- 9.9% and 26.5 +/- 12.0%, respectively, after intramuscular injection. A fivefold difference in the mass of antimony administered intravenously (42.5 mg versus 8.5 mg) had little if any effect on the excretion rate. Total urinary excretion of antimony over the first 48 h after administration of Sb(V) was 83 +/- 6% of the injected amount. The portion of antimony excreted as Sb(III) after administration of Sb(V) was low and variable (1.1-7.6%) over the first 6 h but rose to 50-56% at 28-48 h, indicating gradual conversion of Sb(V) to S(III) in the body.

(93) Following intravenous infusion of Sb tartar emetic (KSb(III) tartrate) to eight male African soldiers suffering from schistosomiasis, 21±4% (range 18-23%) of the dose was excreted in the urine within 72 h (Alves and Blair, 1946).

(94) Bartter et al. (1947) investigated the biokinetics of Sb(III) in seven volunteers receiving ^{124}Sb tartar emetic by intravenous injection. More than 90% of the injected activity was removed from blood within 30 min after injection. Thereafter the blood content declined much more gradually. During the first day urinary and faecal excretion averaged 10.5 +/- 1.9% and 1.5 +/- 0.4%, respectively, of the administered amount. During the first five days urinary and faecal excretion averaged 21.2 +/- 4.6% and 4.4 +/- 1.3%, respectively. Urinary and faecal excretion of antimony measured in one subject over the first 27 d accounted for 66% and 7%, respectively, of the administered amount. The removal half-time from the body in this subject was about 14 d between 1 and 27 days after injection. Based on 44 individual daily measurements of excreta from all seven subjects, the mean daily urinary to faecal excretion ratio was 6.8 (range 0.6-25.8).

(95) Otto et al. (1947) determined antimony levels in blood plasma, red blood cells, and urine of 14 patients after intramuscular injection of trivalent antimony compounds (anthiolimine or monosodium antimony thioglycollate) or pentavalent antimony compounds (antimony sodium gluconate or ethylstibamine). Trivalent antimony showed five-fold higher concentrations in red blood cells than plasma within the first 24 h after injection. Pentavalent compounds showed much lower affinity than trivalent compounds for red blood cells. Average 24-h urinary excretion of antimony was lower for trivalent compounds (11.4% for anthiolimine and 8.1% for monosodium antimony thioglycollate) than pentavalent compounds (43% for antimony sodium gluconate and 17% for ethylstibamine).

(96) Abdallah and Saif (1962) reported studies in which 25 male volunteers were given sodium ^{124}Sb(III)-dimercaptosuccinate (^{124}Sb-DMSA) by intramuscular or intravenous injection. Following intramuscular injection, cumulative excretion accounted for about 25% of administered ^{124}Sb after 1 d, 50% after 15 d, and 68% after 32 d. Following intravenous injection, cumulative excretion accounted for about 35% of the administered ^{124}Sb after 1 d and 63% after 4 d. External measurements indicated relatively high accumulation of activity in the liver. The liver content peaked about 2 d after injection. Two components of retention in the liver are indicated by a plot of the measurements. Approximately 80-85% of the peak

content was removed with a half-time of a few days and the remaining 15-20% had a much longer retention time that could not be quantified over the relatively short observation period.

(97) Taylor (1966) reported measurements of antimony in the urine of workers who had inhaled $SbCl_3$. The data are too sparse to allow a detailed analysis but indicate rapid elimination of absorbed antimony in urine.

(98) Rose and Jacobs (1969) reported a case of acute inhalation of a relatively insoluble form of ^{124}Sb by a worker in a nuclear research facility. The intake could not be estimated with much accuracy by whole-body counting during the first day due to surface contamination of the worker's body. During the first 10 d after intake the authors estimated total faecal excretion to be about 1000 times total urinary excretion of ^{124}Sb. The rate of urinary excretion of ^{124}Sb declined rapidly over the first few days after the incident. In the early weeks after the incident the effective half-life of ^{124}Sb in the body was approximately 30 d, corresponding to a biological half-time of ~60 d. In later months the effective half-life was about the same as the radiological half-life of ^{124}Sb (~60 d), indicating little biological removal of ^{124}Sb from the body. The authors interpreted the data as indicating removal of "transportable material in the tissue" with an effective half-time of 30 d during the early weeks after the incident and much slower removal of non-transportable material from the lungs at later times.

(99) Rees et al. (1980) measured the time-dependent concentrations of antimony in blood plasma and urine of human subjects following intravenous injection of Sb(V) as sodium stibogluconate. The data indicate three phases of removal of antimony from blood plasma, with half-times of 0.2 h (71%), 1.4 h (28%) and 6.9 h (1%). Following intramuscular injection the plasma clearance from 1 to 24 h appeared to be exponential with a biological half-time of ~2.5 h. The renal clearance rate of antimony approximated the glomerular filtration rate. More than 90% of administered antimony was excreted in urine in the first 8 h after intravenous or intramuscular injection.

(100) Chulay et al. (1988) studied blood clearance of antimony in two patients given Sb(V) as sodium stibogluconate and three patients given Sb(V) as meglumine antimoniate. All patients were injected intramuscularly with 10 mg Sb/kg daily for 20 d. The two drugs showed similar biokinetics in blood, with peak blood concentrations appearing about 2 h after the initial injection. In both cases the blood content of antimony could be described by a three-term exponential model representing an initial absorption phase with a half-time of 0.85 h followed by a rapid elimination phase with a mean half-time of 2 h and a slower phase with a mean half-time of 76 h.

(101) Bailly et al. (1991) reported the case of a woman who attempted suicide by ingestion of an unknown amount of Sb(III) as antimony trisulphide (Sb_2S_3, stibnite). Only a small fraction of the intake was absorbed from the gastrointestinal tract. The concentration of antimony in blood was measured over a period of about 130 h after intake. The blood concentration peaked at ~4 h post intake and thereafter decreased bi-exponentially, with estimated biological half-times of ~2.6 h (60%) and 210 h (40%). The urinary excretion rate peaked about 20 h after intake and declined with a half-time of about 46 h over the next 6 d. The concentration of antimony in liver bile peaked about 3 h after intake and from 3-60 h decreased with a half-time of about 12 h. Interpretation of the data for this subject is complicated by the fact that efforts were made to remove antimony from the body by forced diuresis, repeated gastric lavage, and chelation therapy.

(102) Bailly et al. (1991) studied the urinary excretion of antimony in 22 workers employed in the production of the Sb(V) compounds antimony pentoxide and sodium antimoniate. The rate of urinary excretion of antimony during an 8-h shift was highly

correlated with the concentration of antimony in air during the same period, indicating absorption and rapid removal of a portion of inhaled antimony in urine. Exposure to airborne antimony at a concentration of 500 μg/m^3 was estimated to lead to an increase in urinary antimony of 35 μg Sb/g creatinine during an 8-h shift.

(103) Kentner et al. (1995) studied occupational exposure to two antimony compounds that occur in the production of lead batteries: Sb_2O_3 in the casting of grids, and SbH_3 in the formation of lead plates. The concentration of antimony was measured in air in the grid-casting area and formation area and in blood and urine of seven workers from the grid-casting area and 14 workers from the formation area. Comparisons of the concentrations of antimony in air and in blood and urine of the workers suggest similar biokinetics of the two forms of inhaled antimony. At the end of the work shifts the median concentration of antimony in air was 4.5 (1.18-6.6) μg Sb/m^3 in the casting area and 12.4 (0.6-41.5) μg Sb/m^3 in the formation area. The median blood concentrations in pre-shift samples was 2.6 (0.5-3.4) μg Sb/L for the casting area and 10.1 (0.5-17.9) μg Sb/L for the formation area. The average concentration of antimony in urine was 3.9 (2.8-5.6) μg Sb/g creatinine for the casting area and 15.2 (3.5-23.4) μg Sb/g creatinine for the formation area.

(104) Luedersdorf et al. (1987) determined levels of antimony in blood and urine of 109 workers exposed to the oxide of trivalent antimony (Sb_2O_3) in the glass-producing industry. Workers were divided into four groups with different tasks and different levels of exposure to antimony. The concentration ratio of antimony in urine (median value in μg/ml) to antimony in blood (median value in μg/ml) was 1.9 for all 109 workers and varied from 1.1 to 4.5 for the four groups.

(105) Liao et al. (2004) determined levels of five metals including antimony in blood and urine of 103 optoelectronic workers. The concentration ratio of antimony in urine (median value in parts per billion) to antimony in blood (median value in parts per billion) was 2.5 for all 103 workers and varied from 2.2 to 4.7 for three different groups of workers with different tasks and levels of exposure.

(106) The stable antimony content of human tissues has been determined in a number of occupationally or non-occupationally subjects (Smith, 1967; ICRP, 1975; Sumino et al., 1975; Iyengar et al., 1978; Lindh et al., 1980; Gerhardsson et al., 1982; Coughtrey and Thorne, 1983). The reported contents of individual tissues as well as relative contents of different tissues are variable, but the data together with estimates of intake of antimony suggest the existence of long-term components of retention of antimony in bone and soft tissues. Coughtrey and Thorne (1983) estimated on the basis of reported tissue concentrations that bone typically contains about 55% of the total-body content of stable antimony. Newer data from Zhu et al. (2010) on the antimony content of tissues from Chinese males suggest a skeletal content of about 28% of the total body content. Data of Gehardsson et al. (1982) for deceased smelter workers indicate that the total antimony content of liver typically was an order of magnitude greater than that of the kidneys. This conclusion is reported by the data of Zhu et al. (2010) for Chinese males.

Animal studies

(107) Goodwin and Page (1943) studied urinary excretion of antimony by mice following subcutaneous, intravenous, or intramuscular injection of one of three Sb(III) compounds (stibophen, KSb-tartrate, or anthiomaline) or one of five Sb(V)- compounds (NaSb-gluconate, stibamine glucoside, neostibosan, urea-stibamine, or stibacetin). For all compounds and all exposure routes, urinary excretion over the first 48 hours accounted for 50-82% of the administered antimony.

(108) Brady et al. (1945) reported that in four dogs the urinary excretion of radioactive Sb(III) over 36 h after intravenous injection with Sb tartar emeric was 14±8% (range 4 -21%). The urinary excretion in one dog injected intravenously with Sb(III) as sodium antimonyl xylitol was 13.7% in 36 h.

(109) At four days after intramuscular injection of rats with ^{122,124}Sb as $HSbO_3$, blood and bone contained 2% and 0.9%, respectively, of the injected activity (Durbin, 1960). The liver, kidneys, and muscle each contained 0.1% or less of the injected amount. Urinary excretion accounted for 96.5% of total excretion over the four-day period.

(110) Djuric et al. (1962) studied the distribution and excretion of ^{124}Sb in rats after inhalation of an aerosol of $^{124}SbCl_3$ Two rabbits and one dog were administered intratracheal doses of the same compound for comparison. Rapid early loss from the rat lung was followed by slower loss with a half-time on the order of 100 d. The primary site of accumulation of absorbed ^{124}Sb in rats was the red blood cells. Such high accumulation in red blood cells was not evident in the rabbits or dog.

(111) Moskalev (1964) administered ^{124}Sb tartrate emetic to rats by oral or intravenous administration of ^{124}Sb. The liver and skeleton were found to be important repositories for antimony over the first 8 d following either route of administration, but the division of activity between these two organs depended strongly on the route of administration. Comparison with earlier results by the same author indicated that the distribution following intravenous administration also depended strongly on the physicochemical state of antimony in the initial solution.

(112) In mice receiving ^{124}Sb-KSb tartrate by intraperitoneal injection, about 80% of the administered amount was excreted the first day and 99% during the first three weeks (Rowland, 1968). The concentration of ^{124}Sb in blood decreased by a factor of ~20 from 15 min to 6 h after injection and by a factor of ~2 from 6 h to 24 h after injection. Loss of activity from the liver was slower than from the rest of the body but dropped to 0.5-1% of its peak value after 21 d.

(113) Thomas et al. (1973) exposed three groups of mice to ^{124}Sb aerosols in a system that yielded head-only exposures. The aerosols were produced from a starting solution of Sb tartrate but were formed at different temperatures for each group: 100, 500, or 1100 °C. The activity contained in the material formed at the lowest temperature cleared from the lungs soon after deposition and deposited primarily in bone, which was estimated to receive a much higher radiation dose than the lungs in this case. The activity in the material formed at the two higher temperatures was retained in the lungs for a longer period but gradually accumulated to a large extent in bone, although the lung was estimated to receive a much higher radiation dose than bone in this case. In all three groups the portion of the body burden found in the pelt excluding the head increased from ~7% at 1 d to ~25% at 52 d after exposure.

(114) Felicitte et al. (1974a) investigated the biokinetics of trivalent and pentavalent ^{124}Sb over 32 d following inhalation of relatively soluble aerosols by Syrian hamsters. Whole-body clearance of both aerosols occurred in two phases. More than 90% of the initial body burden was eliminated over the first 7 d after exposure. The remaining activity was eliminated with a biological half-time of about 16 d. No significant difference in excretion patterns was observed between the two aerosols. Systemic activity was found mainly in liver, skeleton, and skin (shaved pelt). Activity in liver generally was higher after inhalation of the trivalent then the pentavalent ^{124}Sb, but the opposite pattern was seen for bone. In blood, ^{124}Sb inhaled in the trivalent form was concentrated in the RBC at all sampling times, with maximum RBC concentration of 6-10 times the plasma concentrations at approximately 24 h after exposure.

For activity inhaled in the pentavalent form, concentrations were greater in plasma than RBC in the early hours after exposure, but the RBC to plasma ratio converged over the first day to that seen for inhaled trivalent ^{124}Sb.

(115) Felicitte et al. (1974b) studied the biokinetics of inhaled ^{124}Sb in groups of beagle dogs exposed to trivalent ^{124}Sb aerosols formed at different temperatures (100, 500, or 1000 °C). Particle sizes were 1.3, 1.0, and 0.3 μm AMAD, respectively, for aerosols formed at these three temperatures. Much of the activity inhaled in the aerosol generated at 100 °C cleared rapidly from the lungs and was excreted in urine at a high rate. Activity inhaled in the aerosols formed at higher temperatures was cleared more slowly from the lungs, and the urinary to faecal excretion rate was much lower at early times than for the aerosol formed at 100 °C. For example, urinary excretion of ^{124}Sb was at least 7 times as great as faecal excretion over the first 24 h following inhalation of the aerosol formed at 100 °C, compared with a urine to faeces ratio of about 0.4 over the same period for the aerosol formed at 500 °C. From 1-32 d post exposure the urinary to faecal excretion ratio was not significantly different for the three aerosols. From 1-21 d post exposure the concentration of ^{124}Sb in RBC was on average 6.7 times that in plasma. Average long-term biological half-lives for total-body ^{124}Sb were 100, 36 and 45 d for ^{124}Sb inhaled in aerosols formed at 100, 500, and 1000 °C, respectively. Systemic activity was found mainly in liver, skeleton, and pelt.

(116) Van Bruwaene et al., (1982) studied the urinary and faecal excretion of inorganic ^{124,125}Sb by lactating cows after oral or intravenous administration. During a 70-d period after intravenous injection about 51% of the administered amount was excreted in the urine and 2.4% was excreted in faeces. Almost 16% of the injected amount was found in tissues at 70 d, but most of this was found in the heart and presumed to have resulted from deposition of antimony in blood vessels near the injection site as had been observed in an earlier animal study with antimony. Different systemic distributions were found for the two exposure routes. Excluding the deposit in the heart, activity retained at 70 d was found mainly in the liver (69% of the body burden), skeleton (7.1%), muscle (7.0%), skin (6.7%), and spleen (6.4%). At 102 days after oral administration the retained activity was found mainly in the skin (43% of the body burden), skeleton (30%), muscle (10%), and liver (7.3%). The high content of antimony in liver and spleen following intravenous injection may have been due to uptake and retention of colloidal antimony.

(117) Bailly et al. (1991) studied the urinary and faecal excretion of Sb(III) by rats after intraperitoneal or intravenous injection of $SbCl_3$. During the first day, urinary and faecal excretion accounted on average for about 8.6% and 31%, respectively, of antimony administered by intraperitoneal injection and 19% and 17%, respectively, of antimony administered intravenously.

3.2.3.2. Biokinetic model for systemic antimony

(118) The structure of the biokinetic model for systemic antimony is shown in Figure 3-1. Transfer coefficients are listed in Table 3-3. These coefficients are based on data for trivalent antimony, which has been studied more than pentavalent antimony and which is expected to be the more frequently encountered form of antimony. For radioisotopes of antimony entering the systemic circulation as pentavalent antimony, the model is expected to underestimate the initial rate of biological removal from the body and overestimate cumulative nuclear transformations in systemic tissues and fluids.

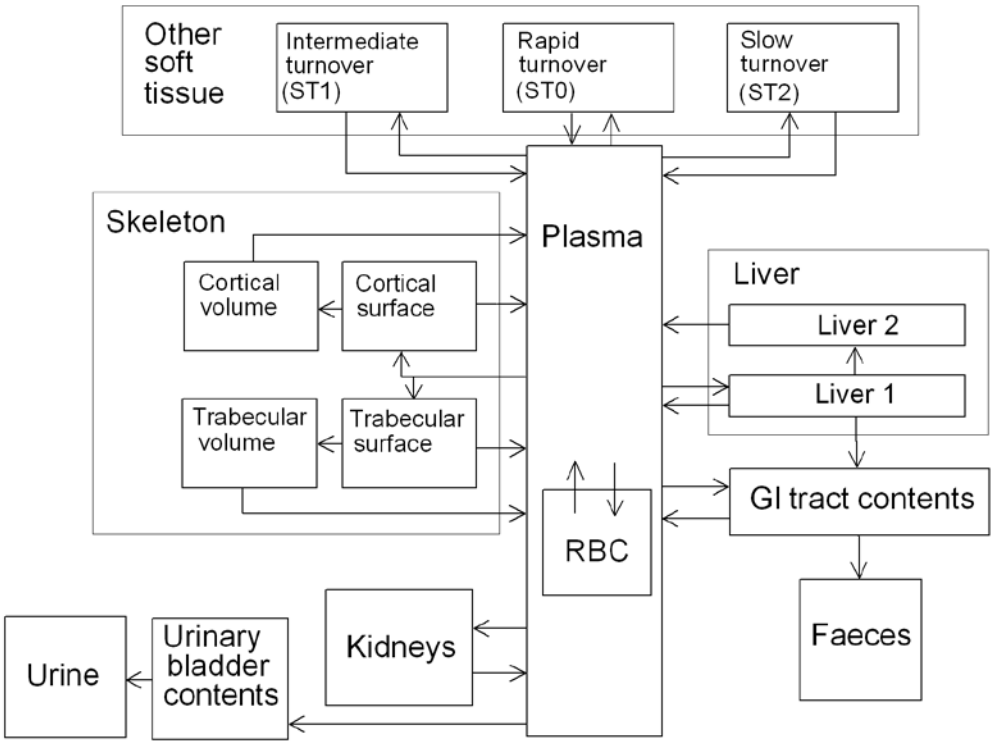

Figure 3-1. Structure of the biokinetic model for systemic antimony.

Table 3-3. Transfer coefficients for systemic antimony

From	To	Transfer coefficient (d^{-1})
Plasma	Small intestine contents	1.0
Plasma	Urinary bladder contents	12
Plasma	Liver 0	4.0
Plasma	Kidneys[a]	0.3
Plasma	RBC	1.25
Plasma	ST0	75
Plasma	ST1	4.35
Plasma	ST2	0.1
Plasma	Cortical bone surface	1.0
Plasma	Trabecular bone surface	1.0
RBC	Plasma	0.0693
Liver 0	Plasma	0.3235
Liver 0	Small intestine contents	0.1155
Liver 0	Liver 1	0.0231
Liver 1	Plasma	0.0347
Kidneys	Plasma	0.231
ST0	Plasma	0.693
ST1	Plasma	0.0693
ST2	Plasma	0.0019
Cortical bone surface	Plasma	0.03396
Trabecular bone surface	Plasma	0.03396
Cortical bone surface	Cortical bone volume	0.000693
Trabecular bone surface	Trabecular bone volume	0.000693
Cortical bone volume	Plasma	0.0000821
Trabecular bone volume	Plasma	0.000493

[a]Assigned to "Other kidney tissue" in the generic model for bone-surface-seeking radionuclides.

(119) It is assumed that antimony leaves blood plasma at the rate 100 d^{-1} (half-time of ~10 min) with 75% moving to the fast-turnover soft-tissue compartment ST0, 1.25% to RBC, 12% to the urinary bladder contents, 1% to the contents of the small intestine, 4% to liver (compartment Liver 0), 0.3% to kidneys, 2% to bone surfaces, 0.1% to the slow-turnover soft-tissue compartment ST2, and the remaining 4.35% to the intermediate-term soft-tissue compartment ST1. Half of the activity deposited on bone surfaces is assigned to cortical bone and half to trabecular bone. The following removal half-times are assigned: 10 d from RBC to plasma, 1 d from ST0 to plasma; 10 d from ST1 to plasma; 1 y from ST2 to plasma; 1.5 d from Liver 0, with 25% moving to the small intestine contents in bile, 5% moving to the longer-term liver compartment Liver 1, and 70% returning to plasma; 20 d from Liver 1 to plasma; 3 d from kidneys to plasma; and 20 d from cortical or trabecular bone surface, with 98% returning to plasma and 2% moving to the corresponding bone volume compartment. The transfer coefficients describing the rates of movement from the bone volume compartments to plasma are the generic turnover rates for cortical and trabecular bone.

(120) The transfer coefficients listed in Table 3-3 yield the following predictions, which are reasonably consistent with the biokinetic database for antimony summarized above. There is an initially rapid disappearance of antimony from blood, with only ~15% of intravenously injected antimony remaining in blood at 30 min and <4% at 1 h after

administration. This rapid phase is followed by a slow phase of disappearance from blood due to accumulation and slow release of antimony by RBC and return of antimony from extravascular spaces to blood. Over the next several days the blood content remains at about 2-3% of the injected amount. The ratio of the concentration of antimony in RBC to that in blood plasma increases to about 5 during the first 24 h after intravenous injection and increases more gradually over the next few weeks. Antimony is removed from the body mainly in urine, with urinary losses representing approximately 17% of intravenously injected antimony after 24 h, 41% after 1 wk, 69% after 1 mo, and 86% after 1 y. The urinary to faecal excretion ratio based on cumulative excretion is about 7. At equilibrium the ratio of the concentration of antimony in urine to that in blood is about 2. Most (>75%) antimony transferred from blood plasma to extravascular spaces following acute input to plasma returns to plasma in the next few days. The liver initially has a higher concentration than other tissues, but most of the initial liver content is lost over several days. At times greater than about one month after intravenous injection the concentration of antimony in the skeleton exceeds that in the liver. About half the total body content remaining at 1 wk after intravenous injection is lost over the next 15 d; about half the content remaining at 1 mo is lost over the next 25 d; and about half the content remaining at 1 y is lost over the next 2 y. From 1 wk to 1 mo after intravenous injection the liver content accounts for 5-6% of total-body antimony. The skeleton content as a fraction of total-body antimony increases from about 11% at 1 wk to about 27% at 1 mo. At equilibrium the skeleton contains about half of total-body antimony. Based on a constant input to blood of 2 μg of antimony per day from environmental sources (Coughtrey and Thorne, 1983), the model predicts a total-body content of 7 mg after 10,000 d. This is reasonably consistent with estimates of the total-body content based on tissue measurements (Coughtrey and Thorne, 1983).

3.2.3.3. Treatment of radioactive progeny

(121) Chain members addressed in the derivation of dose coefficients for antimony isotopes are isotopes of antimony, tellurium, iodine, or xenon. Isotopes of antimony, tellurium, or iodine produced in systemic compartments are assumed to follow the characteristic models for these elements (i.e. the models applied in this report to these elements as parent radionuclides) from their time of production, insofar as application of this assumption is straightforward. This assumption is sometimes ambiguous due to differences in model structures for the different elements. That is, the site of production of a radionuclide may not be clearly identifiable with a specific compartment in its characteristic model. In such cases a transfer rate from the site of production of the radionuclide to the central blood compartment in the radionuclide's characteristic model has been assigned as described below. After reaching its central blood compartment, the radionuclide is assumed to behave as described by its characteristic model.

(122) Tellurium atoms produced at soft-tissue sites in the antimony model that are ambiguous with regard to the characteristic model for tellurium (ST0, ST1, ST2, Liver 0, and Liver 1) are assumed to be transferred to the central blood compartment of that model (plasma) at the rate 0.0693 d^{-1} (half-time of 10 d). This is the rate of removal from all soft tissue compartments in the characteristic model for tellurium. Tellurium produced in RBC is assumed to transfer to plasma at the rate 1000 d^{-1} (a default rate representing rapid transfer between compartments). For modeling convenience, tellurium produced in the central blood compartment of the antimony model is assigned to the central blood compartment in the tellurium model.

(123) Iodine atoms are produced at the following sites in the antimony or tellurium models that are not clearly identifiable with specific compartments of the characteristic model for iodine: blood compartments, liver compartments, kidneys, thyroid (in the tellurium model), compartments within "Other soft tissue", and bone compartments. The following rates of transfer from these compartments to the blood iodide pool of the characteristic model for iodine are assigned: liver compartments or kidneys, 100 d^{-1} (the rate of loss from the liver iodide and kidney iodide compartments in the characteristic model for iodine); blood compartments (excluding central blood compartments, as indicated below) 1000 d^{-1}; Other soft tissue or bone surface compartments, 330 d^{-1} (the highest transfer coefficient to blood in the characteristic model for iodine); thyroid, 36 d^{-1} (the transfer coefficient from the thyroid iodide pool to the blood iodide pool in the characteristic model for iodine); trabecular and cortical bone volume compartments, the reference rates of trabecular and cortical bone turnover. For modeling convenience, iodine atoms produced in the central blood pools of the antimony and tellurium models are assigned to the blood iodide pool in the characteristic model for iodine.

(124) A generic biokinetic model is applied in this report to xenon isotopes produced by decay of a radionuclide in systemic compartments. Xenon produced in bone is assumed to transfer to blood at the rate 100 d^{-1} if produced in bone surface and 0.36 d^{-1} if produced in bone volume. These rates are taken from the model for radon introduced in ICRP *Publication 67* (1993) and applied in this report to radon produced in bone surface and non-exchangeable bone volume, respectively, by decay of a radium isotope. Xenon produced in a soft-tissue compartment is assumed to transfer to blood with a half-time of 20 min. Xenon produced in the central blood compartment in the model for antimony, tellurium, or iodine is assigned to the blood compartment of the xenon model. Xenon produced in any other blood compartment in the antimony, tellurium, or iodine model is assumed to be transferred to blood in the xenon model at the rate 1000 d^{-1}. Xenon entering the blood compartment of the xenon model or produced in that compartment is assumed to be removed from the body (exhaled) at the rate 1000 d^{-1}. Recycling of xenon to tissues via arterial blood is not depicted explicitly in this model for xenon as a daughter radionuclide but is considered in the assignment of the half-times in tissues. The model is intended to yield a conservative average residence time of xenon atoms in the body after their production in systemic pools.

3.3. Individual monitoring

(125) ^{124}Sb may be monitored through Whole Body Counting and/ or Urine bioassay.

Isotope	Monitoring Technique	Method of Measurement	Typical Detection Limit	Achievable detection limit
^{124}Sb	Urine Bioassay	γ-ray spectrometry	1 Bq/L	0.02 Bq/L
^{124}Sb	Lung measurement	γ-ray spectrometry	9Bq*	
^{124}Sb	Whole Body Counting	γ-ray spectrometry	30 Bq	12 Bq

∗ Lung monitoring of ^{124}Sb is not generally used in routine monitoring of workers. Monte Carlo program Visual Monte Carlo was used to simulate the photon emission, to calculate the calibration factor for the geometry and radionuclide, and to calculate the minimum detectable activity (MDA) in the lung. (Hunt et al, 2012)

(126) ^{125}Sb may be monitored through Whole Body Counting and/ or Urine bioassay.

Isotope	Monitoring Technique	Method of Measurement	Typical Detection Limit	Achievable detection limit
^{125}Sb	Urine Bioassay	γ-ray spectrometry	6 Bq/L	0.1 Bq/L
^{125}Sb	Whole Body Counting	γ-ray spectrometry	100 Bq	40 Bq

References

Abdallah, A., Saif, M., 1962. Tracer studies with antimony-124 in man. In: Wolstenholme, G.E.W. and O'Connor, M. (Eds.) Bilharziasis. Churchill, London, pp. 287-309.

Alves, W., Blair, D.M., 1946. Schistosomiasis. Intensive treatment with antimony. Lancet, 247, 9-12.

Bailly, R., Lauwerys, R., Buchet, J.P., Mahieu P., Konings, J., 1991. Experimental and human studies on antimony metabolism: their relevance for the biological monitoring of workers exposed to inorganic antimony, Br. J. Ind. Med. 48, 93–97.

Bartter, F.C., Cowie, D.B., Most, H., Ness, A.T., Forbush, S., 1947. The fate of radioactive tartar emetic administered to human subjects. 1. Blood concentrations and excretion following single and multiple intravenous injections. Amer. J. Trop. Med., 27, 403-416.

Boyd, T.C., Roy, A.C., 1929. Observations on the excretion of antimony in the urine. Indian J. Med. Res., 17, 94-108.

Brady, F.J., Lawton, A.H., Cowie, D.B., Andrews, H.L., Ness, A.T., Ogden, G.E., 1945. Localization of trivalent radioactive antimony following intravenous administration to dogs infected with dirofilaria immitis. Amer. J. Trop. Med., 25, 103-107.

Brahmachari, U.N., Chaudhury, S.C., Das, J., Sen, P.B., 1924. Chemotherapy of antimonial compounds in Kala-azar infection. VIII. Quantitative studies in excretion of antimony (tartar emetic and urea stibamine). Ind. J. Med. Res., 11, 829-838.

Chertok, R.J., Lake, S., 1970. Availability in the dog of radionuclides in nuclear debris from the Plowshare excavation Cabriolet. Health Phys., 19, 405-409.

Chulay, J.D., Fleckenstein, L., Smith, D.H., 1988. Pharmacokinetics of antimony during treatment of visceral leishmaniasis with sodium stibogluconate or meglumine antimoniate. Trans. Roy. Soc. Trop. Med. Hyg., 82, 68.

Coughtrey, P.J., Thorne, M.C., 1983. Antimony. In: Radionuclide distribution and transport in terrestrial and aquatic ecosystems, Vol. 3. Rotterdam, Balkema, A.A., pp. 263-304.

Djuric, D., Thomas, R.G., Lie, R., 1962. The distribution and retention of trivalent antimony in the rat following inhalation. Int. Arch. Gewerbepathol. Gewerbehyg., 19, 529-545.

Durbin, P.W., 1960. Metabolic characteristics within a chemical family. Health Phys., 2, 225-238.

Felicetti, S.A., Thomas, R.G., McClellan, R.O., 1974a. Retention of inhaled antimony-124 in the beagle dog as a function of temperature of aerosol formation. Health Phys., 26, 525–531.

Felicetti, S.A., Thomas, R.G., McClellan, R.O., 1974b Metabolism of two valence states of inhaled antimony in hamsters. Amer. Ind. Hyg. Assoc. J., 35, 292–300.

Garg, S.P., Singh, I.S., Sharma, R.C., 2003. Long term lung retention studies of ^{125}Sb aerosols in humans. Health Phys., 84(4), 457–468.

Gerber, G.B., Maes, J., Eykens, B., 1982. Transfer of antimony and arsenic to the developing organism. Arch. Toxicol. 49, 159-168

Gerhardsson, L., Brune, D., Nordberg, G.F., Wester, P.O., 1982. Antimony in lung, liver and kidney tissue from deceased smelter workers. Scand. J. Work Environ. Health 8(3), 201-8.

Goodwin, L.G., Page, J.E., 1943. A study of the excretion of organic antimonials using a polarographic procedure. Biochem. J. 37, 198-209.

Groth, D.H., Stettler, L.E., Burg, J.R. Busey, W.M., Grant, G.C., Wong, L.J., 1986. Carcinogenic effects of antimony trioxide and antimony ore concentrate in rats. Toxicol. Environ. Health 18, 607–626.

IARC, 1989. Antimony trioxide and antimony trisulfide. Volume 47, 291–305. IARC Monographs on the Evaluation of Carcinogenic Risks to Humans. IARC, Lyon, France.

ICRP, 1975. Report of the Task Group on Reference Man, ICRP Publication 23. Pergamon Press, Oxford.

ICRP, 1981. Limits on Intakes of Radionuclides for Workers. ICRP Publication 30, Part 3. Oxford. Ann. ICRP 6, (2/3).

ICRP, 1993. Age-dependent Doses to Members of the Public from Intake of Radionuclides: Part 2, Ingestion dose coeffcients . ICRP Publication 67. Pergamon Press, Oxford. Ann. ICRP 23, (3/4).

ICRP, 1995. Age-dependent Doses to Members of the Public from Intake of Radionuclides, Part 3, Ingestion dose coefficients, ICRP Publication 69. Ann. ICRP 25(1).

Inaba, J., Nishimura, Y., Ichikawa, R., 1984. Studies on the metabolism of antimony-125 in the rat. NIRS-N-49 (National Institute of Radiological sciences, Chiba, Japan). pp.81-83.

Iyengar, G.V., Kollmer, W.E., Bowen, H.J.M., 1978. The elemental composition of human tissues and body fluids: A complication of values for adults. Verlag Chemic, New York.

Kentner, M., Leinemann, M., Schaller, K.H., Weltle, D., Lehnert, G., 1995. External and internal antimony exposure in starter battery production, Int. Arch. Occup. Environ. Health 67, 119–123.

Khalil, M.B., 1931. The specific treatment of human schistosomiasis (Bilharzias) with special reference to its application on a large scale. Arch. Schiffs Trop. Hyg. 35 (Supp. 2), 1-128.

Liao, Y-H., Yu, H-S., Ho, C-K., Wu, M-T., Yang, C-Y., Chen, J-R., Chang, C-C., 2004. Biological Monitoring of Exposures to Aluminium, Gallium, Indium, Arsenic, and Antimony in Optoelectronic Industry Workers. J. Occ. Env. Med., 46(9), 931-936.

Lindh, U., Brune, D., Nordberg, G., Wester, P., 1980. Levels of antimony, arsenic, cadmium, copper, lead, mercury, selenium, silver, tin and zinc in bone tissue of industrially exposed workers. Sci. Total Environ., 16, 109-116.

Luedersdorf, R., Fuchs, A., Mayer, P., Skulsuksai, G., Schacke, G., 1987. Biological assessment of exposure to antimony and lead in the glass-producing industry. Int. Arch. Occup. Environ. Health., 59(5), 469-74.

McCallum, R.I., 1963. The work of an occupational hygiene service in environmental control. Ann. Occup. Hyg., 6, 55–64.

McCallum, R.I., Day, M.J., Underhill, J., Aird, E.G.A., 1971. Measurement of antimony oxide dust in humans lungs in vivo by X-ray spectrophotometry. Inhaled Particles III, Vol. 2, Proceedings of an International Symposium Organised by the British Occupational Hygiene Society, London, 14 – 23 September 1970, pp. 611–619, (Ed. Walton, W.H.) Unwin Brothers Limited, The Gresham Press, Old Woking, Surrey, England.

Moskalev, Y., 1964. Experiments dealing with distribution of antimony-124 and tellurium-127. AEC-tr-7590, pp.63-72.

Newton, P.E., Bolte, H.F., Daly, I.W., Pillsbury, B.D., Terrill, J.B., Drew, R.T., Ben-Dyke, R., Sheldon, A.W., Rubin, L.F., 1994. Subchronic and chronic inhalation toxicity of antimony trioxide in the rat. Fund. Appl. Tox., 22, 561–576.

Otto, G.F., Maren, T.H., Brown, H.W., 1947. Blood levels and excretion rates of antimony in persons receiving trivalent and pentavalent antimonials. Am. J. Hyg., 46, 193-211.

Rees, P.H., Keating, M.I., Kager, P.A., Hockmeyer, W.T., 1980. Renal clearance of pentavalent antimony (sodium stibogluconate). Lancet 2, 226-229.

Rose, E., Jacobs, H., 1969. Whole-body counter and bioassay results after an acute antimony-124 exposure. In: Handling of Radiation Accidents, International Atomic Energy Agency, Vienna. IAEA-SM-119/30. pp. 589-600.

1811 Rowland, H.A.K., 1968. Stibokinetics III: Studies on mice with 124Sb-labelled potassium antimony
1812 tartrate. Tissue concentrations: Excretion. Trans. Roy. Soc. Trop. Med. Hyg., 62, 795-800.
1813 Smith, H., 1967. The distribution of antimony, arsenic, copper and zinc in human tissue. J. Forensic
1814 Sci. Society, 7, 97-102.
1815 Sumino, K., Hayakawa, K., Shibata, T., Kitamura, S., 1975b. Heavy metals in normal Japanese
1816 tissues. Arch. Environ. Health, 30, 487-494.
1817 Taylor, P.J., 1966. Acute intoxication from antimony trichloride. Brit. J. Indust. Med., 23, 318-321.
1818 Thomas, R.G., Felicetti, S.W., Luchino, R.V., McClellan, R.O., 1973. Retention patterns of antimony
1819 in mice following inhalation of particles formed at different temperatures. Proc. Soc. Exp.
1820 Biol. Med., 144, 544-550.
1821 Van Bruwaene, R., Gerber, G.B., Kirchmann, R., Colard, K., 1982. Metabolism of antimony-124 in
1822 lactating dairy cows. Health Phys., 43, 733-738.
1823 Waitz, J.A., Ober, R.E., Meisenhelder, J.E., Thompson, P.E., 1965. Physiological disposition of
1824 antimony after administration of 124Sb-labelled tartar emetic to rat, mice and monkeys, and
1825 the effects of tris (p-aminophenyl) carbonium pamoate on this distribution. Bull. WHO 33,
1826 537-546.
1827 Zhu, H., Wang, N., Zhang, Y., Wu, Q., Chen, R., Gao, J., Chang, P., Liu, Q., Fan, T., Li, J., Wang, J.
1828 2010. Element contents in organs and tissues of Chinese adult men. Health Phys., 98, 61-73.
1829
1830

4. Tellurium (Z = 52)

4.1. Chemical Forms in the Workplace

(127) Tellurium is a semi-metal or metalloid, which occurs mainly in oxidation states –II, II, IV and VI. Tellurium is in the same chemical series as sulphur and selenium and forms similar compounds. The two anionic forms are known as tellurates (TeO_4^{2-} or TeO_6^{6-}).

(128) Tellurium may be encountered in industry in a variety of chemical forms, including elemental vapour or solid forms, oxides, chlorides, but also as tellurides.

(129) Tellurium-132 is a fission product which is important in the first few days after a criticality accident.

Table 4-1. Isotopes of tellurium addressed in this report

Isotope	Physical half-life	Decay mode
Te-114	15.2 m	EC, B+
Te-116	2.49 h	EC, B+
Te-117	62 m	EC, B+
Te-118	6.00 d	EC
Te-119	16.05 h	EC, B+
Te-119m	4.70 d	EC, B+
Te-121	19.16 d	EC
Te-121m	154 d	IT, EC
Te-123	6.00E+14 y	EC
Te-123m	119.25 d	IT
Te-125m	57.40 d	IT
Te-127	9.35 h	B-
Te-127m	109 d	IT, B-
Te-129[a]	69.6 m	B-
Te-129m	33.6 d	IT, B-
Te-131[a]	25.0 m	B-
Te-131m[a]	30 h	B-, IT
Te-132[a]	3.204 d	B-
Te-133	12.5 m	B-
Te-133m[a]	55.4 m	B-, IT
Te-134	41.8 m	B-

[a] Data for these radionuclides are given in the printed copy of this report. Data for other radionuclides are given on accompanying electronic disk.

4.2. Routes of Intake

4.2.1. Inhalation

(130) A few experimental studies of the behaviour of radio-labelled tellurium (i.e. tracer level) following deposition in the respiratory tract have been identified in the literature. Some information is also available from measurements following inadvertent intakes of irradiated tellurium oxide, from studies of tellurium-132 inhaled by people after the Chernobyl accident, and from toxicology studies of stable tellurium compounds.

Classification of gases and vapours, absorption Types and parameter values

(131) Absorption parameter values and Types, and associated f_A values for gas and vapour forms of tellurium are given in Table 4-2 and for particulate forms in Table 4-3. Common forms of tellurium (e.g. dioxide) are solids at room temperature. Exposures to gas or vapour forms of tellurium are therefore probably relatively unusual compared to exposures to particulate forms, and it is therefore proposed here that particulate form should be assumed in the absence of specific information.

(a) Gases and vapours

(132) Accidental inhalation by two men of tellurium in the form of hexafluoride gas and possibly also tellurium esters was reported by Blackadder and Manderson (1975). However, the information reported related mainly to clinical signs and symptoms. Insufficient information is available to estimate the fraction deposited, or the rate of absorption. Tellurium in gas and vapour forms are assigned the default behaviour for gases and vapours: 100% total deposition (20% ET_2, 10% BB, 20% bb and 50% AI) and Type F absorption (Table 4-2).

(b) Particulate aerosols

Tellurium chloride

(133) Dobryakova (1970) followed the biokinetics of ^{127}Te for 14 days after administration of tellurium chloride to rats by intratracheal instillation. There was rapid absorption from the lungs, but the rate decreased with time. About 40% of the initial lung deposit (ILD) was absorbed at 30 minutes and 70% ILD at 1 day. Subsequent clearance was slow and mainly faecal, with about 6% ILD remaining in the lungs at 14 d. Parameter values estimated here were f_r ~0.7, and s_r of the order of 50 d^{-1}, but decreasing with time, and assignment to Type F.

Elemental tellurium

(134) Geary et al. (1978) investigated the toxicological effects up to 180 days after administration of tellurium to rats by intratracheal instillation. No quantitative information on the biokinetics was reported. However, pigmentation and effects in the lungs and other organs indicate that the tellurium was not absorbed rapidly and completely, but that significant absorption did take place, indicative of Type M rather than Type F or S behaviour.

Tellurium dioxide (TeO_2)

(135) Fehér (1976) followed whole-body retention of ^{123m}Te for up to 45 days after intratracheal instillation of irradiated TeO_2 into rats. The high thyroid uptake of ^{131}I at 1 day indicated correspondingly rapid (Type F) dissolution of the TeO_2 to release the ^{131}I.

(136) Fehér and Andrási (1977) followed whole-body retention of ^{123m}Te for up to 95 days after intake by 10 workers accidentally contaminated with TeO_2 irradiated for the production of ^{131}I. Retention fit a two-component exponential function, with about 75% and 25% retained with effective half-times of about 12 and 70 days respectively. The authors interpreted the results on the basis that the retained activity was homogeneously distributed in the body, assuming rapid dissolution (Type F).

(137) Geary et al. (1978) investigated the toxicological effects up to 180 days after administration of tellurium dioxide to rats by intratracheal instillation. No quantitative information on the biokinetics was reported. However, pigmentation and effects in the lungs

and other organs indicate that the tellurium was not absorbed rapidly and completely, but that significant absorption did take place, indicative of Type M rather than Type F or S behaviour.

Cadmium telluride (CdTe)

(138) As part of a toxicological study, Morgan et al. (1997) measured the concentrations of cadmium and tellurium in lungs and other tissues up to 28 days after administration of cadmium telluride to rats by intratracheal instillation. The lung concentrations of both elements at 28 days was about 30% of that at 1 day, and was accompanied by significant increases in concentrations in extrapulmonary tissues, giving assignment to Type M.

Unspecified compounds

(139) Balonov et al. (2003) summarised the results of *in vivo* measurements made 4 – 8 days after the Chernobyl accident on 65 people evacuated from Pripyat 1.5 d after the accident. Tellurium-132 activity was measurable in 56 persons, and in 28 of them with repeated lung measurements it declined with a half time of 2.5±0.2 d. Taking account of the ^{132}Te decay half-life of 3.3 d gives a lung clearance half time of about 10 d, and a corresponding clearance rate of 0.07 d^{-1}. During the period of measurements the particle clearance rate from the lungs predicted by the HRTM is about 0.01 d^{-1}, suggesting that most of the observed clearance is due to absorption to blood, at a rate (s_s) of about 0.06 d^{-1}. Since the lung measurements started a few days after intake, they do not on their own enable an estimate to be made of the fraction that dissolved rapidly. However, measurements were also made of ^{132}I in the thyroid, which was considered to originate mainly from ^{132}Te deposited the lungs. The mean ratio of ^{132}I activity in thyroid to that of ^{132}Te in lungs was 0.2, but with considerable variation between individuals (range 0.07 to 0.6) (Balonov *et al*, 2003). Analysis was carried out here to make an estimate of f_r based on this ratio. It was assumed that s_r = 100 d^{-1} (default); s_s = 0.06 d^{-1} (see above) and $f_A = f_r * 0.3$ (the default assumption for inhaled materials, see footnote c to Table 4-3, the fractional uptake in the alimentary tract value for ingested soluble forms of tellurium being 0.3). This gave a central estimate for f_r of about 0.3, but with a range similar to that of the ratio of ^{132}I activity in thyroid to that of ^{132}Te in lungs above. Thus the results are consistent with assignment to default Type M, although they indicate faster absorption than assumed by default. Given the uncertainties involved, specific parameter values are not recommended here for tellurium accidentally released from a nuclear reactor.

Rapid dissolution rate for tellurium

(140) Evidence from the tellurium chloride study outlined above suggests a rapid dissolution rate of the order of 50 d^{-1}, which is applied here to all forms of tellurium.

Extent of binding of tellurium to the respiratory tract

(141) Evidence from the tellurium chloride study outlined above suggests that following the rapid phase of absorption about 6% of the ILD clears relatively slowly from the lungs. There is no evidence available that clearance of this material is mainly by absorption to blood, as assumed for material in the ‘bound state’. It is therefore assumed that for tellurium the bound state can be neglected, i.e. f_b = 0.0.

Table 4-2. Deposition and absorption for gas and vapour compounds of tellurium

	Percentage deposited (%)[a]						Absorption	
Chemical form/origin	Total	ET_1	ET_2	BB	bb	AI	Type	f_A
All unspecified compounds	100[b]	0	20	10	20	50	F	0.3

Percentage deposited refers to how much of the material in the inhaled air remains in the body after exhalation. Almost all inhaled gas molecules contact airway surfaces, but usually return to the air unless they dissolve in, or react with, the surface lining. The default distribution between regions is assumed: 20% ET_2, 10% BB, 20% bb and 50% AI.

Table 4-3. Absorption parameter values for inhaled particulate forms of tellurium and for ingested tellurium

		Absorption parameter values[a]			Absorption from the GI tract, f_A
Inhaled particulate materials		f_r	s_r (d^{-1})	s_s (d^{-1})	
Default parameter values[b,c]					
Absorption Type	Assigned forms				
F	Tellurium chloride, tellurium dioxide	1	50	–	0.3
M	Elemental tellurium, cadmium telluride, all unspecified forms[d]	0.1	50	0.005	0.03
S	—	0.001	50	$1x10^{-4}$	$3x10^{-4}$
Ingested materials					
All forms					0.3

[a] It is assumed that for tellurium the bound state can be neglected i.e. $f_b = 0$. The values of s_r for Type F, M and S forms of tellurium (50 d^{-1}) are element-specific.

[b] Materials (e.g. tellurium chloride) are listed here where there is sufficient information to assign to a default absorption Type, but not to give specific parameter values (see text).

[c] For inhaled material deposited in the respiratory tract and subsequent cleared by particle transport to the alimentary tract, the default f_A values for inhaled materials are applied: i.e. the product of f_r for the absorption Type and the f_A value for ingested soluble forms of tellurium (0.3).

[d] Default Type M is recommended for use in the absence of specific information, i.e. if the form is unknown, or if the form is known but there is no information available on the absorption of that form from the respiratory tract.

4.2.2. Ingestion

(142) Kron et al. (1991) studied the renal excretion of stable tellurium by healthy volunteers after oral administration of Te as sodium tellurate (TeO_3), sodium tellurite (TeO_2) and metallic colloid. The calculated fractional absorption values were 0.23±0.09 in 4 volunteers ingesting Na tellurate, 0.21 in a single volunteer ingesting tellurite, and 0.10±0.04 in 3 volunteers ingesting metallic tellurium. Since the main chemical form of tellurium in fission products is sodium tellurite, Kron et al. (1991) proposed that a fractional absorption value of 0.25 should be applied for radiological protection purposes.

(143) Experimental data from several animal species including rats, guinea pigs, rabbits, dogs, sheep and cows gave absorption values in the range 0.2 - 0.5 for water soluble tellurites

(TeO_2) and about 0.1 - 0.25 for tellurates (Barnes et al., 1955; Venugopal and Luckey, 1978; Hollins, 1969; De Meio and Henriques, 1947; Mullen and Stanley, 1974; Taylor, 1996). Chertok and Lake (1970) argued on the basis of absorption studies on dogs that tellurium radionuclides contained in nuclear debris might be unavailable for absorption across the intestinal wall.

(144) In *Publication 30* (ICRP, 1979), an absorption value of 0.2 was recommended. A value of 0.3 was adopted in *Publication 67* (ICRP, 1993) for intakes in food. The data do not support the use of different values for workers and public and therefore an f_A value of 0.3 is used here.

4.2.3. Systemic Distribution, Retention and Excretion

4.2.3.1. Summary of the database

(145) The biokinetics of tellurium in the human body is not well characterized. There are only a few data for human subjects, mainly bioassay measurements following accidental exposure in the workplace. A number of studies deal with the toxicological issues of tellurium incorporation and related side-effects, mainly the occurrence of a sour garlic odour on the breath and in the urine, sweat and excrement resulting from occupational exposure to tellurium. This odour seems to be due to the presence of tiny amounts of dimethyl telluride.

Summary of data for human subjects

(146) Schroeder et al. (1967) estimated the content of tellurium in several human tissues and calculated that the total amount in the body was approximately 600 mg, which would make tellurium one of the most abundant trace elements in the body. The largest amount was found in bone (90%), with much lower amounts in muscle (3%), liver (1.2%) and probably in fat (3%). The amount found in kidney was approximately 3% of that in liver. The concentration in blood serum amounted to 1.07±0.12 $mg \cdot L^{-1}$ (i.e. 0.17%$\cdot L^{-1}$), and that in unwashed erythrocytes to 1.95 $mg \cdot L^{-1}$. However, the values for blood may be unreliable due to analytical problems (Nason and Schroeder, 1967) and were not confirmed by later studies. Van Montfort et al. (1979), for example, found concentrations in blood of unexposed subjects to range between 0.15 and 0.3 $\mu g \cdot L^{-1}$.

(147) Fehér and Andrási (1977) presented the results of a study where an irradiated and cooled suspension of TeO_2-^{131}I was administered to two volunteers. The whole-body retention of tellurium in the first few days after administration was described with a bi-exponential function with effective half-times of 0.7 d (75%) and 10 d (25%). These data are consistent with the whole-body retention measured in ten persons occupationally contaminated with radiotellurium. For these persons no information was available on fast clearance, due to the lack of measurements immediately after the accident, but measurements at later times allowed the determination of longer-term retention components with effective half lives of 11 d (75%) and 45 d. The combined findings of the experimental study and the follow-up of the occupationally exposures suggest that whole body retention can be described by a three-exponential function, with biological half lives of 0.7 d (70%), 12 d (23 %) and 72 d (7 %).

(148) Kron et al. (1991) studied urinary excretion in five healthy volunteers after oral administration of tellurium in different forms (altogether 12 investigations): tellurite (Na_2TeO_4), tellurate (Na_2TeO_3), metallic form, and intrinsically bound in cress (*Lepidium*

sativum). Cress was consumed both with and without oil and vinegar dressing. The three-day urinary excretion varied between 3 and 25%. It was higher for tellurate (9 to 25%) than for tellurite (less than 8%) or metallic tellurium (4 to 9%). After ingestion of tellurium with cress, the amount excreted over three days ranged between 6 and 16%, and was reduced to 3% when dressing was added. For tellurate and metal tellurium most of the excretion occurred in the first 24 h after administration, whereas for cress and tellurite the excretion curve was delayed. For cress this delay presumably indicates a slower absorption of tellurium bound in organic matter as compared to the aqueous solutions. For tellurite the authors assumed a higher retention in the body for this compound as compared to tellurate as an explanation for the lower and slower excretion.

Summary of data from animal studies

(149) DeMeio and Henriques (1947) administered radioactive tellurite to rabbits, rats and dogs and measured the tissue distribution (Table 4-4) and excretion pathways. In rabbits and rats elevated concentrations were measured in kidneys, spleen, heart and lungs, and lower concentrations were found in the liver. In rats the tissue concentrations dropped considerably after one hour. Concentrations in blood averaged 25±4%·L^{-1} at day 1 after intravenous injection in rabbits and 610±390%·L^{-1} in rats at thirty minutes after intraperitoneal administration. In dogs the values dropped from 21±12%·L^{-1} at 1 hour to 6.9±2.5%·L^{-1} at 1 day. About 20 to 23% of tellurite injected intravenously into female dogs was excreted in the urine over 5-6 days, the greatest portion in the first two-three hours. Finally, the authors concluded that less than 1/1000th of the amount of radioactive tellurite injected into rabbits was excreted via the expired air during the 24 hr following administration. On the basis of the observed excretions, the authors argue that about 60% of tellurium injected into dogs remained in their body after 5-6 days.

Table 4-4. Distribution (%/organ) of radiotellurium activity following injection[a]

Organ	Rabbits[b]	Rats[c]	Rats[d]
Kidney	11.6±3.2	6.14±1.90	0.33
Liver	6.6±1.3	6.43±0.60	0.33
Lung	1.4±0.5	0.73±0.12	0.02
Heart	0.66±0.38	0.46±0.15	0.02
Spleen	0.28±0.08	0.72±0.05	0.03

[a] From DeMeio and Henriques (1947).
[b] Intravenous administration. Values are means for up to six animals each and refer to about 1 day after administration.
[c] Intraperitoneal administration. Values are means for up to three animals each and refer to about 0.5 h after administration.
[d] Intraperitoneal administration. Values are for only one animal and refer to about 1 day after administration.

(150) Barnes et al. (1955) administered ^{132}Te orally to rats and guinea pigs and determined the distribution of tellurium in the body at 3-4 days (Table 4-5). About 5.5% and 6.5% was excreted in the urine over 4 days by the guinea pigs and rats, respectively. Fecal excretion plus activity present in the gut amounted to about 93% in the guinea pigs and 80% in the rats. In further experiments, a tellurium solution was injected intravenously into rats, guinea pigs, mice and one rabbit to follow the blood kinetics and investigate the partition between whole blood and plasma. In general, retention in the blood of mice, guinea-pigs and the rabbit was

low (at day 1, 0.5 % in the mice, about 1% in the guinea pigs and 3.2% in the rabbit), whereas in the rats blood retention ranged from 22 to 32%. The biological half-life in the rat was about seven days. Tellurium in the blood appeared to be contained completely in the plasma in guinea pigs and mice, and only a small portion was bound to the corpuscles in the rabbit. By contrast, tellurium activity in the blood of rats was significantly higher than in plasma, suggesting that the rat is unique in retaining tellurium within the red cells. Tellurium in the rabbit's plasma and in the rats' corpuscles was shown to be protein-bound.

Table 4-5. Distribution (%/organ) of ^{132}Te activity following oral administration[a]

Organ	Guinea pigs	Rats
Kidney	0.52±0.06	1.20±0.08
Liver	0.73±0.22	1.13±0.32
Skeleton	0.54±0.08	0.77±0.03
Pelt	0.29±0.02	0.80±0.21
Carcass	0.35±0.10	1.94±0.85
Thyroid	0.01±0.005	0.01±0.005
Blood removed	0.03±0.01	3.60±0.20

[a] From Barnes et al. (1955). Values are means for two animals each and refer to 3-4 days after administration.

(151) Casey et al. (1963) administered a mixture of radionuclides of tellurium and iodine to lactating sheep and found that the transfer to milk was very low (two to three orders of magnitude less than for iodine). Retained tellurium was found mainly in the liver, kidney, lungs. The highest concentration was found in the thyroid, but the total content of the thyroid was small due to its small mass.

(152) Wright and Bell (1966) compared the metabolism of tellurium in sheep and swine. Five animals of each species were orally administered ^{127m}Te as Na_2TeO_3 via a stomach tube, and five more animals received the same compound via injection into the jugular vein. The blood content of ^{127m}Te in the sheep was very low (less than 0.25% of the administered dose) after oral administration. Intravenously injected tellurium was cleared readily from plasma (10% was retained after 2 hr and 2% after 5 d), and only a small portion was recovered in the cell fraction. In swine the peak concentration in whole blood occurred at approximately 30 hours after oral administration, at which time nearly all the ^{127m}Te was in the corpuscular fraction. Clearance of intravenously administered tellurium from plasma was similar to that observed in the sheep, but the corpuscular fraction rose with time (up to 3% at 5 d). The whole blood clearance after iv-administration could be described in terms of two components: a fast component with a biological half-time of about 10 h and a slower component with a half-time of several days. The total organ content at 5 days after intravenous administration is given in Table 4-6. No information was given about skeleton or thyroid.

Table 4-6. Distribution of ^{132}Te 5 d after intravenous administration (% of administered activity)

Organ	Sheep	Swine
Kidney	7.14±0.27	2.08±0.33
Liver	7.95±0.47	7.08±0.33
Lung	1.38±0.02	1.48±0.13
Heart	0.81±0.35	0.29±0.04
Spleen	0.16±0.01	0.37±0.06

[a] From Wright and Bell (1966). Values presented are the average of five subjects each and refer to 5 days after administration.

(153) Sheep as well as swine excreted about 11% of the injected ^{127m}Te in the faeces and 34% in the urine over five days. About two-thirds of the urinary excretion occurred in the first 24 h. After oral administration, sheep excreted 75% in the faeces and 20% in the urine. Swine excreted 70% in the faeces and 19% in the urine, mostly on the second day.

(154) Hollins (1969) studied the metabolism of ^{127m}Te as tellurous acid in rats. The whole body retention after intraperitoneal injection could be described as a bi-exponential function with half-times of 0.8 d (49%) and 13 d (51%), respectively. After oral administration 84% was retained with a half-time of 0.12 d, 11% with 0.8 d and 5% with 12 d. The half-times of the two longer retention terms were the same within the experimental errors as those observed after injection. The highest concentrations of tellurium were observed in the kidneys, blood, liver, spleen, femur and lung. Tellurium in blood was almost entirely bound to the protein content of the red blood cells. The tissues could be divided into three classes according to the retention half-time: lung, blood, liver and heart with a half-time of approximately 10 d; muscle, spleen, and kidney with a half-time of approximately 20 d; and femur (skeleton) with a half-time that was much longer than the duration of the experiment (200 d) and could therefore not be determined with much confidence. About 27% of the injected tellurium was excreted in urine during the first 24 h, and 6% was excreted in faeces. Less than 0.25% of the administered dose was eliminated in the breath in the first 24 h, despite a strong garlic odour.

(155) A series of studies on rats were conducted in the years between 1960 and 1970 in the former USSR and Czechoslovakia. Their findings are summarized by a document of the Health Council of Netherlands (2002). After intravenous injection tellurium was found mainly in the liver (10 to 20%), muscle (around 10%) and skeleton (8 to 24%), and to a lesser extent in the kidneys (2.5-7%). Deposition patterns varied with time from administration, with skeleton being the organ with the greatest retention time. Urinary excretion amounted to 14% of the iv dose on day 1 and 33% in the first week.

(156) Agnew and Cheng (1971) investigated protein binding of tellurium in maternal and fetal tissues after intravenous injection of tellurous acid (H_2TeO_3) labelled with ^{127m}Te into pregnant rats. Activity in whole blood was predominantly in the red cells at all times studied. The fraction in red cells increased from 65% after 15 minutes to about 95% after one week. By far the bulk of the activity in plasma was in a bound form. After 1 hr of circulation, less than 5% of the ^{127m}Te was in unbound form, and only about 0.5% was unbound after one week.

(157) Mullen and Stanley (1974) studied absorption, distribution and milk secretion of radiotellurium in dairy cows and calves. The transfer of tellurium to milk was very low (about 0.25% of the orally administered activity in 13 days). Retained tellurium was found mainly in the liver, bone, and organs of the digestive/ruminal tract. Again, tellurium concentration in

the thyroid was significant (about the same order as in the liver), but due to the tiny mass of this organ the total amount retained was negligible.

(158) Valkonen and Savolainen (1985) administered tellurium in the form of $TeCl_4$ in the drinking water of rats for up to 35 days. The tellurium concentration in liver remained constant with time but increased steadily in blood, kidney and brain. The concentration ratio liver : kidney was 4.1 after 7 days of administration and 2.1 after 35 days. The ratio liver : brain decreased from 8.1 to 1.8 in the same interval.

(159) Morgan et al. (1997) administered cadmium telluride intra-tracheally to rats. After absorption of tellurium into the systemic circulation, significant concentrations were found in the spleen (maximum, 82.8±10.2 $\mu g \cdot g^{-1}$ tissue), kidney (maximum, 8.1±1.3 $\mu g \cdot g^{-1}$ tissue), liver (maximum, 8.8±0.6 $\mu g \cdot g^{-1}$ tissue), femur (maximum 3.5±0.5 $\mu g \cdot g^{-1}$ tissue) and blood (maximum, 5.3±0.2 $\mu g \cdot g^{-1}$ tissue). The maximum concentration was reached at day 14 after administration in all tissues except liver, where the maximum was reached at day 7.

4.2.3.2. Biokinetic model for systemic tellurium

(160) ICRP *Publication 67* (1993) introduced a simple systemic model for tellurium based on findings in animal studies. That model assumed that 50% of tellurium entering blood goes directly to excretion with a half-time of 0.8 days; 25% is translocated to the skeleton, from which it is removed to excretion pathways with a half-time of 10,000 days; and the rest is divided between the kidneys (2.3%), thyroid (0.2%), and remaining tissues (22.5%), from which it is removed to excretion pathways with a biological half-time of 20 days. A urinary to faecal excretion ratio of 4:1 was assumed for systemic tellurium.

(161) In this report the generic model structure for bone-surface-seeking radionuclides is applied to tellurium, with the introduction of the thyroid as a separate compartment primarily to enable the application of the model to tellurium radionuclides produced as progeny of radioiodine. Transfer coefficients of the model are listed in Table 4-6. These coefficients are based predominantly on human data with regard to whole body retention and urinary excretion and on animal data, mainly from studies with swine and guinea pigs, with regard to the organ distribution.

(162) The compartment called Blood in the generic model structure is divided into two compartments: Blood 1, representing blood plasma, and Blood 2, representing red blood cells. It is assumed that tellurium leaves Blood 1 at the rate 1.16 d^{-1} (half-time of ~0.6 d) with 65% moving to the urinary bladder contents, 10.5% to Liver, 8.75% to Blood 2, 5.25% to Bone Surfaces (in the ratio 2:1 between trabecular and cortical), 3.5 % to Kidneys, 0.35% to Thyroid and the remaining 19 % to Soft-Tissue compartment ST. The following removal half-times are assigned: 10 d from Blood 2, Kidney, Thyroid and ST to Blood 1; 10 d from Liver to the small intestine contents (representing removal from the liver in bile); and 50 d from cortical or trabecular bone surface, with 98% returning to Blood 1 and 2% moving to the corresponding bone volume compartment. The transfer coefficients describing the rates of movement from the bone volume compartments to Blood 1 are the generic turnover rates for cortical and trabecular bone.

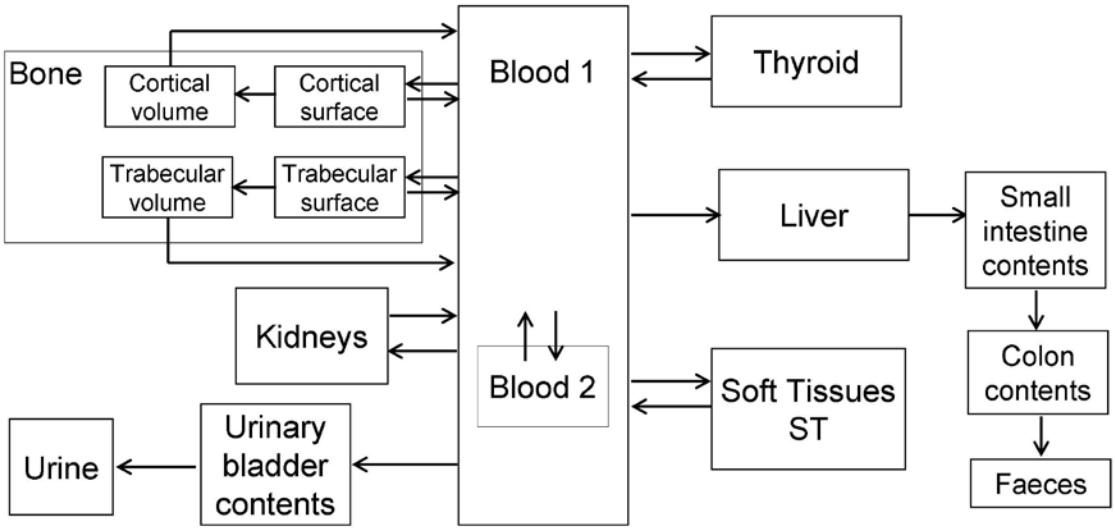

Figure 4-1. The systemic model for tellurium.

Table 4-7. Transfer coefficients for systemic tellurium

From	To	Transfer coefficient (d^{-1})
Blood 1	Urinary bladder contents	0.751
Blood 1	Kidneys	0.0404
Blood 1	Liver	0.1213
Blood 1	Blood 2	0.1011
Blood 1	ST	0.0768
Blood 1	Cortical bone surface	0.0202
Blood 1	Trabecular bone surface	0.0404
Blood 1	Thyroid	0.0040
Blood 2	Blood 1	0.0693
Liver	Small intestine contents	0.0693
Thyroid	Blood 1	0.0693
Kidneys	Blood 1	0.0693
ST	Blood 1	0.0693
Cortical bone surface	Blood 1	0.0116
Trabecular bone surface	Blood 1	0.0116
Cortical bone surface	Cortical bone volume	0.0006931
Trabecular bone surface	Trabecular bone volume	0.0006931
Cortical bone volume	Blood 1	0.0000821
Trabecular bone volume	Blood 1	0.000493

(163) No explicit exhalation pathway was introduced in the model as the available studies indicate that, in spite of the persistent garlic odour experienced after tellurium incorporation, the amount exhaled is negligible.

(164) The transfer coefficients listed in Table 4-7 yield the following predictions, which are reasonably consistent with the biokinetic database for tellurium summarized above. Urinary excretion of systemic tellurium is rapid and amounts to 45% in the first 24 h, 64% after 3 days, 71% after 10 d and 81% after 50 d. These values are in agreement with the urinary excretion observed by Kron et al. (1991) after oral administration of tellurium, taking

into account the absorbed fraction of 0.3. Faecal excretion of intravenous tellurium amounts to 0.54% after 3 days, 4.4% after 10 days and 12.3% after 50 days. Whole body retention is to 55% after one day, 23.8% after 10 d and 2.75% after 100 d, in satisfactory agreement with the data presented by Fehér and Andrási (1977) and with the curve predicted by them, as shown in Figure 4-2. At five days after intravenous injection, 8.2% of the injected amount is contained in the liver, 5.2% in the skeleton, 2.7% in the kidneys and 0.27% in the thyroid. At 100 days the retained fractions are 2.4%, 0.1%, 0.03% and 0.003% for skeleton, liver, kidneys and thyroid respectively.

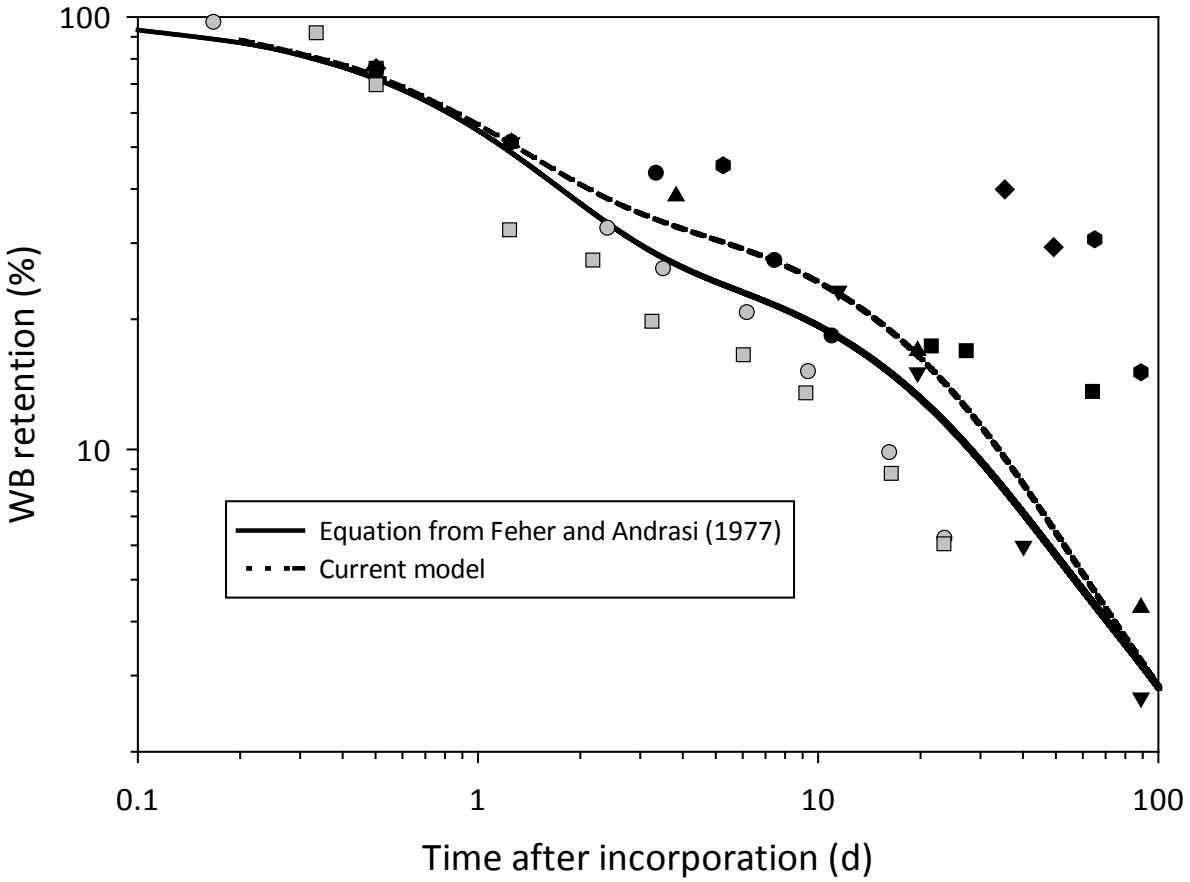

Figure 4-2. Whole body retention for tellurium.

Data from Fehér and Andrási (1977). Grey symbols: retention measured in volunteers after administration of TeO2-^{131}I suspension. Black symbols: retention measured after accidental contamination by workers. Solid line: equation suggested by Fehér and Andrási (1977) on the basis of their data. Dashed line: prediction of the OIR model. For the sake of comparison the workers' values were normalized to the curve prediction for the first available measurement time, as extrapolated from the original graph.

4.2.3.3. Treatment of radioactive progeny

(165) Chain members addressed in the derivation of dose coefficients for tellurium isotopes are isotopes of tellurium, antimony, iodine, or xenon. Isotopes of tellurium, antimony, or iodine produced in systemic compartments are assumed to follow the characteristic models for these elements (i.e. the models applied in this report to these elements as parent radionuclides) from their time of production, insofar as application of this

assumption is straightforward. In some cases, the site of production of antimony or iodine due to decay of a tellurium isotope may not be clearly identifiable with a specific compartment in its characteristic biokinetic model due to differences in model structures for the different elements. In such cases a transfer rate from the site of production of the radionuclide to the central blood compartment in the radionuclide's characteristic model has been assigned as described below. After reaching its central blood compartment, the radionuclide is assumed to behave as described by its characteristic model.

(166) Antimony atoms produced in soft-tissue compartments in the tellurium model that are ambiguous with regard to the characteristic model for antimony (specifically, Liver, Thyroid, and Other) are assumed to be transferred to the central blood compartment of that model (blood plasma) at the rate 0.693 d^{-1} (half-time of 1 d). This is the highest rate of removal from all soft tissue compartments in the characteristic model for antimony. Antimony produced in the compartment of the tellurium model called Blood 2, representing relatively long retention in blood, is assumed to transfer to plasma in the antimony model at the rate 1000 d^{-1} (a default rate representing rapid transfer between compartments). For modelling convenience, antimony produced in the central blood compartment of the tellurium model (Blood 1) is assigned to plasma in the antimony model.

(167) Iodine atoms are produced at the following sites in the tellurium model that are not clearly identifiable with specific compartments of the characteristic model for iodine: compartments of blood, bone, liver, kidneys, thyroid, and other soft tissues (Other). The following rates of transfer from these sites to the blood iodide pool of the characteristic model for iodine are assigned: from compartments of liver or kidneys, 100 d^{-1} (the rate of loss from the liver iodide and kidney iodide compartments in the characteristic model for iodine); from compartments of blood (other than the central blood compartment), 1000 d^{-1}; from compartments of other soft tissues or bone surface, 330 d^{-1} (the highest transfer coefficient to blood in the characteristic model for iodine); from thyroid, 36 d^{-1} (the transfer coefficient from the thyroid iodide pool to the blood iodide pool in the characteristic model for iodine); and from trabecular and cortical bone volume compartments, the reference rates of trabecular and cortical bone turnover. For modelling convenience, iodine produced in the central blood pool of the tellurium model is assigned to the blood iodide pool in the characteristic model for iodine.

(168) A generic biokinetic model is applied in this report to xenon isotopes produced by decay of a radionuclide in systemic compartments. Xenon produced in bone is assumed to transfer to blood at the rate 100 d^{-1} if produced in bone surface and 0.36 d^{-1} if produced in bone volume. These rates are taken from the model for radon introduced in ICRP *Publication 67* (1993) and applied in this report to radon produced in bone surface and non-exchangeable bone volume, respectively, by decay of a radium isotope. Xenon produced in a soft-tissue compartment is assumed to transfer to blood with a half-time of 20 min. Xenon produced in the central blood compartment in the model for tellurium, antimony, or iodine is assigned to the blood compartment of the xenon model. Xenon produced in any other blood compartment in the tellurium, antimony, or iodine model is assumed to be transferred to blood in the xenon model at the rate 1000 d^{-1}. Xenon entering the blood compartment of the xenon model or produced in that compartment is assumed to be removed from the body (exhaled) at the rate 1000 d^{-1}. Partial recycling of xenon to tissues via arterial blood is not depicted explicitly in this model for xenon as a daughter radionuclide but is considered in the assignment of the half-times in tissues. The model is intended to yield a conservative average residence time of xenon atoms in the body after their production in systemic pools.

4.3. Individual monitoring

^{129}Te

(169) ^{129}Te is a γ emitter. Monitoring of ^{129}Te may be accomplished through Whole Body Counting. Urine bioassay may also be used. Because of the short half-life measurements should be done soon after exposure, maximum of 3h after exposure.

Isotope	Monitoring Technique	Method of Measurement	Typical Detection Limit	Achievable detection limit
^{129}Te	Urine Bioassay	γ-ray spectrometry	331 Bq/L	
^{129}Te	Whole Body Counting	γ-ray spectrometry	1070 Bq	

^{131}Te

(170) ^{131}Te is a γ emitter. Monitoring of ^{131}Te may be accomplished through Whole Body Counting, immediately after exposure (up to three hours).

Isotope	Monitoring Technique	Method of Measurement	Typical Detection Limit	Achievable detection limit
^{129}Te	Whole Body Counting	γ-ray spectrometry	428 Bq	

^{131m}Te

(171) ^{131m}Te is a γ emitter. Monitoring of ^{131m}Te may be accomplished through Whole Body Counting. Urine bioassays may also be used. Measurements should be done in a short period after exposure.

Isotope	Monitoring Technique	Method of Measurement	Typical Detection Limit	Achievable detection limit
^{129}Te	Urine Bioassay	γ-ray spectrometry	1.4 Bq/L	
^{129}Te	Whole Body Counting	γ-ray spectrometry	395 Bq	

^{132}Te

(172) ^{132}Te is a γ emitter. Monitoring of ^{131m}Te may be done through Whole Body Counting. Urine bioassays are also used.

Isotope	Monitoring Technique	Method of Measurement	Typical Detection Limit	Achievable detection limit
^{132}Te	Urine Bioassay	γ-ray spectrometry	0.5 Bq/L	
^{132}Te	Whole Body Counting	γ-ray spectrometry	100 Bq	

^{133m}Te

(173) ^{133m}Te is a γ emitter. Monitoring of ^{133m}Te may be accomplished through Whole Body Counting. Urine bioassays may also be used. Measurements should be done immediately after exposure (up to three hours).

Isotope	Monitoring Technique	Method of Measurement	Typical Detection Limit	Achievable detection limit
^{133m}Te	Urine Bioassay	γ-ray spectrometry	114 Bq/L	
^{133m}Te	Whole Body Counting	γ-ray spectrometry	95 Bq	

References

Agnew, W.F., Cheng, J.T., 1971. Protein binding of tellurium-127m by maternal and fetal tissues of the rat. Toxicol. Appl. Pharmacol. 20, 346-356.

Balonov, M., Kaidanovsky, G., Zvonova, I., Kovtun, A., Bouville, A., Luckyanov, N., Voillequé, P., 2003. Contributions of short-lived radioiodines to thyroid doses received by evacuees from the Chernobyl area estimated using early in vivo activity measurements. Radiat. Prot. Dosim. 105 (1–5) 593–599.

Barnes, D.W.H., Cook, G.B., Harrison, G.E., Loutit, J.F., Raymond, W.H.A., 1955. The metabolism of ^{132}tellurium-iodine mixture in mammals. J. Nucl. Energy 1, 218-230.

Blackadder, E.S., Manderson, W.G., 1975. Occupational absorption of tellurium: a report of two cases. Brit. J. Ind. Med. 32, 59–61.

Casey, H.W., Case, A.C., McClellan, R.O., Bustad, L.K., 1963. Metabolism of Te^{132}-I^{132} in lactating sheep. Health Phys. 9, 1223-1226.

Chertok, R.J., Kake, S., 1970. Availability in the dog of radionuclides in nuclear debris from the Plowshare excavation cabriolet. Health Phys. 19, 405-409.

DeMeio, R.H., Henriques, F.C., 1947. Excretion and distribution in tissues studied with a radioactive isotope. J. Biol. Chem. 169, 609-617.

Dobryakova, G.V., 1970. Dynamics of the removal of Te-127 and Ru-106 from rat lungs. In: Moskalev, Yu. I., Editor. Radioaktiv. Izotopy Vnesh. Srede Organizme. pp. 57-63. Moscow: Atomizdat.

Fehér, I. (1976) Investigations of the Internal Radiation Burdens. PhD Thesis (in Hungarian).

Fehér, I. and Andrási, A. (1977) Study on internal contamination due to tellurium isotope mixture. Proc. 4th IRPA congress Vol 2. pp. 421-424. International Radiation Protection Association.

Geary, D. L., Myers, R. C., Nachreiner, D. J. and Carpenter, C. P. (1978). Tellurium and tellurium dioxide: single endotracheal injection to rats. Am. Ind. Hyg. Assoc. J. 39, 100-109.

Health Council of the Netherlands (2002). Committee on Updating of Occupational Exposure Limits. Tellurium and tellurium compounds (excluding TeF6); Health-based Reassessment of Administrative Occupational Exposure Limits. The Hague: Health Council of the Netherlands, 2000/15OSH/055.

Hollins, J.G. (1969) The metabolism of tellurium in rats. Health Phys. 17, 497-505.

ICRP (1979) International Commission on Radiological Protection. Limits on Intakes of Radionuclides for Workers. ICRP Publication 30, Pt.1. ICRP 2, (3/4), 85-87.

ICRP (1993) International Commission on Radiological Protection. Age-dependent Doses to Members of the Public from Intake of Radionuclides. Pt.2. ICRP Publication 67. Ann. ICRP. 23, (3/4), 61-67.

Kron, T., Hansen, Ch. and Werner, E. (1991) Renal excretion of tellurium after peroral administration of tellurium in different forms to healthy humans. J. Trace Elem. Electrolytes Health. Dis. 5, 239-244

Morgan, D.L., Shines, C.J., Jeter, S.P., Blazka, M.E., Elwell, M.R., Wilson, R.E., Ward, S.M., Price, H.C., Moskowitz, P.D., 1997. Comparative pulmonary absorption, distribution, and toxicity of copper gallium diselenide, copper indium diselenide, and cadmium telluride in Sprague-Dawley rats. Toxicology & Applied Pharmacology, 147, 399–410.

Mullen, A.A., Stanley, R.E., 1974. Absorption, distribution and milk secretion of radionuclides by dairy cows. III. Radiotellurium. Health Phys. 27, 279-284.

Nason, A.P., Schroeder, H.A., 1967. Abnormal trace elements in man: tellurium - Erratum. J. Chron. Dis. 20, 671.

Schroeder, H.A., Buckman, J., Balassa, J.J., 1967. Abnormal trace elements in man: tellurium. J. Chron. Dis. 20, 147-161.

Taylor, A., 1996. Biochemistry of tellurium. Biol. Trace Elem. Res. 55(3), 231-239.

Valkonen ,S., Savolainen, H., 1985. Tellurium burden and neurochemical effects in moderate peroral exposure. Bull. Environ. Contam. Toxicol. 34, 170-174.

van Montfort, PFE, Agterdenbos, J., Jütte, B.A.H.G., 1979. Determination of antimony and tellurium in human blood by microwave induced emission spectrometry. Anal. Chem. 51, 1553-1557.

Venugopal, B., Luckey, T.D., 1978. Metal Toxicity ion Mammals. Vol. 2. Plenum Press, New York.

Wright, P.L., Bell, M.C., 1966. Comparative metabolism of selenium and tellurium in sheep and swine. Am. J. Physiol. 20, 6-10.

5. IODINE (Z = 53)

5.1. Chemical Forms in the Workplace

(174) Iodine is a volatile halogen existing mainly in oxidation states –I, 0 and V. The most common chemical forms of iodine in solution are the iodide (I^-) and the iodate (IO_3^-). Iodine may be encountered in industry in a variety of chemical and physical forms, including vapours and gases, organic compounds such as methyl and ethyl iodide, and particulate forms including metal-iodide (NaI, AgI).

(175) ^{131}I, ^{129}I and ^{132}I (from ^{132}Te) are the three main iodine fission products that are released from reactor accidents and that are present in fragments of irradiated fuels. ^{123}I and ^{125}I are used in medicine as tracers for imaging and evaluating the function of the thyroid, and ^{131}I is used in medicine for the treatment of thyroid cancer.

Table 5-1. Isotopes of iodine addressed in this report

Isotope	Physical half-life	Decay mode
I-118	13.7 m	EC, B+
I-119	19.1 m	EC, B+
I-120	81.6 m	EC, B+
I-120m	53 m	EC, B+
I-121	2.12 h	EC, B+
I-123	13.27 h	EC
I-124	4.176 d	EC, B+
I-125[a]	59.40 d	EC
I-126	12.93 d	EC, B+, B-
I-128	24.99 m	B-, EC, B+
I-129[a]	1.57E+7 y	B-
I-130	12.36 h	B-
I-131[a]	8.021 d	B-
I-132	2.295 h	B-
I-132m	1.387 h	IT, B-
I-133	20.8 h	B-
I-134	52.5 m	B-
I-135	6.57 h	B-

[a] Data for these radionuclides are given in the printed copy of this report. Data for other radionuclides are given on accompanying electronic disk.

5.2. Routes of Intake

5.2.1. Inhalation

Absorption Types and Parameter Values

(176) Detailed information on the behaviour of inhaled gases and vapours of iodine is available from studies in human volunteers. Hence, although information is also available from animal experiments, it is not reviewed here. Some information is available on inhaled particulate forms of iodine: as iodide from animal experiments; and associated with irradiated fuel fragments from human exposures.

(177) Absorption parameter values and Types, and associated f_A values for gas and vapour

forms of iodine are given in Table 5-2 and for particulate forms in Table 5-3. Exposures to both gas/vapour forms and particulate forms of iodine are common, and it is therefore proposed here that in the absence of information 50% particulate; 50% gas/vapour should be assumed (ICRP, 2002a).

(a) Gases and vapours

Elemental iodine

(178) Iodine in thyroid measurements were made up to about 4 months after intake on five workers who accidentally inhaled ^{125}I vapours released from an open beaker (Bordell et al., 1972). The thyroid activity fell by about 30% between the first two measurements (at 0.5 and 4 days after the intake), suggesting that most of the absorption to blood had occurred by the time of the first measurement, and indicating Type F behaviour.

(179) Detailed studies have been conducted in human volunteers of the deposition and subsequent biokinetics of iodine inhaled as vapour labelled with ^{132}I (Morgan et al., 1968a; Black and Hounam, 1968). The results confirmed the rapid absorption seen previously in animal experiments. In the experiments conducted by Morgan et al. the iodine was inhaled through a mouthpiece. Respiratory tract deposition was almost complete, and the authors noted that this must be due to the high chemical reactivity of iodine, because it is only sparingly soluble in water. Measurements with collimated detectors showed high deposition in the oral pharynx, and transfer downwards, presumably to the stomach. From these and measurements of systemic activity it was inferred that much of the activity was swallowed and subsequently absorbed from the alimentary tract. The authors concluded that the main site of deposition was the oral pharynx, and while penetration to the trachea and bronchi could not be excluded, it was unlikely that iodine vapour reaches the alveoli. In the experiments conducted by Black and Hounam the iodine was drawn in through the nose and out through the mouth. Using a similar technique, Pattle (1961) reported negligible penetration of the nose and mouth by iodine vapour. However, Black and Hounam found that deposition was not complete (typically ~70%) and estimated that in normal breathing rather less than 50% of iodine vapour would be deposited in the "nasopharyngeal region" and the rest in the tracheobronchial region. Measurements of retention in different parts of the nasal passage were made with collimated detectors from 5 to 100 minutes after deposition. These showed that there was some deposition in the nasal vestibule (ET_1), but the fraction deposited there was not estimated. They estimated a clearance half-time from the nasopharynx of about 30 minutes, but this would not have included clearance during the first few minutes.

(180) Analyses of the results of these human volunteer experiments were carried out by the Task Group to estimate the rate of absorption of iodine from respiratory tract to blood (sr) following its inhalation in elemental form. A compartment model was set up using the updated HRTM and the systemic model for iodine described below, and applied to estimate values of fractional regional deposition and s_r using the reported measurements of ^{132}I in the thyroid and urine. Some parameter values in the systemic model were normalised to the individual subject using reported measurements of ^{132}I in the thyroid and urine following ingestion of ^{132}I-labelled sodium iodide by the same subject. From the reported observations (see above) and for simplicity, it was assumed that deposition occurred only in ET_2 and BB. It was found that the results were insensitive to the ratio of deposition between these regions and the assumption was made of 50% deposition in ET_2 and 50% in BB. On that basis, the rate of absorption of iodine from respiratory tract to blood (s_r) was estimated to be approximately 100 d^{-1}. As described below, based on this assessment, and the results of

studies in which iodine was deposited in the respiratory tract as sodium iodide and in a caesium chloride vector, a value of s_r of 100 d^{-1} is applied here to Type F forms of iodine. Hence for elemental iodine it is assumed here that there is 100% deposition in the respiratory tract but in the upper airways (50% ET_2 and 50% BB), with Type F absorption.

Methyl iodide (CH_3I)

(181) Detailed studies have been conducted in human volunteers of the deposition and subsequent biokinetics of iodine inhaled as CH_3I (Morgan et al., 1967a,b; Morgan and Morgan, 1967). The amount retained varied from 50 to 90% (average 70%), increasing with decreasing number of breaths per minute. It was inferred that most of it deposited in the alveoli. Absorption to blood of the deposited activity was very rapid (estimated half-time about 5 seconds). Subsequent biokinetics were very similar to those of injected iodide, suggesting that the CH_3I is rapidly metabolised. For methyl iodide it is therefore assumed here that there is 70% deposition in the respiratory tract (with default regional distribution, Table 5-2) and Type V absorption.

Ethyl iodide (C_2H_5I)

(182) The retention of ^{132}I-labelled ethyl iodide (C_2H_5I) inhaled by human volunteers was in the range 44 to 62%, slightly lower than the same group of subjects exposed to methyl iodide (53 to 81%) (Morgan *et al*, 1968b). Urinary excretion of ^{132}I also occurred at a slower rate than that following inhalation of ^{132}I-labelled methyl iodide. For ethyl iodide it is therefore assumed here that there is 60% deposition in the respiratory tract (with default regional distribution, Table 5-2) and Type V absorption.

(b) Particulate aerosols

Sodium iodide (NaI)

(183) Iodine inhaled as sodium iodide is rapidly absorbed into blood. Thiéblemont et al. (1965a,b) studied excretion and thyroid uptake of ^{131}I following inhalation of ^{131}I-labelled NaI by rhesus monkeys, and noted that excretion was similar to that for intravenously injected ^{131}I. Perrault et al. (1967) investigated the absorption from the respiratory tract of ^{131}I following inhalation of ^{131}I-labelled NaI by rhesus monkeys. At 13 minutes after the end of a 30-minute exposure, 82% of activity had been absorbed from the respiratory tract to blood. A compartment model fit by the authors to measurements of ^{131}I in lung and blood gave a half-time for absorption between 2.5 and 10 minutes, i.e. a rate of the order of 100 d^{-1}. Dawson et al. (1985) measured absorption of ^{131}I in isolated perfused rabbit lung exposed to an aerosol containing ^{125}I-labelled NaI. They calculated a half-time for absorption of about 10 minutes, corresponding to a rate of ~100 d^{-1}. Although specific parameter values for sodium iodide based on *in vivo* data are available, they are not adopted here. Instead, sodium iodide is assigned to Type F. However, the data are used as the basis for the default rapid dissolution rate for iodine. Hence specific parameter values for sodium iodide would be the same as default Type F iodine parameter values.

Caesium chloride vector

(184) Thomas et al. (1970) followed the biokinetics of ^{131}I for 70 days after inhalation of ^{131}I associated with caesium chloride vector aerosols by rats. Immediately after the 10-minute exposure the lung contained only about 1% of the initial body content. By 24 hours, there were high concentrations in thyroid and pelt. Whole-body retention to 70 days was similar to

that in rats following intravenous injection of ^{131}I. Thus absorption from lungs to blood was rapid, of the order of 100 d^{-1}. The biokinetics of ^{131}I were followed for 30 days after inhalation of ^{131}I associated with caesium chloride vector aerosols by dogs (McClellan and Rupprecht, 1968). It was noted that the maximum thyroid uptake (as a fraction of initial body content) and the time after intake at which the maximum thyroid uptake was reached were very similar for inhaled, ingested, or intravenously injected ^{131}I, which demonstrated the soluble nature of iodide in body fluids. Although specific parameter values for iodine in a caesium chloride vector based on *in vivo* data are available, they are not adopted here. Instead, it is assigned to Type F. However, the data are used as the basis for the default rapid dissolution rate for iodine. Hence specific parameter values would be the same as default Type F iodine parameter values.

Silver iodide (AgI)

(185) Following inhalation of ^{131}I-labelled silver iodide by mice and sheep (Bair, 1961; Willard and Bair, 1961), the ^{131}I was rapidly absorbed from the lungs, even though silver iodide was studied because it is one of the most insoluble iodine compounds in water. Lung retention of ^{110m}Ag following inhalation of ^{110m}Ag-labelled silver iodide by dogs and rats (Morrow et al., 1968) was consistent with assignment to Type M (see silver section). However, Morrow et al. noted that during aerosolisation some conversion to silver oxide probably occurs. Hence it appears that the rapid absorption of ^{131}I observed by Bair et al. is probably not inconsistent with the slow absorption of silver reported by Morrow et al., and iodine inhaled as silver iodide is assigned here to default Type F.

Irradiated fuel fragments

(186) Mirell and Blahd (1989) made whole-body measurements of activity on seven people from about two weeks to several months after exposure to the initial Chernobyl reactor accident plume in Kiev, Ukraine. Biological retention half-times were similar for different radionuclides (23 days for ^{131}I) and different from those expected for systemic retention, indicating that they were trapped in particles and metabolically inert, thus indicating Type M rather than Type F behaviour.

(187) In view of the limited information available, these data are judged to be an insufficient basis to provide specific absorption parameter values. Considerable variability has been observed in the behaviour of caesium associated with irradiated fuel fragments (see caesium section), for which much more information is available. Since this is also likely to be the case for iodine, this form is not assigned specifically to a default Type here.

Default rapid dissolution rate for iodine

(188) Studies with elemental iodine, sodium iodide, and iodine in a caesium chloride vector outlined above give values of s_r of about 100 d^{-1}, which is applied here to all Type F forms of iodine.

Extent of binding of iodine to the respiratory tract

(189) Evidence from the various experimental studies outlined above suggests that there is probably little binding of iodine. It is therefore assumed that for iodine the bound state can be neglected, i.e. $f_b = 0.0$.

Table 5-2. Deposition and absorption for gas and vapour forms of iodine[a]

Chemical form/origin	Fraction deposited (%)[b] Total	ET_1	ET_2	BB	bb	AI	Absorption Type	f_A
Elemental iodine, I_2	100	0	50	50	0	0	F	1.0
Methyl iodide, CH_3I	70[c]	0	14	7	14	35	V	(d)
Ethyl iodide, C_2H_5I	60[c]	0	12	6	12	30	V	(d)
Unspecified[a]	100	0	50	50	0	0	F	1.0

[a] For iodine in unspecified gas or vapour form, the behaviour assumed is the same as that for elemental iodine: 100% deposition (50% ET_2 and 50% BB) with Type F absorption.

[b] *Fraction deposited* refers to how much of the material in the inhaled air remains in the body after exhalation. Almost all inhaled gas molecules contact airway surfaces, but usually return to the air unless they dissolve in, or react with, the surface lining.

[c] Since instantaneous absorption to blood (Type V) is assumed, calculations can be performed assuming direct injection into blood, and the regional deposition does not need to be considered. Nevertheless, for completeness, the deposits in each region are assumed to be distributed in the same proportions as in the default distribution for gases and vapours: 20% ET_2, 10% BB, 20% bb and 50% AI.

[d] Not applicable for absorption Type V, because all activity deposited in the respiratory tract is instantaneously absorbed.

Table 5-3. Absorption parameter values for inhaled particulate forms of iodine and for ingested iodine

Inhaled particulate materials		**Absorption parameter values[a]** f_r	s_r (d^{-1})	s_s (d^{-1})	**Absorption from the alimentary tract, f_A**
Default parameter values[b,c]					
Absorption Type	Assigned forms				
F	Sodium iodide; caesium chloride vector, silver iodide, all unspecified forms[d]	1	100	–	1
M	—	0.2	3	0.005	0.2
S	—	0.01	3	$1x10^{-4}$	0.01
Ingested materials					
All unspecified forms					1

[a] It is assumed that for iodine the bound state can be neglected i.e. $f_b = 0$. The value of s_r for Type F forms of iodine (100 d^{-1}) is element-specific. The values for Types M and S (3 d^{-1}) are the general default values.

[b] Materials (e.g. sodium iodide) are generally listed here where there is sufficient information to assign to a default absorption Type, but not to give specific parameter values (see text).

[c] For inhaled material deposited in the respiratory tract and subsequent cleared by particle transport to the alimentary tract, the default f_A values for inhaled materials are applied: i.e. the product of f_r for the absorption Type and the f_A value for ingested soluble forms of iodine (1.0).

[d] Default Type F is recommended for use in the absence of specific information, i.e. if the form is unknown, or if the form is known but there is no information available on the absorption of that form from the respiratory tract.

5.2.2. Ingestion

(190) The absorption of iodide from the gastrointestinal tract of humans is virtually

complete with reported values of 0.9 and greater (Riggs, 1952; Willard and Bair, 1961; Wayne et al, 1964; Underwood, 1971). Keating and Albert (1949) reported a rate of absorption of about 5% min^{-1} in fasted individuals, with complete absorption within 2 hours. Iodide absorption depends, however, on the redox conditions in the gastrointestinal tract. Mechanistic studies indicate that some oxidizing agents such as chlorine-based disinfectants oxidize the basal iodide content of the gastrointestinal tract and decrease its bioavailability (Bercz et al., 1986).

(191) For other chemical forms, absorption is less complete. Results obtained for iodine administered to humans as thyroxine suggested absorption of 0.80 - 0.85 (Wayne et al., 1964). Similar experiments using ^{125}Iodine incorporated in trypsin and given by direct introduction into the duodenum to one volunteer showed that significant amount of radioactivity appeared in blood within 4 minutes and increased to a maximum by 75 minutes. The total activity absorbed in this experiment was about 11% of the ingested activity (Lake-Bakaar et al., 1980). By contrast, other studies performed on 9 healthy individuals with [^{131}I]-labelled trypsin showed absorption of about 0.78-0.98 with a peak of activity in the plasma 1 hour after administration (Bohe et al., 1986). These authors showed that only free ^{131}I is absorbed into the circulation, demonstrating a deiodinating mechanism in the intestine. This variability in iodine absorption between individuals may be partly explained by genetic polymorphism (Mithen, 2007).

(192) Studies in animals have shown that in dogs, free iodine and iodate are converted to iodide prior to absorption (Cohn, 1932). High values of absorption (>0.7 – 1) have been reported for absorption of iodine and iodide in goats and cattle, as summarized by Coughtrey et al. (1983).

(193) In *Publication 30* (ICRP, 1979), an absorption value$_1$ of 1 was recommended for all chemical forms of I. This value was adopted in *Publication 56* (ICRP, 1989) for dietary intakes. An f_A of 1 is used here for all forms.

5.2.3. Systemic Distribution, Retention and Excretion

5.2.3.1. Summary of the database

Iodine requirements in adult humans

(194) Iodine is an essential component of the thyroid hormones thyroxine (T_4) and triiodothyronine (T_3), which regulate metabolic processes and are critical to growth and development (Utiger, 2001; BEST, 2005; Delange and Dunn, 2005). Several tens of micrograms of inorganic iodide are trapped daily by the adult human thyroid and used for synthesis of T_4 and T_3. T_4 is produced only in the thyroid and represents >90% of the hormonal iodine secreted by the thyroid. About 20% of the circulating T_3 is produced in the thyroid, and the rest is produced from T_4 in extra-thyroidal tissues through a process involving removal of a single iodine atom from T_4. T_3 is more active than T_4 and exerts most of the effects of the thyroid hormones in the body (Greenspan, 2004; BEST, 2005; Bianco and Larsen, 2005).

(195) Iodine is largely recycled by the body after use of T_4 and T_3 by tissues, but the body's supply must be supplemented with dietary iodine due to obligatory losses in excreta. The World Health Organization (WHO) recommends daily intake of 150 µg of iodine by adults and 200 µg during pregnancy and lactation to ensure adequate production of thyroid hormones and prevention of goiter and hypothyroidism (WHO, 2001; FAO/WHO, 2002). WHO defines dietary iodine intake of 50-99 µg d^{-1} (or 50-99 µg L^{-1} urine, assuming a daily

urine volume of 1 L and ignoring losses along other excretion routes) as mild iodine deficiency, 20-49 μg d^{-1} as moderate iodine deficiency, and <20 μg d^{-1} as severe iodide deficiency. Extensive survey data on dietary and urinary iodine (Parr et al., 1992; O'Hare et al., 1998; Iyengar et al., 2004; WHO, 2004; Delange and Dunn, 2005; Caldwell et al., 2005) indicate that iodine intake is at or above recommended levels in much of the world but is mildly to severely deficient in many regions. Daily intake of iodine typically is 30-40% lower in women than in men (Oddie et al., 1970, Fisher et al., 1971; Milakovic et al., 2004, Bilek et al., 2005; Burman, 2006; CDC, 2008). The following reference values for dietary iodine are selected on the basis of worldwide survey data: 130 μg d^{-1} for women, 190 μg d^{-1} for men, and 160 μg d^{-1} as a gender-averaged value.

(196) The following overview of the systemic biokinetics of iodine in adult humans was excerpted from a review by Leggett (2010).

Absorption and distribution of inorganic iodide

(197) Iodine occurs in foods mainly as inorganic iodide. Other forms of iodine in foods are reduced to iodide in the alimentary tract before absorption (Cohn, 1932; WHO, 1989). Absorption is primarily from the small intestine but may occur to some extent from the stomach and other sites along the alimentary tract (Cohn, 1932; Riggs, 1952; Small et al., 1961). Absorption is rapid and nearly complete in most cases. Keating and Albert (1949) estimated an absorption rate of about 5% min^{-1} in fasted individuals, with virtually complete absorption within 2 hours. Absorption was slower when iodide was ingested with food but was virtually complete after about 3 hours. More than 99% of iodine orally administered as potassium iodide was absorbed to blood in normal subjects (Oddie et al., 1964; Fisher et al., 1965).

(198) Absorbed iodide is distributed rapidly throughout the extracellular fluids (ECF). Most of the iodide that leaves blood is recycled to blood within 1-2 h and much of it is recycled within a few minutes (Riggs, 1952; Wayne et al., 1964; Hays and Solomon, 1965).

(199) The iodide ion is largely excluded from most cells but rapidly traverses the red blood cell (RBC) membrane. Equilibration between plasma iodide and RBC iodide occurs in minutes. The concentration of iodide in RBC water is about the same as in plasma water, giving about two-thirds as much iodide in the total RBC as in an equal volume of plasma (Myant et al., 1950; Riggs, 1952).

(200) A substantial portion of iodide entering blood is concentrated in the salivary glands and stomach wall by active transport. It is subsequently secreted into the alimentary tract contents in saliva and gastric juice and nearly completely reabsorbed to blood. As a central estimate the rate of clearance of plasma iodide in saliva plus gastric secretions is about 43 ml/min (range, 36-49 ml/min) (Hays and Solomon, 1965; Harden and Alexander, 1968; Harden et al., 1969). The concentration of iodine in these secretions is on the order of 30 times its concentration in plasma. There is a delay of about 20 min between uptake of iodine by the salivary glands and stomach wall and appearance in the stomach contents, and a delay of about 30 min between the peak concentration in plasma and the peak concentration in secretions into the alimentary tract (Riggs, 1952; Hays and Wegner, 1965).

(201) The thyroid and kidneys are in competition for blood iodide and hence for the body's supply of iodide due to the rapid recycling of total-body iodide through blood. Normally more than 90% of the loss of iodine from the body is due to renal clearance of iodide. Little inorganic iodide is lost in faeces. Sweat does not appear to be an important mode of loss of iodide except perhaps in hot climates or during intense exercise (Wayne et al., 1964; Smyth and Duntas, 2005).

(202) Iodide in blood plasma is filtered by the kidneys at the glomerular filtration rate. About 70% of the filtered iodide is reabsorbed to blood, and the rest enters the urinary bladder contents and is excreted in urine (Bricker and Hlad, 1955; Vadstrup, 1993). Renal clearance expressed as the volume of plasma iodide or blood iodide cleared per unit time is nearly constant over a wide range of plasma concentrations for a given age and gender. As a central estimate, renal clearance is about 37 ml plasma/min for euthyroid adult males (Berson et al., 1952; Wayne et al., 1964; Hays and Solomon, 1965). Renal clearance of iodide expressed as plasma volumes per unit time appears to be about 25-30% lower on average in women than in men, but fractional loss of total-body iodide in urine per unit time is similar for men and women (Wayne et al., 1964; Oddie et al., 1966).

(203) The concentration of radioiodide in the kidneys may exceed that in most extrathyroidal tissues for a brief period after acute input into blood. In rats the peak concentration in the kidneys occurred about 15 min after intravenous injection (Korolev, 1969; Esposito, 1970), at which time the kidneys contained a few percent of the injected amount (Korolev, 1969). In rats and mice the concentration of radioiodine in the kidneys was similar to that of the salivary glands during the early hours after intravenous or intraperitoneal injection (Esposito, 1970; Dadachova et al., 2002). Data on laboratory animals generally indicate that the concentration of radioiodide in the kidneys declines rapidly and is not much greater than that of most other organs by a few hours after administration (Ruegamer, 1953; Ulmer et al., 1959; Moskalev and Yegorova, 1972). Using imaging data for ^{124}I as a tracer for ^{131}I in patients with thyroid cancer, Kolbert et al. (2007) estimated that the dose to kidneys from ^{131}I was on average roughly half of the dose to the salivary glands.

(204) Data on the extent of accumulation of inorganic radioiodide in the liver are variable. It appears from animal data that the liver typically accumulates a few percent of radioiodide soon after ingestion or intravenous administration but much less per gram of tissue than the kidneys (Willard and Bair, 1961; Korolev, 1969; Moskalev and Yegorova, 1972; Dadachova et al., 2002; Zuckier et al., 2004).

Behavior of iodide and organic iodine in the thyroid

(205) The basic unit of cellular organization within the thyroid is the follicle, a spherical structure typically a few hundredths of a millimeter in diameter. Each follicle is composed of a single layer of epithelial cells enclosing a lumen filled with a viscous material called colloid. The colloid consists mainly of thyroglobulin, a protein synthesized by follicular cells and secreted into the lumen. Thyroglobulin serves as a matrix for production and storage of T_4 and T_3 (Kopp, 2005).

(206) Iodide is actively transported from blood plasma into thyroid follicular cells at the plasma membrane. A normal thyroid can concentrate the iodide ion to 20-40 times its concentration in blood plasma. Some of the trapped iodide leaks back into blood, but most of it diffuses across the follicular cell and enters the follicular lumen where it is converted to organic iodine.

(207) Berson and Yalow (1955) studied the kinetics of trapping and binding of intravenously injected ^{131}I by the thyroid in 24 hyperthyroid and 3 euthyroid subjects, first with no inhibition of binding and later with administration of a drug that inhibited binding. They concluded that the rate of binding of trapped iodide is much greater than the rate of return of trapped iodide to blood. When iodide binding was blocked before administration of ^{131}I, activity in the thyroid reached a peak at times varying from several minutes to an hour or more after injection. In about 80% of the cases the rate of loss of trapped ^{131}I from the blocked thyroid was in the range 0.015-0.047 min^{-1} (22-68 d^{-1}).

(208) Robertson et al. (1971) estimated the rate of binding of trapped iodide by the thyroid and the rate of return of trapped iodide to plasma (exit rate) in 15 hyperthyroid and 7 euthyroid subjects by kinetic analysis of time-dependent plasma concentrations and thyroid accumulation of intravenously injected ^{131}I. The estimated binding rate was significantly greater in hyperthyroid than in euthyroid subjects, but no significant difference was found in the exit rate in the two groups. The estimated mean exit rate (+/- standard deviation) for all 22 subjects was 0.025 +/- 0.013 min^{-1} (36 +/- 19 d^{-1}). Estimates of the binding rate averaged 0.110 +/- 0.042 min^{-1} (160 +/- 60 d^{-1}) in the hyperthyroid subjects and 0.066 +/- 0.039 min^{-1} (95 +/- 56 d^{-1}) in the euthyroid subjects.

(209) Iodide is transported across the luminal membrane of the follicular cell into the lumen and oxidized at the cell-colloid interface. The neutral iodine atoms formed by oxidation of iodide are bound (organified) within the lumen to specific residues of the amino acid tyrosine. Some tyrosine residues gain one iodine atom, forming monoiodotyrosine (MIT) and others gain two iodine atoms, forming diiodotyrosine (DIT). T_4 is formed within the lumen by the coupling of two DIT molecules and hence has four iodine atoms, and T_3 is formed within the lumen by coupling of one MIT molecule to one DIT molecule and hence has three iodine atoms. The lumen typically contains 10-15 times more T_4 than T_3.

(210) The thyroid adapts to prolonged reductions or increases in iodine intake by adjusting its rate of uptake of iodide from blood. Adaptation of thyroidal clearance of iodide to dietary intake results in an inverse relation between net 24-h thyroidal uptake of ingested radioiodine (U) and average 24-h urinary excretion of stable iodine (E). The uptake rate U also depends on the mass S of iodine secreted daily by the thyroid. Stanbury et al. (1954) derived the formula $U=S/(S+E)$ or $U=[1+(E/S)]^{-1}$, based on the assumption that daily accumulation of organic iodine by the thyroid is in mass balance with daily secretion S of hormonal iodine. They derived a central estimate for S of 57 μg d^{-1} from measurements of E and U in a relatively large study group, primarily young adult females, with generally low rates of urinary excretion of stable iodine and high incidence of goiter. The formula $U=57/(57+E)$ is still widely used to estimate thyroidal uptake of radioiodine on the basis of urinary iodide (Ermans, 1993; O'Hare et al., 1998).

(211) Zvonova (1989) compiled regional data on dietary intake or urinary excretion of stable iodine, thyroidal uptake of radioiodine, and mass of the thyroid in adult humans. Data were collected for populations in Argentina, West Germany, Russia, Denmark, Scotland, Hungary, West New Guinea, and seven regions in the U.S. Estimated dietary intake Y of stable iodine ranged from 5-10 μg d^{-1} in West New Guinea to 250-700 μg d^{-1} in some regions of the U.S. The mean fractional uptake of ingested radioiodine by the thyroid after 24 h (U) was estimated as 0.14-0.15 for populations with intake >400 μg d^{-1}, 0.16-0.27 for intake of 250-330 μg d^{-1}, 0.41-0.45 for intake of 80-85 μg d^{-1}, 0.54-0.59 for intake of 40-54 μg d^{-1}, and about 0.9 for intake of 5-10 μg d^{-1}. Zvonova derived the relation $U = 85/(85+Y)$ or $U=[1+(Y/85)]^{-1}$ based on an assumed balance of daily thyroidal accumulation of organic iodine and secretion S of hormonal iodine. The value S = 85 μg d^{-1} was derived by fitting the collected data for Y and U.

(212) The formulas of Stanbury et al. (1954) and Zvonova (1989) are both broadly consistent with central estimates of thyroidal uptake of radioiodine in populations with dietary iodine up to a few hundred micrograms per day but substantially underestimate uptake in populations with iodine-rich diet. The underestimates apparently arise because the assumption of balance of thyroidal uptake and hormonal secretion of iodine is invalid at high levels of dietary stable iodine. The rate of accumulation of organic iodine by the thyroid and the rate of loss of iodine from the thyroid both appear to increase at high levels of iodine

intake, but the mass of iodine secreted as thyroid hormones appears to remain unchanged (Koutras et al., 1964; Fisher et al., 1965; Ohtaki, 1967; Nagataki et al., 1967; Harrison, 1968; Fisher and Oddie, 1969a).

(213) In adults with iodine sufficient diet the thyroid typically stores 5-15 mg of hormonal iodine (Riggs, 1952; Fisher and Oddie, 1969b; Hellstern et al., 1978; Handl et al., 1984; Shapiro et al., 1994; Hays, 2001). Estimates of the rate S of secretion of hormonal iodine by the thyroid (μg I d^{-1}) in individual euthyroid adult humans range from less than 30 μg d^{-1} to more than 150 μg d^{-1} (Riggs, 1952; Berson and Yalow, 1954; Ingbar and Freinkel, 1955; Stanbury et al., 1954; Gregerman et al., 1962; Fisher et al., 1965; Fisher and Oddie, 1969a; Zvonova, 1989). Reference values for adults given in reviews and textbooks generally are in the range 55-85 μg d^{-1} (Riggs, 1952; Halnan, 1964; Fisher and Oddie, 1969a; Alexander et al., 1971, DeGroot et al., 1971; Underwood, 1977; Zvonova, 1989). There is a decline of thyroid hormone secretion with increasing adult age, at least after the fifth or sixth decade (Gregerman et al., 1962; Fisher et al., 1965; Oddie et al., 1965; Herrmann et al., 1981; Mariotti, 1995; Sawin, 2005). The secretion rate appears to be about one-third lower on average in women than in men although there is some overlap is measurements for women and men (Ingbar and Freinkel, 1955; Fisher et al., 1965; Oddie et al., 1965). The following reference values of S for workers are based on collected data on thyroidal secretion of iodine as T_4 for ages 18-65 y and the assumption that T_4 represents 90% of total secretion of hormonal iodine: 52 μg d^{-1} for females, 76 μg d^{-1} for males, and 64 μg d^{-1} as a gender-averaged value.

(214) Fractional transfer of iodine from thyroid stores to blood per unit time depends on the size of current stores, the rate of secretion of thyroid hormones, and the extent of leakage of iodide from MIT and DIT deiodinated in follicular cells. For example, assuming first-order kinetics and negligible leakage of iodide to blood, thyroidal stores of 5 mg and a secretion rate of hormonal iodine of 64 μg d^{-1} correspond to a half-time of about 54 d; stores of 10 mg and secretion of 76 mg correspond to a half-time of about 91 d; and stores of 15 mg and a secretion rate of 80 μg d^{-1} correspond to a half-time of about 130 d. Wellman et al. (1970) estimated a mean half-time of about 68 d based on data collected from several studies. In an extensive review of the literature Dunning and Schwartz (1981) determined a range of 21-372 d and a mean of 85 d for adults. Long-term measurements on five workers acutely exposed to ^{125}I vapor indicated an average biological half-time of about 130 d (Bordell et al, 1972). A biological half-time of 90 d is adopted in this report as a reference value for adults.

Behavior of extrathyroidal T_4 and T_3

(215) Upon secretion by the thyroid into blood, T_4 and T_3 are rapidly and almost completely bound to plasma proteins. Little if any enters the RBC. As a result of protein binding, clearance of organic iodine from the circulation is slower than removal of the iodide ion from the circulation. Reported concentrations of protein-bound iodine in blood plasma of euthyroid subjects generally are in the range 3-8 μg / 100 ml and cluster about 5-6 μg / 100 ml (Tucker and Keys, 1951; Oppenheimer et al., 1967; Nicoloff and Dowling, 1968; Pittman et al., 1971; Acland, 1971; Nicoloff et al., 1972).

(216) A number of investigators have studied the kinetics of radio-labeled T_4 after intravenous injection into human subjects (Riggs, 1952; Sterling et al., 1954; Ingbar and Freinkel, 1955; Sterling, 1958; Lennon et al., 1961; Gregerman et al., 1962; Cavalieri and Searle, 1966; Oppenheimer et al., 1967; Nicoloff and Dowling, 1968; Wartofsky et al., 1972; Chopra, 1976; Hays and McGuire, 1980). The removal half-time from blood plasma typically increases from about 1 h at 20-60 min after injection to about 1 wk at equilibrium. Early

disappearance from plasma may represent mainly distribution throughout the extracellular fluids plus uptake by hepatocytes. The slower decline at later times may represent uptake by cells and binding to intracellular proteins throughout the body, reduction to inorganic iodide due to use of the hormones by cells, and biliary secretion followed by faecal excretion of part of the organic iodine entering the liver. External measurements together with liver biopsy data indicate that the liver accumulates roughly 35% (22-52%) of injected T_4 during the first 3-4 hours after administration and contains roughly 25% (14-40%) of extrathyroidal T_4 at equilibrium (Cavalieri and Searle, 1966; Oppenheimer et al., 1967; Nicoloff and Dowling, 1968, Hays and McGuire, 1980).

(217) The kinetics of labeled T_3 has been difficult to determine with much precision, in large part due to interference of iodoproteins generated by metabolism of the injected trace material (Nicoloff et al., 1972; Hays and McGuire, 1980). Human studies indicate high initial uptake of labeled T_3 by the liver but a shorter retention time than T_4 in the liver (Cavalieri et al., 1970). The liver content at equilibrium has been estimated as 5-21% of the total extrathyroidal T_3 pool (Cavalieri et al., 1970; Hays, 1985).

(218) A portion of T_4 or T_3 entering the liver is secreted into the small intestine in bile (Greenspan, 2004). The secreted form is poorly absorbed to blood and is largely excreted in faeces (Hays, 1985). This accounts for about one-fifth of the loss of organic iodine from extrathyroidal tissues, and reduction to iodide and return to the blood iodide pool accounts for the rest (Berson and Yalow, 1954; Ingbar and Freinkel, 1955; Hiss and Dowling, 1962; Choufoer et al., 1963; Anbar et al., 1965; Hays and Solomon, 1969; Pittman et al., 1971; Chopra, 1976). Endogenous faecal excretion of organic iodine can become a major source of loss of iodine during periods of low intake of iodine (Choufoer et al., 1963; Busnardo and Casson, 1965; Kirchgessner et al., 1999).

(219) Animal studies indicate that the concentration of organic iodine in the kidneys is at least as high as that in the liver. For example, in rats receiving daily injections of ^{125}I over a three-week period, the concentration of labeled T_4 in kidneys was similar to that in the liver, about 7 times that in muscle, and more than twice that in heart (Winder and Heninger, 1971). The concentration of labeled T_3 in kidneys was nearly twice that in the liver, 8-9 times that in muscle, and 4 times that in heart.

(220) Most estimates of the mass of extrathyroidal organic iodine at equilibrium are in the range 500-1000 μg. Most estimates of the biological half-life of T_4 in normal subjects are in the range 5-9 d (Sterling et al., 1954; Ingbar and Freinkel, 1955; Gregerman et al., 1962; Anbar et al., 1965; Oppenheimer et al., 1967; Nicoloff and Dowling, 1968; Wartofsky et al., 1972; Chopra, 1976; Hays and McGuire, 1980; ICRP, 1987). The half-life of T_3 is about 1 d (Pittman et al., 1971; Nicoloff et al., 1972; Inada et al., 1975; Chopra, 1976; Bianchi et al., 1978; Hays and McGuire, 1980; BEST, 2005) and that of reverse T_3 (rT_3) is a few hours (Chopra, 1976). Extrathyroidal conversion of T_4 to T_3 or rT_3 results, in effect, in an extension of the half-life of T_4. Measurements on 73 euthyroid males of ages 18-91 y indicate that the rate of T_4 production as well as its turnover rate, representing the combined rate of deiodination and faecal excretion, decrease with age starting some time before age 50 y (Gregerman et al., 1962). The half-life of labeled T_4 was estimated as 6.6 d in young adult males and 8-9 d after the fifth decade of life (Gregerman et al., 1962). In 165 healthy subjects in the age range 18-86 y, measured rates of deiodination of T_4 were similar in male and female subjects in the same age groups (Anbar et al., 1965). The half-time of deiodination of T_4 increased with age from about 8 d in the third decade of life to about 13 in the sixth decade (Anbar et al., 1965).

(221) Nicoloff and Dowling (1968) evaluated the extrathyroidal distribution of ^{131}I-labeled

T_4 in a group of 13 normal subjects. They interpreted external measurements in terms of a four-compartment model representing blood plasma, extracellular fluid, and hepatic and extrahepatic cellular fluid spaces. Their results indicate that the liver cleared T_4 considerably faster than extrahepatic tissues and contained about 14% of extrathyroidal T_4 at equilibrium (Nicoloff and Dowling, 1968). Results of human studies by Oppenheimer et al. (1967) interpreted in terms of a two-compartment model suggest greater accumulation of T_4 in the liver.

(222) In rats receiving daily injections of ^{125}I over a three-week period, the concentration of labeled T_4 in kidneys was similar to that in the liver, about 7 times that in muscle, and more than twice that in heart (Winder and Heninger, 1971). The concentration of labeled T_3 in kidneys was nearly twice that in the liver, 8-9 times that in muscle, and 4 times that in heart.

5.2.3.2. Biokinetic model for systemic iodine

Previous models

(223) A number of physiological systems models have been developed to describe quantitative aspects of the metabolism of iodine as an essential element in humans (Brownell, 1951; Riggs, 1952; Oddie et al., 1955; Hays and Wegner, 1965; Berman et al., 1968; Nicoloff and Dowling, 1968; DeGroot et al., 1971; Alexander et al., 1971; McGuire and Hays, 1981; Bazin et al., 1981; Degon et al., 2008). A three-compartment biokinetic model of iodine developed by Riggs (1952) for applications in physiological and clinical studies has been used by the ICRP for many years as the basis of its biokinetic models for occupational or environmental intake of radioiodine. The ICRP model with parameter values applied to workers in recent reports (ICRP, 1994, 1997) is shown in Figure 5-1. The compartments and paths of transfer represent absorption of dietary iodine to blood as inorganic iodide; competition between thyroidal and renal clearance for circulating inorganic iodide; production, storage, and secretion of hormonal iodine by the thyroid; deiodination of most of the secreted hormonal iodine and recycling of inorganic iodide; and loss of the remainder of secreted hormonal iodine in faeces.

(224) Variations of the Riggs model and some more detailed iodine models been developed for specific applications in radiation protection including: age-specific dosimetry of internally deposited radioiodine for application to environmental exposures (Stather and Greenhalgh, 1983; Johnson, 1987; ICRP, 1989); estimation of doses to patients from medical applications of radioiodine (MIRD, 1975; Robertson and Gorman, 1976; McGuire and Hays, 1981; Hays, 1985; ICRP, 1987; Johannsson et al., 2003); dose to the embryo/fetus or nursing infant from intake of radioiodine by the mother (Berkovski, 1999a,b, 2002; ICRP, 2002b); and reduction of radioiodine dose by administration of potassium iodide (Adams and Bonnell, 1962; Ramsden et al., 1967; Zanzonico and Becker, 2000). The model of Berkovski (1999a,b, 2002) for the pregnant or nursing mother and the model of Johannsson et al. (2003) designed for applications in nuclear medicine of provide relatively detailed descriptions of the early biokinetics of inorganic iodide to allow improved dosimetry of short-lived radioiodine.

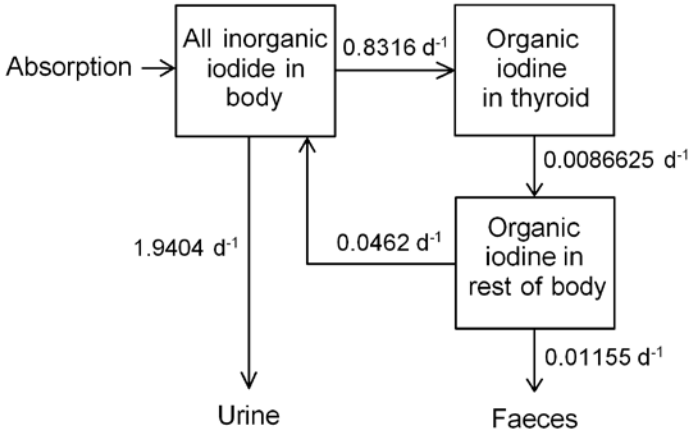

Figure 5-1. Biokinetic model for iodine introduced by Riggs (1952) and widely used in radiation protection, with the ICRP's current parameter values for workers (ICRP, 1994, 1997).

In recent ICRP documents the compartment "All inorganic iodide in body" is called "Blood", the compartment "Organic iodine in thyroid" is called "Thyroid", and the compartment "Organic iodine in rest of body" is called "Rest of body".

Model used in this report

(225) The model for systemic iodine used in this report is taken from a paper by Leggett (2010). The model describes the biokinetics of systemic iodine in terms of three subsystems: circulating (extrathyroidal) inorganic iodide; thyroidal iodine (trapping and organic binding of iodide, and synthesis, storage, and secretion of thyroid hormones); and extrathyroidal organic iodine.

(226) The structure of the model including connections with the alimentary tract is shown in Figure 5-2. Baseline transfer coefficients for a male or female worker are listed in Table 5-4.

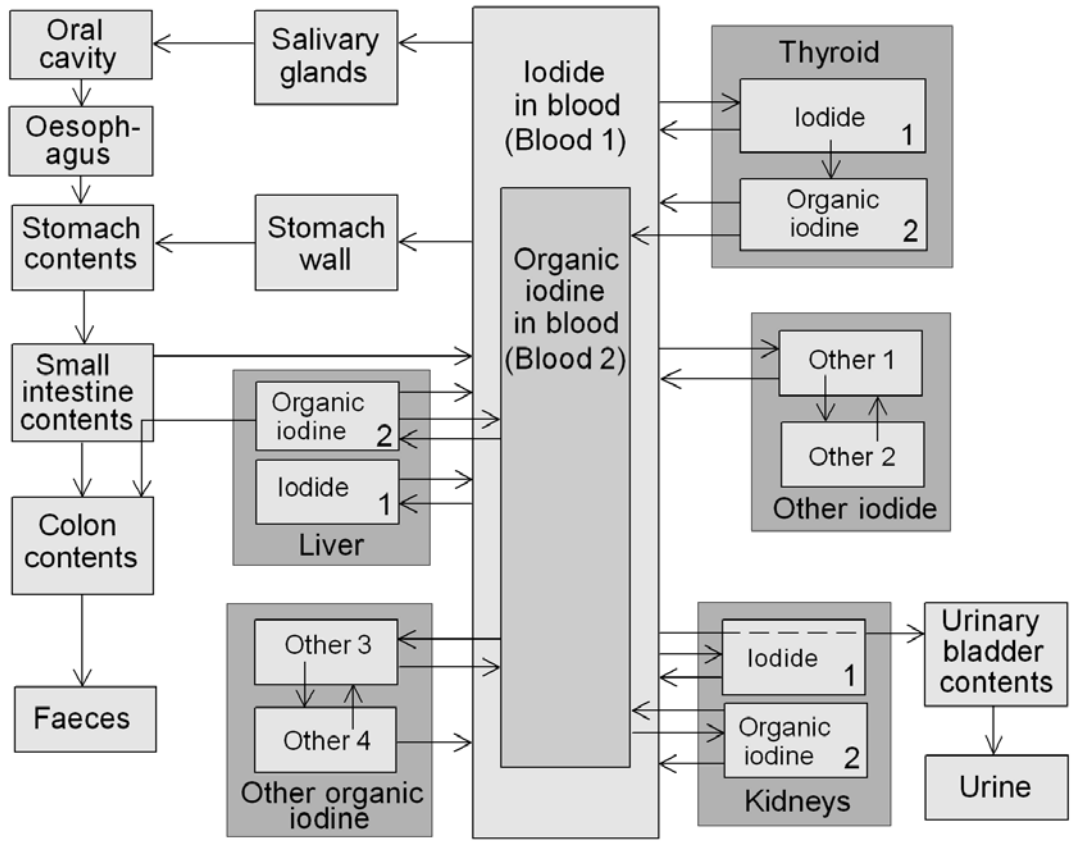

Figure 5-2. Structure of the biokinetic model for systemic iodine used in this report.

(227) The modeled behavior of extrathyroidal inorganic iodide is an extension of a model of Hays and Wegner (1965) based on bioassay and external measurements of ^{131}I in young adult males during the first 3 h after intravenous injection. The present model adds compartments representing inorganic iodide in kidneys and liver and adjusts flow rates to account for differences in model structure and the size of the blood iodide pool compared with the model of Hays and Wegner. The following compartments are used to describe the behavior of extrathryoidal inorganic iodide: a compartment representing iodide in blood plasma plus RBC, treated as a well-mixed pool (Blood 1); Salivary glands; Stomach wall; Liver 1, representing iodide in the liver; Kidneys 1, representing iodide in kidneys; Other 1, representing rapidly exchangeable iodide in extracellular fluids of extrathyroidal tissues other than kidneys and liver; Other 2, representing slowly exchangeable iodide in extrathyroidal tissues other than kidneys and liver; and a series of compartments representing different segments of the alimentary tract as represented in the ICRP's alimentary tract model (ICRP, 2006).

(228) The behavior of iodine in the thyroid is described in terms of two compartments representing inorganic iodide (Thyroid 1) and organic iodine (Thyroid 2). Thyroid 1 receives iodide from Blood 1, feeds iodide to Thyroid 2, and leaks some iodide back to Blood 1. Thyroid 2 converts iodide to organic iodine and transfers organic iodine into the blood organic iodine pool (Blood 2). An arrow representing leakage of activity from Thyroid 2 into Blood 1 is included for application of the model to subjects with unusually high dietary iodine, but the baseline transfer coefficient from Thyroid 2 to Blood 1 is set to zero.

(229) The modeled behavior of extrathyroidal organic iodine is an extension of a model of extrathyroidal T_4 kinetics developed by Nicoloff and Dowling (1968) from measurements of ^{131}I-labeled T_4 in 13 healthy human subjects (7 women and 6 men). The present model adds a compartment representing organic iodine in the kidneys and assumed to have the same rate of exchange with blood plasma per gram of tissue as does the liver. The following compartments are used to describe the behavior of extrathyroidal organic iodine: Blood 2, representing thyroid hormones bound to plasma proteins; Liver 2, representing organic iodine in liver; Kidneys 2, representing organic iodine in kidneys; Other 3, representing rapidly exchangeable organic iodine in extracellular fluids of extrathyroidal tissues other than kidneys and liver; and Other 4, representing slowly exchangeable organic iodine in extrathyroidal tissues other than kidneys and liver.

(230) The kidneys and liver are each divided into two compartments to address the different biokinetics of inorganic iodide and organic iodine. The kidneys are treated explicitly because they accumulate both inorganic iodide and hormonal iodine to a greater extent than most extrathyroidal tissues. The liver is treated explicitly mainly because it is an important repository for hormonal iodine. The iodide content of the liver is addressed for completeness.

(231) Iodine is assumed to be removed from the body only through urinary and faecal excretion. Iodide moves to Urine after transfer from Blood 1 into Urinary bladder contents. This represents the net result of glomerular filtration of iodide, reabsorption of much of the filtered iodide to blood, and transfer of the remainder to the urinary bladder contents followed by excretion in urine. Organic iodine is excreted in faeces after transfer from Liver 2 to Right colon, representing the net result of secretion into the small intestine and transfer of unabsorbed organic iodine to the right colon followed by excretion in faeces.

(232) Assuming that stable iodine intake and excretion are in balance, the transfer coefficient λ from Blood iodide to Thyroid iodide can be estimated in terms of the dietary stable iodine Y ($\mu g\ d^{-1}$) and the rate S of secretion of stable iodine by the thyroid ($\mu g\ d^{-1}$) (Leggett, 2010):

$$\lambda = 16.34 / [0.98(Y/S) - 0.2]\ d^{-1} \qquad \text{(Eq. 5-1)}$$

(233) Thus, λ depends on the ratio Y:S. For example, the ratio Y:S based on reference values for a male worker is Y: S = 190 $\mu g\ d^{-1}$: 76 $\mu g\ d^{-1}$ = 2.5. The same ratio is derived from reference values for a female worker: Y: S = 130 $\mu g\ d^{-1}$: 52 $\mu g\ d^{-1}$ = 2.5. The resulting transfer coefficient based on the above formula is 7.26 d^{-1}.

Table 5-4. Baseline parameter values for the biokinetic model for systemic iodine, applicable to a reference worker.

Pathway	Transfer coefficient (d^{-1})
Blood 1 to Thyroid 1	7.26[a]
Blood 1 to Urinary bladder contents	11.84
Blood 1 to Salivary gland	5.16
Blood 1 to Stomach wall	8.60
Blood 1 to Other 1	600
Blood 1 to Kidneys 1	25
Blood 1 to Liver 1	15
Salivary gland to Oral cavity	50
Stomach wall to Stomach contents	50
Thyroid 1 to Thyroid 2	95
Thyroid 1 to Blood 1	36
Thyroid 2 to Blood 2[b]	0.0077
Thyroid 2 to Blood 1	0[c]
Other 1 to Blood 1	330
Other 1 to Other 2	35
Other 2 to Other 1	56
Kidneys 1 to Blood 1	100
Liver 1 to Blood 1	100
Blood 2 to Other 3	15
Other 3 to Blood 2	21
Other 3 to Other 4	1.2
Other 4 to Other 3	0.62
Other 4 to Blood 1	0.14
Blood 2 to Kidneys 2	3.6
Kidneys 2 to Blood 2	21
Kidneys 2 to Blood 1	0.14
Blood 2 to Liver 2	21
Liver 2 to Blood 2	21
Liver 2 to Blood 1	0.14
Liver 2 to Right colon contents	0.08

[a] Depends on the ratio Y/S, where Y (μg d^{-1}) is dietary intake of stable iodine and S (μg d^{-1}) is the rate of secretion of hormonal stable iodine by the thyroid.

[b] For high intake of stable iodine the outflow from Thyroid 2 is split between Blood 2 and Blood 1 as described by Leggett (2010).

[c] Non-zero only for high intake of stable iodine (Leggett, 2010).

(234) The above formula for the transfer coefficient λ from Blood iodide to Thyroid iodide is applicable to any combination of Y and S that gives a transfer coefficient of at least 2.5 d^{-1}. For lower derived values, the transfer coefficient is set at 2.5 d^{-1}. This coefficient together with baseline values for other coefficients gives a 24-h thyroid content of about 12% of the ingested amount. This appears to be a reasonable average value for dietary iodine between 400 and 2000 μg d^{-1}, although considerably variability is seen between individual subjects.

(235) The reader is referred to the paper by Leggett (2010) for a more detailed description of the basis for the model structure and parameter values.

Model predictions

(236) In the following, predictions of time-dependent activities in tissues and fluids are based on the following transfer rates involving stomach and small intestine contents: 20.57 d^{-1} from stomach contents to small intestine contents as a reference value for adult males for total diet (ICRP, 2006) ; 6 d^{-1} from small intestine contents to colon contents (ICRP, 2006); and 594 d^{-1} from small intestine contents to blood, representing 99% absorption assuming a competing transfer coefficient of 6 d^{-1} from small intestine contents to colon contents.

(237) Figures 5-3 and 5-4 show observations (symbols) and model predictions (curves) of the distribution of radioiodine in the first few hours after intravenous injection into adult humans. The open circles in these figures represent means for nine healthy young adult males (Hays and Solomon, 1965); variability of measurements was reported as mean coefficients of variation, which were approximately 12% and 23% for blood plasma and thyroid, respectively. The close agreement in Figure 5-3 between predictions and the open circles is to be expected because the parameter values dominating model predictions in this case were based in part on these data. The triangles in Figure 5-3 represent median values determined from graphs of data for 5-13 individual euthyroid patients (Berson et al., 1952); individual measurements varied by less than 15% from the estimated medians. The plus signs in Figures 5-3 and 5-4 were determined from graphs of mean values for 9-10 euthyroid subjects (Alexander et al., 1971); variability of measurements was not reported. The model predictions shown in Figure 5-3 are for total blood iodide. The comparison with observed values assumes equilibration between blood plasma and RBC water.

(238) In Figure 5-4 the observations are compared with model-generated curves based on three different values of the transfer coefficient from blood to thyroid. This transfer coefficient is derived from Eq. 5-2 and depends on the ratio Y/S, where Y is dietary stable iodine (μg d^{-1}) and S is daily secretion of hormonal iodine by the thyroid (μg d^{-1}). Estimates of Y and S were not reported for the three study groups addressed in the figure. The group represented by plus signs (subjects of Alexander et al., 1971) was from a region with relatively low dietary iodine, suggesting a ratio Y/S less than the baseline value 2.5. The transfer coefficient based on the ratio Y/S = 2 yields reasonable agreement with thyroidal uptake data for that group as well as data for the healthy young adult male subjects of Hays and Solomon (1965). Short-term urinary data for the third group, represented by the single closed circle, indicate mean iodine intake on the order of 200 μg d^{-1}, suggesting a ratio Y/S greater than the baseline value 2.5. The transfer coefficient based on the ratio Y/S = 3 is consistent with mean 2-hour thyroidal uptake for that group.

(239) Model predictions of the percentage U of ingested radioiodine in the thyroid at 24 h after intake assuming no radioactive decay are compared in Figure 5-5 with observed values for subjects with different levels E of stable iodine in urine. Model predictions are based on the transfer coefficients in Table 5-1 except that the transfer coefficient from Blood 1 to Thyroid 1 was varied with E as described by Eq. 5-3 down to a minimum value of 2.5 d^{-1}. For this comparison the value S was set at the gender-averaged reference value of 64 μg d^{-1}.

(240) The model with baseline parameter values predicts that the thyroid contains about 29% of ingested or intravenously injected iodine at 24 h after intake, assuming no radioactive decay. The content of the thyroid is predicted to peak at about 30% of the ingested or injected amount during the period 24-48 h after intake.

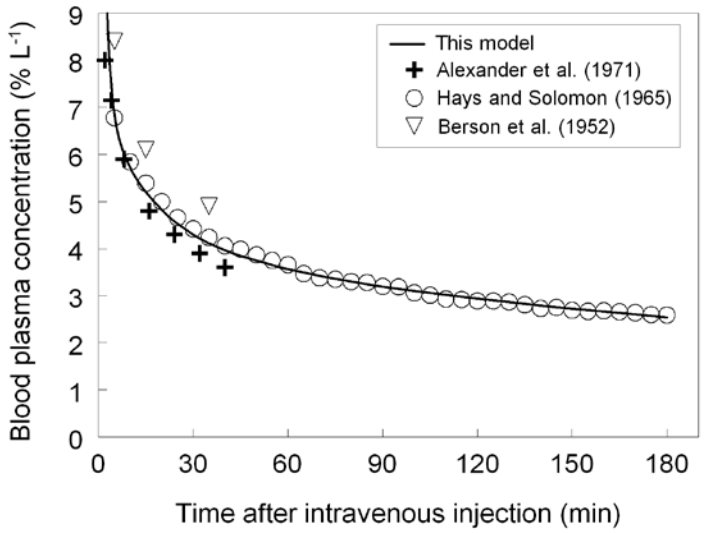

Figure 5-3. Model predictions of clearance of intravenously injected radioiodine from plasma compared with central values determined in three studies.

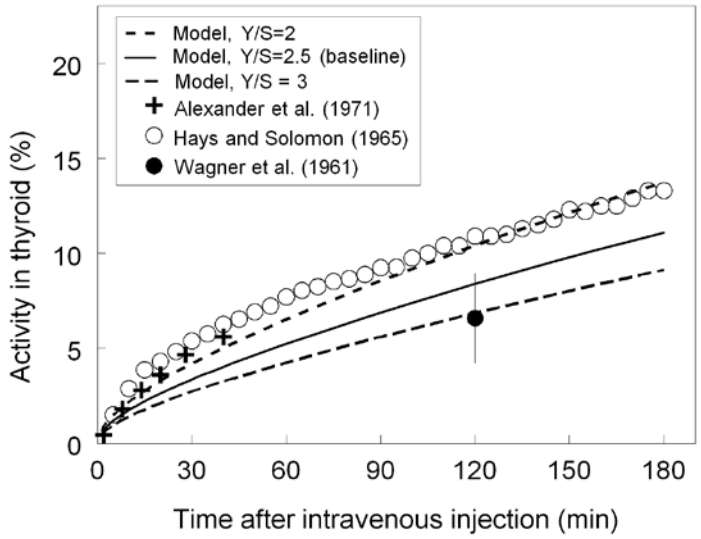

Figure 5-4. Model predictions of thyroidal uptake of intravenously injected ^{131}I compared with mean values of external measurements for three study groups.

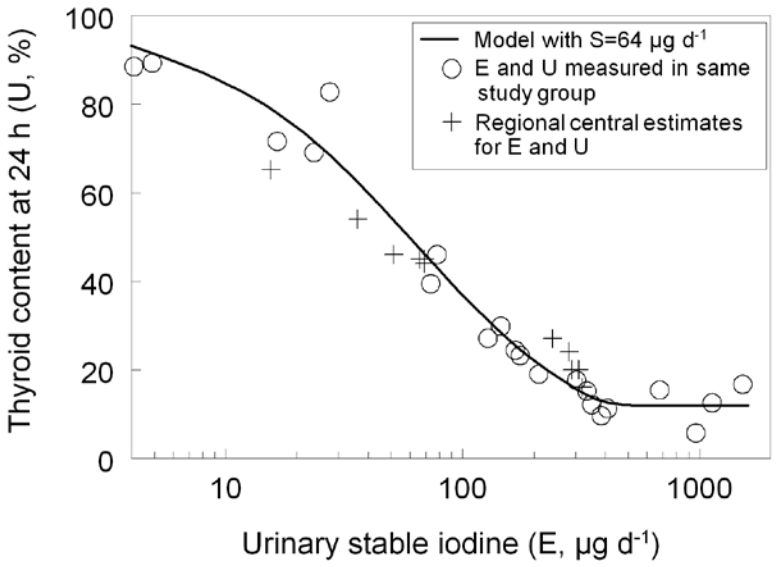

Figure 5-5. Model predictions and observations of 24-h uptake of radioiodine by thyroid (U) as a function of daily urinary excretion of stable iodine (E). After Leggett (2010).

(241) Model predictions of the equilibrium content of iodine in the thyroid, concentration of inorganic iodide and organic iodine in blood, and total extrathoracic contents of inorganic iodide and organic iodide are listed in Table 5-5 for different combinations of dietary iodine Y and thyroidal secretion rate S. The predicted values for each of these quantities based on reference values for dietary stable iodine Y and secretion rate of hormonal iodine S for women, total adult population, and men (see the first three columns of model predictions) are within the ranges of reported values for euthyroid subjects. For example, predictions of the mass of iodide in the thyroid at equilibrium are 6.00, 7.39, and 8.77 g, compared with typical values of 5-15 mg. Predictions of the concentration of organic iodine in blood plasma are 3.9-5.8 μg/dl, compared with commonly reported values of 3-8 μg/dl.

Table 5-5. Model predictions of mass or concentration of iodine in tissues and fluids at equilibrium

Quantity	Dietary iodine(μg d^{-1}) / Thyroidal secretion of organic iodine (μg d^{-1})			
	130 / 52[a]	160 / 64[a]	190 / 76[a]	300 / 100[b]
Iodine in thyroid (μg)	6750	8310	9870	13,000
Iodide in blood plasma (μg dl^{-1})	0.22	0.27	0.32	0.51
Total extrathyroidal inorganic iodide (μg)	58	71	84	135
Organic iodine in blood plasma (μg dl^{-1})	4.3	5.2	6.2	8.2
Total extrathyroidal organic iodine (μg)	520	640	760	1000

[a] Baseline transfer coefficient describing thyroidal uptake (7.26 d^{-1}) is applied because the ratio of daily intake of iodine Y to daily thyroidal secretion S is 2.5.
[b] Transfer coefficient from Blood iodide to Thyroid iodide is 5.96 d^{-1} based on Eq. 5-2.

5.2.3.3. Treatment of radioactive progeny

(242) Chain members addressed in the derivation of dose coefficients for iodine isotopes

are isotopes of iodine, tellurium, antimony, or xenon. Tellurium, antimony, or iodine atoms produced in systemic compartments are assumed to follow the characteristic models for these elements (i.e. the models applied in this report to these elements as parent radionuclides) from their time of production. The implementation of this assumption is not always straightforward. In some cases, the site of production of antimony or tellurium may not be clearly identifiable with a specific compartment in its characteristic biokinetic model due to differences in model structures for the different elements. In such cases a transfer rate from the site of production of the radionuclide to the central blood compartment in the radionuclide's characteristic model has been assigned as described below. After reaching its central blood compartment, the radionuclide is assumed to behave as described by its characteristic model.

(243) Tellurium atoms produced in the blood iodide compartment of the iodine model are assigned to the central blood compartment of the tellurium model. Tellurium atoms produced in the blood organic iodine compartment of the iodine model are assumed to transfer to the central blood compartment of the tellurium model at the rate 1000 d^{-1}. Tellurium atoms produced at soft-tissue sites in the iodine model are assumed to transfer to the central blood compartment of the tellurium model at the rate 0.0693 d^{-1} (half-time of 10 d), which is the rate of removal from all soft tissue compartments in the characteristic model for tellurium.

(244) Antimony produced in the blood iodide compartment of the characteristic model for iodine or the central blood compartment of the characteristic model for tellurium is assigned to the central blood compartment of the characteristic model for antimony. Antimony produced in another blood compartment of the iodine or tellurium model is assumed to transfer to the central blood compartment of the antimony model at the rate 1000 d^{-1}. Antimony produced at any soft-tissue site in the iodine or tellurium model is assumed to transfer to the central blood compartment of the antimony model at the rate 0.693 d^{-1} (half-time of 1 d), which is the highest rate of removal from all soft tissue compartments in the characteristic model for antimony. Antimony produced in a bone compartment of the tellurium model is assumed to behave as if entering that site as a parent radionuclide.

(245) A generic biokinetic model is applied in this report to xenon isotopes produced by decay of radionuclides in systemic pools. Xenon produced in bone is assumed to transfer to blood at the rate 100 d^{-1} if produced in bone surface and 0.36 d^{-1} if produced in bone volume. These rates are taken from the model for radon introduced in ICRP *Publication 67* (1993). Xenon produced in a soft-tissue compartment is assumed to transfer to blood with a half-time of 20 min. Xenon produced in the blood inorganic iodide compartment is assigned to the blood compartment of the xenon model. Xenon produced in the blood organic iodine compartment is assumed to transfer to blood in the xenon model at the rate 1000 d^{-1}. Xenon entering the blood compartment of the xenon model or produced in that compartment is assumed to be exhaled at the rate 1000 d^{-1}.

5.3. Individual monitoring

^{125}I

(246) Thyroid monitoring is generally used for the monitoring of ^{125}I. The urinary excretion rate decreases rapidly with time following intake and so thyroid monitoring is to be preferred until the actual time of intake is known.

(247) Ge detectors, in the thyroid counting configuration, should preferably be used because of the low energy photon emission from ^{125}I.

Isotope	Monitoring Technique	Method of Measurement	Typical Detection Limit	Achievable detection limit
^{125}I	Urine Bioassay	γ-ray spectrometry	1Bq/L	0.4Bq/L
^{125}I	Urine Bioassay	Liquid scintillation counting	1 Bq/L	
^{125}I	Thyroid Counting	γ-ray spectrometry	40 Bq	1 Bq

^{129}I

(248) Thyroid monitoring is generally used for the monitoring of ^{129}I. The urinary excretion rate decreases rapidly with time following intake and so thyroid monitoring is to be preferred unless the actual time of intake is known.

(249) Ge detectors, in the thyroid counting configuration, should preferably be used because of the low energy photon emission from ^{129}I.

Isotope	Monitoring Technique	Method of Measurement	Typical Detection Limit	Achievable detection limit
^{129}I	Urine Bioassay	γ-ray spectrometry	1 Bq/L	0.5 Bq/L
^{129}I	Thyroid Counting	γ-ray spectrometry	40 Bq	8 Bq

^{131}I

(250) In vivo monitoring of the thyroid is the preferential method of monitoring ^{131}I exposures. Iodine-131 can be readily detected using a NaI detector or a germanium detector system. Urinary monitoring is also a reliable method of monitoring for radioiodine. The urinary excretion rate decreases rapidly with time following intake and so thyroid monitoring is to be preferred unless the actual time of intake is known. Use of both measurements, where feasible, can increase confidence in estimated doses.

(251) Although not common in routine monitoring, Whole Body Counting is also feasible in special situations, as for example when thyroid is blocked.

Isotope	Monitoring Technique	Method of Measurement	Typical Detection Limit	Achievable detection limit
^{131}I	Urine Bioassay	γ-ray spectrometry	2 Bq/L	0.3 Bq/L
^{131}I	Thyroid Counting	γ-ray spectrometry, in vivo	25 Bq	1 Bq
^{131}I	Whole Body Counting	γ-ray spectrometry, in vivo	70 Bq	15 Bq

References

Acland, J. D. (1971). The interpretation of the serum protein-bound iodine: A review. J. Clin. Path. 24:187-218.

Adams, G. A.; Bonnell, J. A. (1962). Administration of stable iodide as a means of reducing thyroid irradiation resulting from inhalation of radioactive iodine. Health Phys. 7:127-149.

Alexander, W. D.; Shimmins, J.; Robertson, J. W. K.; Horton, P. W.; McLarty, D. G.; Harden, R. M. (1971). Radioisotope studies of thyroid function and thyroid hormone metabolism. In:

Dynamic studies with radioisotopes in medicine. Proceedings of a symposium. Rotterdam, 31 Aug – 4 Sept, 1970. IAEA, Vienna, 179-190.

Anbar, M.; Guttman, S.; Rodan, G.; Stein, J. A. (1965). The determination of the rate of deiodination of thyroxine in human subjects. J. Clin. Invest. 44:1986-1991.

Bair, W. J. (1961) Deposition, retention, translocation and excretion of radioactive particles. IN Inhaled Particles and Vapours (Edited by C.N. Davies) Pergamon Press, Oxford pp. 192-208.

Bazin, J. P.; Fragu, P.; Di Paola, R.; Di Paola, M.; Tubiana, M. (1981). Early kinetics of thyroid trap in normal human patients and in thyroid diseases. Eur. J. Nucl. Med. 6:317-326.

Bercz, J.P., Jones, L. L., Harrington, R. M., Bawa, R., Condie, L. 1986. Mechanistic aspects of ingested chlorine dioxide on thyroid function: impact of oxidants on iodide metabolism Environ.Health Perspect. 69, 249-254.

Berkovski, V. (1999a) Radioiodine biokinetics in the mother and fetus. Part 1. Pregnant woman. In: Radiation and Thyroid Cancer. World Scientific Publishing. Publication No. EUR 18552 EN. pp.319-325.

Berkovski, V. (1999b) Radioiodine biokinetics in the mother and fetus. Part 2. Fetus. In: Radiation and Thyroid Cancer. World Scientific Publishing. Publication No. EUR 18552 EN. pp.327-332.

Berkovski, V. (2002). New iodine models family for simulation of short-term biokinetics processes, pregnancy and lactation. Food and Nutrition Bulletin 23:87-94.

Berman, M.; Hoff, E.; Barandes, M.; Becker, D. V.; Sonnenberg, M.; Benua, R.; Koutras, D. A. (1968). Iodine kinetics in man – a model. J. Clin. Endocrinol. Metab. 28:1-14.

Berson, S. A.; Yalow, R. S. (1954). Quantitative aspects of iodine metabolism. The exchangeable organic iodine pool, and the rates of thyroidal secretion, peripheral degradation and fecal excretion of endogenously synthesized organically bound iodine. J. Clin. Invest. 33: 1533–1552.

Berson, S. A.; Yalow, R. S. (1955). The iodide trapping and binding functions of the thyroid. J. Clin. Invest. 34:186-204.

Berson, S. A.; Yalow, R. S.; Sorrentino, J.; Roswit, B. (1952). The determination of thyroidal and renal plasma ^{131}I clearance rates as a routine diagnostic test of thyroid dysfunction. J. Clin. Invest. 31:141–158.

BEST (Board on Environmental Studies and Toxicology) (2005). Health implications of perchlorate ingestion. Washington, DC: The National Academy Press.

Bianchi, R.; Zucchelli, G. C.; Giannessi, D. ; Pilo, A. ; Mariani, G. ; Carpi, A. ; Toni, M. G. (1978). Evaluation of triiodothyronine (T_3) kinetics in normal subjects, in hypothyroid, and hyperthyroid patients using specific antiserum for the determination of labeled T_3 in plasma. J. Clin. Endocrinol. Metab. 46:203-214.

Bianco, A. C.; Larsen, P. R. (2005). Intracellular pathways of iodothyronine metabolism. In: Werner and Ingbar's The Thyroid: A Fundamental and Clinical Text, 9th edition, Werner, S. C.; Ingbar, S. H.; Braverman, L. E.; Utiger, R. D., eds. New York: Lippincott Williams & Wilkins; pp. 109-134.

Bilek, R., Bednar, J.; Zamrazil, V. (2005). Spectrophotometric determination of urinary iodine by the Sandell-Kolthoff reaction subsequent to dry alkaline ashing. Results from the Czech Republic in the period 1994-2002. Clin. Chem. Lab. Med. 43:573-580.

Black ,A., Hounam, R.F., 1968. Penetration of iodine vapour through the nose and mouth and the clearance and metabolism of the deposited iodine. Ann. Occup.Hyg. 11, 209-225.

Bohe, M., Borgstrom, A., Genell, S., and Ohlsson, K. (1986) Metabolism of 131I-labelled human pancreatic cationic trypsin after intraduodenal administration. Digestion 34, 127-35.

Bordell, F. L.; Sayeg, J. A.; Wald, N. (1972). In vivo measured effective half-life of ^{125}I in human thyroids. Phys. Med. Biol. 17:365-373.

Bricker, N. S.; Hlad, C. J. (1955). Observations on the mechanism of the renal clearance of ^{131}I. J. Clin. Invest. 34:1057-1072.

Brownell, G. L. (1951). Analysis of techniques for the determination of thyroid function with radioiodine. J. Clin. Endocrinol. 11:1095-1105.

Burman, K. D. (2006). Low iodine diets. In: L. Wartofsky and D. Van Nostrand, Thyroid Cancer, A comprehensive guide to clinical management, Second edition. Totowa, NJ: Human Press. pp. 677-681.

Busnardo, B.; Casson, F. (1965). Aspects of fecal iodine excretion in man. Acta. Isot. (Padova) 31:5-13.

Caldwell, K. L.; Jones, R.; Hollowell, J. G. (2005). Urinary iodine concentration: United States National Health and Nutrition Examination Survey 2001-2002. Thyroid 15:692-699.

Cavalieri, R. R.; Searle, G. L. (1966). The kinetics of distribution between plasma and liver of 131I-labeled L-thyroxine in man : Observations of subjects with normal and decreased serum thyroxine-binding globulin. J. Clin. Invest. 45: 939-949.

Cavalieri, R. R.; Steinberg, M. ; Searle, G. L. (1970). The distribution kinetics of triiodothyronine: Studies of euthyroid subjects with decreased plasma thyroxine-binding globulin and patients with Graves' disease. J. Clin. Invest. 49:1041-1050.

CDC (2008). U.S. Centers for Disease Control and Prevention: National report on biochemical indicators of diet and nutrition in the U.S. population 1999–2002. Available from: http://www.cdc.gov/nutritionreport/index.html.

Chopra, I. J. (1976). An assessment of daily production and significance of thyroidal secretion of 3, 3',5'-triiodothyronine (reverse T_3) in man. J. Clin. Invest. 58:32-40.

Choufoer, J. C.; van Rhijn, M.; Kassenaar, A. A.; Querido, A. (1963). Endemic goiter in Western New Guinea: Iodine metabolism in goitrous and nongoitrous subjects. J. Clin. Endocrinol. Metab. 23:1203-1218.

Cohn, B. N. E. (1932). Absorption of compound solution of iodine from the gastro-intestinal tract. Arch. Intern. Med. 49:950-956.

Coughtrey, P., Jackson, D. and Thorne, M. (1983) Radionuclide distribution and transport in terrestrial and aquatic ecosystems. Vol. 3. A.A. Balkema, Rotterdam. pp.341-346.

Dadachova, E.; Bouzahzah, B.; Zuckier, L. S.; Pestell, R. G. (2002). Rhenium-188 as an alternative to iodine-131 for treatment of breast tumors expressing the sodium/iodide symporter (NIS). Nucl. Med. Biol. 29:13-18.

Dawson, C. A., Skebba, S. C., Lineham, J. H. and Bronikowski, T. A. (1985) Influence of pulmonary embolism on absorption of inhaled iodide-125. J. Appl. Physiol. 58, 1061-1068.

Degon, M.; Chipkin, S.; Hollot, C. V.; Zoeller, T.; Chait, Y. (2008). A computational model of the human thyroid. Math Biosci. 212:22-53.

DeGroot, L. J.; Decostre, P.; Phair, R. (1971). A mathematical model of human iodine metabolism. J. Clin. Endocr. 32:757-765.

Delange, F. M.; Dunn, J. T. (2005). Iodine deficiency. In: Werner and Ingbar's The Thyroid: A Fundamental and Clinical Text, 9th edition, Werner, S. C.; Ingbar, S. H.; Braverman, L. E.; Utiger, R. D., eds. New York: Lippincott Williams & Wilkins; pp. 264-288.

Dunning, D. E.; Schwarz, G. (1981).Variability of human thyroid characteristics and estimates of dose from ingested ^{131}I. Health Phys. 40:661-675.

Ermans, A. M. (1993). Iodine kinetics in iodine deficiency. In: Delange, F.; Dunn, J. T.; Glinoer, D., eds. Iodine deficiency in Europe: A continuing concern. New York: Plenum; pp. 51-56.

Esposito, E. J. (1970). ^{131}I concentration in submaxillary glands and other tissues of rats. J. Dent. Res. 49:459.

FAO/WHO (2002). Chapter 12. Iodine. In: Human vitamin and mineral requirements. Report of a joint FAO/WHO expert consultation. Bangkok, Thialand. Food and Agriculture Organization of the United Nations.World Health Organization. Update of March 12, 2002. pp. 181-194.

Fisher, D. A.; Oddie, T. H. (1969a). Thyroidal radioiodine clearance and thyroid iodine accumulation: Contrast between random daily variation and population data. J. Clin. Endocrinol. Metab. 29:111-115.

Fisher, D. A.; Oddie, T. H. (1969b). Comparison of thyroidal iodine content and turnover in euthyroid subjects: Validity of estimation of thyroid iodine accumulation from short-term clearance studies. J. Clin. Endocrinol. Metab. 29:721-727.

Fisher, D. A.; Oddie, T. H.; Epperson, D. (1965). Effect of increased dietary iodide on thyroid accumulation. J. Clin. Endocrinol. Metab. 25:1580-1590.

Fisher, D. A.; Oddie, T. H.; Thompson, C. S. (1971). Thyroidal thyronine and non-thyronine iodine secretion in euthyroid subjects. J. Clin. Endocrinol. Metab. 33:647-652.

Greenspan, F. S. (2004). The thyroid gland. Chapter 7 in: Greenspan, F. S.; Gardner, D. G. Basic and clinical endocrinology, seventh edition. New York: McGraw-Hill.

Gregerman, R. I.; Gaffney, G. W.; Schock, N. W. (1962). Thyroxine turnover in euthyroid man with special reference to changes with age. J. Clin. Invest. 41:2065-2074.

Halnan, K. E. (1964). The metabolism of radioiodine and radiation dosage in man. Brit. J. Radiol. 37:101-114.

Handl, J.; Kuehn, W.; Hesch, R. D. (1984). Content and heterogeneity of distribution of iodine in human and bovine thyroid glands determined by neutron activation analyses. J. Endocrinol. Invest. 7:97-101.

Harden, R. M.; Alexander, W. D. (1968). The salivary iodide trap in man: Clinical applications. Proc. R. Soc. Med. 61:647–649.

Harden, R. M.; Alexander, W. D.; Shimmins, J.; Chisholm, D. (1969). A comparison between the gastric and salivary concentration of iodide, pertechnetate, and bromide in man. Gut 10:928-930.

Harrison, M. T. (1968). Iodine balance in man. Postgrad. Med. J. 44:69-71.

Hays, M. T. (1985). Radiation dosimetry of radioiodinated thyroid hormones. J. Nucl. Med. 25:1068-1074.

Hays, M. T. (2001). Estimation of total body iodine content in normal young men. Thyroid 7:671-675.

Hays, M. T.; McGuire, R. A. (1980). Distribution of subcutaneous thyroxine, triiodothyronine, and albumin in man : Comparison with intravenous administration using a kinetic mode. J. Clin. Endocrinol. Metab. 51:1112-1117.

Hays, M. T.; Solomon, D. H. (1965). Influence of the gastrointestinal iodide cycle on the early distribution of radioactive iodide in man. J. Clin. Invest. 44:117-127.

Hays, M. T.; Solomon, D. H. (1969). Effects of epinephrine on the peripheral metabolism of thyroxine. J. Clin. Invest. 48:1114-1123.

Hays, M. T.; Wegner, L. H. (1965). A mathematical and physiological model for early distribution of radioiodine in man. J. Appl. Physiol. 20:1319-1328.

Hellstern, P.; Keller, H. E.; Weinheimer, B.; Wesch, H. (1978). Thyroid iodine concentration and total thyroid iodine in normal subjects and in endemic goiter subjects. Clin. Endocrinol. 9:351-356.

Herrmann, J,; Heinen, E.; Kroll, H. J.; Rodorff, K. H.; Krueskemper, H. L. (1981) Thyroid function and thyroid hormone metabolism in elderly people. Klin. Wochenschr. 59:315-323.

Hiss, J. M.; Dowling, J. T. (1962). Thyroxine metabolism in untreated and treated pancreatic steatorrhea. J. Clin. Invest. 41:988-995.

ICRP (1979) International Commission on Radiological Protection. Limits on Intakes of Radionuclides for Workers. ICRP Publication 30, Pt.1. Pergamon Press, Oxford. Ann. ICRP 2, (3/4).

ICRP (1987). International Commission on Radiological Protection. Radiation dose to patients from radiopharmaceuticals. ICRP Publication 53. Oxford: Pergamon Press.

ICRP (1989) International Commission on Radiological Protection. Age-dependent Doses to Members of the Public from Intake of Radionuclides. Pt.1. ICRP Publication 56. Pergamon Press, Oxford. Ann. ICRP 20, (2).

ICRP, 1993. Age-dependent Doses to Members of the Public from Intake of Radionuclides: Part 2, Ingestion Dose Coefficients, ICRP Publication 67. Annals of the ICRP 23 (3/4).

ICRP (1994). International Commission on Radiological Protection. Dose coefficients for intakes of radionuclides by workers, ICRP Publication 68. Oxford: Pergamon Press.

ICRP (1997). International Commission on Radiological Protection. Individual monitoring for internal exposure of workers. Replacement of ICRP Publication 54. ICRP Publication 78. Oxford: Pergamon Press.

ICRP (2002a) Guide for the Practical Application of the ICRP Human Respiratory Tract Model. Supporting Guidance 3. *Annals of the ICRP*, **32**(1-2).

ICRP (2002b). International Commission on Radiological Protection. Basic anatomical and physiological data for use in radiological protection: Reference values. ICRP Publication 89. Oxford: Pergamon Press.

ICRP (2006). International Commission on Radiological Protection. Human alimentary tract model for radiological protection. ICRP Publication 100. Oxford: Pergamon Press.

Inada, M.; Kasagi, K.; Kurata, S.; Kazama, Y.; Takayama, H.; Torizuka, K.; Fukase, M.; Soma, T. (1975). Estimation of thyroxine and triiodothyronine distribution and of the conversion rate of thyroxine to triiodothyronine in man. J. Clin. Invest. 55:1337-1348.

Ingbar, S. H.; Freinkel, N. (1955). Simultaneous estimation of rates of thyroxine degradation and thyroid hormone synthesis. J. Clin. Invest. 34:808-819.

Iyengar, G. V.; Kawamura, H.; Dang, H. S.; Parr, R. M.; Wang, J.; Akhter, P.; Cho, S. Y.; Natera, E.; Miah, F. K.; Dojosubroto, J.; Nguyen, M. S. (2004). Dietary intakes of seven elements of importance in radiological protection by Asian population: Comparison with ICRP data. Health Phys. 86:557–564.

Johansson, L.; Leide-Svegborn, S.; Mattsson, S.; Nosslin, B. (2003). Biokinetics of Iodide in Man: Refinement of Current ICRP Dosimetry Models. Cancer Biotherapy and Radiopharmaceuticals 18:445-450.

Johnson, J. R. (1987). A review of age dependent radioiodine dosimetry. In: Gerber, G. B.; Metivier, H.; Smith, H., eds. Age-related factors in radionuclide metabolism and dosimetry. Dordrecht: Martinus Nijhoff Publishers; pp. 249-260.

Keating, F. R., Jr.; Albert, A. (1949). The metabolism of iodine in man as disclosed with the use of radioiodine. Recent Progr. Hormone Research 4:429-481.

Kirchgessner, M.; He, J.; Windisch, W. (1999). Homeostatic adjustments of iodine metabolism and tissue iodine to widely varying iodine supply in ^{125}I labeled rats. J. Anim. Physiol. Anim. Nutr. 82:238-250.

Kolbert, K. S.; Pentlow, K. S.; Pearson, J. R.; Sheikh, A.; Finn, R. D.; Humm, J. L.; Larson, S. M. (2007). Prediction of absorbed dose to normal organs in thyroid cancer patients treated with ^{131}I by use of ^{124}I PET and 3-dimensional internal dosimetry. Software. J. Nucl. Med. 48:143–149.

Kopp, P. (2005). Thyroid hormone synthesis. In: Werner and Ingbar's The Thyroid: A Fundamental and Clinical Text, 9th edition, Werner, S. C.; Ingbar, S. H.; Braverman, L. E.; Utiger, R. D., eds. New York: Lippincott Williams & Wilkins; pp. 52-76.

Korolev, G. K. (1969). Distribution of iodine-132 and tellurium-132 in the body of rats under intravenous administration. In: Moskalev, Yu. I., ed. Radioactive isotopes and the body. Izdatel'stvo Meditsina. AEC-tr-7195; pp. 175-185.

Koutras, D. A.; Alexander, W. D.; Harden, R. M.; Wayne, E. (1964). Effect of small iodine supplements on thyroid function in normal individuals. J. Clin. Endocrinol. Metab. 24:857-862.

Lake-Bakaar, G., Rubio, C. E., McKavanagh, S., Potter, B. J., and Summerfield, J. A. (1980) Metabolism of 125I-labelled trypsin in man: evidence of recirculation. Gut 21, 580-6.

Leggett, R. W. (2010). A physiological systems model for iodine for use in radiation protection. Radiation Research 174: 496-516.

Lennon, E. J.; Engbring, N. H.; Engstrom, W. W. (1961). Studies of the rate of disappearance of labeled thyroxine from the intravascular compartment. Clin. Invest. 40:996-1005.

Mariotti, S.; Franceschi, C.; Cossarizza, A.; Pinchera, A. (1995). The aging thyroid. Endocrine Reviews 16:686-715.

McClellan, R. O. and Rupprecht, F. C. (Editors) (1968) Radioiodine metabolism in the beagle dog - The importance of age and mode of 131I exposure. Fission Product Inhalation Program Annual Report 1967-1968, LF-39, pp. 122-127. Lovelace Foundation for Medical Education and Research, Albuquerque, New Mexico. Available from National Technical Information Service, Springfield, Virginia.

McGuire, R. A.; Hays, M. T. (1981). A kinetic model of human thyroid hormones and their conversion products. J. Clin. Endocrinol. Metab. 53:852-862.

Milakovic, M.; Berg, G.; Nystro, E.; Lindstedt, G.; Gebre-Medhin, M. (2004). Urinary iodine and thyroid volume in a Swedish population. J. Internal Med. 255:610–614.

MIRD (1975). MIRD dose estimate report no. 5. Summary of current radiation dose estimates to humans from ^{123}I, ^{124}I, ^{125}I, ^{126}I, ^{130}I, ^{131}I, and ^{132}I as sodium iodide. J. Nucl. Med. 16:857-860.

Mirell, S. G., Blahd, W. H. (1989). Biological retention of fission products from the Chernobyl plume. Health Phys. 57 (4), 649-52.

Mithen, R. (2007) Effect of genotype on micronutrient absorption and metabolism: a review of iron, copper, iodine and selenium, and folates. Int J Vitam Nutr Res 77, 205-16.

Morgan, A., Morgan D. J. and Black, A. (1968a) A study of the deposition translocation and excretion of radioiodine inhaled as iodine vapour. Health Phys., 15, 313-322.

Morgan, A., Morgan, D. J. and Arkell, G. M. (1967b) A study of the retention and subsequent metabolism of inhaled methyl iodide. In: Inhaled Particles and Vapours II (C. N. Davies, Ed.) Pergamon Press, Oxford pp. 309-321.

Morgan, A., Morgan, D. J., Evans, J. C. and Lister, B. A. J. (1967a) Studies on the retention and metabolism of inhaled methyl iodide - II. Metabolism of methyl iodide. Health Phys. 13, 1067-1074.

Morgan, D. J. and Morgan, A. (1967) Studies on the retention and metabolism of inhaled methyl iodide - I. Retention of inhaled methyl iodide. Health Phys. 13, 1055-1065.

Morgan, D. J., Black, A., Mitchell, G. (1968b) Retention of inhaled ethyl iodide labeled with iodine-132. Nature, 218 (5147), 1177-1178.

Morrow, P. E., Gibb, F. R., Davies, H. and Fisher, M. (1968) Dust removal from the lung parenchyma: an investigation of clearance stimulants. Toxicol. Appl. Pharmacol. 12, 372-396.

Moskalev, Yu. I.; Yegorova, G. M. (1972). Distribution of iodine-131 in the rat organism following separate and combined exposure to this isotope and cobalt-60 gamma rays. In: Moskalev, Yu. I.; Kalistratova, V. S., eds. Biological effects of radiation from external and internal sources. Meditsina. AEC-tr-7457; pp. 116-122.

Myant, N. B.; Corbett, B. D.; Honour, A. J.; Pochin, E. E. (1950). Distribution of radioiodide in man. Clin. Sci. 9:405-419; 1950.

Nagataki, S.; Shizume, K.; Nakao, K. (1967). Thyroid function in chronic excess iodide ingestion: Comparison of thyroidal absolute iodine uptake and degradation of thyroxine in euthyroid Japanese subjects. J. Clin. Endocr. 27:638-647.

Nicoloff, J. T.; Dowling, J. T. (1968). Estimation of thyroxine distribution in man. J. Clin. Invest. 47:26-37.

Nicoloff, J. T.; Low, J. C.; Dussault, J. H.; Fisher, D. A. (1972). Simultaneous measurement of thyroxine and triiodothyronine peripheral turnover kinetics in man. J. Clin. Invest. 51:473-483.

Oddie, T. H.; Meschan, I.; Wortham, J. (1955). Thyroid function assay with radioiodine. I. Physical basis of study of early phase of iodine metabolism and iodine uptake. J. Clin. Invest. 34: 95–105.

Oddie, T. H.; Fisher, D. A.; Epperson, D. (1965). Effect of exogenous thyroxine on thyroid accumulation and secretion in euthyroid subjects. J. Clin Endocrinol. Metab. 25:1196-1206.

Oddie, T. H.; Fisher, D. A.; Long, J. M. (1964). Factors affecting the estimation of iodine entering the normal thyroid gland using short-term clearance studies. J. Clin Endocrinol. Metab. 24:924-933.

Oddie, T. H.; Fisher, D. A.; McConahey, W. M.; Thompson, C. S. (1970). Iodine intake in the United States: A reassessment. J. Clin Endocrinol. Metab. 30:659-665.

Oddie, T. H.; Meade, J. H.; Fisher, D. A. (1966). An analysis of published data on thyroxine turnover in human subjects. J. Clin. Endocrinol. Metab. 26:425-436.

O'Hare, N. J.; Murphy, D.; Malone, J. F. (1998). Thyroid dosimetry of adult European populations. Brit. J. Radiol. 71:535-543.

Ohtaki, S.; Moriya, S.; Suzuki, H.; Horiuchi, Y. (1967). Nonhormonal iodine escape from the normal and abnormal thyroid gland.

Oppenheimer, J. H.; Bernstein, G.; Hasen, J. (1967).Estimation of rapidly exchangeable cellular thyroxine from the plasma disappearance curves of simultaneously administered thyroxine-I-131 and albumin-I-125. J. Clin. Invest. 46:762-777.

Parr, R. M.; Crawley, H.; Abdulla, M; Iyengar, G. V.; Kumpulainen, J. (1992). Human dietary intakes of trace elements: A global literature survey mainly for the period 1970–91. Data listing and references. Report International Atomic Energy Agency (IAEA). Vienna: IAEA; IAEA-HAHRES-12.

Pattle, R. E. (1961) The retention of gases and particles in the human nose. IN Inhaled Particles and Vapours (Edited by Davies, C. N.) Pergamon Press, Oxford pp. 302-311.

Perrault, G., Thiéblemont, P., Pasquier, C. and Marblé, G. (1967) Cinétique du passage du radioiode soluble à travers les épithéliums respiratoires, après inhalation. Health Phys. 13, 707-718.

Pittman, C. S.; Chambers, J. B.; Read, V. H. (1971). The extrathyroidal conversion rate of thyroxine to triiodothyronine in normal man. J. Clin. Invest. 50:1187-1196.

Ramsden, D.; Passant, F. H.; Peabody, C. O.; Speight, R. G. (1967). Radioiodine uptakes in the thyroid. Studies of the blocking and subsequent recovery of the gland following the administration of stable iodine. Health Phys. 13:633-646.

Riggs, D.S. (1952) Quantitative aspects of iodine metabolism. Pharmacol. Rev. 4, 284-370.

Robertson, J. S.; Gorman, C. A. (1976). Gonadal radiation dose and its genetic significance in radioiodine therapy of hyperthyroidism. J. Nucl. Med. 17:826-835.

Robertson, J. W. K.; Shimmins, J.; Horton, P. W.; Lazarus, J. H.; Alexander, W. D. (1971). Determination of the rates of accumulation and loss of iodide and of protein binding of iodine in the human thyroid gland. In: Dynamic studies with radioisotopes in medicine. Proceedings of a symposium. Rotterdam, 31 Aug – 4 Sept, 1970. IAEA, Vienna, 199-210.

Ruegamer, W. R. (1953). The kinetics of ^{131}I metabolism in the dog and human. Arch. Biochem. Biophys. 47:119-136.

Sawin, C. (2005). Age-related changes in thyroid secretion. In: Werner and Ingbar's The Thyroid: A Fundamental and Clinical Text, 9th edition, Werner, S. C.; Ingbar, S. H.; Braverman, L. E.; Utiger, R. D., eds. New York: Lippincott Williams & Wilkins; pp. 214-219.

Shapiro, B.; Shulkin, B.; Gross, M.; Troncone, L. (1994). Thyroid imaging with radiopharmaceuticals. In: Troncone, L. Shapiro, B.; Satta, M.; Monaco, F. Thyroid Diseases. Basic Science, Pathology, Clinical and Laboratory Diagnoses. CRC Press: 274-292.

Small, M. D.; Bezman, A.; Longarni, A. E.; Fennell, A.; Zamcheck, N. (1961). Absorption of potassium iodide from gastro-intestinal tract. Proc. Soc. Exp. Biol. Med. 106:450-452.

Smyth, P. P. A.; Duntas, L. H. (2005). Iodine uptake and loss – Can frequent strenuous exercise induce iodine deficiency? Horm. Metab. Res. 37:555-558.

Stanbury, J. B.; Brownell, G. L.; Riggs, D. L.; Perinetti, H.; Itoiz, J.; del Castillo, E. B. Endemic goiter. The adaptation of man to iodine deficiency. Cambridge, MA. Harvard University Press. 1954.

Stather, J.W.; Greenhalgh, J.R. (1983). The metabolism of iodine in children and adults. National Radiological Protection Board report NRPB-R140. Chilton, Didcot, June 1983.

Sterling, K. (1958). Radiothyroxine turnover studies in thyroid disease after therapy. J. Clin. Invest. 37:1348-1356.

Sterling, K.; Lashof, J. C.; Man, E. B. (1954). Disappearance from serum of I-131-labeled L-thyroxine and L-triiodothyronine in euthyroid subjects. J Clin Invest. 33:1031–1035.

Thiéblemont, P., Marblé, G., Perrault, G. and Pasquier, C. (1965a) Évaluation de la rétention respiratoire et de l'élimination du radioiode après contamination aérienne du singe. Int. J. Rad. Biol. **9**, 219-231.

Thiéblemont, P., Marblé, G., Perrault, G. and Pasquier, C. (1965b) Charge thyroïdienne en radioiode après contamination respiratoire du singe Macaccus rhesus. Int. J. Rad. Biol. **9**, 233-240.

Thomas, R. L., Scott, J. K. and Chiffelle, T. L. (1970) Metabolism and toxicity of inhaled and injected 131I in the rat. Amer. Ind. Hyg. Assn. J. **31**, 213-220.

Tucker, R. G.; Keys, A. (1951). Concentration of serum protein-bound iodine in normal men. J. Clin. Invest. 30:869-873.

Ulmer, D. D.; Perkins, L. B.; Kereiakes, J. G. (1959). Alterations in iodine-131 distribution in the rat after whole-body x-irradiation. Radiat. Res. 11:810-819.

Underwood J. (1971). Iodine. In: Trace Elements in Human and Animal Nutrition. Academic Press, New York.

Underwood, E.J. (1977). Iodine. In: Trace elements in human and animal nutrition, 4th edition, Academic Press, New York, Chapter 11.

Utiger, R. D. (2001). Thyroid Diseases. In: Endocrinology and Metabolism, 4th edition, Felig, P.; Frohman, L. A., eds. New York: McGraw-Hill; pp. 259-348.

Vadstrup S. (1993). Comparative aspects of iodine conservation in mammals. Comp. Biochem. Physiol. 106A:15-17.

Wartofsky, L.; Martin, D.; Earll, J. M. (1972). Alterations in thyroid iodine release and the peripheral metabolism of thyroxine during acute falciparum malaria in man. J. Clin. Invest. 51:2215-2232.

Wayne, E. J.; Koutras, D. A.; Alexander, W. D. (1964). Clinical aspects of iodine metabolism. Philadelphia, PA: F. A. Davis Co.

Wellman, H. N.; Kereiakes, J. G.; Branson, B. M. (1970). Total- and partial-body counting of children for radiopharmaceutical dosimetry data. In: Cloutier, R. J.; Edwards, C. L.; and Snyder, W. S., eds., Medical Radionuclides: Radiation Dose and Effects. U.S. Atomic Energy Commission, Oak Ridge, TN; pp. 133-156.

WHO (1989). Iodine. In: Toxicological evaluation of certain food additives and contaminants. WHO Food Additives Series, No. 24. World Health Organization. Cambridge, UK: Cambridge University Press. No. 661 on INCHEM. Available online at http://www.inchem.org/documents/jecfa/jecmono/v024je11.htm.

WHO (2001). Assessment of the iodine deficiency disorders and monitoring their elimination. Second edition. Joint publication of International Council for Control of Iodine Deficiency Disorders, United Nations Children's Fund, and World Health Organization (WHO). WHO/NHD/01.1. Geneva: World Health Organization.

WHO (2004). Iodine status worldwide. WHO global database on iodine deficiency. de Benoist, B.; Andersson, M.; Egli, I.; Takkouche, B.; Allen, H., eds. Geneva: Department of Nutrition for Health and Development, World Health Organization.

Willard, D.H. and Bair, W.J. (1961) Behaviour of ^{131}I following its inhalation as a vapour and as a particle. Acta Radiol. **55**, 486-496.

Winder, W. W.; Heninger, R. W. (1971). Effect of exercise on tissue levels of thyroid hormones in the rat. Am. J. Physiol. 221:1139-1143.

Zanzonico, P. B.; Becker, D. V. (2000) Effects of time of administration and dietary iodine levels on potassium iodide (KI) blockade of thyroid irradiation by ^{131}I from radioactive fallout. Health Phys. 78:660-667.

Zuckier, L. S.; Dohan, O.; Li, Y.; Chang, C. J.; Carrasco, N. ; Dadachova, E. (2004). Kinetics of perrhenate uptake and comparative biodistribution of perrhenate, pertechnetate, and iodide by NaI symporter-expressing tissues in vivo. J. Nucl. Med. 45:500-507.

Zvonova, I. A. (1989). Dietary intake of stable I and some aspects of radioiodine dosimetry. Health Phys. 57:471-475.

6. CAESIUM (Z = 55)

6.1. Chemical Forms in the Workplace

(252) Caesium is an alkali metal only present in oxidation state I. It behaves similarly to potassium in the body. Caesium may be encountered in industry in a variety of chemical and physical forms, including soluble inorganic salts (chloride, nitrate) and less soluble sulphate. ^{134}Cs and ^{137}Cs are important fission products and could also be encountered in relatively insoluble fragments of irradiated fuel. ^{137}Cs is commonly used for medical applications as caesium chloride.

Table 6-1. Isotopes of caesium addressed in this report

Isotope	Physical half-life	Decay mode
Cs-125	45 m	EC, B+
Cs-127	6.25 h	EC, B+
Cs-129	32.06 h	EC, B+
Cs-130	29.21 m	EC, B+, B-
Cs-131	9.689 d	EC
Cs-132	6.479 d	EC, B+, B-
Cs-134[a]	2.064 y	B-, EC
Cs-134m	2.903 h	IT
Cs-135	2.3E+6 y	B-
Cs-135m	53 m	IT
Cs-136	13.167 d	B-
Cs-137[a]	30.167 y	B-
Cs-138	33.41 m	B-

[a] Data for these radionuclides are given in the printed copy of this report. Data for other radionuclides are given on accompanying electronic disk.

6.2. Routes of Intake

6.2.1. Inhalation

Absorption Types and parameter values

(253) There is some information on the behaviour of inhaled caesium in man following accidental intakes. Information is also available from experimental studies of caesium in ionic forms (chloride, nitrate), in irradiated fuel fragments and other contaminated dusts associated with nuclear facilities, and in fused aluminosilicate particles (FAP).

(254) Absorption parameter values and Types, and associated f_A values for particulate forms of caesium are given in Table 6-2.

Caesium chloride

(255) Animal experiments have shown that caesium chloride (CsCl) is rapidly and completely absorbed from the respiratory tract following inhalation. Lie (1964) and Thomas (1969) observed that in mice, rats, and guinea pigs killed less than 20 minutes after a 10-minute inhalation exposure to ^{137}CsCl, nearly all the activity had left the lungs, suggesting an absorption rate corresponding to a time of the order of 10 minutes, *i.e.* $s_r \sim 100$ d^{-1}. Stara

(1965) similarly observed that in guinea pigs killed 20 minutes after inhalation of ^{137}CsCl, there had been rapid clearance from the lungs, and by 24 hours the biokinetics of ^{137}Cs were indistinguishable from those following intraperitoneal injection. Morrow et al. (1968) measured a lung retention half time of 0.003 d (~4 minutes) following inhalation of ^{134}CsCl by dogs, giving f_r ~1 and s_r = 200 d^{-1}. Boecker (1969a) noted that following inhalation of ^{137}CsCl by dogs, the lung quickly became one of the tissues to exhibit a low concentration of ^{137}Cs. It was estimated by the Task group from the results of another study in which ^{137}CsCl was inhaled by dogs (Boecker, 1969b) that lung retention at 32 days was <1% of the initial lung deposit (ILD).

(256) Cuddihy and Ozog (1973) deposited ^{137}CsCl directly onto the nasal membranes of Syrian hamsters and followed the biokinetics of the ^{137}Cs for 4 hours. Analysis of the results here gave values of f_r ~1.0 and s_r ~6 d^{-1} ($t_{½}$ ~ 2 hours), slower than in the other studies, possibly because of the experimental techniques used, including the anaesthetic or slower clearance from the nasal passage than from the lungs. Similar observations were made for strontium and barium chlorides which were also administered by Cuddihy and Ozog (see Strontium and Barium Sections).

(257) Hölgye and Malý (2002) followed urinary excretion of ^{137}Cs for 370 days after presumed accidental inhalation of the chloride by a worker. Analysis here showed that the results can be well fit assuming Type F absorption, *i.e.* that absorption from the lungs is rapid compared to transfer from systemic tissues to urine.

(258) Based on the results of the experiments outlined above, specific absorption parameter values for caesium chloride were estimated here to be: f_r = 1 and s_r = 100 d^{-1} (consistent with assignment to default Type F). However, although specific parameter values for caesium chloride based on *in vivo* data are available, they are not adopted separately here. The data are (with those for caesium nitrate) used as the basis for the default rapid dissolution rate for caesium. Hence specific parameter values for caesium chloride would be the same as default Type F caesium parameter values, and therefore caesium chloride is assigned to Type F instead.

Caesium nitrate

(259) Lie (1964) obtained similar results following inhalation of caesium nitrate by rats as for caesium chloride, but few details were given. In rats killed immediately after a 10-minute inhalation exposure, nearly all the activity had left the lungs, suggesting an absorption rate corresponding to a time of the order of 10 minutes, *i.e.* s_r ~ 100 d^{-1}. In view of the few details given, these data are judged to be an insufficient basis to provide specific absorption parameter values and caesium nitrate is therefore assigned to Type F.

Caesium sulphate

(260) Miller (1964) followed distribution and retention of ^{137}Cs in two men following accidental intake (presumed to be inhalation) of caesium sulphate. The distribution along the body was unchanged between 9 and 285 days, implying that absorption from the lungs was complete before the first measurement on day 9, and indicating Type F behaviour. These data are judged to be an insufficient basis to provide specific absorption parameter values and caesium sulphate is therefore assigned to Type F.

Irradiated fuel fragments and other contaminated dusts associated with nuclear facilities.

(261) Studies have been conducted of caesium associated with irradiated fuel fragments, including particles released from the Chernobyl accident, and other materials, more or less

well defined, associated with various nuclear facilities. Such studies indicate that some of the caesium is rapidly absorbed (within days), but a fraction may be retained with the particle matrix and absorbed over a period of months or years. The results of most of these studies indicate Type M behaviour overall, but some indicate Type F and two, partial Type S behaviour.

Chernobyl

(262) Mirell and Blahd (1989) made whole-body measurements of activity on seven people from about two weeks to several months after exposure to the initial Chernobyl reactor accident plume in Kiev, Ukraine. Biological retention half-times were similar for different radionuclides (34 days for ^{137}Cs) and different from those expected for systemic retention, indicating that they were trapped in particles and metabolically inert, thus indicating Type M rather than Type F behaviour.

(263) Kutkov (1998, 2000) reported that about 920 Chernobyl nuclear power plant workers involved in emergency operations on 26-27 April 1986 were examined by means of a semiconductor whole body counter. For 15 of these, who were examined more than five times in the period 40–800 days after the accident, the effective half-time of ^{137}Cs retention in the body ranged from 230 to 590 days with a mean of 360 ± 30 days, much greater than expected for systemic ^{137}Cs (about 110 days). With other information on the characteristics of nuclear fuel particles dispersed in the accident, it was inferred that radionuclides such as ^{137}Cs were trapped in the uranium oxide matrix. Kutkov (1998) reported HRTM parameter values for Chernobyl nuclear fuel particles as: s_p = 4 d^{-1}, s_{pt} = 100 d^{-1}, s_t = 0.002 d^{-1} (and f_1 = 0.002), corresponding to f_r = 0.04, s_r = 104 d^{-1}, and s_s = 0.002 d^{-1}, giving assignment to Type M. However, these reports only summarise the results and little information was given on how the parameter values were derived.

(264) Cuddihy et al. (1989) measured the *in vitro* dissolution of samples of particles released from the Chernobyl accident for up to 60 days. For all radionuclides measured, including ^{137}Cs, 10% dissolved in a few hours, and the rest with a half-time of 160 days. Hence f_r = 0.1, s_r ~10 d^{-1}, and s_s = 0.004 d^{-1}, giving assignment to Type M.

(265) Kutkov and Komaritskaya (1996) measured the *in vitro* leaching (for 122 days) of ^{137}Cs from particles taken from the Chernobyl Shelter. Results indicated f_r ~ 0.3, s_r ~0.04 d^{-1}, and s_s = 0.002 d^{-1}, giving assignment to Type M.

(266) To simulate particles produced in a reactor accident such as that at Chernobyl, Al Rayyes et al. (1993) prepared UO_2 particles labelled with ^{134}Cs by condensation. In distilled water, about 95% dissolved in a few hours, indicating Type F behaviour. However for particles 'matured' in 10% O_2 + 90% CO_2, about 40% remained after 21 days, indicating Type M behaviour.

Other workplace exposures

(267) Hesp (1964) followed whole body retention of ^{137}Cs for 300 days after accidental inhalation by a worker, and also reported measurements in urine, and in the chest. Analysis here showed that the results can be reasonably well fit assuming about 50% Type F and 50% Type M absorption, i. e., f_r is about 0.5, but there is insufficient information to determine s_r and s_s (indicating assignment to Type M overall).

(268) The results of a human study in which *in vivo* measurements were made for over 2 years after accidental inhalation of irradiated uranium indicate Type F behaviour of the caesium present, although measurements of other radionuclides (^{95}Zr-Nb, ^{103}Ru, and ^{144}Ce) indicated Type M or S behaviour (Rundo, 1965).

(269) Raghavendran et al. (1978) followed whole body retention of ^{137}Cs in 12 radiation workers at the Bhaba Atomic Research Centre for between 72 and 456 days. Results were consistent with retention of systemic caesium, indicating Type F behaviour (assuming intake by inhalation).

(270) Froning et al. (2004) followed whole body retention of ^{137}Cs for 16 years after accidental inhalation of high temperature reactor fuel element ash by a worker. Measurements showed that the longest-lived component was concentrated in the thoracic region, suggesting long term lung retention of a relatively insoluble component. The authors found that data up to about 2000 days could be well represented by assuming 77% Type F and 23% Type S. However, subsequent clearance was slower than predicted for default Type S. Analysis here[2] confirmed this assessment, which can be represented by $f_r = 0.77$; $s_r = 100$ d^{-1} and $s_s = 10^{-4}$. Application here of the updated HRTM, which assumes longer retention in the Alveolar-Interstitial region than the original HRTM (see OIR Part 1, Section 3.2.2) gave a better fit to the measurements after 2000 days, but with a smaller 'insoluble' fraction retained, i.e. with a higher value of f_r (~0.9).

(271) Andrieu and Fatome (1979) studied the clearance of mixed fission and activation products in ~1 μm graphite particles following controlled inhalation by a volunteer; data over ~7 years imply partial Type S behaviour for the ^{137}Cs component.

(272) The biokinetics of ^{137}Cs were followed for 6 months after intratracheal instillation into rats of a suspension of residues from a reactor fuel cooling pond (Stradling et al., 1989). Lung retention at 30 days was 2% ILD, giving assignment to Type F. However, insufficient information was published to enable derivation of absorption parameter values.

(273) The biokinetics of ^{137}Cs were followed for 6 months after intratracheal instillation into rats of a complex radionuclide bearing dust from the ventilation grid of the reactor fuel hall of a nuclear power plant (Stradling et al., 1996, 1997). Absorption parameter values: f_r = 0.82; $s_r = 2.7$ d^{-1} and $s_s = 1.4\ 10^{-3}$ d^{-1} derived by ICRP (2002a, Section E4.4), are consistent with assignment to Type M.

(274) Kotrappa et al. (1977) measured *in vitro* the fractions of several radionuclides that dissolved rapidly (within 6 hours) from air samples taken at five working areas in a nuclear power plant. For $^{134+137}$Cs the fraction was between 98% (consistent with Type F) and 38% (indicating possibly Type M behaviour). Dua et al. (1987) measured the *in vitro* dissolution of particles on an air sample from a reactor spent fuel bay for up to 200 days. For all radionuclides measured, including ^{137}Cs, ~40% dissolved with a half-time of 1.2 days, and the rest with a half-time of 155 days. Hence $f_r = 0.4$, s_r ~0.6 d^{-1}, and $s_s = 0.004$ d^{-1}, giving assignment to Type M.

(275) Although specific absorption parameter values were derived from the results of one *in vivo* study, the results from others indicate that the biokinetics of caesium in the forms considered in this section are likely to vary markedly. Caesium associated with irradiated fuel fragments, and other unspecified contaminated dusts from nuclear facilities, is therefore assigned to Type M.

Fused aluminosilicate particles (FAP)

(276) FAP or “fused clay” particles have been extensively used as relatively insoluble particles in inhalation studies, both of biokinetics and of radiation effects. A natural clay mineral is labelled by ion exchange, and the labelled clay particles heated to about 1100˚C, to form aluminosilicate glass microspheres in which the label is incorporated. It has been shown

[2] Data kindly provided by Dr M. Schläger, Forschungszentrum Jülich.

in several animal studies (mouse, rat, guinea pig and dog) that when caesium is incorporated into FAP, a small fraction is rapidly absorbed from the lungs (f_r ~0.1). The rest is absorbed slowly, at rates of the order of 0.001 d^{-1} (Boecker et al., 1974; Snipes et al., 1983; Snipes and McClellan, 1986). In most cases the results give assignment to Type M, but for the largest particles (2.8 μm AMAD) used by Snipes et al. (1983) they give Type S. In view of the variability of the results, and because inhalation exposure to caesium-labelled FAP is so unlikely, specific parameter values for it are not used here, nor is it assigned to a default Type.

Rapid dissolution rate for caesium

(277) Studies with caesium chloride and nitrate outlined above, give values of s_r of about 100 d^{-1}, which is applied here to all Type F forms of caesium.

Extent of binding of caesium to the respiratory tract

(278) Evidence from the caesium chloride studies outlined above suggests that there is probably little binding of caesium. It is therefore assumed that for caesium the bound state can be neglected, i.e. $f_b = 0.0$.

Table 6-2. Absorption parameter values for inhaled and ingested caesium

Inhaled particulate materials		Absorption parameter values[a] f_r	s_r (d^{-1})	s_s (d^{-1})	Absorption from the alimentary tract, f_A
Default parameter values[b,c]					
Absorption Type	Assigned forms				
F	Caesium chloride, nitrate, sulphate	1	100	-	1
M	Irradiated fuel fragments; all unspecified forms[d]	0.2	3	0.005	0.2
S	—	0.01	3	$1x10^{-4}$	0.01
Ingested materials					
Caesium chloride, nitrate, sulphate; all unspecified compounds		–	–	–	1
Relatively insoluble forms (irradiated fuel fragments)		–	–	–	0.1

[a] It is assumed that for caesium the bound state can be neglected, i.e. $f_b = 0.0$. It is assumed that for caesium the bound state can be neglected, i.e. $f_b = 0.0$. The value of s_r for Type F forms of caesium (100 d^{-1}) is element-specific. The values for Types M and S (3 d^{-1}) are the general default values.

[b] Materials (e.g. caesium chloride) are generally listed here where there is sufficient information to assign to a default absorption Type, but not to give specific parameter values (see text).

[c] For inhaled material deposited in the respiratory tract and subsequent cleared by particle transport to the alimentary tract, the default f_A values for inhaled materials are applied: i.e. the product of f_r for the absorption Type (or specific value where given) and the f_A value for ingested soluble forms of caesium (1.0).

[d] Default Type M is recommended for use in the absence of specific information, i.e. if the form is unknown, or if the form is known but there is no information available on the absorption of that form from the respiratory tract.

6.2.2. Ingestion

(279) Human volunteer studies using ^{137}Cs in soluble inorganic form have shown virtually

complete absorption from the alimentary tract (Rosoff et al., 1963; Rundo et al., 1963; Naversten and Liden, 1964; LeRoy et al., 1966). Thus, for example, Rundo et al. (1963) measured an average fractional absorption of 0.99 for 10 normal subjects following the ingestion of ^{137}CsCl and Leroy et al. (1966) measured values from 0.87 to 0.9 on four healthy subjects.

(280) ^{134}Cs and ^{137}Cs incorporated into insoluble particles may be less available for absorption. LeRoy et al. (1966) reported values of 0.29-0.36 for ^{134}Cs contained in microspheres from leachable glass and ingested by three volunteers. These values were about 0.8 when ^{134}Cs was given as caesium silicate to five volunteers.

(281) McKay and Memmott (1991) have shown that absorption of Cs adsorbed onto inorganic sedimentary material was significantly lower than the unity. Experiment with animals showed that absorption of ^{137}Cs from irradiated reactor fuel particles (2 - 10 μm) in adult rats were less than 0.1 (Talbot et al, 1993).

(282) In *Publication 30* (ICRP, 1979), complete absorption from the alimentary tract was assumed for all chemical forms of Cs. In this report, an f_A of 1 is adopted for all forms of Cs, except in situations where it is considered that the material is insoluble (e.g. fuel particles) and a lower f_A value of 0.1 is appropriate.

6.2.3. Systemic Distribution, Retention and Excretion

6.2.3.1. Summary of database

(283) Caesium is a physiological analogue of the lighter alkali metals potassium and rubidium. Caesium has been shown to compete with these elements for both active and passive membrane transport across cell membranes but is generally transported less readily than potassium or rubidium by these processes (Hodgkin, 1947; Sjodin and Beauge, 1967; Edwards, 1982; Latorre and Miller, 1983; Cecchi et al., 1987). *In vitro* studies of the relative selectivity of potassium, caesium, and rubidium by membranes have revealed much about the structure and functions of ionic channels and carriers.

(284) Numerous studies of the biological behavior of caesium in man and laboratory animals have been published since the 1950s due to the importance of the fission-produced isotopes ^{137}Cs and ^{134}Cs as occupational and environment hazards. The retention time of caesium in the human body has been found to vary with age, gender, diet, muscle mass, pregnancy, and diseases that affect the behavior of potassium in the body. Studies on laboratory animals indicate that absorbed caesium initially is heterogeneously distributed in the body with highest concentration in the kidneys but gradually attains a more nearly uniform distribution (Stather, 1970; Moskalev, 1972). Autopsy studies on environmentally exposed humans indicate that caesium concentrations do not differ greatly for different tissues, but higher concentrations generally are found in skeletal muscle than in other measured tissues (Yamagata, 1962; Williams and Leggett, 1987). Measurements on persons briefly exposed to elevated levels of ^{137}Cs in accidents or controlled studies show that whole-body retention for periods up to 3-4 years usually can be represented by the sum of two exponential terms. The long-term component typically represents 85-95% of uptake in adults. The long-term half-time generally is in the range 45-150 days in adults although values on the order of 200 days have been reported (Rundo, 1964; Cryer and Baverstock, 1972; Lloyd et al., 1972, 1973; Leggett, 1986).

(285) Leggett et al. (1998) reviewed data on whole-body retention of caesium in healthy adults from 14 studies involving 2-239 subjects per study. Central estimates of the long-term

half-time in adult males were in the range 79-133 d with an overall mean of about 97 d. Inter-subject variability within a given study generally was small, with a typical coefficient of variation of about 20% and a typical geometric standard deviation of about 1.2. In eight of the 14 studies, retention half-times were measured in both men and women. There was some overlap in half-times for individual male and female subjects, but the mean half-time for females was 15-35% lower than that for males in each of the eight studies.

(286) The long-term half-time of cesium in the body usually is reduced during pregnancy to about two-thirds of the value when not pregnant (Lloyd et al., 1966; Zundel et al., 1969; Melo et al., 1997; Thornberg and Mattsson, 2000).

6.2.3.2. Biokinetic model for systemic caesium

(287) In the model for systemic caesium adopted in ICRP *Publication 30* (1979), caesium is assumed to be uniformly distributed in the body at all times after uptake to blood. Whole-body retention at time t (days) is represented as a sum of two exponential terms:

$$R(t) = a \exp(-0.693t/T_1) + (1 - a) \exp(-0.693t/T_2),$$

where T_1 and T_2 are biological half-times for short-term and long-term components of retention, respectively. Parameter values a = 0.1, T_1 = 2 d, and T_2 = 110 d are applied to the worker. This model is also applied in ICRP *Publication 68* (1994), but explicit excretion pathways are added: 80% of activity leaving the body is assumed to pass through the urinary bladder contents to urine and 20% is assumed to be secreted into the upper large intestine and subsequently excreted in faeces.

(288) The model for systemic caesium used in this report is adapted from a model proposed by Leggett et al. (2003) that is constructed around a dynamic blood flow model involving a number of different blood pools (Leggett and Williams, 1995; Leggett et al., 2006). The dynamic blood flow model is useful, for example, for predicting the blood circulation and tissue accumulation of ultra-short-lived isotopes of caesium or its physiological analogues (Leggett et al., 2006). For application to a caesium isotope with half-life of at least a few minutes, it suffices to treat blood plasma as a well-mixed central compartment. The latter form of the model is used in this report, with the following modifications:

1. In the original model the skeleton is divided into two compartments representing red marrow and all remaining skeletal tissues. In the present version of the model, skeletal caesium is divided into four specific pools that appear to contain nearly all of the skeletal content (Williams and Leggett, 1987): red marrow, cartilage, trabecular bone surface, and cortical bone surface.

2. A simplistic representation of the gastrointestinal (GI) tract used in the original model to describe exchange of caesium between systemic and GI pools is replaced here by the GI portion of the HATM.

(289) The structure of the model as applied in this report is shown in Figure 5-1. Baseline parameter values are listed in Table 6-3. Most of the parameter values were taken from Table 2 of Leggett et al. (2003), which provides baseline values for a reference adult male for the case of a well-mixed plasma pool. Modification or addition of some parameter values was

required due to the structural differences between the present and original versions of the model indicated above. The methods of derivation of the values in Table 6-3 are summarized below.

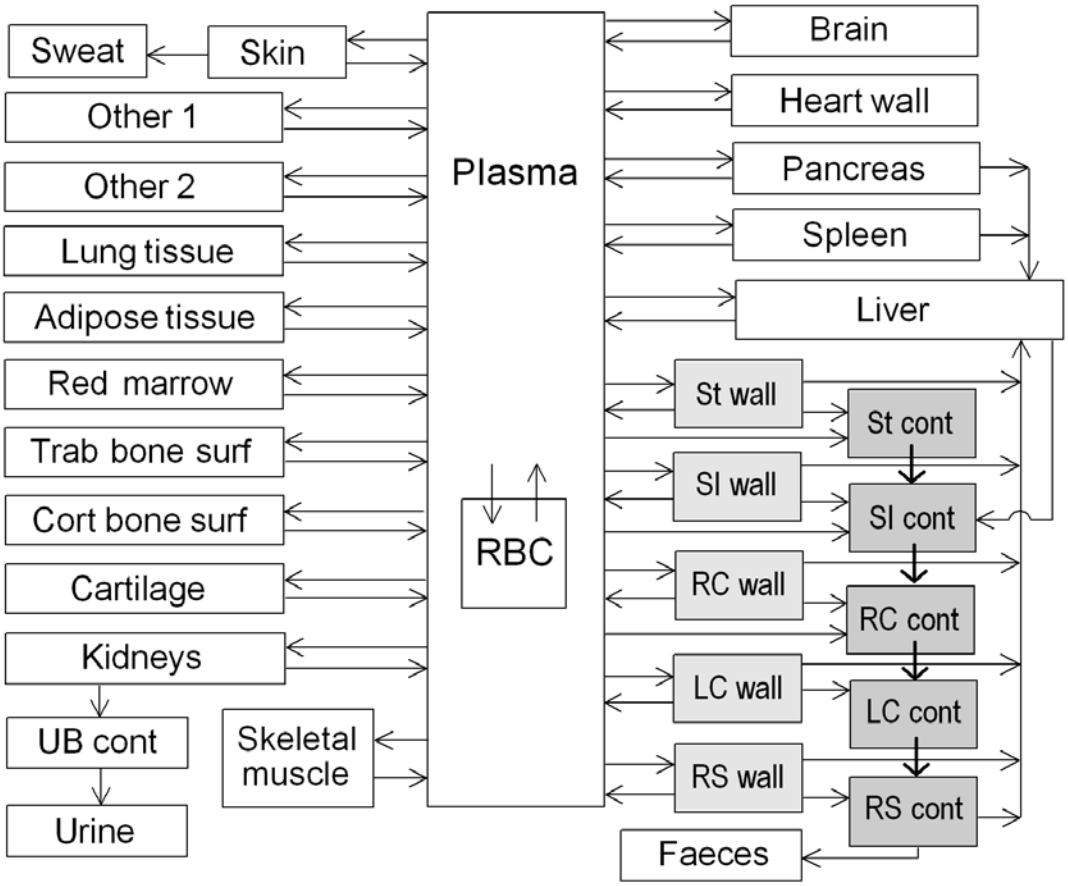

Figure 6-1. Structure of the model for systemic caesium and its exchange with caesium in the alimentary tract. Abbreviations: Trab = trabecular, Cort = cortical, surf = surface, UB = urinary bladder, cont = contents, RBC = red blood cells, St = stomach, SI = small intestine, RC = right colon, LC = left colon, RS = rectosigmoid colon.

(290) The derivation of most parameter values involves reference values for cardiac output and the percentage of cardiac output received by individual tissues. The assumed cardiac output in a resting adult male is 1766 plasma volumes d^{-1}. The assumed distribution of cardiac output is given in Table 6-4.

(291) Movement of caesium is depicted as a system of first-order processes. The transfer coefficient from plasma into a tissue T is estimated as the product of the plasma flow rate to that tissue (1766 plasma volumes per day multiplied by the fraction of cardiac output received by the tissue) and a tissue-specific extraction fraction, E_T. The extraction fraction for a tissue is defined as the fraction of caesium atoms extracted by that tissue during passage of caesium from arterial to venous plasma.

(292) Data on tissue-specific extraction fractions for caesium (Cs) and its physiological analogues potassium (K) and rubidium (Rb) were reviewed by Leggett and Williams (1986, 1988) and Leggett et al. (2003). In general, tissue extraction from plasma decreases in the order $K \geq Rb > Cs$. For example, extraction by the myocardium in dogs was estimated as

0.71 (range, 0.64-0.80) for potassium, 0.65 (0.58-0.76) for rubidium, and 0.22 (0.09-0.30) for caesium (Love et al., 1968; Poe, 1972). More information on extraction fractions was found for potassium and rubidium than for caesium. Data for potassium and rubidium were extrapolated to caesium by applying modifying factors as indicated by data on discrimination between these elements by tissues (Leggett et al., 2003). Initial selections of extraction fractions were modified in some cases after testing the model against reported caesium distributions in the early minutes or hours after administration to laboratory animals (Carr, 1966; Love et al., 1968; Yano et al., 1970; Stather, 1970; Poe, 1972; Moskalev, 1972; Krulik et al., 1980; Gregus and Klaasen, 1986; Nishiyama et al., 1975) or human subjects (Rosoff et al., 1963; Nishiyama et al., 1975). For example, an initially selected extraction fraction of 0.003 for brain was reduced to 0.002 for improved agreement with observations of the time-dependent increase of the caesium content of the brain following acute intake. The final selections of extraction fractions for caesium are as follows: 0.2 for kidneys, walls of the gastrointestinal tract, and heart wall; 0.05 for liver and skin; 0.002 for brain; and 0.1 for all other tissues.

Table 6-3. Transfer coefficients for the model for systemic caesium

From	To	Transfer coefficient (d^{-1})
Plasma	Red blood cells	1.8
Plasma	Skeletal muscle	30.0
Plasma	Liver	19.5
Plasma	Kidneys	67.1
Plasma	Spleen	5.30
Plasma	Pancreas	1.77
Plasma	Skin	4.42
Plasma	Adipose tissue	8.83
Plasma	Brain	0.424
Plasma	Heart wall	14.1
Plasma	Lung tissue	4.42
Plasma	Red marrow	5.3
Plasma	Cartilage	3.0
Plasma	Trabecular bone surface	1.59
Plasma	Cortical bone surface	1.06
Plasma	Stomach wall	3.53
Plasma	Stomach content	4.52
Plasma	Small intestine wall	35.3
Plasma	Small intestine content	1.05
Plasma	Right colon wall	5.65
Plasma	Right colon content	0.02
Plasma	Left colon wall	5.65
Plasma	Rectosigmoid colon wall	2.83
Plasma	Other 1	9.71
Plasma	Other 2	0.00353
Red blood cells	Plasma	0.257
Muscle	Plasma	0.0751
Liver	Plasma	2.14
Liver	Small intestine content	0.113
Kidneys	Urinary bladder content	1.68

Kidneys	Plasma	31.9
Spleen	Plasma	5.03
Spleen	Liver	0.265
Pancreas	Plasma	1.68
Pancreas	Liver	0.0883
Skin	Plasma	0.867
Skin	Excreta	0.0159
Adipose tissue	Plasma	1.77
Brain	Plasma	0.0848
Heart wall	Plasma	8.07
Lung tissue	Plasma	1.47
Red marrow	Plasma	0.706
Cartilage	Plasma	0.2
Trabecular bone surface	Plasma	0.212
Cortical bone surface	Plasma	0.212
Stomach wall	Plasma	4.16
Stomach wall	Liver	0.219
Stomach wall	Stomach content	0.21
Small intestine wall	Plasma	9.87
Small intestine wall	Liver	0.519
Small intestine wall	Small intestine content	0.21
Right colon wall	Plasma	6.86
Right colon wall	Liver	0.361
Right colon wall	Right colon content	0.21
Left colon wall	Plasma	6.86
Left colon wall	Liver	0.361
Left colon wall	Left colon content	0.21
Rectosigmoid colon wall	Plasma	6.86
Rectosigmoid colon wall	Liver	0.361
Rectosigmoid colon wall	Rectosigmoid colon content	0.21
Other 1	Plasma	0.762
Other 2	Plasma	0.00141

(293) The transfer coefficient from a tissue T to plasma is based on the relative contents of caesium in plasma and T at equilibrium (Table 6-4), as estimated from collected studies of stable and radioactive caesium in living human subjects and cadavers (Williams and Leggett, 1987; Leggett et al., 2003). If T exchanges caesium only with plasma, the transfer coefficient R_2 from T to plasma is determined as $R_2 = R_1 \times P/A$, where A and P are the fractions of total-body caesium in the tissue and plasma at equilibrium and R_1 is the transfer coefficient from plasma to T.

Table 6-4. Reference distribution of cardiac output and steady-state distribution of stable caesium in an adult male[a]

Compartment	Caesium content at equilibrium (% of total body)	Blood flow rate (% of cardiac output)
Plasma	0.2	--
Red blood cells (RBC)	1.4	--
Skeletal muscle	80	17
Liver	2.0	6.5 (arterial) + 19 (portal)
Kidneys	0.4	19
Spleen	0.2	3.0
Pancreas	0.2	1.0
Stomach wall	0.154	1.0
Small intestine wall	0.667	10
Right colon wall	0.152	1.6
Left colon wall	0.152	1.6
Rectosigmoid colon wall	0.076	0.8
GI contents[b]	0.4	--
Red marrow	1.5	3.0
Trabecular bone[c]	1.5	0.9
Cortical bone[c]	1.0	0.6
Cartilage	3.0	--
Skin	1.0	5.0
Heart wall	0.35	4.0
Lung tissue	0.6	2.5
Brain	1.0	12
Adipose tissue	1.0	5.0
Other[d]	3.05	5.5
Totals	100	100

[a] Based on estimates of Leggett et al. (2003). Values for GI tissue compartments based on estimate for total GI tissue and mass fractions of individual tissues. Division of skeletal caesium based on a review by Williams and Leggett (1987).

[b] Sum of contents of stomach, small intestine, right colon, left colon, and rectosigmoid colon.

[c] In the model, all caesium in bone is assumed to reside on bone surface.

[d] In the model, Other is divided into compartments Other 1 and Other 2 with fast and slow exchange with plasma, respectively. Other 1 receives 5.498% of cardiac output and contains 2.55% of total-body caesium at equilibrium. Other 2 receives 0.002% of cardiac output and contains 0.5% of total-body caesium at equilibrium.

(294) The use of extraction fractions and the equilibrium distribution for caesium to derive transfer coefficients between plasma and tissues is illustrated for skeletal muscle. The transfer coefficient from plasma to skeletal muscle is estimated as 0.1 x 0.17 x 1766 d^{-1} = 30.022 d^{-1}, where 0.1 is the estimated extraction fraction for skeletal muscle, 0.17 is the reference fraction of cardiac output going to skeletal muscle, and 1766 d^{-1} is the reference cardiac output in plasma volumes per day. The transfer coefficient from skeletal muscle to plasma is 0.002 x 30.022 d^{-1} / 0.8 = 0.0751 d^{-1}, where 0.002 and 0.8 are, respectively, fractions of total-body caesium in plasma and skeletal muscle at equilibrium. Derived parameter values are rounded to three significant digits in Table 6-3.

(295) The concept of an extraction fraction does not apply to red blood cells (RBC). The

transfer coefficients between plasma and RBC are derived from observed transfer rates for potassium and comparative data on potassium and caesium. The transfer coefficient for potassium from plasma to RBC is estimated from data from several experimental studies as 6 d^{-1} (Leggett and Williams, 1986, 1988). The rate of transfer of caesium into RBC is roughly 0.3 times that of potassium in humans, rabbits, and rats (Love and Burch, 1953; Forth et al, 1963; Gyorgyi and Kanyar, 1973) and thus is estimated as 0.3 x 6 d^{-1} = 1.8 d^{-1}. The transfer coefficient from RBC to plasma can be determined from the caesium inflow rate (1.8 d^{-1}) and the equilibrium fractions of caesium in plasma and RBC, respectively. Based on the reference steady-state content of RBC (as a fraction of total-body caesium; see Table 6-4) the transfer coefficient from RBC to plasma is 1.8 d^{-1} x 0.002 / 0.014 = 0.257 d^{-1}.

(296) The concept of an extraction fraction also does not apply to cartilage, which contains no blood vessels but receives nutrients via a permeable matrix in contact with extravascular fluids. The simplifying assumption is made here that cartilage receives caesium directly from plasma and returns caesium to plasma. Transfer coefficients describing exchange between plasma and cartilage are set to depict rapid uptake and subsequently elevated concentration of radiocaesium in cartilage as observed in different animal species (Nelson et al., 1961; Ekman, 1961; Furchner et al., 1964) and to yield a cartilage content of 3% of total-body caesium at equilibrium (Williams and Leggett, 1987).

(297) For a compartment T that receives caesium from plasma but loses caesium to multiple compartments, the total outflow rate R from T is derived as illustrated above for skeletal muscle, and additional information is used to divide R into transfer coefficients representing different paths of movement. For example, the derived rate of loss R from skin is divided into transfer coefficients R_1 and R_2 representing the rate of loss from skin to plasma and the rate of loss from skin to sweat, respectively. The value for R_2 is set for consistency with data of Yamagata et al. (1966) on the appearance of activity in sweat after ingestion of ^{132}Cs by a human subject, and R_1 is determined as $R - R_2$. As a second example, the compartment representing the stomach wall is assumed to return caesium to plasma via the portal vein and to lose caesium to the stomach contents due to cell sloughing. The total rate of loss R (4.59 d^{-1}) from the stomach wall to all destinations is derived as illustrated earlier for skeletal muscle. The transfer coefficient from the stomach wall to the stomach contents representing cell sloughing is set at 0.21 d^{-1}, an estimated average cell sloughing rate from GI tract tissues to GI contents (Leggett et al., 2003). The rate of loss of caesium from the stomach wall via the portal vein is calculated as the total removal rate from stomach wall minus the rate of cell sloughing: 4.59 d^{-1} – 0.21 d^{-1} = 4.38 d^{-1}. Outflow from the stomach wall via the portal vein is divided between the plasma and liver compartments on the basis of the extraction fraction for liver (0.05). That is, the transfer coefficient from the stomach wall to the liver is 0.05 x 4.38 d^{-1} = 0.219 d^{-1}, and the transfer coefficient from the stomach wall to plasma is 0.95 x 4.38 d^{-1} = 4.16 d^{-1}.

(298) Some of the transfer coefficients are based on a combination of basic physiological data and empirical data for caesium. For example, the rate of transfer of caesium into the gastrointestinal tract in liver bile is estimated as 5% of total outflow from the liver based on data on the rate of bile flow in man and observed concentration ratios for caesium in liver and bile in different animal species. A total outflow rate from the liver of 2.25 d^{-1} is based on the derived transfer coefficient from plasma to liver of 19.5 d^{-1} and the assumption that the liver contains 2% of total-body caesium at equilibrium. The transfer coefficient from liver to bile is calculated as 0.05 x 2.25 d^{-1} = 0.113 d^{-1}.

(299) Urinary excretion of caesium is depicted as transfer from plasma to a well-mixed kidney compartment and division of outflow from that compartment to plasma and the

contents of the urinary bladder. Transfer from plasma to kidneys is represented as an effective extraction fraction times the blood flow rate to kidneys, where the effective extraction fraction includes atoms temporarily retained in the tubules after filtration at the glomerulus as well as atoms entering kidney tissue directly from blood plasma. The division of kidney outflow between plasma and urinary bladder contents is set for consistency with short-term urinary excretion data for healthy adult males (Lloyd et al., 1972, 1973). It is assumed that the renal deposit represents the only source of urinary caesium. That is, it is assumed that none of the urinary caesium arises from filtered or secreted atoms that pass to the urinary bladder without being retained in kidney tissue.

(300) Endogenous faecal excretion is assumed to arise from transfer of caesium into the contents of the alimentary tract in saliva, gastric juices, pancreatic secretions, liver bile, and other secretions. It is assumed that 99% of the secreted activity that reaches the small intestine is reabsorbed to blood and that absorption occurs only in the small intestine.

(301) The model depicts a small component of very long-term retention observed in human subjects involved in the accident in Goiania, Brazil (Melo et al., 1997, 1998) and in experimental studies on rats that received ^{137}Cs by intraperitoneal injection (Thomas and Thomas, 1968). In eight adult human subjects involved in the Goiania accident, this small component of retention had an estimated half-time on the order of 500 d and represented an estimated 0.01-0.25% of uptake to blood, with estimates falling between 0.04% and 0.07% for five of the eight subjects. In rats, this component represented less than 0.01% of injected ^{137}Cs and had a half-time of 150-200 d. The physiological basis for this retention component is not known. It is represented in the model as a compartment called “Other 2” that is assumed to receive 0.002% of cardiac output and to contain 0.5% of total-body caesium at equilibrium. This long-term component of retention does not represent an important contribution to dose per unit intake of radiocesium but can be important for interpretation of bioassay data collected at times remote from exposure.

(302) As is the case for the original model, the present version of the model can be used to simulate the effect of binding of caesium to Prussian Blue (PB) or other unabsorbed material in the gut. The simulation is carried out by changing the relative fractions of caesium assumed to move from the small intestine contents to blood and to the right colon contents. If it is assumed that all caesium entering the small intestine is carried by PB to the right colon contents and is eventually excreted in faeces, the long-term retention half-time for the adult male decreases by about 60%. Melo et al. (1998) found that oral administration of PB reduced the long-term retention half-time by an average of 69% (range, 36-83%) in 11 adult male subjects. Ruwei et al. (1985) found an average reduction in the half-time of about 50% in five subjects. Madshus et al. (1966) found an average reduction of 64% in two subjects.

6.2.3.3. Treatment of radioactive progeny

(303) Four caesium isotopes addressed in this report have radioactive progeny that may contribute significantly to dose estimates for the parent, depending to some extent on the assumed behavior of the progeny: ^{125}Cs, ^{127}Cs, ^{134m}Cs, and ^{137}Cs. Cesium-134m ($T_{1/2}$ = 2.9 h) decays to ^{134}Cs ($T_{1/2}$ = 2.06 y), which presumably behaves as if entering its site of production as a parent radionuclide. The other three cesium isotopes decay to radionuclides that are expected to migrate to some extent from the parent radionuclide.

(304) Cesium-125 ($T_{1/2}$ = 45 m) decays to the noble gas ^{125}Xe ($T_{1/2}$ = 16.9 h), which decays to ^{125}I ($T_{1/2}$ = 59.4 d). Xenon-125 produced by decay of ^{125}Cs in bone is assumed to transfer to blood at the rate 100 d^{-1} if produced in a bone surface compartment and 0.36 d^{-1} if

produced in a bone volume compartment. These rates are taken from the model for radon introduced in ICRP *Publication 67* (1993) and applied in this report to radon produced in bone surface and non-exchangeable bone volume, respectively, by decay of a radium isotope. Xenon produced in a soft-tissue compartment is assumed to transfer to blood with a half-time of 20 min. Xenon entering blood is assumed to be removed from the body (exhaled) at the rate 1000 d^{-1}, corresponding to a half-time of 1 min. Partial recycling of xenon to tissues via arterial blood is not depicted explicitly in this model for xenon as a daughter radionuclide but is considered in the assignment of the half-times in tissues. The model is intended to yield a conservative average residence time of xenon atoms in the body after their production in systemic pools.

(305) Iodine-125 produced by serial decay of ^{125}Cs and ^{125}Xe is assumed to follow the characteristic model for iodine (the model applied in this report to iodine as a parent radionuclide) from its time of production in a compartment of the caesium model that is identifiable with a compartment of the characteristic model for iodine. For example, the compartments of the caesium model representing liver and kidneys are assumed to correspond to the compartments for liver iodide and kidney iodide in the characteristic model for iodine. When produced in a compartment that is not identifiable with a compartment in the characteristic model for iodine, ^{125}I generally is assumed to transfer rapidly to blood (at the rate 330 d^{-1}, the highest transfer rate to blood in the iodine model) and then to follow the characteristic model for iodine. An exception is that ^{125}I produced in red blood cells is assumed to transfer to the iodide blood pool in the iodine model at the rate 1000 d^{-1}.

(306) Caesium-127 ($T_{1/2}$ = 6.25 h) decays to the noble gas ^{127}Xe ($T_{1/2}$ = 36.4 d). In this case inclusion of decays of the progeny based on the xenon model described above has a negligible effect on dose estimates for the parent due to the relatively long half-life of the xenon isotope.

(307) Cesium-137 ($T_{1/2}$ = 30.2 y) decays to ^{137m}Ba ($T_{1/2}$ = 2.55 min). Wasserman et al. (1959) demonstrated considerable dissociation of ^{137m}Ba from ^{137}Cs in rats at 4-7 d after intraperitoneal administration of ^{137}Cs/^{137m}Ba, despite the short half-life of ^{137m}Ba. Barium-137m was found to exceed equilibrium proportions in bone, blood, and plasma by factors of 3.3, 3.9, and 14, respectively. Some soft tissues were moderately deficient in ^{137m}Ba, while others showed little or no deviation from equilibrium. The authors concluded nevertheless that soft tissues likely were the main source of the excess ^{137m}Ba in plasma and that red blood cells probably also contributed to the excess. Skeletal muscle was not sampled but seems likely to have been a major contributor to the excess ^{137m}Ba in plasma and bone as it presumably contained the preponderance of systemic ^{137}Cs after 4-7 d.

(308) The model applied in this report to barium as a parent radionuclide was modified in the following ways for application to ^{137m}Ba produced in systemic pools by decay of ^{137}Cs: (1) compartments and pathways not relevant to the short-term behavior of systemic barium were eliminated; and (2) the rate of exchange of barium between plasma and a rapid-turnover soft-tissue compartment as well as the rates of transfer of barium to tissues and excretion pathways were increased to provide an improved fit to blood clearance data for human subjects immediately following intravenous injection of ^{133}Ba (Newton et al., 1991). Kinetic studies with radioisotopes of barium and other alkaline earth elements indicate that these elements initially leave plasma with a half-time of a few minutes and equilibrate rapidly with an extravascular pool about three times the size of the plasma pool (Newton et al., 1991; Leggett, 1992). Studies of the short-term behavior of ^{133m}Ba in human subjects indicate that the important repositories for barium during the early minutes after intravenous administration are bone and colon (Korsunskii et al., 1986). The following systemic model

for ^{137m}Ba produced by decay of ^{137}Cs is based on these considerations and the findings of Wasserman et al. (1959) regarding the dissociation of ^{137m}Ba from ^{137}Cs in rats. Barium produced in skeletal muscle and red blood cells transfers to plasma at the rate 1000 d^{-1}, the default value for extremely rapid transfer between systemic compartments. Barium produced in all other soft tissue compartments transfers to plasma at the rate 200 d^{-1} (half-time of 5 min), chosen to yield at most a moderate deficiency of ^{137m}Ba in these tissues compared with equilibrium values. Barium produced in bone decays at its site of production. Barium transfers from plasma to: trabecular bone surface at the rate 19.4 d^{-1}, cortical bone surface at 15.6 d^{-1}, right colon contents at 40.3 d^{-1}, urinary bladder contents at 4.48 d^{-1}, and a compartment representing all soft tissues at 184 d^{-1}. The transfer coefficient from the soft tissue compartment back to plasma is 61.4 d^{-1}. Barium entering the urinary bladder or right colon contents follows the generic excretion models. The transfer coefficients from plasma to bone surface compartments and excretion pathways are two times the corresponding values given in the model for barium as a parent. The rates of transfer between plasma and the soft tissue compartment are set to fit the early plasma clearance data of Newton et al. (1991) for human subjects, with the constraint that the transfer coefficient from soft tissues to plasma is one-third the coefficient from plasma to soft tissues. This constraint implies that the content of the soft-tissue compartment is three times that of plasma at equilibrium. The model predicts that the plasma content of ^{137m}Ba at 4-7 d after injection of ^{137}Cs to blood is 13-16 times the equilibrium value, which is consistent with findings of Wasserman et al. (1959) for rats. The bone content of ^{137m}Ba at 4-7 d is predicted to be roughly 2 times the equilibrium value compared with the ratio 3.3 determined by Wasserman and coworkers. The high rate of migration of ^{137m}Ba from its sites of production to bone indicated by the findings for rats could not be reproduced while remaining consistent with reported biokinetic data, e.g. blood clearance data, for barium in human subjects.

6.2.3.4. Differences with gender

(309) The long-term biological half-time of caesium in the total body, representing roughly 90% of absorbed caesium, typically is about one-fourth (15-35%) lower in women than in men and about one-third lower in pregnant than in non-pregnant women. During lactation there is substantial transfer of caesium from blood to the mammary glands to milk (ICRP, 2004).

6.3. Individual monitoring

(310) ^{134}Cs internal exposures may be detected using urinalysis or in vivo Whole Body counting.

Isotope	Monitoring Technique	Method of Measurement	Typical Detection Limit	Achievable detection limit
^{134}Cs	Urine Bioassay	γ-ray spectrometry	1 Bq/L	0.04 Bq/L
^{134}Cs	Whole Body Counting (shielded room)	γ-ray spectrometry, in vivo	20-40 Bq	11 Bq
^{134}Cs	Lung Monitoring	γ-ray spectrometry, in vivo	9 Bq*	

* Lung monitoring of ^{134}Cs is not generally used in routine monitoring of workers. Monte Carlo program Visual Monte Carlo was used to simulate the photon emission, to calculate the calibration factor for the geometry and radionuclide, and to calculate the minimum detectable activity (MDA) in the lung. (Hunt et al, 2012)

(311) ^{137}Cs internal exposures are detected by gamma spectroscopy using the 0.661 MeV gamma ray from its daughter ^{137m}Ba (T1/2 =2.5 min), which is produced in approximately 94.4 % of decays of ^{137}Cs and exists in secular equilibrium with ^{137}Cs in the body. Gamma spectroscopy is used for in vivo measurements and for excreta analysis.

Isotope	Monitoring Technique	Method of Measurement	Typical Detection Limit	Achievable detection limit
^{137} Cs	Urine Bioassay	γ-ray spectrometry from ^{137m}Ba	1-5 Bq/L	0.1 Bq/L
^{137} Cs	Lung monitoring	γ-ray spectrometry from^{137m}Ba	11 Bq*	
^{137} Cs	Whole Body Counting (shielded room)	γ-ray spectrometry from^{137m}Ba	25-60 Bq	16 Bq

* Lung monitoring of ^{137}Cs is not generally used in routine monitoring of workers. Monte Carlo program Visual Monte Carlo was used to simulate the photon emission, to calculate the calibration factor for the geometry and radionuclide, and to calculate the minimum detectable activity (MDA) in the lung. (Hunt et al, 2012)

References

Al Rayyes, A.H., Ronneau, C., Stone, W.E., Genet, M.J., Ladière, J., Cara. J., 1993. Radiocaesium in Hot particles: solubility vs chemical speciation. J. Environ. Radioact., 21, 143-151.

Andrieu, L., Fatome, M., 1979. Évolution lontaine inattenfue d'une contamination interne. Radioprotection 14(3), 135-143.

Boecker, B. B., Cuddihy, R.G., Hahn, F F., McClellan, R.O., 1974. A seven year study of the pulmonary retention and clearance of 137Cs inhaled in fused aluminosilicate particles by the beagle dog. Inhalation Toxicology Research Institute Annual Report 1973–1974, LF–49, pp. 48–52. Lovelace Biomedical and Research Foundation, Albuquerque, New Mexico. Available from National Technical Information Service, Springfield, Virginia.

Boecker, B.B., 1969a. The metabolism of ^{137}Cs inhaled as ^{137}CsCl by the beagle dog. Proc. Soc. Exp. Biol. Med. 30, 966-971.

Boecker, B.B., 1969b. Comparison of ^{137}Cs metabolism in the beagle dog following inhalation and intravenous injection. Health Phys., 16, 785–788

Carr, E.A., 1966. Pharmacology of radioactive caesium salts. In: Andrews GA, Kniseley RM, Wagner HN, editors. Radioactive Pharmaceuticals, Proceedings of a symposium held at Oak Ridge Associated Universities, Nov 1-4, 1965, USAEC; CONF-651111, pp. 619-634.

Cecchi, X., Wolff, D., Alvarez, O., Latorre, R., 1987. Mechanisms of Cs^+ blockade in a $Ca2^+$-activated K^+ channel from smooth muscle. Biophys. J., 52, 707-716

Cryer, M.A., Baverstock, K.F., 1972. Biological half-time of ^{137}Cs in man. Health Phys., 23, 394-395.

Cuddihy, R.G., Finch, G.L., Newton, G.J., Hahn, F.F., Mewhinney, J.A., Rothenberg, S.J., Powers, D.A., 1989. Characteristics of radioactive particles released from the Chernobyl nuclear reactor. Environ. Sci. Technol., 23, 89–95.

Cuddihy, R.G., Ozog, J.A., 1973. Nasal absorption of CsCl, $SrCl_2$, $BaCl_2$, and $CeCl_3$ in Syrian Hamsters. Health Phys., 25, 219–224.

Dua, S.K., Maniyan, C.G., Kotrappa, P., 1987. Inhalation exposures during operations in spent fuel bays. Radiat. Prot. Dosim., 19, 165–172.

Edwards, C., 1982. The selectivity of ion channels in nerve and muscle. Neuroscience 7, 1335-1366.

Ekman, L., 1961, Distribution and excretion of radio-cesium in goats, pigs and hens. Acta Vet. Scand. 2 (Suppl. 4):1-83.

Forth, W., Oberhausen, E., Pfleger, K., Weske, G., 1963. Beitrag zur Kloumarung der Ursachen der Anreicherung von Caesium-137 im Organismus. Experientia, 19, 25-26.

Froning, M., Kozielewski, T., Schlager, M., Hill, P., 2004. A case study of the long-term retention of ^{137}Cs after inhalation of high temperature reactor fuel element ash, Radiat. Prot. Dosim., 111(1), 55-58.

Furchner, J. E.; Trafton, G. A.; Richmond, C. R. , 1964. Distribution of cesium-137 after chronic exposure in dogs and mice. Proc. Soc. Exp. Biol. Med. 116:375-378.

Gregus, Z., Klaassen, C.D., 1986. Disposition of metals in rats: A comparative study of fecal, urinary, and biliary excretion and tissue distribution of eighteen metals. Toxicol Appl. Pharmacol., 85, 24-38.

Gyorgyi, S., Kanyar, B., 1973. Comparison of Cs-137 and K-42 transport of rat erythrocytes by means of a tracer kinetic model. In: Bujdoso E. Proceedings of the IRPA second European congress on radiation protection, pp. 263-268.

Hesp, R., 1964. The retention and excretion of caesium-137 by two male subjects. In Assessment of Radioactivity in Man. Vol. II. IAEA, Vienna, pp. 61-74.

Hodgkin, A.L., 1947. The effect of potassium on the surface membrane of an isolated axon. J. Physiol., 106, 319-340.

Hölgye, Z., Malý, M., 2002. A case of repeated accidental inhalation contamination of a male subject with ^{137}Cs. Health Phys., 82(4), 517-520.

ICRP, 1979. Limits for intakes of radionuclides by workers. ICRP Publication 30, Part 1. Oxford: Pergamon Press.

ICRP, 1989. Age-dependent Doses to Members of the Public from Intake of Radionuclides. Part 1. ICRP Publication 56. Ann. ICRP 20(2).

ICRP, 1993. Age-dependent Doses to Members of the Public from Intake of Radionuclides. Part 2.Ingestion dose coefficients. ICRP Publication 67. Ann. ICRP 23(3-4).

ICRP, 1994. Dose coefficients for intake of radionuclides by workers. ICRP Publication 68, Ann. ICRP 24 (4).

ICRP, 2002a. Supporting Guidance 3. Guide for the Practical Application of the ICRP Human Respiratory Tract Model. Ann. ICRP 32(1-2).

ICRP, 2002b. Basic anatomical and physiological data for use in radiological protection: reference values. ICRP Publication 89, Ann. ICRP 32 (3-4).

ICRP, 2004. Doses to infants from ingestion of radionuclides in monthers' milk. ICRP Publication 95. Ann ICRP 34 (3-4).

Korsunskii, V.N., Tarasov, N.F., Naumenko, A.Z., 1981. Clinical evaluation of Ba-133m as an osteotropic agent. ORNL/TR-86/30 (7 pgs); Translated from the Russian UDC 616.71-006-073.916, Meditsinskaya Radiologiya No. 10, pp. 45-48.

Kotrappa, P., Bhat, I.S., Vashi, V.D., 1977. Particle size and solubility characteristics of aerosols in Pu processing areas and BWR type power reactors. IN Proceedings of the Fourth International Congress of the International Radiation Protection Association (IRPA) Paris Vol. 3, pp. 771–774.

Krulik, R., Farska, I., Prokes, J., Tykva, R., 1980. Distribution of caesium in the organism and its effect on the nucleotide metabolism enzymes. Int. Pharmacopsychiat. 15, 157-165.

Kutkov, V.A., 1998. Application of human respiratory tract models for reconstruction of the size of aerosol particles through the investigation of radionuclides behaviour in the human body. Radiat. Prot. Dosim., 79, 265–268.

Kutkov, V.A., 2000. Results of in vivo monitoring of the witnesses of the Chernobyl accident. Radiat. Prot. Dosim. 89, 193-197.

Kutkov, V.A., Komaritskaya, O.I., 1996. In vitro solubility of Chernobyl nuclear fuel aerosol with respect to collective behaviour of its radionuclides. In : Proc. IRPA 9, Vienna, 2, 445-447.

Latorre, R., Miller, C., 1983. Conduction and selectivity in potassium channels. J Membr. Biol. 71:11-30.

Leggett, R. W., 1992. A generic age-specific biokinetic model for calcium-like elements. Radiat. Prot. Dosim., 41,183-198.

Leggett, R.W., 1986. Predicting the retention of caesium in individuals. Health Phys., 50, 747-759.

Leggett, R.W., Bouville, A., Eckerman, K.F., 1998. Reliability of the ICRP's systemic biokinetic models. Radiat. Prot. Dosim., 79, 335-342.

Leggett, R.W., Williams, L.R., 1986. A model for the kinetics of potassium in healthy humans. Phys. Med. Biol., 31, 23-42.

Leggett, R.W., Williams, L.R., 1988. A biokinetic model for rubidium in humans. Health Phys., 55, 685-702.

Leggett, R.W., Williams, L.R., 1995. A proposed blood circulation model for Reference Man. Health Phys., 69, 187-201.

Leggett, R. W.; Williams, L. R.; Eckerman, K. F. (1999). A blood circulation model for reference man. In: Proceedings of the 6th Annual Radiopharmaceutical Dosimetry Symposium; A. T. S.-Stelson, M. G. Stabin, and R. B. Sparks, eds. (Oak Ridge, TN: Oak Ridge Institute for Science and Education); pp. 487-499.

Leggett, R.W., Williams, L.R., Melo, D.R., Lipsztein, J.L., 2003. A physiologically based biokinetic model for caesium in the human body. The Science of the Total Environment 317, 235-255.

LeRoy, G.V., Rust, J.H., Hasterlik, R.J., 1966. The Consequences of Ingestion by Man of Real and Simulated Fallout. Health Phys., 12, 449-473.

Lie, R., 1964. Deposition and retention of ^{137}Cs in the rat following inhalation of the chloride and the nitrate. Health Phys., 10, 1071–1076.

Lloyd, R.D., Mays, C.W., McFarland ,S.S., Zundel, W.S., Tyler, F.H., 1972. Rb-86 and Cs-137 metabolism in persons affected by muscle disease. In: University of Utah Report COO-119-247, University of Utah College of Medicine. Salt Lake City, UT, pp. 1-72.

Lloyd, R.D., Mays, C.W., McFarland, S.S., Zundel, W.S., Tyler, F.H., 1973. Metabolism of Rb-83 and Cs-137 in persons with muscle disease. Radiat Res., 54, 463-478.

Lloyd, R.D., Zundel, W.S., Mays, C.W., Wagner, W.W., Pendelton, R.C., 1966. Enhanced Cs-137 elimination in pregnant and dystrophic humans. Radiat. Res., 27, 548.

Love, W.D., Burch, G.E., 1953. A comparison of K-42, Rb-86, and Cs-134 as tracers of potassium in the study of cation metabolism of human erythrocytes in vitro. J. Lab. Clin. Med., 41, 351-362.

Love, W.D., Ishihara, Y., Lyon, L.D., Smith, R.O., 1968. Differences in the relationships between coronary blood flow and myocardial clearance of isotopes of potassium, rubidium, and caesium. American Heart J., 76, 353-355.

Madshus, K., Stromme, A., Bohne, F., Nigrovic, V., 1966. Diminution of radiocaesium body-burden in dogs and human beings by Prussian Blue. Int. J. Radiat. Biol., 10, 519-520.

McKay, W.A., Memmott, S.D., 1991. An investigation of the availability of 137Cs and 239 + 240Pu for gut absorption in winkles following cooking and in vitro simulated gastro-intestinal digestion. Food Addit. Contam., 8, 781-786.

Melo, D.R., Lipsztein, J.L., Oliveira, C.A., Lundgren, D.L., Muggenburg, B.A., Guilmette, R.A., 1997. A biokinetic model for ^{137}Cs. Health Phys., 73, 320-332.

Melo, D.R., Lipsztein, J.L., Oliveira, C.A., Lundgren, D.L., Muggenburg, B.A., Guilmette, R.A., 1998. Prussian Blue decorporation of ^{137}Cs in humans and beagle dogs. Radiat. Prot. Dosim., 79, 473-476.

Miller, C.E., 1964. Retention and distribution of ^{137}Cs after accidental inhalation. Health Phys. 10, 1065–1070.

Mirell, S. G., Blahd, W.H., 1989. Biological retention of fission products from the Chernobyl plume. Health Phys., 57, 649–652.

Morrow,P.E., Gibb,F.R., Davies, H., Fisher, M., 1968. Dust removal from the lung parenchyma: an investigation of clearance stimulants. Toxicol. Appl. Pharmacol., 12, 372-396.

Moskalev,Yu., I. 1972. Distribution and acceleration of radioisotope excretion. Distribution of caesium-137 in the animal organism. AEC-TR-7512, pp. 4-19.

Naversten, Y., Liden, K., 1964. Half-life studies of radiocaesium in humans. In: Assessment of radioactivity in man, Vol II (Vienna: IAEA), pp. 79-87.

Nelson, A.; Ullberg, S.; Kristoffersson, H.; Ronnback, C., 1961. Distribution of radiocesium in mice. Acta Radiol. 55:374-384.

Newton, D., Harrison, G.E., Kang, C., Warner, A. J., 1991. Metabolism of injected barium in six healthy men. Health Phys., 61, 191-201.

Nishiyama, H., Sodd, V.J., Schreiber, T.J., Loudon, R.G., Saenger, E.L., 1975. Imaging of pulmonary tumors with ^{129}Cs. In: Subramanian, G., Rhodes, B.A., Cooper, J.F., Sodd, V.J., (Eds.), Radiopharmaceuticals, New York, NY, The Society of Nuclear Medicine, pp. 482-490.

Poe, N.D., 1972. Comparative myocardial uptake and clearance characteristics of potassium and caesium. J. Nucl. Med., 13:557-560.

Raghavendran, K., Satbhai, P.D., Abhyankar, B., Unnikrishnan, K., Somasundaram, S., 1978. Long-term retention studies of ^{131}I, ^{137}Cs and ^{60}Co in Indian workers, Health Phys., 34, 185-188.

Rosoff, B., Cohn, S.H., Spencer, H.I., 1963. Caesium-137 metabolism in man, Radiat. Res., 19, 643-654.

Rundo, J., 1964. The metabolism of biologically important radionuclides. VI. A survey of the metabolism of caesium in man. Brit. J. Radiol., 37, 108-114.

Rundo, J., 1965. A case of accidental inhalation of irradiated uranium. Brit. J. Radiol., 38, 39–50.

Rundo, J., Mason, J., Newton, D., Taylor, B., 1963. Biological half-life of caesium in man in acute and chronic exposure. Nature, Lond., 200, 188-189.

Ruwei, M.A., Yueru, J., Songling, W., 1985. Study of ^{137}Cs metabolism in humans. In: Assessment of radioactive contamination in man (Vienna: IAEA), IAEA-SM-276/59, pp. 499-506.

Sjodin, R.A., Beauge, L.A., 1967. The ion selectivity and concentration dependence of cation coupled active sodium transport in squid giant axons. Curr. Mod. Biol., 1, 105-115.

Snipes, M.B., Boecker, B.B., McClellan, R.O., 1983. Retention of monodisperse or polydisperse aluminosilicate particles inhaled by dogs, rats, and mice. Toxicol. Appl. Pharmacol., 69, 345–362.

Snipes, M.B., McClellan, R.O., 1986. Model for deposition and long-term disposition of ^{134}Cs-labeled fused aluminosilicate particles inhaled by guinea pigs. Inhalation Toxicology Research Institute Annual Report 1985–1986, LMF–115, pp. 91–95. Lovelace Biomedical & Environmental Research Institute, Albuquerque, New Mexico. Available from National Technical Information Service, Springfield, Virginia.

Stara, J.F., 1965. Tissue distribution and excretion of caesium-137 in the guinea pig after administration by three different routes. Health Phys., 11, 1195–1202.

Stather, J.W., 1970. An analysis of the whole-body retention of caesium-137 in rats of various ages. Health Phys., 18, 43-52.

Stradling, G.N., Pellow, P.G., Hodgson, A., Fell, T.P., Phipps, A., Pearce, M., Rance, E., Ellender, M., Taskaeva, M., Penev, I., Guentchev, T., 1996. Dose coefficient and assessment of intake of a radionuclide bearing dust formed at the Kozloduy Nuclear Power Plant, NRPB-M679, Chilton.

Stradling, G.N., Pellow, P.G., Hodgson, A., Fell, T.P., Phipps, A., Pearce, M., Taskaeva, M., Penev, I., Guentchev, T., 1997. Assessment of intake of a complex radionuclide bearing dust formed at a nuclear power plant. J. Radioanal. Nucl. Chem., 226(1-2), 7-14.

Stradling, G.N., Stather, J.W., Gray, S.A., Moody, J.C., Ellender M., Collier, C.G., 1989. Assessment of intake of an actinide-bearing dust formed from the pond storage of spent magnox fuel. Radiat. Prot. Dosim., 26, 201–206.

Talbot, R.J., Newton, D., Segal, M.G., 1993. Gastrointestinal absorption by rats of Cs-137 and Sr-90 from uranium octoxide fuel particles: implications for radiation doses to man after a nuclear accident. Radiat. Prot. Dosim. 50: 39-43.

Thomas, R.G., Thomas, R.L., 1968. Long-term retention of Cs-137 in the rat. Health Phys., 15, 83-84.

Thomas, R.L., 1969, Deposition and initial translocation of inhaled particles in small laboratory animals. Health Phys., 16, 417-428.

Thornberg, C., Mattsson, S., 2000. Increased ^{137}Cs metabolism during pregnancy. Health Phys., 78, 502-506.

Wasserman, R.H., Wardock, A.R., Comar, C.L., 1959. Metabolic dissociation of short-lived barium-137m from its caesium-137 parent. Science 129:568-569.

Williams, L.R., Leggett, R.W., 1987. The distribution of intracellular alkali metals in Reference Man. Phys. Med. Biol. 32, 173-190.

Yamagata, N., 1962. Balance of potassium, rubidium, and caesium between Japanese people and diet and assessments of their biological half-times, Nature, 196, 83-84.

Yamagata, N., Iwashima, K., Nagai, T., Watari, K., Iinuma, T.A., 1966. In vivo experiment on the metabolism of caesium in human blood with reference to rubidium and potassium. J. Radiat. Res., 7, 29-46.

Yano, Y., Van Dyke, D., Budinger, T.F., Anger, H.O., Chu, P., 1970. Myocardial uptake studies with ^{129}Cs and the scintillation camera. J. Nucl. Med., 11, 663-668.

Zundel, W.S., Tyler, F.H., Mays, C.W., Lloyd, R.D., Wagner, W.W., Pendleton, R.C., 1969. Short half-times of caesium-137 in pregnant women. Nature, 221, 89-90.

7. BARIUM (Z = 56)

7.1. Chemical Forms in the Workplace

(312) Barium is an alkaline earth element, which mainly occurs in oxidation states II. It is a chemical analogue of calcium. Chemical forms encountered in industry include simple inorganic salts such as chlorides, sulphates and carbonates. Barium sulphate is used as an X-ray radiocontrast agent for imaging the human gastrointestinal tract. ^{133}Ba is routinely used as a standard source in the calibration of gamma-ray detectors in nuclear physics studies.

Table 7-1. Isotopes of barium addressed in this report

Isotope	Physical half-life	Decay mode
Ba-124	11.0 m	EC, B+
Ba-126	100 m	EC, B+
Ba-127	12.7 m	EC, B+
Ba-128	2.43 d	EC
Ba-129	2.23 h	EC, B+
Ba-129m	2.16 h	EC, B+
Ba-131	11.50 d	EC
Ba-131m	14.6 m	IT
Ba-133[a]	10.52 y	EC
Ba-133m	38.9 h	IT, EC
Ba-135m	28.7 h	IT
Ba-139	83.06 m	B-
Ba-140[a]	12.752 d	B-
Ba-141	18.27 m	B-
Ba-142	10.6 m	B-

[a] Data for these radionuclides are given in the printed copy of this report. Data for other radionuclides are given on accompanying electronic disk.

7.2. Routes of Intake

7.2.1. Inhalation

Absorption Types and parameter values

(313) No direct information was found on the behaviour of inhaled barium in man. Information is available from experimental studies of barium as chloride, sulphate or in fused aluminosilicate particles (FAP).

(314) Absorption parameter values and Types, and associated f_A values for particulate forms of barium are given in Table 7-2.

Barium chloride

(315) Cember et al. (1961) reported that more than 99% of barium administered to rats by intratracheal injection of $^{133}BaCl_2$ had cleared from the lungs within 3 hours. Cuddihy and Griffith (1972) observed very rapid, and almost complete, absorption of $^{140}BaCl_2$ following inhalation of ^{140}Ba–^{140}La by dogs, consistent with assignment to Type F. They developed a biokinetic model to represent the results, and with it estimated a rate of transfer of Ba from

the respiratory tract to blood of 25 d^{-1} ($t_{½}$ ~ 40 minutes). In the model, a small fraction (0.3%) of the deposit in the pulmonary region was retained indefinitely. This was not discussed: it could represent a small "bound" component, or systemic barium in lung tissues and blood. In a complementary experiment, alimentary tract absorption of ^{140}Ba following administration of $^{140}BaCl_2$ to dogs by gavage was 7%. However, Cuddihy and Griffith noted that reported values of alimentary tract absorption reported in the literature for $BaCl_2$ varied greatly. In subsequent studies (Cuddihy et al., 1974) of dogs that inhaled $^{133}BaCl_2$, essentially all of the existing body content was measured in the skeleton 16 d after the exposure. *In vitro* dissolution of the same material showed >99.9% dissolved at a rate of 14 d^{-1} ($t_{½}$ ~ 1 hour). Cuddihy and Ozog (1973) deposited $^{140}BaCl_2$ directly onto the nasal membranes of Syrian hamsters: the results give an absorption rate of about 7 d^{-1} ($t_{½}$ ~ 2 hours). This is somewhat slower than in other studies, possibly because of the experimental techniques used, including the anaesthetic or slower clearance from the nasal passage than from the lungs. Similar observations were made for strontium and caesium chlorides which were also administered by Cuddihy and Ozog (see Strontium and Caesium Sections).

(316) Based on the results of the experiments outlined above, specific absorption parameter values for barium chloride were estimated by the Task group to be: f_r = 1 and $s_r = 20\ d^{-1}$ (consistent with assignment to default Type F). However, although specific parameter values for barium chloride based on *in vivo* data are available, they are not adopted here, because inhalation exposure to it is so unlikely. Instead, barium chloride is assigned to Type F. However, the data are used as the basis for the default rapid dissolution rate for barium. Hence specific parameter values for barium chloride would be the same as default Type F barium parameter values.

Barium carbonate

(317) For details see the section on carbon. Measurements of lung retention of ^{14}C following pulmonary intubation of barium ^{14}C-labelled carbonate into rats, and accidental inhalation by man, indicate assignment to Type F.

Barium sulphate.

(318) Morrow et al. (1964) observed a biological half time in the lungs of 8 d following inhalation of $^{131}BaSO_4$ by a dog, corresponding to a rate of absorption of about 0.1 d^{-1}, and assignment to Type F. Cuddihy et al. (1974) followed the behaviour of ^{133}Ba for 16 d after inhalation of $^{133}BaSO_4$ by dogs. *In vitro* dissolution tests of the same material gave f_r = 0.9, s_r = 0.4 d^{-1} ($t_{½}$ ~ 2 d) and s_s = 0.0017 d^{-1} ($t_{½}$ ~ 400 d), consistent with absorption Type F. These values were incorporated in a biokinetic model, which gave predictions in good agreement with the observed *in vivo* behaviour. In similar experiments with heat-treated (900˚C) $^{133}BaSO_4$ (Cuddihy et al., 1974), *in vitro* dissolution tests gave f_r = 0.2, s_r = 0.07 d^{-1} ($t_{½}$ ~ 10 d) and s_s = 0.038 d^{-1} ($t_{½}$ ~ 18 d), consistent with absorption Type M. Again, biokinetic model predictions using these values were in reasonable agreement with the observed behaviour.

(319) $^{133}BaSO_4$ has also been used as an effectively insoluble test material to study the retention and clearance of particles deposited in the trachea in several species (Patrick and Stirling, 1977; Takahashi and Patrick, 1987; Takahashi et al., 1993; Patrick and Stirling, 1997). Most of these studies were of short duration (typically a week), and absorption was not considered to be a significant clearance pathway. In one, however, measurements were made for 6 months, and included tissue distribution data, which indicate Type M behaviour (Takahashi and Patrick, 1987). In rats, about 1% of the material deposited on the distal

trachea was retained with a half-time of 88 days, and the main clearance route identified was to lymph nodes, suggesting an absorption rate of less than 0.01 d^{-1}.

(320) Overall, a wide range of absorption rates has been observed, possibly due to differences in the method of preparation of the $BaSO_4$. Specific parameter values are therefore not proposed and $BaSO_4$ is assigned to Type M.

Fused aluminosilicate particles (FAP)

(321) FAP or "fused clay" particles have been extensively used as relatively insoluble particles in inhalation studies, both of biokinetics and of radiation effects. A natural clay mineral is labelled by ion exchange, and the labelled clay particles heated to about 1100˚C, to form aluminosilicate glass microspheres in which the label is incorporated. Cuddihy et al. (1974) followed the behaviour of ^{133}Ba for 512 d after inhalation of ^{133}Ba-FAP by dogs. *In vitro* dissolution tests (duration 120 d) of the same material gave $f_r = 0.12$, $s_r = 0.13\ d^{-1}$ ($t_{½} \sim 5$ d) and $s_s = 0.0016\ d^{-1}$ ($t_{½} \sim 430$ d), consistent with absorption Type M. These were incorporated in a biokinetic model, which gave predictions in good agreement with the observed behaviour.

Rapid dissolution rate for barium

(322) Studies with barium chloride outlined above give values of s_r of about 20 d^{-1}, which is applied here to all Type F forms of barium.

Extent of binding of barium to the respiratory tract

(323) Evidence from the barium chloride studies outlined above suggests that there is probably little binding of barium. It is therefore assumed that for barium the bound state can be neglected, i.e. $f_b = 0.0$.

Table 7-2. Absorption parameter values for inhaled and ingested barium

Inhaled particulate materials		Absorption parameter values[a] f_r	s_r (d^{-1})	s_s (d^{-1})	Absorption from the alimentary tract, f_A
Default parameter values[b,c]					
Absorption Type	Assigned forms				
F	Barium chloride, carbonate	1	20		0.2
M	Barium sulphate; all unspecified forms[d]	0.2	3	0.005	0.04
S	—	0.01	3	$1x10^{-4}$	0.002
Ingested materials					
Soluble forms					0.2
Insoluble form (sulphate, titanate)					$1x10^{-4}$

[a] It is assumed that for barium the bound state can be neglected, i.e. $f_b = 0.0$. The value of s_r for Type F forms of barium (20 d^{-1}) is element-specific. The values for Types M and S (3 d^{-1}) are the general default values.

[b] Materials (e.g. barium chloride) are listed here where there is sufficient information to assign to a default absorption Type, but not to give specific parameter values (see text).

[c] For inhaled material deposited in the respiratory tract and subsequent cleared by particle transport to the alimentary tract, the default f_A values for inhaled materials are applied: i.e. the product of f_r for the absorption Type (or specific value where given) and the f_A value for ingested soluble forms of barium (0.2).

[d] Default Type M is recommended for use in the absence of specific information, i.e. if the form is unknown, or if the form is known but there is no information available on the absorption of that form from the respiratory tract.

7.2.2. Ingestion

(324) Barium absorption depends on its chemical form. Barium sulfate is poorly absorbed from the gastrointestinal tract of adults (Figueroa et al., 1968; Boender and Verloop, 1969), while acid-soluble barium salts (e.g. acetate, carbonate, chloride, nitrate, hydroxide…) are readily dissolved in gastric acid and absorbed (Leggett, 1992a). Other factors are known to affect absorption. In animals, fasting and low calcium concentration in the gut may increase barium absorption by a factor 2 to 3 (Taylor et al., 1962, Della Rosa et al., 1967, Cuddihy and Griffith, 1972).

(325) Figueroa et al. (1968) fed five patients with stable barium sulfate and recovered 97.7-103% of the barium given orally in the stools after 5 days. In another study using stable barium sulfate and barium titanate, average urinary excretion by five to nine human subjects during the 24h after oral intake varied from about 0.16 to 0.26 $\mu g.g^{-1}$ ingested (Clavel et al., 1987) leading other authors to conclude that absorption of these forms should be in the order of 10^{-4} (Leggett, 1992a).

(326) LeRoy et al. (1966) found the absorption of ^{133}Ba from simulated fall-out to be highly variable. Absorption could only be detected by whole-body counting in 4 of the 8 subjects and in these it varied between 0.01 and 0.15. The analysis of barium in human excreta (Harrison et al., 1956) suggested absorption of about 0.07 and the fraction of dietary barium excreted in the urine of 2 subjects in a balance study was 0.02 and 0.06 (Tipton et al., 1969). In five female cancer patients with normal gut function, absorption of ^{140}Ba added to orange juice as the chloride was about 0.08 with a range of 0.03 - 0.16. Studies in which the absorption of Ba and Ra have been compared in rats, dogs, sheep, pigs and cows have shown similar levels of absorption of the two elements (Garner, 1960; Taylor et al., 1962; Della Rosa et al., 1967; Sansom and Garner, 1966).

(327) In *Publication 30* (ICRP, 1979), absorption was taken to be 0.1 for all forms of Ba.

However, as concluded by Leggett (1992a), absorption for soluble forms of barium may be higher. On the basis of chemical similarity with Ra, and similar absorption values reported for the two elements, a value of 0.2 was adopted in *Publication 67* (ICRP, 1993).

(328) An f_A of 0.2 for adults is recommended here for direct ingestion of soluble forms of barium. For insoluble forms such as barium sulfate or titanate, an f_A of 10^{-4} is recommended.

7.2.3. Systemic Distribution, Retention and Excretion

7.2.3.1. Summary of the database

(329) The alkaline earth element barium is a physiological analogue of the alkaline earth elements calcium, strontium, and radium but has different biokinetics from those elements due to discrimination by biological membranes and hydroxyapatite crystals of bone. The biokinetics of barium resembles that of radium much more closely than that of calcium or strontium.

(330) Retention and distribution of barium have been determined in controlled studies involving healthy human subjects (ICRP, 1973, 1993; Leggett, 1992a). There is also information on the biokinetics of barium in other animal species (ICRP, 1993, Leggett, 1992b). Data for human subjects or laboratory animals used in the development of the model for systemic barium used in this report are summarized below in the discussion of the basis for parameter values.

7.2.3.2. Biokinetic model for systemic barium

(331) The generic model structure for bone-volume-seeking radionuclides was used in ICRP *Publication 67* (1993) to model the systemic biokinetics of barium. The same model structure is applied in this report. The compartments and paths of movement as applied to barium are summarized below.

(332) Blood plasma is treated as a uniformly mixed pool that contains all barium in blood and exchanges activity with soft tissues and bone surfaces. Soft tissues are divided into three compartments corresponding to fast, intermediate, and slow return of activity to plasma (compartments ST0, ST1, and ST2, respectively). The liver and kidneys are not addressed separately in the model for barium but are included implicitly in the soft tissue compartments. Bone is divided into cortical and trabecular bone, and each of these bone types is further divided into bone surfaces and bone volume. Bone volume is viewed as consisting of two pools, one that exchanges with activity in bone surface for a period of weeks or months and a second, non-exchangeable pool from which activity can be removed only by bone restructuring processes. Activity depositing in the skeleton is assigned to bone surface. Over a period of days a portion of the activity on bone surfaces moves to exchangeable bone volume and the rest returns to plasma. Activity leaves exchangeable bone volume over a period of months, with part of the activity moving to bone surfaces and the rest to non-exchangeable bone volume. The rate of removal from non-exchangeable bone volume is assumed to be the rate of bone turnover, with different turnover rates applying to cortical and trabecular bone. Barium is assumed to be lost from the body only by urinary and fecal excretion.

Parameter values

(333) The parameter values for barium applied in ICRP *Publication 67* (1993) to an adult

member of the public are adopted in this document for application to workers. The basis for the parameter values is summarized below.

(334) The biological behavior of injected or ingested barium has been investigated in several controlled studies involving human subjects (Bauer and Carlsson, 1957; Leroy et al., 1966; Harrison et al., 1967; Harrison, 1981; Korsunskii et al., 1981; Newton et al., 1977, 1991, 2001) and several animal species (Richmond et al., 1960, 1962a, 1962b; Farnham and Rowland, 1965; Ellsasser et al., 1969; Hardy et al., 1969; Wood et al., 1970; Cuddihy and Griffith, 1972; Stather, 1974; Domanski et al., 1980). It has been shown that the biokinetics of barium is similar but not identical to that of radium. For example, data for a healthy 60-y-old male human injected with ^{223}Ra and ^{133}Ba indicate similar retention of these radionuclides in blood and in the total body for several days after injection but a slightly more rapid decline of whole-body ^{223}Ra after a few weeks (Harrison et al., 1967, Newton et al., 1977). In human studies, administered radium and barium isotopes have been excreted primarily in faeces (Schales, 1964; Harrison et al., 1967; Maletskos et al., 1969; Korsunskii et al., 1981) and have shown fairly similar fecal excretion rates for at least a month after injection (Harrison et al., 1967). Barium appears to be eliminated in urine at a greater rate than radium (Harrison et al., 1967), but urinary excretion constitutes only a small fraction of total excretion of both elements in humans (Harrison et al., 1967, Korsunskii et al., 1981, Newton et al., 1991). In a study of the fate of ^{226}Ra and ^{133}Ba acutely ingested by eight beagles from 43 to 1500 days of age, Della Rosa et al. (1967) found that these two radionuclides were absorbed and retained with nearly the same efficiency in each animal, with 30-d retention of barium being slightly greater as an average than that of radium. In cows, radium and barium behaved similarly with regard to secretion into the gut, resorption from bone, and concentration in pigmented tissue but differed in their rates of secretion into milk, loss in urine, and whole-body accretion (Sansom and Garner, 1966).

(335) Kinetic analysis of plasma disappearance curves for normal subjects intravenously injected with radioisotopes of calcium, strontium, barium, or radium indicates that these elements initially leave plasma at a rate of several hundred plasma volumes per day and equilibrate rapidly with an extravascular pool roughly three times the size of the plasma pool (Heaney, 1964; Harrison et al., 1967; Hart and Spencer, 1976). Total transfer rates from plasma of 70 d^{-1} yield reasonable fits to plasma disappearance curves for barium and radium at times greater than 1-2 h after injection (Leggett, 1992a). The rapid early removal from plasma is not addressed in this model.

(336) Fractional deposition of barium in the fast-turnover soft-tissue compartment ST0 is determined as the balance after other deposition fractions have been assigned. As discussed below, deposition fractions of 0.25 for bone, 0.1 for intermediate-term soft tissues (ST1), 0.002 for long-term soft tissues (ST2), and 0.32 for excretion pathways are assigned to barium, leaving 0.328 for ST0. The derived transfer rate from plasma to ST0 is 0.328 x 70 d^{-1} = 23 d^{-1}. Based on the assumed relative amounts of barium in ST0 and plasma, the transfer rate from ST0 to plasma is set at one-third the transfer rate from plasma to ST0, or 7.67 d^{-1}.

(337) Data on intermediate-term retention of injected barium in human soft tissues are largely qualitative but indicate that little barium remains in soft tissues by a few days after injection (Korsunskii et al., 1981; Newton et al., 1991). This conclusion is consistent with direct measurements of injected, ingested, or inhaled barium in tissues of laboratory animals (Garner, 1960; Loutit and Russell, 1961; Bligh and Taylor, 1963; Wood et al., 1970; Cuddihy and Griffith, 1972). *In vitro* measurements indicate that barium competes with calcium for transport across cell membranes and in some cases may be transported in preference over calcium but may not be sequestered at intracellular sites that sequester calcium or strontium

(Mullins, 1959; Shine et al., 1978; Carafoli, 1987; Tsien et al., 1987). Comparative data on the distributions of intravenously injected strontium and barium in rats (Bligh and Taylor 1963) indicate similar deposition of these elements in soft tissues but a much higher rate of loss of barium than strontium from soft tissues. In this model it is assumed that barium is deposited in the intermediate-term soft-tissue compartment ST1 to the same extent as calcium or strontium (deposition fraction = 0.1) but returns to plasma at a much higher rate than those elements. A removal half-time of 1 d for barium is broadly consistent with soft-tissue data on laboratory animals and qualitative information for human subjects. The derived transfer rate from plasma to ST1 is 0.1 x 70 d^{-1} = 7 d^{-1} and from ST1 to plasma is ln(2)/ 1 d = 0.693 d^{-1}.

(338) Despite the low intermediate-term retention of injected barium in soft tissues, a non-trivial portion of total-body barium can be found in human soft tissues after chronic exposure (Schroeder et al., 1972; ICRP, 1973, 1975; Schlenker et al., 1982). Much of this may reside in small, relatively insoluble deposits of barium sulphate (Garner, 1960; Schroeder et al., 1972; Van Middlesworth and Robison, 1975; Doig, 1976). In this model, compartment ST2 is used to account for nearly all the barium in soft tissues during chronic intake. The deposition fraction for compartment ST2 is set for consistency with the estimate that 4.7% of total-body Ba resides in soft tissues of the average adult (Schlenker et al., 1982), taking account of the projected contribution of ST1 and assuming that the removal half-time from ST2 to plasma is the same as estimated for calcium (5 y). It is assumed that 0.2% of barium leaving plasma enters ST2. The derived transfer rate from plasma to ST2 is 0.002 x 70 d^{-1} = 0.14 d^{-1} and from ST2 to plasma is ln(2)/5 y = 0.00038 d^{-1}.

(339) Data from human and animal studies indicate that the rate of loss of alkaline earth elements from bone over the first few months after injection increases in the order calcium < strontium < barium < radium, and fractional long-term retention increases in the reverse order. Some element-specific parameter values are required to account for these differences, but most of the parameter values describing bone kinetics are generic, that is, the same for each of these alkaline earth elements. The basis for applying generic values is discussed in earlier sections on calcium and strontium. Essentially, kinetic analysis of whole-body retention data for humans and more direct examination of alkaline earth kinetics in laboratory animals do not reveal distinct differences between these elements with regard to the following: early accumulation in bone as a fraction of activity reaching blood; initial division between trabecular and cortical bone; early rate of loss from bone, interpreted for purposes of the present model as transfer from bone surfaces to plasma; the fraction subject to intermediate-term retention in bone, interpreted as transfer from bone surfaces to exchangeable bone volume; and the rate of removal from bone at times remote from uptake, interpreted as removal of non-exchangeable activity due to bone resorption. The following generic parameter values are applied (see the earlier sections on calcium and strontium): fractional deposition in bone = 0.25; fractional deposition in trabecular bone = 1.25 times that on cortical bone; half-time on bone surface = 1 d, with 5/6 transferring to plasma and 1/6 to exchangeable bone volume; removal rate from non-exchangeable trabecular and cortical bone volume = 18% and 3% y^{-1}, respectively. The transfer rates for barium derived from these generic parameter values are as follows: plasma to trabecular bone surface = (1.25/2.25) x 0.25 x 70 d^{-1} = 9.72 d^{-1}; plasma to cortical bone surface = (1/2.25) x 0.25 x 70 d^{-1} = 7.78 d^{-1}; trabecular or cortical bone surface to the corresponding exchangeable bone volume compartment = (1/6) × ln(2)/1 d = 0.116 d^{-1}, trabecular or cortical bone surface to plasma is (5/6) × ln(2)/1 d = 0.578 d^{-1}; trabecular bone volume to plasma, 0.000493 d^{-1}; and non-exchangeable cortical bone volume to plasma, 0.0000821 d^{-1}.

(340) Observed differences in the behavior of alkaline earth elements in bone are accounted for by differences in the rate of removal from the exchangeable bone volume compartments and the fraction transferred from exchangeable to non-exchangeable bone volume. It is assumed, in effect, that calcium, strontium, barium, and radium are all equally likely to become temporarily incorporated in bone mineral after injection into blood but that the likelihood of reaching a non-exchangeable site in bone crystal decreases in the order calcium > strontium > barium > radium. Fractional transfers of calcium, strontium, barium, and radium from exchangeable to non-exchangeable bone volume are set at 0.6, 0.5, 0.3, and 0.2, respectively, and the balance is assumed to return to bone surfaces. The removal half-times from exchangeable bone volume are set at 100 d, 80 d, 50 d, and 30 d, respectively. These values are set to achieve reasonable consistency with whole-body retention curves for humans injected with radioisotopes of the alkaline earth elements (e.g. Harrison et al., 1967; Newton et al., 1991). The assumed fractional transfers to non-exchangeable bone volume are also reasonably consistent with results of *in vitro* measurements. For example, under conditions approximating physiological, Neuman (1964) found that calcium incorporated into forming hydroxyapatite crystals is 65% non-exchangeable, and Stark (1968) determined discrimination factors relative to calcium of 0.93 for strontium, 0.56 for barium, and 0.32 for radium in forming crystals. Such *in vitro* results have varied to some extent with experimental conditions, length of aging of the crystals, and the definition of discrimination (Neuman, 1964; Stark, 1968).

(341) For barium, the above estimates of the removal half-time from exchangeable bone volume and the fractional transfers to non-exchangeable bone volume and bone surface yield the following transfer rates: exchangeable to non-exchangeable bone volume (cortical or trabecular), 0.3 x ln(2)/50 d = 0.0042 d^{-1}; exchangeable bone volume to bone surface, 0.7 x ln(2)/50 d = 0.0097 d^{-1}.

(342) Based on estimates from human studies (Harrison et al., 1967; Newton et al., 1991), it is estimated that about 32% of barium leaving plasma is deposited in excretion pathways and that the ratio of urinary to faecal excretion is about 1:9. The derived transfer rate from plasma to the urinary bladder contents is $0.1 \times 0.32 \times 70\ d^{-1} = 2.24\ d^{-1}$ and from plasma to the contents of the right colon is $0.9 \times 0.32 \times 70\ d^{-1} = 20.16\ d^{-1}$.

(343) Newton et al. (1991, 2001) conducted a long-term study of the biokinetics of ^{133}Ba in six healthy adult male subjects. Data for the first ~3 y of that study were considered in the development of the systemic model (Leggett, 1992b) adopted in ICRP *Publication 67* (1993) and used in the present document. External measurements of whole-body retention of ^{133}Ba in each subject were continued until recently (Newton et al., 2001), providing a check on model predictions through ~13 y post injection. Model predictions are compared in Figure 6-1 with the reported data.

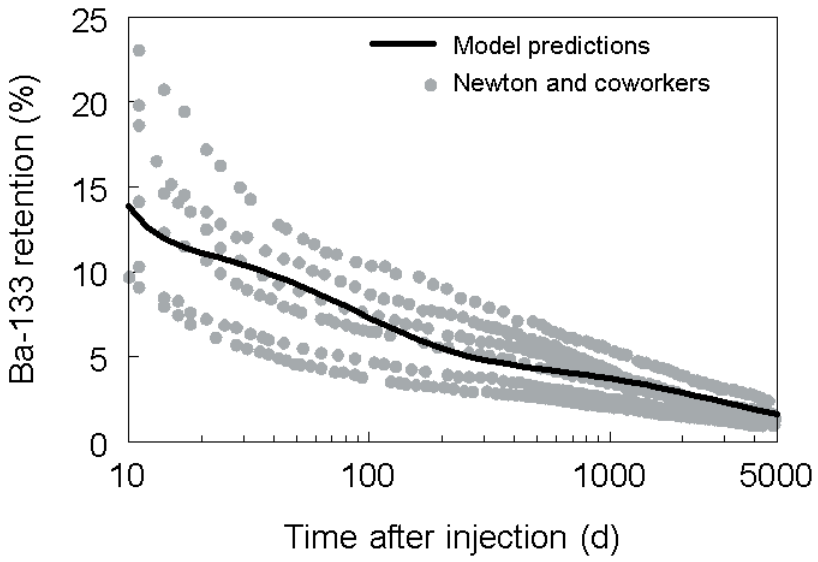

Figure 7-1. Comparisons of measured whole-body retention of ^{133}Ba intravenously injected into six healthy men (Newton et al., 1991, 2001) with predictions of the systemic biokinetic model adopted in ICRP *Publication 67* (1993) and used in this report. Data for the first ~3 y post injection were used in the construction of the model.

Table 7-3. Transfer rates (d^{-1}) for barium.

Pathway	Transfer rate (d^{-1})
Plasma to urinary bladder contents	2.2400E+00
Plasma to right colon	2.0160E+01
Plasma to trabecular bone surface	9.7200E+00
Plasma to cortical bone surface	7.7800E+00
Plasma to ST0	2.3000E+01
Plasma to ST1	7.0000E+00
Plasma to ST2	1.4000E-01
Trabecular bone surface to plasma	5.7800E-01
Trabecular bone surface to exch volume	1.1600E-01
Cortical bone surface to plasma	5.7800E-01
Cortical bone surface to exchangeable volume	1.1600E-01
ST0 to Plasma	7.6700E+00
ST1 to Plasma	6.9300E-01
ST2 to Plasma	3.8000E-04
Exchangeable trabecular bone volume to surface	9.7000E-03
Exchangeable to nonexchangeable trabecular bone volume	4.2000E-03
Exchangeable cortical bone volume to surface	9.7000E-03
Exchangeable to nonexchangeable cortical bone volume	4.2000E-03
Nonexchangeable cortical bone volume to plasma	8.2100E-05
Nonexchangeable trabecular bone volume to plasma	4.9300E-04

7.2.3.3. Treatment of radioactive progeny

(344) Several of the barium isotopes addressed in this report have radioactive progeny that may contribute significantly to dose coefficients for the internally deposited barium parent. These progeny are isotopes of barium, caesium, lanthanum, or cerium.

(345) Barium, caesium, lanthanum, and cerium atoms produced in systemic compartments by radioactive decay are assumed to follow the characteristic models for these elements (i.e. the models applied in this report to these elements as parent radionuclides) from their time of production, insofar as application of this assumption is straightforward. This assumption is sometimes ambiguous due to differences in model structures for the different elements. That is, the site of production of a radionuclide may not be clearly identifiable with a specific compartment in its characteristic model. In such cases a transfer rate from the site of production of the radionuclide to the central blood compartment in the radionuclide's characteristic model has been assigned as described below. After reaching its central blood compartment, the radionuclide is assumed to behave as described by its characteristic model.

(346) A caesium atom produced in a soft tissue compartment of the barium model is assumed to transfer to the central blood compartment of the characteristic model for cesium at the rate 1000 d^{-1}, a default value used in this report to describe rapid biological transfer. Caesium produced in a non-exchangeable bone compartment of the barium model transfers to the central blood compartment at the rate of bone turnover. Caesium produced in bone surface or exchangeable bone volume transfers to the central blood compartment at the rate of removal from bone surface compartments given in the characteristic model for caesium (0.212 d^{-1}). A caesium atom produced in the blood compartment of the barium model is assumed to be produced in the central blood compartment of the characteristic model for caesium.

(347) The characteristic model for lanthanum and cerium (the same model is applied to both elements) will appear in a later part of this series. The reader is referred to a paper by Taylor and Leggett (2003) for a description of the model. In this report, a lanthanum or cerium atom produced in a soft-tissue compartment of the barium model is assumed to transfer to the blood compartment of the lanthanum/cerium model with a half-time of 0.5 d. This is the shortest biological half-time for any soft tissue compartment in that model. A lanthanum or cerium atom produced in a bone compartment of the barium model is assumed to behave as if deposited in that compartment as a parent radionuclide. With regard to the biokinetics of lanthanum or cerium, no distinction is made between production in an exchangeable or a non-exchangeable bone volume compartment of the barium model. In either case the assigned removal rate to the corresponding marrow compartment is the rate of bone turnover.

7.3. Individual monitoring

^{133}Ba

(348) Monitoring of ^{133}Ba is usually accomplished through urine bioassay.

Isotope	Monitoring Technique	Method of Measurement	Typical Detection Limit	Achievable detection limit
^{133}Ba	Urine Bioassay	γ-ray spectrometry	0.6 Bq/L	0.06 Bq/L
^{133}Ba	Whole Body Counting	γ-ray spectrometry	100 Bq	32 Bq

^{140}Ba

(349) Monitoring of ^{140}Ba is usually accomplished through urine bioassay. Whole Body Counting may also be used.

Isotope	Monitoring Technique	Method of Measurement	Typical Detection Limit	Achievable detection limit
^{140}Ba	Urine Bioassay	γ-ray spectrometry	1 Bq/L	0.1 Bq/L
^{140}Ba	Whole Body Counting	γ-ray spectrometry	80 Bq	51 Bq

References

Bauer, G.C.H., Carlsson, A., 1957. Lindquist, B. Metabolism of Ba-140 in man. Acta Orth. Scand. 26, 241-257.

Bligh, P.H., Taylor, D.M., 1963. Comparative studies of the metabolism of strontium and barium in the rat. Biochem. J. 87, 612-618.

Boender, C.A., Verloop, M.C., 1969. Iron absorption, iron loss and iron retention in man: studies after oral administration of a tracer dose of 59FeSO4 and 131-BaSO4. Br. J. Haematol., 17, 45-58.

Carafoli, E., 1987. Intracellular calcium homeostasis Ann. Rev. Biochem. 56, 395-433.

Cember, Watson, J.A., Novak, M.E., 1961. The influence of radioactivity and lung burden on the pulmonary clearance rate of barium sulphate. Am. Ind. Hyg. Assoc. J., 22, 27–32.

Clavel, J.P., Lorillot, M.L., Buthiau, D., Gerbet, D., Heitz, F., Galli, A., 1987. Intestinal absorption of barium during radiological studies. Therapie 42, 239-43.

Cuddihy, R.G., Ozog, J.A., 1973. Nasal absorption of CsCl, $SrCl_2$, $BaCl_2$ and $CeCl_3$ in Syrian hamsters. Health Phys., 25, 219–224.

Cuddihy, R.G., Griffith, W.C., 1972. A biological model describing tissue distribution and whole-body retention of barium and lanthanum in beagle dogs after inhalation and gavage. Health Phys., 23, 621-633.

Cuddihy, R.G., Hall, R.P., Griffith, W.C., 1974. Inhalation exposure to barium aerosols: physical, chemical and mathematical analysis. Health Phys., 26, 405–416.

Della Rosa, R.J., Goldman, M., Wolf, H.G., 1967. Uptake and retention of orally administered Ra-226 and Ba-133: A preliminary report, University of California at Davis, Report 472-114, pp. 40-41;

Doig, A.T., 1976. Baritosis: a benign pneumoconiosis. Thorax 31, 30-39.

Domanski, T., Witkowska, D., Garlicka, I., 1980. Influence of age on the discrimination of barium in comparison with strontium during their incorporation into compact bone. Acta Physiol. Pol., 31, 289-296.

Ellsasser, J.C., Farnham, J.E., Marshall, J.H., 1969. Comparative kinetics and autoradiography of Ca-45 and Ba-133 in ten-year-old beagle dogs. J. Bone Jt. Surg. 51A, 1397-1412.

Farnham, J.E., Rowland, R.E., 1965. The retention of Ba-133 in beagles. In: Radiological physics division annual report, July 1964 through June 1965, Argonne National Laboratory; ANL-7060; 70-73.

Figueroa, W.G., Jordan, T., Basset, S.H., 1968. Use of barium sulfate an an unabsorbable fecal marker. Am. J. Cin. Nutr., 21, 1239-1245.

Garner, R.J., 1960. Distribution of radioactive barium in eye tissues. Nature 184, 733-734.

Hardy, E., Rivera, J., Fisenne, I., Pond, W., Hogue, D., 1969. Comparative utilization of dietary radium-226 and other alkaline earths by pigs and sheep. In: Sikov, M.R., Mahlum, D.D. (Eds.), Radiation biology of the fetal and juvenile mammal. Proc. 9th Annual Hanford Biology Symposium at Richland, Washington, May 5-8, 1969. U.S. AEC, Division of Technical Information, 183-190.

Harrison, G.E., 1981. Whole body retention of the alkaline earths in adult man. Health Phys., 40, 95-99.

Harrison, G.E., Carr, T.E.F., Sutton, A., 1967. Distribution of radioactive calcium, strontium, barium and radium following intravenous injection into a healthy man. Int. J. Radiat. Biol., 13, 235-247.

Harrison, G.E., Raymond, W.H.A., Tretheway, H.C., 1956. The estimation of barium and strontium in biological materials by activation analysis with special reference to the turnover of strontium in man. In: Proc. International Conference on the Peaceful uses of Atomic Energy. Vol. 11, Biological effects of radiation. New York, United Nations, 156-159.

Hart, H.E., Spencer, H., 1976. Vascular and extravascular calcium interchange in man determined with radioactive calcium. Radiat. Res., 67, 149-161.

Heaney, R.P., 1964. Evaluation and interpretation of calcium-kinetic data in man. Clin. Orthop. Rel. Res., 31, 153-183.

ICRP, 1973. Alkaline Earth Metabolism in Adult Man. ICRP Publication 20, Pergamon Press, Oxford.

ICRP, 1979. Limits on Intakes of Radionuclides for Workers. ICRP Publication 30, Pt.1. Ann. ICRP 2. (3/4).

ICRP, 1993. Age-dependent doses to members of the public from intake of radionuclides, Part 2. Publication 67, Ann. ICRP 23(3/4).

Korsunskii, V.N., Tarasov, N.F., Naumenko, A.Z., 1981. Clinical evaluation of Ba-133m as an osteotropic agent. ORNL/TR-86/30 (7 pgs); Translated from the Russian UDC 616.71-006-073.916, Meditsinskaya Radiologiya No. 10, pp. 45-48.

Leggett, R.W., 1992a. Fractional absorption of ingested barium in adult humans. Health Phys., 62, 556-61.

Leggett, R.W., 1992b. A generic age-specific biokinetic model for calcium-like elements. Radiat. Prot. Dosim., 41, 183-198.

LeRoy, G.V., Rust, J.H., Hasterlik, R.J., 1966. The consequences of ingestion by man of real and simulated fallout. Health Phys., 12, 449-473.

Loutit, J.F., Russell, R.S., (Eds.), 1961. Progress in Nuclear Energy, Series VI, Biological Sciences. Vol. 3, The entry of fission products into food chains. Pergamon Press, New York.

Maletskos, C.J., Keane, A.T., Telles, N.C., Evans, R.D., 1969. Retention and absorption of Ra-224 and Th-234 and some dosimetric considerations of Ra-224 in human beings. In: Mays, C.W., Jee, W.S.S., Lloyd, R.D., Stover, B.J., Dougherty, J.H., Taylor, G.N. (Eds.), Delayed effects of bone-seeking radionuclides, edSalt Lake City, UT. University of Utah Press, 29-49.

Morrow, P.E., Gibb, F.R., Johnson, L., 1964. Clearance of insoluble dust from the lower respiratory tract. Health Phys., 10, 443–555.

Mullins, L.J., 1959. The penetration of some cations into muscle. J. Gen. Physiol., 42, 817-829.

Neuman, W.F., 1964. Blood-bone exchange. In: Frost, H.M., (Ed.), Bone biodynamics, Boston, Little, Brown, and Co, 393-408.

Newton, D., Ancill, A.K., Naylor, K.E., Eastell, R., 2001. Long-term retention of injected barium-133 in man. Radiat. Prot. Dosim., 97, 231-240.

Newton, D., Harrison, G.E., Kang, C., Warner, A. J., 1991. Metabolism of injected barium in six healthy men. Health Phys., 61, 191-201.

Newton, D., Rundo, J., Harrison, G.E., 1977. The retention of alkaline earth elements in man, with special reference to barium. Health Phys., 33, 45-53.

Patrick, G., Stirling, C., 1977. The retention of particles in large airways of the respiratory tract. Proc. R. Soc. Lond. B., 198, 455–462.

Patrick, G., Stirling, C., 1997. Slow clearance of different-sized particles from rat trachea. J. Aero. Med., 10, 55–65.

Richmond, C.R., Furchner, J.E., Trafton, G.H., 1962a. Retention and excretion of orally administered Ba-133 by mice. Los Alamos Scientific Laboratory Report LAMS-2780, 17-25.

Richmond, C.R., Furchner, J.E., Trafton, G.H., 1962b. Retention and excretion of orally administered Ba-133 by rats. Los Alamos Scientific Laboratory Report LAMS-2780, 26-34.

Richmond, C.R., Furchner, J.E., Trafton, G.H., 1960. Retention of Ba-133 in mice, rats, and dogs. Los Alamos Scientific Laboratory Report LAMS-2455, 24-31.

Sansom, B.F., Garner, R.J., 1966. The metabolism of radium in dairy cows. Biochem. J. 99, 677-81.

Schales, F., 1964. The excretion of thorium X and its daughter products after intravenous injection in man. In: Assessment of radioactivity in man, Vol. II, Vienna, IAEA, 267-276.

Schlenker, R.A., Keane, A.T., Holtzman, R.B., 1982. The retention of Ra-226 in human soft tissue and bone; implications for the ICRP 20 alkaline earth model. Health Phys., 42, 671-693.

Schroeder, H.A., Tipton, I.H., Nason, A.P., 1972. Trace metals in man: strontium and barium. J. Chron. Dis., 25, 491-517.

Shine, K.I., Douglas, A.M., Ricchiuti, N.V., 1978. Calcium, strontium, and barium movements during ischemia and reperfusion in rabbit ventricle. Circ. Res., 43, 712-720.

Stark, G., 1968. Studies on synthetic hydroxyapatite crystals with regard to metabolism of calcium, strontium, barium and radium in bone. I. The discrimination against calcium. Biophysik., 5, 42-54.

Stather, J.W., 1974. Distribution of P-32, Ca-45, Sr-85 and Ba-133 as a function of age in the mouse skeleton. Health Phys., 26, 71-79.

Takahashi, S., Patrick, G., 1987. Long term retention of ^{133}Ba in the rat trachea following local administration as barium sulfate particles. Radiat. Res., 110, 321–328.

Takahashi, S., Kubota, Y., Sato, H., Matsuoka, O., 1993. Retention of ^{133}Ba in the trachea of rabbits, dogs and monkeys following local administration of $^{133}BaSO_4$ particles. Inhalation Toxicology 5, 265–273.

Taylor, D.M., Bligh, P.H., Duggan, M.H., 1962. The absorption of calcium, strontium, barium, and radium from the gastrointestinal tract of the rat. Biochem. J., 83, 25-29.

Taylor, D.M., Leggett, R.W. 2003. A generic biokinetic model for predicting the behaviour of the lanthanide elements in the human body. Radiat. Prot. Dosimetry, 105, 193-198.

Tipton, I.H., Stewart, P.L., Dickson, J., 1969. Patterns of elemental excretion in long term balance studies. Health Phys., 16, 455-462.

Tsien, R.W., Hess, P., McCleskey, E.W., Rosenberg, R.L., 1987. Calcium channels: Mechanisms of selectivity, permeation, and block. Ann. Rev. Biophys. Biophys. Chem., 16, 265-290.

Van Middlesworth, L., Robison, W.L., 1975. Thyroid concentration of barium and radium. Int. J. Nucl. Med. Biol., 2, 1-4.

Wood, S.K., Farnham, J. E., Marshall, J.H., 1970. Ca-45, Ba-133, and Ra-226 in 6-to 10-year-old beagle dogs: A 100-day study. In: Radiological Physics Division annual report, Center for Human Radiobiology, July 1969 through June 1970; Argonne, IL: Argonne National Laboratory; ANL-7760, Part II, Biology and Medicine, 110-132.

8. IRIDIUM (Z = 77)

8.1. Chemical Forms in the Workplace

(350) Iridium is a transition metal, which occurs mainly in oxidation states III and IV. Iridium may be encountered in industry in a variety of chemical and physical forms, including oxides (IrO_2, Ir_2O_3), chlorides and fluorides. Iridium also forms a number of organometallic compounds, such as iridium carbonyl.

(351) Iridium-192 is used as a gamma radiation brachytherapy source for the treatment of cancer.

Table 8-1. Isotopes of iridium addressed in this report

Isotope	Physical half-life	Decay mode
Ir-182	15 m	EC, B+
Ir-183	58 m	EC, B+
Ir-184	3.09 h	EC, B+
Ir-185	14.4 h	EC, B+
Ir-186	16.64 h	EC, B+
Ir-186m	1.92 h	EC, B+, IT
Ir-187	10.5 h	EC, B+
Ir-188	41.5 h	EC, B+
Ir-189	13.2 d	EC
Ir-190	11.78 d	EC
Ir-190m	1.12 h	IT
Ir-190n	3.087 h	EC, IT
Ir-192[a]	73.827 d	B-, EC
Ir-192n	241 y	IT
Ir-193m	10.53 d	IT
Ir-194	19.28 h	B-
Ir-194m	171 d	B-
Ir-195	2.5 h	B-
Ir-195m	3.8 h	B-, IT
Ir-196m	1.40 h	B-

[a] Data for these radionuclides are given in the printed copy of this report. Data for other radionuclides are given on accompanying electronic disk.

8.2. Routes of Intake

8.2.1. Inhalation

Absorption Types and parameter values

(352) Some information was found on the behaviour of inhaled iridium in man following accidental intakes. Information is available from experimental studies of iridium chloride and elemental iridium.

(353) Absorption parameter values and Types, and associated f_A values for particulate forms of iridium are given in Table 8-2.

Iridium chloride

(354) Kreyling et al. (2002) followed the biokinetics of ^{192}Ir for 7 days after intratracheal instillation of $^{192}IrCl_3$ into rats. By 7 days, about 8% of the initial lung deposit (ILD) remained in the lungs, 10% ILD in soft tissues and bone, and smaller amounts in other tissues; 60% was excreted in urine and 10% in faeces (mostly in the first three days). Similar results (unpublished) were obtained following inhalation (Kreyling, 2010). Analysis here gave f_r approximately 0.9. There is insufficient information to estimate other parameter values precisely, but the low fecal excretion suggests that the rapid dissolution rate is high compared to particle transport rates from the upper respiratory tract, 100 d^{-1}, or more. The results thus indicate assignment to Type F.

Elemental iridium (metal/oxide)

(355) Casarett et al. (1960) followed the biokinetics of ^{192}Ir for 28 days after inhalation by rats of the aerosol formed by nebulising an aqueous suspension of ^{192}Ir-labelled iridium. They estimated that about 95% of the initial deposit (ID) deposited in the upper respiratory tract. Only about 0.2% ID was retained in the lungs after 2 days, clearing with a half-time of about 23 days. Immediately after inhalation about 5% ID was found in the carcass, which reduced to about 0.5% by 14 days, with a corresponding increase in urinary excretion. These results suggest that the rapid dissolution rate is high compared to the particle transport rate from the upper respiratory tract, 100 d^{-1}, or more. On that assumption, analysis by the task group gave f_r approximately 0.1, indicating assignment to Type M or S.

(356) Kreyling and co-workers have used ^{192}Ir-labelled particles produced with a spark generator (an intermittent arc between two electrodes in argon) as relatively inert particles to study the biokinetics of inhaled ultrafine particles, especially particle transport pathways. The aerosol, produced by evaporation and condensation, consists of agglomerates of primary particles of about 2-5 nm diameter. Analysis showed the iridium nanoparticles to be oxidised at the surface (Szymczak et al., 2006). The aerosol was administered (via an endotracheal tube) to rats which were intubated and ventilated, to avoid extrathoracic deposition and to optimize deep lung deposition. In a complementary experiment in which a suspension of the particles was administered via the oesophagus, no detectable ^{192}Ir was observed in urine (Kreyling et al., 2002), which suggests that fractional absorption from the alimentary tract f_A <0.0001.

(357) Kreyling et al. (2002) followed the biokinetics of ^{192}Ir for 7 days after inhalation (via an endotracheal tube) by rats of 15-nm and 80-nm count median diameter (CMD) agglomerates of ^{192}Ir-labelled particles, or intratracheal instillation of a particle suspension (15-nm CMD). By 7 days after inhalation 47% and 36% of the deposited 15- and 80-nm particles had cleared, predominantly to faeces. Following inhalation of both aerosols urinary excretion by 7 days was ~2% ILD, and following instillation ~0.1% ILD. For both aerosols, a few percent of the ILD was found in tissues other than the lung, but most of this ^{192}Ir was attributed to particle translocation, rather than dissolution. Semmler et al. (2004) followed the biokinetics of ^{192}Ir for 180 days after inhalation (via an endotracheal tube) of 15-nm CMD agglomerates of ^{192}Ir-labelled particles. As in the study by Kreyling et al. (2002), only small fractions of ILD were found in tissues other than the lung, and most was attributed to particle translocation. Based on these results, those of Kreyling et al. (2002), and unpublished excretion data (Kreyling, 2010) parameter values assessed here were $f_r = 0.0$ and $s_s = 0.01$ d^{-1}, giving assignment to Type M.

(358) Cool et al. (1979) followed lung retention and excretion of ^{192}Ir for two years after accidental inhalation of iridium aerosol (produced by cutting into a source) by two workers. Biological retention half times assessed from lung retention and fecal excretion were in the

range 700 – 3000 days, and it was reported that urine samples showed only “low activity”, indicating assignment to Type S.

(359) Whole-body retention of ^{192}Ir was followed for four months after accidental inhalation by a worker of aerosol (considered to be metal or oxide) produced by grinding the tip of an electrode, which had been used to seal ^{192}Ir sources for industrial radiography by electro-welding (IAEA, 1999). Partial-body monitoring showed the highest count rate above the chest. There was little clearance after 13 days, indicating assignment to Type S.

^{192}Ir-labelled carbon

(360) Kreyling et al. (2009) produced carbon chain aggregates (~25-nm CMD) containing a small fraction (< 1%) of ^{192}Ir ultrafine (2-5 nm) particles by spark discharge between an ^{192}Ir-labelled iridium electrode and a graphite rod. At 24 hours after inhalation (via an endotracheal tube) by rats, particle translocation to tissues (measured by ^{192}Ir activity) was less than for 20-nm pure iridium (see above).

Rapid dissolution rate for iridium

(361) The experimental information for iridium chloride and elemental iridium suggests that the rate is high compared to particle transport rates from the upper respiratory tract, 100 d^{-1}, or more, but is insufficient to provide an estimate. There is therefore no justification for choosing a rate different from the general default value of 30 d^{-1}, which is applied here to all Type F forms of iridium.

Extent of binding of iridium to the respiratory tract

(362) Information from the iridium chloride study outlined above suggests that about 10% of iridium deposited in the lungs in soluble form is retained. However there is no evidence that it is retained in the bound state rather than in particulate form. It is therefore assumed that for iridium the bound state can be neglected, i.e. $f_b = 0.0$.

Table 8-2. Absorption parameter values for inhaled and ingested iridium

Inhaled particulate materials		Absorption parameter values[a] f_r	s_r (d^{-1})	s_s (d^{-1})	Absorption from the alimentary tract, f_A
Default parameter values[b,c]					
Absorption Type	Assigned forms				
F	Iridium chloride	1	30	–	0.01
M	All unspecified forms[d]	0.2	3	0.005	0.002
S	Elemental iridium	0.01	3	$1x10^{-4}$	$1x10^{-4}$
Ingested materials					
All unspecified forms					0.01

[a] It is assumed that for iridium the bound state can be neglected i.e. $f_b = 0$. The values of s_r for Type F, M and S forms of iridium (30, 3 and 3 d^{-1}, respectively) are the general default values.

[b] Materials (e.g. iridium chloride) are listed here where there is sufficient information to assign to a default absorption Type, but not to give specific parameter values (see text).

[c] For inhaled material deposited in the respiratory tract and subsequent cleared by particle transport to the alimentary tract, the default f_A values for inhaled materials are applied: i.e. the product of f_r for the absorption Type and the f_A value for ingested soluble forms of iridium (0.01).

[d] Default Type M is recommended for use in the absence of specific information, i.e. if the form is unknown, or if the form is known but there is no information available on the absorption of that form from the respiratory tract.

8.2.2. Ingestion

(363) No human data are available on the absorption of iridium from the gastrointestinal tract.

(364) The fractional absorption of iridium, administered as chloride ($Na_2{}^{192}IrCl6$), has been measured in several mammalian species (mouse, rat, monkey and dog) and ranged from 0.01 in mice to about 0.04 in monkeys (Furchner et al., 1971).

(365) In *Publication 30* (ICRP, 1979), an absorption value of 0.01 was recommended. Since no new data on the gastrointestinal absorption seem to be available, an f_A value of 0.01 is adopted here for all chemical forms.

8.2.3. Systemic Distribution, Retention and Excretion

8.2.3.1. Summary of the database

Data for human subjects

(366) Data on the biokinetics of iridium in human subjects are primarily from cases of accidental inhalation of ^{192}Ir (Cool et al., 1979; Kelsey and Mettler, 2001; Brodsky and Wald, 2004). The case studies provide little information on the systemic behavior of iridium.

Data for laboratory animals

(367) Casarett et al. (1960) studied the biokinetics of acutely inhaled metallic ^{192}Ir in rats. The count median diameter of the particles was 0.07 μm with a geometric standard deviation of about 1.5. Several rats were sacrificed immediately after exposure for determination of deposition in the respiratory tract, and pairs of rats were sacrificed at 3 h after exposure and at 1, 3, 6, 9, 13, and 14 d after exposure. Excretion was measured in some animals up to 28 d. Mean deposition in the respiratory tract was ~58% of the inhaled activity. More than 95% of the deposition was in the upper respiratory tract. The half-time of the initial phase of clearance was 2-4 h, and the half-time of a second phase was ~24 h. Activity was found in the liver in two rats immediately after exposure and in one rat at 3 h after exposure, amounting to about 0.2-0.6% of the deposited amount. In other rats, no significant activity was found in the liver or other tissues excluding skin except for spleen in two rats (0.14% at time zero and 0.02% at 3 d) and bone in two rats (0.55% at time zero and 0.14% at 3 h). Small but measurable activities were found in skin throughout the 28-day study. Urinary and fecal excretion accounted for <4% and >96% of the deposited amount, respectively, over 28 days. The urinary excretion rate averaged over 48-hour periods was on the order of 1%/day for 0-2 d, 0.1%/day for 10-12 d, and 0.01%/day for 26-28 d.

(368) Durbin et al. (1957, 1960) described the results of tracer studies with ^{190}Ir or ^{192}Ir in

rats. Kidney, liver, and spleen were the main deposition sites. Excretion was mainly in urine. After intravenous injection 36% was excreted in urine in the first 4 h. At 1 d the liver, kidneys, bone, blood, and muscle of rats contained 19.3%, 4%, 3.1%, 6.4%, and 5.6% and excretion accounted for 43.5% of the administered amount. By 33 d, 45% was excreted in urine and 35% in faeces, and about 12% remained in liver, skin, and muscle.

(369) Furchner et al. (1971) studied the systemic behavior of ^{192}Ir in mice, rats, monkeys, and dogs after oral administration, intravenous injection, or intraperitoneal injection of $Na_2{}^{192}IrCl_6$. Cumulative urinary excretion during the first two days after oral intake averaged 0.86% of the administered amount in mice, 2.02% in Mystromys rats, 0.96% in Sprague-Dawley rats, 1.34% in monkeys, and 3.54% in dogs. These results indicate that average fractional uptake by the gastrointestinal tract was higher than the value 0.01 applied to iridium in ICRP *Publication 68* (1994). Whole-body retention over several months following intravenous or intraperitoneal injection was similar in dogs, mice, Mystromys rats, and Sprague-Dawley rats (Figure 8-1). Monkeys showed lower excretion rates initially than dogs, mice, or rats but a faster drop in the body burden than the other species at times remote from injection (Figure 8-1). Whole-body retention in all species could be described in terms of three components with average biological half-times on the order of a few hours, a week, and several months (120-375 d). On average the rapid phase of loss represented about 20% (9-27%) of the administered amount, compared with mean excretion of 43.5% in rats receiving ^{190}Ir or ^{192}Ir chloride by intravenous injection as reported by Durbin (1960). The long-term component represented at least 46% of the administered amount in all species. As illustrated in Table 8-3, whole-body retention curves based on the different animal species and different modes of injection give fairly similar cumulative activities in the body for iridium isotopes with a range of half-lives. The distribution of activity was determined in rats over the first 120 d after intraperitoneal injection. The retention times in individual organs roughly paralleled that in the whole body. Highest concentrations were found in spleen, kidneys, and liver, in that order. The concentration in bone was a factor of 2-3 lower than that of liver but higher than the average concentration in the body. The liver, kidneys, and bone contained roughly 15%, 5%, 1-2%, and 10% of total-body content, respectively, during the observation period. The authors concluded from comparison with injection data of Durbin et al. (1957) for rats that the rate of loss of iridium from the body depends on the chemical form reaching blood.

(370) Ando et al. (1989) determined the distribution of ^{192}Ir in rats at 3, 24, and 48 h after intravenous injection of $H_2{}^{192}IrCl_6$. Cumulative urinary excretion at 3 h represented 79.8% of injected ^{192}Ir. At all three observation times the highest concentration was found in the kidneys, followed by liver. In contrast to findings of Durbin et al. (1957) and Furchner et al. (1971), the concentration of iridium in the spleen was an order of magnitude lower than that of kidney and a factor of 3-4 lower than that of liver.

(371) Hirunuma et al. (1997) studied uptake, retention, and excretion of 17 trace elements including iridium in Wistar rats over the first 6 d after oral intake of radioisotopes of these elements in a hydrochloric acid solution. Iridium was found in liver, kidney, and intestinal tissue, with the kidneys generally showing the highest concentration. Iridium was not detectable by the multi-tracer technique in brain, skeletal muscle, bone, spleen, testes, or blood. On Day 3 the liver, kidneys, and intestines contained about 0.35%, 0.26%, and 0.13%, respectively, of the administered iridium. On Day 6 these three organs contained about 0.11%, 0.13%, and 0.04%, respectively, of the administered iridium. Over the 6-day study about 90% of the administered iridium was excreted in faeces and 7.7% was excreted in urine, indicating that most of the absorbed iridium was excreted during the short study period.

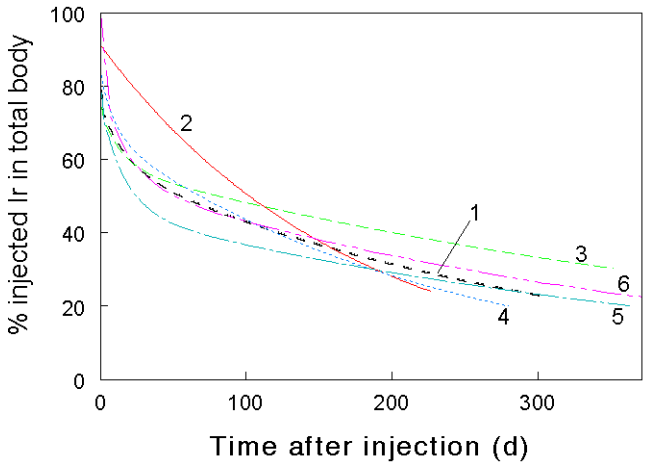

Figure 8-1. Whole-body retention of 192Ir in laboratory animals following intravenous (iv) or intraperitoneal (ip) injection of $Na_2{}^{192}IrCl_6$ (curve fits reported by Furchner et al., 1971). Curve 1 = dogs, iv injection, observation period 304 d; 2 = monkeys, iv, 227 d; 3 = mice, iv, 352 d; 4 = rats, iv, 280 d; 5 = mice, ip, 364 d; 6 = rats, ip, 371 d.

Table 8-3. Cumulative activities of iridium isotopes in the whole body based on retention curves derived by Furchner et al. (1971). Values for a given isotope are normalized to the value for that isotope in dogs.

Isotope	Half-life	Dogs[a]	Monkeys[a]	Mice[a]	Rats[a]	Mice[b]	Rats[b]
Ir-190	11.78 d	1.0	1.3	1.0	1.1	0.8	1.0
Ir-192	73.827 d	1.0	1.2	1.1	1.0	0.7	1.0
Ir-192n	241 y	1.0	0.8	1.7	0.8	0.6	1.2
Ir-194	19.28 h	1.0	1.1	1.0	1.0	1.0	1.1
Ir194m	171 d	1.0	1.1	1.2	1.0	0.7	1.1

[a] intravenous injection
[b] intraperitoneal injection

8.2.3.2. Biokinetic model for systemic iridium

(372) Biokinetic data for iridium summarized above indicate that whole-body retention is not predictable on the basis of body size and does not vary greatly from one species to another. Three phases of excretion of absorbed or intravenously injected iridium are indicated: a rapid phase of loss, primarily in urine, with a half-time of a few hours; an intermediate phase of loss with a half-time on the order of 1-2 wk; and a slow phase of loss with a half-time of several months. The fraction of uptake associate with each of these phases is variable and depends on the form of iridium reaching blood. For example, the fraction associated with the rapid phase of loss in urine has varied from <0.1 to 0.8 or more. The rate of loss from individual tissues roughly parallels that in the whole body. Concentrations of iridium in the kidneys and liver are much higher than those in most other tissues. Elevated uptake of iridium by the spleen is indicated by some data, but findings are inconsistent. Data on rats indicate that the liver contains roughly 15-20% of the systemic content during the first few months after input to blood. Most studies indicate that kidneys and bone accumulate less

iridium than does the liver.

(373) The structure of the biokinetic model for systemic iridium is shown in Figure 8-2. Transfer coefficients are listed in Table 8-4. Whole-body retention data of Furchner et al. (1971) for dogs were used as a guide for model parameters. The retention data for dogs are typical of the studied species.

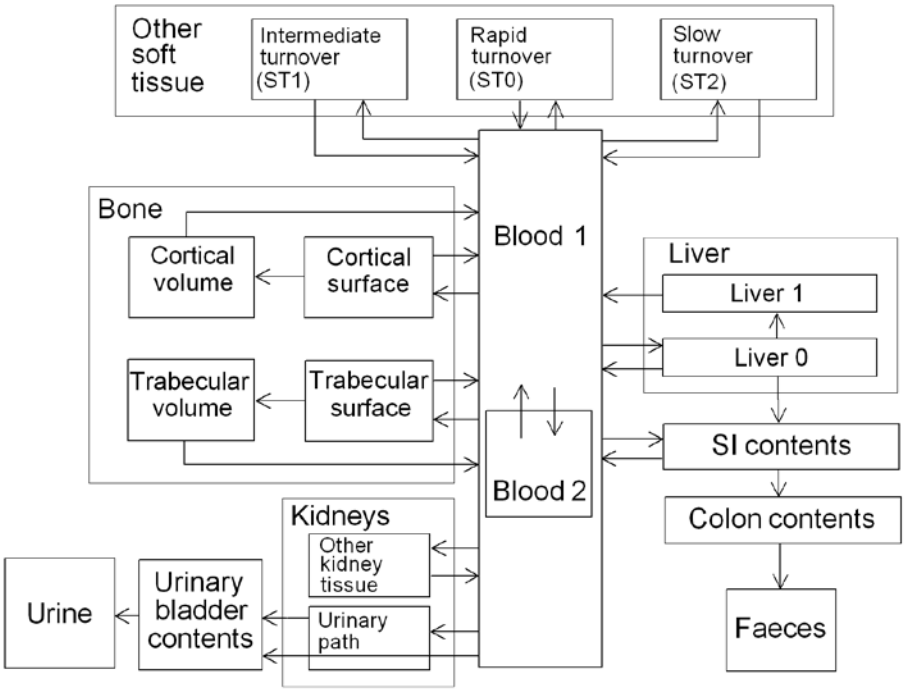

Figure 8-2. Structure of the biokinetic model for systemic iridium.

Table 8-4. Transfer coefficients for systemic iridium

From	To	Transfer coefficient (d^{-1})
Blood 1	Small intestine contents	4.0
Blood 1	Urinary bladder contents	12
Blood 1	Liver 1	12
Blood 1	Urinary path	4.0
Blood 1	Other kidney tissue	2.0
Blood 1	Blood 2	27
Blood 1	ST0	15
Blood 1	ST1	15
Blood 1	ST2	1.0
Blood 1	Cortical bone surface	4.0
Blood 1	Trabecular bone surface	4.0
Blood 2	Blood 1	0.693
Liver 1	Blood 1	0.0231
Liver 1	Small intestine contents	0.0462
Liver 1	Liver 2	0.0693
Liver 2	Blood 1	0.00693
Urinary path	Urinary bladder contents	0.139
Other kidney tissue	Blood 1	0.00693
ST0	Blood 1	0.0693
ST1	Blood 1	0.00693
ST2	Blood 1	0.00095
Cortical bone surface	Blood 1	0.0185
Trabecular bone surface	Blood 1	0.0185
Cortical bone surface	Cortical bone volume	0.00462
Trabecular bone surface	Trabecular bone volume	0.00462
Cortical bone volume	Blood 1	0.0000821
Trabecular bone volume	Blood 1	0.000493

(374) In the model for iridium, urinary excretion is assumed to arise from transfer of activity from blood into the urinary bladder contents and transfer from blood to the kidneys (Urinary path) and subsequent release to the urinary bladder contents over a period of days. Fecal excretion is assumed to arise in part from biliary secretion into Small intestine contents from a liver compartment (Liver 1) and in part from secretion from Blood 1 into Small intestine contents. The parameter values are set so that the two sources of faecal excretion contribute equally to endogenous faecal excretion of iridium, in the absence of specific data on relative contributions of these sources. Deposition fractions and removal half-times for compartments are set to reproduce different phases of loss of iridium from the total body observed in laboratory animals.

(375) Clearance of iridium from blood is modeled on the basis of human data for the chemically related element ruthenium (Veronese et al., 2003, 2004). Blood is divided into two compartments called Blood 1 and Blood 2. Iridium entering blood is assigned to Blood 1, which is a rapid-turnover pool. Blood 2 is a more slowly exchanging pool that contains the preponderance of activity in blood except for a short period soon after acute uptake of iridium. Activity leaves Blood 1 at the rate 100 d^{-1}, corresponding to a half-time of ~10 min, with 27% of outflow going to Blood 2 and the remaining 73% divided among tissue

compartments, urinary bladder contents, and gastrointestinal contents. Activity moves from Blood 2 back to Blood 1 with a half-time of 1 d.

(376) In addition to the 27% of outflow from Blood 1 assigned to Blood 2, outflow from Blood 1 is assumed to be distributed as follows: 12% to Liver, 6% to Kidneys, 8% to Bone, 12% to the Urinary bladder contents, 4% to Small intestine contents, and the remainder (31%) to Other. Activity entering Liver is assigned to a compartment called Liver 1 that has relatively fast turnover. Two-thirds of the activity entering Kidneys (4% of outflow from Blood 1) is assigned to Urinary path and one-third (2%) to Other kidney tissue; thus, a total of 12% + 4% = 16% of activity leaving Blood 1 enters the urinary excretion pathways. Activity depositing in bone is divided equally between Cortical bone surface and Trabecular bone surface. Activity entering Other is divided as follows: fast-turnover compartment ST0, 15%; intermediate turnover compartment ST1, 15%; and slow-turnover compartment ST2, 1%.

(377) Activity transfers from Liver 1 with a half-time of 5 d, with one-third going to the Small intestine contents (biliary secretion), one-half to Liver 2, and one-sixth to Blood 1. Activity transfers from Liver 2 to Blood 1 with a half-time of 100 d. Activity transfers from Urinary path to Urinary bladder contents with a half-time of 5 d and from Other kidney tissues to Blood 1 with a half-time of 100 d. Activity in soft-tissue compartments ST0, ST1, and ST2 returns to Blood 1 with half-times of 10 d, 100 d, and 2 y, respectively. Activity leaves Cortical and Trabecular bone surface with a half-time of 30 d, with 80% returning to Blood 1 and 20% entering the corresponding bone volume compartment. Activity is transferred from the bone volume compartments to Blood 1 at the rate of bone turnover.

(378) As illustrated in Figure 8-3, model predictions approximate whole-body retention of iridium as determined in dogs after intravenous injection with ^{192}Ir (Furchner et al., 1971).

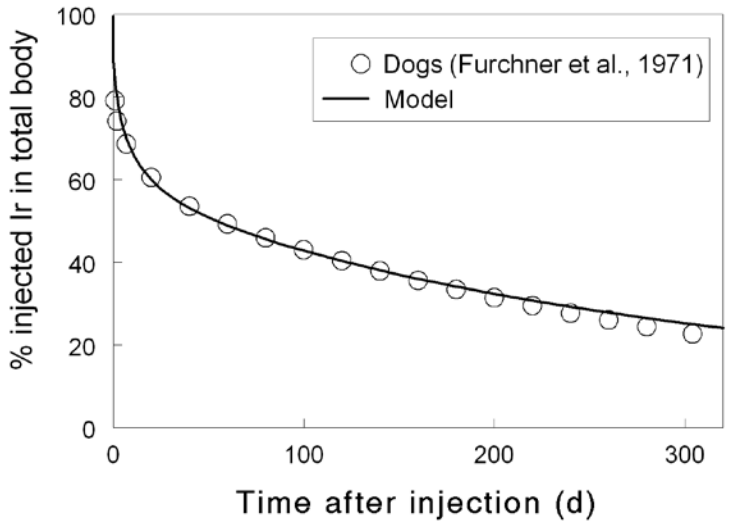

Figure 8-3. Comparison of model predictions of whole-body retention of iridium with observations for dogs. Data points derived from whole-body retention curve reported by Furchner et al. (1971) for dogs intravenously injected with $Na_2{}^{192}IrCl_6$.

8.2.3.3. Treatment of radioactive progeny

(379) Chain members addressed in the derivation of dose coefficients for isotopes of iridium are isotopes of platinum, osmium, and rhenium. Independent kinetics of chain members is assumed.

(380) Platinum and osmium are members of the platinum group, which also contains iridium, ruthenium, rhodium, and palladium. These six metals are chemically similar and generally are found together in ores.

(381) The systemic biokinetics of ingested, inhaled, or injected platinum has been studied in laboratory animals, mainly rats, and to some extent in human subjects (Durbin et al., 1957; Durbin, 1960; Lange et al., 1973; Smith and Taylor, 1974; Litterst et al., 1976; Yoakum et al., 1975; Moore et al., 1975a,b,c; Hirunuma et al., 1997). Platinum shows a high rate of urinary excretion in the early days after administration. Some but not all studies also indicate a relatively high rate of faecal excretion. Following intravenous administration of platinum isotopes as the chloride to rats, highest concentrations generally were found in the kidneys, followed by the liver (Durbin et al., 1957; Moore et al., 1975a,b,c). At 1 mo the rats contained roughly 10-15% of the intravenously injected activity.

(382) Biokinetic studies of platinum in human subjects have focused on the behavior of the antitumor agent cis-diamminedichloroplatinum (II) (DDP) (Lange et al., 1973; Smith and Taylor, 1974). In these studies the biokinetics of the platinum label was similar to the behavior of other forms of platinum following their administration to laboratory animals. Following intravenous administration of ^{195m}Pt-labeled DDP to two cancer patients, approximately 35% of the injected activity was excreted in urine during the first 3.5 d (Smith and Taylor, 1974). At most a few percent of the activity was excreted in faeces during that time. Based on external measurements, the liver accumulated an estimated 10% of the injected activity during the first day. The biological removal half-times of activity from the liver and total body from days 1-7 were estimated as 8 d and 10 d, respectively. The study period was too short to determine any longer-term components of retention.

(383) Biokinetic studies on rodents (Durbin et al., 1957; Durbin, 1960; Weininger et al., 1990; Jamre et al., 2011) indicate that the systemic behavior of osmium is broadly similar to that of platinum and the other members of the platinum group. The systemic distribution of osmium at 1 d after intravenous injection closely resembled that of platinum (Durbin et al., 1957; Durbin, 1960). Highest concentrations of intravenously injected osmium and generally occur in the kidneys and liver. Excretion of osmium is primarily in urine. Durbin and workers (Durbin et al., 1957; Durbin, 1960) found that the rate of excretion of osmium was initially higher than that of other members of the platinum group. This may reflect differences in the administered forms of these elements or experimental conditions; osmium was administered as $NaHOsO_5$ or OsO_4, while the other elements were administered as chloride compounds. Also, studies on mice indicate that the excretion rate of osmium depends on the pH of the injected solution, with longest retention observed at relatively low pH (Weininger et al., 1990). The total-body retention curves over the first four weeks following intravenous administration of osmium to mice at relatively low pH (4.5-5.1) were similar to the retention pattern observed by Moore et al. (1975a,b,c) for systemic platinum in rats.

(384) In this report the same biokinetic model is applied to both osmium and platinum as progeny of systemic iridium. The model is a modification of the characteristic biokinetic model for ruthenium used in this report. The ruthenium model is modified by shifting a portion of the deposition in bone and soft tissue compartments ST1 and ST2 to the urinary bladder content and kidneys. Specifically, the ruthenium model is modified for application to osmium and platinum as iridium progeny by the following changes in transfer coefficients:

Blood 1 to Cortical bone surface, reduced from 6 d^{-1} to 3 d^{-1}; Blood 1 to Trabecular bone surface, reduced from 2 d^{-1} to 1 d^{-1}; Blood 1 to ST1, reduced from 5 d^{-1} to 2.5 d^{-1}; Blood 1 to ST2, reduced from 5 d^{-1} to 2.5 d^{-1}; Blood 1 to Urinary bladder content, increased from 17 d^{-1} to 23 d^{-1}; Blood 1 to Kidneys 1 (urinary path), increased from 7.76 d^{-1} to 10.67 d^{-1}; and Blood 1 to Kidneys 2 (other kidney tissue), increased from 0.24 d^{-1} to 0.33 d^{-1}. These modifications leave the total outflow rate from the central blood compartment, Blood 1, unchanged at 100 d^{-1}.

(385) An osmium or platinum atom produced by radioactive decay in a systemic compartment is assigned the model for these elements described above from its time of production. This is straightforward for osmium and platinum atoms because their preceding chain members are also members of the platinum group, and all members of this group have the same model structure. Each compartment in the model for osmium and platinum is identified with the iridium compartment with the same name.

(386) Rhenium is a member of Group VIIA of the period table and exhibits chemical and biokinetic properties remarkably close to those of the adjacent Group VIIA element technetium (Durbin et al., 1957; Deutsch et al., 1986; Yanaga et al., 1996, Dadachova et al., 2002; Zuckier et al., 2004). Rhenium and technetium presumably become covalently bound with oxide ions to form the structurally similar anions perrhenate (ReO_4^-) and pertechnetate (TcO_4^-) in the body and in many environment settings. These two anions have important medical applications as close physiological analogues of iodide, with the important exception that there is little if any organic binding of perrhenate or pertechnetate in the thyroid. The systemic biokinetic model applied in this report to technetium as a member of ruthenium chains (see the section on ruthenium) is also applied to rhenium as a member of iridium chains.

8.3. Individual monitoring

(387) ^{192} Ir may be detected in urine or Whole Body counting.

Isotope	Monitoring Technique	Method of Measurement	Typical Detection Limit	Achievable detection limit
^{192}Ir	Urine Bioassay	γ-ray spectrometry	0.5Bq/L	
^{192}Ir	Whole Body Counting	γ-ray spectrometry	97Bq	
^{192}Ir	Lung Monitoring	γ-ray spectrometry	6 Bq*	

* Lung monitoring of ^{192}Ir is not generally used in routine monitoring of workers. Monte Carlo program Visual Monte Carlo was used to simulate the photon emission, to calculate the calibration factor for the geometry and radionuclide, and to calculate the minimum detectable activity (MDA) in the lung. (Hunt et al, 2012)

References

Ando, A., Ando, I., Hiraki, T., Hisada, K. 1989. Relation between the location of elements in the periodic table and various organ-uptake rates. Nucl. Med. Biol. 16: 57-69.

Brodsky, A., Wald, N., 2004. Experiences with early emergency response and rules of thumb. In: Brodsky, A.; Johnson, R.H., Jr., Goans, R.E., (Eds.), Public protection from nuclear, chemical, and biological terrorism. Health Physics Society 2004 Summer School. Madison, Wisconsin: Medical Physics Publishing; 2004, Chapter 20, pp. 335-371.

Casarett, L.J., Bless, S., Katz, R., Scott, J.K., 1960. Retention and fate of iridium-192 in rats following inhalation. J. Amer. Ind. Hyg. Assoc. 21, 414-418.

Cool, D.A., Cool, W.S., Brodsky, A., Eadie, G.G., 1979. Estimation of long-term biological elimination of insoluble iridium-192 from the human lung. Health Phys. 36, 629–632.

Dadachova, E.; Bouzahzah, B.; Zuckier, L. S.; Pestell, R. G. 2002. Rhenium-188 as an alternative to iodine-131 for treatment of breast tumors expressing the sodium/iodide symporter (NIS). Nucl. Med. Biol. 29:13-18.

Deutsch, E.; Libson, K.; Vanderheyden, J. L.; Ketring, A. R.; Maxon, H. R. 1986. The chemistry of rhenium and technetium as related to the use of isotopes of these elements in therapeutic and diagnostic nuclear medicine. Int. J. Rad. Appl. Instrum. B 13:465-477.

Durbin, P.W., 1960. Metabolic characteristics within a chemical family. Health Phys. 2, 225-238.

Durbin, P.W., Scott, K.G., Hamilton, J.G., 1957. Distribution of radioisotopes of some heavy metals in the rat. University of California (Berkely) Publ. Pharmocol. 3, 1-34.

Furchner, J.E., Richmond, C.R., Drake, G.A., 1971. Comparative metabolism of radionuclides in mammals-V. Retention of ^{192}Ir in the mouse, rat, monkey and dog. Health Phys. 20, 375-382.

Hirunuma, R., Endo, K., Yanaga, M., Enomoto, S., Ambe, S., Tanaka, A., Tozawa, M., Ambe, F., 1997) The use of a multitracer technique for the studies of the uptake and retention of trace elements in rats. Appl. Radiat. Isot. 48, 727-733.

IAEA, 1999. Intercomparison and biokinetic model validation of radionuclide intake assessment. Case 6: Single intake of ^{192}Ir. IAEA-TECDOC-1071 pp. 48-49.

ICRP, 1979. Limits on Intakes of Radionuclides for Workers. ICRP Publication 30, Part 2. Pergamon Press, Oxford. Ann. ICRP 4 (3/4).

ICRP, 1994. Dose Coefficients for Intakes of Radionuclides by Workers. ICRP Publication 68. Ann. ICRP 24(4).

Jamre, M.; Salek, N.; Jalilian, A. R.; Moghaddam, L.; Shamsaee, M.; Mazidi, M.; Ghannadi-Maragheh, M. 2011. Development of an in vivo radionuclide generator by labeling bleomycin with 191Os. J. Radioanal. Nucl. Chem. 290:543-549.

Kelsey, C.A., Mettler, Jr., F.A., 2001. Iridium-192 acid skin burn in Alburquerque, New Mexico, U.S.A. Chapter 29. In: Gusev, I.A., Guskova, A.K., Mettler, Jr., F.A., (Eds.), Medical management of radiation accidents, 2nd edition; New York: CRC Press, pp. 421-423.

Kreyling, W.G., 2010. Personal communication.

Kreyling, W.G., Semmler, M., Erbe, F., Mayer, P., Takanaka, S., Schulz, H., Oberdörster, G. and Ziesenis, A., 2002. Translocation of ultrafine insoluble iridium particles from lung epithelium to extrapulmonary organs is size dependent but very low. Journal of Toxicology and Environmental Health, Part A, 65 (20), 1513–1530.

Kreyling, W.G., Semmler-Behnke, M., Seitz, J., Scymczak, W., Wenk, A., Mayer, P., Takenaka, S., Oberdörster, G., 2009. Size dependence of the translocation of inhaled iridium and carbon nanoparticles aggregates from the lungs of rats to the blood and secondary target organs. Inhalation Toxicology, 21 (S1), 55–60.

Lange, R. C.; Spencer, R. P.; Harder, H. C. 1973. The anti-tumor agent cis-Pt(NH3)2Cl2: Distribution studies and dose calculations for 193mPt and 195mPt. J. Nucl. Med. 14:191-195.

Litterst, C. L.; Gram, T. E.; Dedrick, R. L.; Leroy, A. F.; Guarino, A. M. 1976. Distribution and disposition of platinum following intravenous administration of cis-diamminedichloroplatinum (II) (NSC119875) to dogs. Cancer Res. 36:2340-2355.

Moore, W.; Hysell, D.; Crocker, W.; Stara, J. 1975a. Whole body retention in rats of different 191Pt compounds following inhalation exposure. Environ. Health Persp. 12:35-39.

Moore, W.; Hysell, D.; Hall, L.; Campbell, K.; Stara, J. 1975b. Preliminary studies on the toxicity and metabolism of palladium and platinum. Environ. Health Persp. 10:63-71.

Moore, W.; Malanchuk, M.; Crocker, W.; Hysell, D.; Cohen, A.; Stara, J. F. 1975c. Biological fate of a single administration of 191Pt in rats following different routes of exposure. Environ Res. 9:152-158.

Semmler, M., Seitz, J., Erbe, F., Mayer, P., Heyder, J., Oberdörster, G. and Kreyling, W.G., 2004. Long-term clearance kinetics of inhaled ultrafine insoluble iridium particles from the rat lung, including transient translocation into secondary organs. Inhal. Tox., 16, 453 – 459

Smith, P. H. S.; Taylor, D. M. 1974. Distribution and retention of the antitumor agent 195mPt-cis-dichlorodiammine platinum (II) in man. J. Nucl. Med. 15:349-351.

Szymczak, W., Menzel, N., Kreyling, W.G., Wittmaack, K., 2006. TOF-SIMS characterisation of spark-generated nanoparticles made from pairs of Ir–Ir and Ir–C electrodes. International Journal of Mass Spectrometry 254, 70–84.

Veronese, I., Cantone, M.C., Giussani, A., Maggioni, T., Birattari, C., Bonardi, M., Groppi, F., Garlaschelli, L., Werner, E., Roth, P., Höllriegl, V., Louvat, P., Felgenhauer, N., Zilker, Th., 2003. Stable tracer investigations in humans for assessing the biokinetics of ruthenium and zirconium radionuclides. Rad. Prot. Dosim. 105, 209–212.

Veronese, I., Giussani, A., Cantone, M.C., Birattari, C., Bonardi, M., Groppi, F., Höllriegl, V., Roth, P., Werner, E., 2004. Influence of the chemical form on the plasma clearance of ruthenium in humans. Appl. Radiat. Isot. 60, 7-13.

Weininger, J.; Issachar, D.; Lubin, E.; Zabari, M.; Trumper, J. 1990. Influence of PH adjustment agents on the biologic behavior of osmium-191 impurity in iridium-191m generator eluates. J. Nucl. Med. 31:523-525.

Yanaga, M.; Enomoto, S.; Hirunuma, R.; Iuruta, R.; Endo, K.; Tanaka, A.; Ambe, S.; Tozawa, M.; Ambe, F. (1996). Multitracer study on uptake and excretion of trace elements in rats. Appl. Radiat. Isot. 47:235-246.

Yoakum, A. M.; Steward, P. L.; Sterrett, J. E. 1975. Method development and subsequent analysis of biological tissues for platinum, lead and manganese content. Environ. Health Persp. 10:85-93.

Zuckier, L. S.; Dohan, O.; Li, Y.; Chang, C. J.; Carrasco, N. ; Dadachova, E. 2004. Kinetics of perrhenate uptake and comparative biodistribution of perrhenate, pertechnetate, and iodide by NaI symporter-expressing tissues in vivo. J. Nucl. Med. 45:500-507.

9. Lead (Z = 82)

9.1. Chemical Forms in the Workplace

(388) Lead is a soft metal which mainly occurs in oxidation states II and IV. Lead may be encountered in industry in a variety of chemical and physical forms, including oxides (PbO, PbO_2, Pb_2O_3, Pb_3O_4), chlorides, sulphides, fluorides, nitrates, and also as organic vapour compounds (tetra-ethyl, tetra-methyl). Lead may also be present in uranium mines and mills. Molten lead is used as a coolant in lead cooled fast reactors.

(389) ^{210}Pb originates from the decay of ^{238}U and ^{234}Th, and ^{212}Pb from the decay of ^{232}Th.

Table 9-1. Isotopes of lead addressed in this report

Isotope	Physical half-life	Decay mode
Pb-194	12 m	EC, B+, A
Pb-195m	15 m	EC, B+
Pb-196	37 m	EC,B+
Pb-197m	43 m	EC, B+, IT
Pb-198	2.4 h	EC
Pb-199	90 m	EC, B+
Pb-200	21.5 h	EC
Pb-201	9.33 h	EC, B+
Pb-202	5.25E+4 y	EC, A
Pb-202m	3.53 h	IT, EC
Pb-203	51.873 h	EC
Pb-204m	67.2 m	IT
Pb-205	1.53E+7 y	EC
Pb-209	3.253 h	B-
Pb-210[a]	22.20 y	B-, A
Pb-211	36.1 m	B-
Pb-212[a]	10.64 h	B-
Pb-214[a]	26.8 m	B-

[a] Data for these radionuclides are given in the printed copy of this report. Data for other radionuclides are given on accompanying electronic disk.

9.2. Routes of Intake

9.2.1. Inhalation

Absorption Types and parameter values

(390) Information is available from experimental studies of the behaviour of lead inhaled in a variety of forms by both animals and man. In particular, studies have been conducted to improve assessment of risks from exposure to radioisotopes of lead inhaled as decay products of radon, and from exposure to stable lead as an atmospheric pollutant, e.g. from petrol engine exhaust.

(391) Absorption parameter values and Types, and associated f_A values for particulate forms of lead are given in Table 9-2. Parameter values are not given for the gas and vapour forms considered here because occupational exposure to radioisotopes in such forms is

unlikely. Exposures to gas and vapour forms of lead are relatively unusual compared to exposures to particulate forms, and therefore it is proposed here that particulate form is assumed in the absence of information (ICRP, 2002b). However, for radiation protection purposes, the most important exposures to radioisotopes of lead are as decay products of radon. Specific consideration is given here to studies of the absorption of lead administered in that form, and to studies using other ionic forms (e.g. nitrate) that were designed to investigate the absorption of radon decay products from the respiratory tract. Dose coefficients for isotopes of lead inhaled as radon decay products are given in the radon section, where factors such as the relevant aerosol size distribution are addressed. Otherwise, exposures to radioisotopes of lead occur most often as decay products associated with intakes of uranium, thorium or radium.

(a) Gases and vapours

Tetra ethyl lead (TEL)

(392) Heard et al. (1979) followed the biokinetics of ^{203}Pb for about a week after inhalation of ^{203}Pb-labelled tetra-methyl lead (TEL) vapour by four healthy male volunteers. Initial deposition averaged 37% of the inhaled vapour. There was rapid uptake of ^{203}Pb from the lungs, with the first blood samples taken 3 minutes after intake indicating ~10% of the deposit in the cells and ~30% in the plasma; and hence an absorption rate greater than 100 d^{-1}. The systemic behaviour was different from that of inorganic lead. Loss from blood was much faster: concentrations in both fractions fell by two orders of magnitude in the first 10 hours. At 1 hour >50% of ^{203}Pb deposited from inhalation was present in the liver, remaining fairly constant during the remaining 6 days of observation. About 20% of the ^{203}Pb-TEL deposited was lost by exhalation within 48 hours. These results indicate about 40% deposition in the respiratory tract with Type F absorption for TEL.

Tetra methyl lead (TML)

(393) Three of the subjects in the study of TEL above inhaled ^{203}Pb-labelled tetra-methyl lead (TML) in separate studies (Heard et al., 1979). Initial deposition averaged 51% of the inhaled vapour. The behaviour of ^{203}Pb inhaled as TML was similar to that for TEL, with rapid uptake of ^{203}Pb from the lungs, except that initially more ^{203}Pb was in the cells than in the plasma. About 40% of the ^{203}Pb-TEL deposited was lost by exhalation within 48 hours. These results indicate about 50% deposition in the respiratory tract with Type F absorption for TEL.

(394) However, although specific parameter values for TEL and TML based on *in vivo* data could be assessed, they are not adopted here, because inhalation exposure to it is so unlikely. Furthermore the systemic behaviour of lead inhaled in these forms differs from that of the model adopted here. The information is, however, useful for comparison with the behaviour of lead inhaled in ionic form, which is absorbed from the lungs much more slowly than lead inhaled in these organic forms.

(b) Lead as a decay product of radon

(395) In this section studies are considered in which ^{212}Pb (half-life 11 hours) formed from decay of ^{220}Rn (half-life 56 seconds) and ^{216}Po (half-life 0.15 seconds), or ^{214}Pb (half-life 27 minutes) formed from decay of ^{222}Rn (half-life 3.8 days), and ^{218}Po (half-life 3.1 minutes) was inhaled directly, while still airborne. For decay schemes, see the thorium and uranium sections. Studies in which lead ions were inhaled as nitrate or chloride, or in which lead ions

(either formed from decay of ^{220}Rn and ^{216}Po, or as nitrate) were administered to the respiratory tract in a liquid medium, which are also relevant to lead as a decay product of radon, are considered below in the section on particulate forms.

Lead as an unattached decay product of radon

(396) Booker et al. (1969) followed lung retention, blood concentration and fecal excretion of ^{212}Pb for up to 3 d after inhalation (by mouth) of unattached ^{212}Pb (vapour, formed from decay of ^{220}Rn/^{216}Po) by one volunteer. In a complementary experiment, the amount of ^{212}Pb in blood was measured at times up to 2 d after intravenous injection of ^{212}Pb into the same volunteer. Of the initial deposit in the respiratory tract, 37% was recovered in faeces during the first 3 d, which the authors attributed to high deposition in the upper airways. Overall, clearance from the chest occurred with a half-time of about 10 hours.

(397) Detailed analyses, of this and other studies, were carried out here (i.e. by the Task Groups), to estimate absorption parameter values appropriate for short-lived radon progeny. The studies by James et al. (1977) and Greenhalgh et al. (1979, 1982) outlined below, which were designed to investigate the early clearance of lead ions deposited in the lungs, showed a rapid phase: about 10–40% absorbed with a half-time of about 15 minutes, and evidence that some of the slow phase was due to binding. Specific consideration was therefore given here to the rapid absorption phase and the bound state. For this experiment, absorption parameter values were assessed from the lung, blood and fecal data published by Booker et al. (1969) using a subject-specific systemic model, and assuming an absorption model with a rapid dissolution rate (s_r) of 67 d^{-1} (half-time 15 minutes) and slow dissolution (s_s) and uptake (s_b) rates of 1.7 d^{-1} (10-hour half-time). Other parameter values were assessed to be f_r = 0.36 and f_b = 0.82, which gives rapid absorption of about 6% of the initial deposit [f_r*(1–f_b)]. Activity deposited in the upper respiratory tract retained in particulate form would mainly clear by mucociliary action to faeces, whereas activity retained in the bound state would not. This potentially enables a distinction to be made between the two pathways (provided s_r, and hence transfer to the bound state, is fast compared to particle transport). The faecal measurement was lower than the predicted value, even with the high bound fraction estimated, and suggests that s_r is > 67 d^{-1}. However, because the result was only for one volunteer and because of measurement uncertainties, it was judged here that it did not provide a better basis for estimating s_r than the information on which the value of 67 d^{-1} was based.

(398) Butterweck et al. (2001, 2002) carried out volunteer experiments to determine the absorption rate of unattached radon progeny. Twenty-one volunteers were exposed in a radon chamber with well-controlled aerosol and radon progeny conditions. The aerosol was predominantly unattached radon progeny. Eleven volunteers inhaled by mouth and seven by nose. Measurements were made of radon gas and progeny (^{214}Pb and ^{214}Bi) in blood samples taken at the end of a 30-minute exposure (Butterweck et al., 2002). *In vivo* measurements of the head and chest were carried out over a 30-minute period, starting approximately 7 minutes after exposure (Butterweck et al,. 2001). No clearance from the head (other than physical decay) was observed over this period, indicating that small fractions of the unattached ^{214}Pb and ^{214}Bi were absorbed rapidly to blood (s_r >> 100 d^{-1}), as measured by the blood sample, while the rest (fraction f_b) was bound to tissues (or stationary mucus). Assuming a rapid dissolution rate (s_r) of 1000 d^{-1} with f_r = 1.0 and an uptake rate from the bound state (s_b) of 1.7 d^{-1}, Butterweck et al. (2002) estimated that f_b was in the range 0.7–0.85 for radon progeny (without distinguishing between ^{214}Pb and ^{214}Bi). In this study the fraction of the initial deposit that was rapidly absorbed [f_r*(1–f_b)] was in the range 0.15–0.3, which is more than observed in the study by Booker et al. (1969) (see above). These data were re-evaluated here

using a systemic model based on the ICRP *Publication 67* model for lead (ICRP, 1993) but modified to take account of the early rapid exchange between plasma and extravascular fluid. Assuming s_r = 1000 d^{-1} with f_r=1 they estimated f_b was ~0.7 for lead. The longer-duration measurements made by Booker et al. (1969) are consistent with assignment to Type F.

(399) Bianco et al. (1974) followed chest retention and blood concentration of ^{212}Pb for up to 2 d after inhalation by dogs (via endotracheal tube) of unattached ^{212}Pb (formed from decay of ^{220}Rn/^{216}Po, effective diffusion diameter of about 11 nm). Fitting a single exponential function to the chest data (after correction for ^{212}Pb in blood) gave an average biological half-time for lung clearance of about 12 hours with values in the range 7 – 20 hours. The corresponding absorption half-time would be greater, because no correction was made for mucociliary clearance. However, some would have occurred before the first chest measurement took place, and similarly there could have been some rapid absorption that was not observed. There is insufficient information in the paper for more detailed analysis.

Lead as a radon decay product attached to ambient aerosols

(400) Booker et al. (1969) followed blood concentration, urinary and fecal excretion of ^{212}Pb in two volunteers for up to 3 d after inhalation (by mouth) of an aerosol formed by mixing ^{212}Pb (formed from decay of ^{220}Rn/^{216}Po) with particles (condensation nuclei, mainly 0.05–5 µm diameter). In complementary experiments, the amount of ^{212}Pb in blood was measured at times up to 2 d after intravenous injection of ^{212}Pb into the same volunteers. Of the initial respiratory tract deposit (IRTD), only 2–3% was recovered in faeces during the first 3 d, which the authors attributed to low deposition in the upper airways. Overall clearance from the chest was deduced from the blood measurements to occur with a half-time of about 10 hours. The authors noted that this was similar to that observed following inhalation of unattached ^{212}Pb (see above), even though it was expected that for ^{212}Pb attached to particles there was relatively greater deposition in the lower than in the upper respiratory tract, and suggesting similar rates of absorption to blood in both cases.

(401) Hursh et al. (1969) followed lung retention, blood concentration, urinary and fecal excretion of ^{212}Pb in ten volunteers for up to 3 d after inhalation (by mouth) of an aerosol formed by mixing ^{212}Pb (formed from decay of ^{220}Rn/^{216}Po) with natural room aerosol. On average about 3% IRTD was excreted in urine in the first 24 hours, and total fecal excretion (in 24 – 76 hours) was about 3% IRTD. The authors estimated that on average clearance of ^{212}Pb from lungs to systemic tissues occurred with a half time of 6.5 hours, although they inferred (from detailed measurements of urinary excretion) that some lead was absorbed promptly from the lungs. They noted that ^{212}Pb in blood and systemic tissues made a significant contribution to uncertainty in the lung measurements, but complementary intravenous injection experiments, which would have enabled direct correction to be made, were not carried out.

(402) Hursh and Mercer (1970) followed lung retention, blood concentration, and urinary and fecal excretion of ^{212}Pb in four volunteers for up to 3 d after inhalation (by mouth) of an aerosol formed by mixing ^{212}Pb (formed from decay of ^{220}Rn/^{216}Po) with natural room aerosol. In complementary experiments, the amount of ^{212}Pb in blood was measured at times up to 2 d after intravenous injection of ^{212}Pb into the same volunteers. On average about 2% IRTD was excreted in urine in the first 24 hours and total fecal excretion (in 34 – 50 hours) was 0.35% IRTD: the authors inferred that the latter suggested low deposition in ciliated airways. They noted that in two subjects the blood lead appeared to increase more rapidly than for the other two, and that this suggested that ^{212}Pb inhaled as freshly generated ^{212}Pb of very small diameter may be more readily absorbed from the lung parenchyma to blood than

an aged aerosol associated with larger diameter particles. However, the authors noted that "the determination is not sufficiently precise to establish this relationship." They estimated that, on average, clearance of ^{212}Pb from lungs to systemic tissues occurred with a half time of 10.5 to 11.5 hours, after correcting for activity outside the lungs.

(403) Singh et al. (1986) reported that concentrations of ^{210}Pb (half-life 22 years) in the lungs of uranium miners obtained at autopsy were several times higher than concentrations of ^{238}U, ^{234}U or ^{230}Th. This indicated that there were sources of intake of ^{210}Pb in addition to uranium ore dust. The authors suggested several possibilities, one of which was inhalation of ^{210}Pb present in the mine air but not associated with ore dust. If this originated from radon in the mine air it suggests that it was retained in the lungs in a relatively insoluble (Type M or S) form.

(404) Marsh and Birchall (1999) re-evaluated the published data from experiments in which volunteers inhaled ^{212}Pb attached to condensation nuclei or to 'natural' particles in room air (Booker et al., 1969; Hursh et al., 1969; Hursh and Mercer, 1970) to estimate an absorption half-time for lead, assuming a single component. The best estimate obtained was 10 hours with a 95% confidence interval of ±2 hours, which gave an absorption rate of about 1.7 d^{-1}. A more detailed analysis of these and other studies was carried out here to estimate absorption parameter values appropriate for short-lived radon progeny, giving specific consideration to the rapid absorption phase (see paragraph above on lead as an unattached decay product of radon). The published data from experiments in which volunteers inhaled ^{212}Pb attached to condensation nuclei were re-evaluated with a two-component model. Assuming s_r = 67 d^{-1} (half-time 15 min) values of f_r and s_s of 0.06 and 1.4 d^{-1} (half-time 12 h) respectively were estimated. However, the information did not permit assessment of f_b as for unattached ^{212}Pb (see above), because there was low deposition in the upper respiratory tract (and for Booker et al., 1969, no direct measurements of activity in the lungs).

(405) Based on these studies and those below on ionic lead, lead nitrate and lead oxide, bound state parameter values for lead of f_b = 0.5 and s_b = 1.7 d^{-1} were chosen here (see below). For the studies of radon as a decay product above, and ionic lead below, specific parameter values were estimated of about f_r = 0.3, s_r = 100 d^{-1}, s_s = 1.7 d^{-1}, f_b = 0.8 and s_b = 1.7 d^{-1}, i.e. a somewhat higher value of f_b. Note that (neglecting particle transport) the fraction of the initial deposit in the respiratory that is absorbed into blood in the rapid phase is given by f_r*(1 – f_b), thus these parameter values are consistent with rapid absorption of 0.3*(1 – 0.8) = 0.06. A similar fractional rapid absorption would be obtained with f_b = 0.5 and f_r = 0.12. Absorption parameter values: f_r = 0.1, s_r = 100 d^{-1}, s_s = 1.7 d^{-1}, f_b = 0.5 and s_b = 1.7 d^{-1} (consistent with assignment to default Type F) are used here for lead as a short-lived decay product of radon.

(c) Particulate aerosols

Ionic lead

(406) Greenhalgh et al. (1978, 1979) investigated the absorption of lead ions (^{203}Pb or ^{214}Pb) instilled into the bronchi of rabbits or rats in different media. In rabbits, the average amounts in blood at 20 and 42 minutes after instillation (estimated at about 4% and 7% respectively of the amount instilled) were similar, whether instilled in lead nitrate solution or in fresh rat mucus (both isotopes), or in isotonic saline (^{203}Pb). The authors inferred that about 10% of instilled lead was absorbed in a rapid phase with a half-time of about 10 minutes. In rats, systemic absorption of ^{203}Pb at 30 minutes after instillation in water, isotonic saline or hypertonic saline was similar, averaging 42% of the amount instilled, but

higher than in rabbits (~13%). It was somewhat higher when instilled as nitrate (53%), and in 0.1N HCl (61%).

(407) Greenhalgh et al. (1982) investigated the rapid clearance phase of radon decay products by comparing the biokinetics of ionic ^{212}Pb with those of insoluble radiolabelled particles (^{88}Y-labelled fused aluminosilicate, FAP) instilled together onto the nasal mucosa of rats. The ^{88}Y-FAP acted as a tracer for deposition and mucociliary clearance. The suspension was prepared by collecting ^{216}Po ions from the decay of ^{220}Rn in a chamber onto an electrode, and transferring the ^{212}Pb formed to distilled water: a suspension of the ^{88}Y-FAP in water was allowed to dry out, and the ^{212}Pb solution was added to the container. Activity retained in the head, and blood concentration, were followed for 100 minutes. By the end of the experiment about 8% of the ^{212}Pb had been absorbed (rate about 66 d^{-1}). (Thus rapid absorption of the initial deposit [f_r*(1–f_b)] was about 8%.) Nevertheless, the fraction of the initial deposit remaining in the nose was greater for ^{212}Pb (~40%) than for the particles (~30%). The authors concluded that some of the ^{212}Pb was retained by binding either to static mucus or epithelial tissue, and developed a two phase (sol and gel) model of mucociliary clearance to explain the results. Analysis carried out here, assuming slow dissolution (s_s) and uptake (s_b) rates of 1.7 d^{-1} (10-hour half-time, see paragraph above on lead as an unattached decay product of radon) gave absorption parameter values of f_r = 0.35, s_r = 60 d^{-1} (half-time 17 minutes), and f_b = 0.7.

Lead nitrate ($Pb(NO_3)_2$)

(408) James et al. (1977) followed the biokinetics of ^{212}Pb for up to 100 minutes after instillation of ^{212}Pb-nitrate into the trachea or bronchioles of rabbits. (The solution was prepared by collecting ^{216}Po ions from the decay of ^{220}Rn in a chamber onto an electrode, and transferring the ^{212}Pb formed to distilled water containing stable lead nitrate carrier.) From both sites approximately 20% of deposited ^{212}Pb was absorbed to blood with a half-time of about 4 minutes (250 d^{-1}), and the remainder with a half-time estimated at about 9 h (1.8 d^{-1}). Insoluble radiolabelled particles were instilled simultaneously into the bronchioles of one rabbit to act as a tracer for mucus. It was found that despite absorption to blood, the ^{212}Pb cleared more slowly than the particles, and it was inferred that this indicated slow diffusion of ^{212}Pb through the epithelium (i.e. that some binding occurs). It was reported that by the end of the experiment (2 hours after instillation) more of the ^{212}Pb remaining in the lungs was associated with mucus than with epithelium.

(409) Chamberlain et al. (1978) administered to four volunteers an aerosol of ^{203}Pb-labelled nitrate (AMAD in the range 0.4–0.8 µm), formed by adding nitrogen to the flame produced by burning ^{203}Pb-labelled tetra-ethyl lead in propane. Measurements of ^{203}Pb in the chest, blood and excreta were made for about 4 days. Complementary measurements were also made of ^{203}Pb in the legs, to correct lung measurements for systemic ^{203}Pb, based on the results of similar measurements made after intravenous injection of ^{203}Pb. Lung retention was represented by a three-component exponential function with half-times of 1.0 hours (26%); 2.2 hours (33%); and 10 hours (41%) (rates of 17, 7.6 and 1.7 d^{-1} respectively). Clearance was almost entirely by systemic uptake: only a small percentage of the initial lung deposit (ILD) was cleared by mucociliary action and swallowed. Chamberlain et al. (1978) noted that lead nitrate was far more soluble *in vitro* than indicated by the lung measurements, and suggested that the mechanism for transferring lead from lung fluid to blood is a relatively slow process, which determines the overall transfer rate.

(410) Ballou et al. (1986) measured lung retention and tissue distribution of ^{232}U, ^{228}Th, ^{224}Ra, ^{212}Pb, ^{212}Bi and ^{208}Tl at 24 hours after intratracheal instillation into rats of ^{232}U nitrate with its decay products. (For further information, see the uranium inhalation section.) For

^{212}Pb, on average 2.1% ILD was measured in the lungs at 1 day. Correcting for the physical decay of ^{212}Pb gives retention of 10% ILD at 1 day.

(411) Moody et al. (1994b); Moody and Stradling, 1992) measured the tissue distribution of ^{228}Th, ^{212}Pb, ^{212}Bi and ^{208}Tl, at times from 6 hours to 7 days after intratracheal instillation into rats of a nitrate solution of ^{228}Th in equilibrium with its decay products. (Radon-220 is a precursor of ^{212}Pb, but it is unlikely that a significant amount was lost from solution before deposition in the lungs, because of its short half life of 56 seconds. Its average half distance of diffusion in water was estimated to be 50 µm by Ballou and Hursh, 1972.) For ^{212}Pb, on average 8.4% of the initial lung deposit (ILD) was measured in the lungs at 6 hours and 1.2% ILD at 1 day: clearance was much faster than that of the parent ^{228}Th. Correcting for the physical decay of ^{212}Pb gives retention of 12.5% ILD at 6 hours and 5.6% ILD at 1 day. From these results it was assessed here, assuming either (i) that the retained lead was in particulate form, i.e. a slow dissolution (s_s) rate of 1.7 d^{-1} with no bound state (f_b=0) or (ii) that the retained lead was in the bound state with an uptake rate (s_b) of 1.7 d^{-1} with no slow dissolution (f_r=1) (see paragraphs above on lead as a decay product of radon), that s_r was ~50 d^{-1} (half-time ~20 min) with f_r ~0.75 or f_b ~0.25 respectively, i.e. about 75% cleared rapidly in either case. Later measurements were not included because of possible significant contributions to measured ^{212}Pb from decay of higher members of the chain.

(412) Based on these studies and others, bound state parameter values for lead of f_b = 0.5 and s_b = 1.7 d^{-1} were chosen (see below). It is noted that (neglecting particle transport) the fraction of the initial deposit in the respiratory that is absorbed into blood in the rapid phase is given by f_r *(1 – f_b), which for f_b = 0.5, gives f_r *(0.5). For the study in which lead nitrate were inhaled by human volunteers (Chamberlain et al., 1978), ~50% ILD was cleared rapidly (components with half times less than 3 hours), suggesting a value for f_r of ~1.0. Specific parameter values derived for lead nitrate would be close to those for Type F (including the bound state parameters for lead), and therefore lead nitrate is assigned here to Type F.

Lead chloride ($PbCl_2$)

(413) Morrow et al. (1980) followed lung retention and blood concentration of ^{203}Pb in eight volunteers for up to 4 d after inhalation (by mouth) of an aerosol formed by nebulising a sodium chloride vector solution to which carrier-free $^{203}PbCl_2$ was added, giving an AMAD of ~0.25 µm. Lung retention was represented by a two-component exponential function with on average (after correction for systemic ^{203}Pb and physical decay) 7% clearing at a rate of 0.023 min^{-1} (33 d^{-1}, half-time 30 minutes) and 93% at a rate of 0.00088 min^{-1} (1.3 d^{-1}, half-time 13 hours). The corresponding absorption rates would be lower, because of particle transport to the alimentary tract. However, at this aerosol size deposition in the upper respiratory tract would have been relatively low, and so the contribution would be small, at least to the slow phase. The authors noted that the blood data suggested that the rapid phase could be due to absorption rather than mucociliary clearance. Some mucociliary clearance and some rapid absorption would have occurred before the first chest measurement took place, shortly after aerosol administration. Without fecal clearance measurements, estimates of specific absorption parameter values could not be made here: the results are consistent with assignment to Type F.

Lead hydroxide ($Pb(OH)_2$)

(414) Morrow et al. (1980) followed lung retention and blood concentration of ^{203}Pb in nine volunteers for up to 4 d after inhalation (by mouth) of a $Pb(OH)_2$ - NaCl aerosol formed by nebulising a sodium chloride vector solution to which carrier-free $^{203}PbCl_2$, stable lead

chloride and sodium hydroxide were added, giving an AMAD of ~0.25 µm. Lung retention was represented by a two-component exponential function with on average (after correction for systemic ^{203}Pb and physical decay) 12% clearing at a rate of 0.012 min^{-1} (17 d^{-1}, half-time 60 minutes) and 88% at a rate of 0.00081 min^{-1} (1.2 d^{-1}, half-time 14 hours). The authors noted that the results were not significantly different from those obtained with carrier-free lead chloride (see above) despite differences in chemical form and mass. As for the chloride, estimates of specific absorption parameter values could not be made: the results are consistent with assignment to Type F.

(415) Stradling et al. (2005; Moody et al., 1994a) measured the tissue distribution of ^{228}Th, ^{212}Pb, ^{212}Bi and ^{208}Tl, at times from 1 to 168 days after intratracheal instillation into rats of a suspension of ^{228}Th hydroxide in equilibrium with its decay products. For ^{212}Pb, on average 2.7% ILD was measured in the lungs at 1 day, when administered with a low mass (50 pg) of thorium, (5% ILD when administered with a high mass, 6.5 µg, of thorium). Clearance was much faster than that of the parent ^{228}Th. Correcting for the physical decay of ^{212}Pb gives retention of 13% ILD at 1 day. From this result it was assessed here that s_r was greater than 2 d^{-1} (half-time ~8 hours). Alternatively, assuming f_r = 1, and s_r = 100 d^{-1} gave f_b = 0.8. Later measurements were not included because of possible significant contributions to measured ^{212}Pb from decay of higher members of the chain. There was insufficient information to quantify a slower phase as seen in other studies of soluble forms of lead: its presence would give a higher value for s_r. The results are consistent with assignment to Type F, to which lead hydroxide is assigned.

Lead oxide (PbO and Pb_3O_4)

(416) Rendall et al. (1975) measured lead levels in blood (only) of baboons that inhaled red lead oxide (Pb_3O_4): either as a “coarse” (mass median diameter, MMD, 6 µm) or “fine” (MMD 2 µm) aerosol at similar mass concentrations. There is insufficient information to assess absorption parameter values, but blood levels were higher following exposure to coarse than to fine dust. Since it is likely that for the coarse dust deposition in the upper respiratory tract (URT) was higher and deposition in the lungs lower than for the fine dust, the results suggest that there was rapid absorption from the URT and/or the alimentary tract.

(417) Boudene et al. (1977) measured tissue distribution and excretion in rats for 6 days following inhalation (whole body) of an aerosol formed by passing nebulised gasoline labelled with organic ^{210}Pb with air through a tube furnace at 600°C. Lung clearance was rapid, reducing to 11% ILD at 24 hours and 1% ILD at 6 days. There is detailed information on the biokinetics (nine time points within the first day) but large uncertainties on the deposition pattern (extrathoracic and pelt). From the results, parameter values assessed here, assuming that the lead which was not cleared in the rapid phase was retained in the bound state (f_r =1) were s_r ~5 d^{-1} (half-time ~3 hours); f_b ~0.2 and s_b ~0.5 d^{-1} (half-time ~33 hours), giving assignment to Type F.

(418) Chamberlain et al. (1978) administered to six volunteers an aerosol of ^{203}Pb-labelled oxide (AMAD in the range 0.4–0.8 µm), formed by eliminating nitrogen from the flame produced by burning ^{203}Pb-labelled tetra-ethyl lead in propane. Measurements of ^{203}Pb in the chest, blood and excreta were made for about 4 days. Complementary measurements were also made of ^{203}Pb in the legs, to correct lung measurements for systemic ^{203}Pb, based on the results of similar measurements made after intravenous injection of ^{203}Pb. Lung retention was represented by a four-component exponential function with half-times of 0.5 hours (25%); 2.9 hours (32%); 9.8 hours (25%) and 38 hours (18%) (rates of 33, 5.7, 1.7 and 0.4 d^{-1} respectively). Clearance was almost entirely by systemic uptake: only a small percentage of

the initial lung deposit (ILD) was cleared by mucociliary action and swallowed. Chamberlain et al. (1978) noted that (in contrast to nitrate and motor exhaust aerosols) the lead oxide was less soluble *in vitro* than indicated by the lung measurements, and suggested that this might be because of efficient fluid flow in the lungs.

(419) Rhoads and Sanders (1985) followed the biokinetics of lead in rats for 91 days after inhalation of non-radioactive PbO. Lung retention was represented by a two-component exponential function with half-times of 1 day (93%) and 89 days (7%), consistent with assignment to Type F.

(420) Lung retention of lead oxide inhaled by human volunteers was similar to that of lead nitrate (Chamberlain et al., 1978), and therefore specific parameter values derived from them would also be close to those for Type F (including the bound state parameters for lead), and therefore lead oxide is assigned here to Type F.

Lead difluoride (PbF_2)

(421) Stradling et al. (2005; Moody et al., 1994a) measured the tissue distribution of ^{228}Th, ^{212}Pb, ^{212}Bi and ^{208}Tl, at times from 1 to 168 days after intratracheal instillation into rats of a suspension of ^{228}Th fluoride in equilibrium with its decay products. For ^{212}Pb, on average 6.0% ILD was measured in the lungs at 1 day, when administered with a low mass (60 pg) of thorium. Correcting for the physical decay of ^{212}Pb gives retention of 28% ILD at 1 day. Clearance was faster than that of the parent ^{228}Th. From this result it was assessed here that s_r was at least 1 d^{-1} (half-time ~8 hours). Later measurements were not included because of possible significant contributions to measured ^{212}Pb from decay of higher members of the chain. There was insufficient information to quantify a slower phase as seen in other studies of soluble forms of lead: its presence would give a higher value for s_r. (However, when administered with a high mass, 6.5 µg, of thorium, 18% ILD of ^{212}Pb was measured in the lungs at 1 day. Correcting for the physical decay of ^{212}Pb gives retention of ~80% ILD at 1 day, similar to that of the parent thorium.) The results indicate Type F behaviour and lead difluoride is assigned to Type F.

Lead in fresh or age-aggregated motor exhaust (including lead dibromide, $PbBr_2$)

(422) Although mainly related to environmental, rather than occupational, exposure, information relating to lead in motor exhaust and tobacco smoke is included here for completeness.

(423) Chamberlain et al. (1975, 1978) administered various aerosols derived from ^{203}Pb-labelled motor exhaust to several volunteers. Measurements of ^{203}Pb in the chest, blood and excreta were made for up to about 4 days. Complementary measurements were also made of ^{203}Pb in the legs, to correct lung measurements for systemic ^{203}Pb, based on the results of similar measurements made after intravenous injection of ^{203}Pb. (Absorption from the alimentary tract following ingestion of exhaust particles collected on filters was also determined.) In most cases, patterns of lung clearance and systemic uptake were similar to those found by these authors for lead inhaled as nitrate or oxide (see above), often in the same volunteers. For fresh motor exhaust, Chamberlain et al. (1978) represented lung retention by a three-component exponential function with half-times of 1.2 hours (27%); 2.3 hours (39%); and 8.1 hours (34%) (rates of 14, 7.2 and 2.1 d^{-1} respectively). Clearance was almost entirely by systemic uptake: only a small fraction of the ILD was cleared by mucociliary action and swallowed. For aged exhaust (stored and in some cases exposed to ultraviolet light) a fourth component was needed: about 10%-15% was retained with a half-time of 40-220 hours. (Chamberlain et al., 1975, reported only that most of the ^{203}Pb in the lungs was retained with

a half-time of about 6 hours, and the rest cleared more slowly.) Most studies of the composition of exhaust lead (e.g. Habibi 1973) have identified complex mixtures of lead oxides, halides and ammonium salts, together with sulphates and carbonaceous material. This suggests that Type F behaviour may be characteristic of many lead compounds other than those for which specific information is available. In particular, since lead dibromide was an important constituent of lead in motor exhaust, it suggests that, like lead chloride, it should be assigned to Type F.

Lead-210 in cigarette smoke tar

(424) A brief summary is given here: for further information see the polonium section. Lead-210 and its decay product, ^{210}Pb, are inhaled in cigarette smoke (Desideri et al., 2007). Martell (1974) reported that ^{210}Pb concentrates in resinous material in tobacco leaves, forming insoluble particles during combustion. Cohen et al. (1979) measured ^{210}Po concentrations in the tracheobronchial tree and lung parenchyma in autopsy tissues from smokers and non-smokers, and attributed differences to the retention of insoluble particles containing ^{210}Pb/^{210}Po in cigarette smoke. Cohen et al. (1985) measured ^{210}Po in the lungs of rats after exposure to cigarette smoke enriched in ^{210}Pb/^{210}Po: results indicate Type M or S behaviour for both the ^{210}Pb and ^{210}Po.

Mineral dust

(425) A potentially important source of intake of ^{210}Pb in particulate aerosols arises from airborne mineral dusts containing the natural long-lived parent. In this case the absorption rate will probably be determined by the dissolution rate of the mineral matrix in lung fluids. Measurements have been made of the dissolution in simulated lung fluid of samples of coal fly ash (Kalkwarf et al., 1984) and condensate from calcining phosphate rock dust (Kalkwarf and Jackson, 1984) for 60 days. By this time the amounts of ^{210}Pb dissolved were <0.2% and <5% respectively, indicating assignment to Type S in both cases.

Uranium ore dust

(426) Duport et al. (1991) measured the dissolution in simulated lung fluid of long lived radionuclides in uranium ore dust from Canadian mines. (For further information see the uranium section relating to uranium ore dust and to decay products of uranium formed in the respiratory tract). For high grade ore, measurements were made for up to 60 days. Results were presented as undissolved fractions as functions of time, and showed two components, which were expressed as Class D (rapid) and Class Y (slow) fractions. For ^{210}Pb the rapidly dissolved fraction was 0.28. HRTM parameter values fitted to the ^{210}Pb data by Marsh et al. (2011) were: f_r = 0.26, s_r = 3.9 d^{-1} and s_s = 0.001 d^{-1}, indicating assignment to Type M. For ^{210}Pb, no effects of size were observed in total dissolution over 40 days for particles in size ranges 7–10, 3–7, 1–3 and <1 µm. For low grade and medium grade ores, measurements were made for 12 days, but only on samples of relatively coarse dust, the smallest fraction being <37 µm. For ^{210}Pb, rapidly dissolved fractions were lower, <0.01, indicating assignment to Type S.

Thorium dioxide

(427) Hodgson et al. (2000, 2003) measured the tissue distribution of ^{228}Th, ^{212}Pb, ^{212}Bi and ^{208}Tl, at times from 1 to 168 days after intratracheal instillation into rats of suspensions of ^{232}Th dioxide enriched with ^{228}Th, in equilibrium with its decay products, with geometric diameters of about 0.4 and 2 µm. (For further information, see the thorium inhalation

section.) There was little absorption of the thorium itself, consistent with assignment to Type S. The activity of ^{212}Pb in the lungs was about 50% and 80% of that of the thorium at 1 day for the 0.4 and 2 µm particles respectively, and 25% and 70% at later times. The lower concentrations of ^{212}Pb were attributed to diffusion of ^{220}Rn (thoron) and recoil of the progeny from alpha particle decay.

Decay products of lead formed in the respiratory tract

(428) The general approach to treatment of decay products formed in the respiratory tract is described in Part 1, Section 3.2.3. In summary, it is expected that generally the rate at which a particle dissociates is determined by its matrix, and hence the physico-chemical form of the inhaled material. It is recognised that nuclei formed by alpha decay within a particle matrix may be expelled from it into the surrounding medium by recoil, but to implement this routinely would add greatly to the complexity of calculations. It is expected that the behaviour of soluble (e.g. Type F) material in the respiratory tract would depend on its elemental form, i.e. that of the decay product. Nevertheless, for simplicity, in this series of documents the absorption parameter values of the parent are, by default, applied to all members of the decay chain formed in the respiratory tract. Exceptions are made for noble gases formed as decay products, which are assumed to escape from the body directly, at a rate of 100 $d^{-1,}$ in addition to other routes of removal.

(429) For decay schemes of lead isotopes in the natural decay series, including ^{214}Pb, ^{212}Pb and ^{210}Pb, see the uranium and thorium sections. Studies specifically comparing the behaviour of lead with that of its decay products (bismuth and thallium isotopes) are summarised here. For further information, see the bismuth inhalation section.

(430) Drew (1971) reported that the tissue distributions of ^{212}Pb (half-life 11 hours) and ^{212}Bi (half-life 61 minutes) activities were similar in rats following exposure to ^{220}Rn (thoron) and its decay products for 2 days. However, the exposure situation was complex, because the ^{212}Pb and ^{212}Bi in tissues originated from inhalation of ^{220}Rn, and its decay within the body, inhalation of ^{212}Pb and ^{212}Bi, and also their ingestion from food and preening of fur. It is therefore difficult to estimate how much of the ^{212}Bi originated from decay of ^{212}Pb in the lungs. Furthermore, ^{212}Bi would have grown in rapidly between dissection of the animals and measurements of activities in tissues. Thus the activities of ^{212}Bi present *in vivo* may have been significantly lower than those measured.

(431) As noted above, measurements have been made of the tissue distributions of ^{212}Pb and its decay products, ^{212}Bi and ^{208}Tl, following administration to rats of ^{228}Th in various chemical forms (nitrate, hydroxide, fluoride, dioxide), in equilibrium with its decay products. In all these studies the distributions of ^{212}Bi and ^{208}Tl were similar to each other and those of the parent ^{212}Pb. Because their physical half-lives are so short (61 minutes and 3 minutes respectively) measurements made at 6 hours onwards would be mainly of activity formed from decay of ^{212}Pb within the body, rather than from intake of ^{212}Bi (or ^{208}Tl). The similar distributions of ^{212}Bi (and ^{208}Tl) to those of ^{212}Pb might suggest that there was not rapid movement of ^{212}Bi from the site (e.g. the lungs) in which it was formed by decay of ^{212}Pb. However, ^{212}Bi (and ^{208}Tl) would have grown in rapidly between dissection of the animals and measurements of activities in tissues. Without detailed information (which is not available) about the time which elapsed between dissection of the animals and measurements, it is not possible to correct for this ingrowth and hence estimate the absorption rates of the bismuth or thallium formed as a decay products in the lungs. However, since the half-life of ^{208}Tl is so short (as is that of ^{207}Tl present in the ^{235}U decay series, 5 minutes), the absorption rate of thallium would have to be very high to influence dose assessments.

(432) As described above, Butterweck et al. (2001, 2002) measured radon gas, ^{214}Pb and ^{214}Bi in blood samples taken from volunteers at the end of a 30-minute inhalation exposure to unattached radon progeny. *In vivo* measurements of the head and chest were also carried out. Assuming a rapid dissolution rate (s_r) of 1000 d^{-1} with f_r=1 and an uptake rate from the bound state (s_b) of 1.7 d^{-1}, Butterweck et al. (2002) estimated that the rapid absorption of the initial deposit is in the range 0.15–0.3 and the remaining fraction is bound with f_b in the range 0.7–0.85, for "radon progeny" (without distinguishing between ^{214}Pb and ^{214}Bi). However, Butterweck et al. (2002) also estimated "absorption rates" for ^{214}Pb and ^{214}Bi from their activities in the blood sample and the estimated respiratory tract deposition, assuming that absorption from respiratory tract to blood could be represented by a single rate constant (s_r) i.e. f_r=1 and f_b=0, although this model seems inconsistent with the *in vivo* measurements. They obtained absorption half-times of ~60 minutes for ^{214}Pb and ~25 minutes for ^{214}Bi, suggesting that there was greater absorption of ^{214}Bi than of ^{214}Pb by the end of the exposure when the blood sample was taken.

(433) As noted above, Singh et al. (1986) measured concentrations of ^{210}Pb (half-life 22 years) in the lungs of uranium miners obtained at autopsy. In most (six out of eight) cases several years elapsed between death and analysis, so that, regardless of its concentration in the lungs at death, ^{210}Po would have reached equilibrium with ^{210}Pb. For the other two miners the analysis was within a few months of death, and the authors inferred that the results indicated that the ^{210}Po and ^{210}Pb were in equilibrium at the time of death.

Rapid dissolution rate for lead

(434) The absorption of lead from the respiratory tract following deposition in ionic form has been studied extensively. There have been human volunteer and laboratory animal studies of the biokinetics of lead inhaled in several ionic forms: as a decay product of radon and as nitrate, chloride, hydroxide, fluoride and oxide. There have also been laboratory animal studies in which solutions of ionic lead were instilled onto the nasal and bronchial epithelium to study the absorption of lead in more detail. Most of these show a similar pattern. As noted by Morrow et al. (1980), where absorption from the respiratory tract to blood has been represented by a single overall absorption rate, half-times of about 10 hours were obtained for several different forms of lead. For some inhalation studies, the duration of exposure and delay before the first measurement mean that a minor rapid component (time scale of minutes) would not have been observed. However, in studies with sufficient data, two components are generally observed, a rapid phase, with between about 10% and 75% clearing with a half-time between a few minutes and an hour (rate between about 20 and 200 d^{-1}: the rest with a half-time of about 10 hours (rate about 1.7 d^{-1}). Exceptions are the human volunteer studies of lead as an unattached decay product of radon (Booker et al., 1969, Butterweck et al., 2001, 2002): the results indicate a rate for the rapid phase > 100 d^{-1}. Studies of lead inhaled as a decay product of radon give values of s_r of about 100 d^{-1}, which is applied here to all Type F forms of lead.

Extent of binding of lead to the respiratory tract

(435) There is strong evidence for a bound state for lead, on a time scale relevant to its inhalation as a decay product of radon. As noted above, the absorption of lead from the respiratory tract following deposition in ionic form has been extensively studied. In studies with sufficient data, two components are generally observed, a rapid phase (10–75% clearing in less than an hour) and the rest with a half-time of about 10 hours.

(436) This similarity in the half-time associated with slow uptake of lead in several

different ionic forms suggests that it is a characteristic of the element rather than determined by dissociation of the different forms. The slow phase was not observed when lead was inhaled in organic form (tetra-ethyl or tetra-methyl lead): the rate of uptake observed (~50% in a few minutes), seems consistent with the size of the molecules. Uptake of inorganic ionic lead was much slower, indicating that some mechanism slows down its uptake to blood.

(437) The question of whether the slow phase of absorption of ionic lead represented binding to respiratory tract components has been considered for over 30 years. Chamberlain et al. (1978) noted that lead nitrate was far more soluble *in vitro* than indicated by the lung measurements, and suggested that the mechanism for transferring lead from lung fluid to blood is a relatively slow process, which determines the overall transfer rate.

(438) Hursh and Mercer (1970) complemented their inhalation studies of lead as a radon decay product (see above) with ultrafiltration experiments (transfer though dialysis membrane): the ^{212}Pb aerosol was collected electrostatically onto a metal plate, and dispersed ultrasonically into the liquid medium tested. In distilled water or heparinised plasma less than 1% was ultrafilterable, but this was greatly increased by addition of citrate. The authors attributed the low fraction without added citrate to binding of lead to the dialysis membrane (distilled water) or proteins (plasma).

(439) Most directly, James et al. (1977) and Greenhalgh et al. (1982) compared the biokinetics of ionic ^{212}Pb with those of insoluble radiolabelled particles instilled together onto the bronchiolar epithelium of rabbits or nasal mucosa of rats. Despite some rapid absorption into blood, the ^{212}Pb cleared more slowly than the particles. The authors concluded that some of the ^{212}Pb was retained by binding either to static mucus or epithelial tissue. However, a similar clearance half-time has been observed with ionic lead deposited predominantly in the alveolar region (see above, e.g. lead as a radon decay product attached to ambient aerosols), which does not have a mucus lining, suggesting that there is binding to the epithelium.

(440) For the experiment by Booker et al. (1969) in which a volunteer inhaled unattached ^{212}Pb (see above), absorption parameter values assessed here (assuming an absorption model with s_r = 67 d^{-1} and s_s = s_b= 1.7 d^{-1}) were f_r = 0.36 and f_b = 0.82. Neglecting the bound state (assuming f_b = 0) underestimated lung retention and overestimated fecal excretion. Similar parameter values were assessed here from the results of the experiment by Greenhalgh et al. (1982). Butterweck et al. (2002) estimated f_b to be in the range 0.7–0.85, assuming that f_r = 1, from the results of their experiments in which volunteers inhaled unattached radon decay products: f_b was estimated here to be ~0.7 for lead from these data.

(441) Note that (neglecting particle transport) the fraction of the initial deposit in the respiratory tract that is absorbed into blood in the rapid phase is given by f_r*(1 – f_b). For the studies in which lead nitrate and lead oxide were inhaled by human volunteers (Chamberlain et al., 1978), about 60% ILD was cleared rapidly (components with half times less than 3 hours). (There was little mucociliary clearance and fecal excretion.) These results suggest a lower value of f_b than the estimates made for lead as a decay product of radon. Similarly, f_b values of about 0.25 were estimated here for lead nitrate instilled into rats or lead oxide inhaled by rats based on the data of Moody et al. (1994b) and Boudene et al. (1977) respectively.

(442) On the basis of all these results, a bound fraction with f_b = 0.5 and a rate of uptake s_b = 1.7 d^{-1} is adopted here for lead. There is experimental evidence that lead in soluble form deposited in the conducting airways is retained in a bound state. It is therefore assumed here that these bound state parameter values apply throughout the respiratory tract (ET_2, BB, bb and AI regions).

Table 9-2. Absorption parameter values for inhaled and ingested lead

Inhaled particulate materials	Absorption parameter values[a] f_r	s_r (d^{-1})	s_s (d^{-1})	Absorption from the alimentary tract, f_A[b]
Specific parameter values[c]				
Lead as a decay product of radon	0.1	100	1.7	0.02
Default parameter values[d]				
Absorption Type	Assigned forms			
F	Lead dichloride, dibromide, difluoride, hydroxide, nitrate, oxide, all unspecified forms[e]	1	100	–	0.2
M	—	0.2	3	0.005	0.04
S	Mineral dusts	0.01	3	0.0001	0.002
Ingested material				
All forms				0.2

[a] It is assumed that for lead the bound fraction f_b is 0.5 with an uptake rate s_b = 1.7 d^{-1}, and that this applies throughout the respiratory tract (ET_2, BB, bb and AI regions). The value of s_r for Type F forms of lead (100 d^{-1}) is element-specific. The values for Types M and S (3 d^{-1}) are the general default values.

[b] For inhaled material deposited in the respiratory tract and subsequent cleared by particle transport to the alimentary tract, the default f_A values for inhaled materials are applied: i.e. the product of f_r for the absorption Type (or specific value where given) and the f_A value for ingested soluble forms of lead (0.2).

[c] See text for summary of information on which parameter values are based, and on ranges of parameter values observed in different studies. For lead as a decay product of radon, specific parameter values are used for dissolution in the lungs, but a default value of f_A (footnote b).

[d] Materials (e.g. lead dichloride) are listed here where there is sufficient information to assign to a default absorption Type, but not to give specific parameter values (see text).

[e] Default Type F is recommended for use in the absence of specific information, i.e. if the form is unknown, or if the form is known but there is no information available on the absorption of that form from the respiratory tract.

9.2.2. Ingestion

(443) Lead absorption has been studied extensively in man and animals (See review in ICRP, 1993). Factors shown to affect absorption of Pb include ingestion of milk, calcium and iron status, protein deficiency, vitamin D and fasting. Of these, fasting causes the greatest variation in uptake. For example, James et al. (1985) measured absorption in volunteers given ^{203}Pb acetate in water to be about 0.65 after a 12h fast compared with about 0.04 when taken with a meal. At 3h after a meal, absorption averaged about 0.16 with a range of 0.05 to 0.5, and after 5h the average was about 0.45 with a range of 0.3 to 0.65. Individual variation was also shown by Blake (1976) who measured absorption ranging from 0.1 to 0.7 in ten volunteers given ^{203}Pb chloride. Heard and Chamberlain (1982) showed that fasting values of about 0.4 to 0.5 by giving ^{203}Pb as chloride to volunteers in distilled water were reduced to 0.1 to 0.2 in tea, coffee or beer.

(444) Leggett (1993) suggest in its age-specific kinetic model of lead metabolism in humans, to assign an f_1 value of 0.15 in adults.

(445) The *Publication 30* (ICRP, 1980) derived an absorption value of 0.2 that was applied in *Publication 67* (ICRP, 1993) to dietary intakes. An f_A of 0.2 is used here for direct ingestion of all forms of lead.

9.2.3. Systemic Distribution, Retention and Excretion

9.2.3.1. Summary of the database

(446) Following intravenous administration of radiolead to human subjects, the injected activity initially cleared from blood at a rate of 1 min^{-1} or greater (Wells et al., 1975; Chamberlain et al., 1978). A minimum blood content of about one-third of the injected amount was reached within 2-3 min, at which time roughly three-fourths of activity in blood resided in red blood cells (RBC). Increased activity in blood was then seen for 24-48 h as the tracer returned from extravascular spaces and accumulated in RBC (Booker et al., 1969; Wells et al., 1975; Chamberlain et al., 1978). Within a few hours after injection, 99% or more of activity in blood was bound in or on RBC (Hursh et al., 1969; Booker et al., 1969; Wells et al., 1975; Chamberlain et al., 1978; Everson and Patterson, 1980; DeSilva, 1981; Manton and Cook, 1984; Heard and Chamberlain, 1984).

(447) At 1-2 d after introduction of radiolead into adult humans by injection or inhalation, the blood contained 40-75% (mean 58 ± 12%) of the amount reaching the circulation (Hursh and Suomela, 1968; Booker et al., 1969; Hursh et al., 1969; Wells et al., 1975; Chamberlain et al., 1978; Morrow et al., 1980; Heard and Chamberlain, 1984). Over the next few weeks, activity was cleared from blood with a biological half-time on the order of 15-20 days (Rabinowitz et al., 1973, 1974, 1976; Wells et al., 1975; Heard and Chamberlain, 1984).

(448) Soon after introduction of radiolead into blood plasma, the tracer is largely available for diffusion into extravascular fluids and filtration by the kidneys (Vander et al., 1977; Chamberlain et al., 1978; Heard and Chamberlain, 1984). Under steady-state conditions, however, most of the lead in plasma is bound to proteins (Griffin and Matson, 1972).

(449) The liver contained about 10-15% of administered radiolead at 1 d after intravenous injection into adult humans (Heard and Chamberlain, 1984), baboons (Cohen et al., 1970), or dogs (Lloyd et al., 1975). Most of the activity deposited in the liver was removed with a biological half-time of a few weeks. Autopsy measurements on chronically exposed adult humans indicate that the liver typically contains about 2-3% of total-body lead. The blood-to-liver concentration ratio in chronically exposed persons typically is about 0.2 (Blanchard and Moore, 1970, 1971; Hamilton et al., 1972; ICRP, 1975; Gross et al., 1975; Barry, 1975,198l).

(450) Part of the loss of lead from the liver can be accounted for by biliary secretion into the gastrointestinal content, but return of lead from the liver to blood also must be postulated to explain the limited losses in faeces. Estimates of the contribution of biliary secretion to total faecal excretion of lead are variable. For example, data of Rabinowitz et al. (1976) indicate that biliary secretion represents no more than half of all endogenous secretion of lead into the gastrointestinal tract, while data of Ishihara and Matsushiro (1986) suggest that hepatic bile is the main route of faecal elimination of absorbed lead from the body.

(451) Results of experimental studies on dogs and rodents indicate that the kidneys accumulated as much as 15-20% of intravenously injected radiolead within the first 1-2 h, most of the accumulated activity represented filtered lead, and a substantial portion of the early accumulation was reabsorbed or lost in urine within a few hours (Morgan et al., 1977; Victery et al., 1979; Keller and Doherty, 1980). In rats, the kidneys contained roughly 10% of the intravenously injected amount after 1 day but less than 2% after 9 days. In baboons

receiving radiolead by intravenous injection, the kidneys contained about 4% of the administered amount after 1 day, 0.6% after 30 days, and 0.1% after 60 days (Cohen et al., 1970). In dogs receiving ^{210}Pb by intravenous injection, the kidneys contained about 0.5% of the administered activity at 1 month (Lloyd et al., 1975). Comparison of the decline of renal and hepatic activity from 1 d to about 2 mo after intravenous administration of radiolead to baboons (Cohen et al., 1970) indicate that the removal half-time from the kidneys is roughly half of that from the liver, if each of these organs were treated as a single compartment. This agrees with estimates for baboons exposed to lead by daily ingestion over a period of a few months (Mallon, 1983).

(452) Gradual loss of lead from RBC, liver, kidneys, and other soft tissues over the first few weeks can be accounted for by a slow loss in urine and faeces and a continual increase in skeletal lead. Typically, 3-5% of injected or absorbed lead is lost in urine during the first day. The urinary to faecal excretion ratio is about 2 during days 3-14 after absorption of lead to blood in humans. About 30% of intravenously injected radiolead is removed in urine and faeces during the first 20 days (Hursh and Suomela, 1968; Hursh et al., 1969; Hursh and Mercer, 1970; Booker et al., 1969; Wells et al., 1975; Chamberlain et al., 1978; Heard and Chamberlain, 1984).

(453) In baboons (Cohen et al., 1970) and human subjects (Heard and Chamberlain, 1984), there was evidence of rapid skeletal uptake of about 10-15% of intravenously administered lead. The skeletal content remained nearly constant over the next 2-3 d and then slowly increased over an extended period as activity returned from RBC and soft tissues to plasma. In human subjects the skeleton contained roughly 20% of the injected amount after 20 d. Autopsy data for persons chronically exposed to environmental lead indicate that the skeletal content of lead increases throughout life and represents 90% or more of systemic lead by the fifth decade (Tipton and Cook, 1963; Gross et al., 1975; Barry, 1975, 1981; Leggett, 1993).

(454) Skeletal behaviour of lead appears to be qualitatively similar to that of the alkaline earth elements and quantitatively similar to that of barium or radium, if account is taken of the slower deposition of lead in the skeleton due to competition from RBC (Hursh, 1973; Lloyd et al., 1975; Domanski and Trojanowska, 1980; Heard and Chamberlain, 1984). Lead has been used frequently as a marker of bone growth and osteon formation, and a close resemblance to calcium has been demonstrated in such studies (Vincent, 1957; Lacroix, 1960; Scheiman-Tagger and Brodie, 1964; Hong et al., 1968; Yen and Shaw, 1977). Lead is incorporated into the crystalline structure of bone, where it replaces calcium ions (MacDonald et al., 1951; Verbeeck et al., 1981; Miyake et al., 1986).

(455) Autoradiographs of bone sections from baboons injected with ^{210}Pb indicate that a portion of skeletal activity remains near bone surfaces at 1 to 2 months after administration, as appears to be the case for radium and barium. Studies on human subjects indicate that the distribution of lead in bone may be skewed toward bone surfaces for at least a few months after exposure, but the subjects generally have been exposed to heavy levels of lead that could affect bone metabolism (Lindh et al., 1978; Flood et al., 1988). Burial of lead beneath the surfaces in regions of bone formation has been observed, and there is evidence that lead is eventually distributed throughout the bone volume (Vincent, 1957; Lacroix, 1960; Scheiman-Tagger and Brodie, 1964; Hong et al., 1968; Yen and Shaw, 1977; Lindh et al., 1978; Hu et al., 1989). In beagles, long-term skeletal retention of lead is similar to that of strontium and radium (Hursh, 1973; Lloyd et al, 1975). Because lead is incorporated into the bone crystal, long-term losses from bone presumably are largely controlled by the rate of bone resorption.

(456) In a study of the comparative behaviour of injected lead, calcium, and barium in bone of rabbits, Domanski and Trojanowska (1980) found that the build-up of lead in bone is

similar to that of barium and greater than that of calcium when related to integrated activity in plasma. Similar results for lead and calcium were obtained by Heard and Chamberlain (1984) for humans injected with radioisotopes of these two elements. A relatively low uptake of lead by the skeleton at early times compared with radium, for example, apparently reflects a competition for lead with RBC that does not occur to a significant extent for the alkaline earth elements. The later build-up in the skeleton results from the gradual release of activity from RBC and the relatively longer retention of lead in the skeleton than in RBC.

9.2.3.2. Biokinetic model for systemic lead

(457) The biokinetic model for systemic lead used in this report is the model applied to adult members of the public in ICRP *Publication 67* (1993) and to workers in *Publication 68* (1994). The model is a simplification of a model of Leggett (1993), which provides more detail concerning the initial exchange of lead between plasma and extravascular spaces, its kinetics in RBC, and its distribution in soft tissues.

(458) The model structure is shown in Figure 9-1. Parameter values for a reference worker are listed in Table 9-2. Lead-specific parameter values (all parameter values other than those based on bone remodeling rates) were based on results of: controlled studies of on human subjects receiving stable or radioactive lead by injection, acute inhalation, or acute ingestion; long-term balance studies on human subjects; autopsy measurements on environmentally exposed humans; bioassay and autopsy measurements on occupationally exposed persons; and radioisotopic studies on laboratory animals, primarily non-human primates and dogs.

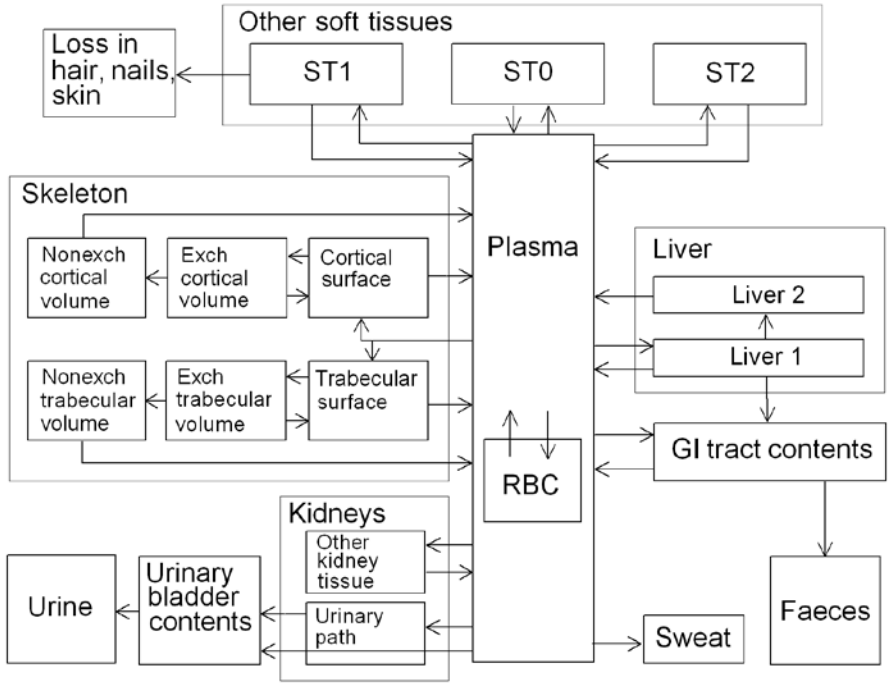

Figure 9-1. Structure of the biokinetic model for systemic lead. Abbreviations: RBC = Red Blood Cells, Exch = Exchangeable, Nonexch = Non-exchangeable.

The primary parameter values such as compartment deposition fractions and biological half-times underlying the transfer coefficients given in Table 9-3 are summarized below. The reader is referred to the paper by Leggett (1993) for a detailed discussion of the conceptual basis of the model and the data sets used in the development of parameter values.

(459) An early, rapid exchange of lead that occurs between plasma and extravascular spaces (Leggett, 1993) is not addressed in the present model. It is assumed here that lead leaves plasma at a rate of 70 d-1 and that a substantial portion of activity leaving plasma goes to a rapid-turnover soft tissue compartment called ST0 that is three times as large as the plasma compartment. Inflow and outflow rates selected for RBC yield an estimate of roughly 58% of injected lead in RBC at l-2 days after injection. It is assumed that 40% of outflow from plasma deposits in RBC. A biological half-time of 5 d for lead in RBC is set to yield a net half-time in blood (elongated by recycling) of about 20 days in the time between a few days and a few weeks after injection, based on data for humans.

Table 9-3. Transfer coefficients in the biokinetic model for systemic lead

From	To	Transfer oefficient (d^{-1})
Plasma	Urinary bladder content	1.75
Plasma	Right colon content	0.7
Plasma	Trabecular bone surface	4.86
Plasma	Cortical bone surface	3.89
Plasma	ST0	22.16
Plasma	ST1	0.7
Plasma	ST2	0.14
Plasma	Liver 1	4.9
Plasma	Urinary path	2.45
Plasma	Other kidney tissue	0.0245
Plasma	RBC	28
Plasma	Excreta (sweat)	0.42
RBC	Plasma	0.139
Trabecular bone surface	Plasma	0.5
Trabecular bone surface	Exch trabecular bone volume	0.5
Cortical bone surface	Plasma	0.5
Cortical bone surface	Exch cortical bone volume	0.5
Exch trabecular bone volume	Trabecular bone surface	0.0185
Exch trabecular bone volume	Nonexch trabecular bone volume	0.0046
Exch cortical bone volume	Cortical bone surface	0.0185
Exch cortical bone volume	Nonexch cortical bone volume	0.0046
Nonexch trabecular bone volume	Plasma	0.000493
Nonexch cortical bone volume	Plasma	0.0000821
Liver 1	Plasma	0.0312
Liver 1	SI content	0.0312
Liver 1	Liver 2	0.00693
Liver 2	Plasma	0.0019
Urinary path	Urinary bladder content	0.139
Other kidney tissue	Plasma	0.0019
ST0	Plasma	7.39
ST1	Plasma	0.00416
ST2	Plasma	0.00038
ST1	Excreta (Hair, skin, nails)	0.00277

RBC = Red Blood Cells, Exch = Exchangeable, Nonexch = Non-exchangeable

(460) Urinary and faecal excretion rates were based on observations of the fate of

intravenously injected radiolead in human subjects. It is assumed that 6% of outflow from plasma enters urinary excretion pathways. Part of this (2.5%) is assumed to pass instantaneously through the kidneys to the bladder content, and the rest (3.5%) is assumed to deposit in the renal tubules and to be released to the bladder content over a period of days. It is assumed that 1.7% of outflow from plasma enters the intestinal content either directly or indirectly: 1% passes directly into the right colon content, and 10% of the deposition in liver (7% of outflow from plasma) is secreted into the SI content. Because lead entering the SI content is subject to reabsorption to blood, the model predicts that slightly less than 1.7% of outflow from plasma is excreted in faeces.

(461) Loss of lead in sweat is assumed to represent 0.6% of outflow from plasma. A fourth excretion pathway, representing loss of lead in hair, skin, and nails, is depicted as outflow from soft-tissue compartment ST1 (described below). The predicted loss of lead from the body through this fourth pathway is equivalent to 0.4% of outflow from plasma.

(462) The liver is assumed to consist of two compartments, one with relatively short retention (Liver 1) and one with relatively long retention (Liver 2). Activity entering the liver is assigned to Liver 1. A small portion of the activity leaving Liver 1 is assigned to Liver 2, but most of the outflow is divided between plasma and the small intestine. Parameter values describing uptake, retention, and removal of lead by the liver were based on biokinetic studies of radiolead in human subjects, baboons, and dogs, and blood-to-liver concentration ratios observed in persons chronically exposed to low levels of environmental lead. It is assumed that 7% of lead leaving plasma deposits in Liver 1; the removal half-time from Liver 1 is 10 days; 10% of activity leaving Liver 1 deposits in Liver 2; and the remaining 90% of outflow from Liver 1 is evenly divided between plasma and SI content. The removal half-time from Liver 2 is 1 y.

(463) The kidneys are assumed to consist of two compartments, one with relatively short retention (Urinary path) and one with relatively long retention (Other kidney tissue). The Urinary path receives lead from plasma and loses activity to the urinary bladder content. Other kidney tissue exchanges lead slowly with plasma. Parameter values describing uptake, retention, and removal of lead by the kidneys were based on biokinetic studies of radiolead in baboons, dogs, and rats, and blood-to-liver concentration ratios observed in persons chronically exposed to low levels of environmental lead. It is assumed that 3.5% of outflow from plasma deposits in the urinary path and 0.035% deposits in other kidney tissue. The removal half-time from the urinary path to the urinary bladder content is 5 d. The removal half-time from other kidney tissue is 1 y.

(464) Other soft tissues are divided into compartments ST0, ST1, and ST2 representing fast (hours), moderate (months), and slow (years) return of lead to plasma. These are not physically identifiable compartments. They are defined on a kinetic basis, for reasonable agreement with estimates of the lead content of soft tissues other than liver and kidneys during chronic exposure or as a function of time after acute intake of lead. The underlying datasets include results of a variety of studies on laboratory animals and human subjects. Compartments ST1 and ST2 are assigned 1% and 0.2% of outflow from plasma, respectively. The fast-turnover compartment is assigned 31.66% of outflow from plasma, where the last three digits reflect an adjustment of the initially assigned deposition fraction to account for 100% of outflow from plasma. The biological half-times in ST0, ST1, and ST2 are approximately 2.25 h, 100 d, and 5 y, respectively. Outflow from the intermediate-term compartment ST1 is divided between plasma (60%) and an excretion compartment representing loss of lead in hair, skin, and nails (40%).

(465) Parameter values describing the bone kinetics of lead at early to intermediate times

after uptake to blood are based on studies of radiolead in adult humans, baboons, and dogs, and analogy with radium. Bone surface is assumed to receive 12.5% of outflow from plasma. The assumed division between trabecular and cortical surface is based on analogy with radium. Lead is removed from bone surface at a rate of 1 d^{-1}, with 50% returning to plasma and 50% entering exchangeable bone volume. The rates of transfer from the exchangeable bone volume compartments to bone surface and to non-exchangeable bone volume are based on analogy with radium. The assumed rate of removal from each bone volume compartment to plasma is the reference bone turnover rate for that bone type (ICRP, 2002a).

9.2.3.3. Treatment of radioactive progeny

Dosimetrically significant lead progeny

(466) Several lead isotopes addressed in this report have radioactive progeny that contribute significantly to dose coefficients for the internally deposited lead parent. The dosimetrically significant members of lead chains are isotopes of gold, mercury, thallium, lead, bismuth, or polonium. The biokinetic models applied to these elements as progeny of systemic lead are described below.

Gold

(467) The biokinetics of gold has been investigated extensively in human subjects and laboratory animals in studies related to its medical applications, particularly the use of stable gold for treating rheumatoid arthritis and short-lived radioactive gold as an imaging agent (Freyberg, et al., 1942; Block, et al., 1942, 1944; Jeffrey et al., 1958; Lawrence, 1961; Rubin et al., 1967; McQueen and Dykes, 1969; Mascarenhas et al., 1972; Sugawa-Katayama et al., 1975; Gottlieb, 1979, 1983; Jellum et al., 1980; Massarella and Pearlman, 1987; Andersson et al., 1988; Bacso et al., 1988; Brihaye and Guillaume, 1990). Also, several studies have addressed the biological behavior of gold as a radioactive contaminant in the workplace or environment (Durbin, 1960; Fleshman et al., 1966; Chertok and Lake, 1971a, 1971b, 1971c; Silva et al., 1973). Development of a representative biokinetic model for systemic gold in adult humans is complicated by the apparent dependence of reported data on the mode of administration, chemical form, administered mass, and other study conditions. The following general properties appear to be typical of gold administered in relatively soluble form. Much of the gold reaching blood is excreted in the first week or two, but a nontrivial portion is retained for several weeks or months. Excretion is primarily in urine. Most of the retained amount is found in the kidneys, liver, and blood. Most of the gold found in blood is bound to plasma proteins.

(468) The following model is applied in this report to radioisotopes of gold produced in systemic compartments following intake of a lead parent. Gold leaves the central blood compartment (Blood 1) at the rate 1 d^{-1} and is distributed as follows: 10% to Blood 2 (a blood compartment with relatively slow turnover), 30% to Urinary bladder content, 10% to Right colon content, 10% to Kidneys, 10% to Liver, 5% to Red marrow (active marrow), 1% to Spleen, 1% to Trabecular bone surface, 1% to Cortical bone surface, 0.06% to Testes, 0.02% to Ovaries, 10% to ST2 (a soft tissue compartment with slow turnover), and the remaining 11.92 % to ST1 (a soft tissue compartment with a moderate turnover time). Gold transfers from Blood 2 to Blood 1 with a half-time of 5 d; from Liver, ST1, Spleen, Testes, Ovaries, Red marrow, Trabecular bone surface, and Cortical bone surface to Blood 1 with a half-time of 10 d; from Kidneys to Urinary bladder content with a half-time of 10 d; and from Other 2 to Blood with a half-time of 50 d. Gold produced by radioactive decay in a blood

compartment that is not identifiable with a blood compartment of the gold model is assumed to transfer to Blood 1 at the rate 1000 d^{-1}. Gold produced in a soft-tissue compartment that is not identifiable with a compartment in the gold model is assumed to transfer to Blood 1 with a half-time of 10 d. Gold produced in a compartment of trabecular or cortical bone volume is assumed to transfer to Blood 1 at the reference turnover rate for that bone type.

Mercury

(469) The model for mercury produced in systemic compartments by radioactive decay is based on biokinetic data for human subjects and laboratory animals exposed to inorganic forms of mercury, primarily divalent mercury salts (Friberg, 1956; Rothstein and Hayes, 1960; Cember, 1962; Hayes and Rothstein, 1962; Berlin and Ullberg, 1963; Clarkson and Rothstein, 1964; Joselow et al., 1967; Johnson and Johnson, 1968; Berlin et al., 1969; Brown et al., 1975; Jugo, 1976; Hursh et al., 1976, 1980; Cherian et al., 1978; Berlin, 1986; Newton and Fry, 1978; Jonsson et al., 1999). Retention data for mercury entering the body as a vapor are also considered for times remote from intake, as the biokinetics of this initial form of mercury gradually converges to that seen after intake of divalent mercury salts. Studies of animals administered divalent mercury salts indicate initially rapid disappearance of mercury from blood, but a substantial portion of the injected amount is retained in blood after several hours. Animal and human studies indicate that as much as 30-40% of divalent mercury reaching blood is deposited in the kidneys and is retained there with a half-time on the order of 50 (35-90) d. In rats injected with inorganic divalent mercury, the kidneys and liver accounted for about 10% of the systemic burden after 4 h, 40% after 1 d, 70% after 6 d, 88% after 15 d, and 91% after 52 d. In human subjects, more than half of absorbed inorganic mercury is removed from the body in urine. Initially, the rate of fecal excretion is much higher than that of urinary excretion, but this relation reverses over a few weeks as the kidney content builds up and the content of other systemic tissues declines. In addition to losses in urine and faeces, mercury is removed from the systemic fluids and tissues by exhalation as mercury vapor, and small amounts are lost through sweat, hair, and other routes. External measurements on human subjects exposed to inorganic mercury suggest that much of the mercury deposited in soft tissues other than kidneys is removed over a period of a few weeks. In rats receiving mercury chloride by intravenous or intramuscular injection, a slow phase of excretion with a half-time of 3 mo or more was apparent by 2 mo after injection. A component of retention in the body with a half-time on the order of 100 d is also indicated by long-term measurements of urinary mercury following human exposure to inorganic mercury.

(470) The systemic model for mercury as a member of a lead chain consists of the following compartments: Plasma 1 (diffusible mercury), Plasma 2 (protein-bound mercury), RBC, Kidneys, Liver, Spleen, Red marrow (active marrow), Testes, Ovaries, Cortical bone surface, Trabecular bone surface, and compartments ST1 and ST2 representing two phases of loss from remaining soft tissues. Mercury absorbed to blood or reentering blood from tissues is assigned to Plasma 1. The total transfer coefficient from Plasma 1 to all destinations is 16.636 h^{-1} corresponding to a half-time of 1 h. Outflow from Plasma 1 is divided as follows: 4% to RBC, 12% to Plasma 2, 35% to Kidneys, 20% to Liver, 10% to Small intestine content, 3% to Red marrow, 0.6% to Spleen, 0.036% to Testes, 0.012% to Ovaries, 3.5% to ST2, 5% to Excreta (excretion other than urine and faeces), 1% to Cortical bone surface, 1% to Trabecular bone surface, and the remaining 4.852% to ST1. Mercury transfers from RBC to Plasma 1 with a half-time of 3 d, from Plasma 2 to Plasma 1 with a half-time of 1 d, from Kidneys to Urinary bladder content with a half-time of 35 d, from bone surface compartments to Plasma 1 with a half-time of 20 d, from ST1 to Plasma 1 with a half-time of 20 d, and from

ST2 to Plasma 1 with a half-time of 100 d. Mercury is removed from Liver with a half-time of 10 d, with outflow from Liver equally divided between Plasma 1 and SI content. Mercury transfers from Red marrow, Spleen, Testes, and Ovaries to Plasma 1 with a half-time of 20 d. Mercury is absorbed from SI content to Plasma 1 based on the reference absorption fraction for ingested inorganic mercury, and the unabsorbed portion transfers to the Right colon content and is eventually excreted in faeces. Mercury produced in a soft-tissue compartment that is not identifiable with a compartment in the mercury model is assumed to transfer to the central blood compartment of the mercury model with a half-time of 20 d. Mercury produced in a compartment of cortical or trabecular bone volume is assumed to transfer to the central blood compartment at the reference turnover rate for that bone type.

Thallium

(471) The biokinetics of thallium has been investigated extensively in human subjects and laboratory animals, due mainly to the importance of radio-thallium in nuclear medicine and many occurrences of accidental or malicious poisoning with stable thallium (Gettler and Weiss, 1943; Barclay et al., 1953; Lie et al., 1960; Gehring and Hammond, 1967; Potter et al., 1971; Bradley-Moore et al., 1975; Strauss et al., 1975; Atkins et al., 1977; Suzuki et al., 1978; Berger et al., 1983; Nakamura et al., 1985; Gregus and Klaassen, 1986; Krahwinkel et al., 1988; Lathrop et al., 1989; Blanchardon et al., 2005). Comparisons of the disappearance of radioisotopes of thallium, potassium, and rubidium from blood and their uptake by tissues of laboratory animals suggest a close relation in the movement of these elements, presumably associated with their similar ionic radii (Gehring and Hammond, 1967; Strauss et al., 1975). These elements are rapidly removed from plasma, and their early distributions are determined largely by the distribution of cardiac output. After entering the cell, thallium is released more slowly than potassium or rubidium, but the mean residence time of thallium in the body is less than that of potassium or rubidium due to a higher rate of clearance from plasma to excretion pathways. Most reported removal half-times of thallium from the adult human body are in the range 9-13 d (Atkins et al., 1977; Krahwinkel et al., 1988; Blanchardon et al., 2005). Chen et al. (1983) reported two components of retention of thallium: 7d for 63% and 28 d for 37% of the injected amount. It appears that faecal excretion typically represents more than half of cumulative excretion of thallium over a period of weeks following its acute intake, although some relatively short-term human studies have suggested that excretion of thallium is primarily in urine (cf. Barclay et al., 1953; Lathrop et al., 1975; Atkins et al., 1977; Blanchardon et al., 2005).

(472) The following model is applied in this report to radioisotopes of thallium produced in systemic compartments following intake of a lead parent. Thallium leaves the central blood compartment (Plasma) at the rate 200 d^{-1} (corresponding to a half-time of 5 min) and is distributed as follows: 2.5% to RBC, 0.75% to Urinary bladder content, 1.75% to Right colon content, 5% to Kidneys, 5% to Liver, 1.5% to Red marrow (active marrow), 0.2% to Spleen, 0.045% to Testes, 0.015% to Ovaries, 7.5% to Trabecular bone surface, 7.5% to Cortical bone surface, and 68.24% to ST0 (remaining soft tissues). Thallium returns from RBC to Plasma at the rate 3.7 d^{-1} and from tissue compartments to Plasma at the rate 2.5 d^{-1}. Thallium produced by radioactive decay in a blood compartment that is not identifiable with a blood compartment of the thallium model is assumed to transfer to Plasma at the rate 1000 d^{-1}. Thallium produced in a soft-tissue compartment that is not identifiable with a compartment of the thallium model is assumed to transfer to Plasma at the rate 2.5 d^{-1}. Thallium produced in a compartment of cortical or trabecular bone volume is assumed to transfer to Plasma at the reference turnover rate of that bone type.

Lead

(473) The systemic model for lead as a progeny of a lead parent is based on the characteristic model for lead applied in this series of reports. The structure of the characteristic model is modified by the addition of four compartments that are explicitly identified in models for some elements appearing in lead chains: Red marrow (active marrow), Spleen, Testes, and Ovaries. Each of these compartments is assumed to exchange lead with the central blood compartment of the lead model (Plasma). Transfer coefficients for the added compartments are selected for reasonable consistency with the biokinetic database underlying the characteristic model for lead and with the retention curve for total soft tissues based on the characteristic model. The specific changes to the characteristic model for lead are as follows: (1) the transfer coefficients from Plasma to compartments added to the characteristic model for lead are 0.015 d^{-1} for Red marrow, 0.002 d^{-1} for Spleen, 0.00045 d^{-1} for Testes, and 0.00015 d^{-1} for Ovaries; (2) the transfer coefficient from Plasma to ST1 is reduced from 0.70 d^{-1} to 0.69 d^{-1}, and the coefficient from Plasma to ST2 is reduced from 0.14 d^{-1} to 0.138 d^{-1}; and (3) the assigned transfer coefficient from each of the added compartments back to Plasma is 0.002 d^{-1}. Lead produced in a blood compartment of a preceding chain member that is not identifiable with a blood compartment of the lead model is assigned the transfer rate 1000 d^{-1} to Plasma.

Bismuth

(474) The systemic model for bismuth as a progeny of lead is based on the characteristic model for bismuth applied in this series of reports. The structure of the characteristic model is modified by the addition of four compartments that are explicitly identified in models for some elements appearing in lead chains: Red marrow (active marrow), Spleen, Testes, and Ovaries. Each of these compartments is assumed to exchange bismuth with the central blood compartment (plasma). Transfer coefficients are selected for reasonable consistency with the biokinetic database underlying the characteristic model for bismuth and with the retention curve for total soft tissues based on that original model. The specific changes to the characteristic model for bismuth are as follows: (1) the transfer coefficients from plasma to the added compartments are 0.3 d^{-1} for Red marrow, 0.02 d^{-1} for Spleen, 0.003 d^{-1} for Testes, and 0.001 d^{-1} for Ovaries; (2) the transfer coefficient from plasma to the Other soft-tissue compartment ST1 is reduced from 4.2 d^{-1} to 3.976 d^{-1}, and the coefficient from plasma to the Other soft tissue compartment ST2 is reduced from 1.3 d^{-1} to 1.2 d^{-1}; and (3) the assigned transfer coefficient from each of the added compartments back to plasma is 0.007 d^{-1} (half-time of 100 d). Bismuth produced in a blood compartment that is not identifiable with a compartment of the bismuth model is assumed to transfer to the plasma compartment of the bismuth model at the rate 1000 d^{-1}. Bismuth produced in a trabecular or cortical bone volume compartment is assumed to transfer to plasma at the reference turnover rate for that bone type.

Polonium

(475) The model for polonium produced in systemic compartments following intake of a lead isotope is a simplified version of the model applied in this report to polonium absorbed to blood following its inhalation as a parent radionuclide. It is assumed that polonium leaves the central blood compartment of the model (Plasma) at the rate 100 d^{-1} and distributes as follows: 5% to red blood cells (RBC), 3% to plasma proteins (Plasma P), 28% to Liver, 28% to Kidneys, 1.2% to Bone surface, 3.3% to Red marrow (active marrow), 1.6% to Spleen, 0.1% to Testes, 0.05% to Ovaries, 4% to a soft-tissue compartment with a relatively long

retention time (ST2), and the remaining 25.755% to a soft-tissue compartment with a relatively short retention time (ST1). Activity entering Liver is equally divided between compartments Liver 1 and Liver 2. Of the 28% of outflow from Plasma depositing in Kidneys, 24% is assigned to the urinary path (Kidneys 1) and 4% is assigned to other kidney tissue (Kidneys 2). Activity entering Bone surface is equally divided between Cortical bone surface and Trabecular bone surface. Activity transfers to Plasma from each of the compartments RBC, Plasma P, ST1, Liver 2, Red marrow, Spleen, and Kidneys 2 with a half-time of 7 d. Activity transfers from Liver 1 to Small intestine content with a half-time of 5 d, from Kidneys 1 to Urinary bladder content with a half-time of 4 d, from Trabecular and Cortical bone surface to Plasma with a half-time of 30 d, from ST2 to Plasma with a half-time of 100 d, and from Testes and Ovaries to Plasma with a half-time of 50 d. Polonium produced in a soft-tissue compartment of a preceding chain member that is not identifiable with a compartment in the polonium model is assumed to move to Plasma with a half-time of 7 d. Polonium produced in a compartment of cortical or trabecular bone volume is assumed to transfer to Plasma at the reference rate of turnover of that bone type.

9.3. Individual monitoring

^{210}Pb

(476) Urine bioassay is used for the monitoring of ^{210}Pb. In addition, when necessary, measurements of the concentration in faeces may be performed. For refined monitoring of ^{210}Pb skeleton burdens, in vivo measurements of the cranium and knee might be performed.

Isotope	Monitoring Technique	Method of Measurement	Typical Detection Limit	Achievable detection limit
^{210}Pb	Urine Bioassay	Beta proportional counting	0.1 Bq/L	0.01 Bq/L
^{210}Pb	Faeces Bioassay	Beta proportional counting	0.04 Bq/24h	
^{210}Pb	Cranium Measurement	γ-ray spectrometry		16 Bq
^{210}Pb	Knee Measurement	γ-ray spectrometry		14 Bq

^{212}Pb

(477) In vivo monitoring, lung and Whole Body Counting, are the main techniques used to determine ^{212}Pb intakes.

Isotope	Monitoring Technique	Method of Measurement	Typical Detection Limit	Achievable detection limit
^{212}Pb	Whole Body Counting	γ-ray spectrometry	80 Bq	50Bq
^{212}Pb	Lung Counting	γ-ray spectrometry	9 Bq	8Bq

^{214}Pb

(478) In vivo monitoring, lung and Whole Body Counting, are the main techniques used to determine ^{214}Pb intakes

Isotope	Monitoring Technique	Method of Measurement	Typical Detection Limit	Achievable detection limit
^{214}Pb	Whole Body Counting	γ-ray spectrometry	90 Bq	50 Bq
^{214}Pb	Lung Counting	γ-ray spectrometry	16 Bq	

References

Andersson, L.; Hallstadius, L.; Strand, S.-E. 1988. Biokinetics and dosimetry for 195Au, evaluated in an animal model. Eur. J. Nucl. Med. 14:393-399.

Atkins, H. L.; Budinger, T. F.; Lebowitz, E.; Ansari, A. N.; Greene, M. W.; Fairchild, R. G.; Ellis, K. J. 1977. Thallium-201 for medical use, 3. Human distribution and physical imaging properties. J. Nucl. Med. 18:133-140.

Bacso, J.; Uzonyi, I.; Dezso, B. 1988. Determination of gold accumulation in human tissues caused by gold therapy using x-ray fluorescence analysis. Appl. Radiat. Isot. 39:323-326.

Ballou, J.E., Gies, R.A., Case, A.C., Haggard, D.L., Buschbom, R.L., Ryan, J.L., 1986. Deposition and early disposition of inhaled 233UO2(NO3)2 and 232UO2(NO3)2 in the rat. Health Phys. 51, 755–771.

Ballou, J.E., Hursh, J.B., 1972. The measurement of thoron in the breath of dogs administered inhaled or injected ThO2. Health Phys., 22, 155–159.

Barclay, R. K.; Peacock, W. C.; Karnofsky, D. A. 1953. Distribution and excretion of radioactive thallium in the chick embryo, rat, and man. J. Pharmacol. Exp. Ther.107:178-187.

Barry, P.S.I., 1975. A comparison of lead concentrations in human tissues. Br. J. Znd. Med. 32, 119-139.

Barry, P.S.I., 1981. Concentrations of lead in tissues of children. Br. J. Ind. Med. 38, 61-71.

Berger, C. D.; Lane, B. H.; Hamrick, T. 1983. Clearance of 202Tl contaminate following intravenous injection of 201Tl. Health Phys. 45:999-1001.

Berlin, M. (1986) Mercury. In: Friberg, L.; Nordberg, G. F.; Vouk, V. B., eds. Handbook of the toxicology of metals, Vol. II. New York: Elsevier; 387-445.

Berlin, M.; Fazackerley, J.; Nordberg, G. 1969. The uptake of mercury in the brains of mammals exposed to mercury vapor and to mercuric salts. Arch. Environ. Health 18, 719-729.

Berlin, M.; Ullberg, S. (1963) Accumulation and retention of mercury in the mouse. Arch. Environ. Health 6, 589-601.

Bianco, A., Gibb, F.R., Morrow, P.E., 1974. Inhalation study of a submicron size lead-212 aerosol. In: Snyder, W.S. (Ed.), 3rd Int. Congress of the IRPA, Washington D.C., 9–14 Sept. 1973., USAEC CONF-730907, pp. 1214–1219.

Blake, K., 1976. Absorption of lead-203 From gastrointestinal tract of man. Enviromental Research. 11, 1-4.

Blanchard, R.L., Moore, J.B., 1971. Body burden, distribution and internal dose of Pb-210 and Po-210 in a uranium miner population. Health Phys. 21, 499-518.

Blanchard, R. L., Moore, J.B., 1970. Pb-210 and Po-210 in tissues of some Alaskan residents as related to consumption of caribou or reindeer meat. Health Phys. 18, 127-134.

Block, W. D.; Buchanan, O. H.; Freyberg, R. H. (1942). Metabolism, toxicity and manner of action of gold compounds used in the treatment of arthritis. IV. Studies of the absorption, distribution and excretion of gold following the intramuscular injection of gold thioglucose and gold calcium thiomalate. J. Pharmacol. Exp. Ther. 76:355-357.

Block, W. D.; Buchanan, O. H.; Freyberg, R. H. (1944). Metabolism, toxicity and manner of action of gold compounds used in the treatment of arthritis. V. A comparative study of the rate of

absorption, the retention, and the rate of excretion of gold administered in different compounds. J. Pharmacol. Exp. Ther. 82, 391-398.

Booker, D.V., Chamberlain, A.C., Newton, D., Stott, A.N., 1969. Uptake of radioactive lead following inhalation and injection. Br. J. Radiol. 42, 457–466.

Boudene, C., Malet, D., Masse, R., 1977. Fate of 210Pb inhaled by rats. Toxicol. Appl. Pharmacol. 41, 271–276.

Bradley-Moore, P. R.; Lebowitz, E.; Greene, M. W.; Atkins, H. L.; Ansari, A. N. (1975). Thallium-201 for medical use, 2. Biologic behavior. J. Nucl. Med. 16:156-160.

Brihaye, C.; Guillaume, M. (1990). 195Au biokinetics and dosimetry. Eur. J. Nucl. Med. 16:369-371.

Brown, K. W.; McFarlane, J. C.; Bernhardt, D. E. (1975) Accidental inhalation of mercury-203. Health Phys. 28, 1-4.

Butterweck, G., Schuler, C., Vezzu, G., Muller, R., Marsh, J.W., Thrift, S., Birchall, A., 2002. Experimental determination of the absorption rate of unattached radon progeny from respiratory tract to blood. Radiat. Prot. Dosimetry, 102, 343–348.

Butterweck, G., Vezzù, G., Schuler, Ch., Müller, R., Marsh, J.W., Thrift, S., Birchall, A., 2001. In-vivo measurement of unattached radon progeny deposited in the human respiratory tract. Radiat. Prot. Dosim. 94, 247–250.

Cember, H. (1962) The influence of the size of the dose on the distribution and elimination of inorganic mercury, Hg(NO3)2, in the rat. Amer. Ind. Hyg. Assoc. J. 23, 304-313.

Chamberlain, A.C., Clough, W.S., Heard, M.J., Newton, D., Stott, A.N.B., Wells, A.C., 1975. Uptake of lead by inhalation of motor exhaust. Proc. R. Soc. Lond. B. 192, 77–110.

Chamberlain, A.C., Heard, M.J., Little, P., Newton, D., Wells, A.C., Wiffen, R.D., 1978. Investigations into lead from motor vehicles. UK Atomic Energy Authority Report AERE-R 9198. HMSO, London.

Chen, C. T.; Lathrop, K. A.; Harper, P. V.; Bartlett, R. D.; Stark V. J.; Fultz, K. R.; Faulhaber, P. F. (1983). Quantitative measurement of long term in vivo thallium distribution in the human. J. Nucl. Med., 24:P50.

Cherian, M. G.; Hursh, J. B.; Clarkson, T. W.; Allen, J. (1978) Radioactive mercury distribution in biological fluids and excretion in human subjects after inhalation of mercury vapor. Arch. Environ. Health 33, 109-114.

Chertok, R. J.; Lake, S. (1971a) Availability in the peccary pig of radionuclides in nuclear debris from the plowshare excavation buggy. Health Phys. 20, 313-316.

Chertok, R. J.; Lake, S. (1971b) Biological availability of radionuclides produced by the plowshare event schooner - I. Body distribution in domestic pigs exposed in the field. Health Phys. 20, 317-324.

Chertok, R. J.; Lake, S. (1971c) Biological availability of radionuclides produced by the plowshare event schooner - II. Retention and excretion rates in peccaries after a single oral dose of debris. Health Phys. 20, 325-330.

Clarkson, T.; Rothstein, A. (1964) The excretion of volatile mercury by rats injected with mercuric salts. Health Phys. 10, 1115-1121.

Cohen, B.S., Eisenbud, M., Wrenn, M.E., Harley, N.H., 1979. Distribution of polonium-210 in the human lung. Radiat. Res. 79, 162-168.

Cohen, B.S., Harley, N.H., Tso, T.C., 1985. Clearance of polonium-210-enriched cigarette smoke from the rat trachea and lung. Toxicol. Appl. Pharmacol. 79, 314-322.

Cohen, N., Eisenbud, M., Wrenn, M.E., 1970. The Retention and Distribution of Lead-210 in the Adult Baboon. Progress report, Radioactivity studies, New York University Medical Center, New York.

Desideri D., Meli, M.A., Feduzi, L., Roselli, C., 2007. 210Po and 210Pb inhalation by cigarette smoking in Italy. Health Phys. 92(1) 58-63.

DeSilva, P.E., 1981. Determination of lead in plasma and studies on its relationship to lead in erythrocytes. Br. J. Ind. Med. 38,209-217.

Domanski, T., Trojanowska, B., 1980. Studies on metabolic kinetics of lead and alkaline earth elements (Ca, Ba). Acta Physiol. Pol. 31, 439-447.

Drew, R.T., 1971. 212Pb distribution studies in the rat. Health. Phys. 20, 617–623.

Duport, P., Robertson, R., Ho, K., Horvat, F., 1991. Flow-through dissolution of uranium-thorium ore dust, uranium concentrate, uranium dioxide, and thorium alloy in simulated lung fluid. Radiat. Prot. Dosim. 38(1/3), 121-133.

Durbin, P. W. (1960) Metabolic characteristics within a chemical family. Health Phys. 2, 225-238.

Everson, J., Patterson, C.C., 1980. "Ultra-clean" isotope dilution/mass spectrometric analyses for lead in human blood plasma indicate that most reported values are artificially high. Clin. Chem. 26, 1603-1607.

Fleshman, D; Krotz, S.; Silva, A. (1966). The metabolism of elements of high atomic number. UCRL 14739:69-86.

Flood, P.R., Schmidt, P.F., Wesenberg, G.R., Gadeholt, H., 1988. The distribution of lead in human hemopoietic tissue and spongy bone after lead poisoning and Ca-EDTA chelation therapy. Arch. Toxicol. 62, 295-300.

Freyberg, R. H.; walter d. Block, W. D.; Levey, S. (1942). Metabolism, toxicity and manner of action of gold compounds used in the treatment of arthritis. III. Complete excretion studies and comparison of intravenous and intramuscular administration of some gold salts. Ann. Rheum. Dis. 3:77-89.

Friberg, L. (1956) Studies of the accumulation, metabolism and excretion of inorganic mercury (203Hg) after prolonged subcutaneous administration to rats. Acta Pharmacol. et Toxicol. 12, 411-427.

Gehring, P. J.; Hammond, P. B. (1967). The interrelationship between thallium and potassium in animals. J. Pharmacol. Exp. Ther. 155:187-201.

Gettler, A. O.; Weiss, L. (1943). Thallium poisoning. III. Clinical toxicology of thallium. Amer. J. Clin. Pathol. 13: 422-429.

Gottlieb, N. L. (1983). Comparison of the kinetics of parenteral and oral gold. Scand. J. Rheumatol. 12:10-14.

Greenhalgh, J.R., Birchall, A., James, A.C., Smith, H., Hodgson, A., 1982. Differential retention of 212Pb ions and insoluble particles in nasal mucosa of the rat. Phys. Med. Biol. 27, 837–851.

Greenhalgh, J.R., James, A.C., Smith, H., Hodgson, A., 1979. Absorption of lead ions from the lung. NRPB/ R&D3. Annual Research and Development Report 1978 pp. 38–42.

Greenhalgh, J.R., James, A.C., Smith, H., Stubberfield, D.R., 1978. Absorption of lead from the bronchial region of the lung. NRPB/ R&D2. Annual Research and Development Report 1977 pp. 65–70.

Gregus, Z.; Klaassen, C. D. 1986. Disposition of metals in rats: A comparative study of fecal, urinary, and biliary excretion and tissue distribution of eighteen metals. Toxicol. Appl. Pharmacol. 85:24-38.

Griffin, R.M., Matson, W.R., 1972. The assessment of individual variability to trace metal insult: low-molecular-weight metal complexing agents as indicators of trace metal insult. Amer. Indus. Hyg. Assoc. 33, 373-377.

Gross, S.B., Pfitzer, E.A., Yeager, D.W., Kehoe, R.A., 1975. Lead in human tissues. Toxicol. Appl. Pharmacol. 32, 638-651.

Habibi, K., 1973. Characterisation of particulate matter in vehicle exhaust. Environ. Sci. Technol. 7, 223–234.

Hamilton, E.I., Minski, M.J., Cleary, J.J., 1972. The concentration and distribution of some stable elements in healthy human tissues from the United Kingdom. Sci. Total Environ. 1, 341-374.

Hayes, A. D.; Rothstein, A. 1962. The metabolism of inhaled mercury vapor in the rat studied by isotope techniques. J. Pharmacol. 38, 1-10.

Heard, M., Chamberlain, A., 1982. Effect of minerals and food on uptake from the gastrointestinal tract in humans. Human Toxicology. 1. 411–415.

Heard, M.J., Chamberlain, A.C., 1984. Uptake of Pb by human skeleton and comparative metabolism of Pb and alkaline earth elements. Health Phys. 47,857-865.

Heard, M.J., Wells, A.C. Newton, D., Chamberlain, A.C., 1979. Human uptake and metabolism of tetra-ethyl and tetra-methyl lead vapour labelled with lead-203. In: Heavy Metals in the Environment (London: CEP Consultants).

Hodgson, S.A., Rance, E.R., Stradling, G.N., Hodgson, A., Fell, T.P., Youngman, M.J., Moody, J.C., Ansoborlo, E., 2000. Biokinetics of thorium dioxide and its decay products in the rat after alveolar deposition: implications for human exposure. Chilton, NRPB-M1192.

Hodgson, S.A., Stradling, G.N., Hodgson, A., Smith, T.J., Youngman, M.J., Moody, J.C., Ansoborlo, E., 2003. Biokinetics and assessment of intake of thorium dioxide. Radiat. Prot. Dosim. 105, 115–118.

Hong, Y.C., Yen, P.K.-J., Shaw, J.H., 1968. An analysis of the growth of the cranial vault in rabbits by vital staining with lead acetate. Calc. Tiss. Res. 2, 271-285.

Hu, H., Milder, F.L., Burger, D.E., 1989. X-ray fluorescence: Issues surrounding the application of a new tool for measuring burden of lead. Environ. Res. 49, 295-317.

Hursh, J. B.; Greenwood, M. R.; Clarkson, T. W.; Allen, J.; Demuth, S. (1980) The effect of ethanol on the fate of mercury vapor inhaled by man. J. Pharmacol. Exp. Ther. 214, 520-527.

Hursh, J.B., 1973. Retention of Pb-210 in beagle dogs. Health Phys. 25, 29-35.

Hursh, J.B., Brown, C., 1969. Tissue distribution of 212Bi in rats. Proc. Soc. Exp. Biol. Med. 131, 116-120.

Hursh, J.B., Mercer, T.T., 1970. Measurement of 212Pb loss rate from human lungs. J. Appl. Physiol 28, 268–274.

Hursh, J.B., Schraub, A., Sattler, E.L., Hofmann, H.P., 1969. Fate of 212Pb inhaled by human subjects. Health Phys. 16, 257–267.

Hursh, J.B., Suomela, J., 1968. Absorption of Pb-212 from the gastrointestinal tract of man. Acta Radiol. Ther. Phys. Biol. 7, 108-120.

Hursh, J.B.; Clarkson, T. W.; Cherian, M. G.; Vostal, J. J.; Mallie, R. V. (1976) Clearance of mercury (Hg-197, Hg-203) vapor inhaled by human subjects. Arch. Environ. Health 31, 302-309.

ICRP 1994. Dose Coefficients for Intakes of Radionuclides by Workers, ICRP Publication 68. Ann. ICRP 24(4).

ICRP 2002a. Basic anatomical and physiological data for use in radiological protection: Reference values, ICRP Publication 89, Ann. ICRP 32(3/4).

ICRP 2002b. Guide for the Practical Application of the ICRP Human Respiratory Tract Model. ICRP Supporting Guidance 3 Ann. of the ICRP 32(1–2).

ICRP, 1975. Report of the Task Group on Reference Man, ICRP Publication 23. Oxford, Pergamon Press.

ICRP, 1980. Limits on Intakes of Radionuclides for Workers. ICRP Publication 30, Pt.2. Ann. ICRP 4(3/4).

ICRP, 1993. Age-dependent Doses to Members of the Public from Intake of Radionuclides: Part 2, Ingestion dose coefficients. ICRP Publication 67. Ann. ICRP 23. (3/4).

Ishihara, N., Matsushiro, T., 1986. Biliary and urinary excretion of metals in humans. Arch. Environ. Health 41, 324-330.

James, A.C., Greenhalgh, J.R., Smith, H., 1977. Clearance of lead-212 ions from rabbit bronchial epithelium to blood. Phys. Med. Biol. 22, 932–948.

James, H., Hilburn, M., Blair, J., 1985. Effects of meal times on uptake of lead from the gastrointestinal tract in humans. Hum Toxicol., 4, 401-407.

Jeffrey M. R.; Freundlich, H. F.; Bailey, D. M. (1958). Distribution and excretion of radiogold in animals. Ann. rheum. Dis. 17:52-60.

Jellum, E.; Munthe, E.; Guldal, G.; Aaseth, J. (1980). Fate of the gold and the thiomalate part after intramuscular administration of aurothiomalate to mice. Ann. Rheum. Dis. 39:155-158.

Johnson, J. E.; Johnson, J. A. (1968) A new value for the long component of the effective half-retention time of 203Hg in the human. Health Phys. 14, 265-266.

Jonsson, F.; Sandborgh-Englund, G.; Johanson, G. A. (1999) Compartmental model for the kinetics of mercury vapor in humans. Toxicol. Appl. Pharmacol. 155, 161-168.

Joselow, M. M.; Goldwater, L. J.; Weinberg, S. B. (1967) Absorption and excretion of mercury in man. XI. Mercury content of "normal" human tissues. Arch. Environ. Health 15, 64-66.

Jugo, S. (1976) Retention and distribution of 203HgCl2 in suckling and adult rats. Health Phys. 30, 241-243.

Kalkwarf, D.R., Jackson, P.O., 1984. Lung-clearance classification of radionuclides in calcined phosphate rock dust. PNL-5221, Richland, WA. Pacific Northwest Laboratory Reports.

Kalkwarf, D.R., Jackson, P.O., Hardin, J.M., 1984. Lung-clearance classification of radionuclides in coal fly ash. Health Phys. 47, 37–45.

Keller, C. A., Doherty, R. A. 1980. Distribution and excretion of lead in young and adult female mice. Environ Res 21, 217-228.

Krahwinkel, W.; Herzog, H.; Feinendegen, L. E. (1988). Paramacokinetics of thallium-201 in normal individuals after routine myocardial scintigraphy. J. Nucl. Med. 29:1582-1586.

Lacroix, P., 1960. Ca-45 autoradiography in the study of bone tissue. In: Bone as a tissue (Rodahl K, Nicolson JT, Brown EM, Eds). New York, McGraw-Hill, pp. 262-279,

Lathrop, K. A.; Harper, P. V.; Gloria, I. V.; Rich, M. (1975). Intestinal localization of Tl-201. J. Nucl. Med. 16:545.

Lathrop, K. A.; Tsui, B. M. W.; Chen, C.-T.; Harper, P. V. (1989). Multiparameter extratrapolation of biodistribution data between species. Health Phys. 57, Suppl. 1:121-126.

Lawrence, J. S. (1961). Studies with radioactive gold. Ann. Rheum. Dis. 20:341-352.

Leggett, R.W., 1993. An age-specific kinetic model of lead in humans. Environ. Health Perspect. 101, 598-616.

Lie, R.; Thomas, R. G.; Scott, J. K. (1960). The distribution and excretion of thallium-204 in the rat, with suggested MPC's and a bioassay procedure. Health Phys. 2:334-340.

Lindh, U., Brune, D., Nordberg, G., 1978. Microprobe analysis of lead in human femur by proton induced x-ray emission (PIXE). Sci. Total Environ. 10, 31-37.

Lloyd, R.D., Mays, C.W., Atherton, D.R., Bruenger, F.W., 1975. 210Pb studies in beagles. Health Phys. 28, 575-583.

MacDonald, N.S., Ezmirlian, F., Spain, P., McArthur, C., 1951. The ultimate site of skeletal deposition of strontium and lead. J. Biol. Chem. 189, 387-399.

Mallon, R.P., 1983. A metabolic model of lead kinetics based upon measured organ burdens during chronic exposure experiments with infant and juvenile baboons. Dissertation. New York University.

Manton, W.I., Cook, J.D., 1984. High accuracy (stable isotope dilution) measurements of lead in serum and cerebrospinal fluid. Br. J. Ind. Med. 41, 313-319.

Marsh J.W., Gregoratto, D., Karcher, K., Nosske D., Bessa Y., Blanchardon E., Hofmann W., Tomasek, L., 2011. Dosimetric calculations for uranium miners for epidemiological studies. Radiat. Prot. Dos. pp. 1-13, doi:10.1093/rpd/ncr310.

Marsh, J.W., Birchall, A., 1999. Determination of lung-to-blood absorption rates for lead and bismuth that are appropriate for radon progeny. Radiat. Prot. Dosim. 83, 331–337.

Martell, E.A., 1974. Radioactivity of tobacco trichomes and insoluble cigarette smoke particles. Nature 249, 215-217.

Mascarenhas, B. R.; Granda, J. L.; Freyberg, R. H. (1972). Gold metabolism in patients with rheumatoid arthritis treated with gold compounds – reinvestigated. Arthritis and Rheumatism 15:391-402.

Massarella, J. W.; Pearlman, R. S. (1987). Gold disposition in the rat: Studies of its plasma half-life and its urinary, biliary and fecal elimination pathways. J. Pharmacol. Exp. Ther. 243:247-257.

McQueen, E. G.; Dykes, P. W. (1969). Transport of gold in the body. Ann. Rheum. Dis. 28:437-442.

Miyake, M., Ishigaki, K., Suzuki, T., 1986. Structure refinements of Pb2+ ion-exchanged apatites by x-ray powder pattern-fitting. J. Solid State Chem. 61, 230-235.

Moody, J.C., Davies, C.P., Stradling, G.N., 1994a. Biokinetics of thorium and daughter radionuclides after deposition in the rat lung as fluoride and hydroxide. In: Mohr, U., Dungworth, D.L., Mauderly, J.L., Oberdörster, G. (Eds.), Proc. Fourth International Inhalation Symposium, Hannover, March 1–5, 1993. Toxic and Carcinogenic Effects of Solid Particles in the Respiratory System, pp. 611–614.

Moody, J.C., Stradling, G.N., 1992. Biokinetics of thorium and daughter radionuclides after deposition in the rat lung. J. Aerosol Sci. 23, S523–S526.

Moody, J.C., Stradling, G.N., Pearce, M.J., Gray, S.A., 1994b. Biokinetics of Thorium and Daughter Radionuclides after Deposition in the Rat Lung as Nitrate: Implications for Human Exposure. NRPB-M525, Chilton, UK.

Morgan, A., Holmes, A., Evans, J.C., 1977. Retention, distribution, and excretion of lead by the rat after intravenous injection. Br. J. Ind. Med. 34, 37-42.

Morrow, P.E., Better, F., Amato, F., Gibb, F.R., 1980. Pulmonary retention of lead: an experimental study in man. Environ. Res. 21 373–384.

Nakamura, K.; Nishiguchi, I.; Takagi, Y.; Kubo, A.; Hashimoto, S. (1985). Distribution of 201Tl in blood. Radioisotopes. 34:550-554.

Newton, D.; Fry, F. A. (1978) The retention and distribution of radioactive mercuric oxide following accidental inhalation. Ann. Occup. Hyg. 21, 21-32.

Potter, G. D.; Vattuone, G. M.; McIntyre, D. R. (1971). The fate and implications of ingested 204Tl in a dairy cow and a calf. Health Phys. 20:657-662.

Rabinowitz, M. B., Wetherill, G.W., Kopple, J.D., 1974. Studies of human lead metabolism by use of stable isotope tracers. Environ. Health Perspect. 5-7, 145-153.

Rabinowitz, M.B., Wetherill, G.W., Kopple, J.D., 1973. Lead metabolism in the normal human: Stable isotope studies. Science 182, 725-727.

Rabinowitz, M.B., Wetherill, G.W., Kopple, J.D., 1976. Kinetic analysis of lead metabolism in healthy humans. J. Clin. Invest 58, 260-270.

Rendall, R.E.G., Baily, P., Soskolne, C. L., 1975. The effect of particle size on absorption of inhaled lead. Am. Ind. Hyg. Assoc. J. 36, 207–213.

Rhoads, K., Sanders, C.L., 1985. Lung clearance, translocation, and acute toxicity of arsenic, beryllium, cadmium, cobalt, lead, selenium, vanadium, and ytterbium oxides following deposition in rat lung. Environ. Res. 36, 359–378.

Rothstein, A.; Hayes, A. D. (1960) The metabolism of mercury in the rat studied by isotope techniques. J. Pharmacol. Exp. Ther. 130, 166-176.

Rubin, M.; Sliwinski, A.; Photias, M,; Feldman, M.; Zvaifler, N. (1967). Influence of chelation on gold metabolism in rats. Proc. Soc. Exp. Biol. Med. 124:290-296.

Scheiman-Tagger, E., Brodie, A.G., 1964. Lead acetate as a marker of growing calcified tissues. Anat. Rec. 150, 435-440.

Silva, A. J.; Fleshman, D. G.; Shore, B. (1973). The effects of penicillamine on the body burdens of several heavy metals. Health Phys. 24:535-539.

Singh, N.P., Bennett, D.B., Wrenn, M.E., 1986. Concentrations of 210Pb and its states of equilibrium with 238U, 234U, and 230Th in U miners' lungs. Health Phys., 51, 501–507.

Stradling, G.N., Davies, C.P., Moody, J.C., Gray, S.A., Wilson, I., Ellender, M., 2005. Biokinetics of thorium and daughter radionuclides after deposition as fluoride and hydroxide in the rat lung: implications for occupational exposure. NRPB-DA/05/2005, Chilton, UK.

Strauss, H. W.; Harrison, K.; Langan, J. K.; Lebowitz, E.; Pitt, B. (1975). Thallium-201 for myocardial imaging. Circulation 51:641-645.

Sugawa-Katayama, Y.; Koishi, H.; Danbara, H. (1975). Accumulation of gold in various organs of mice injected with gold thioglucose. J. Nutr. 105:957-962.

Suzuki, M.; Morikawa, M.; Tomita, K.; Yoshida, A.; Suwo, M.; Matsushima, H.; Kato, M.; Ueda, N.; Yamada, H.; Hazue, M. (1978). Thallous chloride-201Tl – Fundamental studies on its behavior and clinical evaluation. Kaku Igaku. Japanese J. Nucl. Med. 15:27-40.

Tipton, I.H., Cook, M.J., 1963. Trace elements in human tissue. Part II. Adult subjects from the United States. Health Phys. 9, 103-145.

Vander, A.J., Taylor, D.L., Kalitis, K., Mouw, D.R., Victery, W., 1977. Renal handling of lead in dogs: Clearance studies. Am. J. Physiol. 233, F532-F538.

Verbeeck, R.M., Lassuyt, C.J., Heijligers, H.J., Driessens, F.C., Vrolijk, J.W., 1981. Lattice parameters and cation distribution of solid solutions of calcium and lead hydroxyapatite. Calc. Tiss. Int. 33, 243-247.

Victery, W., Vander, A.J., Mouw, D.R., 1979. Renal handling of lead in dogs, stop-flow analysis. Am. J. Physiol. 237, F408-F414.

Vincent, J., 1957. Les remaniements de l'os compact marque a l'adie de plomb. Revue Belge de Path. et Med. Exper. 26, 168-172.

Wells, A.C., Venn, J.B., Heard, M.J., 1975. Deposition in the lung and uptake to blood of motor exhaust labelled with Pb-203. In: Walton, W.H., McGovern, B. (Eds.), Inhaled Particles IV, pp. 175-189. Proceedings of a Symposium of the British Occupational Hygiene Society, Edinburgh.

Yen, P. K., Shaw, J. H. 1977. Remodeling of compact bone studied with lead acetate as an intravital stain. J Dent. Res. 56, 961-966.

10. BISMUTH (Z = 83)

10.1. Chemical forms in the workplace

(479) Bismuth is a metalloid which mainly occurs in oxidation state III. Arsenic and antimony are good chemical analogues of bismuth. Bismuth is encountered in industry in a variety of chemical and physical forms, including oxides, chlorides, fluorides, iodides, and sulphides.

(480) Several isotopes of bismuth with short half-lives occur within the radioactive disintegration chains of actinium, radium and thorium.

Table 10-1. Isotopes of bismuth addressed in this report

Isotope	Physical half-life	Decay mode
Bi-200	36.4 m	EC, B+
Bi-201	108 m	EC, B+
Bi-202	1.72 h	EC, B+
Bi-203	11.76 h	EC, B+
Bi-204	11.22 h	EC, B+
Bi-205	15.31 d	EC, B+
Bi-206	6.243 d	EC, B+
Bi-207	32.9 y	EC, B+
Bi-208	3.68E+5 y	EC
Bi-210[a]	5.013 d	B-, A
Bi-210m	3.04E+6 y	A
Bi-212	60.55 m	B-, A
Bi-213	45.59 m	B-, A
Bi-214[a]	19.9 m	B-, A

[a] Data for these radionuclides are given in the printed copy of this report. Data for other radionuclides are given on accompanying electronic disk.

10.2. Routes of Intake

10.2.1. Inhalation

Absorption Types and parameter values

(481) Very little information from which parameter values can be assessed is available from experimental studies of the behaviour of bismuth deposited in the respiratory tract.

(482) Absorption parameter values and Types, and associated f_A values for particulate forms of bismuth are given in Table 10-2. For radiation protection purposes, the most important exposures to radioisotopes of bismuth are as decay products of radon. Dose coefficients for isotopes of bismuth inhaled as radon decay products are given in the radon section, where factors such as the relevant aerosol size distribution are addressed. Otherwise, exposures to radioisotopes of bismuth occur most often as decay products associated with intakes of uranium, thorium or radium.

(a) Bismuth as a decay product of radon

(483) In this section studies are considered in which ^{212}Bi (half-life 61 minutes) formed

from decay of ^{220}Rn (half-life 56 seconds) ^{216}Po (half-life 0.15 seconds) and ^{212}Pb (half-life 11 hours), or ^{214}Bi (half-life 20 minutes) formed from decay of ^{222}Rn (half-life 3.8 days), ^{218}Po (half-life 3.1 minutes) and ^{214}Pb (half-life 27 minutes) was inhaled directly, while still airborne. For decay schemes, see the thorium and uranium sections. Studies in which bismuth ions were administered to the respiratory tract in a liquid medium, which might also be relevant to bismuth as a decay product of radon, are considered below in the section on particulate forms.

(484) Drew (1971) reported that the tissue distributions of ^{212}Pb and ^{212}Bi activities were similar in rats following exposure to ^{220}Rn (thoron) and its decay products for 2 days. However, the exposure situation was complex, because the ^{212}Pb and ^{212}Bi in tissues originated from inhalation of ^{220}Rn and its decay within the body, inhalation of ^{212}Pb and ^{212}Bi, and also their ingestion from food and preening of fur. It is therefore difficult to estimate how much of the ^{212}Bi originated from intake of ^{212}Bi, and how much from decay of ^{212}Pb in the body.

(485) Butterweck et al. (2001, 2002) carried out volunteer experiments to determine the absorption rate of unattached radon progeny. (For further information see the lead inhalation section.) Volunteers inhaled an aerosol which was predominantly unattached radon progeny. Measurements were made of ^{222}Rn, ^{214}Pb and ^{214}Bi in blood samples taken at the end of a 30-minute exposure (Butterweck et al., 2002). *In vivo* measurements of the head and chest were carried out over a 30-minute period, starting approximately 7 minutes after exposure (Butterweck et al., 2001). No clearance from the head (other than physical decay) was observed over this period for ^{214}Pb, indicating that a small fraction of the unattached ^{214}Pb was absorbed rapidly to blood ($s_r >> 100$ d^{-1}), as measured by the blood sample, while the rest (fraction f_b) was bound to tissues (or stationary mucus). Assuming a rapid dissolution rate (s_r) of 1000 d^{-1} with f_r=1.0 and an uptake rate from the bound state (s_b) of 1.7 d^{-1}, Butterweck et al. (2002) estimated values of f_b in the range 0.7–0.85, for radon progeny (without distinguishing between ^{214}Pb and ^{214}Bi) from the blood measurements. However, Butterweck et al. (2002) also estimated "absorption rates" for ^{214}Pb and ^{214}Bi from their activities in the blood sample and the estimated respiratory tract deposition, assuming that absorption from respiratory tract to blood could be represented by a single rate constant (s_r) i.e. f_r =1 and f_b =0, although this model seems inconsistent with the *in vivo* measurements. They obtained absorption half-times of ~60 minutes for ^{214}Pb and ~25 minutes for ^{214}Bi, suggesting that there was greater absorption of ^{214}Bi than of ^{214}Pb by the end of the exposure when the blood sample was taken.

(486) Hursh et al. (1969) followed lung retention, blood concentration, urinary and fecal excretion of ^{212}Pb in ten volunteers for up to 3 d after inhalation (by mouth) of an aerosol formed by mixing ^{212}Pb (formed from decay of ^{220}Rn/^{216}Po) with natural room aerosol. (For further information see the lead inhalation section.) Measurements of ^{212}Bi were also made, but because of its short half-life fecal excretion of ^{212}Bi could not be determined. Initial deposition of ^{212}Bi in the lungs was ~10% of the ^{212}Pb activity, as expected because of its lower concentration in the air. Measurements of urinary excretion of ^{212}Bi were reported for one subject. Hursh and Mercer (1970) measured ^{212}Bi activities in blood and urine in four volunteers after inhalation of an aerosol formed by mixing ^{212}Pb with natural room aerosol. (For further information see the lead inhalation section). However, the results were not reported "to conserve space and because the findings were in all cases similar to those reported earlier" with reference to Hursh et al. (1969). Marsh and Birchall (1999) used the measurements of urinary excretion of ^{212}Bi reported by Hursh et al. (1969) to estimate the absorption rate for bismuth. They took account of ingrowth from decay of its parent ^{212}Pb in

the lungs and following systemic uptake. They assumed that absorption of both lead and bismuth could be represented by a single component i.e. $f_r = 1$ and $f_b = 0$. In the analysis the absorption half-time for lead was fixed at 10 hours. The best fit was obtained with an absorption half-time for bismuth of 13 hours, suggesting Type F behaviour. However, the authors noted that this value should be treated with caution as it was based on data from a single subject. A more detailed analysis of the results of human volunteer studies of inhaled radon progeny was carried out here (i.e. by the Task Groups), to estimate absorption parameter values appropriate for short-lived radon progeny, giving specific consideration to the rapid absorption phase and binding. (For further information see the lead inhalation section.) However, for the study by Hursh et al. (1969) the information available did not permit assessment of f_b.

(b) Particulate aerosols

(487) In all of the studies summarised below, except that of Greenhalgh et al. (1977) who administered $^{207}BiCl_3$, isotopes of uranium or thorium with their decay products were administered by intratracheal instillation into rats, and measurements were made of the lung retention and tissue distribution of ^{228}Th, ^{212}Pb, ^{212}Bi and ^{208}Tl at times from 6 or 24 hours onwards. In all these studies the distributions of ^{212}Bi (and ^{208}Tl) were similar to those of the parent ^{212}Pb. Because their physical half-lives are so short (61 minutes and 3 minutes respectively) measurements made at 6 hours onwards would be mainly of activity formed from decay of ^{212}Pb within the body, rather than from intake of ^{212}Bi. The similar distributions of ^{212}Bi and ^{208}Tl (allowing for the 36% branching ratio for the formation of ^{208}Tl from decay of ^{212}Bi) to those of ^{212}Pb might suggest that there was not rapid movement of ^{212}Bi from the site (e.g. the lungs) in which it was formed by decay of ^{212}Pb. However, ^{212}Bi (and ^{208}Tl) would have grown in rapidly between dissection of the animals and measurements of activities in tissues. Thus the activities of ^{212}Bi (and ^{208}Tl) measured may have been significantly higher than those present *in vivo*, and without detailed information (which is not available) about the time which elapsed between dissection of the animals and measurements, it is not possible to correct for this and hence estimate the absorption rate of the bismuth from the respiratory tract.

Bismuth chloride ($BiCl_3$)

(488) Greenhalgh et al. (1977) followed the lung retention of ^{207}Bi for about an hour after instillation of ^{207}Bi instilled as $BiCl_3$ solution into the bronchi of rabbits. There was little clearance in this time and the amount of ^{207}Bi in blood after 90 minutes was <1% of that instilled. The authors estimated that the clearance half-time was greater than 1 day. This appears to have been a pilot study that was not followed up.

Bismuth nitrate ($Bi(NO_3)_3$)

(489) Ballou et al. (1986) measured lung retention and tissue distribution of ^{232}U, ^{228}Th, ^{224}Ra, ^{212}Pb, ^{212}Bi and ^{208}Tl at 24 hours after intratracheal instillation into rats of ^{232}U nitrate with its decay products. (For further information, see the uranium inhalation section.) Moody et al. (1994a; Moody and Stradling, 1992) measured the tissue distribution of ^{228}Th, ^{212}Pb, ^{212}Bi and ^{208}Tl, at times from 6 hours to 7 days after intratracheal instillation into rats of a nitrate solution of ^{228}Th in equilibrium with its decay products. (For further information, see the thorium and lead inhalation sections.) In both studies the distributions of ^{212}Bi (and ^{208}Tl) were similar to those of ^{212}Pb. However, no estimate could be made by the task group of the rate of absorption of the ^{212}Bi from the lungs (see above).

Bismuth hydroxide ($Bi(OH)_3$)

(490) Moody et al. (1994b; Stradling et al., 2005) measured the tissue distributions of ^{228}Th, ^{212}Pb, ^{212}Bi and ^{208}Tl, at times from 1 to 28 days after intratracheal instillation into rats of a suspension of ^{228}Th hydroxide in equilibrium with its decay products. (For further information, see the thorium and lead inhalation sections.) The distributions of ^{212}Bi (and ^{208}Tl) were similar to those of ^{212}Pb. However, no estimate could be made here of the rate of absorption of the ^{212}Bi from the lungs (see above).

Bismuth fluoride ($BiCl_3$)

(491) Moody et al. (1994b; Stradling et al., 2005) measured the tissue distributions of ^{228}Th, ^{212}Pb, ^{212}Bi and ^{208}Tl, at times from 1 to 28 days after intratracheal instillation into rats of a suspension of ^{228}Th fluoride in equilibrium with its decay products. (For further information, see the thorium and lead inhalation sections.) The distributions of ^{212}Bi (and ^{208}Tl) were similar to those of ^{212}Pb. However, no estimate could be made here of the rate of absorption of the ^{212}Bi from the lungs (see above).

Thorium dioxide

(492) Hodgson et al. (2000, 2003) measured the tissue distributions of ^{228}Th, ^{212}Pb, ^{212}Bi and ^{208}Tl, at times from 1 to 168 days after intratracheal instillation into rats of suspensions of ^{232}Th dioxide enriched with ^{228}Th, in equilibrium with its decay products. (For further information, see the thorium and lead inhalation sections.) There was little absorption of the thorium itself, consistent with assignment to Type S. The activity of ^{212}Pb in the lungs was lower than of that of the thorium, which was attributed to diffusion of ^{220}Rn (thoron) and recoil of the progeny from alpha particle decay. The distributions of ^{212}Bi (and ^{208}Tl) were similar to those of ^{212}Pb. However, no estimate could be made here of the rate of absorption of the ^{212}Bi from the lungs (see above).

Decay products of bismuth formed in the respiratory tract

(493) The general approach to treatment of decay products formed in the respiratory tract is described in Part 1, Section 3.2.3. In summary, it is expected that generally the rate at which a particle dissociates is determined by its matrix, and hence the physico-chemical form of the inhaled material. It is recognised that nuclei formed by alpha decay within a particle matrix may be expelled from it into the surrounding medium by recoil, but to implement this routinely would add greatly to the complexity of calculations. It is expected that the behaviour of soluble (e.g. Type F) material in the respiratory tract would depend on its elemental form, i.e. that of the decay product. Nevertheless, for simplicity, in this series of documents the absorption parameter values of the parent are, by default, applied to all members of the decay chain formed in the respiratory tract. Exceptions are made for noble gases formed as decay products, which are assumed to escape from the body directly, at a rate of 100 d^{-1}, in addition to other routes of removal.

(494) For decay schemes of bismuth isotopes in the natural decay series: ^{210}Bi, ^{211}Bi, ^{212}Bi, and ^{214}Bi, see the uranium and thorium sections. Studies specifically comparing the behaviour of bismuth with that of its decay product (thallium) are summarised here.

(495) As noted above, measurements have been made of the tissue distributions of ^{212}Bi and its decay product, ^{208}Tl, following administration to rats of ^{228}Th in various chemical forms (nitrate, hydroxide, fluoride, dioxide), in equilibrium with its decay products. In all these studies the distributions of ^{212}Bi (and ^{208}Tl) were similar to each other and those of the

parent ^{212}Pb. Because their physical half-lives are so short (61 minutes and 3 minutes respectively) measurements made at 6 hours onwards would be mainly of activity formed from decay of ^{212}Pb within the body, rather than from intake of ^{212}Bi (or ^{208}Tl). However, the half-life of ^{208}Tl (3 minutes) is so short that it would easily reach equilibrium with ^{212}Bi between dissection of the animals and measurements of activities in tissues. It is not possible to correct for this ingrowth and hence estimate the absorption rate from the respiratory tract of the thallium formed as a decay product of bismuth. However, since the half-life of ^{208}Tl is so short (as is that of ^{207}Tl present in the ^{235}U decay series, 5 minutes), the absorption rate would have to be very high to influence dose assessments.

Rapid dissolution rate for bismuth

(496) Inferences drawn from the three studies outlined above, which might provide information on the rapid dissolution rate for bismuth, are contradictory. Greenhalgh et al. (1977) estimated that the lung retention half-time was greater than 1 day following instillation of $^{207}BiCl_3$ into the bronchi of rabbits: much slower absorption than that of lead over the period (one hour) of measurement. Marsh and Birchall (1999) estimated the absorption rate for bismuth using measurements of urinary excretion of ^{212}Bi by a volunteer following inhalation of attached radon decay products reported by Hursh et al. (1969). They assumed that absorption of both lead and bismuth could be represented by a single component i.e. f_r = 1 and f_b = 0. The best fit was obtained with an absorption half-time for bismuth of 13 hours, very similar to that obtained for lead, i.e. s_r ~1 d^{-1}. Butterweck et al. (2002) assessed that absorption of ^{214}Bi was faster than that of ^{214}Pb during inhalation of unattached radon progeny.

(497) The main use for absorption parameter values for bismuth is in assessing doses from inhaled radon decay products. A value of s_r of 1 d^{-1}, based on the assessment of Marsh and Birchall (1999) is adopted here. The short-lived isotopes of bismuth (^{214}Bi, ^{212}Bi and ^{211}Bi) formed as a decay product of radon have radioactive decay constants >> 1 d^{-1}, so the bismuth absorption rate will have little influence in assessing doses from inhaled radon decay products.

Extent of binding of bismuth to the respiratory tract

(498) There is insufficient information to estimate the extent of any bound state. It is therefore assumed by default that f_b = 0.

Table 10-2. Absorption parameter values for inhaled and ingested bismuth

Inhaled particulate materials		Absorption parameter values[a] f_r	s_r (d^{-1})	s_s (d^{-1})	Absorption from the alimentary tract, f_A
Default parameter values[c]					
Absorption Type	Assigned forms				
F	Bismuth as a decay product of radon	1	1	–	0.05
M	All unspecified forms[d]	0.2	1	0.005	0.01
S	—	0.01	1	$1x10^{-4}$	$5x10^{-4}$
Ingested material					
All forms					0.05

[a] It is assumed that for bismuth the bound state can be neglected, i.e. $f_b = 0$. The values of s_r for Type F, M and S forms of bismuth (1 d^{-1}) are element-specific.

[b] For inhaled material deposited in the respiratory tract and subsequent cleared by particle transport to the alimentary tract, the default f_A values for inhaled materials are applied: i.e. the product of f_r for the absorption Type (or specific value where given) and the f_A value for ingested soluble forms of bismuth (0.05).

[c] Materials (e.g. bismuth as a decay product of radon) are listed here where there is sufficient information to assign to a default absorption Type, but not to give specific parameter values (see text).

[d] Default Type M is recommended for use in the absence of specific information, i.e. if the form is unknown, or if the form is known but there is no information available on the absorption of that form from the respiratory tract.

10.2.2. Ingestion

(499) There are few available data on bismuth absorption in human and animals. It has been stated that basic salts of bismuth are only poorly absorbed from the gastrointestinal tract (Sollman, 1957) and suggested that the fractional absorption of dietary bismuth from the gastrointestinal tract is about 0.08 (ICRP, 1975).

(500) The absorption of bismuth from five ^{205}Bi compounds was studied in man (Dresow at al., 1992). From single oral doses of these five compounds, less than 0.1% bismuth was absorbed and excreted in the urine, with a significantly higher absorption from the colloidal subcitrate and gallate compounds (about 0.04%) than from salicylate, nitrate and aluminate (0.002 to 0.005%). Koch et al. have studied the pharmacokinetics of bismuth following administration of single or multiple oral doses of ranitidine bismuth citrate to healthy subjects (Koch et al., 1996a,b). They showed that bismuth absorption from ranitidine bismuth citrate was below 0.5% of the dose, and bismuth elimination was predominantly by renal secretion. Boertz et al. (2009) studied the biotransformation and excretion of bismuth after ingestion of 215 mg of colloidal bismuth subcitrate by 20 male volunteers. Bismuth absorption in the stomach and upper intestine was very low, and a total of 0.03 to 1.2% of the ingested Bi was eliminated in the urine during the 56 hours test.

(501) The bioavailability of ^{205}Bi from various oral bismuth preparations was also studied in rats (Dresow et al., 1991). The intestinal absorption, calculated from ^{205}Bi whole body retention and accumulated urinary excretion was very low, but significantly higher (about 0.3%) from bismuth citrates (Bi citrate and colloidal Bi subcitrate) as compared to bismuth nitrate, salicylate, gallate and alluminate (0.04 to 0.11%).

(502) The ICRP *Publication 30* recommended an absorption value of 0.05 to apply to all

chemical forms (ICRP, 1980).

(503) The most recent studies confirm this absorption value for bismuth and an f_A of 0.05 is therefore adopted here for direct ingestion of all chemical forms.

10.2.3. Systemic Distribution, Retention and Excretion

10.2.3.1. Summary of the database

(504) Bismuth has been used since the late 1700s as a therapeutic agent for a number of disorders of the human body. For example, it has been used externally on burns and inflamed skin; orally for gastrointestinal inflammations, ulcers, and as an opaque medium for x-ray examinations; and intramuscularly for treatment for syphilis (Sollman, 1957). Serious adverse affects including death have sometimes occurred. Successful treatments often have involved maintenance of maximal nontoxic concentrations of bismuth. The optimal dosages have been worked out by measurement and estimation of absorption, distribution, and excretion, both clinically and in animal studies.

(505) The systemic biokinetics of bismuth has been found to vary with the route of administration and the form administered. Concentration of particulate or colloidal forms is particularly high in the reticuloendothelial (RE) system (Eridani et al., 1964; Einhorn et al., 1964).

(506) In the early period after acute input to blood, most forms of bismuth are rapidly cleared from plasma to extracellular fluids and excretion pathways. For example, 75% or more of bismuth in human plasma intravenously injected into rats or bismuth citrate intravenously injected into humans left the circulation in the first 5-10 min (Hursh and Brown, 1969; Coenegracht and Dorleyn, 1961; Newton et al., 2001). After the rapid equilibration between blood plasma and extracellular fluids the disappearance of bismuth from blood is much slower. In a human subject receiving ^{207}Bi citrate by intravenous injection, about 6% of the injected amount remained in blood after 1 h, 1% after 7 h, and 0.5% after 1 d (Newton et al., 2001).

(507) Data on the distribution of bismuth in blood are inconsistent. Some investigators have concluded that bismuth shows little affinity for erythrocytes (Benet, 1991; Koch et al., 1996a), while others have concluded that bismuth in blood is present primarily in erythrocytes (D'Souza and Francis, 1987; Rao and Feldman, 1990; Newton et al., 2001).

(508) In studies involving continued oral dosing of human subjects for 6-8 weeks with bismuth compounds, there was a continual rise in plasma concentration and the urinary excretion rate (Froomes et al., 1989). Apparent steady-state levels were reached after about 18 days (range 7-29 days). Renal clearance of bismuth from normal volunteers and gastritis patients averaged 22.2 ml/min. Elimination half-lives based on declining concentrations of bismuth in plasma and urine were 20.7 and 21.6 days, respectively. Similarly, in patients with bismuth encephalopathy, Boiteau et al. (1976) found plasma elimination half-times of about 13-22 days and urine half-times of about 10-20 days. Data of Loiseau and coworkers (1976) indicated a half-time in plasma of about 23 days.

(509) The pharmacokinetics of bismuth was studied in 60 healthy male subjects, ages 19-40 y, for single oral administration of ranitidine bismuth citrate and for twice daily doses for 28 days in 27 healthy male subjects, ages 20-49 y (Koch et al., 1996a,b). After single administration the concentration of bismuth in plasma typically peaked after 30-45 min and declined with a half-time initially on the order of 1 h. The bismuth concentrations in plasma for 15 subjects measured up to 154 d after the last intake indicated three components of

removal with average half-times of 20 min, 11.1 h, and 20.7 d.

(510) Gavey et al. (1989) measured the bismuth concentration in plasma and urine in nine patients before, during, and after treatment with tripotassium dicitrato bismuthate for six weeks. The 24-h urinary clearance of bismuth was estimated as 19.4 and 19.8 plasma volumes per day based on data for 3 and 6 weeks after the start of exposure, assuming a plasma volume of 3000 ml.

(511) Most forms of bismuth show high deposition in the kidneys and subsequent clearance to urine (Durbin, 1960; Eridani et al., 1964; Matthews et al., 1964; Russ et al., 1975; Pieri and Wegmann, 1981; Slikkerveer and de Wolff, 1989). Human subjects injected with bismuth citrate excreted a third or more of the administered bismuth in urine during the first day (Coenegracht and Dorleyn, 1961; Newton et al., 2001). Lower excretion rates have been observed for some forms used in clinical studies. For example, about 13% of bismuth injected as citrate adsorbed on charcoal was excreted in urine during the first day (Coenegracht and Dorleyn, 1961), 2-3% of bismuth injected as phosphate appeared in urine the first day (Coenegracht and Dorleyn, 1961), and as little as 5% of bismuth injected as a salicylate suspension is excreted in urine during the first 3 wk after injection (Sollmann, 1957). Microscopic studies of the epithelium of the proximal renal tubules have shown accumulations of bismuth in the nucleus, cytoplasm, and possibly the lysosomes (Slikkerveer and de Wolff, 1989).

(512) Clinical data indicate that fecal excretion constitutes 4-10% of total excretion of bismuth with oil solutions, 6-22% with "watery" solutions, and 12% with oil suspensions (Sollmann, 1957). In rats and rabbits, fecal excretion arising to a large extent from biliary secretion accounts for 10-20% of the total excretion of bismuth (Pieri and Wegmann, 1981; Vienet et al., 1983, Gregus and Klaassen, 1986).

(513) In a study of the fate of intravenously injected tracer doses of ^{206}Bi in human subjects, Coenegracht and Dorleyn (1961) concluded from in vivo measurements that ^{206}Bi injected as citrate was taken up and retained to a large extent by the liver and spleen. They suggested that injected bismuth citrate may form complexes with plasma proteins and that the size of the bismuth protein complexes will largely determine the initial distribution of bismuth in the body. A high rate of urinary excretion of ^{206}Bi in the first few days after injection presumably represented activity that did not attach to plasma proteins or was released fairly quickly from these proteins.

(514) Extended retention of a portion of the administered bismuth has been reported for relatively insoluble bismuth compounds used in clinical applications (Sollmann, 1957). Autopsy measurements have been interpreted as indicating that the total bismuth stored in the body for an extended period may be as much as 7% of the administered amount (Sollmann, 1957), with approximate relative concentrations (wet weight) of bismuth in different organs being as follows: kidney, 33; liver, 6.8; spleen, 1.6; colon, 1.3; lung, 0.9; brain, 0.6; and blood, 0.5 (Sollmann and Seifter, 1942). The kidneys and liver each contained nearly 10% of the total found in the body (Sollman, 1957).

(515) Buijs and coworkers (1985) found ^{207}Bi ($T_{1/2}$ = 38 y) remaining in two human subjects treated a quarter century earlier with ^{206}Bi injections contaminated with small amounts of ^{207}Bi. They estimated from measurements of the rate of decline of total-body ^{207}Bi and from assumptions on the early rate of excretion of bismuth that 7% of injected bismuth is retained with a half-time close to 20 y. Buijs's estimate applies to bismuth injected as phosphate or as citrate adsorbed on charcoal, the two forms known to be administered to at least one of the subjects. These two forms are taken up to some extent by the RE system (Coenegracht and Dorleyn, 1961), and it appeared from external measurements that the long-

retained activity in the two human subjects was associated largely with organs of this system (Buijs et al., 1985).

(516) Newton et al. (2001) studied the biokinetics of bismuth in a healthy male volunteer after intravenous injection with ^{207}Bi citrate. They estimated that the liver contained 60% of the body content at 3 d. An estimated 55% was lost in excreta, primarily urine, during the first 47 h. Longer-term losses were much slower. Approximately 0.6% of the injected amount remained at 924 d. The long-term half-time was estimated as 1.9 y.

(517) Studies on rats indicate elevated deposition in the kidneys and sometimes in the liver, but the systemic distribution varies with the form of bismuth reaching blood. For example, the ratio of the concentration in the kidneys to that in the liver averaged roughly 15 at 2 h after intravenous (iv) injection with bismuth nitrate (Gregus and Klaassen, 1986); 10 at 2 h after iv injection of bismuth in human plasma (Hursh and Brown, 1969); 5 at 2-48 h after iv injection with bismuth citrate (Pieri and Wegmann, 1981); 50 at 6-48 h after intraperitoneal injection with bismuth citrate (Russ et al., 1975); 20 at 72-144 h after iv injection with bismuth nitrate (Vienet et al., 1983); and 40 at 2-6 h after intraperitoneal injection of bismuth in a carbonate buffer (Zidenberg-Cherr et al., 1987).

(518) In studies on rabbits, the liver was generally a more important repository for bismuth than the kidneys (van den Werff, 1965). The systemic distribution of ^{206}Bi was determined from a few days up to about 2 wk after intravenous administration of different forms, including citrate or phosphate in 5% charcoal suspension in saline, nitrate, phosphate in 5% glucose, and acetate in saline solution. Distributions varied considerably from one form of ^{206}Bi to another. As averages over all animals studied, all forms of ^{206}Bi administered, and all observation times, the liver, kidneys, skeleton, and remaining tissues contained about 38%, 18%, 17%, and 22%, respectively, of the body burden. Typically, the portion of the total-body content in the skeleton increased with time while the portions in liver and kidneys decreased with time.

(519) Deposition of bismuth in bone has also been observed in rats (Eridani et al., 1964; Hursh and Brown, 1969; Russ et al., 1975; Gaucher et al., 1979; Gregus and Klaassen, 1986). Reported values for uptake and retention by bone are highly variable and may depend on the administered form of bismuth. At 4 d after intramuscular injection of ^{206}Bi into rats as BiOCl or BiO(OH), 14.4% of the administered dosage was found in the kidneys, 6.6% in liver, 1.5% in bone, and 0.6% in muscle (Durbin, 1960). About three-fourths of the administered activity was excreted in the first four days, mainly in urine. In rats receiving ^{206}Bi citrate by intraperitoneal injection, total-body activity declined from about 59% of the administered activity at 6 h to about 12-18% at 3-5 d (Russ et al., 1975). Bone contained about 4-7% of the administered amount at 0.5 h and roughly 1% from 1 to 6 d. The kidney content declined from almost 40% of the administered amount at 0.5 h to roughly 12% at 3-6 d. The liver content was <1% of the administered amount from 0-6 d.

(520) Data for dogs injected with ^{224}Ra (Lloyd et al., 1982) or ^{228}Th indicate that there is considerable migration of ^{212}Bi ($T_{1/2}$ = 60.6 min) from its parent, ^{212}Pb, in bone surfaces, red blood cells, and some soft tissues, and that much of the migrating bismuth accumulates in the kidneys or is quickly eliminated in urine. In human subjects who inhaled ^{212}Pb, ^{212}Bi escaped more quickly from red blood cells than did its parent ^{212}Pb, and the rate of urinary excretion of ^{212}Bi was 3-4 times that of ^{212}Pb (Hursh et al, 1969). In bone, ^{210}Bi tends to remain to a large extent with ^{210}Pb at times remote from exposure, indicating that bismuth probably does not readily escape from Pb in bone volume.

10.2.3.2. Systemic model

(521) The structure of the biokinetic model for systemic bismuth is shown in Figure 10-1. Transfer coefficients are listed in Table 10-3.

(522) It is assumed that bismuth leaves blood plasma at the rate 400 d^{-1} (half-time of approximately 2.5 min) with three-fourths moving to the fast-turnover soft-tissue compartment ST0 representing extracellular fluids in the present model. Outflow of the remaining one-fourth is divided as follows: 20% to urinary bladder contents, 4% to the contents of the right colon, 30% to liver (compartment Liver 0), 30% to the urinary path, 5% to other kidney tissue, 5% to bone surfaces, 0.5% to RBC, 1.3% to the slow-turnover soft-tissue compartment ST2, and the remaining 4.2% to the intermediate-term soft-tissue compartment ST1. Half the activity deposited on bone surfaces is assigned to cortical bone and half to trabecular bone. The following removal half-times are assigned: 15 min from ST0 to plasma; 2 d from Liver 0, with 60% moving to the small intestine contents in bile and 40% moving to Liver 1; 10 d from Liver 1 to Plasma; 1 d from the urinary path to urinary bladder contents; 5 d from other kidney tissue to Plasma; 20 d from bone surface or ST1 to Plasma; 4 d from RBC to Plasma; and 600 d from ST2 to Plasma.

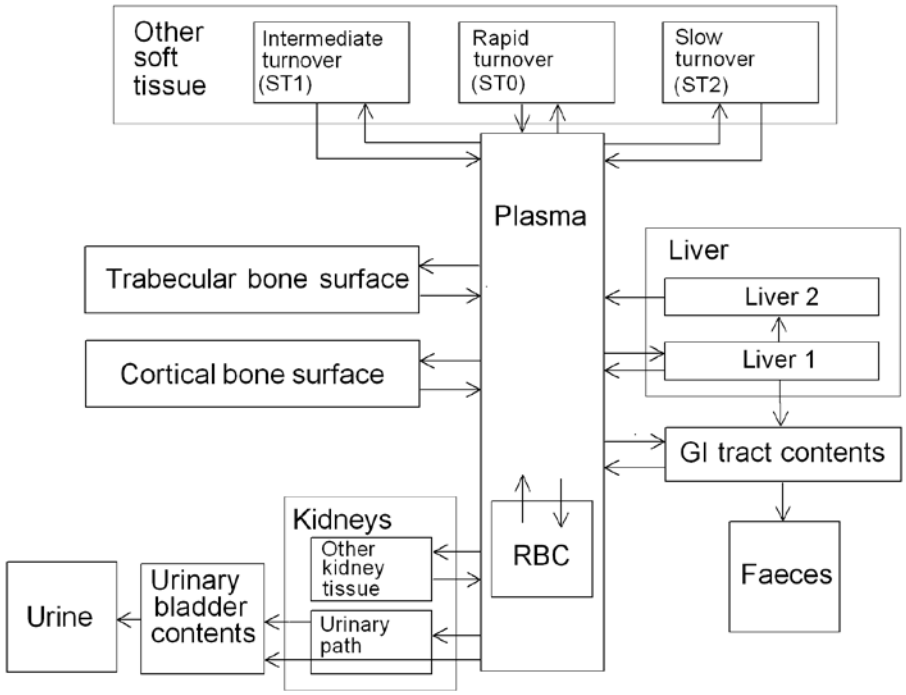

Figure 10-1. Structure of the biokinetic model for systemic bismuth.

Table 10-3. Parameter values for systemic model for bismuth

From	To	Transfer coefficient (d^{-1})
Plasma	Urinary bladder contents	20
Plasma	Right colon contents	4.0
Plasma	RBC	0.5
Plasma	ST0	300
Plasma	ST1	4.2
Plasma	ST2	1.3
Plasma	Liver 0	30
Plasma	Kidneys (urinary path)	30
Plasma	Other kidney tissue	5.0
Plasma	Cortical bone surface	2.5
Plasma	Trabecular bone surface	2.5
RBC	Plasma	0.173
ST0	Plasma	66.54
ST1	Plasma	0.0347
ST2	Plasma	0.00116
Liver 0	Small intestine contents	0.208
Liver 0	Liver 1	0.139
Liver 1	Plasma	0.0693
Kidneys (urinary path)	Urinary bladder contents	0.693
Other kidney tissue	Plasma	0.139
Cortical bone surface	Plasma	0.0347
Trabecular bone surface	Plasma	0.0347

(523) Model predictions are compared with the human injection data of Newton et al. (2001) in Figures 10-1 to 10-3.

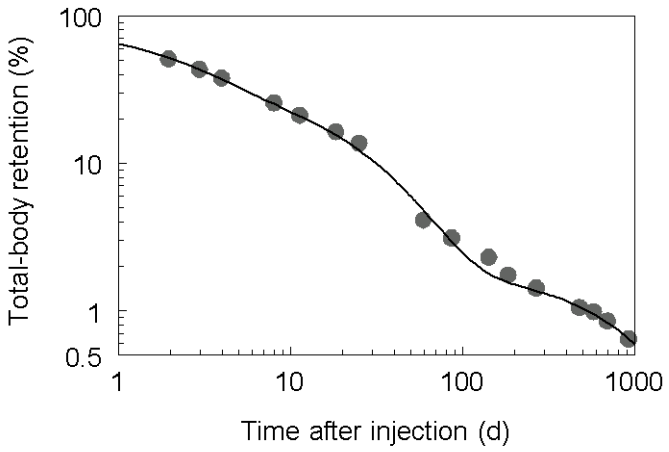

Figure 10-2. Model predictions of total-body retention of intravenously injected bismuth compared with observations of Newton et al. (2001) for a human subject intravenously injected with ^{207}Bi citrate. Retention through Day 25 estimated from excretion measurements and for subsequent times from external measurements.

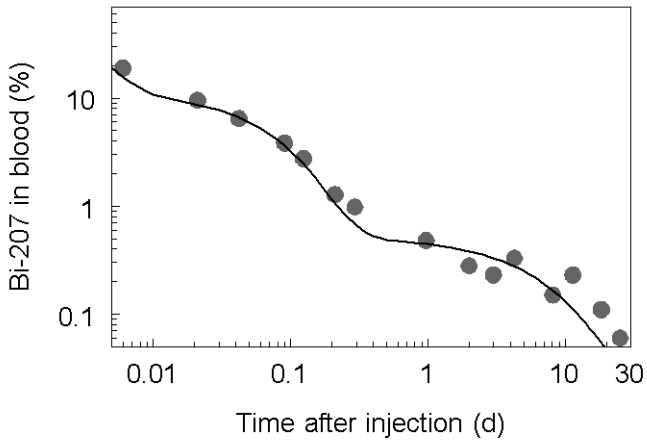

Figure 10-3. Model predictions of blood retention of intravenously injected bismuth compared with observations of Newton et al. (2001) for a human subject intravenously injected with ^{207}Bi citrate.

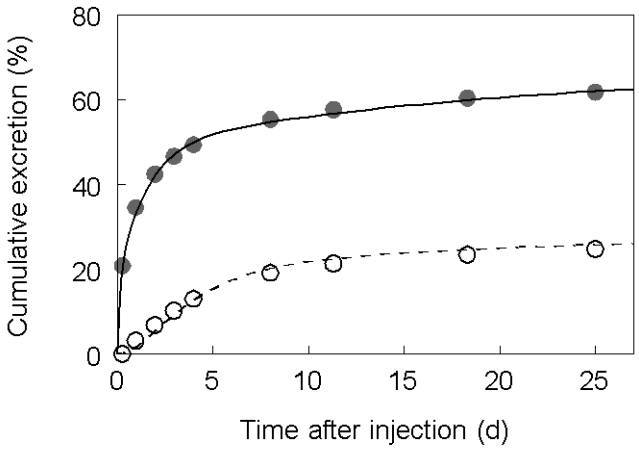

Figure 10-4. Model predictions of cumulative urinary and faecal excretion of intravenously injected bismuth compared with observations of Newton et al. (2001) for a human subject intravenously injected with ^{207}Bi citrate.

10.2.3.3. Treatment of radioactive progeny

(524) The members of bismuth chains considered in the calculations of dose coefficients for bismuth isotopes are isotopes of lead, polonium, thallium, bismuth, or mercury. The systemic models for these elements as progeny of bismuth isotopes are the same as their systemic models as progeny of lead isotopes. They are described in the section on lead.

10.3. Individual monitoring

^{210}Bi

(525) Urine bioassay is used for the monitoring of ^{210}Bi.

Isotope	Monitoring Technique	Method of Measurement	Typical Detection Limit	Achievable detection limit
^{210}Bi	Urine Bioassay	γ-ray spectrometry	1-5 Bq/L	0.9Bq/L

^{214}Bi

(526) Whole Body counting is used for the monitoring of ^{214}Bi.

Isotope	Monitoring Technique	Method of Measurement	Typical Detection Limit	Achievable detection limit
^{214}Bi	Whole Body Counting	γ-ray spectrometry	200 Bq	36 Bq

References

Ballou, J.E., Gies, R.A., Case, A.C., Haggard, D.L., Buschbom, R.L., Ryan, J.L., 1986. Deposition and early disposition of inhaled $^{233}UO_2(NO_3)_2$ and $^{232}UO_2(NO_3)_2$ in the rat. Health Phys. 51, 755–771.

Benet, L.Z., 1991. Safety and pharmacokinetics: Colloidal bismuth subcitrate. Scand. J. Gastroenterol. 26 (Suppl. 185), 29-35.

Boertz, J., Hartmann, L., Sulkowski, M., Hippler, J., Mosel, F., Diaz-Bone, R., Michalke, K., Rettenmeier, A., Hirner, A., 2009. Determination of trimethylbismuth in the human body after ingestion of cooloidal bismuth subcitrate. Drug Metabolism and Disposition. 37 (2): 352-358;

Boiteau, H.L., Cler, J.M., Mathe, J.F., Delobel, R., Feve, J.R., 1976. Relations entre l'evolution des encephalopathies bismuthiques et les taux de bismuth dans le sang et dans les urines. Eur. J. Toxicol. 9, 233-239.

Buijs, W. C.; Corstens, F.H., Beentjes, L.B., 1985. ong-term retention of ^{207}Bi in the human body after injection of ^{206}Bi. Health Phys. 49, 1267-1269.

Butterweck, G., Schuler, Ch., Vezzù, G., Müller, R., Marsh, J.W., Thrift, S., Birchall, A., 2002. Experimental determination of the absorption rate of unattached radon progeny from respiratory tract to blood. Radiat Prot Dosim. 102, 343–348.

Butterweck, G., Vezzù, G., Schuler, Ch., Müller, R., Marsh, J.W., Thrift, S., Birchall, A., 2001. In-vivo measurement of unattached radon progeny deposited in the human respiratory tract. Radiat. Prot. Dosim. 94, 247–250.

Coenegracht, J.M., Dorleyn, M., 1961. The distribution of intravenously administered tracer doses of Bi-206 compounds in the human body. J. Belge de Radiologie 44, 485-504.

D'Souza, R.W., Francis, W.R., 1987. Bioavailability and pharmacokinetics of bismuth in the rat. Pharm. Res. 4:S115 (abstract).

Dresow, B., Fisher, R., Gabbe, E., Wendel, J., Heinrich, H., 1992. Bismuth absorption from 205Bi-labelled pharmaceutical bismuth compounds used in the treatment of peptic ulcer disease. Scan. J. Gastroenterol. 27(4): 333-336.

Dresow, B., Nielsen, P., Fisher, R., Wendel, J. Gabbe, E., Heinrich, H., 1991. Bioavailibility of bismuth from 205Bi-labelled pharmaceutical oral Bi-preparations in rats. Arch. Toxicol. 65(8), 646-650.

Drew, R.T., 1971. ^{212}Pb distribution studies in the rat. Health. Phys. 20, 617–623.

Durbin, P.W., 1960. Metabolic characteristics within a chemical family. Health Phys. 2, 225-238.

Einhorn, J., Engstedt, L., Franzen, S., Lundell, G., 1964. Distribution of colloidal bismuth intravenously and intraarterially administered in man. Acta Radiol. 2, 443-448.

Eridani, S., Balzarini, M., Taglioretti, D., 1964. The distribution of radiobismuth in the rat. Br. J. Radiol. 37, 311-314.

Froomes, P.R.A., Wan, A.T., Keech, A.C., McNeil, J.J., McLean, A.J., 1989. Absorption and elimination of bismuth from oral doses of tripotassium dicitrato bismuthate. Eur. J. Clin. Pharmacol. 37, 533-536.

Gaucher, A., Netter, P., Faure, G., 1979 Bismuth-induced osteoarthropathies. Med. J. Aust. 24:129-130.

Gavey, C.J., Szeto, M.-L., Nwokolo, C.U., Sercombe, J., Pounder, R.E., 1989. Bismuth accumulates in the body during treatment with tripotassium dicitrato bismuthate. Aliment. Pharmacol. Therap. 3, 21-28.

Greenhalgh, J.R., James, A.C., Smith, H., 1977. Clearance of radon daughters from the lung. NRPB/R&D1 Annual Research and Development Report 1976 pp. 49–51, Chilton, UK.

Gregus, Z., Klaassen, C.D., 1986. Disposition of metals in rats: a comparative study of fecal, urinary, and biliary excretion and tissue distribution of eighteen metals. Toxicol. Appl. Pharmacol. 85, 24-38.

Hodgson, S.A., Rance, E.R., Stradling, G.N., Hodgson, A., Fell, T.P., Youngman, M.J., Moody, J.C., Ansoborlo, E., 2000. Biokinetics of thorium dioxide and its decay products in the rat after alveolar deposition: implications for human exposure. NRPB-M1192, Chilton, UK.

Hodgson, S.A., Stradling, G.N., Hodgson, A., Smith, T.J., Youngman, M.J., Moody, J.C., Ansoborlo, E., 2003. Biokinetics and assessment of intake of thorium dioxide. Radiat. Prot. Dosim. 105, 115–118.

Hursh, J. B., Brown, C., 1969. Tissue distribution of ^{212}Bi in rats. Proc. Soc. Exp. Biol. Med. 131:116-120.

Hursh, J.B., Mercer, T.T., 1970. Measurement of ^{212}Pb loss rate from human lungs. J. Appl. Physiol 28, 268–274.

Hursh, J.B., Schraub, A., Sattler, E.L., Hofmann, H.P., 1969. Fate of ^{212}Pb inhaled by human subjects. Health Phys. 16, 257–267.

ICRP, 1980. Limits for intakes of radionuclides by workers. ICRP Publication 30. Part 2. Oxford: Pergamon Press.

ICRP 1975. Reference Man: Anatomical, Physiological and Metabolic characteristics. ICRP Publication 23. Oxford, Pergamon Press.

Koch, K.M., Davis, I.M., Gooding, A.E., Yin, Y., 1996a. Pharmacokinetics of bismuth and ranitidine following single doses of ranitidine bismuth citrate. Br. J. Clin. Pharmacol. 42, 201-205.

Koch, K.M., Kerr, B.M., Gooding, A.E., Davis, I.M., 1996b. Pharmacokinetics of bismuth and ranitidine following multiple doses of ranitidine bismuth citrate. Br. J. Clin. Pharmacol. 42:207-211.

Lloyd, R.D., Mays, C.W., Taylor, G.N., Atherton, D.R., Bruenger, F.W., Jones, C.W., 1982. Radium retention, distribution, and dosimetry in beagles. Radiat. Res. 92, 280-295.

Loiseau, P., Henry, P., Jallon, P., Legroux, M., 1976. Encephalopathies myocloniques iatrogenes aux sels de bismuth. J. Neurol. Sci. 27, 133-143.

Marsh, J.W., Birchall, A., 1999. Determination of lung-to-blood absorption rates for lead and bismuth that are appropriate for radon progeny. Radiat. Prot. Dosim. 83, 331–337.

Matthews, C.M.E., Dempster, W.J., Kapros, C., Kountz, S., 1964. The effect of bismuth 206 irradiation on survival of skin homografts. Br. J. Radiol. 37, 306-310.

Moody, J.C., Davies, C.P., Stradling, G.N., 1994b. Biokinetics of thorium and daughter radionuclides after deposition in the rat lung as fluoride and hydroxide. In: Mohr U., Dungworth, D.L., Mauderly, J.L., Oberdörster, G (Eds.), Proc. Fourth International Inhalation Symposium, Hannover, March 1–5, 1993. Toxic and Carcinogenic Effects of Solid Particles in the Respiratory System, pp. 611–614.

Moody, J.C., Stradling, G.N., 1992. Biokinetics of thorium and daughter radionuclides after deposition in the rat lung. J. Aerosol Sci. 23, S523–S526.

Moody, J.C., Stradling, G.N., Pearce, M.J., Gray, S.A., 1994a. Biokinetics of Thorium and Daughter Radionuclides after Deposition in the Rat Lung as Nitrate: Implications for Human Exposure. NRPB-M525, Chilton, UK.

Newton, D., Talbot, R.J., Priest, N.D., 2001. Human biokinetics of injected bismuth-207. Human Exper. Toxicol. 20, 601-609.

Pieri, F., Wegmann, R., 1981. Radiopharmaceutical study of Bi-citrate in the rat. Compartmental distribution. Cell. Molecul. Biol. 27, 57-60.

Rao, N., Feldman, S., 1990. Disposition of bismuth in the rat: I. Red blood cell and plasma protein binding. Pharm. Res. 7, 188-191.

Russ, G. A., Bigler, R.E., Tilbury, R.S., Woodard, H.Q., Laughlin, J.S., 1975. Metabolic studies with radiobismuth. I. Retention and distribution of 206Bi in the normal rat. Radiat. Res. 63, 443-454.

Slikkerveer, A., de Wolff, F.A., 1989. Pharmacokinetics and toxicity of bismuth compounds. Med. Toxicol. Adverse Drug Exp. 4, 303-323.

Sollmann, T.A., 1957. Manual of Pharmacology and its Applications to Therapeutics and Toxicology. Philadelphia: W.B. Saunders Co.

Sollmann, T., Seifter, J., 1942. Intravenous injections of soluble bismuth compounds: their toxicity, and their sojourn in the blood and organs. J. Pharmacol. Exp. Ther. 74, 134-154.

Stradling, G.N., Davies, C.P., Moody, J.C., Gray, S.A., Wilson, I., Ellender, M., 2005. Biokinetics of thorium and daughter radionuclides after deposition as fluoride and hydroxide in the rat lung: implications for occupational exposure. NRPB-DA/05/2005, Chilton, UK.

Van der Werff, J. Th., 1965. Radioactive bismuth ^{206}Bi. Experimental studies and clinical applications. Acta Radiological Suppl. 243, 1-89.

Vienet, R., Bouvet, P., Istin, M., 1983. Kinetics and distribution of 206Bi in the rat and the rabbit: a model. Int. J. Appl. Radiat. Isot. 34, 747-753.

Zidenberg-Cherr, S., Parks, N.J., Keen, C.L., 1987. Tissue and subcellular distribution of bismuth radiotracer in the rat: considerations of cytotoxicity and microdosimetry for bismuth radiopharmaceuticals. Radiat. Res. 111, 119-129.

11. POLONIUM (Z = 84)

11.1. Chemical forms in the workplace

(527) Polonium is a metalloid which mainly occurs in oxidation states IV. Bismuth and tellurium are good chemical analogues of polonium. Polonium may be encountered in industry in a variety of chemical and physical forms, including oxides, hydroxides, acidic polonium vapours, inorganic salts (bromides, chlorides, and iodides) and also volatile organic forms such as dimethyl and dibenzyl-polonium. A mixture or alloy of polonium and beryllium can be used as a neutron source. Polonium is produced by the decay of ^{220}Ra and ^{222}Ra, which respectively belong to the ^{232}Th and ^{238}U natural radioactive series. The main polonium isotope presents in the environment is ^{210}Po.

Table 11-1. Isotopes of polonium addressed in this report

Isotope	Physical half-life	Decay mode
Po-203	36.7 m	EC, B+, A
Po-204	3.53 h	EC, A
Po-205	1.66 h	EC, B+, A
Po-206	8.8 d	EC, A
Po-207	5.898 h	EC, B+, A
Po-208	2.90 y	A, EC
Po-209	102 y	A, EC
Po-210[a]	138.376 d	A

[a] Data for these radionuclides are given in the printed copy of this report. Data for other radionuclides are given on accompanying electronic disk.

11.2. Routes of Intake

11.2.1. Inhalation

(528) The most important widespread exposures to radioisotopes of polonium are as decay products of radon. The alpha-emitting isotopes ^{218}Po (half-life 3 minutes) and ^{214}Po (half-life 160 µs) give rise to most of the dose from inhalation of the short-lived decay products of ^{222}Rn, as do ^{216}Po (half-life 0.15 s) and ^{212}Po (half-life 310 ns) for those of ^{220}Rn (thoron). For the decay schemes see the uranium and thorium sections. Dose coefficients for isotopes of polonium inhaled as short-lived radon decay products are given in the radon section, where factors such as the relevant aerosol size distribution are addressed.

(529) Otherwise, inhalation of ^{210}Po (half-life 138 d) arises through its formation as the last radioactive member of the ^{238}U decay series, and through its use as a high specific activity alpha-emitting source. It may be present in mineral dusts containing the whole series, or in the atmosphere as a decay product of ^{222}Rn via relatively long-lived ^{210}Pb (half-life 22 years). Workers in uranium and others mines are exposed to both. There is evidence that atmospheric ^{210}Pb accumulates on growing tobacco leaves, leading to intakes of ^{210}Pb and ^{210}Po by smokers.

(530) Applications of ^{210}Po as a high specific activity alpha-emitter include electrostatic charge eliminators, and neutron sources. The high specific activity gives rise to special issues, notably the spontaneous formation of ^{210}Po aerosol above ^{210}Po samples. Borisov (1999)

showed that ^{210}Po on open surfaces releases particles ranging from individual ^{210}Po atoms to aggregates of >3000 atoms. Borisov (1999) also reported that gaseous polonium is present in aerosols containing ^{210}Po, resulting in some penetration of fibrous filters, and that the gaseous fraction formed in moist air resembles polonium hydride (PoH_2), which is unstable, decomposing to polonium and hydrogen.

Absorption types and parameter values

(531) Information is available on the behaviour of polonium following deposition in the respiratory tract from animal experiments with several chemical forms, and from some accidental human intakes.

(532) However, the behaviour of ionic (soluble) Po following deposition in the respiratory tract is difficult to determine because ionic solutions (e.g. chloride) are unstable at neutral pH and in many biological media, resulting in colloid formation. Adsorption of polonium onto surfaces has caused experimental problems, e.g. in determining amounts administered. All the experiments described below used ^{210}Po, because of its relatively long half-life and availability, but as its yield of penetrating photons is very low, direct external counting could not be used to estimate initial deposits or whole body content *in vivo*. Analysis of experimental data to derive absorption parameter values is difficult. Excretion of systemic polonium is mainly fecal, and so fecal excretion does not enable particle transport from the respiratory tract to be easily distinguished from absorption. There is also significant absorption of polonium in the alimentary tract (~10%), and in inhalation experiments, with high deposition in the extrathoracic airways and rapid clearance to the alimentary tract, this contributed to early uptake to blood, along with the rapid phase of absorption from the respiratory tract. Studies of polonium hydroxide colloid administered to rats by intratracheal instillation and nose-only inhalation are considered first, because they provide the most detailed information on the rapid phase of absorption. In deriving absorption parameter values from the results of studies using rats, the systemic model structure described in section 3 below was used, but it was modified using information from the polonium hydroxide studies (Thomas and Stannard 1964; Casarett 1964) and from intravenous injection experiments in rats conducted at the same institute (Stannard 1964).

(533) Absorption parameter values and Types, and associated f_A values for particulate forms of polonium are given in Table 11-2.

Polonium hydroxide colloid ($PoO(OH)_2$)

(534) Thomas and Stannard (1964) studied the tissue distribution and excretion of ^{210}Po after intratracheal administration into rats of a freshly neutralised solution of ^{210}Po in 0.5N HCl. This preparation was termed "polonium hydroxide colloid" by Morrow and Della Rosa (1964), referring to Morrow et al. (1964) who investigated the formation of polonium colloids. According to Morrow and Della Rosa (1964) it consists almost entirely of colloid particles less than 50 Å (5 nm) in diameter. One group of 30 rats was used to study the short-term biokinetics, with emphasis on lung clearance: seven were sacrificed during the first 24 hours, and the rest at times up to 62 d (further details are given in Thomas and Stannard 1956). Another 39 were used for a long-term experiment with measurements up to 478 d. Lung retention at 1, 10 and 60 d after administration was estimated to be ~70%, 45% and 5% of the initial lung deposit (ILD) (after correction for incomplete recovery in ^{210}Po measurements, and blood-borne ^{210}Po). The distribution of systemic activity was broadly similar to that observed following intravenous injection into rats of a similar ^{210}Po preparation (Stannard 1964). The fecal to urine excretion ratio was >20 during the first week, during

which about 4% ILD was excreted in faeces, presumably reflecting particle transport from the bronchial tree to the alimentary tract. After 10 days the ratio was ~10, similar to that observed after intravenous injection (Stannard 1964), indicating that most of the excretion was systemic. Analysis carried out here (i.e. by the Task Group) of the results of the short-term (62-d) study, assuming that the ^{210}Po retained in the lungs was in particulate form rather than bound (f_b = 0, see below) gave absorption parameter values of f_r = 0.5; s_r = 2 d^{-1} and s_s = 0.02 d^{-1}. Analysis of the results of the long-term study gave similar values of f_r and s_r, but a lower value of s_s, ~0.01 d^{-1}. (Both sets of parameter values give assignment to Type M.)

(535) Casarett (1964) followed the distribution and excretion of ^{210}Po following brief (20-minute) nose-only exposure of 44 rats to polonium hydroxide colloid (neutralised ^{210}Po chloride) carried on a sodium chloride vector aerosol (count median diameter, CMD, 0.05 µm). Further details are given by Casarett (1958). Six rats were sacrificed immediately after exposure, the rest in pairs at times up to 30 d, including nine time points in the first 24 hours, giving unusually detailed information on the rapid phase of respiratory tract clearance for an inhalation experiment. Complete urine and fecal collections were made for each rat, which also enabled the "dose", *i.e.* the initial total deposit (ITD) in each rat to be estimated. The measurements of activity distribution were complemented by a comprehensive autoradiographic study. The amounts of ^{210}Po in the alimentary tract and faeces in the first three days indicate that about 60% ITD was deposited in the upper respiratory tract (URT, the skinned head and trachea) and bronchial tree. (However, this might also have included some ingestion of ^{210}Po deposited on the pelt during preening.) The particle clearance rate to the alimentary tract was estimated here to be about 10-15 d^{-1} (half-time of 1.5 hours). The assumption that this clearance was predominantly by particle transport sets an upper limit of ~10 d^{-1} on the rapid absorption rate (s_r). Casarett (1964, p. 158) reported that "During exposure, about 20% of the deposited load left the lung and was translocated to other tissues..." which would imply a value of s_r of the order of 100 d^{-1}. The basis for this inference is not apparent from the tissue or blood data presented in that paper, but Casarett (1958 pp. 151-152) relates it to the presence of ~25% ITD in the "residual carcass", in the first few measurements (which fell to ~4% ITD by 1 d, and remained at that level thereafter). However, it appears that this might well have included most if not all of the pelt, and it is plausible that the transient high ^{210}Po content could have been due to external contamination. Since it seems inconsistent with amounts in blood and other tissues, it was not included in analyses carried out here. Similarly, Casarett (1964) noted that the appearance of high excretion (~4% ITD) in urine in the first 12 hours was evidence for rapid absorption. However, whereas the urinary excretion rate was much higher during the first few days (> 1% ITD d^{-1}) than subsequently (typically < 0.1% ITD d^{-1}), this was not observed after intratracheal instillation of similar material (Thomas and Stannard 1964), for which the rate was ~0.07% d^{-1} during the first week. It seems plausible that the high early excretion rate after inhalation was due to contamination from the pelt, as noted by Kimball and Fink (1950). Bailey et al. (1985) similarly observed much higher urinary excretion of ^{85}Sr by rats in the first few days after nose-only inhalation than after instillation of ^{85}Sr-labelled fused aluminosilicate particles, and that most of the activity in such samples was removed by filtration, and was therefore probably particulate contamination. The early urine data were not therefore included in analyses here. Lung retention at 10 and 30 days after exposure was ~37% and 17% of the lung content at the end of exposure. As for the instillation experiment, the fecal to urine excretion ratio after 10 days was ~10, similar to that observed after intravenous injection (Stannard 1964), indicating that most of the excretion was systemic.

(536) The content of the upper respiratory tract (URT, based on the skinned head and

trachea) fell rapidly from ~30% ITD immediately after exposure, to ~2% ITD at 8 – 24 hours. Casarett (1958 p. 166) alluded to retention of ~2% ITD in the trachea throughout the 30-d study period. He considered it more likely to represent ^{210}Po in associated structures (e.g. lymphatic tissues) than ^{210}Po in transit from lungs to alimentary tract. This could be evidence of a bound fraction, but could include contributions from other sources, such as systemic ^{210}Po (see below). Autoradiographs of the lungs throughout the 30 d showed both clusters of alpha tracks, and many individual tracks, indicating the presence of both particulate and ionic ^{210}Po. Casarett (1958 p. 97) judged that most of the ^{210}Po in the lungs appeared to be in particulate form.

(537) Analysis carried out here, assuming that the ^{210}Po retained in the lungs was in particulate form rather than bound (f_b = 0, see below) gave absorption parameter values of f_r = 0.1; s_r = 2 d^{-1} and s_s = 0.03 d^{-1}, giving assignment to Type M. The values of s_r and s_s are in good agreement with those derived above for the short-term instillation experiment. The value of f_r is lower, which might reflect a difference resulting from the method of administration, or a higher proportion of colloidal material in the inhalation experiment. The value of s_r (rounded to 2 d^{-1}) was therefore used in the analyses of results of other experiments with similar forms of polonium, but for which there were insufficient data to define s_r.

(538) Smith et al. (1961) determined the distribution of ^{210}Po at approximately 1, 4 and 5 months after inhalation by six dogs of polonium hydroxide colloid (neutralised ^{210}Po chloride) carried on a sodium chloride vector aerosol (CMD, 0.04 µm), similar to that inhaled by rats (Casarett 1964). Urine and fecal excretion were also measured. Further details (including daily excretion and additional tissue measurements) are given by Smith et al. (1960). However, there are differences in some of the results reported in the two documents. (Some, but not all, could be attributed to decay correction being made in the 1961 paper but not in the 1960 report.) Since the 1961 paper refers to the other as an earlier version, it was used as the definitive source in analyses carried out here. About 50% of the ITD cleared in ~3 d, which was attributed to clearance from the URT, suggesting that the rapid dissolution rate is slow compared to particle transport from the URT. The other ~50% of ^{210}Po in the body was retained with a half-time of 37 d. Lung retention after 30 days as a fraction of the remaining body content decreased with a half-time of 36 d. Since particle transport from the lungs of dogs is so slow, this would have been mainly by absorption. Analysis carried out here gave values of f_r ~0.3 and s_s = 0.03 d^{-1}, assuming that the ^{210}Po retained in the lungs was in particulate form rather than bound (f_b = 0, see below); and that s_r = 2 d^{-1} (based on the more detailed studies with polonium hydroxide in rats, see above). These are in broad agreement with the studies in rats described above, and also give assignment to Type M. Autoradiography of tissues from dogs sacrificed at 28 and 29 d showed uniform distribution of ^{210}Po as single tracks, except for lesser concentrations in and on tissues of the bronchial tree. (This might suggest lung retention in the bound state rather than particulate form, see below.)

(539) Morrow and Della Rosa (1964) studied the tissue distribution and excretion of ^{210}Po after intratracheal administration to seven rabbits of a freshly neutralised stock solution of ^{210}Po in 0.5N HCl. Further details are given by Morrow and Della Rosa (1956). For two rabbits the neutralised solution was aged for a week in order to increase the fraction of polonium colloid, but no differences in retention characteristics were noted between the two preparations, and the results were combined. At 2 d after administration the lungs contained about 60% ILD. The authors estimated that of the 40% cleared about half was in the alimentary tract and contents and half (*i.e.* ~20% ILD) absorbed into blood, indicating a value

of f_r ~0.2. Since the first measurement was at 1 day, only a lower limit on s_r can be set of ≥ 1 d^{-1}. At 10 and 30 d the lungs contained about 24% and 2% ILD, respectively. These values are significantly lower than those obtained in the experiments with rats (45% and 18% respectively, Thomas and Stannard, 1964). From 2 to 30 d lung retention could be represented by a single exponential function with a rate of 0.12 d^{-1} (half-time ~5.7 d). This is an upper limit on s_s, because some of the clearance was due to particle transport. However, the rate of particle transport from the rabbit lung is not known. (Rabbits have not often been used to study alveolar clearance.) The authors estimated that ~60% ILD had been absorbed from the lung by 30 d, which suggests that absorption was the dominant clearance process and hence that s_s is likely to be in the range 0.05 - 0.1 d^{-1}. This is much faster than assessed for rats or dogs, and would give assignment to Type F. Another inter-species difference, compared to rats, is the much higher urinary excretion in rabbits than in rats, the ratio of faecal to urine excretion being about 0.5 after 10 d. Higher urinary excretion in rabbits than in rats was also observed after intravenous injection (Silberstein et al., 1950a). In four other rabbits the ^{210}Po was attached to silver particles (<10 µm diameter) before neutralisation (only reported in Morrow and Della Rosa, 1956). The biokinetics of ^{210}Po were broadly similar to those following administration of hydroxide colloid alone. Lung clearance was even faster: retention could be represented by a single exponential function with a rate of 0.25 d^{-1} (half-time ~2.8 d). Surprisingly, this did not appear to result from greater particle transport to the alimentary tract, but to greater absorption: whole body retention and urinary excretion were higher, and fecal excretion was lower. Complementary autoradiographic studies (on the same rabbits, with or without silver particles) were reported by Casarett (1958). It was noted that most of the activity was usually found in one lung lobe. As in the rat studies, autoradiographs of the lungs throughout the 28 d showed both clusters of alpha tracks, and many individual tracks, indicating the presence of both particulate and ionic ^{210}Po.

(540) Although specific parameter values for polonium hydroxide based on *in vivo* data are available, they are not adopted here, because inhalation exposure to it is unlikely, and because they are similar to those for default Type M. Instead, polonium hydroxide is assigned to Type M.

Polonium chloride ($PoCl_2$; $PoCl_4$)

(541) Berke and DiPasqua (1964) followed the biokinetics of ^{210}Po in rats for 60 d after a 5-hour whole-body exposure to ^{210}Po chloride carried on a sodium chloride vector aerosol (CMD 0.1 µm). However, whereas the aerosols administered in the studies described in the section on polonium hydroxide colloid were neutralised, in this experiment the solution was acidified (0.1N HCl). This might have resulted in a greater proportion of the ^{210}Po being in ionic, rather than colloidal form. Further details are given by Berke and DiPasqua (1957). With a relatively long exposure and few early measurements (immediately after exposure, 1 and 3 d) there is little information to define s_r. The whole body exposure resulted in extensive contamination of the pelt, which would have affected early excretion measurements. Preening would have led to ingestion of an indeterminate amount of ^{210}Po, and absorption from the alimentary tract to blood, making it difficult to estimate early uptake from the respiratory tract. Lung retention of ^{210}Po at 10, 30 and 60 d was about 44%, 15% and 10% of the ILD (based on the estimated lung content at the end of exposure). These results are similar to those observed following administration of polonium hydroxide (Casarett 1964, Thomas and Stannard 1964, see above). Activity in the URT (skinned head) was about 12% of the body content (excluding pelt and alimentary tract) immediately after exposure. This fell rapidly to about 3% of the body content, and remained at that level throughout the experiment. Berke

and DiPasqua (1957) suggested that this might be due to continuing ingestion e.g. of excreta. Analyses carried out here gave absorption parameter values of f_r = 0.4 and s_s = 0.01 d^{-1}, assuming that the ^{210}Po retained in the lungs was in particulate form rather than bound (f_b = 0, see below); and that s_r = 2 d^{-1} (based on the more detailed studies with polonium hydroxide, see above). These parameter values give assignment to Type M. The value of s_s is broadly similar to values derived from studies using polonium hydroxide (see above). A central value of 0.015 d^{-1} was therefore used in the analyses of results of other experiments with similar forms of polonium, but for which there were insufficient data to define s_s.

(542) Although specific parameter values for polonium chloride based on *in vivo* data are available, they are not adopted here, because inhalation exposure to it is unlikely, and because they are similar to those for default Type M. Instead, polonium chloride is assigned to Type M.

Volatilised polonium (oxide)

(543) Kimball and Fink (1950) investigated the biokinetics of ^{210}Po for 10 d after a brief inhalation of volatilised polonium by rats. The aerosol was produced by deposition of ^{210}Po from solution onto a nickel foil, through which a current was passed until it was red hot. The chemical form was not investigated, but oxide is mentioned in the report. Measurements of the diffusion coefficient of Po ions newly formed by decay of radon indicate that they exist in a variety of chemical forms as a result of interaction with components of air (see e.g. Busigin et al., 1981). According to Chu and Hopke (1988), Po ions are rapidly converted to PoO_2^+ in the presence of oxygen. In one experiment (individual nose-only inhalation for 10–60 s), lung retention fell to ~60% ILD at 24 hours, and ~10% ILD at 10 d. The authors assessed that lung clearance was mainly by absorption to blood. Although data were not given, it was stated that (when extreme precautions were taken) animals sacrificed within a few minutes of exposure showed only traces of activity outside the respiratory tract, suggesting that the rapid absorption was on a time-scale of hours rather than minutes. In another experiment, (group of 20 rats, simultaneous head-only 15-minute inhalation) lung clearance appeared to be slower, falling from ~40% ILD at 24 hours to ~30% ILD at 10 d. Analyses carried out here gave values of f_r ~0.4 for both experiments, assuming that the ^{210}Po retained in the lungs was in particulate form rather than bound (f_b = 0, see below); and that s_r = 2 d^{-1} and s_s = 0.015 d^{-1} (based on more detailed studies with polonium hydroxide, see above). These parameter values give assignment to Type M. Retention of material in the URT (based on the skinned head and trachea) was reported, of the order of 10% of the estimated initial deposit in the URT. This could be evidence of a bound fraction, but could include contributions from other sources, such as systemic ^{210}Po (see below). Autoradiography of lungs from a rat sacrificed immediately after inhalation showed uniform distribution of ^{210}Po in alveolar tissue and clear deposition throughout bronchi and bronchioles. However, the authors noted that by 24 hours after inhalation autoradiography showed only a little remaining in the bronchial walls.

(544) Although specific parameter values for volatilised polonium based on *in vivo* data are available, they are not adopted here, because of the uncertainty on them, and because they are similar to those for default Type M. Instead, volatilised polonium is assigned to Type M.

Mineral dusts

(545) Intakes of ^{210}Po in particulate aerosol form can arise from exposure to airborne mineral dusts containing the natural long-lived parent ^{210}Pb. In this case the absorption rate will probably be determined by the dissolution rate of the mineral matrix in lung fluids. Measurements have been made of the dissolution in simulated lung fluid of samples of coal

fly ash (Kalkwarf et al., 1984) and condensate from calcining phospate rock dust (Kalkwarf and Jackson 1984) for 60 days. By this time the amounts of ^{210}Po dissolved were <0.2% and <1% respectively, indicating assignment to Type S in both cases.

Polonium condensed with cigarette smoke tar

(546) Although mainly related to environmental, rather than occupational, exposure information relating to ^{210}Po in tobacco smoke is included here for completeness. Polonium-210 and its precursor, ^{210}Pb, are inhaled in cigarette smoke (Holtzman 1967; Little and Radford 1967; Parfenov 1974; Cross 1984; Skwarzec et al., 2001; Desideri et al., 2007). Higher concentrations of ^{210}Po have been measured in the lungs of smokers than in non-smokers, indicating that not all the ^{210}Pb and ^{210}Po inhaled are readily soluble (Little et al., 1965; Rajewsky and Stahlhofen 1966; Holtzman and Ilcewicz 1966). It has been reported that ^{210}Pb is concentrated in resinous material in the tips of trichomes (hairs) on the surfaces of tobacco leaves, which forms relatively insoluble particles during combustion (Martell 1974; Radford and Martell, 1975). The ^{210}Po present probably vaporises during combustion, but grows in from decay of ^{210}Pb after deposition in the respiratory tract.

(547) Cohen et al., (1979) measured the concentration of ^{210}Po in the tracheobronchial tree (TB) and parenchyma (alveolar interstitial, AI region) of tissues obtained at autopsy from smokers, ex-smokers, and non-smokers. In non-smokers, the ratio of ^{210}Po concentration in TB to that in AI was ~3 (resulting mainly from systemic ^{210}Pb/^{210}Po). In smokers and ex-smokers, the ratio was ~1: the higher concentration of ^{210}Po in the parenchyma was attributed to the retention of relatively insoluble particles containing ^{210}Pb/^{210}Po inhaled in cigarette smoke. Cohen et al. (1980) measured the dissolution (in physiological saline at 37°C) of alpha-activity of cigarette smoke collected on membrane filters. No decrease in activity was observed (estimated upper limit on dissolution ~20%), although there was a considerable reduction in sample mass. Cohen et al. (1985) measured ^{210}Po in the lungs of rats at times during exposure for 6 months to smoke from cigarettes enriched in ^{210}Pb/^{210}Po, and up to 5 months afterwards. A two-component compartment model was fit to measurements of lung retention following the end of exposure: a good fit was obtained with 90% cleared at a rate of 0.036 d^{-1} (half-time 19 d) and 10% was cleared at a rate of 0.0055 d^{-1} (half-time 125 d). This indicates Type M or S behaviour for both the ^{210}Pb and the ^{210}Po.

Unknown form (accidental exposures of workers)

(548) Follow-up data for many cases of apparently acute inhalation of ^{210}Po by workers have been reported, but in a high proportion only urine (and in some cases blood) measurements were reported, and in such cases little can be inferred about respiratory tract absorption (see e.g. Naimark 1948, 1949, and section 3 below). Some cases are considered here: in most of these, urine and fecal excretion measurements were reported. The biokinetic models used in this document predict that for inhalation of a 5-µm AMAD aerosol by a reference worker, the ratio of daily fecal excretion to daily urinary excretion (F/U) is fairly constant from about 10 d after intake, being ~3 for default Type F or Type M ^{210}Po (which does not allow a distinction to be made between them), and ~40 for Type S. However, in their review, Leggett and Eckerman (2001) pointed out that a technique widely used for routine workplace monitoring of ^{210}Po in urine involved spontaneous deposition of ^{210}Po onto a metal disc, without prior acid digestion, and this could underestimate the activity present. In none of the cases considered in this section was it reported that acid digestion was used prior to ^{210}Po deposition onto a metal disc, and so any conclusions must be treated with caution, since the urine measurements may have been underestimated, and the ratio F/U overestimated.

(549) Foreman et al. (1958) reported excretion data for two physicists who were exposed to ^{210}Po for at most a few minutes after the rupture of a Po-Be source, for ~200 d after the incident (urinary excretion for both, and faecal excretion for one). Both urinary and faecal excretion showed at least two phases. The estimated biological half-time of the first (rapid) urinary component, representing about 6% of total urinary excretion, was 0.75 d. The ratio F/U was approximately 20 over the period 10–100 d, suggesting behaviour between Types M and S. Analysis here, using the systemic model described in section 3, and the updated HRTM (inhalation of a 5-µm AMAD aerosol by a reference worker) with s_r = 2 d^{-1}, gave estimated parameter values f_r = 0.02 d^{-1}, s_s = 0.001 d^{-1}.

(550) Sheehan (1964) analyzed blood, urine, and faeces of a worker who inhaled ^{210}Po in acid vapours. Measurements apparently started several days after exposure. Urine and blood both showed a biological half-time of 43 d. Total urinary and faecal excretion determined for days 47-52 post exposure indicated a ratio F/U of 6.5, suggesting behaviour between Types M and S, but closer to Type M.

(551) Scott and West (1975) measured excretion of ^{210}Po in urine and faeces for 160 d, starting an estimated 2 days after the presumed accidental inhalation by a worker of material from a ^{210}Po source. Contamination was found throughout the room. Although the paper's summary refers to "an exposure to 210-Po oxide...", the only information on chemical form given is that the source was made by vapour-depositing polonium metal onto a metal disc. Only ~3% of the estimated activity deposited in the respiratory tract was excreted in the urine. (The urine data showed very high day-to-day variation.) The ratio F/U was in the range 20-30 over the period 10 - 110 d, suggesting behaviour between Types M and S.

(552) Ilyin (2001) reported measurements on a worker who died as a result of a large accidental intake of ^{210}Po by inhalation (no information was given on its form). Reported activities retained at death, 13 days after intake, were: whole body 100 MBq, lungs 13 MBq, kidney 4.5 MBq and liver 21 MBq. The daily excretion rate was reported to be 1.6 MBq d^{-1} (urine 25.5%, faeces 33.8%, vomit 32.4%, saliva 7.1% and sweat 1.2%). Harrison et al. (2007) discussed the reported symptoms in relation to estimated tissue doses. They obtained a consistent fit to the urine and post-mortem tissue measurements using the *Publication 66* Type M default values of s_r (100 d^{-1}) and s_s (0.005 d^{-1}) but with higher values of f_r and fractional intestinal absorption than the default values. Analysis here, using the systemic model described in section 3, and the updated HRTM (inhalation of a 5-µm AMAD aerosol by a reference worker) with s_r = 2 d^{-1}, s_s = 0.005 d^{-1}, and f_A constrained to 0.1*f_r (see Table 11-2, footnote c), gave a consistent fit to post-mortem tissue measurements with f_r ~0.7. The result was insensitive to the choice of s_r. The F/U ratio was lower (~1.3) than predicted by the systemic model used here, but may have been affected by the response to the radiation, which included severe vomiting.

Default rapid dissolution rate for polonium

(553) Studies with polonium hydroxide colloid give values of s_r of about 2 d^{-1}. This is close to the general default value of 3 d^{-1} for Type M and S materials, and in view of the uncertainties in assessing absorption parameter values for polonium, a value of 3 d^{-1} is also applied here to all Type F forms of polonium.

Extent of binding of polonium to the respiratory tract

(554) The studies with polonium hydroxide, chloride, and volatilised polonium (oxide) all suggest that there is respiratory tract retention of polonium deposited in ionic (soluble) form. However, whether this is retained in particulate or bound form is unclear. Because of colloid

formation at and around neutral pH, some colloid formation before deposition in the respiratory tract almost certainly occurred with polonium hydroxide, and may have occurred with the other materials. Similarly colloid formation may well have occurred after deposition. Thus formation of some particulate material would be expected.

(555) The high proportion of systemic excretion going to faeces makes it difficult to distinguish clearance by absorption from clearance by particle transport and hence the extent of any bound fraction. As noted above, in several studies, retention of ^{210}Po in the upper respiratory tract (URT) was noted, and might be considered to be evidence of a bound fraction. However, this was usually based on retention in the skinned head, which would have included ^{210}Po in soft tissues, blood and lymphatics. Clearance from the URT appeared to be slower than from the lungs: if retention in the respiratory tract were due predominantly to a bound fraction, then the rate of uptake to blood should be similar from the URT and lungs. Autoradiographic studies which complemented the radiochemical measurements of activity distribution and excretion also indicated the presence of both particulate and ionic ^{210}Po. The latter might be considered to be evidence of a bound fraction, but some would have been systemic or blood-borne. Another indication of retention in a bound, rather than particulate form, is the similarity in the retention kinetics of different chemical forms administered, suggesting the retention is characteristic of the element rather than related to dissolution of different particulate forms (see lead section). Thus there are indications that there might well be some binding of polonium. However, the information is insufficient to estimate the extent of the bound state with confidence. Although it is not clear that the bound state for polonium is negligible, it is assumed by default that $f_b = 0$.

Table 11-2. Absorption parameter values for inhaled and ingested polonium

Inhaled particulate materials		Absorption parameter values[a]			Absorption from the alimentary tract, f_A
		f_r	s_r (d^{-1})	s_s (d^{-1})	
Default parameter values[b,c]					
Absorption Type	Assigned forms				
F	—	1	3	–	0.1
M	Chloride, hydroxide, volatilised polonium, all unspecified forms[d]	0.2	3	0.005	0.02
S	—	0.01	3	$1x10^{-4}$	0.001
Ingested material					
All chemical forms					0.1

[a] It is assumed that for polonium the bound state can be neglected, *i.e.* $f_b = 0.0$. The value of s_r for Type F forms of polonium (3 d^{-1}) is element-specific. The values for Types M and S (3 d^{-1}) are the general default values.

[b] Materials (e.g. polonium chloride) are generally listed here where there is sufficient information to assign to a default absorption Type, but not to give specific parameter values (see text).

[c] For inhaled material deposited in the respiratory tract and subsequent cleared by particle transport to the alimentary tract, the default f_A values for inhaled materials are applied: i.e. the product of f_r for the absorption Type and the f_A value for ingested soluble forms of polonium (0.1).

[d] Default Type M is recommended for use in the absence of specific information, i.e. if the form is unknown, or if the form is known but there is no information available on the absorption of that form from the respiratory tract.

11.2.2. Ingestion

(556) Fractional absorption of ^{210}Po from the alimentary tract has been measured in human subjects and in animals (see review in Harrison et al., 2007; Scott, 2007).

(557) A male patient being treated for chronic myeloid leukaemia was reported to be volunteer for ingestion of 7Bq/Kg body mass in drinking water. Blood concentrations and urinary excretion after administration were about one-tenth of corresponding values obtained in other subjects after intravenous injection of polonium chloride, suggesting an f_1 of 0.1(Silberstein et al., 1950b;Fink 1950). Leggett and Eckerman (2001) reanalysed these data and estimated that absorption was at least 0.15.

(558) The absorption of ^{210}Po in animals has been reported for rats, guinea pigs and cats. In rats, the fractional absorption has been reported as 0.03-0.06 for an unspecified chemical form (Anthony et al., 1956) and 0.06 for the chloride (Della Rosa et al., 1955). In a study of two rats exposed by gavage to approximately 20MBq/Kg body mass of freshly neutralized ^{210}Po-chloride, fractional absorption was estimated as 0.024 and 0.048 (Cohen et al., 1989). Haines et al. (1993) obtained values for rats of 0.05 for the nitrate forms. For ^{210}Po administered as the citrate, absorption was reported as 0.07 - 0.09 in rats and guinea pigs. After administration by gavage of 0.52 Mbq /Kg body mass to rats (chemical form not specified) the f_1 was found to be 0.03-0.05 (Spoerl and Anthony 1956).

(559) Fractional absorption in animals seems to be identical in males and females. Stannard (1964) reported average f_1 values of 0.05 for male rats and 0.045 for female rats based on balanced studied after correcting for the amount of Po assumed to be excreted into the intestine via the bile (see review in Scott 2007).

(560) In a series of experiments by Morrow et al., (1964) cats were administered by gavage either a colloidal hydroxide or soluble citrate form of ^{210}Po. After placing ^{210}Po in the stomach, 0.6 to 1.6% were absorbed, independent of chemical form over a 7h-period. However, significant differences were found for the two isotopes when the solution was placed in isolated duodenal loops of the small intestine. During a 10h-period, absorption was up to 40 times greater for the citrate solution. The authors indicated that in the stomach, gastric acidity converted the colloidal ^{210}Po to a soluble form, making absorption comparable to the monomeric citrate form.

(561) In *Publication 30* (ICRP, 1979), an f_1 value of 0.1 was recommended. A higher value of 0.5 applied to Po in foodstuff (ICRP 1993). In this report, an f_A value of 0.1 is used for all chemical forms in the workplace.

11.2.3. Systemic Distribution, Retention and Excretion

11.2.3.1. Summary of the database

Human subjects - occupational data

(562) Leggett and Eckerman (2001) reviewed records of about 1500 former polonium workers and estimated urinary half-times for numerous cases of apparently elevated, acute exposure. Approximately 95% of the derived effective half-times were in the range 8-52 d, corresponding to a range of biological half-times of 8.5-83 d. The mean, median, and mode of the effective half-times were approximately 30 d, 30 d, and 34 d, corresponding to biological half-times of 38 d, 38 d, and 45 d, respectively.

(563) Silverman (1944) reported data for a male worker who was exposed while handling a

foil containing 44.4 GBq of ^{210}Po. Daily urine sampling and weekly fecal sampling began immediately and continued for 64 d. Biological half-times of 34.9 d and 29.3 d were derived from urinary and fecal excretion data, respectively.

(564) Sheehan (1964) described a case in which a worker punctured his finger with a wire contaminated with ^{210}Po. Daily urinary excretion of ^{210}Po decreased by about a factor of 4 during the first 2-3 d after the incident and then decreased with a biological half-time of about 29 d over the next 14 wk.

(565) Testa (1972) described a case in which a 59-y-old woman contaminated her hands by cleaning a chemical hood where a ^{210}Po nitrate solution had been handled. Both ingestion intake (from a habit of finger sucking) and absorption through the skin were suspected. Urinary excretion measurements were initiated about one week after the incident. These data indicated a biological half-time of 29 d, but an early, rapid component may have been missed since the first measurement was at day 7 or 8, and the urinary excretion rate fell by more than a factor of 2 between the first measurement and the second, which was made about 10 d later.

(566) A solution containing ^{210}Po was accidentally splashed on the face of a female technician at Mound (Cohen et al., 1989). Measurements of ^{210}Po in urine, faeces, and blood over several months indicate biological half-times of 13.1 d, 28.6 d, and 20.3 d, respectively.

(567) Wraight and Strong (1989) described a case in which a worker was exposed to ^{210}Po through a puncture wound of the thumb. The authors derived biological half-times of 35 d, 40 d, and 26 d from measurements of ^{210}Po in urine, faeces, and blood, respectively. Fecal excretion of ^{210}Po was highly variable, and only one fecal measurement was made at times greater than about 1 mo after the incident. Urinary data for this subject may be more precisely described in terms of two excretion phases with biological half-times of about 5 d (representing about 30% of total urinary excretion) and 42 d (Leggett and Eckerman, 2001).

(568) Follow-up data for several cases of apparently acute inhalation of ^{210}Po by workers have been reported (e.g. see Naimark 1948, 1949; Spoerl 1951; Jackson and Dolphin 1966). Estimated biological half-times for individual subjects, based for the most part on urinary excretion data, generally fall in the range 20-60 d. Central estimates for relatively large groups of workers usually are in the range 30-50 d. These half-times reflect combined retention times in the respiratory tract and systemic tissues. Selected incidents are described below.

(569) Foreman et al. (1958) reported urinary and fecal excretion data for two physicists who were exposed to airborne ^{210}Po for at most a few minutes after the rupture of a Po-Be source. Both urinary and fecal excretion showed at least two phases. The estimated biological half-time of the first (rapid) urinary component, representing about 6% of total urinary excretion, was 0.75 d. The estimated biological half-time of the first fecal component, representing roughly 60% of total fecal excretion, was about 0.6 d. Urinary as well as fecal data for times greater than a few days after exposure indicate a biological half-time of about 40 d, based on reevaluation of the plotted data (Leggett and Eckerman, 2001).

(570) Sheehan (1964) analyzed blood, urine, and faeces of a worker who inhaled ^{210}Po in acid vapors. Measurements apparently started several days after exposure. Urine and blood both showed a biological half-time of 43 d. Total urinary and fecal excretion determined for days 47-52 post exposure indicated a faeces to urine ratio of 6.5. The technique used to measure ^{210}Po in urine did not involve wet-ashing of samples and thus could have underestimated urinary excretion of ^{210}Po (Fellman et al., 1989).

(571) Scott and West (1975) measured excretion of ^{210}Po in urine and faeces of a worker following accidental inhalation of material thought to consist of small particles of ^{210}Po oxide. Urine sampling began about 2 d after the exposure, and fecal sampling began 2 d later.

A biological half-time of 33 d was estimated from the urinary excretion data, but the data are highly variable and not closely represented by a single half-time.

Human subjects - controlled studies

(572) Silberstein et al. (1950b) measured ^{210}Po in the urine, faeces, and blood of four volunteers (Subjects 1-4) who were administered ^{210}Po chloride by intravenous injection and in a fifth volunteer (Subject 5) who ingested ^{210}Po chloride. Subject 1 was suffering from generalized lymphosarcoma, Subject 2 from acute lymphatic leukemia, and Subjects 3-5 from chronic myeloid leukemia. Observations on Subjects 1, 2, 3, 4, and 5 were continued for up to 43, 6, 71, 13, and 228 d, respectively. Biological half-times fitted to the time-dependent concentration of ^{210}Po in urine, faeces, or blood of these subjects varied somewhat with the observation period and also showed considerable intersubject variability. For the subjects who were followed for several weeks or months (Subjects 1, 3, and 5), urinary excretion data indicate half-times of 30-50 d for the period starting 1 wk after exposure; fecal excretion data indicate half-times of 33-52 d for this period; and data for red blood cells indicate half-times of 12-48 d for this period. Urinary excretion data for the first week after administration yield biological half-times as short as 3 d.

(573) Excretion data for the subject of Silberstein et al. who ingested ^{210}Po chloride (Subject 5) were reanalyzed in an attempt to determine fractional absorption from the GI tract. Under the assumption that all fecal excretion at times greater than one week after ingestion was due to secretion of systemic ^{210}Po into the GI tract, it is estimated that endogenous fecal excretion represented at least 14% of ingested ^{210}Po. Measurements of urinary excretion indicate that approximately 0.5% of the ingested amount was removed in urine. Thus, it appears that at least 14.5% of the ingested amount was absorbed to blood. The estimate of 0.5% for urinary excretion may be an underestimate due to problems with the measurement technique (Fellman et al., 1989).

(574) Subject 2 of Silberstein et al. died of acute lymphatic leukemia six days after injection of ^{210}Po. The distribution of ^{210}Po was determined from tissue samples taken about one hour after his death. The usefulness of the data for this subject are limited not only by the fact that he was terminally ill but also because estimated recovery of polonium was substantially greater than 100%, probably due to substantial overestimates of the mass of some tissues. For example, skin was estimated to represent 18% of body weight, which is about fourfold greater than the relative mass of skin given in the ICRP's Reference Man document (ICRP, 1975). For purposes of the present study, the distribution of polonium in the human subject has been recalculated on the basis of current information on typical organ weights and by constraining organ contents to achieve mass balance.

(575) Hunt and Allington (1993) determined urinary ^{210}Po in six subjects who had ingested crab meat containing elevated concentrations of this radionuclide. Urinary excretion rates were determined for periods of 9-21 d in five of the subjects. Biological half-times of 3-8 d are indicated by these short-term data. Comparison of fecal excretion data with the ingested amounts indicates that fractional absorption to blood ranged from about 0.6 to more than 0.9 in the six subjects. Urinary excretion over the first 7 d represented 0.4-1.1% of the absorbed amount in four of the subjects and 5.1% in a fifth subject. It is not evident whether these data for ingestion of biologically incorporated polonium are pertinent to occupational exposures to ^{210}Po, but the data demonstrate the potentially high absorption of some forms of polonium from the GI tract and the potentially high variability in the biokinetics of absorbed polonium.

Laboratory animals

(576) Data on the biokinetics of polonium in laboratory animals was reviewed by Leggett and Eckerman (2001). The systemic behavior of polonium is qualitatively similar among species in most respects, but some species differences have been identified. For example, the blood cells of rats appear to have an unusually high affinity for polonium absorbed after ingestion, and rabbits show an unusually high rate of loss of polonium from the body.

11.2.3.2. Biokinetic model for systemic polonium

(577) A biokinetic model for systemic polonium proposed by Leggett and Eckerman (2001) is used in this report. The model structure is shown in Figure 11-1. Transfer coefficients are given in Table 11-3. The basis for each of the transfer rates is discussed below.

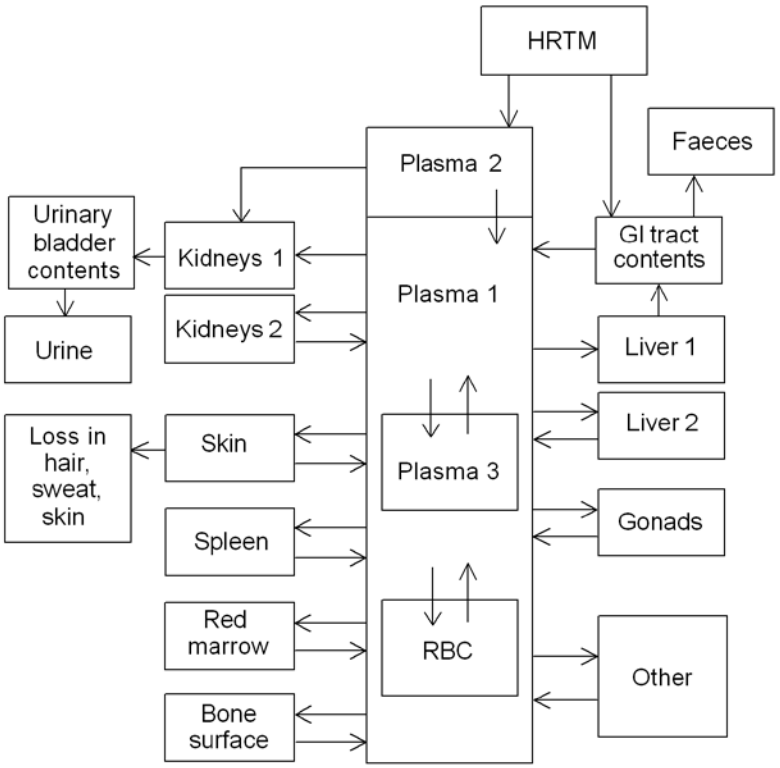

Figure 11-1. Structure of the biokinetic model for systemic polonium.

Table 11-3. Transfer coefficients in the model for systemic polonium.

From	To	Transfer coefficient (d^{-1})
Plasma 2	Plasma 1	800
Plasma 2	Kidneys 1	200
Plasma 1	Plasma 3	4
Plasma 1	RBC	6
Plasma 1	Liver 1	17.5
Plasma 1	Liver 2	17.5
Plasma 1	Kidneys 1	5
Plasma 1	Kidneys 2	5
Plasma 1	Skin	5
Plasma 1	Red Marrow	4
Plasma 1	Bone Surface	1.5
Plasma 1	Spleen	2
Plasma 1	Testes	0.1
Plasma 1	Ovaries	0.05
Plasma 1	Other	32.35
Plasma 3	Plasma 1	0.099
RBC	Plasma 1	0.099
Liver 1	GI Tract	0.139
Liver 2	Plasma 1	0.099
Kidneys 1	Urinary Bladder	0.173
Kidneys 2	Plasma 1	0.099
Skin	Plasma 1	0.00693
Skin	Excreta	0.00693
Red Marrow	Plasma 1	0.099
Bone Surface	Plasma 1	0.0231
Spleen	Plasma 1	0.099
Gonads	Plasma 1	0.0139
Other	Plasma 1	0.099

Blood

(578) Data on non-human primates indicate that there is a rapid phase of removal of polonium from blood, followed by one or more slower phases of removal (Cohen et al., 1989). The rapid phase represented about 80-90% of intravenously injected polonium and had a half-time on the order of 10-40 min. The remainder was removed with a half-time of about 8-19 d in the baboon and about 37 d in the tamarin. The slower phase of removal appears to be associated with attachment of polonium to red blood cells and plasma proteins (Thomas 1964, Cohen et al., 1989).

(579) The relative quantities of polonium associated with red blood cells and plasma proteins varies with species, but in all species the total amount of polonium in red blood cells exceeds that in plasma at most times after absorption or injection of polonium into blood (Silberstein et al., 1950a; Smith et al., 1961; Thomas, 1964; Cohen et al., 1989). There was considerable inter- and intra-subject variability in the relative quantities of ^{210}Po in red blood cells and plasma determined in human subjects administered ^{210}Po by intravenous injection or ingestion, but the content of red blood cells averaged about 1.5 times that of plasma

(Silberstein et al., 1950b).

(580) The initial behavior of polonium in blood may depend on the route of exposure. After exposure by inhalation or wounds there is generally an early, rapid loss of polonium in urine (Foreman et al., 1958; Smith et al., 1961; Casarett, 1964; Wraight and Strong, 1989) that appears to be absent or less pronounced after exposure by other routes.

(581) The model for blood was designed to depict rapid and slow phases of removal such as those observed in non-human primates (Cohen et al., 1989); to approximate blood retention data for human subjects (Silberstein et al., 1950a), non-human primates (Cohen et al., 1989, Fellman et al., 1994), and dogs (Parfenov and Poluboyarinova, 1969); and to depict a higher rate of urinary excretion of polonium after exposure through inhalation or wounds than after exposure by other routes. Variation in the rate of urinary excretion with route of exposure is modelled by using different receptor compartments in plasma with different rates of transfer to the urinary excretion pathways. Specifically, a compartment called Plasma 2 is assumed to receive inflow to blood from the respiratory tract or wounds, and a compartment called Plasma 1 is assumed to receive inflow to blood from all other sources, including polonium that returns from systemic tissues to blood. Outflow from Plasma 2 is assumed to be rapid (half-time of 1 min, corresponding to a transfer rate of 1000 d^{-1}) and is divided between Plasma 1 and a kidney compartment (Kidneys 1) that feeds the urinary bladder contents. This scheme yields an initially higher rate of urinary excretion for exposure by inhalation or wounds than for other routes. As default values, 80% of outflow from Plasma 2 is assigned to Plasma 1 and 20% is assigned to Kidneys 1. Assignment of a higher percentage to Kidneys 1 may be indicated in cases where the observed urinary excretion rate falls rapidly during the first few days after acute intake of polonium. This is because an unusually rapid decline in the urinary excretion rate may indicate that an unusually high fraction of the amount entering the systemic circulation was rapidly cleared by the kidneys.

(582) A third plasma compartment, called Plasma 3, is used to represent protein-bound, or non-diffusible polonium in plasma. Red blood cells are represented by a single compartment, called RBC.

(583) The removal half-time from Plasma 1 is assumed to be 10 min, corresponding to a total transfer rate of 100 d^{-1}. Plasma 3 is assumed to receive 4% and RBC is assumed to receive 6% of the polonium atoms that leave Plasma 1 (i.e. the deposition fractions for Plasma 3 and RBC are 0.04 and 0.06, respectively). The removal half-time from either RBC or Plasma 3 back to Plasma 1 is assumed to be 7 d. The term half-time refers here to the estimated half-time that would be seen if there were no recycling of polonium between compartments, and that the “apparent” or “externally viewed” half-time in blood will be greater than 7 d due to recycling of polonium.

Liver and faecal excretion

(584) Data for laboratory animals (Smith et al., 1961; Parfenov and Poluboyarinova, 1969, Fellman et al., 1994) and one human subject (Silberstein et al., 1950b) indicate that a substantial portion of injected or absorbed polonium deposits in the liver. It appears that much of the initial uptake by the liver may be removed with a half-time of a few days, and the remainder may be lost over a period of weeks. Endogenous fecal excretion of polonium appears to arise mainly from biliary secretion from the liver (Silberstein et al., 1950b; Fellman et al., 1994).

(585) In this model the liver is assumed to consist of two compartments, called Liver 1 and Liver 2. Liver 1 is used to represent relatively rapid removal of polonium from the liver and to account for biliary secretion of polonium, which appears to decline rapidly with time. Liver 2 is used to describe relatively long-term retention in the liver.

(586) The total liver is assumed to receive 35% of the outflow from Plasma 1, with half of this amount depositing in Liver 1 and half depositing in Liver 2. Polonium is assumed to be removed from Liver 1 to the contents of the small intestine with a half-time of 5 d and from Liver 2 to Plasma 1 with a half-time of 7 d. Passage from Plasma 1 to Liver 1 to the contents of the small intestine is assumed to be the sole source of endogenous fecal excretion of polonium.

Kidneys and urinary excretion

(587) In this model the kidneys are assumed to consist of two compartments, called Kidneys 1 and Kidneys 2. Kidneys 1 represents polonium that is eventually removed to the urinary bladder contents after filtration at the glomerulus and deposition in the renal tubules. Kidneys 2 represents polonium that is eventually returned to blood after entering kidney tissue, either from nutrient blood or the tubular lumen. For simplicity, polonium entering either Kidneys 1 or Kidneys 2 is assumed to transfer directly from Plasma 1. Also, there is assumed to be no direct transfer of filtered polonium into the urinary bladder contents. That is, filtered polonium is assumed to reside temporarily in kidney tissue before being transferred to the urinary bladder contents.

(588) Parameter values describing renal retention of polonium were chosen to fit retention data for man, baboons, and dogs. Kidneys 1 and Kidneys 2 are each assumed to receive 5% of polonium atoms that leave Plasma 1. The removal half-time from Kidneys 1 to bladder urine is assumed to be 4 d, and the removal half-time from Kidneys 2 to Plasma 1 is assumed to be 7 d.

(589) After parameter values describing fecal excretion of polonium had been selected, parameter values describing urinary excretion were set, in part, to yield a (cumulative) fecal-to-urinary excretion ratio, F:U, of about 3. The typical value of F:U for man has not been established. The selected value of 3 is a compromise, based on a fairly wide range of values determined for human subjects and non-human primates. The selected value is slightly lower than the value determined for tamarins (Cohen et al., 1989; Fellman et al., 1989) and higher than the value determined for baboons (Fellman et al., 1989). The true ratio seems likely to be lower than the values of 10 or more determined by Silberstein et al. (1950b) for human subjects, in view of findings of Fellman et al. (1989) that the measurement technique of Silberstein substantially underestimates the concentration of polonium in urine, at least in baboons and tamarins. Results of a modern study on a human subject exposed through a puncture wound seem consistent with the relatively low urinary-to-fecal excretion ratio determined by Silberstein and coworkers (Wraight and Strong, 1989); however, the technique for measuring urinary polonium was not described, and conclusions concerning F:U were based on an uncertain curve fit to scattered fecal excretion data. Reported ratios F:U for human subjects exposed to ^{210}Po by inhalation are in the range 6.5-70 but provide only upper-bound estimates of F:U for systemic polonium, for two reasons: (1) a substantial portion of ^{210}Po found in faeces may have been transported from the lungs to the gastrointestinal tract without having been absorbed to blood; and (2) at least some of the reported values were based on a measurement technique that may substantially underestimate the concentration of ^{210}Po in urine.

(590) The measurement technique used by Silberstein et al. (1950b) and some later

investigators involved spontaneous deposition of ^{210}Po from raw urine onto a suitable metal disc. Recovery was estimated by plating ^{210}Po from samples that had been spiked with known amounts of ^{210}Po. There is evidence from studies on laboratory animals, however, that ^{210}Po excreted in urine is not plated with the same efficiency as ^{210}Po added to urine, unless the samples have been digested with acid prior to deposition (Fellman et al., 1989). Although it is tempting to adjust older urinary excretion data for human subjects to account for potentially low recovery of ^{210}Po as indicated by results for laboratory animals, such adjustments would involve substantial uncertainties because recovery of metabolized ^{210}Po from raw urine appears to depend on species as well as time since exposure (Fellman et al., 1989), and because there is some question as to whether inaccuracies in older methods are as great as indicated by modern reconstructions of those methods. Moreover, reported data on urinary excretion of ^{210}Po often have not been accompanied by a description of the measurement technique.

Spleen

(591) The spleen is represented as a single compartment in exchange with Plasma 1. Parameter values were set for reasonable consistency with spleen retention data for baboons, dogs, and one human subject (Leggett and Eckerman, 2001). It is assumed that the spleen receives 2% of the outflow from Plasma 1 and that the removal half-time from spleen to Plasma 1 is 7 d.

Skin

(592) Data on laboratory animals and man indicate that skin initially takes up a few percent of polonium that enters plasma but retains polonium more tenaciously than most other tissues. At times remote from acute intake, skin may contain half or more of the systemic burden. Much of the skin content is found around hair follicles (Soremark and Hunt 1966). Hair has a relatively high polonium content at times remote from exposure (Mayneord and Hill 1964).

(593) In this model, skin is represented as a single compartment that receives 5% of polonium that leaves Plasma 1. The removal half-time from skin is assumed to be 50 d. Half of polonium leaving skin is assumed to be lost in excreta (hair, skin, sweat) and the other half is assumed to return to Plasma 1.

(594) In baboons, pelt contained 53% of the body content at 91 d post injection (Fellman et al., 1989). In dogs, the pelt contained 44%, 43%, 54% and 51% of total-body polonium at 116, 131, 146, and 149 d after inhalation (Smith et al., 1961). Model predictions are reasonably consistent with these data.

Skeleton

(595) Experimental data on laboratory animals indicate that about 5% of the injected or absorbed amount deposits in the skeleton. Soon after exposure, most of the skeletal deposition is found in the marrow spaces and appears to be associated primarily with active marrow (ICRP, 1993). A smaller amount found in the mineralized skeleton may be associated with organic material in bone. The bone deposit may be retained longer than most soft-tissue polonium.

(596) In this model, the skeleton is represented as two compartments, identified with red marrow and bone surface. It is assumed that these compartments receive, respectively, 4% and 1.5% of polonium leaving Plasma 1, and that both compartments lose polonium to Plasma 1. The removal half-time from red marrow is assumed to be 7 d, and the removal half-time from bone surface is assumed to be 30 d.

Gonads

(597) Data on uptake and retention of polonium by testes or ovaries are variable but indicate elevated concentrations compared with most tissues (Silberstein et al., 1950b, Blanchard and Moore 1971; Cohen et al., 1989; Naylor et al., 1991). In this model, the testes and ovaries are each considered as a single compartment that exchanges polonium with Plasma 1. These compartments are assumed to receive, respectively, 0.1% and 0.05% of polonium leaving Plasma 1. The removal half-time from each of these compartments is assumed to be 50 d.

Other tissues

(598) Remaining tissues and fluids are lumped into a compartment called Other that is assumed to exchange polonium with Plasma 1. Parameter values for this compartment were chosen for consistency with data on baboons (Cohen et al., 1989). Other is assumed to receive 32.35% of polonium leaving Plasma 1, which is the amount not accounted for in the sum of deposition fraction for all explicitly identified compartments. The removal half-time from Other to Plasma 1 is assumed to be 7 d.

11.2.3.3. Treatment of radioactive progeny

(599) Dosimetrically significant progeny of polonium isotopes addressed in this report are isotopes of bismuth or lead. The models for these two elements produced in systemic compartments following intake of a polonium isotope are based on their characteristic models, i.e. the systemic models applied in this series of reports to bismuth and lead as parent radionuclides.

(600) For application to bismuth and lead as progeny of polonium, the characteristic models for bismuth and lead are modified by adding compartments representing the following tissues that are explicitly identified in the polonium model: spleen, skin, red marrow, testes, and ovaries. The model revisions are similar for each element and are summarized here for bismuth. Each of these tissues is represented in the bismuth model as a single compartment. The five compartments are extracted from the intermediate- and long-term compartments of Other soft tissues (ST1 and ST2, respectively). Transfer coefficients between the added compartments and the central blood compartment are based on the biokinetic database for bismuth summarized elsewhere in this series of reports, together with the requirements that the total outflow rate of bismuth from blood and integrated activities of long-lived bismuth isotopes in total soft tissues remain unchanged from the characteristic model for bismuth (except for small changes due to rounding of parameter values).

(601) The specific changes to the characteristic model for bismuth are as follows: (1) the transfer coefficient from the central blood compartment (plasma) to ST1 is reduced from 4.2 d^{-1} to 3.7 d^{-1}, and the coefficient from plasma to ST2 is reduced from 1.3 d^{-1} to 1.2 d^{-1}; (2) the following transfer coefficients from plasma to the added compartments are assigned: to Red marrow, 0.3 d^{-1}, to Spleen, 0.02 d^{-1}, to Skin, 0.3 d^{-1}, to Testes, 0.003 d^{-1}, to Ovaries, 0.001 d^{-1}; (3) the assigned transfer coefficient from Red marrow, Spleen, Skin, Testes, and Ovaries to plasma is 0.007 d^{-1}; and (4) the following transfer coefficients are assigned to bismuth produced in compartments of the polonium model that are not identifiable with compartments of the bismuth model: Plasma 2 to the plasma compartment of the bismuth model, 1000 d^{-1}; Plasma 3 to the plasma compartment of the bismuth model, 1000 d^{-1}; and Other to the plasma compartment of the bismuth model, 0.0347 d^{-1} (based on removal rate from ST1 to plasma in

the model for bismuth).

(602) The specific changes to the characteristic model for lead are as follows: (1) the transfer coefficient from the central blood compartment (Plasma) to ST1 is reduced from 0.70 d^{-1} to 0.65 d^{-1}, and the coefficient from Plasma to ST2 is reduced from 0.14 d^{-1} to 0.13 d^{-1}; (2) the following transfer coefficients from Plasma to the added compartments are assigned: to Red marrow, 0.015 d^{-1}, to Spleen, 0.002 d^{-1}, to Skin, 0.04 d^{-1}, to Testes, 0.00045 d^{-1}, to Ovaries, 0.00015 d^{-1}; (3) the assigned transfer coefficient from Red marrow, Spleen, Skin, Testes, and Ovaries to Plasma is 0.002 d^{-1}; and (4) the following transfer coefficients are assigned to lead produced in compartments of the polonium model that are not identifiable with compartments of the lead model: Plasma 2 to Plasma, 1000 d^{-1}; Plasma 3 to Plasma, 1000 d^{-1}; Other to Plasma, 0.00416 d^{-1} (based on removal rate from ST1 to Blood 1 in the model for lead).

(603) For modelling convenience, the compartment in the polonium model named Plasma 1 is identified with the compartment in the bismuth model named Plasma and the compartment in the lead model named Plasma. For example, a bismuth atom produced in Plasma 1 is assumed to be produced in the plasma compartment of the bismuth model, and a lead atom produced in Plasma 1 is assumed to be produced in the plasma compartment of the lead model.

11.3. Individual monitoring

^{210}Po

(604) Monitoring of ^{210}Po intakes is accomplished through urine bioassay, using a technique that involves wet acid digestion followed by alpha spectrometry.

Isotope	Monitoring Technique	Method of Measurement	Typical Detection Limit	Achievable detection limit
^{210}Po	Urine Bioassay	alpha spectrometry	1 mBq/L	0.1 mBq/L

References

Anthony, D.S., Davis, R.K., Cowden, R.N., Jolley, W.P., 1956. Experimental data useful in establishing maximum single and multiple exposure to polonium. In: Proceedings of the International Conference on the Peaceful Uses of Atomic Energy, Vol. 13, pp.215-218. United Nations, New York.

Bailey, M.R., Hodgson, A., Smith, H., 1985. Respiratory tract retention of relatively insoluble particles in rodents. J. Aerosol Sci., 16, 279–293.

Berke H.L., Dipasqua A.C. 1957. The distribution and excretion of polonium^{210} after inhalation. University of Rochester Atomic Energy Project, Report UR-495.

Berke, H.L., Dipasqua, A.C., 1964. Distribution and excretion of polonium-210. VIII. After inhalation by the rat. Radiat Res 5 (suppl.), 133-147.

Blanchard, R.L., Moore, J.B., 1971. Body burden, distribution and internal dose of Pb-210 and Po-210 in a uranium miner population. Health Phys. 21, 499-518.

Borisov, N.B., 1999. On the 275th Anniversary of the Russian Academy of Sciences, Research on polonium aerosols and appropriate safety measures under the leadership of I. V. Petryanov-Sokolov. Atomic Energy. 86 (6) 385–387.

8011 Casarett, L.J. 1958. A study of the pharmacodynamics of polonium administered via the lungs. PhD
8012 Thesis, University of Rochester.
8013 Casarett, L.J. 1964. Distribution and excretion of polonium-210. IX. Deposition, retention, and fate
8014 after inhalation by nose-only exposure, with notes on mechanics of deposition and clearance
8015 and comparison of routes of administration. Radiat Res 5 (suppl.), 148-165.
8016 Chu, K.-D., Hopke P.K., 1988. Neutralization kinetics for polonium-218. Environ. Sci. Technol., 22,
8017 711-717.
8018 Cohen, B.S., Eisenbud, M., Wrenn, M.E., Harley, N.H., 1979. Distribution of polonium-210 in the
8019 human lung. Radiat. Res. 79, 162-168.
8020 Cohen, N., Fellman, A.L., Hickman, D.P., Ralston, L.G., Ayres, L.S., 1989. Primate polonium
8021 metabolic models and their use in estimation of systemic radiation doses from bioassay
8022 data. Mound Laboratory.
8023 Cohen,B.S., Eisenbud, M., Harley, N.H., 1980. Alpha Radioactivity in cigarette smoke. Radiat Res
8024 83, 190-196.
8025 Cohen, B.S., Harley, N.H., Tso,T.C., 1985. Clearance of polonium-210-enriched cigarette smoke
8026 from the rat trachea and lung. Toxicol. Appl. Pharmacol. 79, 314-322.
8027 Cross F.T., 1984. Radioactivity in cigarette smoke issue. Health Phys. 46(1) 205-209.
8028 Della Rosa, J.R., Thomas, R.G., Stannard, J.N., 1955. The acute toxicity and retention of orally
8029 administered polonium-210. University of Rochester, UR-392.
8030 Desideri D., Meli M.A., Feduzi L., Roselli, C., 2007. ^{210}Po and ^{210}Pb inhalation by cigarette smoking
8031 in Italy. Health Phys. 92(1) 58-63.
8032 Fellman, A., Ralston, L., Hickman, D., Ayres, L., Cohen, N., 1994. Polonium metabolism in adult
8033 female baboons. Radiat. Res. 137, 238-250.
8034 Fellman, A., Ralston, L., Hickman, D., Ayres, L., Cohen, N., 1989. The importance of acid digestion
8035 of urine prior to spontaneous deposition of ^{210}Po. Health Phys. 57, 615-6221.
8036 Fink, R.M., 1950. (Ed.), Biological studies with polonium, radium, and plutonium. New York:
8037 McGraw-Hill.
8038 Foreman, H., Moss, W., Eustler, B.C., 1958. Clinical experience with radioactive materials.
8039 American Journal of Roentgenology Radium Therapy and Nuclear Medicine 79, 1071-
8040 1079.
8041 Haines, J.W., Naylor, G.P.L., Pottinger, H., Harrison, J.D., 1993. Gastrointestinal absorption and
8042 retention of plonium in adult and newborn rats and guinea pigs. Int. J. Radiat. Biol. 64, 127-
8043 132.
8044 Harrison, J.D., Leggett, R.W., Lloyd D., Phipps, A.W., Scott, B.R., 2007. Polonium-210 as a poison.
8045 J. Radio. Prot. 27, 17–40.
8046 Holtzman, R.B., Ilcewicz, F.H., 1966. Lead-210 and polonium-210 in tissues of cigarette smokers.
8047 Sci. 153, 1259-1260.
8048 Holtzman, R.B., 1967. Polonium-210 in bronchial epithelium of cigarette smokers. Sci. 155, 607.
8049 Hunt, G.J., Allington, D.J., 1993. Absorption of environmental polonium-210 by the human gut. J.
8050 Radiol. Prot. 13, 119-126.
8051 ICRP, 1975. Report of the Task Group on Reference Man. ICRP Publication 23. Oxford: Pergamon
8052 Press.
8053 ICRP, 1979. Limits on Intakes of Radionuclides for Workers. ICRP Publication 30, Pt.1. Ann. ICRP
8054 2, (3/4).
8055 ICRP, 1993. Age-dependent Doses to Members of the Public from Intake of Radionuclides. Pt.2.
8056 ICRP Publication 67. Ann. ICRP. 23, (3/4).
8057 Ilyin, L.A., 2001. Radiation Medicine. Guidance for Medical Researchers and Health Management.
8058 Vol 2. Radiation Damage of Humans. Ed. A. Yu. Bushmanov et al. (Moscow: AT) ISBN 5-
8059 86656-114-X.
8060 Jackson, S., Dolphin, G.W., 1966. The estimation of internal radiation dose from metabolic and
8061 urinary excretion data for a number of important radionuclides. Health Phys. 12, 481-500.

Kalkwarf, D.R., Jackson, P.O., 1984. Lung-clearance classification of radionuclides in calcined phosphate rock dust. PNL-5221.. Richland, Washington, Pacific Northwest Laboratory.

Kalkwarf, D.R., Jackson, P.O., Hardin, J.M., 1984. Lung-clearance classification of radionuclides in coal fly ash. Health Phys. 47, 37-45.

Kimball, C.P., Fink, R.M., 1950. Inhalation of volatilized polonium by rats. In: Fink, R.M., editor. Biological studies with polonium, radium, and plutonium. New York: McGraw-Hill, pp. 89–111.

Landinskaya, L.A., Parfenov, Y.D. Popov, D.K., Federova, A.V., 1973. ^{210}Pb and ^{210}Po content of air, weater, foodstuffs and the human body. Arch. Environ. Health 27, 254-258.

Leggett, R.W., Eckerman, K.F., 2001. A systemic biokinetic model for polonium. Sci. Total Environ. 275, 109-125.

Little, J.B., Radford, E.P., Jr. 1967. Polonium-210 in bronchial epithelium of cigarette smokers. Sci. 155, 606-607.

Little, J.B., Radford, E.P., Jr., McCombs, H.L., Hunt, V.R., 1965. Distribution of polonium-210 in pulmonary tissues of cigarette smokers. N. Engl. J. Med. 273, 1343-1351.

Martell, E.A. 1974. Radioactivity of tobacco trichomes and insoluble cigarette smoke particles. Nature 249, 215-217.

Mayneord, W.V., Hill, C.R., 1964. Total counting and spectroscopy in the assessment of alpha activity in human tissues. In: Assessment of radioactivity in man, Vol. 1. IAEA, Vienna, Austria, 291-309.

Morrow, P.E., Della Rosa, R.J., 1956. The fate of polonium^{210} colloid and polonium^{210} tagged silver particles following intratracheal administration to rabbits. University of Rochester Atomic Energy Project, Report UR-478.

Morrow, P.E., Della Rosa, R.J., 1964. Distribution and excretion of polonium-210. VII. Fate of polonium colloid after intratracheal administration to rabbits. Radiat Res 5 (suppl.), 124-132.

Morrow, P.E., Della Rosa, R.J., Casarrett L.J., Miller, G.J., 1964. Investigations of the colloidal properties of polonium-210 solutions using molecular filters. Radiat Res 5 (suppl.), 1-15.

Naimark, D.H., 1948. Acute exposure to polonium (medical study of three human cases). Mound Laboratory, Report MLM-67.

Naimark, D.H. 1949. Effective half-life of polonium in the human. Mound Laboratory, Report MLM-272.

Naylor, G.P.L., Bonas, H.E., Haines, J.W., Ham, G.J., Harrison, J.D., Sundaram, S., Dayan, A.D., 1991. The gastrointestinal absorption and tissue distribution of alpha-emitting actinide isotopes and polonium-210. The British Nuclear Energy Society Conference: Occupational Radiation Protection, Guernsey. Thomas Telford, London. 291-296.

Parfenov, Y. 1974. Polonium-210 in the environment and in the human organism. At. Energy Rev. 12, 75-143.

Parfenov, Yu. D., Poluboyarinova, Z.I., 1969. Dynamics of polonium-210 exchange in dogs after a single subcutaneous administration. Radioactive isotopes and the body, Yu. I. Moskaleve, ed. Izdatel'stvo Medisina. Moscow. 1969. AEC-tr-7195, pp. 128-135.

Radford, E.P., Martell, E.A., 1975. Polonium-210: lead-210 ratios an index of residence times of insoluble particles from cigarette smoke in bronchial epithelium. Walton, W.H. and McGovern, B. 2, 567-581. 1975. Oxford, Pergamon Press. Proc. of an international symposium organized by the British Occupational Hygiene Society, Edinburgh. 22-9-1975.

Rajewsky, B., Stahlhofen, W., 1966. Polonium-210 activity in the lungs of cigarette smokers. Nature 209, 1312-1313.

Scott, B.R., 2007. Health risk evaluations for ingestion exposure of humans to polonium-210. Dose Response 5: 94-122;

Scott, L.M., West, C.M., 1975. Excretion of 210-Po oxide following accidental inhalation. Health Phys. 28, 563-565.

Sheehan, W.E., 1964. Effective half-life of polonium. Proc. 10th annual bioassay and analytical

chemistry meeting. Conf. 727, pp. 32-38.
Silberstein, H.E., Minto, W.L., Fink, R.M. 1950a. Intravenous injection of polonium in a rabbit. In: Biological Studies With Polonium, Radium and Plutonium (Ed. by R.M. Fink), pp. 117-119. New York, McGraw-Hill.
Silberstein, H.E., Valentine, W.N., Minto, W.L., Lawrence, J.S. & Fink, R.M. 1950b. Studies of polonium metabolism in human subjects. Intravenous studies, comparison of intravenous studies, oral administration. In: Fink, R.M. (Ed.), Biological Studies With Polonium, Radium and Plutonium, pp. 122-148. New York, McGraw-Hill.
Silverman, L.B., 1994. Excretion activity analyses as a monitor for postum exposures. Final report No. 10. Mound Laboratory. MLM-1443. Miamisburg, Ohio.
Skwarzec, B., Ulatowski, J., Struminska, D.I., Borylo, A., 2001. Inhalation of 210Po and 210Pb from cigarette smoking in Poland. J. Environ. Radioact. 57, 221-230.
Smith, F.A., Morrow, P.E., Gibb, F.R., Della Rosa, R.J., Casarett, L.J., Scott, J.K., Morken D.A. and Stannard, J.N. 1960. Distribution and excretion studies in dogs exposed to an aerosol containing polonium-210. University of Rochester Atomic Energy Project, Report UR-566.
Smith, F.A., Morrow, P.E., Gibb, F.R., Della Rosa, R.J., Casarett, L.J., Scott, J.K., Morken, D.A., Stannard, J.N. 1961. Distribution and excretion studies in dogs exposed to an aerosol containing polonium-210. Am. Ind. Hyg. Assoc. J. 22, 201-208.
Soremark, R., Hunt, V.R., 1966. Autoradiographic studies of the distribution of polonium-210 in mice after a single intravenous injection. Int. J. Rad. Biol. 11, 43-50.
Spoerl, E., Anthony, D.S. 1956. Biological research related to polonium. In : Polonium. United States Atomic Energy Commission Technical Information Service Extension, July 1956, Oak Ridge, TN.
Spoerl, E.S., 1951. A derived biological half-life of polonium in humans. Mound Laboratory, MLM-626. Report for biological research, 72-76.
Stannard, J.N., 1964. Distribution and excretion of polonium-210. I. Comparison of oral and intravenous routes in the rat. Radiat. Res. 5 (suppl.), 49-59.
Testa, C., 1972. Indirect methods used at CNEN for the evaluation of internal contamination. In: Assessment of radioactive contamination in man. IAEA-SM-150/18, Vienna, pp. 405-421.
Thomas, R.G., 1964. The binding of polonium by red cells and plasma proteins. Radiat. Res. Suppl. 5, 29-39.
Thomas, R.G., and Stannard, J.N., 1956. The metabolism of polonium-210 administered by intratracheal injection to the rat. University of Rochester Atomic Energy Project, Report UR-430.
Thomas, R.G., Stannard, J.N., 1964. Distribution and excretion of polonium-210. VI. After intratracheal administration in the rat. Radiat. Res. 5 (suppl.), 106-123.
Wraight, J.C., Strong, R.A., 1989. Case study on the retention and excretion of internally deposited polonium. Radiation protection - theory and practice. Proc. of the 4th International Symposium, Malvern, pp 227-230.

12. Radon (Z = 86)

12.1. Chemical forms in the workplace

(605) Radon is an inert (noble) gas that is encountered in elemental form either as a gas, or dissolved, usually in water.

(606) Three isotopes of radon are considered in this section, ^{222}Rn, ^{220}Rn and ^{219}Rn (Table 12-1). They are usually encountered as decay products of radium isotopes (^{226}Ra, ^{224}Ra and ^{223}Ra), which are members of the three natural radioactive decay series, headed by the primordial radionuclides ^{238}U, ^{232}Th and ^{235}U respectively (Figures 12-1 to 12-3). Because of their origins, the isotopes ^{222}Rn, ^{220}Rn, ^{219}Rn are commonly known as radon, thoron and actinon respectively. The two isotopes ^{222}Rn and ^{220}Rn are the main sources of exposure from radon of importance for radiation protection.

Table 12-1. Isotopes of radon addressed in this report

Isotope	Physical half-life	Decay mode
Rn-222 (radon)	3.8 days	Alpha
Rn-220 (thoron)	56 seconds	Alpha
Rn-219 (actinon)	4.0 seconds	Alpha

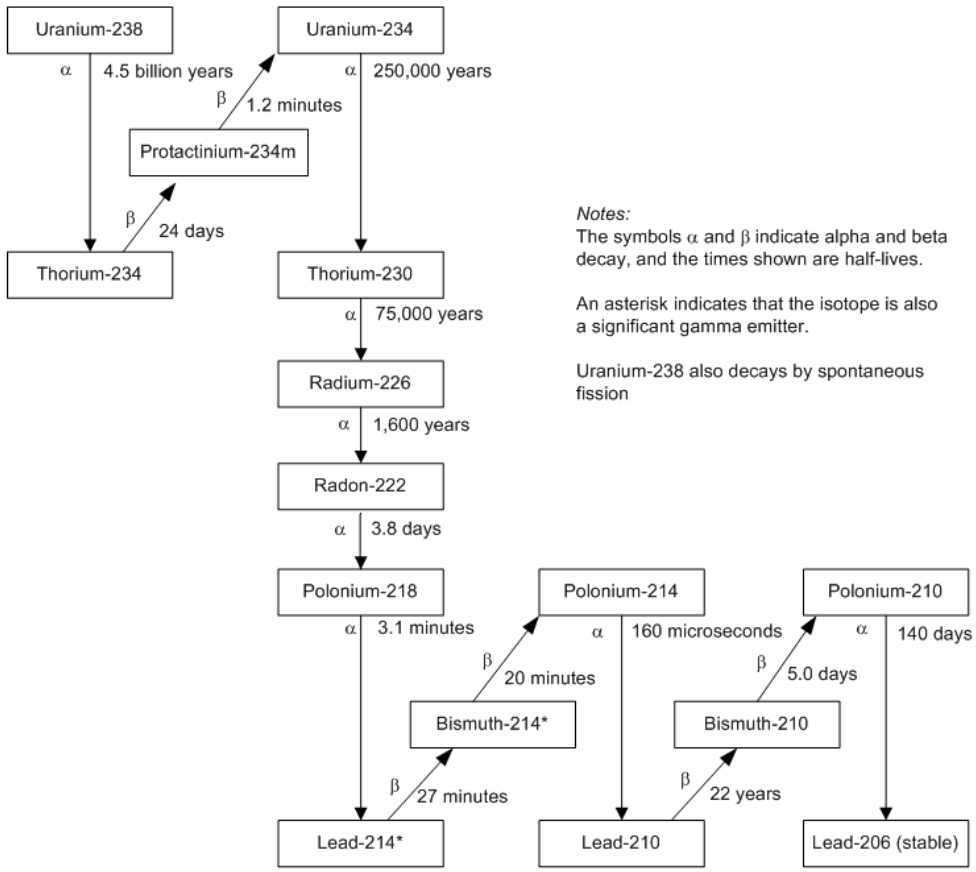

Figure 12-1. Natural decay series: Uranium-238

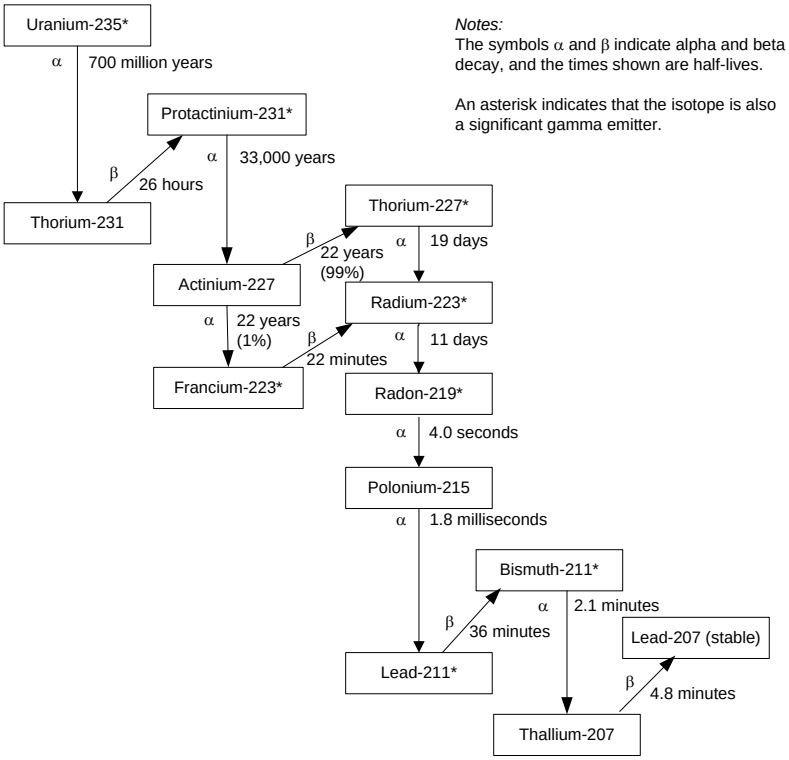

Figure 12-2. Natural decay series: Uranium-235

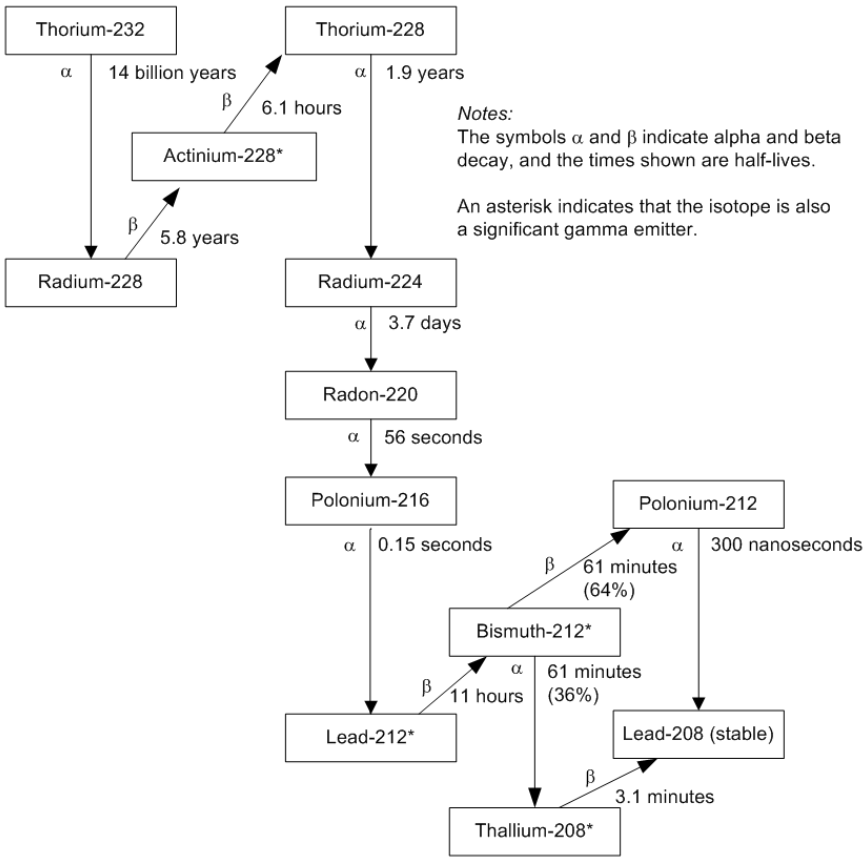

Figure 12-3. Natural decay series: Thorium-232

(607) Uranium, radium and thorium occur naturally in soil and rocks and provide a continuous source of radon. Radon can escape from the Earth's crust either by molecular diffusion or by convection and as a consequence is present in the air outdoors and in all buildings including workplaces. The build up of activity concentrations of radon and its short-lived decay products within enclosed spaces gives rise to a radiation hazard. This applies particularly to workplaces such as underground mines, tourist caves, and water supply facilities where ground water with a high radon concentration is treated or stored.

(608) In general the problems posed by radon (^{222}Rn) are much more widespread than those posed by thoron (^{220}Rn). Because thoron (^{220}Rn) has a short half-life (56 s), it is less able than radon (^{222}Rn) to escape from the point where is formed. As a consequence, building materials are the most usual source of indoor thoron exposure. In contrast, radon (^{222}Rn), which has a half-life of 3.8 days can diffuse in soil more than a meter from the point where it is formed. As a result the ground underneath buildings is usually the main source of indoor radon (^{222}Rn). Because actinon (^{219}Rn) has an even shorter half-life (4 s) its contribution to workplace exposure is generally low and in most situations can be ignored. Dose coefficients for it and its short-lived decay products are discussed in Section 12.5.4.

(609) Radon (^{222}Rn), thoron (^{220}Rn) and actinon (^{219}Rn) gases decay into a series of solid short-lived radioisotopes (Figures 12-1 to 12-3). The resulting aerosol is created in two steps (Figure 12-4). After decay of the radon gas, the freshly formed radionuclides react rapidly (< 1 s) with trace gases and vapours and grow by cluster formation to form particles around 1 nm in size. These are referred to as unattached progeny. The unattached radionuclides may also attach to existing aerosol particles in the atmosphere within 1 – 100 s forming the so-called attached progeny. The attached progeny can have a trimodal activity size distribution which can be described by a sum of three lognormal distributions (Porstendörfer, 2001). These comprise the nucleation mode with an activity median thermodynamic diameter (AMTD) between 10 nm and 100 nm, the accumulation mode with AMTD values of 100 – 450 nm and a coarse mode with activity median aerodynamic diameter, AMAD > 1 μm. Generally, the greatest activity fraction is in the accumulation mode.

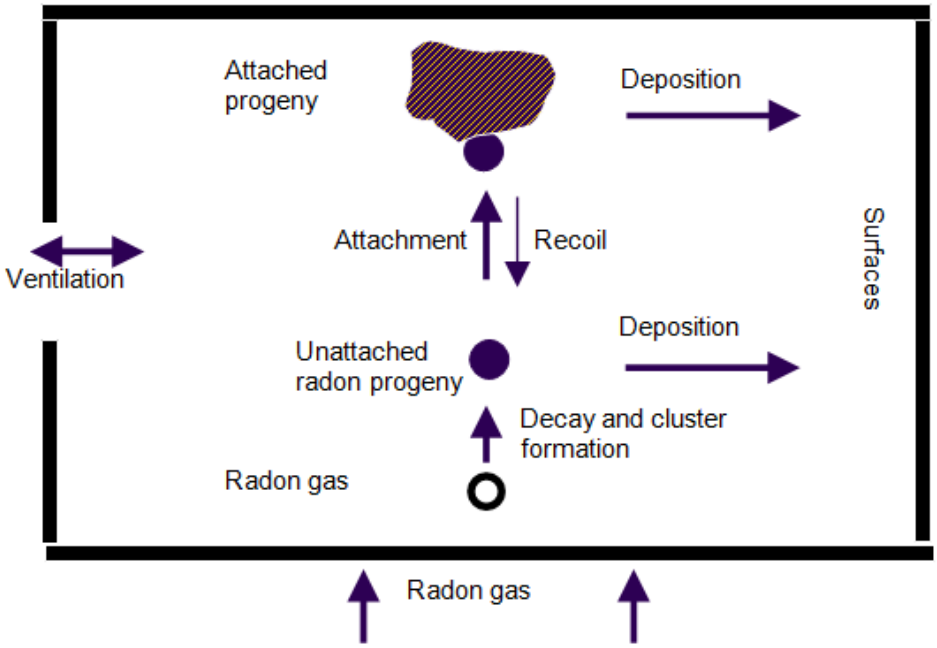

Figure 12-4. Schematic representation of the behaviour of radon progeny in an enclosed space, (NRC, 1991; Porstendörfer, 1994)

(610) Because radon progeny in the air can be removed by plate-out (i.e. by deposition on surfaces) and ventilation, the activity concentrations of the short-lived radon progeny in the air are less than that of the radon gas. This is quantified by the equilibrium factor, F which is a measure of the degree of disequilibrium between the radon gas and its progeny (see below). If the activity concentrations of the short-lived radon progeny were equal to the activity concentration of the radon gas (i.e. secular equilibrium had been reached) then F would be 1. However, because of plate-out and ventilation, F is in practice always less than 1; typically for ^{222}Rn, F is 0.4 for indoor air and 0.2 for force-ventilated mines.

(611) For exposures to radon (^{222}Rn) and thoron (^{220}Rn) gas, inhalation of their short-lived decay products generally gives much higher contributions to effective dose than inhalation of the gas itself (Figures 12-1 to 12-3). Following inhalation of the short-lived progeny most of their decay takes place in the lung before clearance can occur, either by absorption into blood or by particle transport to the alimentary tract. As a consequence the lung dose contributes more than 95% of the effective dose. Because of the importance of this route of exposure, detailed consideration is given below to exposures to radon and thoron decay products. Exceptionally, dose coefficients are given here for simultaneous intakes of radon with its short-lived decay products, under exposure conditions representative of two different types of workplace.

12.2. Special quantities and units

(612) Special quantities and units are used to characterise the concentration of radon and its short-lived progeny in the air, and the resulting inhalation exposure.

Concentration

(613) The dose to the lung mainly arises from the inhalation of the short-lived radon progeny and the alpha particles emitted during their decay and that of their short-lived progeny. The quantity 'potential alpha energy concentration (PAEC)' of the radon progeny mixture was historically used as a measure of concentration that was an indicator of dose and risk. The potential energy, $\varepsilon_{p,i}$ of an atom, *i*, in the decay chain of radon (^{222}Rn) is the total alpha energy emitted during the decay of this atom to stable ^{210}Pb. The PAE per unit of activity (Bq) of radionuclide, *i*, is $\varepsilon_{p,i} / \lambda_{r,i}$ where λ_r (in s^{-1}) is the radioactive decay constant. The PAE per atom and per unit activity are listed in Table 12-2 for the short-lived progeny of radon (^{222}Rn) and thoron (^{220}Rn). The PAEC, c_p, of any mixture of short-lived radon progeny in air is the sum of the PAE of these atoms present per unit volume of air. Thus, if c_i (in Bq m^{-3}) is the activity concentration of decay product nuclide *i*, the PAEC of the progeny mixture is

$$c_p = \sum_i c_i \left(\varepsilon_{p,i} / \lambda_{r,i} \right) \qquad \textbf{(Eq. 12-11)}$$

(614) The SI unit of this quantity is J m^{-3} (1 J m^{-3} = 6.242 10^{12} MeV m^{-3}).

(615) The historical unit of PAEC that was used in the mining industry is the working level (WL). A concentration of 1 WL is defined, in ICRP *Publication 65* (ICRP, 1993), as any combination of the short-lived radon progeny in 1 m^3 of air that will result in the emission of 1.300 10^8 MeV of alpha energy (i.e. a PAEC of 1.300 10^8 MeV m^{-3}).

(616) The so-called equilibrium equivalent concentration (EEC) is defined as the activity

concentration of radon gas, in equilibrium with its short-lived progeny which would have the same potential alpha energy concentration as the existing non-equilibrium mixture. It can therefore be calculated as follows for a given radon progeny mixture:

$$EEC = \frac{\sum_i c_i \left(\varepsilon_{p,i} / \lambda_{r,i}\right)}{\sum_i \left(\varepsilon_{p,i} / \lambda_{r,i}\right)} \qquad \textbf{(Eq. 12-2)}$$

(617) One WL equals approximately 3750 Bq m^{-3} of EEC of ^{222}Rn (radon gas) or approximately 275 Bq m^{-3} of EEC of ^{220}Rn (thoron gas).

Table 12-2. Potential alpha energy per atom and per unit activity for radon (^{222}Rn) and thoron (^{220}Rn) progeny.

Nuclide	Half-life	Potential alpha energy			
		per atom		per unit of activity	
		MeV	10^{-12} J	MeV Bq^{-1}	10^{-10} J Bq^{-1}
Radon (^{222}Rn) progeny:					
^{218}Po	3.05 min	13.69	2.19	$3.615\ 10^{3}$	5.79
^{214}Pb	26.8 min	7.69	1.23	$1.784\ 10^{4}$	28.6
^{214}Bi	19.9 min	7.69	1.23	$1.325\ 10^{4}$	21.2
^{214}Po	164 μs	7.69	1.23	$2\ 10^{-3}$	$3\ 10^{-6}$
Total at equilibrium, per Bq of ^{222}Rn				$3.471\ 10^{4}$	55.6
Thoron (^{220}Rn) progeny:					
^{216}Po	0.15 s	14.6	2.34	3.16	$5.1\ 10^{-3}$
^{212}Pb	10.64 h	7.8	1.25	$4.312\ 10^{5}$	691
^{212}Bi[a]	60.6 min	7.8	1.25	$4.090\ 10^{4}$	65.5
^{212}Po	304 ns	8.78	1.41	$3.85\ 10^{-6}$	$6.2\ 10^{-9}$
Total at equilibrium, per Bq of ^{220}Rn				$4.721\ 10^{5}$	756

[a] ^{212}Bi decays into ^{212}Po and ^{208}Tl with branching ratio of 64% and 36%.

Equilibrium factor, F

(618) The equilibrium factor, F is defined as the ratio of the EEC to the radon gas concentration. In other words, it is the ratio of the PAEC for the actual mixture of radon decay products to that which would apply at radioactive equilibrium.

Exposure

(619) The PAE exposure is defined as the time integral of the PAEC in air. The SI unit of PAE exposure is J h m^{-3} and the historical unit applied to uranium mining is the working level month (WLM). The WLM is defined as the cumulative exposure from breathing an atmosphere at a concentration of 1 WL for a working month of 170 hours. The relationship between the historical and SI units is as follows:

1 WLM = 3.54 mJ h m^{-3}

1 mJ h m^{-3} = 0.282 WLM

(620) One WLM equals approximately $6.37\ 10^{5}$ Bq h m^{-3} of EEC of ^{222}Rn (radon gas) or approximately $4.68\ 10^{4}$ Bq h m^{-3} of EEC of ^{220}Rn (thoron gas). In terms of SI units, 1 J h m^{-3}

equals approximately 1.80 10^8 Bq h m^{-3} of EEC of ^{222}Rn gas or approximately 1.32 10^7 Bq h m^{-3} of EEC of ^{220}Rn gas. For ^{222}Rn, if the exposure is expressed in terms of the radon gas concentration then the two units are related via the equilibrium factor: 1 WLM = (6.37 10^5 / F) Bq h m^{-3} or 1 J h m^{-3} = (1.80 10^8 / F) Bq h m^{-3}.

(621) Because of its short half-life, the gas activity concentration of thoron (^{220}Rn) can vary substantially across an enclosed space and so it is not possible to use thoron gas concentration in dose evaluation. Therefore, for control purposes, the PAEC of the thoron progeny should be determined; that is, the EEC of thoron should be controlled. In ICRP *Publication 65* (ICRP, 1993), it was stated that 'for protection against thoron, it is usually sufficient to control the intake of the decay product, ^{212}Pb, which has a half-life of 10.6 hours'. This is because the PAE per unit activity inhaled is about 10 times higher for ^{212}Pb than for other thoron progeny (Table 12-2). However, in this report doses are calculated for exposures of thoron and its decay products, considering intakes of ^{212}Pb as well as ^{212}Bi and ^{220}Rn.

Unattached fraction, f_p

(622) The unattached fraction, f_p is defined as the fraction of the potential alpha energy concentration (PAEC) of the short-lived progeny that is not attached to the ambient aerosol. The magnitude of f_p primarily depends on the concentration of particles of ambient aerosol, Z and can be estimated with the semi-empirical equations given by Porstendörfer, (2001):

Radon (^{222}Rn) progeny: $$f_p = \frac{414}{Z\ (cm^{-3})} \qquad \text{(Eq. 12-3)}$$

Thoron (^{220}Rn) progeny: $$f_p = \frac{150}{Z\ (cm^{-3})} \qquad \text{(Eq. 12-4)}$$

(623) Porstendörfer and his colleagues measured the unattached fraction of radon and thoron progeny using a single screen diffusion battery with 50% penetration for 4 nm diameter particles. A condensation nuclei counter was used to measure Z for particle diameters > 5 nm. Equation (3) agrees fairly well with data for 2000 < Z < 7 10^5 cm^{-3} (Porstendörfer, 2001). At lower particle concentrations (Z< 400 cm^{-3}), the agreement with data is poor (Cheng et al., 1997). Also the above equation may underestimate f_p in situations where the radon progeny is far from equilibrium as is the case in some modern mines, which are ventilated at a high rate to reduce radon concentrations (Cavallo et al., 1999). Because of the relatively long radioactive half-life of the thoron decay product ^{212}Pb (10 h), the f_p value for the thoron progeny is lower than that for the radon progeny under the same conditions. Reasonable agreement was obtained between equation (4.4) and the data of Tschiersch et al., 2007, for 900 < Z < 3 10^4 cm^{-3}.

Correlation between F and f_p

(624) For indoor air, F is weakly correlated with the unattached fraction, f_p (Vaupotič, 2007; Vaupotič and Kobal, 2006, Marsh et al., 2002; Huet et al., 2001a; Vargas et al., 2000; Chen et al., 1998; Tokonami, et al., 1996a; NRC, 1991; Vanmarcke, et al., 1989). This negative correlation between F and f_p has also been observed in a tourist cave (Vaupotič, 2008). The correlation can be explained as follows for conditions where the ventilation rate is relatively low: When the aerosol particle concentration is high the unattached fraction is low, and the equilibrium factor is relatively high as more of the radon progeny are attached

and stay in the air. More stay in the air because plate-out rates (i.e. deposition rates) for the aerosol attached nuclides are significantly lower than that for the unattached nuclides (Porstendörfer, 1994). Taking account of this negative correlation between F and f_p, it has been shown that for indoor air the radon gas concentration is a better index of dose than the PAEC under a range of aerosol conditions normally encountered (Vargas et al., 2000; Marsh and Birchall, 1998; Vanmarcke, et al., 1989; James et al., 1988). On this basis and because of practical considerations, radon gas measurements are generally carried out in homes and indoor workplaces. However, in mines with forced ventilation, the correlation between F and f_p is unlikely, so control of radon exposure in mines should be in terms of PAE exposure.

12.3. External dose

(625) Radon progeny in the ambient air can plate-out (i.e. deposit) on surfaces including human skin. The alpha particles emitted will deliver a dose to the outer layers of the skin in areas exposed to the atmosphere such as neck and face whereas skin protected by clothing and hair will in general receive a minimal dose (AGIR, 2009). The amount of radon progeny depositing on the skin for a given air concentration mainly depends on the deposition velocity, which in turn depends on particle size and air movement. The BEIR VI report (NRC, 1999) gives values of absorbed dose rate to exposed areas of the skin as a result of domestic exposure to ^{222}Rn based on the work of Harley and Robbins (1992) and of Eatough and Henshaw (1992). The latter authors give estimates of equivalent dose to skin of 1.4 10^{-8} Sv per Bq h m^{-3} (range 0.97 10^{-8} to 9.710^{-8} Sv per Bq h m^{-3}) for ^{222}Rn and 1.1 10^{-7} Sv per Bq h m^{-3} (range 0 to 7.2 10^{-7} Sv per Bq h m^{-3}) for EEC of ^{220}Rn. These values relate to the basal cell layer of the face and neck with an assumed epidermal thickness of 50 μm. The values for ^{222}Rn were calculated assuming F= 0.5 (and f_p =0.03), so the estimated equivalent dose to skin in terms of mSv per WLM for indoor exposure is about 18 mSv per WLM (range 12 to 124 mSv per WLM). The estimated range mainly reflects the uncertainties in the deposition velocity of the radon progeny. As the tissue weighting factor for the skin is 0.01, this skin dose contributes a small amount to the overall effective dose (Table 12-15).

(626) Charles (2004), point out that currently there is no definitive answer to the location and the identity of the target cells in the skin that play a dominate role in the induction of skin cancer. It has generally been assumed by several authors that the basal cell layer of the epidermis is the target cell layer. However, there are existing animal data that imply that the target cells are in the underlying dermis, in which case they may lie too deep to receive any significant dose from radon progeny on skin surface. In this report, the calculation of effective dose from exposure to radon and its progeny does not include dose to skin from radon progeny deposited on skin surface.

(627) The external dose from submersion in a cloud of radon and its decay products is not considered in this report.

12.4. Routes of Intake

12.4.1. Inhalation

(628) Consideration is given to the two components of exposure:

- Inhalation of the short-lived decay products;
- Inhalation of radon gas.

(629) Absorption parameter values for radon decay products are addressed in the inhalation sections of the elements (lead, bismuth and polonium) and are given in Table 12-3. As described in OIR part 1, Section 3.2.3 shared kinetics are assumed in the respiratory tract. However, analysis has shown that the application of independent kinetics in the respiratory tract rather than shared kinetics would make little difference to the lung dose; less than about 5%.

(630) Information is available on the behaviour of inhaled radon and other inert gases in man. This information is given in Section 12.4.3, which describes the biokinetic model for radon following inhalation and ingestion.

Table 12-3. Absorption parameter values for inhaled radon progeny

Inhaled radon progeny	Dissolution parameter values			Uptake parameter values		Absorption from the alimentary tract, f_A
	f_r	s_r (d^{-1})	s_s (d^{-1})	f_b	S_b (d^{-1})	
Polonium	1	3	–	–	–	0.1
Lead	0.1	100	1.7	0.5	1.7	0.02
Bismuth	1	1	–	–	–	0.05

Inhalation of the short-lived decay products of ^{222}Rn

(631) Aerosol characteristics need to be defined in order to calculate doses from inhaling radon progeny. The activity size distribution of the radon progeny aerosol can be very variable and depends upon the exposure scenario. For the purposes of dose calculation, aerosol parameter values are given for indoor workplaces and mines (Table 12-4). However, for completeness measured values of aerosol parameters for tourist caves, water supply facilities and thermal spas are also discussed. Because the absolute risk of lung cancer from inhaling radon and its progeny is greatly influenced by tobacco smoking, choosing aerosol parameter values other than those given in Table 12-4 is considered generally not to be warranted for radiation protection purposes.

(632) The relative activity size distribution of unattached radon progeny clusters depends on the concentration of water vapour, trace gases and the electrical charge distribution of the radionuclides in the air. Porstendörfer (2001) found that under 'normal' conditions of humidity and radon concentration, the activity size distribution of the unattached progeny can be approximated with three lognormal distributions. The AMTD values measured were 0.6 nm, 0.85 nm, and 1.3 nm with geometric standard deviations (σ_g) of about 1.2. In places with high radon concentrations, the fraction with the greatest AMTD value (1.3 nm) was not observed. The neutralisation rate of the unattached clusters increases with radon concentration and so it is likely that modes below 1 nm are mainly associated with neutral clusters, whereas modes above 1 nm are charged clusters (Porstendörfer et al., 2005). Huet et al. (2001b) also measured the size distribution for the unattached radon progeny and found a unimodal distribution with median diameters between 0.5 and 1.5 nm and values of σ_g between 1.2 and 1.4. Other workers have also measured a unimodal distribution in the range 0.7 – 1.7 nm (Cheng et al., 1997; El-Hussein, et al., 1998; Mohammed, 1999; El-Hussein, 2005). For the purposes of dose calculation and for simplicity, a unimodal distribution with an AMTD of 0.9 nm and a σ_g of 1.3 is assumed here for all exposure scenarios.

(633) The size of the unattached radon progeny is assumed to remain constant in the lung (NRC, 1991). However, some of the ambient aerosols, to which radon progeny attach, are

unstable in saturated air (i.e. hygroscopic) and are assumed to grow very quickly on inhalation by a given factor (Sinclair et al., 1974; NRC, 1991). For modelling purposes and simplicity, it is assumed that the AMTD increases by the hygroscopic growth factor (*hgf*) instantaneously as the particle enters the nose or mouth. Assumed values for the *hgf* are given in Table 12-4 for different exposure scenarios.

(634) Porstendörfer (1996) pointed out that results of experimental studies show that the differences between the activity size distribution of the individual decay products attached on aerosol particles are negligible. Therefore, for simplicity and for dosimetry purposes, the aerosol distribution of each of the short-lived ^{222}Rn progeny (i.e. of ^{218}Po, ^{214}Pb and ^{214}Bi) is assumed to be the same.

(635) Low pressure cascade impactors, which measure the aerodynamic diameter, can be used to measure the activity size distribution of the attached progeny. Such results are expressed in terms of an AMAD with a σ_g for a given mode of the attached size distribution (Reineking et al., 1994). However, measurements carried out with diffusion batteries measure the thermodynamic diameter and the results are expressed in terms of AMTD with a σ_g for a given mode. For particle sizes less than 500 nm diffusion is the dominate mechanism of deposition in the respiratory tract and the AMTD is the parameter that characterises deposition by diffusion.

Table 12-4. Aerosol parameter values for different exposure scenarios for 222Rn progeny

Exposure scenario	f_p [a, b]	Equilibrium factor, F	Attached aerosol characteristics in the ambient air[c]							
			Mode, i	f_{pi}	$AMAD_i$ (nm)	Density, ρ_i ($g\ cm^{-3}$)	Shape factor, χ_i	$AMTD_i$ (nm)	σ_{gi}	hgf_i[d]
Indoor workplace	0.1	0.4	n	0.2	30	1.4	1.1	24	2.0	2.0
			a	0.8	250	1.4	1.1	213	2.0	2.0
Mine	0.01	0.2	a	1.0		0.7[e]	1.0[e]	250	2.0	1.0

[a] f_p = unattached fraction in terms of the potential alpha energy concentration (PAEC).

[b] The unattached progeny are assumed to have an AMTD of 0.9 nm with $\sigma_g = 1.3$, and unit density and shape factor.

[c] Indices i = n and a represent the accumulation and nucleation modes. f_{pi} = fraction of attached PAEC for mode i. σ_{gi} = geometric standard deviation of mode i. hgf_i = hygroscopic growth factor for mode i.

[d] It is assumed that the AMTD increases by *hgf* instantaneously as the particle enters the nose or the mouth. For simplicity, the hygroscopically enlarged particles are assumed to have unit density and shape factor.

[e] The values chosen for the density (ρ) and shape factor (χ) for a diesel powered mine aerosol are based on the measurements of the effective density, (i.e. ρ/χ) of diesel exhaust particles and is assumed to be $\rho/\chi = 0.7\ g\ cm^{-3}$ (Park et al., 2003; Olfert et al., 2007).

Indoor workplaces

(636) Published data on activity size distributions in indoor workplaces other than homes are relatively sparse. Reichelt et al. (2000) carried out activity size measurements of radon progeny at several workplaces including offices, workshops, factories, kitchens, agricultural facilities and public buildings like schools, hospitals and art galleries. Porstendörfer (2001) summarised their results and suggested dividing indoor workplaces into two categories: workplaces in rooms without coarse particles, and workplaces with coarse particles generated by human activities and dispersion processes. Calculated values of the equivalent dose to the lung per unit exposure for the two categories differed by less than 10% (Porstendörfer, 2001). In this report workplaces in rooms without coarse particles are considered.

(637) The parameter values of the activity size distribution for the attached radon progeny assumed for indoor workplaces (Table 12-4) are based primarily on the measurement results of Porstendörfer (2001) and on results published for homes. Marsh et al. (2002) summarises measurement results for homes published in the literature since 1980.

(638) For an aged aerosol (i.e. without additional aerosols), the presence of a nucleation mode is not always measured but can be observed when additional aerosols are produced (Marsh et al., 2002; Huet et al., 2001b; Tu et al., 1991; NRC, 1991). For an aged aerosol, Huet et al. (2001b) found that the attached size distribution consisted only of the accumulation mode. However, intercomparison measurements performed in a house in Germany, without additional aerosols, showed nucleation and accumulation modes with the fraction of the attached PAEC in the nucleation mode (f_{pn}) being about 0.2 (Reineking et al., 1994). Measurements of the activity size distribution of the attached progeny in a dwelling in Okinawa, Japan also showed a nucleation mode with an activity fraction of 0.14 (Kranrod et al., 2009). The mean AMAD of the nucleation mode was about 30 nm with a σ_g of 1.6. Porstendörfer (2001) reported values of f_{pn} between 0.2 and 0.5 for workplaces. The AMAD of the nucleation mode was reported to be between 15 to 40 nm with a σ_g ranging between 1.6 and 2.2. A f_{pn} value of 0.2 is assumed here for indoor workplaces. An AMAD of 30 nm with a σ_g of 2.0 is assumed for the nucleation mode.

(639) Indoor measurements of the AMAD of the accumulation mode show a wide range of values, typically between 110 – 370 nm (Huet et al., 2001b, Porstendörfer, 2001, Mohammed, 1999, El-Hussein et al., 1998; Tu et al., 1991; Tu and Knutson, 1988). A central value of 250 nm is assumed here with a σ_g of 2.0.

(640) Sinclair et al. (1974) found that atmospheric particles in their laboratory increased in diameter by about a factor of 2 when the relative humidity increased from zero to 98%. For indoor workplaces a hygroscopic growth factor (hgf) of 2.0 is assumed here for the ambient aerosol. The density (g cm^{-3}) and the shape factor of these hygroscopically enlarged particles are taken to be unity.

(641) Measurements of the unattached fraction, f_p, in indoor workplaces such as schools and offices show a wide range of values, typical between 3% and 15% and with some values greater than 20% (Vaupotič, 2008b; Porstendörfer, 2001; Yu et al., 1998; Tokonami et al., 1996b; Hattori et al., 1995, Hattori and Ishida, 1994). Typical values of f_p in homes range between 4% and 20% with some values greater than 40% (Kranrod et al., 2009; El-Hussein, 2005; Mohamed, 2005; Vargas, et al., 2000; Tokonami, et al., 1996a; Yu, et al., 1996; Hopke, et al., 1995; Reineking and Porstendörfer, 1990; Chen, et al., 1988; Kojima and Abe, 1988). A representative value of $f_p = 0.1$ is chosen for indoor workplaces.

(642) The value of the equilibrium factor, F, depends mainly on the indoor ventilation rate due to opening/shutting of windows, use of electric fans, air conditioners and dehumidifiers.

(Iyogi et al., 2003; Iimoto, 2000; Iimoto et al., 2001; Chen, et al., 1998). Typically, mean values of F ranged from 0.3 to 0.6 for schools, kindergardens, offices, nuclear power plant, factories and cafes (Labidi et al., 2010; Vaupotič, 2008b, Maged, 2006; Misdaq and Amghar, 2005; Iyogi et al., 2003; Misdaq and Flata, 2003; Tokonami et al., 2003, 1996; Yu et al., 2000, 1998; Hattori et al., 1995; Hattori and Ishida, 1994). In its 2000 report, UNSCEAR assumed an F value of 0.4 for indoor exposures, based mainly on measurements in dwellings in the USA (Hopke et al., 1995) and in India (Ramachandran and Subba Ramu, 1994). A F value of 0.4 is assumed here for indoor workplaces, which is in agreement with the value given in ICRP *Publication 65* (ICRP, 1993).

Mines

(643) Characterising the aerosol parameters for mines is difficult because of the highly variable conditions and because of the different types of mining conditions such as use of diesel or electric powered equipment, different ventilation rates, and the type of heating used during the winter months (Marsh et al., 2008; Cavallo, 2000).

(644) Measurements were made of the activity size distribution in two mines in the USA in Colorado and New Mexico (Cooper et al., 1973). Because the measurements were made during wintertime, it is likely that the incoming ventilation air was heated by burning propane gas. However, it is not clear from the report whether the heaters were being used when the measurements were made. Both mines used diesel engines. The measurements were carried out with a low pressure impactor having five stages and a backup filter. However, its resolution was relatively poor. These data were reanalysed by Cavallo (1998) using modern unfolding techniques. The reanalysed data showed that for the Colorado mine the AMAD of the principal mode ranged from 111 nm to 303 nm with a mean of 200 nm. The mean value of σ_g was 2.0. Four out of the nine spectra had a secondary mode with a peak around 30 nm containing about 20-25% of the PAEC. However, given the poor resolution of the impactor the authors did not consider this secondary mode in their dose calculations. For the New Mexico mine, the mean values of the AMAD and σ_g of the accumulation modes were 140 nm and 2.9 respectively (Cavallo, 1998).

(645) Measurements were carried out in four uranium mines in New Mexico, USA during the summer of 1971 (George et al., 1975). All four mines were diesel powered with one of the mines being much less active than the others. The activity size measurements obtained with a diffusion battery were reanalysed by Knutson and George (1990). Twenty six spectra were obtained; nine of the spectra were unimodal with a mean AMTD of 150 nm (80 – 210 nm) and a σ_g of about 2.7, and 11 spectra had both unattached and accumulation modes. The remaining six spectra showed one activity peak at 100 – 200 nm and another at 5 – 10 nm. The average value of the equilibrium factor was 0.17.

(646) During the summer of 1978 measurements were carried out with a diffusion battery in a Canadian diesel powered uranium mine (Busgin et al., 1981). An AMTD of about 100 nm with a σ_g of 1.9 was measured in an exhaust ventilation area of the mine. The unattached fraction of ^{218}Po was estimated to be less than 2%. Based on the measured particle concentration (10^5 cm^{-3}), f_p is calculated to be about 0.4%. The same group also carried out a second set of measurements during the winter of 1985 in two mines in Canada; one mine used diesel equipment and the other used electrically powered equipment (Kahn et al., 1987). In the diesel powered mine the AMTD was about 90 nm with a σ_g of 1.8 whereas in the electrically powered mine the AMTD was about 50 nm with a σ_g of 1.8. The measurements were carried out with a set of diffusion batteries which had relatively poor resolution.

(647) Activity size measurements have been performed at a diesel powered uranium mine

in France, at the Bellezane mining centre during the summer of 1989 (Boulaud and Chouard, 1992). The gallery cross section was 10 m^2 with mean air velocities of about 1 m s^{-1}. A combination of a cascade impactor in series with a diffusion battery was used to carry out the measurements. The AMTD ranged from 150 nm to 210 nm with a mean of 178 nm. The aerosol concentration was also measured; mean values per half day varied from 6 10^4 to 9 10^4 cm^{-3}. This indicates f_p values of less than about 1%.

(648) Butterweck et al. (1992) carried out activity size measurements in underground mines in Germany with a low pressure cascade impactor and a high volume impactor. The unattached fraction was also measured with wire screens. Their results showed that with diesel engines, the diesel aerosol dominates the mine aerosol resulting in a very low unattached fraction; 0.1% - 2.5% with a mean of 0.7%. In the diesel powered slate mine, they found that during working hours the AMAD of the accumulation mode was about 200 nm with a σ_g of about 2.0. During non-working hours the AMAD increased to about 350 nm. For the other active mines in Germany (barite: Dreislar, Bad Lauterberge; iron: Salzgitter; uranium: Groβ-Schloppen), the mean values of the AMAD ranged from 180 – 270 nm during working hours. The equilibrium factor value ranged from 0.3 to 0.6 with a mean of 0.45.

(649) Solomon et al. (1993, 1994) carried out activity size distributions measurements in an underground uranium mine, at Olympic Dam, South Australia. Measurements were carried out with a serial graded screen array and a diffusion battery. In areas of the mine where there were large diesel-powered vehicles, the AMTD of the accumulation mode ranged from 200 to 300 nm. The average value of the AMTD was 250 nm with a σ_g of about 2.5. In the areas of the mine where there were no vehicles or the ventilation intakes were close by, the AMTD values were smaller in the range 90-200 nm with a mean of 150 nm. The mean value of the unattached fraction throughout the mine was about 3% to 4% and the mean value of the equilibrium factor was about 0.2.

(650) Measurements have been carried out to characterise the aerosol in a wet underground uranium mine in northern Saskatchewan, Canada (Cavallo, 1997, 2000; Cavallo et al., 1999, Wu-Tu et al., 1997). This mine used state-of-the art mining technology and used diesel powered equipment extensively. Because of the exceptionally high grade ore, the mine ventilation rate was very high; about 3.6 10^4 m^3 min^{-1}, which was estimated to be about one air change per 3 minutes. The average air velocity in the main decline was about 5 m s^{-1} (12 mph). Measurements were carried out in the winter of 1995 and in the summer of 1996. An impactor with a graded screen array was used to determine the size distribution over a range of particle sizes of 0.6 to 5000 nm. During the winter months the temperature inside the mine was maintained at 5ºC by direct burning of propane gas to heat the ventilation air. As a result, the mine aerosol consisted of particles from the combustion of propane gas as well as diesel particles. The winter time measurements carried out at a stope and a drilling area where miners were working showed predominately a two modal distribution for the attached progeny. The fraction of the attached PAEC associated with the nucleation and accumulation modes were about 65%, and 35%, and the mean values of the AMAD were about 60 nm and 330 nm respectively. The unattached fraction (f_p) was about 1%. Winter time measurements were also carried out at a bolt-storage bay next to a major mine exhaust. Most of these measurements showed that the attached progeny consisted of the nucleation mode containing about 97% of the attached PAEC, on average, with AMAD values between 50 and 75 nm. The coarse mode accounted for the remaining 3% of attached PAEC with an AMAD between 2 and 8 μm. Typically f_p was less than 2% and the mean value of the AMTD of the unattached progeny was less than 1 nm. The results of the summer time measurements of 1996 showed that throughout the mine the AMAD values ranged from 50 nm to 120 nm with

a mean value of 85 nm and σ_g of about 2.0. The average value of f_p was about 6% whereas the expected value based on particle concentration was 0.3%. This unexpected high value of f_p was theoretically shown to occur under conditions when the radon progeny is far from equilibrium as was the case in this Canadian mine, which was ventilated at a high rate (Cavallo et al., 1999). The average value of the equilibrium factor was 0.08.

(651) Tokonami, et al. (2005) measured the activity size distribution in an underground mine located in the Gifu prefecture region of Japan. A cascade impactor with ten stages and a graded screen array were used for the measurements. The AMTD of the unattached progeny was 0.8 nm with a σ_g of 1.5. The activity size distribution of the attached progeny was represented by a single mode having an AMAD of 162 nm with a σ_g of 3.1.

(652) Based on the measurements of Cooper et al. (1973) in US mines and the measurements of Bigu and Kirk (1980) in Canadian mines, a panel of experts from the National Research Council (NRC, 1991) recommended an AMTD of 250 nm in areas of active mining and a f_p value of 0.5%. In areas of transport and maintenance work (i.e. haulage drifts), a f_p value of 3% was assumed. In these areas a lower AMTD value of 150 nm was assumed based on the measurement data of George et al., 1975, which was reanalysed by Knutson and George (1990).

(653) Aerosol parameter values are given for a diesel powered mine with medium to good ventilation (Table 12-4). These chosen values are mainly based on the measurements carried out in mines in Australia (Solomon et al., 1993, 1994), France (Bouland and Chouland, 1992) and Germany (Butterweck et al., 1992). For diesel powered mines it is assumed that the aerosol does not increase in size in the respiratory tract because diesel aerosols are hydrophobic (Cavallo, 2000; Weingartner et al., 1997).

(654) For a diesel powered mine it is assumed that the aerosol is mainly dominated by the diesel aerosol. Several workers have calculated the effective density of diesel exhaust particles from measurements of the thermodynamic diameter (d_{th}) and aerodynamic diameter (d_{ae}) of the exhaust particles (Park et al., 2003; Olfert et al., 2007). The effective density is the ratio of the particle density (ρ) and shape factor (χ). Results indicate that the effective density decreases with increasing d_{th} in the size range from 50 – 300 nm. This mainly occurs because particles become more highly agglomerated as size increases. The smaller particles are more compact than the larger particles and therefore have a higher effective density. Typically, the effective density varies from 1.2 to about 0.3 g cm^{-3} depending on size and fuel composition; higher effective densities are observed for high sulphur fuel. The chosen values for the effective density of the aerosol in diesel powered mines are based on the measurements of Park et al. (2003) and Olfert et al. (2007).

(655) It is acknowledged that the exposure conditions in mines today are significantly different from those 10 to 20 years ago and that the chosen aerosol parameter values are not necessarily representative of mines today. However, there are currently no published data on aerosol characteristics in modern mines.

Tourist caves

(656) Information on exposure conditions in tourist caves is given here for completeness. Reference parameter values for tourist caves are not given in this report.

(657) Typically there is no additional ventilation in tourist caves as forced ventilation may alter the humidity inside the cave affecting some of the geological formations that attract tourists. As a result radon concentrations can reach high levels of several thousand Bq m^{-3} (Butterweck et al., 1992; Sainz et al., 2007). Several measurements have been carried out in natural caves to characterise the aerosols.

(658) Butterweck et al. (1992) carried out activity size measurements in a natural tourist cave, in Postojna, Slovenia, with a low pressure cascade impactor and a high volume impactor. The unattached fraction was also determined from wire screen measurements. The AMAD of the accumulation mode ranged from 120 nm to 290 nm with a mean of 230 nm. The mean σ_g value of the accumulation mode was 2.2. The f_p value varied from 6% to 16% with a mean of 10%. The average value of the particle concentration was about 3000 cm^{-3}. The F value range from about 0.3 to 0.5 with a mean of 0.4.

(659) Solomon, et al. (1992) used a parallel wire screen diffusion battery and a serial graded screen array battery to measure the activity size distribution of the radon progeny in a limestone cave, Victoria, Australia. Measurements were carried out over a 3 day period during October 1990 at different sites in the cave. The accumulation mode had an AMTD of 170 nm and the unattached mode had an AMTD of 1.1 nm. The f_p value throughout the cave varied from 11% to 18% whereas the F factor varied from 0.2 to 0.5. The average f_p value weighted by the occupancy of the tour guides in each sampling site was 14%. Measurements of the radon concentration carried out during June and October indicated that the radon concentration is relatively constant throughout the year.

(660) Measurements have been carried out over a 3 day period during the summer of 1994 in the Carlsbad Caverns, in southern New Mexico to determine air exchange rate, aerosol characteristics and radon progeny activity size distributions (Cheng et al., 1997). During the summer months the outside air temperature is much greater than inside the cave, which keeps the cave air stagnant. The mean ventilation rate was measured to be 2 10^{-3} h^{-1}, which was estimated to be one air exchange every 18 days. The measured particle concentration was very low; average daily values were between 280 and 385 cm^{-3}. As a result the measured f_p values were high; values ranged from 25% to 60% with a mean of 44%. The average value of F was 0.4. The activity size measurements were carried out with a graded diffusion battery. The AMTD of the unattached particles were between 0.6 and 0.8 nm, and the attached mode had a peak > 50 nm. It was noted that the particle concentration measurements made in the same area of the cave during summer months by Wilkening and Romero (1981) were more than twice as high, indicating f_p values lower by a factor of 2 or more.

(661) Sainz et al. (2007) carried out radon concentration and particle concentration measurements in tourist caves located in the region of Cantabria in the North of Spain. The results of the particle concentration measurements were 464 cm^{-3} in the Castillo cave and 1514 cm^{-3} in the Monedas cave. This indicates f_p values of 86% and 26% respectively.

(662) Measurements of the unattached fraction and equilibrium factor have been carried out in the Postojna Cave, Slovenia for 10-15 days during summer and winter months of consecutive years from 1998 to 2001 (Vaupotič, 2008a). Measurements were carried out at the railway station in the cave and at the lowest point of a walking tour. There is no forced ventilation in the cave; however during the winter months there is a natural draught of air from the cave to the outdoors as the temperature in the cave is greater than the outdoor temperature, whereas in the summer months this draught is minimal. As a consequence, the radon concentration in the cave is higher in the summer compared with the winter. The measurement results show that unattached fraction is higher in the summer compared with the winter. At the lowest point of the cave, mean values of f_p were about 60% in the summer and about 12% in the winter; the mean values of F were about 0.3 in the summer and 0.6 in the winter. Values of F were negatively correlated with f_p. At the railway station during the summer, mean values of f_p and F were 17% and 0.6 respectively.

(663) Rosvenská, et al. (2008) measured the unattached fraction, equilibrium factor and the particle size spectrum in the Bozkov dolomite cave, Czech Republic. The f_p value was low

and varied between 1% and 3%. The F value was about 0.7. The activity size distribution was theoretically determined from the particle size distribution. For the attached progeny the AMAD and σ_g of three modes were calculated: 140 nm with σ_g = 1.7; 720 nm with σ_g = 1.4 and 1.9 μm with σ_g = 1.9. The fraction of the PAEC associated with each mode was not given.

Water Supply facilities and Spas

(664) Information on exposure conditions in water supply facilities and spas is given here for completeness. Reference parameter values for water supply facilities and spas are not given in this report.

(665) High levels of ^{222}Rn gas concentrations in indoor air have been measure at water supply facilities where ground water with a high radon concentration is treated or stored (Trautmannsheimer, 2003). Porstendörfer and Reineking (1999) measured the activity size distribution at a water supply station in Germany. About 84% of the attached PAEC was associated with the accumulation mode, having an AMAD of 300 nm with a σ_g=1.8. The remaining 16% of the attached PAEC was associated with the nucleation mode, having an AMAD of 50 nm with a σ_g=1.5. They reported a f_p value of 0.05. The relative humidity at a water supply station was reported to be close to 100% (Porstendörfer, 2001).

(666) Thermal spa facilities have been used for medical therapy and rehabilitation centres as well as for recreational purposes. Radon emanating from the thermal waters is an additional source of radiation exposure to the working personnel as well as to the bathers. Measurements of ^{222}Rn in air in thermal spas have shown that the dominant mechanism by which ^{222}Rn is released from water to air is during bath filling and to a lesser extent during bathing as a result of water agitation (Vogiannis et al., 2004a, Lettner et al., 1996). During bathtub filling, F is initially low but then gradually increases and reaches a peak with a time delay preceding a ^{222}Rn peak. Correspondingly, the f_p value is initially high but then decreases and reaches a minimum. Average values of F and f_p have been reported for measurements carried out in treatment/bath rooms, rest rooms and reception rooms of spas in Greece (Vogiannis et al., 2004b, 2004c); average values of f_p range from 0.06 to 0.12 and F values range from 0.2 to 0.4. However, Geranios et al. (2004) reported higher values of f_p of about 0.23 in a treatment room and a reception room of the spa of Loutra Eipsou, Greece. Values of F measured in treatment rooms of spas in Slovenia and Austria range from 0.14 – 0.45 (Vaupotič and Kobal , 2001; Lettner et al., 1996). In two Spanish spas, the estimated average F value was 0.6 (Soto and Gómez, 1999).

Inhalation of the short-lived decay products of ^{220}Rn

(667) Thoron (^{220}Rn) decays into the short-lived progeny of ^{216}Po, ^{212}Pb, and ^{212}Bi (Figure 12-2, Table 12-2. As can be seen from Table 12-2, the PAE per unit activity of ^{212}Pb is about 10 times higher than for other thoron progeny. As a consequence, ICRP *Publication 65* (ICRP, 1993) states that "For protection against thoron, it is usually sufficient to control the intake of the decay product, lead-212, which has a half-life of 10.6 hours." In this report the intake of ^{212}Bi is also considered, but most of the dose arises from the intake of ^{212}Pb. The activity size distribution of ^{212}Bi attached on aerosols is assumed to be the same as that for ^{212}Pb.

(668) Published data on the activity size distributions of the thoron decay product, ^{212}Pb are relatively sparse. It has been suggested that because of the longer radioactive half-life of ^{212}Pb compared with that of ^{222}Rn progeny that the aerosol size of attached ^{212}Pb is likely to be larger compared with that of ^{222}Rn progeny (Khan et al., 1987). The longer half-life means

that atoms of ^{212}Pb can spend more time in the vicinity of aerosols leading to increased coagulation of aerosols and larger particle sizes. However, measurements show that the median diameters of the accumulation mode for ^{212}Pb and the radon decay product, ^{214}Pb are similar at least for 'typical' indoor air (Becker et al., 1984; Reineking et al., 1992). For the purposes of dose calculation, aerosol parameter values for thoron progeny are given in Table 12-5 for indoor workplaces and mines.

(669) The size distribution of the unattached thoron progeny is assumed to be the same as that for ^{222}Rn progeny. A unimodal lognormal distribution with an AMTD of 0.9 nm with a σ_g of 1.3 is assumed for all exposure scenarios. This is in agreement with what is measured for indoor and mining environments, where the unattached ^{212}Pb was found to have particle sizes around 1 nm (Chen, et al., 1997). Measurements carried out in a radon test chamber, as part of an intercomparison exercise, also showed medium diameters less than 1 nm for unattached ^{212}Pb (Cheng, et al., 2000).

Table 12-5. Aerosol parameter values for different exposure scenarios for thoron (^{220}Rn) progeny.

Exposure scenario	f_p [a, b]	Attached aerosol characteristics in the ambient air[c]							
		Mode, i	f_{pi}	$AMAD_i$ (nm)	Density, ρ_i (g cm^{-3})	Shape factor, χ_i	$AMTD_i$ (nm)	σ_{gi}	hgf_i[d]
Indoor workplace	0.02	n	0.14	40	1.4	1.1	32	2.0	2.0
		a	0.86	200	1.4	1.1	170	1.8	2.0
Mine	0.005	a	1.0		0.7	1.0	250	2.0	1.0

[a] f_p = unattached fraction in terms of the potential alpha energy concentration (PAEC).
[b] The unattached progeny are assumed to have an AMTD of 0.9 nm with σ_g = 1.3, and unit density and shape factor.
[c] Indices i = n and a represent the accumulation and nucleation modes. f_{pi} = fraction of attached PAEC for mode i. σ_{gi} = geometric standard deviation of mode i. hgf_i = hygroscopic growth factor for mode i.
[d] It is assumed that the AMTD increases by *hgf* instantaneously as the particle enters the nose or the mouth. For simplicity, the hygroscopically enlarged particles are assumed to have unit density and shape factor.

Indoor air

(670) Becker et al. (1984), measured the activity size distribution of ^{212}Pb in different buildings in the city of Göttingen, and in the countryside of Germany. Measurements were carried out with a high volume cascade impactor. The size distribution of the attached aerosol could be approximated by a log-normal distribution. Values of AMAD ranged from 120 nm to 290 nm with a mean of 200 nm. The mean value of σ_g was 2.9. The mean value of the AMAD for the city results was similar to that of the countryside results but the σ_g for the countryside results was larger.

(671) Reineking et al. (1992) measured the activity size distribution of ^{212}Pb in seven rooms of different houses in Germany. Measurements were performed with a low pressure cascade impactor. For separating unattached from aerosol-associated thoron progeny, a single screen with a 50% penetration for 4 nm diameter particles was used. The AMAD of the accumulation mode was about 200 nm with a σ_g of 1.8. Between 6% and 20% of the attached activity was associated with the nucleation mode with a mean of 14%. The nucleation mode had an AMAD less than 80 nm. These results were also reported by Porstendörfer (2001). Porstendörfer reports that the nucleation mode has an AMAD between 30 to 50 nm with a σ_g of about 2. Porstendörfer noted that the fraction of the attached ^{212}Pb activity associated with

the nucleation mode is lower than the corresponding values for radon (^{222}Rn) progeny. The unattached fraction (fp) of thoron progeny for 'typical' indoor air with aerosol particle concentration of (5-15) $\times$ 10^3 cm^{-3} is between 0.01 and 0.03.

(672) Zhang et al. (2010) measured activity size distributions of ^{212}Pb in countryside and city dwellings of China. There were no appreciable differences among the particle size distribution from dwellings within the same area and under the same climate conditions. However, the particle size distribution measured in countryside dwellings were lower than in city dwellings. In city dwellings of Beijing, the AMAD of ^{212}Pb was about 150 nm with a σ_g of 2.0 and in the suburbs of Beijing the AMAD was about 110 nm with a σ_g of 2.0. For some of the countryside dwellings of Yangjiang, Guuangdong Province, which were mainly made of brick, the mean AMAD was 80 nm with a σ_g of 2.9. For the cave dwellings of Datong, Shanxi Province, the mean AMAD was 50 nm with a σ_g of 3.1.

(673) The aerosol parameter values assumed for thoron progeny for indoor workplaces are based on the measurements of Reineking et al., 1992 and on the values recommended by Porstendörfer, 2001 (Table 12-5).

Mine

(674) The activity size distribution of ^{212}Pb was measured with a diffusion battery in a Canadian diesel powered uranium mine during the summer of 1978 (Busgin et al., 1981). Measurements were carried out in an exhaust ventilation area of the mine where there was no work of any kind in progress. The average value of the AMTD was found to be about 90 nm with a σ_g from 1.5 to 2.3. The same group also carried out a second set of measurements during the winter of 1985 in a diesel powered mine and in an electrical powered mine (Kahn et al., 1987). The mean AMTD of ^{212}Pb was about 100 nm with a σ_g of 1.7 in the diesel powered mine whereas in the electrically powered mine the mean AMTD was about 70 nm with a σ_g of 2.0. The thoron (^{220}Rn) WL was similar to the ^{222}Rn WL in the electric powered mine but less than the ^{222}Rn WL in the diesel powered mine.

(675) Butterweck et al. (1992) carried out activity size measurements in underground mines in Germany with a low pressure cascade impactor and a high volume impactor. Measurements were made at a uranium mine (Groβ-Schloppen), an iron mine (Salzgitter) and at a barite mine (Bad Lauterberge). The activity size distribution of ^{212}Pb could be approximated by a unimodal log-normal distribution described by the AMAD and σ_g. During working hours mean values of the AMAD of ^{212}Pb ranged from 150 – 290 nm with a σ_g ranging from 2 – 3.1. For the Barite mine of Bad Lauterberge, the mean value AMAD of ^{212}Pb was 290 nm during working hours but increased to 400 nm outside working hours. Measurements were also carried out at a disused silver mine at Lautenthal, which was open to tourists; the mean value of AMAD was 310 nm (range: 270 – 340 nm) and the σ_g was 2.4 (range: 2.1 – 3.6). In most of these mines, the activity size distributions of the accumulation mode of ^{212}Pb were broadly similar to the corresponding size distribution of the ^{222}Rn progeny, ^{214}Pb/^{214}Bi.

(676) The activity size distribution for thoron (^{220}Rn) progeny assumed for the mining environment is given in Table 12-5. These values are the same as those assumed for radon (^{222}Rn) progeny for mine (Table 12-4) apart from assuming a lower unattached fraction. Because of the longer half-life of ^{212}Pb, more of the lead is likely to be attached. However, the value of f_p also depends upon the ventilation rate; higher unattached fractions are expected for high ventilation rates.

Reference values for regional deposition of inhaled ^{222}Rn and ^{220}Rn progeny aerosols

Radon (^{222}Rn) progeny

(677) The aerosol distributions for the attached ^{222}Rn progeny (^{218}Po, ^{214}Pb and ^{214}Bi) in the ambient air are given in Table 12-4 for indoor workplaces and mines. Taking account of hygroscopic growth, the assumed aerosol characteristics of the attached progeny in the respiratory tract are given in Table 12-6. The unattached mode of the short-lived ^{222}Rn progeny (i.e. of ^{218}Po and ^{214}Pb) is assumed to have an AMTD of 0.9 nm with σ_g = 1.3, and unit density and shape factor for both exposure scenarios (Section 12.4.1.1). Table 12-7 gives the corresponding regional depositions in the respiratory tract for each mode of the assumed aerosol distribution of ^{222}Rn progeny.

Table 12-6. Attached aerosol characteristics in the respiratory tract for ^{222}Rn progeny

Exposure scenario	Attached aerosol characteristics in the respiratory tract					
	Mode[a], i	$AMAD_i$ (nm)	Density, ρ_i (g cm^{-3})	Shape factor, χ_i	$AMTD_i$ (nm)	σ_{gi} [b]
Indoor workplace	Nucl.	48	1.0	1.0	48	2.0
	Acc.	427	1.0	1.0	427	2.0
Mine	Acc.	197	0.7	1.0	250	2.0

[a] Indices i = 'Nucl.' and 'Acc.' represent the nucleation and accumulation modes respectively.
[b] σ_{gi} = geometric standard deviation of mode i.

Table 12-7. Deposition of inhaled ^{222}Rn progeny aerosols in respiratory tract regions. Values are given for each mode of the assumed aerosol distribution for indoor workplaces and mines.

Exposure scenario	Mode[a]	Deposition in regions (%)[(b)]					
		ET_1	ET_2	BB	bb	AI	Total
All	Unatt.	53.33	28.71	7.585	8.633	0.3920	98.65
Indoor workplace	Nucl.	4.458	2.401	1.084	7.627	31.79	47.36
	Acc.	8.643	4.654	0.5289	1.540	9.04	24.41
Mine	Acc.	3.150	1.696	0.4087	2.164	9.95	17.37

[a] 'Unatt.' = unattached mode, 'Nucl.' = nucleation mode, and 'Acc.' = accumulation mode.
[b] The degree of precision of the values is given for computational purposes and does not reflect the certainty with which they are known.

Thoron (^{220}Rn) progeny

(678) The aerosol distributions for the attached thoron progeny (^{212}Pb and ^{212}Bi) in the ambient air are given in Table 12-5 for indoor workplaces and mines. Taking account of hygroscopic growth, the assumed aerosol characteristics of the attached progeny in the respiratory tract are given in Table 12-8. The unattached mode of the short-lived ^{220}Rn decay product, ^{212}Pb is assumed to have an AMTD of 0.9 nm with σ_g = 1.3, and unit density and shape factor for both indoor workplaces and mines. Table 12-9 gives the corresponding regional depositions in the respiratory tract for each mode of the assumed aerosol distribution of ^{220}Rn progeny.

Table 12-8. Attached aerosol characteristics in the respiratory tract for ^{220}Rn progeny

Exposure scenario	Attached aerosol characteristics in the respiratory tract						
	Mode[a], i	$AMAD_i$ (nm)	Density, (ρ_i) (g cm^{-3})	Shape factor, χ_i	$AMTD_i$ (nm)	σ_{gi} [b]	
Indoor workplace	Nucl.	64	1.0	1.0	64	2.0	
	Acc.	340	1.0	1.0	340	2.0	
Mine	Acc.	197	0.7	1.0	250	2.0	

[a] Indices i = 'Nucl.' and 'Acc.' represent the nucleation and accumulation modes respectively.
[b] σ_{gi} = geometric standard deviation of mode i.

Table 12-9. Deposition of inhaled ^{220}Rn progeny aerosols in respiratory tract regions. Values are given for each mode of the assumed aerosol distribution for indoor workplaces and mines.

Exposure scenario	Mode[a]	Deposition in regions (%)[b]					
		ET_1	ET_2	BB	bb	AI	Total
All	Unatt.	53.33	28.71	7.585	8.633	0.3920	98.65
Indoor workplace	Nucl.	3.701	1.993	0.895	6.231	26.79	39.60
	Acc.	6.335	3.411	0.467	1.768	9.35	21.33
Mine	Acc.	3.150	1.696	0.4087	2.164	9.95	17.37

[a] 'Unatt.' = unattached mode, 'Nucl.' = nucleation mode, and 'Acc.' = accumulation mode.
[b] The degree of precision of the values is given for computational purposes and does not reflect the certainty with which they are known.

Inhalation of radon gas

(679) The biokinetic model for radon gas described in Section 12.4.3.2 is used to calculate doses from inhalation of radon gas. Although, radon is chemically inert, the radon gas can be absorbed into the blood stream from the lung, where it moves rapidly within the body. Radon gas absorbed to pulmonary blood is distributed in arterial blood to tissues and is then transferred from tissue to venous blood. The gas is carried in the venous blood to pulmonary blood where some of it exhaled, while the rest returns to artery blood and the cycle continues. The transfer rates between blood and tissues depend on blood flow rates, tissue and blood volumes, and on the relative solubility of radon in tissues and blood represented by tissue-to-blood partition coefficients. Transfer rate constants from lung air-to-blood, blood-to-tissues, tissues-to-blood, and blood-to-lung air are given in Section 12.4.3.2. Equilibrium concentrations in tissues, blood and lung air are reached for continuous chronic exposure to a given radon concentration. The time it takes for ^{222}Rn to reach equilibrium concentrations in tissues varies from several minutes to a few days depending upon their blood supply and the tissue-to-blood partition coefficient. However, the value of the equilibrium concentration of ^{222}Rn in a tissue can be calculated directly from the ambient concentration, the tissue-to-blood partition coefficient, and the blood-to-air partition coefficient.

(680) The equivalent doses to regions of the respiratory tract arising from the radon gas within the airways are calculated assuming that the radon gas within the airways equilibrates rapidly with the ambient concentration (Section 12.4.3.2). However, Absorbed Fractions (AFs) have not been calculated for a source consisting of the volume of the gas within the airways. Because there is little loss of energy within the air in the airways, the AFs for non-penetrating radiations can be approximated by assuming the activity in the volume of the gas within the airways can be replaced by the same activity uniformly deposited on the surface ('surface' in ET_1 and ET_2, 'mucus layers' in BB and bb, 'AI' in AI). For this purpose, Table

12-10 gives reference volumes of the respiratory tract regions for reference worker (ICRP, 1994).

Table 12-10. Reference volumes of respiratory tract regions for calculating doses from gases within the airways for Reference worker [a,b]

Region	Volume (m^3)
ET1	2.500E-06
ET2	3.375E-05
BB	3.901E-05
bb	6.265E-05
AI	3.720E-03

[a] Values given to four significant figures for precision in calculation.
[b] Taken from ICRP *Publication 68*; Table A.1, page 23. In ICRP *Publication 68* there is a transcript error for the reference volume of bb; this has been corrected here.

12.4.2. Ingestion

(681) Radon is soluble in water, and if high concentrations are found in drinking water this may be an important source of exposure. Volunteer experiments have shown that radon is readily absorbed from the alimentary tract into blood (Section 12.4.3.1). Kursheed (2000) assumed that ingested radon follow the pathway of water out of the stomach and is absorbed to blood only via the small intestine. However, important issues relating to the dosimetry of radon gas from ingestion relate to the residence time of radon in the stomach and the extent to which radon diffuses into the wall of the stomach. As a result of different assumptions regarding these two issues published estimates of dose to the stomach wall per unit intake of ingested ^{222}Rn vary by a factor of about 200 (von Döbeln and Lindell, 1964; Hursh et al., 1965; Suomela and Kahlos, 1972; Crawford-Brown, 1989; Brown and Hess, 1992; Harley and Robbins, 1994; Sharma et al., 1996; NAS, 1999; Khursheed, 2000). The rate of removal of radon from the stomach assumed in the dose calculations has varied from a few minutes to a few hours. The following approaches illustrate the variety of assumptions that have been made concerning accumulation of radon in the stomach wall. Hursh and coworkers (1965) assumed that the stomach wall contains radon at the same concentration as occurs in the stomach contents at all times following ingestion and that the radon is uniformly distributed in the wall. A committee of the U.S. National Academy of Sciences (NAS, 1999) assumed that the time-integrated concentration of radon at the depth of the radiosensitive cells in the stomach wall is 30% of the time-integrated concentration in the contents. Harley and Robbins (1994) assumed on the basis of the structure and secretory properties of the stomach wall that any radon that diffuses from the contents into the wall does not reach a depth at which the alpha emissions could irradiate the stem cells. Kursheed (2000) pointed out that improved fits were obtained between the model predictions and the data of Hursh et al. (1965) if the site of absorption into blood is only the small intestine.

(682) The biokinetic model for radon gas following ingestion assumed in this report is described in Section 12.4.3.2. In this model it is assumed that radon gas does not diffuse from Stomach contents to Stomach wall but that radon is absorbed to blood via the small intestine.

12.4.3. Biokinetic model for radon gas

12.4.3.1. Summary of the database

(683) The noble gases are chemically inert but are absorbed to blood from the lungs or gastrointestinal tract and retained in systemic tissues to some extent, due in part to their solubility in blood and tissues. Much of the gas that reaches blood is cleared by the lungs in a single pass, but a portion is partitioned between the blood and tissues. The rate of transfer of the gas from blood to a tissue can be estimated on the basis of the fraction of cardiac output received by the tissue. The rate of return from a tissue to blood depends on both the blood perfusion rate and the relative solubility of the gas in blood and the tissue, represented by a gas-specific tissue-to-blood partition coefficient. The partition coefficient for two compartments is defined as the ratio of the concentrations of the gas in the compartments at equilibrium. Some experimentally determined tissue-to-blood partition coefficients for the noble gases radon, xenon, and krypton are listed in Table 12-11. Half-times for the buildup or washout of these gases are a few minutes for tissues with a rich blood supply and low to moderate partition coefficients but are much greater for fatty tissues because of their poor blood supply and high tissue-to-blood partition coefficient. Within an hour after acute intake or the start of continuous intake of radon, xenon, or krypton, body fat contains most of the systemic content.

Table 12-11. Partition coefficients for radon, xenon, and krypton[a]

Organ/blood	Radon	Xenon	Krypton
Fat	11	8-10	5.50
Muscle	0.36	0.70	1.09
Bone	0.36[b]	0.41	
Kidney	0.66	0.65	~1.0
Liver	0.71	0.70	1.1
Brain	0.72	0.75	~1.0
Heart	0.51		
Testes	0.43		0.85
GI tract	0.70[b]	0.80	
Lung	0.70[b]	0.70	
Spleen	0.70[b]		
Skin	0.36[b]		
Blood/air	0.43	0.18	0.06

[a] Nussbaum and Hursh, 1957; Conn, 1961; Kirk et al., 1975; Bell and Leach, 1982; Peterman and Perkins, 1988; NAS, 1999; Khursheed, 2000.

[b] Values assigned by Bernard and Snyder (1975).

(684) The partition coefficients for radon given in Table 12-11 were derived from radon solubility coefficients quoted by Bernard and Snyder (1975), which in most cases were based on in vivo rat data of Nussbaum and Hursh (1957). The values for bone and skin were based on radon solubility in physiological saline.

Ingestion of ^{222}Rn by volunteers

(685) A number of investigators have used measurements of ^{222}Rn in breath or external measurements of the short-lived chain member ^{214}Bi to estimate whole-body retention of radon in human subjects after ingestion of elevated levels in water or other material

(Vaternahm, 1922; Fernau and Smereker, 1933; Meyer, 1937; Anderson and Nilsson, 1964; von Dobeln and Lindell, 1964; Hursh et al., 1965; Suomela and Kahlos, 1972; Gosink et al., 1990; Brown and Hess, 1992). Reported rates of loss of radon from the body are variable, probably due in large part to differences in experimental conditions such as the timing of intake of radon relative to meals, the level of physical activity of the subjects after intake of radon, and the length of the observation period. Retention half-times in the range 30-70 min have been reported in several studies involving relatively short observation periods. Multiple retention components with half-times varying from a few minutes to several hours have been determined in some studies with relatively long observation periods.

(686) Hursh et al. (1965) used periodic measurements of breath to estimate total-body retention of ^{222}Rn following acute intake of ^{222}Rn in water by each of two subjects on two occasions. In three of the four individual experiments the radon was ingested two hours after a normal light breakfast. In the fourth experiment the radon was ingested 10 min after a heavy breakfast. Retention was longer in the fourth experiment than in the first three, presumably due to a longer retention time in the full stomach. Retention of radon in the subjects with empty stomach could be expressed as a sum of three exponential terms corresponding to half-times of about 11 min (61%), 19 min (34%), and 3 h (5%). Retention in the subject with full stomach could be expressed as a sum of three exponential terms corresponding to half-times of about 12 min (39%), 58 min (51%), and 5 h (10%). Hursh and coworkers interpreted the data as indicating that much of the ingested radon mixes with the stomach contents, diffuses out through the stomach walls into the splanchnic venous blood system, and passes through the liver and up into the right heart to the lung where much of the absorbed amount is rapidly lost in the expired air. Uptake of radon by systemic tissues was assumed to be divided mainly among three pools: liver, fat, and other. Fat was estimated to contain only a small portion of the systemic burden in the early minutes after intake but a major portion after 2-3 h.

(687) Suomela and Kahlos (1972) used external measurements of the ^{222}Rn chain member ^{214}Bi to estimate whole-body retention of radon in 10 healthy adult male subjects who ingested radon-rich water as a single intake. A single exponential function with biological half-time in the range 30-50 min was found to describe the elimination of ^{222}Rn reasonably well in some cases over observation periods of up to about 6 h. In other cases a second component with half-time 1.5-2 h was evident within the 6-h observation period. Suomela and Kahlos compared their findings with results from earlier studies of retention of ^{222}Rn ingested in water by human subjects (Andersson and Nilsson, 1964; Döbeln and Lindell, 1964; unpublished study by Mays, 1972; Hursh et al., 1965). The retention curves determined by Hursh et al. (1965) for a full and empty stomach bounded the retention curves determined in other studies over the first 6 h after intake.

(688) Gosink et al. (1990) used breath measurements to estimate the rate of loss of ^{222}Rn from a 51-year-old male subject (1.96 m, 112 kg) in different experiments involving consumption of water with a moderately high natural concentration of ^{222}Rn. During a period of relatively high physical activity the subject eliminated virtually all the ingested ^{222}Rn during the first 4 h after intake. During mild activity the biological half-time was 45-65 min. For a sedentary or sleeping period a biological half-time was estimated as 11.2 h for a substantial portion of the ingested radon. For the sedentary case the subject exhaled <3% of ingested ^{222}Rn per hour after the first hour.

(689) Brown and Hess (1992) conducted 41 tests on 38 human subjects, ages 9-85 y, to measure elimination rates of ^{222}Rn in expired breath following acute intake of ^{222}Rn in drinking water. The levels of physical activity of the subjects ranged from inactive to marathon level. The percentage of elimination of ^{222}Rn from the body during the first 30 min

after intake ranged from 12 to 68%. The elimination rate showed a moderate correlation with the time passed since eating. Estimated retention half-times ranged from 17 to 400 min.

Inhalation of inert gases by volunteers

(690) In a series of experiments, Harley and coworkers (1951, 1994) studied the retention of inhaled radon by subjects following exposures to constant, elevated concentrations of radon in air for periods up to 8.5 h. Measurements of ^{222}Rn in periodic breath samples after the end of exposure were used to infer the rate of loss of ^{222}Rn from the body. About the same peak total-body content of radon (~850 Bq) was estimated following exposure for 8.5 h at an air concentration of 25.9 Bq/L and for 7 h at 22.2 Bq/L, suggesting that saturation may have been approached. Following both the 7-h and 8.5-h exposures the activity remaining in the body at the end of exposure showed five distinct components of retention. In the more detailed study involving exposure for 8.5 h, about 8% of the total expired radon was removed with a half-time of 23 s, 9% with a half-time of 4.5 min, 18% with a half-time of 41 min, 32% with a half-time of 3.4 h, and 33% with a half-time of 18 h. These retention half-times are broadly similar to half-times observed in human subjects following inhalation of xenon or krypton (Susskind et al., 1977; Ellis et al., 1977).

(691) Susskind et al. (1977) used in vivo measurements to estimate retention of inhaled ^{127}Xe in 12 human subjects. Five components of retention with average biological half-times of 21.7 s, 3.05 min, 0.40 h, 2.71 h, and 10.4 h were determined. The half-time of the slowest component of clearance ranged from 7.4 h to 17.0 h and correlated highly with total-body fat as a percent of body weight (Figure 12-5). The mean half-time (+/- standard deviation) of this component for five subjects with body fat representing less than one-third of total-body weight was 8.4 +/- 0.7 h. On average the slowest component of clearance represented approximately 13% of the retained activity, excluding the rapid clearance represented by the retention components with half-times 21.7 s and 3.05 min.

(692) Ellis et al. (1977) studied total-body retention of ^{79}Kr in 16 subjects by whole-body external counting following a 10-min or 30-min inhalation period. The retention data were resolved into a five-component exponential curve with average half-times of 21.5 s, 4.74 min, 0.33 h, 2.41 h, and 7.0 h. The last three retention components represented on average 61.7%, 29.6%, and 9.4% of the retained activity, excluding the rapid clearance represented by the retention components with half-times of 21.5 s and 4.74 min. The half-time of the long-term component ranged from about 4.2 h to 9.6 h and correlated significantly with the estimated percentage of total body fat (Figure 12-5). The mean half-time (+/- standard deviation) for six subjects with body fat representing less than one-third of body weight was 5.5 +/- 0.7 h.

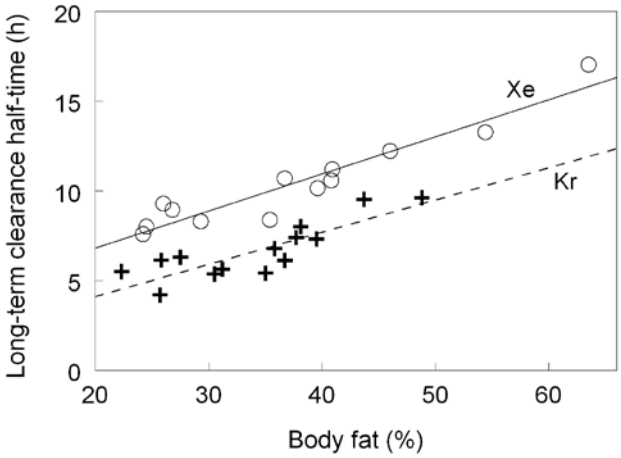

Figure 12-5. Relation of body fat (% of body weight) and long-term clearance half-time of inhaled Xe or Kr. Data on Xe from Susskind et al. (1977). Data on Kr from Ellis et al. (1977).

Loss of noble gas from the body other than through exhalation

(693) Loss of radon or other noble gases through skin, urine, or faeces is expected to be small compared with loss through exhalation. Limited measurements of radon or its progeny in urine following ingestion of high levels of radon in drinking water indicated that urinary excretion did not represent a significant mode of loss (Hursh et al., 1965; Gosink et al., 1990). On the basis of a mechanistic biokinetic model of inert gases in the human body, Peterman and Perkins (1988) estimated that loss of xenon through the skin amounts to about 0.6% of its loss through the lungs.

12.4.3.2. Biokinetic model for systemic radon

(694) Compartmental biokinetic models have been developed for a number of inert gases, including radon, on the basis of physical laws governing transfer of a non-reactive and soluble gas between materials (Kety, 1951; Bell and Leach, 1982; Peterman and Perkins, 1988; Sharma et al., 1997; NAS 1999; Khursheed 2000; Yu and Kim, 2004). The biokinetics of such a gas is assumed to be determined by the blood-to-air partition coefficient and the blood perfusion rates, tissue-to-blood partition coefficients, and volumes of the tissues represented by the compartments of the model. As depicted in the standard modelling approach, an inert gas entering the lung air after inhalation or entering pulmonary blood after absorption from the gastrointestinal contents equilibrates instantly between lung air and pulmonary blood, with relative concentrations in the two pools determined by their volumes and blood-to-air partition coefficients. Gas retained in the pulmonary blood is distributed in arterial blood to tissues in proportion to the percentage of cardiac output received by each tissue. The transfer rate from a tissue to venous blood is determined by the blood perfusion rate, the volume of the compartment, and the tissue-to-blood partition coefficient. The gas is carried in the venous blood to the pulmonary blood. The cycle continues until the body burden is depleted due to exchange between pulmonary blood and lung air and loss from the body in expired air.

(695) For a given tissue, a set of differential equations can be derived by considerations of mass balance and equilibrium. As an example, consider a systemic tissue that receives blood only from the arterial pool and leaves in the venous stream. The rate of change of the activity

of inert gas in a tissue is F_i ($C_{B\text{-}A} - C_{B\text{-}V}$), where F_i is the blood flow rate (L min^{-1}) through the systemic tissue, $C_{B\text{-}A}$ is the activity gas concentration (Bq L^{-1}) in non-pulmonary arterial blood and $C_{B\text{-}V}$ is the activity gas concentration in non-pulmonary venous blood. In the standard modeling approach it is assumed that the perfusion of the gas in tissues is instantaneous, allowing equilibrium to achieve between venous blood and tissue such that $C_{B\text{-}V} = C_i/P_i$, where C_i is the activity concentration of the gas in the tissue and P_i is the tissue-blood partition coefficient. Thus, for a given organ the differential equation describing the rate of change of the activity of gas Q_i in a tissue, is:

$$\frac{dQ_i}{dt} = F_i\left(C_{B-A} - \frac{C_i}{P_i}\right) - \lambda_r Q_i \qquad \textbf{(Eq. 12-5)}$$

where λ_r is the radioactive rate constant for the inert gas. To express the above equation in terms of activity of gas, Q, it can be rewritten as:

$$\frac{dQ_i}{dt} = \frac{F_i}{V_{B-A}} Q_{B-A} - \frac{F_i}{P_i V_i} Q_i - \lambda_r Q_i \qquad \textbf{(Eq. 12-6)}$$

where $V_{B\text{-}A}$ is the volume of the non-pulmonary arterial blood and V_i is the volume of the tissue. So the transfer rate constant from arterial blood to tissue is $F_i/V_{B\text{-}A}$ and the transfer rate constant from tissue to venous blood is $F_i/(P_iV_i)$. The blood flow rate (F_i) through a systemic tissue, *i* is given by the product of the cardiac output and the fraction of the cardiac output going to tissue, *i* (ICRP, 2002). The volume of a systemic tissue is calculated from its mass and specific gravity.

(696) The biokinetic model for radon used in this report is based largely on the theoretical considerations summarised above but includes some empirical features and simplifications. As a first step, a detailed biokinetic model involving three blood compartments representing pulmonary, arterial, and venous blood and 20 compartments representing systemic tissues was developed for radon on the basis of these theoretical considerations. That model was then simplified for use in this report by dividing blood into two rather than three compartments, pooling several tissue compartments with broadly similar time-dependent radon concentrations, and replacing the theoretical model of instantaneous exchange of radon between lung air and pulmonary blood with a first-order system consistent with the ICRP's general modelling approach for inhaled activity. Also, the theoretical considerations as applied to bone were replaced by a dosimetrically cautious bone model involving exchange of radon between blood and bone surfaces.

(697) The structure of the model used in this report is shown in Figure 12-6. Baseline transfer coefficients are listed in Table 12-12.

(698) Blood is divided into arterial and venous blood (Blood-A and Blood-V, respectively). These compartments are assumed to represent 27%, and 73%, respectively, of the total blood volume based on reference sizes of blood pools summarized in ICRP *Publication 89* (2002). The reference total blood volume is 5.3 L in the adult male and 3.9 L in the adult female (ICRP, 2002).

(699) Fat is represented as two compartments with equal volumes but different blood perfusion rates as a way of depicting the two phases of relatively long-term retention (several hours) observed in human subjects following inhalation of radon or radioisotopes of xenon or

krypton. The blood perfusion rate of Fat 1 is assumed to be four times higher than that of Fat 2, which implies that the removal half-time from Fat 2 is four times greater than the removal half-time from Fat 1.

(700) For continuous inhalation of radon, it is assumed that the activity concentration in respiratory tract (RT) air rapidly reaches equilibrium with the activity concentration in the environment, C_{env}. The transfer rate from RT air to environment, λ is assumed to be 2600 d^{-1} (half-time 23 s). The removal half-time of 23 s is based on observed half-times for the rapid phase of exhalation of radon, xenon, or krypton by human subjects immediately after a period of continuous inhalation (Harley et al., 1951; Susskind et al., 1977; Ellis et al., 1977). The removal half-time does depend on breathing rate but for dosimetry purposes it is assumed to be constant. The rate at which activity enters the RT air space is assumed to be $\lambda\ C_{env}\ V_{RT\text{-}air}$ (Bq d^{-1}), where $V_{RT\text{-}air}$ is the average volume of the RT air space (3.858 L for male, ICRP, 1994). In order to use the model to calculate the number of disintegrations in the respiratory tract (RT) air space, this rate is partitioned to each region of the HRTM according to its fractional volume (Table 12-10).

(701) It is assumed that the radon in RT air diffuses to Blood-A rapidly, allowing equilibrium to achieve between Blood-A and RT air such that $C_{B\text{-}A} = C_{RT\text{-}air}\ P_{b\text{-}air}$, where $P_{b\text{-}air}$ is the blood to air partition coefficient, (Table 12-11) and $C_{RT\text{-}air}$ is the activity concentration in RT air. On the basis of mass balance and equilibrium the rate of change of activity in the RT air is given by:

$$\frac{dQ_{RT-air}}{dt} = \lambda C_{env} V_{RT-air} - \lambda Q_{RT-air} + F\ \left(C_{B-V} - C_{RT-air} P_{b-air}\right) - \lambda_r Q_{RT-air} \qquad \textbf{(Eq. 12-7)}$$

where F (L min^{-1}) is the cardiac output. To express the above equation in terms of activity of gas, Q, it can be rewritten as:

$$\frac{dQ_{RT-air}}{dt} = \lambda C_{env} V_{RT-air} - \lambda Q_{RT-air} + \frac{F}{V_{B-V}} Q_{B-V} - \frac{F\ P_{b-air}}{V_{RT-air}} Q_{RT-air} - \lambda_r Q_{RT-air} \qquad \textbf{(Eq. 12-8)}$$

(702) From equation (4.8) it can be seen that the transfer rate constant from Blood-V to RT-air is $F/V_{B\text{-}V}$ and the transfer rate constant from RT-air to Blood-A is $F\ P_{b\text{-}air}/V_{RT\text{-}air}$.

(703) Radon ingested in drinking water or other material is transferred from Stomach contents to Small intestine contents at a material-specific stomach emptying rate. The default transfer coefficient from Stomach contents to Small intestine contents are reference values for total diet (ICRP, 2002, 2006): 20.57 d^{-1} for adult males and 15.16 d^{-1} for adult females.

(704) Radon is transferred from Small intestine contents to Liver at the rate 5994 d^{-1}. This corresponds to an absorption fraction of 0.999 based on a reference transfer coefficient of 6 d^{-1} from the small intestine contents to the right colon contents (ICRP, 2002, 2006).

(705) With exceptions described later, derivations of transfer coefficients between systemic compartments are based on the blood flow rates, compartment volumes, and tissue-to-blood partition coefficients listed in Table 12-13. The blood flow rates are taken from ICRP *Publication 89* (2002). The compartment volumes are based on reference tissue masses for adults (ICRP, 2002), together with the following specific gravities based on information summarized in ICRP *Publication 23* (1975) and *Publication 89* (2002): fat, 0.92; red marrow, 1.0; all other soft tissues, 1.04. The tissue-to-blood partition coefficients are based on estimates listed in Table 12-11. A rounded partition coefficient of 0.4 for Other was based on

the estimate of 0.36 for skeletal muscle, which represents much of the volume of Other. The specific gravity and tissue-to-blood partition coefficient for red marrow are based on reference masses of active marrow and total marrow given in ICRP *Publication 89* (2002) and the assumptions that red marrow is composed of active marrow plus fat and represents half the mass of total marrow. In other words, the specific gravity and tissue-to-blood partition coefficient for red marrow were calculated assuming red bone marrow is composed of about 40% fat (ICRP, 1975).

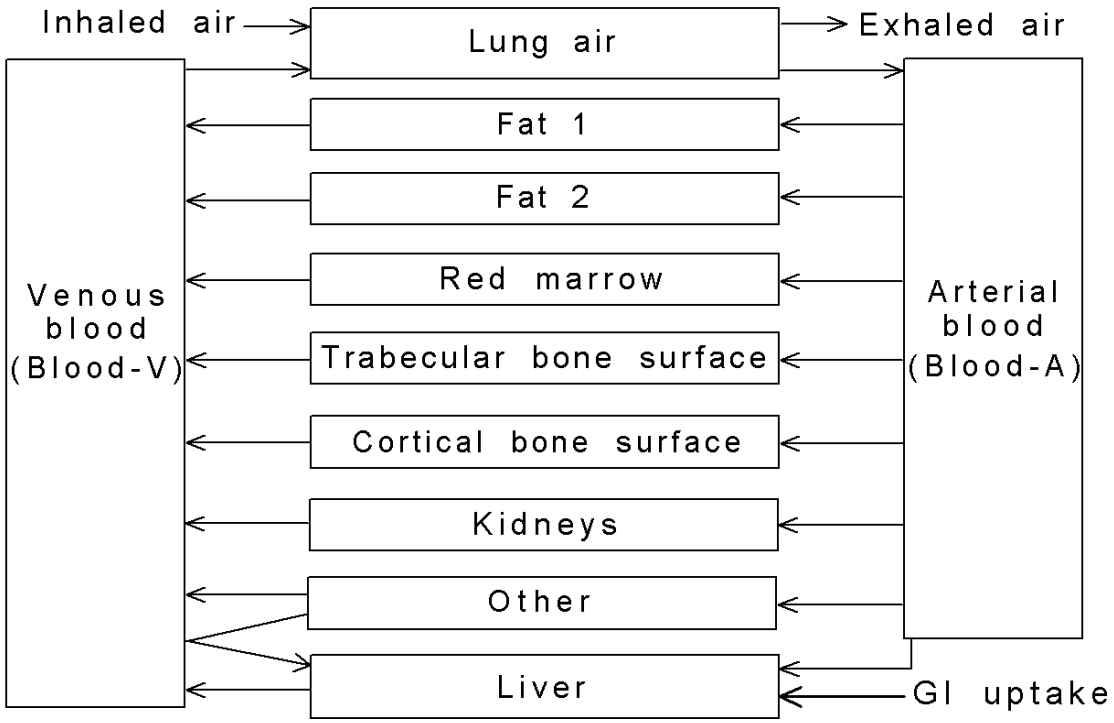

Figure 12-6. Structure of the biokinetic model for systemic radon

(706) The derivation of transfer coefficients is illustrated for the reference adult male. Radon is cleared from Blood-A at the rate 6.5 L min^{-1} x 1440 min d^{-1} / 1.431 L = 6541 d^{-1}, where 1.431 L = 0.27 x 5.3 L is the volume of Blood-A. Radon is transferred from Blood-V to lung air at the rate 6.5 L min^{-1} x 1440 min d^{-1} / 3.869 L = 2419 d^{-1}, where 3.869 L = 0.73 x 5.3 L is the volume of Blood-V. The transfer coefficient from Blood-A to Kidneys, for example, is 0.19 x 6541 d^{-1} = 1243 d^{-1}, where 0.19 is the fraction of cardiac output received by the kidneys in the reference adult male. The transfer coefficient from Kidneys to Blood-V is 1440 min d^{-1} x 0.19 x 6.5 L min^{-1} / (0.298 L x 0.7) = 8525 d^{-1}, where 0.298 L is the volume of the kidneys and 0.7 is the kidneys-to-blood partition coefficient.

(707) Tissue compartments other than Liver receive radon only from Blood-A. In addition to Blood-A, Liver receives a portion of outflow from Other, representing radon that leaves the splanchnic tissues, as well as radon absorbed from the alimentary tract following its

ingestion. Activity leaving tissue compartments is assigned to Blood-V, except that the portion of outflow from Other representing outflow from splanchnic tissues is assigned to Liver. The fraction of outflow from Other assigned to Liver is 19/(19+46) = 19/65, based on estimated blood flows of 19% and 46%, respectively, of cardiac output through splanchnic and non-splanchnic tissues within Other.

(708) As a dosimetrically cautious approach, radon depositing in bone is assigned to bone surface. Transfer coefficients from Blood-A to Trabecular bone surface and Cortical bone surface are based on the reference blood flow rates of 0.9% and 0.6% to trabecular and cortical bone, respectively expressed as a % of cardiac output (ICRP, 2002). Transfer coefficients from these bone surface compartments to Blood-V were not derived by the same methods as applied to other tissue compartments due to difficulties in determining meaningful volumes and partition coefficients for bone surface. Rather, the transfer coefficient from each bone surface compartment to Blood-V is taken as 100 d^{-1}, which is the value estimated in ICRP *Publication 67* for radon produced on bone surface by radioactive decay of radium isotopes.

(709) Figure 12-7 compares model predictions derived from the baseline parameter values in Table 12-12 with observations of total-body retention in adult male subjects exposed acutely to elevated levels of ^{222}Rn in drinking water. Two sets of predictions are shown, one based on relatively fast transfer of radon from the stomach to the small intestine ($T_{1/2}$ = 15 min), and one based on relatively slow transfer ($T_{1/2}$ = 1 h). The predicted total-body retention pattern based on a half-time of 15 min in the stomach is reasonably similar to the retention pattern observed for subjects who ingested radon two hours after a light breakfast (Hursh et al., 1965). The predicted retention pattern based on a half-time of 1 h in the stomach is reasonably similar to the pattern observed by the same investigators for a subject who ingested radon 10 min after a heavy breakfast.

(710) Figure 12-8 compares model predictions with observations of the rate of exhalation of ^{222}Rn by an adult male following exposure to a constant, elevated concentration (25.9 Bq/L) of radon in a closed room for 8.5 h (Harley et al., 1951). The rate of exhalation of radon at the end of the 8.5-h exposure was 132 Bq/min. This indicates a radon inhalation rate of 132 Bq/min and is consistent with the breathing rate (B_r) of 5 L air/min estimated by Harley and coworkers. A transfer rate λ of 2600 d^{-1} (1.8 min^{-1}) from RT air to environment is estimated from the fastest component (half-time of 23 s) of the exhalation rate of radon determined in the human study. The estimated volume of lung air involved in the radon exchange with blood is $V_{L\text{-}air}=B_r/\lambda=2.8$ L. Based on a lung air volume of 2.8 L, the transfer coefficient from RT air to Blood-A is $F\ P_{b\text{-}air}/\ V_{L\text{-}air}$ = 1437 d^{-1}, where F is cardiac output in blood volumes per day and $P_{b\text{-}air}$ is the blood-to-air partition coefficient. This case-specific estimate of the transfer coefficient from RT-air to Blood-A was used in the model simulation rather than the baseline value 1043 d^{-1} listed in Table 12-12. All other model parameters were assigned their baseline values. A radon inhalation rate of 190,000 Bq/d (132 Bq/min) was assumed.

12.4.3.3. Treatment of radioactive progeny

(711) The radon isotopes addressed in this report as parent radionuclides are ^{222}Rn, ^{220}Rn, and ^{219}Rn. Their radioactive progeny considered in the determination of dose coefficients are isotopes of lead, polonium, bismuth, and thallium. Radioisotopes of mercury, astatine, and radon also appear in the ^{222}Rn chain, but their contributions to tissue doses following intake of ^{222}Rn are negligible.

(712) The systemic models for lead, polonium, bismuth, and thallium as radon progeny are based on their characteristic systemic models as modified for their application as lead progeny (see the section on lead). The following additions are made to their models as lead progeny: lead, polonium, bismuth, or thallium produced in respiratory tract air (RT-air) is assumed to be exhaled at the rate 1000 d^{-1}; polonium produced in a blood compartment for which its biokinetics is not defined is assumed to transfer to the central blood compartment of the polonium model at the rate 1000 d^{-1}; lead produced in a soft-tissue compartment for which its biokinetics is not defined is assumed to transfer to the central blood compartment of the lead model at the rate 7.39 d^{-1} (the highest transfer rate from tissues to blood in the lead model); and bismuth produced in a soft-tissue compartment for which its biokinetics is not defined is assumed to transfer to the central blood compartment of the bismuth model at the rate 66.542 d^{-1} (the highest transfer rate from tissues to blood in the bismuth model).

Table 12-12. Transfer coefficients in the systemic model for radon

		Transfer coefficient (d^{-1})	
From	To	Adult male	Adult female
Environment	RT air	(a)	(a)
RT air	Environment	2600	2600
Blood-A	Fat 1	261.6	548.6
Blood-A	Fat 2	65.41	137.2
Blood-A	Kidneys	1243	1372
Blood-A	Liver	425.2	524.4
Blood-A	Trab bone surface	58.9	72.6
Blood-A	Cort bone surface	39.3	48.4
Blood-A	Red marrow	196.2	242.0
Blood-A	Other	4252	5123
Fat 1	Blood-V	4.48	5.68
Fat 2	Blood-V	1.12	1.42
Kidneys	Blood-V	8525	7803
Liver	Blood-V	1970	586.1
Trab bone surface	Blood-V	100	100
Cort bone surface	Blood-V	100	100
Red marrow	Blood-V	34.1	42.0
Other	Blood-V	260.3	302.7
Other	Liver	107.5	149.8
Blood-V	RT air	2419	2984
RT air	Blood-A	1043	1043
Stomach Content	SI Content	20.57	15.16
SI Content	Liver	5994	5994

(a) The rate at which activity enters the respiratory tract (RT) air space is assumed to be $\lambda\ C_{env}\ V_{RT\text{-}air}$ (Bq d^{-1}), where λ is the transfer coefficient from environment to RT air space (2600 d^{-1}), C_{env} is the concentration of radon in the environment (Bq L^{-1}), and $V_{RT\text{-}air}$ (L) is the average volume of the respiratory tract air space (3.858 L for male, ICRP, 1994). This rate is partitioned to each region of the HRTM according to its fractional volume (Table 12-10).

9275

Table 12-13. Reference blood flow rates, compartment volumes, and blood:tissue partition coefficients used to derive transfer coefficients.

Compartment	Blood flow rate[a] (% of cardiac output)		Volume[b] (L)		Blood:Tissue partition coefficient[c]
	Male	Female	Male	Female	
Fat 1	4	6.8	7.61	9.24	11
Fat 2	1	1.7	7.61	9.24	11
Kidneys	19	17	0.298	0.264	0.7
Liver			1.73	1.35	0.7
Arterial	6.5	6.5			
Total	25.5	27			
Trabecular bone surface	0.9[d]	0.9[d]	--	--	--
Cortical bone surface	0.6[d]	0.6[d]	--	--	--
Red marrow	3	3	1.83	1.35	4.5
Other	65	63.5	41.35	29.80	0.4
Blood	--	--	5.3	3.9	--
Blood-A	--	--	1.431	1.053	--
Blood-V	--	--	3.869	2.847	--
Cardiac output (L min^{-1})	6.5	5.9	--	--	--

[a] From ICRP *Publication 89* (2002).
[b] Based on reference tissue masses given in ICRP *Publication 89* (2002) and specific gravities listed in the text.
[c] See Table 12-11 and discussions in text of partition coefficients for Red marrow and Other.
[d] See discussion in text.

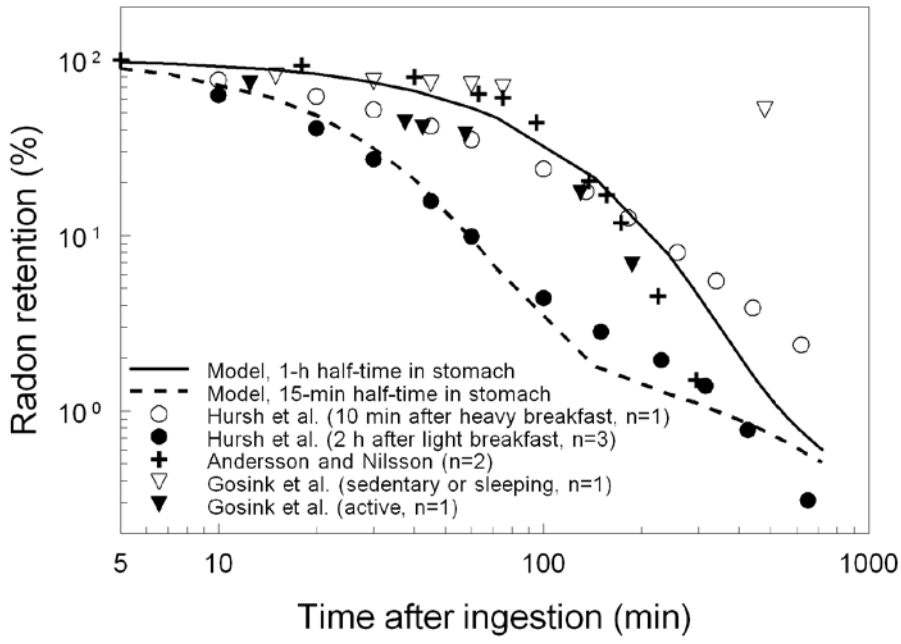

9276
9277 **Figure 12-7. Comparison of model predictions and observations of total-body retention of**
9278 **radon following its ingestion in drinking water**

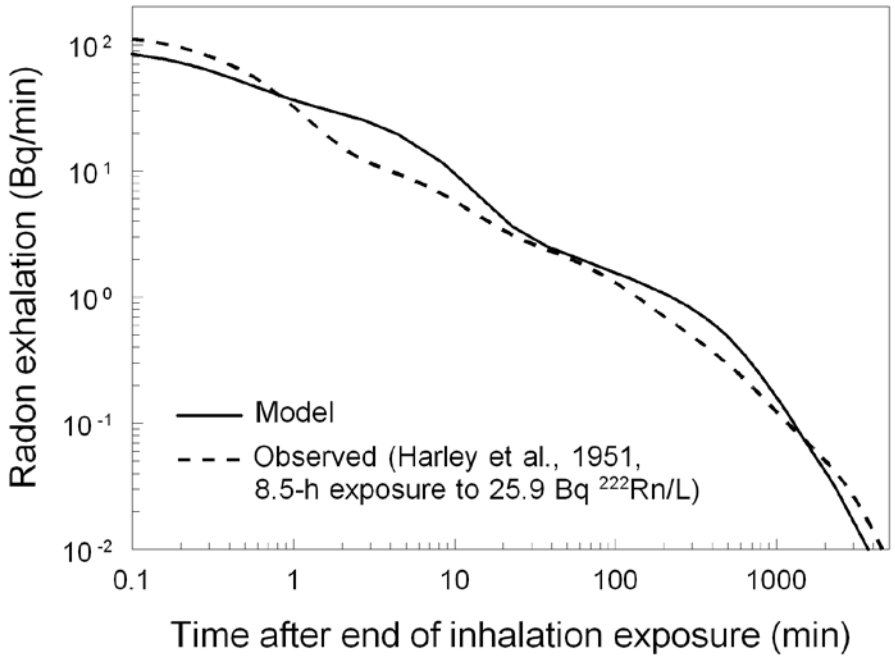

Figure 12-8. Comparison of model predictions and observations of the exhalation rate of radon following continuous exposure to a high concentration of radon in air for 8.5 hours

12.5. Dosimetry

12.5.1. Calculation of dose conversion factor arising from the inhalation of radon progeny.

(713) The effective doses arising from the inhalation of the short-lived radon progeny are calculated in terms of Sv per PAE exposure, (i.e. in units of Sv per J h m^{-3} or in units of Sv per WLM). The intakes of activity of the radon progeny, I_i (in Bq) for a subject exposed to 1 WLM are given by Eq. 12-9. :

$$I_i = C_i \; B t \qquad \textbf{(Eq. 12-9)}$$

where C_i (in Bq m^{-3}) is the activity concentration of the decay product *i* corresponding to a radon progeny mixture of 1 WL, B (in m^3 h^{-1}) is the average breathing rate and *t* (in h) is the exposure period of 170 h.

(714) In practice, the activity concentrations of radon progeny will vary with particular environmental conditions of exposure. However, Marsh and Birchall (2000) showed that for intakes of short-lived ^{222}Rn progeny, the equivalent dose to the lung per WLM is relative insensitive to F (i.e. to the activity ratios of the radon progeny). This is because the WL is defined in terms of the PAEC and because the fraction of alpha energy absorbed by the target tissues in the lung is similar for ^{218}Po and ^{214}Po per disintegration. Based on measurements of the activity concentration of ^{218}Po, ^{214}Pb, and ^{214}Bi carried out indoors (Reineking and Porstendörfer, 1990; Kojima and Abe, 1988) the following activity ratios of ^{222}Rn progeny are assumed for dosimetry:

Unattached: ^{218}Po : ^{214}Pb : ^{214}Bi = 1 : 0.1 : 0

Attached: ^{218}Po : ^{214}Pb : ^{214}Bi = 1 : 0.75 : 0.6

(715) For thoron (^{220}Rn) progeny, the activity ratios assumed are the ones proposed by the committee of the National Research Council (NRC, 1991); activity ratios of ^{212}Pb : ^{212}Bi of 1.0:0 and 1.0:0.25 were assumed for the unattached and attached modes respectively. Because ^{216}Po contributes less than 0.001% to the PAEC, it can be ignored for dosimetry purposes.

(716) The activity concentrations of radon progeny that correspond to a radon progeny mixture of 1 WL for either the unattached or the attached progeny can be calculated by assuming the above activity ratios and by applying Eq. 12-1. These values are given in Table 12-14.

Table 12-14. Activity concentrations, Ci of a mixture of short-lived radon (^{222}Rn) or thoron (^{220}Rn) progeny that gives 1 WL for either the unattached or the attached progeny

Nuclide	Activity concentration, Bq m^{-3}	
	Unattached	Attached[a]
Radon (^{222}Rn) progeny[b]:		
^{218}Po	2.41 10^{4}	5.21 10^{3}
^{214}Pb	2.41 10^{3}	3.91 10^{3}
^{214}Bi	0	3.13 10^{3}
Thoron (^{220}Rn) progeny[c]:		
^{212}Pb	3.01 10^{2}	2.94 10^{2}
^{212}Bi	0	7.36 10^{1}

[a] For simplicity, it is assumed that the activity ratios of the radon progeny for each of the attached modes are the same.

[b] Activity ratios of ^{218}Po : ^{214}Pb : ^{214}Bi of 1.0:0.1:0 and 1.0:0.75:0.60 are assumed for the unattached and attached modes respectively.

[c] Activity ratios of ^{212}Pb : ^{212}Bi of 1.0:0 and 1.0:0.25 are assumed for the unattached and attached modes respectively.

(717) For the average breathing rate, B, the ICRP default value for a reference worker of 1.2 m^{3} h^{-1} is assumed for all exposure scenarios (ICRP, 1994). Regarding exposures in a mine, this value is similar to the average breathing rate of 1.3 m^{-3} h^{-1} estimated from a study of 620 underground miners carrying out heavy work in a gold mine in South Africa (ICRP *Publication 66*, para. B76, ICRP, 1994). It is also consistent with the breathing rates derived by Ruzer et al. (1995) for personnel (0.9 ± 0.4 m^{-3} h^{-1}), assistant drillers (1.1 ± 0.5 m^{-3} h^{-1}) and drillers (1.4 ± 0.5 m^{-3} h^{-1}) working underground in a metal mine in Tadjikistan.

(718) The effective dose per WLM arising from the inhalation of the short-lived radon progeny is calculated by combining the intakes, I_i (derived from Eq. 12-9) with the effective dose coefficients (Sv per Bq) for the individual radon progeny. The following equation is applied:

$$E\ (Sv\ \ per\ \ WLM) = \sum_{i=1}^{3} \sum_{j} I_{j,i}\ \ f_{pj}\ \ E_{j,i} \qquad \textbf{(Eq. 12-10)}$$

where index *j* corresponds to the aerosol mode of the activity size distribution; j=1, 2, and 3 for the unattached, nucleation and accumulation modes respectively. The f_{pj} value is the

fraction of the PAEC associated with mode *j*. The index *i* corresponds to the inhaled decay product; in the case of ^{222}Rn progeny, *i* =1, 2, and 3, which corresponds to ^{218}Po, ^{214}Pb and ^{214}Bi respectively. The symbol $E_{j,i}$ is the effective dose coefficient (in Sv per Bq) for decay product *i* with an activity size distribution for mode *j*. In the case of ^{222}Rn progeny, the intakes $I_{j,1}$, $I_{j,2}$ and $I_{j,3}$ are the intakes of ^{218}Po, ^{214}Pb and ^{214}Bi respectively, which result in an exposure of 1 WLM for either the unattached progeny (j=1) or for the attached progeny (j=2,3).

(719) Table 12-15 gives calculated values of the effective dose per unit exposure for indoor workplaces and mines in terms of PAE exposure (mSv per WLM or mSv per mJ h m^{-3}) and in terms of radon gas exposure (Sv per Bq h m^{-3}). For exposures to ^{222}Rn progeny, the units Sv per WLM can be converted to Sv per Bq h m^{-3} of ^{222}Rn gas exposure by multiplying by (F/6.37 10^5 WLM per Bq h m^{-3}). For exposures to thoron (^{220}Rn) the units Sv per WLM can be converted to Sv per Bq h m^{-3} of EEC of ^{220}Rn by multiply by (1/4.68 10^4 WLM per Bq h m^{-3} of ECC of ^{220}Rn).

(720) The committed equivalent doses to organs arising from the inhalation of ^{222}Rn progeny and from ^{220}Rn progeny are given in the accompanying electronic disk.

Table12-15. Calculated values of effective doses per unit exposure to radon progeny for indoor workplaces and mines. Dose from inhaling ^{222}Rn or ^{220}Rn gas is excluded.

Place	Unattached fraction[a], f_p	F[b]	Effective dose per unit exposure[c]		
			mSv per WLM	mSv per mJ h m^{-3}	Sv per Bq h m^{-3}
Radon (^{222}Rn) progeny:					
Indoor workplace	0.1	0.4	21	5.9	$1.3\ 10^{-8}$
Mine	0.01	0.2	11	3.0	-
Thoron (^{220}Rn) progeny:					
Indoor workplace	0.02	-			[d]
Mine	0.005	-			[d]

[a] f_p = unattached fraction in terms of the potential alpha energy concentration (PAEC).
[b] F = equilibrium factor.
[c] 1 WLM = (6.37 10^5/F) Bq h m^{-3}; 1 WLM = 3.54 mJ h m^{-3}
[d] In terms of Sv per Bq h m^{-3} of EEC of ^{220}Rn

Inhalation of short-lived decay products of actinon ^{219}Rn

(721) Because actinon (^{219}Rn) has a very short half-life (4s) it is less able than radon (^{222}Rn; half-life 3.8 d) or thoron (^{220}Rn; half-life 56 s) to escape from the point of where it is formed. As a consequence, exposures to ^{219}Rn and its progeny in the workplace are low and can generally be ignored. However, there may be some unusual situations where it is appropriate to calculate doses from inhaling ^{219}Rn and its progeny. For example, Crawford (1980) reported that radiological surveys at former uranium ore processing facilities showed that there were a number of sites with high levels of airborne ^{219}Rn decay products. Further investigation showed that these sites had been used for the storage of a precipitate, which was formed during processing pitchblende ore and found to have a relatively high content of ^{227}Ac and a low content of ^{226}Ra. In such cases, for radiation protection purposes, it is normally sufficient to control exposures on the basis of the intake of ^{211}Pb. This is because the PAE per unit activity of ^{211}Pb is about 15 times higher or more than for other actinon progeny. However, for completeness, in the accompanying electronic disk dose coefficients (Sv Bq^{-1}) are given for both ^{211}Pb and ^{211}Bi. To our knowledge there have been no activity size

measurements of actinon progeny. Dose coefficients have been calculated separately for the unattached, nucleation and accumulation modes with size characteristics (AMTD, σ_g) equal to that assumed for ^{222}Rn progeny in indoor work places (Table 12-4 and Table 12-6), because the half-life of ^{211}Pb (36 minutes) is much closer to that of the ^{222}Rn decay product ^{214}Pb (27 minutes) than that of the ^{220}Rn decay product ^{212}Pb (11 h). For these modes the regional deposition in the respiratory tract are given in Table 12-7.

12.5.2. Inhalation of radon gas

(722) The equilibrium effective dose rate for continuous chronic exposure to unit concentration of ^{222}Rn is ? Sv per Bq h m^{-3}. The corresponding equilibrium equivalent dose rates to organs are given in the accompanying electronic disk. The equilibrium effective dose can be expressed in terms of potential alpha energy exposure for a given F value; for F=0.4 the effective dose arising from the inhalation of ^{222}Rn gas alone is ? mSv per WLM (? Sv per J h m^{-3}) and for F=0.2 effective dose is ? mSv per WLM (? Sv per J h m^{-3}). Comparing these numbers with the effective doses arising from the inhalation of radon progeny shows that the dose from inhaling radon gas is only a small component; less than 10%.

(Data will be provided in the final version of this document.)

12.5.3. Ingestion of radon

(723) Equivalent doses to organs per unit activity of ^{222}Rn ingested are given in the accompanying electronic disk. The effective dose per unit intake of ingested ^{222}Rn is ? Sv per Bq.

(Data will be provided in the final version of this document.)

12.5.4. Use of dose coefficients for radon-222 and radon-220 and their short lived decay products

(724) For the radioisotopes of most elements, dose coefficients are given in this report series for different exposure conditions (mainly different chemical forms) with the advice that in situations where more specific data are available, and estimated doses warrant more detailed consideration, site specific dose coefficients may be calculated.

(725) Radioisotopes of radon represent a special case since there is substantial direct evidence of lung cancer induction resulting from inhalation of ^{222}Rn and its radioactive progeny (ICRP, 2000). Epidemiological data clearly show that tobacco smoke is a more powerful lung carcinogen that accounts for many more lung cancer cases than radon inhalation (ICRP, 2010). Background lung cancer rates in different populations will differ according to smoking prevalence and will change with time as habits change. In transporting risk estimates for radiation induced cancer across populations and calculating overall and relative detriment values, ICRP does not take account of smoking statistics. Thus, it should be recognised that ICRP nominal risk coefficients and dose coefficients apply to a mixed population of smokers and non-smokers.

(726) Dose coefficients are given in this publication for the inhalation of radon isotopes and their progeny in two situations of exposure:- Indoor Workplaces and Mines. The value for Indoor Workplaces should also be applied to other situations of exposure, including those in tourist caves, water supply facilities and spas. The task group calculated similar dose coefficients for indoor workplaces, tourist caves, water supply facilities and spas. In

circumstances of occupational exposure to radon and progeny which require the application of the system of protection and the calculation of worker doses, it is envisaged that the appropriate reference dose coefficient will be applied. Employers may also wish to make assessments of risk to their workers. It would then be appropriate to take account of the specific conditions of exposure (aerosol characteristics, equivalent factors, etc) in the calculation of lung dose, and of the individual characteristics of workers, including smoking habits, in estimating the associated risks.

References

AGIR (Advisory Group on Ionising Radiation) (2009). Radon and public health. *Doc HPA*, RCE-11, ISBN 978-0-85951-644-0. Available at www.hpa.org.uk.

Andersson, I. O.; Nilsson, I. (1964). Exposure following ingestion of water containing radon-222. In: IAEA Symposium on Assessment of Radioactivity in Man: Vienna, IAEA, pp. 317-326.

Becker, H. K., Reineking, A., Scheibel, H. G. and Porstendörfer, J. (1984). Radon daughter activity size distributions. Radiat. Prot. Dosim., 7(1-4), 147-150.

Bell, C. M. J.; Leach, M. O. (1982). A compartmental model for the investigation of the influence of physiological factors on the rate of Xe-133 and Ar-37 from the body. Phys. Med. Biol. 27:1105–1117.

Bernard, S. R.; Snyder, W. S. (1975). Metabolic models for estimation of internal radiation exposure received by human subjects from inhalation of noble gases. ORNL Report 5046, pp. 197-204.

Bigu, J. and Kirk, B. (1980). Determination of the unattached radon daughter fractions in some uranium mines. Presented at the workshop on attachment of radon daughters, measurements techniques and related topics, October 30, 1980, University of Toronto. (Report available from CANMET, P.O. Box 100, Elliot Lake, Ontario, Canada).

Boulaud, D., & Chouard, J. C. (1992). Submicron sized aerosol and radon progeny measurements in a uranium mine. Radiat. Prot. Dosim., 45(1-4), 91-94.

Brown, W. L.; Hess, C. T. (1992). Measurement of the biotransfer and time constant of radon from ingested water by human breath analysis. Health Phys. 62:162-170.

Busgin, A., van der Vooren, A., & Phillips, C. R. (1981). Measurements of the total and radioactive aerosol size distribution in a Canadian uranium mine. American Industrial Hygiene Association Journal, 42, 310-314.

Butterweck, G., Porstendörfer, J., Reineking A. and Kesten J. (1992). Unattached Fraction and the Aerosol Size Distribution of the Radon Progeny in a Natural Cave and Mine Atmospheres. Radiat. Prot. Dosim., 45(1-4), 167-170.

Cavallo, (1997). Understanding aerosols in uranium mines in order to compute the lung dose for uranium miners. J. of Aerosol Sci., 28, Suppl. 1, S435- S436.

Cavallo, (2000). Understanding mine aerosols for radon risk assessment. J. Environ. Radioactivity 51, 99-119.

Cavallo, A. J. (1998). Reanalysis of 1973 activity-weight particle size distribution measurements in active US uranium mines. Aerosol Science and Technology, 29, 31-38.

Cavallo, A., Hutter, A., Shebell, P. (1999). Radon progeny unattached fraction in an atmosphere far from radioactive equilibrium. Health Physics, 76 (5), pp. 532-536.

Charles, M. W. (2004). The skin in radiological protection ─ recent advances and residual unresolved issues. Radiat. Prot. Dos., 109(4), 323-330.

Chen, R. T., Cheng, Y.-S., Hopke, P. K., Tung, C.-J. and Pourprix, M. (1997). Electrical mobility and size distribution of aged 212Pb nanometer carriers in nitrogen gas. J. Aeerosol Sci. Vol. 28(8), 1465-1477.

Chen C.-J., Liu C.-C., Lin Y.-M. (1998). Measurement of equilibrium factor and unattached fraction of radon progeny in Kaohsiung, Taiwan. Appl. Radiat. Issot. 49(12) 1613-1618.

Cheng, Y.-S., Chen, T.-R., Wasiolek, P. T., Van Engen, A. (1997). Radon and radon progeny in the Carlsbad caverns. Aerosol Science and Technology, 26, 74-92.

Cheng, Y.-S., Chen, R. T., Yeh, H. C., Bigu, J, Holub, R., Tu, K., Knutson, E. O. and Falk, R. (2000). Intercomparison of activity size distribution of thoron progeny and a mixture of radon and thoron progeny. J. Environ. Radioactivity 51, 59-78.

Conn, H. L. (1961). Equilibrium distribution of radioxenon in tissue: Xenon-hemoglobin association curve. J. Appl. Physiol. 16:153-157.

Cooper, J. A., Jackson, P. O., Langford, J.C., Petersen, M. R., and Stuart, B. O. (1973). Characteristics of attached radon-222 daughters under both laboratory and field conditions with particular emphasis on the underground uranium mine environment. Report to the U.S. Bureau of Mines; Contract Report H0220029, Battelle Pacific Northwest Laboratories.

Correia, J.; Weise, S.; Callahan, R.; Strauss, H. (1987). The Kinetics of ingested Rn-222 in humans determined from measurements with Xe-133 (Boston: Massachusetts General Hospital).

Crawford, D. J. (1980). Radiological characteristics of ^{219}Rn. Health Physics, 39, 449-461.

Crawford-Brown, D. J. (1989). The biokinetics and dosimetry of radon-222 in the human body following ingestion of groundwater. Environ. Geochem. Health 11:10-17.

Dundulis, W. P.; Bell, W. J.; Keene, B. E.; Dostie, P. J. (1984). Radon-222 in the gastrointestinal tract: A proposed modification of the ICRP Publication 30 model. Health Phys. 47:243–252.

Eatough, J. P., Henshaw, D. L. (1992). Radon and thoron associated dose to the basal layer of the skin. Phys. Med. Biol. 37, 955-67.

El-Hussein, A. (2005). A study on natural radiation exposure in different realistic living rooms. Journal of Environmental Radioactivity 79 355-367.

El-Hussein, A., Ahmed, A. and Mohammed, A. (1998). Radiation dose to the Human Respiratory Tract from inhalation of radon-222 and its progeny. Appl. Radiat. Isot. Vol. 49, No. 7, pp. 783-790.

Ellis, K. J.; Cohn, S. H.; Susskind, H.; Atkins, H. L. (1977). Kinetics of inhaled krypton in man. Health Phys. 33:515-522.

Fernau, A.; Smereker, H. (1933). Concerning the remaining radioactive substance in organisms due to radon emanation. Strahlentherapie 46:365-373.

George, A. C., Hinchliffe, L., and Sladowski, R. (1975). Size distribution of radon daughters in uranium mine atmospheres. American Industrial Hygeine Association Journal, 36, 484.

Geranios, A. Nikolopoulos, D., Louizi, A, et al., 2004. Multiple radon survey in spa of Loutra Edipsou (Greece). Radiat. Prot. Dosim. 112(2), 251-258.

Gosink, T. A.; Baskaran, M.; Holleman D. F. (1990). Radon in the human body from drinking water. Health Phys. 59: 919-924.

Harley, J. H.; Jetter, E.; Nelson, N. (1951). Elimination of radon from the body. New York, NY: U.S. Atomic Energy Commission, New York Operations Office; Report No. 3. Reissued as Health and Safety Report, HASL-32 (1958). New York: U.S. Atomic Energy Commission. New York Operations Office. Also see: Harley, J. H.; Jetter, E.; Nelson, N. (1994). Elimination of radon from the body. Environmental International 20:573-584.

Harley, N. H., Robbins E. S. (1992). ^{222}Rn alpha dose to organs other than the lung. Radiat. Prot. Dosim. 45, 617-622.

Harley, N. H.; Robbins, E. S. (1994). A biokinetic model for 222Rn gas distribution and alpha dose in humans following ingestion. Environ. Int. 20:605-610.

Hattori, T. and Ishida, K. (1994). Equilibrium factor and unattached fraction of radon in nuclear power plants. Radiat. Prot. Dosim., **55**(3), 191-197.

Hattori, T. Ichiji, T., and Ishida, K. (1995). Behaviour of radon and its progeny in a Japanese office. Radiat. Prot. Dosim., **62**(3), 151-155.

Hopke, P., Jenson, B., Li, C. S., Montassier, N. Wassiolek, P., Cavallo, A. J., Gatsby K. Scocolow, R. H. and James, A. C. (1995). Assessment of the exposure to and dose from radon decay products in normally occupied homes. Environ. Sci. Technol. 29: 1359-1364 (1995).

Huet, C. Tymen, G., Boulaud, D., (2001a). Long-term measurements of equilibrium factor and unattached fraction of short-lived radon decay products in dwelling – comparison with Praddo Model. Aerosol Science and Technology 35, 553-563.

Huet, C. Tymen, G., Boulaud, D., (2001b). Size distribution, equilibrium ratio and unattached fraction of radon decay products under typical indoor domestic conditions. The Science of the Total Environment, 272, 97-103.

Hursh, J. B.; Morken, A.; Thomas, P. D.; Lovaas, A. (1965). The fate of radon ingested by man. Health Phys. 11:465-476.

ICRP (1975). International Commission on Radiological Protection, Report of the Task Group on Reference Man, ICRP Publication 23. Oxford: Pergamon Press.

ICRP (1993). *Protection against radon-222 at home and at work*. ICRP Publication 65. Annals of the ICRP 23(2), Pergamon Press, Oxford.

ICRP (1994a). *Human respiratory tract model for radiological protection.* ICRP Publication 66. Annals of the ICRP, 24(1-3), Pergamon Press, Oxford.

ICRP (1994b). Dose coefficients for intakes of radionuclides by workers. ICRP Publication 68. Annals of the ICRP, 24(4), Pergamon Press, Oxford.

ICRP (2002). International Commission on Radiological Protection. Basic anatomical and physiological data for use in radiological protection: Reference values. ICRP Pub. 89. Ann. ICRP, 32(3-4). Oxford: Pergamon Press.

ICRP (2006). International Commission on Radiological Protection. Human Alimentary Tract Model for Radiological Protection. ICRP Publication 100. Ann. ICRP, 26(1-2). Oxford: Pergamon Press.

Iimoto, T. (2000). Time variation of the radon equilibrium factor in reinforced concrete dwelling. Radiat. Prot. Dosim., 92(4), 319-321

Iimoto, T., Kosako, T. and Sugiura, N. (2001). Measurements of summer radon and its progeny concentrations along with environmental gamma dose rates in Taiwan. Journal of Environmental Radioactivity, 57 (1), 57-66

Iyogi, T., Ueda, S., Hisamatsu, S., Kondo, K., Sakurai, N. and Inaba, J. Radon concentrations in indoor occupational environments in Aomori Prefecture, Japan. (2003). Journal of Environmental Radioactivity 67, 91-108.

James, A C, Strong, J C, Cliff, K D, and Stranden. (1988). The significance of equilibrium and attachment in radon daughter dosimetry. Radiat. Prot. Dosim., 24, 451-455.

Kahn, A., Bandi, F., Gleasur, R.W., Phillips, C.R., & Duport, P. (1987). Underground measurements of aerosol and activity distributions of radon and thoron progeny. P.K. Hopke, Radon and its decay products Washington, DC: (p. 219), The American Chemical Society.

Kety, S. G. (1951). The theory and applications of the exchange of inert gases at lung and tissue. Pharmacol. Rev. 3:1-41.

Khursheed, A. (2000). Doses to systemic tissues from radon gas. Radiat. Prot. Dosim. 88:171-181.

Kirk, W. P.; Parish, P. W; Morken, D. A. (1975); *In vivo solubility of Kr-85 in guinea pig tissues.* Health Physics 28, 249-261 (1975).

Knutson, E. O., and George, A. C. (1990). Reanalysis of the data on the particle size distribution of radon progeny in uranium mines. Proceedings of the 29th life sciences symposium, indoor radon and lung cancer: reality or myth? October 16-19, Part 1. Edited by F. T. Cross. Pacific Northwest Laboratories Richland, WA (p. 149).

Kojima, H. and Abe, S. (1988). Measurements of the total and unattached radon daughters in a house. Radiat. Prot. Dosim., 24(1/4), 241- 244.

Kranrod, C., Tokonami, S., Ishikawa, T., Sorimachi, A., Janik, M., Shigaki, R., Furukawa, M., Chanyotha, S. and Chankow, N. (2009). Mitgation of the effective dose of radon decay products through the use of an air cleaner in a dwelling in Okinawa, Japan. Applied Radiation and Isotopes 67(6), 1127-1132.

Labidi, S., Al-Azmi, D., Mahjoubi, H., Ben Salah, R. (2010). Radon in elementary schools in Tunisia. Radiopotection, 45(2), 209-217.

Leggett, R. W.; Williams, L. R. (1995). A proposed blood circulation model for reference man. Health Phys. 69:187-201.

Lettner, H., Hubmer, A.K., Rolle, R., Steinhäusler, F. (1996). Occupational exposure to radon in treatment facilities of the radon-spa Badgastein, Austria. Environ. Intern 22 (1), S399-S407.

Maged, A. F. (2006). Radon concentrations in elementary schools in Kuwait. Health Phys. 90(3), 258-262.

Marsh J W and Birchall A (1998). Sensitivity analysis of the weighted equivalent lung dose per unit exposure from radon progeny. NRPB-M929 Health Protection Agency, Chilton, Didcot, Oxon, OX11 ORQ, UK.

Marsh, J. W., Bessa, Y., Birchall, A., Blanchardon, E., Hofmann, W., Nosske. D. and L. Tomasek (2008). *Dosimetric models used in the Alpha-Risk project to quantify exposure of uranium miners to radon gas and its progeny*. Radiat. Prot. Dosim., 130(1) 101-106.

Marsh, J.W., Birchall, A., Butterweck, G., Dorrian, M.-D., Huet, C., Ortega, X., Reineking, A., Tymen, G., Schuler, Ch., Vargas, A., Vezzu, G. and Wendt. J. (2002). *Uncertainty analysis of the weighted equivalent lung dose per unit exposure to radon progeny in the home*. Radiat. Prot. Dosim., 102(3), 229-248.

Meyer, S. (1937). Physical foundations of radon cures. Strahlentherapie. 58:656-663.

Misdaq, M. A. and Amghar, A. (2005). Radon and thoron emanation from various marble materials: impact on the workers. Radiation Measurements 39, 421-430.

Misdaq, M. A. and Flata, K. (2003). The influence of the cigarette smoke pollution and ventilation rate on alpha activities per unit volume due to radon and its progeny. Journal of Environmental Radioactivity, 67, 207-218.

Mohammed, A. (1999). Activity size distributions of short-lived radon progeny in indoor air. Radiat. Prot. Dosim., 86(2), 139-145.

Mohammed, A. (2005). Study on radon and radon progeny in some living rooms. Radiat. Prot. Dosim., 117(4), 402-407.

NAS (1999). Risk assessment of radon in drinking water. National Research Council. National Academy of Sciences. Washington, D.C.: National Academy Press.

National Research Council, (1991). Comparative Dosimetry of Radon in Mines and Homes. National Academy Press (Washington, DC). ISBN 0-309-04484-7 (1991).

Nickell, W.B. (2005). Skelton J Breast fat and fallacies: more than 100 years of anatomical fantasy. Journal of Human Lactation, 21(2):126-130

NRC (National Research Council), (1999). Health effects of exposure to radon. Washinghton, DC: National Academy Press; BEIR VI, ISBN: 0-309-05645-4.

Nussbaum, E. and Hursh, J. B. (1958). Radon solubility in fatty acids and triglycerides. J Phys. Chem. 62, 81-84.

Nussbaum, E.; Hursh, J. B. (1957). Radon solubility in rat tissues. Science 125:552.

Olfert, J. S., Symonds, J. P. R. and Collings, N. (2007). The effective density and fractal dimensions of particles emitted from a light-duty vehicle with a diesel oxidation catalyst. Aerosol Science **38** 69-82.

Park, K., Cao, F., Kittelson, D. B. and McMurry, P. H. (2003). Relationship between particle mass and mobility for diesel exhaust particles. Environ. Sci. Technol. **37**, 577-583.

Peterman, B. F.; Perkins C. J. (1988). Dynamics of radioactive chemically inert gases in the human body. Radiat. Prot. Dosim. 22:5–12.

Porstendörfer, J (1994). Tutorial/Review: Properties and behaviour of radon and thoron and their decay products in the air. J. Aerosol Sci., 25(2), 219-263.

Porstendörfer, J (1996). Radon: Measurements related to dose. Environmental International, Vol. 22, Suppl. 1, pp. S563-S583.

Porstendörfer, J (2001). Physical parameters and dose factors of the radon and thoron decay products. Radiat. Prot. Dosim., 94(4), 365-373.

Porstendörfer, J., Pagelkopf, P. and Gründel, M. (2005). Fraction of the positive ^{218}Po and ^{214}Pb

clusters in indoor air. Radiat. Prot. Dosim., 113(3), 242-351.
Porstendörfer, J. and Reineking, A. (1999). Radon: Characteristics in air and dose conversion factors. Health Phys. 76(3), 300-305.
Ramachandran, T.V. and Subba Ramu, M.C. (1994). Variation of equilibrium factor F between radon and its short-lived decay products in an indoor atmosphere. Nuclear Geophysics, 8 (5), pp. 499-503.
Ramsay, D. T. ; Kent, J. C.; Hartmann, R. A. ; Hartmann, P. E. (2005). Anatomy of the lactating human breast redefined with ultrasound imaging. J. Anat. 206:525–534.
Reichelt, A., Lehmann, K.H., Reineking, A., Porstendörfer, J., Schwedt, J. and Streil, T. (2000). Radon at workplaces. In: Proc. IRPA-10, Hiroshima, Japan, 14-19 May (2000).
Reineking, A., Butterweck, G., Kesten, J. and Porstendörfer J (1992). Thoron gas concentration and aerosol characteristics of thoron decay products. Radiat. Prot. Dosim., 45(1/4), 353-356.
Reineking A, Knutson E A, George A C, Solomon S B, Kesten J, Butterweck G and Porstendorfer J (1994). Size distribution of unattached and aerosol-attached short-lived radon decay products: some results of intercomparison measurements. Radiat. Prot. Dosim., 56(1-4), 113-118.
Reineking, A and Porstendörfer, J. (1990). "Unattached" fraction of short-lived Rn decay products in indoor and outdoor environments: an improved single-screen method and results. Health Physics, 58(6) 715-727.
Richardson, R. B.; Eatough, J. P.; Henshaw, D. L. (1991). Dose to red bone marrow from natural radon and thoron exposure. Br. J. Radiol. 64:608-624.
Rosvenská, K., Thinová, L., Ždímal, V. (2008). Assessment of the dose from radon and its decay products in the Bozkov dolomite cave. Radiat. Prot. Dosim., 130(1), 34-37.
Ruzer, L. S., Nero A.V. and Harley N. H. (1995). *Assessment of lung deposition and breathing rate of underground miners in Tadijikistan*. Radiat. Prot. Dosim., 58, 261-268.
Sainz, C., Quidós, L. S., Fuente, I., Nicolás, J., Quidós, L. (2007). Analysis of the main factors affecting the evaluation of the radon dose in workplaces: The case of the tourist caves. Journal of Hazardous Materials, 145, 368-371.
Sharma, N.; Hess, C. T.; Thrall, K. D. (1997). A compartment model of water radon contamination in the human body. Health Phys. 72:261-268.
Sinclair, D., Countess, R. J. and Hoopes, G. S (1974). Effect of relative humidity on the size of atmospheric aerosols particles. Atmos. Environ., 8, 1111-1117.
Solomon, S. B., Cooper, M. B., O'Brien, R. S., Wilkinson, L., (1992). Radon exposure in a limestone cave. Radiat. Prot. Dosim., 45(1-4), 171-174.
Solomon, S. B., Wilks, M., O'Brien, R. S. and Ganakas, G. (1993). Particle sizing of airborne radioactivity field measurements at Olympic Dam. Report ARL/TR113. ISSN 0157-1400. Australian Radiation Laboratory, Lower Plenty Road, Yallambie VIC 3085.
Solomon, S. B., O'Brien, R. S., Wilks, M. and James, A. C. (1994) Application of the ICRP's new respiratory tract model to an underground uranium mine. Radiat. Prot. Dosim., **53**(1-4), 261-268.
Soto, J., Gómez, J. (1999). Occupational doses from radon in Spanish spas. Health Phys. 76(4), 398-401.
Suomela, M.; Kahlos, H. (1972). Studies on the elimination rate and the radiation exposure following ingestion of Rn-222 rich water. Health Phys. 23:641-652.
Susskind, H.; Atkins, H. L.; Cohn, S. H.; Ellis, K. J.; Richards, P. (1977). Whole-body retention of radioxenon. J. Nucl. Med. 18:462-471.
Tokonami, S., Fukutsu, K., Yamada, Y., Yatabe, Y. (2005). Particle size measurement of radon decay products using MOUDI and GSA. In: High Levels of Natural Radiation and Radon Areas: Radiation Dose and Health Effects (T. Sugahara et al., eds.). International Congress Series 1276, 278-280, Elsevier.

Tokonami, S., Iimoto, T. and Kurosawa. (1996a). Continuous measurement of the equilibrium factor, F and the unattached fraction, fp of radon progeny in the environment. Environmental International, 22, Suppl. 1, S611-S616.

Tokonami, S., Matsumoto, M. Furukawa, M., Fujimoto, K., Fujitaka, K., and Kurosawa, R. (1996b). Behavior of radon and its progeny at working place. In: Proc. IRPA-9.

Trautmannsheimer, M., Schindlmeier, W., Börner, K. (2003). Radon concentration measurements and personnel exposure levels in Bavarian water supply facilities. Health Phys. 84(1), 100-110.

Tschiersch, J., Li, W. B. and Meisenberge, O. (2007) Increased indoor thoron concentrations and implication to inhalation dosimetry. Radiat. Prot. Dosim., 127(1-4), 73-78.

Tu K W and Knutson E O. (1988) Indoor radon progeny particle size distribution measurements made with two different methods. . Radiat. Prot. Dosim., 24(1/4) 251-255.

Tu K W, Knutson E O and George A C. (1991) *Indoor radon progeny aerosol size measurements in urban, surban, and rural regions.* Aerosol Science and Technolgy 15 170-178.

Vanmarcke, H., Berkvens, P. and Poffijn, A. (1989) Radon versus Rn daughters. Health Physics, 56(2), 229-231.

Vargas, A., Ortega, X. and Porta, M. (2000). Dose conversion factor for radon concentration in indoor environments using a new equation for the F-f_p correlation. Health Phys. 78(1): 80-85.

Vaternahm, T. (1922). Comparative investigation of the radon capacity of exhaled breath after drinking of radon ladened water and oil. Zschr. Phys. Diat. Ther. 26:361-364.

Vaupotič, J. (2007) Nano-size radon short-lived progeny aerosols in Slovenian kindergartens in wintertime. Chemosphere, 69 (6), 856-863.

Vaupotič, J. (2008a). Nanosize radon short-lived decay products in air of the Postojna Cave. Science of the total environment 393 27-38.

Vaupotič, J. (2008b). Levels of nanosize radon decay products in indoor air: A comparison for different environments. Coll. Antropol. 32 Suppl. 2 99-104.

Vaupotič, J. and Kobal, I (2001). Radon exposure in Slovenia spas. Radiat. Prot. Dosim. 97(3) 265-270

Vaupotič, J. and Kobal, I. (2006) Effective doses in schools based on nanosize radon progeny aerosols. Atmospheric Environment, 40 (39), 7494-7507.

Vogiannis, E. Nikolopoulos, D., Halvadakis, C. P (2004a). Contribution of 222Rn-bearing water to the occupational exposure in thermal baths. Environmental International 30, 621-629.

Vogiannis, E., Nikolopoulos, D., Loouizi, A., Halvadakis, C. P. (2004b). Radon exposure in the thermal spas of Lesvos island—Greece. Radiat. Prot. Dos., 111(1), 121-127.

Vogiannis, E., Nikolopoulos, D., Loouizi, A., Halvadakis, C. P. (2004c). Radon variations during treatment in thermal spas of Lesvos Island (Greece). J. Environ. Radioactivity., 76, 283-294.

von Döbeln, W.; Lindell, B. (1964). Some aspects of radon contamination following ingestion. Arkiv für Fysik 27:531-572.

Weingartner, E., Burtscher, H. and Baltensperger, U. (1997) Hygroscopic properties of carbon and diesel soot particles. Atmospheric Environ. 31 2311-2327.

Wilkening, M. H., Romero, V. (19781). 222Rn and atmospheric electrical parameters in the Carlsbad caverns. J. Geophys. Res. 86:9911-9916.

Wu-Tu, K., Fisenne, I. M. and Hutter, A. R. (1997). Short - and long-lived radionuclide particle size measurements in a uranium mine. Report EML-588, Environmental Measurements Laboratory, U.S. [www.eml.doe.gov/publications/reports/eml588.pdf]

Yu, D.; Kim, J. K. (2004). A physiologically based assessment of human exposure to radon released from groundwater. Chemospher 54:639-645.

Yu, K. N., Cheung, T., Guan, Z. J., Mui, B. W. N. and Ng, Y. T. (2000). ^{222}Rn, ^{220}Rn and their progeny concentrations in offices in Hong Kong. Journal of Environmental Radioactivity 48 211 – 221.

9742 Yu, K. N., Young, M. C. E. and Li, K. C. (1996). A survey of radon properties for dwellings for
9743 Hong Kong. Radiat. Prot. Dosim., 63(1) 55-62.
9744 Yu, K. N., Young, M. C. E., Stokes, M. J. and Tang, K. K. (1998). Radon properties in offices.
9745 Health Phys. 75(2) 159-164.
9746 Zhang, L. Guo, Q. and Zhuo, W. (2010). Measurement of the ^{212}Pb particle size distribution indoors.
9747 Radiat. Prot. Dosim., 141(4), 371-373.
9748

13. Radium (Z = 88)

13.1. Chemical Forms in the Workplace

(727) Radium is an alkaline earth element, which mainly occurs in oxidation states II. It is a chemical analogue of calcium. Chemical and physical forms encountered in industry include oxides, nitrates, chlorides, sulphates, and luminising residues. Radium can be found in trace amounts in uranium ores. A mixture of radium and beryllium is used as a neutron source. ^{224}Ra, ^{226}Ra and ^{228}Ra are the most common isotopes of radium. ^{223}Ra is currently under investigation for use in medicine as a treatment for bone metastases.

Table 13-1. Isotopes of radium addressed in this report

Isotope	Physical half-life	Decay mode
Ra-223	11.43 d	A
Ra-224	3.66 d	A
Ra-225	14.9 d	B-
Ra-226[a]	1600 y	A
Ra-227	42.2 m	B-
Ra-228[a]	5.75 y	B-
Ra-230	93 m	B-

[a] Data for these radionuclides are given in the printed copy of this report. Data for other radionuclides are given on accompanying electronic disk.

13.2. Routes of Intake

13.2.1. Inhalation

Absorption Types and parameter values

(728) Several studies have been reported on the behaviour of inhaled radium in man following accidental intakes, especially of the sulphate, which was used in powder form in gamma-ray sources. However, it is difficult to estimate the contribution of absorption to lung clearance in such cases, because the systemic excretion of radium is predominantly by the faecal route. Information is available from experimental studies of radium as nitrate, or in fly ash.

(729) Absorption parameter values and Types, and associated f_A values for particulate forms of radium are given in Table 13-2.

Radium nitrate ($Ra(NO_3)_2$)

(730) Following administration of $^{232}UO_2(NO_3)$ with its decay products to rats by intratracheal instillation (Ballou et al., 1986), about 3% of the ^{224}Ra present was retained in the lung after 1 day, consistent with assignment to Type F. (For further information see the uranium inhalation section.)

(731) Following administration of $Ra(NO_3)_2$ (alone or with thorium nitrate) to rats by intratracheal instillation (Moody and Stradling 1992; Moody et al., 1994), about 14% of the initial lung deposit (ILD) was retained in the lung after 6 hours and ~5% ILD after 1 or 7 days. From the results, it was assessed here that f_r was about 0.95 and s_r about 10 d^{-1}, but it was not possible to estimate s_s.

(732) Based on the results of the experiments outlined above, specific absorption parameter values for radium nitrate were estimated here to be: $f_r = 1$ and $s_r = 10$ d^{-1} (consistent with assignment to default Type F). However, although specific parameter values for radium nitrate based on *in vivo* data are available, they are not adopted here, because inhalation exposure to it is unlikely. Instead, radium nitrate is assigned to Type F. However, the data are used as the basis for the default rapid dissolution rate for radium. Hence specific parameter values for radium nitrate would be the same as default Type F radium parameter values.

Radium sulphate ($RaSO_4$)

(733) Marinelli et al. (1953) reported measurements on six people following accidental inhalation of a mixture of radium and barium sulphates, resulting from rupture of a capsule. The observed lung retention half-time of 120 d suggested that the material was relatively insoluble. Looney and Archer (1956) reported measurements on two men, also following the inhalation of a mixture of radium and barium sulphates from a damaged source. The results from both studies are difficult to interpret.

Coal fly ash

(734) Kalkwarf et al. (1984) measured the *in vitro* dissolution of radionuclides in 11 samples of coal fly ash (3–5 size fractions from three sources). Less than 0.2% of the ^{226}Ra present dissolved during the 60 days, indicating Type S behaviour.

Uranium ore dust

(735) Duport et al. (1991) measured the dissolution in simulated lung fluid of long lived radionuclides in uranium ore dust from Canadian mines. (For further information see the uranium section relating to uranium ore dust and to decay products of uranium formed in the respiratory tract). For high grade ore, measurements were made for up to 60 days. Results were presented as undissolved fractions as functions of time, and showed two components, which were expressed as Class D (rapid) and Class Y (slow) fractions. For ^{226}Ra the rapidly dissolved fraction was 0.12. HRTM parameter values fitted to the ^{210}Pb data by Marsh et al. (2011) were: $f_r = 0.11$, $s_r = 7.3$ d^{-1} and $s_s = 0.0004$ d^{-1}, indicating assignment to Type M. For ^{226}Ra, no effects of size were observed in total dissolution over 40 days for particles in size ranges 7–10, 3–7, 1–3 and <1 µm. For low grade and medium grade ores, measurements were made for 12 days, but only on samples of relatively coarse dust, the smallest fraction being <37 µm. For ^{226}Ra, rapidly dissolved fractions were lower, 0.07, indicating assignment to Type S.

Other compounds

(736) In another case of human inhalation, Toohey et al. (1984) reported a lung retention half-time of 120 d. However, the radium compound was unknown, (Ra-contaminated dust from grinding old rubber liners from ion-exchange tanks). It was considered by the authors to be insoluble, because the amount recovered in fecal excretion corresponded closely to the amount clearing from the lungs.

Decay products of radium formed in the respiratory tract

(737) The general approach to treatment of decay products formed in the respiratory tract is described in Part 1, Section 3.2.3. In summary, it is expected that generally the rate at which a particle dissociates is determined by its matrix, and hence the physico-chemical form

of the inhaled material. It is recognised that nuclei formed by alpha decay within a particle matrix may be expelled from it into the surrounding medium by recoil, but to implement this routinely would add greatly to the complexity of calculations. It is expected that the behaviour of soluble (e.g. Type F) material in the respiratory tract would depend on its elemental form, i.e. that of the decay product. Nevertheless, for simplicity, in this series of documents the absorption parameter values of the parent are, by default, applied to all members of the decay chain formed in the respiratory tract. Exceptions are made for noble gases formed as decay products, which are assumed to escape from the body directly, in addition to other routes of removal. For calculation purposes it is assumed that radon formed as a decay product within the respiratory tract escapes from the body at a rate of 100 d^{-1}, in addition to other routes of removal. (For further information see Part 1, Section 3.2.3, and the section on decay products of thorium formed in the respiratory tract.

(738) For decay schemes of radium isotopes in the natural decay series, including ^{223}Ra, ^{224}Ra, ^{226}Ra and ^{228}Ra, see the uranium and thorium sections.

(739) Studies specifically comparing the behaviour of radium with that of its decay products (lead, bismuth and thallium isotopes) are summarised here. For further information on these elements, see the lead and bismuth inhalation sections.

(740) Studies relating to the loss from the body (emanation) of radon formed in the lungs are summarised in the section on decay products of thorium formed in the respiratory tract, even though radium is its immediate predecessor. It was considered useful to have the relevant information in one place, and to avoid repetition. The most important practical application of radon emanation is measurement of exhaled ^{220}Rn to assess intakes of relatively insoluble thorium (thoron-in-breath measurements) and most studies investigating radon formed in the respiratory tract involved thorium deposited in the lungs.

(741) Ballou et al. (1986) measured lung retention and tissue distribution of ^{232}U, ^{228}Th, ^{224}Ra, ^{212}Pb, ^{212}Bi and ^{208}Tl at 24 hours after intratracheal instillation into rats of ^{232}U nitrate with its decay products. (For further information, see the uranium inhalation section.) As noted above, for ^{224}Ra, ~3% ILD was retained in the lungs at 24 hours. For the first descendant measured, ^{212}Pb, ~2.1% ILD was measured in the lungs: correcting for the physical decay of ^{212}Pb gives retention of 10% ILD at 24 hours. However, measurements of ^{212}Pb are difficult to interpret, being partly of material administered with the parent ^{224}Ra, and partly formed from its decay in the lungs. Furthermore, the ^{212}Pb measured could have been higher than that present *in vivo* because of ingrowth of ^{212}Pb between dissection and measurement. If not due to ingrowth, the greater fractional retention of lead could reflect its slower absorption than that of radium observed when administered separately.

(742) As described in the lead inhalation section, measurements have been made of the tissue distributions of ^{212}Pb and its decay products, ^{212}Bi and ^{208}Tl, following administration to rats of ^{228}Th in various chemical forms (nitrate, hydroxide, fluoride, dioxide) in equilibrium with its decay products. These included ^{224}Ra, but it was not measured. In all these studies the distributions of ^{212}Bi and ^{208}Tl were similar to each other and those of the parent ^{212}Pb. In the study of thorium nitrate (Moody et al., 1994; Moody and Stradling, 1992) a complementary study was carried out with ^{226}Ra (see radium nitrate above). For ^{212}Pb, on average 8.4% ILD was measured in the lungs at 6 hours and 1.2% ILD at 1 day (clearance was much faster than that of the ^{228}Th). Correcting for the physical decay of ^{212}Pb gives retention of 12.5% ILD at 6 hours and 5.6% ILD at one day. This is similar to that found for ^{226}Ra (see above), suggesting similar overall clearance of radium and lead over this period.

Rapid dissolution rate for radium

(743) From the results of studies with radium nitrate outlined above, the value of s_r was assessed to be about 10 d^{-1}, which is applied here to all Type F forms of radium.

Extent of binding of radium to the respiratory tract

(744) Evidence from the radium nitrate studies outlined above suggests that there is probably little binding of radium. It is therefore assumed that for radium the bound state can be neglected, i.e. $f_b = 0.0$.

Table 13-2. Absorption parameter values for inhaled and ingested radium

Inhaled particulate materials		Absorption parameter values[a] f_r	s_r (d^{-1})	s_s (d^{-1})	Absorption from the alimentary tract, f_A
Default parameter values[b,c]					
Absorption Type	Assigned forms				
F	Nitrate	1	10	–	0.2
M	All unspecified forms[d]	0.2	3	0.005	0.04
S	—	0.01	3	0.0001	0.002
Ingested materials					
All forms					0.2

[a] It is assumed that for radium the bound state can be neglected, i.e. $f_b = 0.0$. The value of s_r for Type F forms of radium (10 d^{-1}) is element-specific. The values for Types M and S (3 d^{-1}) are the general default values.

[b] Materials (e.g. radium nitrate) are generally listed here where there is sufficient information to assign to a default absorption Type, but not to give specific parameter values (see text).

[c] For inhaled material deposited in the respiratory tract and subsequent cleared by particle transport to the alimentary tract, the default f_A values for inhaled materials are applied: i.e. the (rounded) product of f_r for the absorption Type (or specific value where given) and the f_A value for ingested soluble forms of radium (0.2).

[d] Default Type M is recommended for use in the absence of specific information, i.e. if the form is unknown, or if the form is known but there is no information available on the absorption of that form from the respiratory tract.

13.2.2. Ingestion

(745) Radium is a good chemical analogue of barium and calcium, and its absorption depends on its chemical form. Factors affecting absorption of radium are various. It seems that ageing significantly decreases radium absorption by a factor of 2 to 4 compared to adults (Taylor et al., 1962), whereas fasting and low calcium intake increases its absorption (Taylor et al., 1962, Della Rosa et al., 1967).

(746) Data from balance studies reviewed by the ICRP Task Group on Alkaline Earth Metabolism in Adult Man (ICRP, 1973) indicated the fraction of radium absorbed from food or drinking water to be between 0.15 and 0.21. Results from a study of a single human volunteer who ingested a known quantity of radium suggested a higher value from 0.14 to 0.7, depending on the method of calculation (Seil et al., 1915). Normal elderly subjects ingesting mock radium dial paint containing $^{224}RaSO_4$ absorbed an average of about 0.2 (Maletskos et al., 1966, 1969).

(747) In the *Publication 30* (ICRP, 1979) an absorption value of 0.2 was adopted and that was also applied to dietary intakes in *Publication 67* (1993).

(748) An f_A of 0.2 is used in this report for all forms of radium.

13.2.3. Systemic Distribution, Retention and Excretion

13.2.3.1. Biokinetic database

(749) The alkaline earth element radium is a physiological analogue of the alkaline earth elements calcium, strontium, and barium but has different biokinetics from those elements due to discrimination by biological membranes and hydroxyapatite crystals of bone. The biokinetics of radium resembles that of barium much more closely than that of calcium or strontium.

(750) Retention and distribution of radium have been determined in a number of persons who were briefly exposed to radium isotopes (ICRP, 1973, 1993; Leggett, 1992). There is also extensive information on the biokinetics of radium in laboratory animals, particularly dogs (ICRP, 1993, Leggett, 1992). Data for human subjects and laboratory animals used in the development of the model are summarized below in the discussion of the basis for parameter values.

13.2.3.2. Biokinetic model for systemic radium

(751) The model for systemic radium applied in this report is a modification of the model adopted in ICRP *Publication 67* (1993). In the earlier version of the model the liver was represented as a single compartment, and the kidneys were not depicted explicitly but were included as part of Other soft tissues. In the present version the kidneys are also depicted explicitly, and both the liver and kidneys are modelled as two compartments representing relatively fast and relatively slow loss of radium.

(752) The structure of the present model is shown in Figure 13-1. Blood plasma (called “Blood” in Figure 13-1) is treated as a uniformly mixed pool that contains all radium in blood, exchanges activity with soft tissues and bone surfaces, and loses activity to urinary and faecal excretion pathways. Soft tissues are divided into compartments representing two phases of loss from the liver, two phases of loss from the kidneys, and three phases of loss from remaining soft tissues. Bone is divided into cortical and trabecular bone. Each of these bone types is further divided into bone surfaces and bone volume. Bone volume is viewed as consisting of two pools, one that exchanges with activity in bone surface over a period of months and a second, non-exchangeable pool from which activity is removed only by bone restructuring processes. Activity depositing in the skeleton is assigned to bone surface. Over a period of days a portion of the activity on bone surfaces moves to exchangeable bone volume and the rest returns to plasma. Activity leaving exchangeable bone volume is divided between bone surfaces and non-exchangeable bone volume. The assigned rate of removal from non-exchangeable bone volume is the reference rate of bone turnover for trabecular or cortical bone.

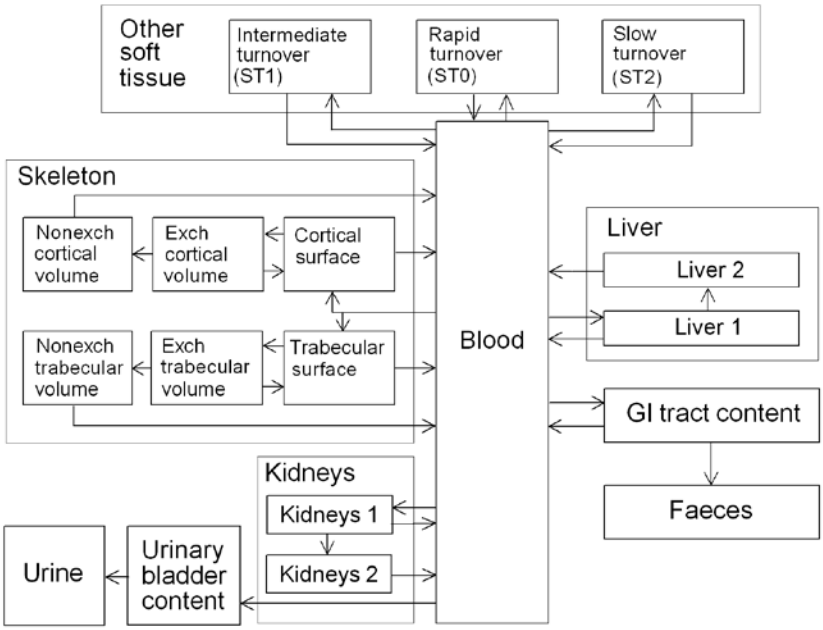

Figure 13-1. Model for systemic radium used in this report.

Parameter values

(753) Retention and distribution of radium have been determined in a number of persons who were briefly exposed to radium isotopes (Schlundt et al., 1933; Norris et al., 1955; Mays et al., 1962, 1963; Miller and Finkel, 1965; Harrison et al., 1967; ICRP, 1973; Parks et al., 1978; Harrison, 1981; Schlenker et al., 1982; Parks and Keane, 1983; Keane and Schlenker, 1987). These data can be supplemented with extensive biokinetic data for radium in beagles (Wood et al., 1970; Lloyd et al., 1976a,b, 1982, 1983a,b,c,d; Parks et al., 1978) and with human and beagle data for barium, a chemical and physiological analogue of radium. In extrapolation of data from beagles to man, consideration must be given to the relatively low rate of faecal excretion of heavy alkaline earths in beagles (Van Dilla et al. ,1958; Della Rosa et al., 1967; Cuddihy and Griffith, 1972) compared with human subjects (Harrison et al., 1967; Newton et al., 1991).

(754) Kinetic analysis of plasma disappearance curves for normal subjects intravenously injected with radioisotopes of calcium, strontium, barium, or radium indicates that these elements initially leave plasma at a rate of several hundred plasma volumes per day and equilibrate rapidly with an extravascular pool roughly three times the size of the plasma pool. Total transfer rates from plasma of 70 d^{-1} yield reasonable fits to plasma disappearance curves for radium and barium at times greater than 1-2 h after injection (Leggett, 1992). The rapid early removal from plasma is not depicted in this model.

(755) Soft tissues apparently contain a substantial portion of systemic radium for a period of days or weeks after its uptake to blood (Hursh and Lovaas, 1963; Atherton et al., 1965; Harrison et al., 1967; Hardy et al., 1969; Schlenker et al., 1982; Qiyue et al., 1988). Based on a review of data on ^{226}Ra in human soft tissues, Schlenker et al. (1982) estimated that soft-tissue retention rises to about 58% of whole body retention at 18 d after single intake and then falls steadily to 33% at 100 d and 6% at 1000 d. These estimates relied on assumptions and features of the ICRP's alkaline earth model introduced in the 1970s (ICRP, 1973). A model-free fitting procedure would yield somewhat lower estimates at early times. Harrison et al. (1967) inferred from measurements on a human subject receiving ^{223}Ra by intravenous

injection that extracellular fluids of soft tissues of man contain about one-fourth of administered radium at 24 h. In adult beagles, soft tissues contained about 62% of the total-body burden of intravenously injected ^{224}Ra at 1 h, 29% at 1 d, and 12% at 7 d (Lloyd et al., 1982). The liver and kidneys contained on average about one-third of the total ^{226}Ra in soft tissues from 7-1190 d after its intravenous administration to adult beagles (Atherton et al., 1965).

(756) Autopsy measurements of environmental ^{226}Ra in adult humans indicate that soft tissues contain 10-30% of total-body ^{226}Ra (Hursh and Lovaas, 1963; Rajewsky et al., 1965; Maletskos et al., 1969; ICRP, 1973; Qiyue et al., 1988). These estimates have been based on means or pooled samples for several subjects, which may give misleading results since measured ^{226}Ra concentrations are likely to be asymmetically distributed in the population. Using median values of ^{226}Ra to Ca ratios obtained from the literature, Schlenker et al. (1982) estimated that soft tissues contain 5.5-6% of the natural Ra-226 in the total body.

(757) In the present model, fractional deposition of radium in the fast-turnover soft-tissue compartment ST0 is determined as the balance after other deposition fractions have been assigned. As discussed below, deposition fractions of 0.25 for bone, 0.05 for intermediate-term soft tissues (ST1), 0.001 for long-term soft tissues (ST2), 0.06 for liver, 0.02 for kidneys, and 0.32 for excretion pathways are assigned to radium, leaving 0.299 for ST0. The derived transfer rate from plasma to ST0 is $0.299 \times 70\ d^{-1} = 20.93\ d^{-1}$. Based on the assumed relative amounts of radium in ST0 and plasma, the transfer rate from ST0 to plasma is set at one-third the transfer rate from plasma to ST0, or $6.98\ d^{-1}$.

(758) The biokinetics of radium in the liver is modeled on the basis of observations of the behavior of ^{224}Ra and ^{226}Ra in adult beagle dogs (Glad et al., 1960; Atherton et al., 1965; Lloyd et al., 1982). The liver consists of compartments Liver 1 and Liver 2 with fast and slow turnover, respectively. Radium transfers from plasma to Liver 1 and is removed from Liver 1 with a half-time of 1 d, with 99.7% returning to plasma and 0.3% moving to Liver 2. Radium transfers from Liver 2 to plasma with a half-time of 1 y.

(759) The biokinetics of radium in the kidneys is also based on data for adult beagle dogs (Glad et al., 1960; Atherton et al., 1965; Lloyd et al., 1982). The kidneys are divided into compartments Kidneys 1 and Kidneys 2 with fast and slow turnover, respectively. Radium transfers from plasma to Kidneys 1 and is removed from Kidneys 1 with a half-time of 8 h, with 99.7% returning to plasma and 0.3% moving to Kidneys 2. Radium transfers from Kidneys 2 to plasma with a half-time of 1 y.

(760) The removal half-time from the long-term soft-tissue compartment ST2 to plasma is assumed to be 5 y, the same as applied in the models for calcium, strontium, and barium. Fractional deposition of radium in ST2 is set to yield reasonable agreement with autopsy data for persons exposed over a short period to relatively high levels of ^{226}Ra and persons exposed over their lifetimes only to natural levels of ^{226}Ra (Schlenker et al., 1982). It is assumed that 0.1% of radium leaving plasma enters ST2. The derived transfer rate from plasma to ST2 is $0.001 \times 70\ d^{-1} = 0.07\ d^{-1}$ and from ST2 to plasma is $\ln(2)/5\ y = 0.00038\ d^{-1}$.

(761) Data from human and animal studies indicate that the rate of loss of alkaline earth elements from bone over the first few months after injection increases in the order calcium < strontium < barium < radium, and fractional long-term retention increases in the reverse order. Some element-specific parameter values are required to account for these differences, but most of the parameter values describing bone kinetics are generic, that is, the same for each of these alkaline earth elements. The basis for applying generic values is discussed in earlier sections on calcium and strontium. Essentially, kinetic analysis of whole-body retention data for humans and more direct examination of alkaline earth kinetics in laboratory

animals do not reveal distinct differences between these elements with regard to the following: early accumulation in bone as a fraction of activity reaching blood; initial division between trabecular and cortical bone; early rate of loss from bone, interpreted for purposes of the present model as transfer from bone surfaces to plasma; the fraction subject to intermediate-term retention in bone, interpreted as transfer from bone surfaces to exchangeable bone volume; and the rate of removal from bone at times remote from uptake, interpreted as removal of non-exchangeable activity due to bone resorption. The following generic parameter values are applied (see the earlier sections on calcium and strontium): fractional deposition in bone = 0.25; fractional deposition in trabecular bone = 1.25 times that on cortical bone; half-time on bone surface = 1 d, with 5/6 transferring to plasma and 1/6 to exchangeable bone volume; removal rate from non-exchangeable trabecular and cortical bone volume = 18% and 3% y^{-1}, respectively. The transfer rates for radium derived from these generic parameter values are as follows: plasma to trabecular bone surface = $(1.25/2.25) \times 0.25 \times 70\ d^{-1} = 9.72\ d^{-1}$; plasma to cortical bone surface = $(1/2.25) \times 0.25 \times 70\ d^{-1} = 7.78\ d^{-1}$; trabecular or cortical bone surface to the corresponding exchangeable bone volume compartment = $(1/6) \times \ln(2)/1\ d = 0.116\ d^{-1}$, trabecular or cortical bone surface to plasma is $(5/6) \times \ln(2)/1\ d = 0.578\ d^{-1}$; trabecular bone volume to plasma, $0.000493\ d^{-1}$; and non-exchangeable cortical bone volume to plasma, $0.0000821\ d^{-1}$.

(762) Observed differences in the behavior of alkaline earth elements in bone are accounted for by differences in the rate of removal from the exchangeable bone volume compartments and the fraction transferred from exchangeable to non-exchangeable bone volume. It is assumed, in effect, that calcium, strontium, barium, and radium are all equally likely to become temporarily incorporated in bone mineral after injection into blood but that the likelihood of reaching a non-exchangeable site in bone crystal decreases in the order calcium > strontium > barium > radium. Fractional transfers of calcium, strontium, barium, and radium from exchangeable to non-exchangeable bone volume are set at 0.6, 0.5, 0.3, and 0.2, respectively, and the balance is assumed to return to bone surfaces. The removal half-times from exchangeable bone volume are set at 100 d, 80 d, 50 d, and 30 d, respectively. These values are set to achieve reasonable consistency with whole-body retention curves for humans injected with radioisotopes of the alkaline earth elements (e.g. Harrison et al., 1967; Newton et al., 1977; Harrison, 1981; Newton et al., 1991). The assumed fractional transfers to non-exchangeable bone volume are also reasonably consistent with results of in vitro measurements. For example, under conditions approximating physiological, Neuman (1964) found that calcium incorporated into forming hydroxyapatite crystals is 65% non-exchangeable, and Stark (1968) determined discrimination factors relative to calcium of 0.93 for strontium, 0.56 for barium, and 0.32 for radium in forming crystals. Such in vitro results have varied to some extent with experimental conditions, length of aging of the crystals, and the definition of discrimination (Neuman, 1964; Stark, 1968).

(763) For radium, the above estimates of the removal half-time from exchangeable bone volume and the fractional transfers to non-exchangeable bone volume and bone surface yield the following transfer rates: exchangeable to non-exchangeable bone volume (cortical or trabecular), $0.2 \times \ln(2)/30\ d = 0.0046\ d^{-1}$; exchangeable bone volume to bone surface, $0.8 \times \ln(2)/30\ d = 0.0185\ d^{-1}$.

(764) Based on estimates from human studies (Looney et al., 1956; Schales, 1964; Harrison et al., 1967; Maletskos et al.. 1969, Newton et al., 1991), it is estimated that 32% of radium leaving plasma is deposited in excretion pathways and that the ratio of urinary to faecal excretion is 1:36. The derived transfer rate from plasma to the urinary bladder contents

is 0.606 d^{-1} and from plasma to the contents of the right colon is 21.8 d^{-1}.

(765) The transfer coefficients of the model for systemic radium in the worker are summarized in Table 13-3.

13.2.3.3. Treatment of radioactive progeny

Dosimetrically significant progeny of radium

(766) The radioactive progeny of radium isotopes addressed in this report are isotopes of radon, polonium, lead, bismuth, thallium, actinium, thorium, radium, francium, or astatine.

Radon

(767) A generic model is applied in this series of reports to radon, xenon, and krypton produced in systemic compartments by decay of a parent radionuclide. These gases are assigned the model for transfer of radon from bone to blood introduced in ICRP *Publication 67* (1993) but are assigned element-specific rates of transfer from soft tissues to blood. Specifically, radon, xenon, or krypton produced in non-exchangeable bone volume, exchangeable bone volume, or bone surface transfers to blood at the rate 0.36 d^{-1}, 1.5 d^{-1}, or 100 d^{-1}, respectively. Radon produced in a soft-tissue compartment transfers to blood with a half-time of 30 min, compared with a half-time of 20 min for xenon and 15 min for krypton. Radon, xenon, or krypton produced in blood or entering blood after its production in a systemic compartment is removed from the body (exhaled) at the rate 1000 d^{-1}, corresponding to a half-time of 1 min.

Table 13-3. Transfer coefficients for radium

From	To	Transfer coefficient (d-1)
Blood	Urinary bladder content	0.606
Blood	Right colon content	21.79
Blood	Trabecular bone surface	9.72
Blood	Cortical bone surface	7.78
Blood	ST0	20.93
Blood	ST1	3.5
Blood	ST2	0.07
Blood	Liver 1	4.2
Blood	Kidneys 1	1.4
Trabecular bone surface	Blood	0.578
Trabecular bone surface	Exch trabecular bone volume	0.116
Cortical bone surface	Blood	0.578
Cortical bone surface	Exch cortical bone volume	0.116
ST0	Blood	6.98
ST1	Blood	0.693
ST2	Blood	0.00038
Liver 1	Blood	0.691
Liver 1	Liver 2	0.00208
Liver 2	Blood	0.0019
Kidneys 1	Blood	2.073
Kidneys 1	Kidneys 2	0.00624
Kidneys 2	Blood	0.0019
Exch trabecular bone volume	Trabecular bone surface	0.0185
Exch trabecular bone volume	Nonexch trabecular bone volume	0.0046
Exch cortical bone volume	Cortical bone surface	0.0185
Exch cortical bone volume	Nonexch cortical bone volume	0.0046
Nonexch cortical bone volume	Blood	0.0000821
Nonexch trabecular bone volume	Blood	0.000493

Polonium

(768) The model for polonium produced in systemic compartments following intake of a radium isotope is a simplified version of the model applied in this report to polonium absorbed to blood following its inhalation as a parent radionuclide. It is assumed that polonium leaves the central blood compartment of the model (Plasma) at the rate 100 d^{-1} and distributes as follows: 5% to red blood cells (RBC), 3% to plasma proteins (Plasma P), 28% to Liver, 28% to Kidneys, 1.2% to Bone surface, 3.3% to Trabecular marrow, 1.1% to Cortical marrow, 1.6% to Spleen, 0.1% to Testes, 0.05% to Ovaries, 4% to a soft-tissue compartment with a relatively long retention time (ST2), and the remaining 24.65% to a soft-tissue compartment with a relatively short retention time (ST1). Activity entering Liver is equally divided between compartments Liver 1 and Liver 2. Of the 28% of outflow from Plasma depositing in Kidneys, 24% is assigned to the urinary path (Kidneys 1) and 4% is assigned to other kidney tissue (Kidneys 2). Activity entering Bone surface is equally divided between Cortical bone surface and Trabecular bone surface. Activity transfers to Plasma from each of the compartments RBC, Plasma P, ST1, Liver 2, Trabecular marrow, Cortical

marrow, Spleen, and Kidneys 2 with a half-time of 7 d. Activity transfers from Liver 1 to Small intestine content with a half-time of 5 d, from Kidneys 1 to Urinary bladder content with a half-time of 4 d, from Trabecular and Cortical bone surface to Plasma with a half-time of 30 d, from ST2 to Plasma with a half-time of 100 d, and from Testes and Ovaries to Plasma with a half-time of 50 d. Polonium produced in a soft-tissue compartment of a preceding chain member that is not identifiable with a compartment in the polonium model is assumed to move to Plasma with a half-time of 7 d. Polonium produced in a compartment of cortical or trabecular bone volume is assumed to transfer to Plasma at the reference rate of turnover of that bone type.

Lead

(769) The systemic model for lead as a progeny of radium is based on the characteristic model for lead applied in this series of reports. The structure of the characteristic model is modified by the addition of five compartments that are explicitly identified in models for some elements appearing in radium chains: Trabecular marrow, Cortical marrow, Spleen, Testes, and Ovaries. Each of these compartments is assumed to exchange lead with the central blood compartment of the lead model (Plasma). Transfer coefficients are selected for reasonable consistency with the biokinetic database underlying the characteristic model for lead and with the retention curve for total soft tissues based on that original model. The specific changes to the characteristic model for lead are as follows: (1) the transfer coefficients from Plasma to compartments added to the characteristic model for lead are 0.015 d^{-1} for Trabecular marrow, 0.005 d^{-1} for Cortical marrow, 0.002 d^{-1} for Spleen, 0.00045 d^{-1} for Testes, and 0.00015 d^{-1} for Ovaries; (2) the transfer coefficient from Plasma to ST1 is reduced from 0.70 d^{-1} to 0.681 d^{-1}, and the coefficient from Plasma to ST2 is reduced from 0.14 d^{-1} to 0.136 d^{-1}; and (3) the assigned transfer coefficient from each of the added compartments back to Plasma is 0.002 d^{-1}. Lead produced in a blood compartment of a preceding chain member that is not identifiable with a blood compartment of the lead model is assigned the transfer rate 1000 d^{-1} to Plasma.

Bismuth

(770) The systemic model for bismuth as a progeny of radium is based on the characteristic model for bismuth applied in this series of reports. The structure of the characteristic model is modified by the addition of five compartments that are explicitly identified in models for some elements appearing in radium chains: Trabecular marrow, Cortical marrow, Spleen, Testes, and Ovaries. Each of these compartments is assumed to exchange lead with the central blood compartment of the bismuth model. Transfer coefficients for these added compartments are selected for reasonable consistency with the biokinetic database underlying the characteristic model for bismuth and with the retention curve for total soft tissues based on that original model. The specific changes to the characteristic model for bismuth are as follows: (1) the transfer coefficients from plasma to the added compartments are 0.3 d^{-1} for Trabecular marrow, 0.1 d^{-1} for Cortical marrow, 0.02 d^{-1} for Spleen, 0.003 d^{-1} for Testes, and 0.001 d^{-1} for Ovaries; (2) the transfer coefficient from plasma to the Other soft-tissue compartment ST1 is reduced from 4.2 d^{-1} to 3.876 d^{-1}, and the coefficient from plasma to the Other soft tissue compartment ST2 is reduced from 1.3 d^{-1} to 1.2 d^{-1}; and (3) the assigned transfer coefficient from each of the added compartments back to plasma is 0.007 d^{-1} (half-time of 100 d). Bismuth produced in a blood compartment that is not identifiable with a compartment of the bismuth model is assumed to transfer to the plasma compartment of the bismuth model at the rate 1000 d^{-1}. Bismuth produced in a trabecular or cortical bone volume

compartment is assumed to transfer to plasma at the reference turnover rate for that bone type.

Thallium

(771) The section on lead contains a summary of biokinetic information on systemic thallium and a biokinetic model for thallium produced in systemic compartments following intake of a radioisotope of lead. The following modified version of that model is applied to thallium produced in systemic compartments following intake of a radioisotope of radium. Thallium leaves the central blood compartment (Plasma) at the rate 200 d^{-1} (corresponding to a half-time of 5 min) and is distributed as follows: 2.5% to RBC, 0.75% to Urinary bladder content, 1.75% to Right colon content, 5% to Kidneys, 5% to Liver, 1.5% to Trabecular marrow, 0.5% to Cortical marrow, 0.2% to Spleen, 0.045% to Testes, 0.015% to Ovaries, 7.5% to Trabecular bone surface, 7.5% to Cortical bone surface, and 67.74% to ST0 (remaining soft tissues). Thallium returns from RBC to Plasma at the rate 3.7 d^{-1} and from tissue compartments to Plasma at the rate 2.5 d^{-1}. Thallium produced by radioactive decay in a blood compartment that is not identifiable with a compartment of the thallium model is assumed to transfer to Plasma at the rate 1000 d^{-1}. Thallium produced in a soft-tissue compartment that is not identifiable with a compartment of the thallium model is assumed to transfer to Plasma at the rate 2.5 d^{-1}. Thallium produced in a compartment of cortical or trabecular bone volume is assumed to transfer to Plasma at the reference turnover rate of that bone type.

Actinium

(772) Studies on laboratory animals indicate that the systemic behavior of actinium is broadly similar to that of americium (USEPA, 1999; NCRP, 2009). The model for systemic americium adopted in ICRP *Publication 67* (1993) is applied here to actinium as a progeny of radium. Actinium produced in a compartment of a preceding chain member that is not identifiable with a compartment in the actinium model is assumed to transfer to the central blood compartment of the actinium model at the following rate: 0.0019 d^{-1} (half-time of 1 y) if produced in the liver; and at the rate of bone turnover if produced in the exchangeable bone volume compartment of trabecular or cortical bone.

Thorium

(773) The systemic model applied to thorium as a parent radionuclide in this series of reports is also applied to thorium produced in systemic compartments following intake of a radium isotope. Thorium produced in an exchangeable bone volume compartment in the model of a preceding chain member is assumed to transfer to the central blood compartment of the thorium model at the rate of bone turnover.

Radium

(774) The model for radium as a parent radionuclide is also applied to radium produced by serial decay of members of a radium chain. Radium produced in a compartment of a preceding chain member that is not identifiable with a compartment in the radium model is assumed to transfer to the central blood compartment of the radium model at the following rates: 1000 d^{-1} if produced in a blood compartment and 0.693 d^{-1} (half-time of 1 d) if produced in a soft-tissue compartment. The value 0.693 d^{-1} is the transfer coefficient from the intermediate-term soft tissue compartment ST1 to blood in the characteristic model for radium.

Francium and astatine

(775) Radioisotopes of francium and astatine appearing in radium chains considered in this report have half-lives varying from <1 s to 22 min. These short-lived radionuclides are assumed to decay at their sites of production.

13.3. Individual Monitoring

^{226}Ra

(776) ^{226}Ra intakes are generally determined though analysis of its excretion in urine. Several measurement techniques may be used: alpha spectrometry, beta counting in a proportional counter or liquid scintillation counting, after chemical separation and emanation of ^{222}Rn into a scintillation cell for measurement of photon emissions from its short-lived progeny.

Isotope	Monitoring Technique	Method of Measurement	Typical Detection Limit	Achievable detection limit
^{226}Ra	Urine Bioassay	α spectrometry	10 m Bq/L	
^{226}Ra	Urine Bioassay	Emanation	5 mBq/L	
^{226}Ra	Urine Bioassay	Proportional counter	4 mBq/L	
^{226}Ra	Urine Bioassay	Liquid scintillation counting	3mBq/L	
^{226}Ra	Faeces Bioassay	Proportional Counter	16mBq/24h	

^{228}Ra

(777) ^{228}Ra intakes may be determined though analysis of its excretion in urine, using beta counting in a proportional counter or liquid scintillation counting, after chemical separation Bioassay monitoring using faeces samples is also possible.

(778) Ra-228 cannot be detected directly by in vivo measurement. The lung content of Ra-228 can be inferred from a measurement of its immediate decay product, Ac-228.

Isotope	Monitoring Technique	Method of Measurement	Typical Detection Limit	Achievable detection limit
^{228}Ra	Urine Bioassay	Beta Proportional counter	1 Bq/L	0.01 Bq/L
^{228}Ra	Urine Bioassay	Liquid scintillation counting	50mBq/L	
^{228}Ra	Faeces Bioassay	Beta Proportional counter	0.1Bq/24h	
^{228}Ra	LungCounting	γ-ray spectrometry of ^{228}Ac	40 Bq	15 Bq

References

Atherton, D.R., Stover, B.J., Mays, C.W., 1965. Soft tissue retention of Ra-226 in the beagle. Health

Phys. 11, 101-108.
Ballou, J.E., Gies, R.A., Case, A.C., Huggard, D.L., Buschbom, R.L., Ryan, J.L., 1986. Deposition and early disposition of inhaled $^{233}UO_2(NO_3)_2$ and $^{232}UO_2(NO_3)_2$ in the rat. Health Phys. 51, 755–771.
Cuddihy, R.G., Griffith, W.C., 1972. A biological model describing tissue distribution and whole-body retention of barium and lanthanum in beagle dogs after inhalation and gavage. Health Phys., 23, 621-633.
Della Rosa, R.J., Goldman, M., Wolf, H.G., 1967. Uptake and retention of orally administered Ra-226 and Ba-133: A preliminary report, University of California at Davis, Report 472-114, pp. 40-41.
Glad, B. W.; Mays, C. W.; Fisher, W. 1960. Strontium studies in beagles. Radiat. Res. 12, 672-681.
Hardy, E., Rivera, J., Fisenne, I., Pond, W., Hogue, D., 1969. Comparative utilization of dietary radium-226 and other alkaline earths by pigs and sheep. In: Sikov, M.R., Mahlum, D.D. (Eds), Radiation biology of the fetal and juvenile mammal. Proc. of the ninth annual Hanford biology symposium at Richland, Washington, May 5-8, 1969; U. S. AEC, Division of Technical Information, 183-190.
Harrison, G.E., 1981. Whole body retention of the alkaline earths in adult man. Health Phys., 40, 95-99.
Harrison, G.E., Carr, T.E.F., Sutton, A., 1967. Distribution of radioactive calcium, strontium, barium and radium following intravenous injection into a healthy man. Int. J. Radiat. Biol., 13, 235-247.
Hursh, J.B., Lovaas, A., 1963. Radium-226 in bone and soft tissues of man. Nature 198, 265-268.
ICRP, 1973. Alkaline Earth Metabolism in Adult Man, Publication 20, Pergamon Press, Oxford.
ICRP, 1979. Limits on Intakes of Radionuclides for Workers. ICRP Publication 30, Part 1. Ann. ICRP 2. (3/4).
ICRP, 1993. Age-dependent Doses to Members of the Public from Intake of Radionuclides: Part 2, Ingestion dose coefficients . ICRP Publication 67. Ann. ICRP 23. (3/4).
ICRP, 1995. Age-dependent Doses to Members of the Public from Intake of Radionuclides: Part 4 Inhalation dose coefficients. ICRP Publication 71. Ann. ICRP 25(3-4), 393-405.
Kalkwarf, D.R., Jackson, P.O., Hardin, J.M., 1984. Lung-clearance classification of radionuclides in coal fly ash. Health Phys., 47, 37–45.
Keane, A.T., Schlenker, R.A., 1987. Long-term loss of radium in 63 subjects exposed at ages 6 to 46. In: Age-related factors in radionuclide metabolism and dosimetry, ed. G. B. Gerber, H. Metivier, H. Smith. Proceedings of a workshop in Angers, November 26-28, 1986; Dordrecht: Martinus Nijhoff Publishers, 127-135.
Leggett, R.W., 1992. A generic age-specific biokinetic model for calcium-like elements, Radiation Protection Dosimetry 41, 183-198.
Lloyd, R.D., Bruenger, F.W., Jones, C.W., Taylor, G.N., Mays, C.W., 1983a. Retention in mature beagles injected at 5 years of age. Radiat. Res., 94, 210-216.
Lloyd, R.D., Bruenger, F.W., Mays, C.W., Jones, C.W., 1983b. Skeletal radon-to-radium ratios in neonatal, juvenile and mature beagles and in adult St. Bernards. Health Phys. 44:61-63.
Lloyd, R.D., Jones, C.W., Bruenger, F.W., Atherton, D.R., Mays, C.W., 1983c. Radium retention and dosimetry in juvenile beagles. Radiat. Res., 94, 295-304.
Lloyd, R.D., Taylor, G.N., Jones, C.W., Mays, C.W., 1983d. Radium retention and dosimetry in the St. Bernard. Radiat. Res., 95, 150-157.
Lloyd, R.D., Mays, C.W., Atherton, D.R., 1976a. Distribution of injected Ra-226 and Sr-90 in the beagle skeleton. Health Phys., 30, 183-189.
Lloyd, R.D., Mays, C.W., Atherton, D.R., Taylor, G.N., Van Dilla, M.A., 1976b. Retention and skeletal dosimetry of injected Ra-226, Ra-228, and Sr-90 in beagles. Radiat. Res., 66, 274-287.
Lloyd, R.D., Mays, C.W., Taylor, G.N., Atherton, D.R., Bruenger, F.W., Jones, C.W., 1982. Radium-224 retention, distribution, and dosimetry in beagles. Radiat. Res., 92, 280-295.

10308 Looney, W.B., Hursh, J.B., Archer, V.E., Steadman, L.T., Colodzin, M., 1956. A summary of radium
10309 and thorium excretion in humans. In: Proceedings of the international conference on the
10310 peaceful uses of atomic energy. Vol. 11. Biological effects of radiation. United Nations, pp.
10311 55-64.
10312 Looney, W.B., Archer, V.E., 1956. Radium inhalation accident - radium excretion study. Am. J.
10313 Roentgenol. Rad. Ther. Nucl. Med., 75, 548-558.
10314 Maletskos, C.J., Keane, A.T., Telles, N.C., Evans, R.D., 1969. Retention and absorption of Ra-224
10315 and Th-234 and some dosimetric considerations of Ra-224 in human beings. In: Delayed
10316 effects of bone-seeking radionuclides, ed. by C.W. Mays, W.S.S. Jee, R.D. Lloyd, B.J.
10317 Stover, J.H. Dougherty, G.N. Taylor, Salt Lake City, UT, University of Utah Press, 29-49.
10318 Maletskos, C.J., Keane, A.T., Trelles, N.C., Evans, R.D., 1966. The metabolism of intravenously
10319 administered radium and thorium in human beings and the relative absorption from the
10320 human gastrointestinal tract of radium and thorium in simulated radium dial paints. Annual
10321 Report MIT-952-3, Radioactivity Center, Inst Technology, Cambridge, MA. Pp.202-317.
10322 Marinelli, L.D., Norris, W.P., Gustafson, P.F., Speckman, T.W., 1953. Transport of radium sulfate
10323 from the lung and its elimination from the human body following single accidental
10324 exposures. Radiology 61, 903–915.
10325 Mays, C.W., Christensen, W.R., Lloyd, R.D., Atherton, D.R., Parmley, W.W., Pitchford, G.S., 1962.
10326 Radium studies in a man soon after injection. In: Research in radiobiology, COO-226, Univ.
10327 of Utah, 71-77.
10328 Mays, C.W., Lloyd, R.D., Christensen, W.R., Atherton, D.R., Pitchford, G.S., 1963. Radium
10329 metabolism in a man. Radiat. Res., 19, 210.
10330 Miller, C.E., Finkel, A.J., 1965. A re-examination of retention patterns in patients who received
10331 radium by multiple injections 33 years earlier. In: Health division gamma-ray spectroscopy
10332 group annual report, July 1964 through June 1965, Argonne National Laboratory, ANL-
10333 7217; 5-90.
10334 Moody, J.C., Stradling, G.N., 1992. Biokinetics of thorium and daughter radionuclides after
10335 deposition in the rat lung. J. Aerosol Sci., 23, Suppl. 1, S523–S526.
10336 NCRP 2009. Management of persons contaminated with radionuclides. NCRP Report No. 161.
10337 National Council on Radiation Protection and Measurements: Bethesda, Maryland.
10338 Neuman, W.F., 1964. Blood-bone exchange. In: Bone biodynamics, ed. by H.M. Frost. Boston: Little,
10339 Brown, and Co, 393-408.
10340 Newton, D., Harrison, G.E., Kang, C., Warner, A.J., 1991. Metabolism of injected barium in six
10341 healthy men. Health Phys., 61, 191-201.
10342 Newton, D., Rundo, J., Harrison, G.E., 1977. The retention of alkaline earth elements in man, with
10343 special reference to barium. Health Phys., 33, 45-53.
10344 Norris, W.P., Speckman, T.W., Gustafson, P.F., 1955. Studies on the metabolism of radium in man.
10345 Am. J. Roentgenol., Radium Ther. Nucl. Med., 73, 785-802.
10346 Parks, N.J., Keane, A.T., 1983. Consideration of age-dependent radium retention in people on the
10347 basis of the beagle model. Health Phys., 44, 103-112.
10348 Parks, N.J., Pool, R.R., Williams, J.R., Wolf, H.G., 1978. Age and dosage-level dependence of
10349 radium retention in beagles. Radiat. Res., 75, 617-632.
10350 Qiyue, H., Zhonghon, Z., Shijun, L., 1988. Radium-226: Concentration and distribution in human
10351 bone. Chin. J. Radiol. Med. Prot. 8:224-225 (abstract).
10352 Rajewsky, B., Belloch-Zimmermann, V., Loehr, E., Stahlhofen, W., 1965. Ra-226 in human
10353 embryonic tissue, relationship of activity to the stage of pregnancy, measurement of natural
10354 Ra-226 occurrence in the human placenta. Health Phys., 11, 161-169.
10355 Schales, F., 1964. The excretion of thorium X and its daughter products after intravenous injection in
10356 man. In: Assessment of radioactivity in man, Vol. II, Vienna, IAEA, 267-276.
10357 Schlenker, R.A., Keane, A.T., Holtzman, R.B., 1982. The retention of Ra-226 in human soft tissue
10358 and bone; implications for the ICRP 20 alkaline earth model. Health Phys., 42, 671-693
10359 1982.

Schlundt, H., Nerancy, J.T., Morris, J.P., 1933. The detection and estimation of radium in living persons. IV. The retention of soluble radium salts administered intravenously. Am. J. Roentgenol., Radium Ther., 30, 515-522.

Seil, H, Viol, C, Gorden, M., 1915. The elimination of soluble radium salts taken intravenously and per os. Radium., 5, 40-44.

Stark, G., 1968. Studies on synthetic hydroxyapatite crystals with regard to metabolism of calcium, strontium, barium and radium in bone. I. The discrimination against calcium. Biophysik, 5, 42-54.

Taylor, D.M., Bligh, P.H., Duggan, M.H., 1962. The absorption of calcium, strontium, barium, and radium from the gastrointestinal tract of the rat. Biochem. J., 83, 25-29.

Toohey, R.E., Sha, J.Y., Urnezis, P.W., Hwang, E.Y., 1984. An unusual case of radium exposure. Argonne National Laboratory Environmental Research Division Annual Report July 1982 – June 1983, ANL–83–100 Part II, 15–20.

USEPA 1999. Cancer risk coefficients for environmental exposure to radionuclides. Federal Guidance Report No. 13, EPA 402-R-99-001. Prepared by Eckerman, K. F.; Leggett, R. W.; Nelson, C. B.; Puskin, J. S.; Richardson, A. C. B. Office of Radiation and Indoor Air. US Environmental Protection Agency: Washington, D.C.

Van Dilla, M.A., Stover, B.J., Floyd, R.L., Atherton, D.R., Taysum, D.H., 1958. Radium (Ra-226) and radon (Em-222) metabolism in dogs. Radiat. Res., 8, 417-437.

Wood, S.K., Farnham, J.E., Marshall, J.H., 1970. Ca-45, Ba-133, and Ra-226 in 6-to 10-year-old beagle dogs: A 100-day study. In: Radiological Physics Division annual report, Center for Human Radiobiology, July 1969 through June 1970; Argonne, IL: Argonne National Laboratory; ANL-7760, Part II, Biology and Medicine, 110-132.

14. Thorium (Z = 90)

14.1. Chemical Forms in the Workplace

(779) Thorium is an actinide element which occurs mainly in oxidation state IV. It is naturally abundant in the earth and the main ores are thorite, thorianite, and monazite, the latter occurring mainly as mineral sand. Thorium may be encountered in industry in a variety of chemical and physical forms, such as oxides (ThO_2), hydroxides, nitrates, fluorides and sulphates.

(780) Thorium-232 can be used as fuel in a nuclear reactor to absorb slow neutrons and to produce ^{233}U, which is fissile.

Table 14-1. Isotopes of thorium addressed in this report

Isotope	Physical half-life	Decay mode
Th-226	30.57 m	A
Th-227	18.68 d	A
Th-228[a]	1.912 y	A
Th-229[a]	7.34E+3 y	A
Th-230[a]	7.538E+4 y	A
Th-231	25.52 h	B-
Th-232[a]	1.405E+10 y	A
Th-233	22.3 m	B-
Th-234[a]	24.10 d	B-
Th-236	37.5 m	B-

[a] Data for these radionuclides are given in the printed copy of this report. Data for other radionuclides are given on accompanying electronic disk.

14.2. Routes of Intake

14.2.1. Inhalation

Absorption Types and parameter values

(781) Information is available on the biokinetic behaviour of thorium after deposition of various chemical forms in the respiratory tract after accidental human exposure, and from experimental studies with animals, mainly rats.

(782) Absorption parameter values and Types, and associated f_A values for particulate forms of thorium are given in Table 14-2. In referring to default types it should be noted that the biokinetic behaviour of thorium is exceptional in that, following deposition of water-soluble forms in the lungs, a minor fraction of the lung deposit is absorbed very rapidly, after which absorption is minimal. This indicates that there are no commonly encountered Type F forms of thorium.

Thorium chloride ($ThCl_4$)

(783) Boecker et al. (1963) conducted a series of experiments to determine the effect of the mass of thorium deposited in the lungs on its disposition, by following the biokinetics of ^{234}Th (half-life 24 days) for up to 90 days after inhalation of the chloride by rats. They observed that soon after exposure a fraction of the thorium deposited in the lungs was

absorbed into the body, but after this the thorium organ contents remained approximately constant: the lung content decreased with time, with excretion of thorium predominantly in faeces. Similar behaviour has been observed following deposition of other water-soluble thorium compounds in the lungs: see below. It suggests that the fraction of thorium that is not absorbed rapidly is retained in the lungs in particulate form, rather than bound to respiratory tract tissues. They also found that the fraction of the thorium initial lung deposit (ILD) that was absorbed, and the fractions excreted in the urine and faeces, did not appear to be affected by variation in the mass of the ILD by a factor of 10^5. This was in contrast to mass-dependent biokinetics observed by Thomas et al. (1963) following injection by different routes, including intratracheal instillation. It was considered that this might be due to the relatively high local concentrations that occurred in the injection studies, compared to the more diffuse (in both space and time) distribution following inhalation. At the first measurement of distribution, made <1 hour after exposure, the "Remainder" tissue (taken by the authors to represent activity absorbed from the lungs), contained about 10% ILD, and showed little further change. This indicated that the absorption rate corresponds to a time constant of less than an hour, i.e. that s_r was more than 20 d^{-1}. However, it was not very much greater, because it appeared that clearance from the upper respiratory tract (URT) was mainly to the alimentary tract. At this time there were similar amounts of thorium in the URT and in the alimentary tract plus contents, indicating that the particle transport rate from the URT was about 20 d^{-1}: this was assumed in all the assessments carried out here (*i.e.* by the Task Group) for thorium inhaled by rats. The lung content decreased from about 85% ILD at 6 d to 28% ILD at 84 d. Absorption parameter values of f_r = 0.06, s_r = 90 d^{-1} and s_s = 0.002 d^{-1} were assessed here. Retention in lung and carcass were represented well, without the need to introduce the bound state.

(784) Boecker (1963) followed the biokinetics of ^{234}Th for 32 days after inhalation of the chloride by rats. At the first measurement of distribution, made <1 hour after exposure, the "Remainder" tissue contained ~7% ILD, which increased to ~15% at 2 days onwards. Absorption parameter values of f_r = 0.13, s_r = 20 d^{-1} and s_s = 0.004 d^{-1} were assessed here. Boecker also found that thorium in rats exposed up to five times behaved similarly to thorium in rats exposed only once.

Water-soluble forms of thorium and Type F thorium

(785) Based on the results of the experiments outlined above, and those with thorium citrate and nitrate below, specific dissolution parameter values of f_r = 0.1, s_r = 50 d^{-1} and s_s = 0.005 d^{-1} (consistent with assignment to default Type M) are used here for water-soluble forms of thorium, including chloride. It should be noted that with an initial uptake as high as ~10% ILD, it is difficult to estimate the low value of s_s. This consideration also applies to the following compounds that are assigned to Type M. Since the estimated values of s_s are close to the Type M default value of 0.005, it was used. The values of s_r, with those estimated for chloride (below), are also used here to assign the specific value of s_r for Type F thorium. Default Type F thorium (with dissolution parameter values: f_r = 0.1, s_r = 50 d^{-1}) is nevertheless retained as an option.

Thorium citrate

(786) Thomas et al. (1963) measured the tissue distribution of ^{234}Th at times from 7 to 19 days after intratracheal instillation into rats as the citrate, as a preliminary to inhalation experiments (see below for citrate, and above for chloride). There was no obvious change with time and mean values were reported. When administered at tracer level, ~3% ILD

remained in the lungs and ~50% was absorbed (deposited in systemic organs). When administered with carrier, ~10% ILD remained in the lungs, and ~15% was absorbed, indicating Type F and Type M behaviour respectively.

(787) Boecker (1963) followed the biokinetics of ^{234}Th for 32 days after inhalation of the citrate by rats. The first measurement of distribution was made soon (<1 hour) after exposure. The "Remainder" tissue, taken by the author to represent activity absorbed from the lungs, already contained about 40% ILD, and showed little further change. This was more than found for the chloride in a similar experiment (~10% ILD, see above) but suggests that as for the chloride s_r was more than 20 d^{-1}, but not much greater. About 60% ILD remained in the lungs at 7 days, much more than after intratracheal instillation (see above) and it was suggested that the difference was an artefact of the instillation procedure. Absorption parameter values of f_r = 0.14, s_r = 70 d^{-1} and s_s = 0.01 d^{-1} were assessed here, giving assignment to Type M.

(788) Based on the results of the experiments outlined above, and those with thorium chloride (above) and nitrate (below), specific absorption parameter values of f_r = 0.1, s_r = 50 d^{-1} and s_s = 0.005 d^{-1} (consistent with assignment to default Type M) are used here for water-soluble forms of thorium, including citrate. The values of s_r, with those estimated for chloride (above), are also used here to assign the specific value for Type F thorium.

Thorium nitrate ($Th(NO_3)_4$)

(789) Ballou et al. (1986) measured the tissue distributions of ^{232}U and its decay products at 24 hours after their intratracheal instillation into rats as nitrates. (For further information see the uranium inhalation section, and the section below on decay products of thorium formed in the respiratory tract.) For ^{228}Th, lung retention was 52% ILD, much higher than for the other radionuclides, with deposition in the skeleton at 12% ILD, broadly similar to the behaviour observed after instillation of thorium sulphate (see below).

(790) Gray et al. (1991) measured the tissue distribution of $^{230+232}$Th at times between 7 and 252 days after administration to rats by inhalation or intratracheal instillation of thorium nitrate with an ILD of about 5 µg thorium. Following inhalation, lung retention decreased from 73% ILD to 12.6% ILD between 7 and 252 days. It was estimated that about 10% was absorbed by 7 days, with little subsequent change. Thus the overall behaviour was similar to that observed for inhaled chloride and citrate (see above). With the first measurement at 7 days, there is no information on which s_r can be estimated. Stradling et al. (2004) derived two sets of parameter values from the data: assuming a "low" value for s_r of 3 d^{-1}, gave f_r = 0.07 and s_s = 0.00035 d^{-1}; assuming a "high" value for s_r of 100 d^{-1}, gave f_r = 0.04 and s_s = 0.0005 d^{-1}. Values of s_r in the range 20–90 d^{-1} were obtained here from the results of inhalation experiments with chloride and citrate (see above). Taking a central value of 50 d^{-1}, a good fit to the data was obtained here with f_r = 0.04 and s_s = 0.0008 d^{-1}, giving assignment to Type M. Very similar values were obtained for the data following instillation (f_r = 0.05 and s_s = 0.0008 d^{-1}).

(791) Gray et al. (1991) also followed the biokinetics of thorium after intratracheal instillation into rats of thorium nitrate with ILDs of about 2 pg or 3 ng thorium, with the first measurement at 1 or 7 days and the last at 28 or 84 days. Assuming s_r = 50 d^{-1}, and s_s = 0.0008 d^{-1} (as in the longer-term studies) values of f_r of about 0.3 were obtained here for both (giving assignment to Type M). Thus a larger fraction was absorbed rapidly when these lower masses were instilled, as observed by Thomas et al. (1963) for thorium citrate.

(792) Moody et al. (1994a; Moody and Stradling, 1992) measured the tissue distributions of ^{228}Th, ^{212}Pb, ^{212}Bi and ^{208}Tl, at times from 6 hours to 7 days after intratracheal instillation

into rats of a nitrate solution of ^{228}Th in equilibrium with its decay products (ILD 17 ng Th). (For further information see the section below on decay products of thorium formed in the respiratory tract.) For thorium, about 20% ILD was absorbed by 6 hours, with little subsequent change, indicating that s_r was more than 4 d^{-1}. They also measured the tissue distribution of ^{228}Th at times from 1 to 84 days after instillation of Th nitrate (ILD 32 ng). Assuming s_r = 50 d^{-1}, and s_s = 0.0008 d^{-1} (as above) values of f_r of 0.2 and 0.14 respectively were obtained here.

(793) Stradling et al. (2005a) measured the tissue distribution of ^{228}Th at times from 1 to 84 days after intratracheal instillation into rats of a nitrate solution of ^{228}Th. Absorption was somewhat greater for an ILD of 1.6 pg thorium than for an ILD of 0.17 µg thorium. Assuming s_r = 50 d^{-1}, and s_s = 0.0008 d^{-1} (as above) values of f_r of 0.35 and 0.25 were obtained here. The behaviour of thorium was not significantly affected by the presence of uranium when they were administered together (for further information, see section on decay products of uranium formed in the respiratory tract).

(794) Thus similar overall behaviour was reported in these experiments, with absorption to blood largely complete by the time of the first measurement. The studies with citrate and chloride outlined above suggest that following inhalation there is little effect of mass on the biokinetics of thorium, but following instillation the rapidly absorbed fraction decreases with mass instilled. Similarly, for thorium nitrate administered by instillation, the fraction of ILD absorbed rapidly tends to decrease with increasing ILD. Values of f_r estimated here varied from 0.05 to 0.35, (giving assignment to Type M) with the lowest value at the highest ILD. A value of f_r = 0.04 was obtained from the results of the only inhalation experiment with thorium nitrate (Gray et al., 1991). Based on the results of the experiments outlined above, and those with thorium chloride and citrate, specific absorption parameter values of f_r = 0.1, s_r = 50 d^{-1} and s_s = 0.005 d^{-1} (consistent with assignment to default Type M) are used here for water-soluble forms of thorium, including nitrate.

Thorium sulphate ($Th(SO_4)_2$)

(795) Scott et al. (1952) measured the tissue distribution of ^{234}Th at 4 days after intratracheal instillation into rats of thorium sulphate solution (with carrier). About 35% ILD remained in the lungs and 4% was deposited in systemic organs indicating somewhat less absorption than for instillation of thorium citrate (see above), but also indicating Type M behaviour. Since the thorium sulphate was administered in solution the specific parameter values adopted here for water-soluble forms of thorium (f_r = 0.05, s_r = 50 d^{-1}, and s_s = 0.001 d^{-1}) are also applied to thorium sulphate.

Thorium fluoride (ThF_4)

(796) Stradling et al. (2005b; Moody et al., 1994b) measured the tissue distributions of ^{228}Th, ^{212}Pb, ^{212}Bi and ^{208}Tl, at times from 1 to 168 days after intratracheal instillation into rats of a suspension of ^{228}Th or $^{228+232}$Th fluoride (ILD 60 pg or 6.5 µg thorium) in equilibrium with the decay products of ^{228}Th. (For further information see the section below on decay products of thorium formed in the respiratory tract.) As for the water-soluble forms (see above) absorption of thorium to blood was largely complete by the time of the first measurement. However, the authors noted that although the tissue distribution of systemic thorium was independent of mass or chemical form administered, the fraction excreted rapidly in urine was much higher than observed for the nitrate, and suggested that this might reflect the transfer of ultrafine particles through the kidneys. Lung retention at 168 days was greater with the higher mass than with the lower mass administered (25% vs 8% ILD),

presumably because particle transport was impaired. Estimated absorption in the first day was greater for an ILD of 60 pg (12% ILD) than for an ILD of 6.5 µg thorium (6% ILD). Assuming s_r = 50 d^{-1}, (as above, since most absorption took place within 1 d) values of f_r of 0.10 and 0.06, respectively and values of s_s of 0.003 d^{-1} and 0.001 d^{-1} respectively were obtained here, giving assignment to Type M. The parameter values assessed are similar to those adopted here for water-soluble forms of thorium (f_r = 0.1, s_r = 50 d^{-1} and s_s = 0.005 d^{-1}) and therefore these specific absorption parameter values are also used here for thorium fluoride.

Thorium hydroxide ($Th(OH)_4$)

(797) Albert (1966), in a review of lung retention of thorium, referred to a study in which about 2% ILD of the thorium was absorbed from the lungs in 2 months after intratracheal instillation of $Th(OH)_4$ into rats (Thomas R. G., The Metabolism of Thorium-230 (Ionium) Administered by Intratracheal Injection to the Rat. USAEC Report UR-40, University of Rochester, January 1957).

(798) Stradling et al. (2005b; Moody et al., 1994b) measured the tissue distributions of ^{228}Th, ^{212}Pb, ^{212}Bi and ^{208}Tl at times from 1 to 168 days after intratracheal instillation into rats of a suspension of ^{228}Th or $^{228+232}$Th hydroxide (ILD 50 pg or 6.5 µg thorium) in equilibrium with the decay products of ^{228}Th. (For further information see the section below on decay products of thorium formed in the respiratory tract.) Results were similar to those obtained for the fluoride. Absorption to blood was largely complete by the time of the first measurement. However, the authors noted that although the tissue distribution of systemic thorium was independent of mass or chemical form administered, the fraction excreted rapidly in urine was much higher than observed for the nitrate, and suggested that this might reflect the transfer of ultrafine particles through the kidneys. Lung retention at 168 days was greater with the higher mass than with the lower mass administered (17% vs 8% ILD), presumably because particle transport was impaired. Estimated absorption in the first day was somewhat greater for an ILD of 50 pg (8% ILD) than for an ILD of 6.5 µg thorium (6% ILD). Assuming s_r = 50 d^{-1}, (as above, since most absorption took place within 1 d) values of f_r of 0.07 and 0.06, respectively and values of s_s of 0.002 d^{-1} and 0.001 d^{-1} respectively were obtained here, giving assignment to Type M. The parameter values assessed are similar to those adopted here for water-soluble forms of thorium (f_r = 0.1, s_r = 50 d^{-1} and s_s = 0.005 d^{-1}) and therefore these specific absorption parameter values are also used here for thorium hydroxide.

Thorium dioxide (ThO_2)

(799) Hodge and Thomas (1959) reported that high concentrations of thorium were found in the lungs and lymph nodes of dogs sacrificed 7 years after 2-year inhalation exposure to ThO_2. Few details are given but the authors inferred that negligible amounts of thorium had cleared from the lungs in 7 years, indicating Type S behaviour.

(800) Newton et al. (1981) followed the retention of ^{228}Th for 7 years in a man who became internally contaminated, presumably through its inhalation in oxide form. The first measurements were made about 500 days after the presumed time of intake. The authors assessed that by this time only a small fraction of the ^{228}Th in the body was in the lungs, suggesting Type M rather than Type S behaviour.

(801) Ballou and Hursh (1972) followed retention of ^{228}Th in the lungs of dogs for 150 days after inhalation of ThO_2, by *in vivo* measurements of exhaled thoron (^{220}Rn) and ^{208}Tl gamma emissions over the thorax, and *post mortem* measurements of ^{228}Th in the lungs. At

14 days, about 1% ILD was in the body outside the lungs, indicating that f_r was ~0.01. The authors estimated lung retention half-times of 350–500 days, suggesting Type S behaviour. (See also the section below on decay products of thorium formed in the respiratory tract.)

(802) Lamont et al. (2001) measured the dissolution rates in simulated lung fluid of freshly prepared and aged samples of ThO_2 for 100 days. The fractions dissolved over 100 days were ~$2x10^{-6}$ and $1x10^{-5}$ respectively. The higher value for the aged oxide was attributed to radiolytic damage and consequent increase in surface area. Most of the dissolution occurred in the first day or so, giving values of f_r ~$2x10^{-6}$ and $1x10^{-5}$, and values of s_s less than ~10^{-7} d^{-1} and 10^{-8} d^{-1} respectively.

(803) Hodgson et al. (2000, 2003) measured the tissue distributions of ^{228}Th, ^{212}Pb, ^{212}Bi and ^{208}Tl, at times from 1 to 168 days after intratracheal instillation into rats of suspensions of ^{232}Th dioxide enriched with ^{228}Th in equilibrium with its decay products, with two different particle sizes (geometric diameters about 0.4 and 2 µm). About 1% ILD was measured in the carcass at the first measurement (6 hours), with no further measurable increase, showing that s_r was not less than about 10 d^{-1}. The authors derived absorption parameter values of f_r = 0.02, s_r = 10 d^{-1} and s_s = $1x10^{-6}$ d^{-1}, giving assignment to Type S. However, they considered that the value of f_r should not be regarded as typical of ThO_2. They referred to *in vitro* dissolution tests (Lamont et al., 2001, see above) which showed much lower values of f_r. In view of this, specific parameter values are not adopted for thorium dioxide, which is assigned to Type S, but it should be recognised that absorption could be even lower than assumed for default Type S.

Thorium ore and refinery dusts

(804) Measurements of thorium decay products in the chest and exhaled air of nearly 200 former thorium refinery workers, made three or more years after the end of exposure to a range of compounds from monazite ore to thorium nitrate, indicate long-term retention and hence Type S behaviour for at least some of the material (Stehney et al., 1980; Rundo et al., 1981). (See also the section below on decay products of thorium formed in the respiratory tract.) Analysis of autopsy tissues from five workers showed excess concentrations of thorium in lung and lymph nodes (Mausner 1982; Stehney and Lucas 2000). The authors noted that the large amounts of ^{232}Th remaining in the lungs 6–30 years after the end of employment supported the long-term lung retention assumed in the original HRTM.

(805) Maniyan et al. (2000) carried out repeated *in vivo* measurements of the decay product ^{208}Tl in the chest of four workers at a monazite processing plant. They had previous chronic inhalation exposure for 25 to 30 years mainly to thorium hydroxide and phosphate. Measurements, which extended over periods of ~500–1200 days, indicated a clearance half-life for thorium in the chest of ~1000 days. However it was recognised that because of the long exposure there were contributions to the measurements from activity in lymph nodes and skeleton.

(806) Jaiswal et al. (2004) reported that the ratios of daily urinary excretion to lung content of thorium in five workers exposed chronically (10–32 years) at a plant that processed thorium concentrate (hydroxide) to produce thorium nitrate and oxide, were consistent with the predictions of the HRTM and ICRP *Publication 69* systemic Th model (ICRP 1994b; 1995a) assuming Type S, but not Type M.

(807) As part of a programme of measurements of the dissolution in simulated lung fluid of thorium and uranium in dusts to which workers were exposed (see below), Duport et al. (1991) observed negligible dissolution of ^{232}Th in samples of Ni-ThO_2 (2%Th: 98%Ni) alloy from a plant that produced heat and corrosion resistant alloys for aircraft industries.

Uranium ore dust

(808) There is experimental evidence that thorium present in uranium ore dust is retained in the lungs longer than other constituents of the particle matrix (Stuart and Beasley 1967; Stuart and Jackson 1975). Similarly, Fisher et al. (1983) measured significantly higher activity levels of ^{234}U and ^{238}U than of the decay product ^{230}Th in excreta samples obtained from active uranium millers, indicating that clearance of uranium in the inhaled ore dust was faster than that of thorium. In contrast, Wrenn et al. (1985) measured ^{230}Th concentrations similar to those of ^{234}U in the lungs of five uranium miners. In a later study (Singh et al., 1987) the same group found ^{230}Th to ^{234}U concentrations ratios >1 in the lungs of three uranium miners and two uranium millers. They concluded that overall, dissolution in the human lungs of uranium and thorium in uranium ore dust was similar. For further information see the section on decay products of uranium formed in the respiratory tract.

(809) Duport et al. (1991) measured the dissolution in simulated lung fluid of long lived radionuclides in uranium ore dust from Canadian mines. (For further information see the sections on decay products of uranium and thorium formed in the respiratory tract). For high grade ore, measurements were made for up to 60 days. Results were presented as undissolved fractions as functions of time, and showed two components, which were expressed as Class D (rapid) and Class Y (slow) fractions. For ^{238}U and ^{230}Th, the rapidly dissolved fractions were 0.25 and 0.15 respectively, indicating assignment to Type M. (HRTM parameter values fitted to the ^{230}Th data by Marsh *et al.*, 2011, were: f_r = 0.14, s_r = 4.6 d^{-1} and s_s = 0.0007 d^{-1}). For both radionuclides, no effects of size were observed in total dissolution over 40 days for particles in size ranges 7–10, 3–7, 1–3 and <1 µm. For low grade and medium grade ores, measurements were made for 12 days, but only on samples of relatively coarse dust, the smallest fraction being <37 µm. For ^{238}U, rapidly dissolved fractions were greater than those measured in the high grade ores: ~0.33 and 0.5 for low and medium grade ores respectively. Measurements were also made of ^{232}Th in low grade ore, and a much lower fraction obtained, 0.01, indicating assignment to Type S.

(810) Reif (1994) measured the dissolution rates in simulated lung fluid of thorium residues from two different uranium mill tailings in the USA for 100 days. Dissolution parameter values calculated were s_s = 6.4x10^{-4} d^{-1} for one compound, and f_r = 0.3, s_r = 0.23 d^{-1} and s_s = 4.1x10^{-3} d^{-1} for the second compound, indicating assignment to Type S and Type M respectively.

(811) Bečková and Malátová (2008) measured dissolution for 26 days of ^{238}U, ^{234}U and ^{230}Th in simulated serum ultrafiltrate of uranium ore dust collected on personal air filters in a mine in the Czech Republic. The dust contained no measurable ^{232}Th series radionuclides. Moderate dissolution of both uranium isotopes was observed, indicating assignment to Type M. (For further information see the uranium inhalation section.) In contrast no dissolution of ^{230}Th was detected, indicating assignment to Type S.

Other mine dusts

(812) Chen et al. (1995) followed lung retention of thorium by measurements of exhaled thoron in a worker involved in crushing ore containing iron, rare earths and thorium (~0.04%). This worker's lung content was the highest found in a survey of over 100 workers at the mine (Chen et al., 1988), and he suffered from pneumoconiosis. About 40% of the thorium remaining in the lungs when exposure stopped cleared within about a year, but there was very little further clearance during the following 5 years, indicating Type S behaviour of at least some of the dust.

Environmental thorium

(813) Although mainly related to public, rather than worker exposure, information relating to environmental thorium is included here for completeness.

(814) Measurements of environmental levels of thorium in autopsy tissues from members of the public showed that the fraction of thorium in the lungs (~25% of the estimated total body content) was considerably greater than that of plutonium (~5%), and suggested a long term lung retention half-time for thorium of between 1 and 8 y (Wrenn et al., 1981; Singh et al., 1983). The concentrations of thorium in the lymph nodes were 10-20 times those in the lungs in autopsy tissues from members of the public (Hamilton et al., 1972; Ibrahim et al., 1983; Singh et al., 1983; Wrenn et al., 1985; Sunta et al., 1987).

(815) Jaiswal et al. (2004) found good agreement between measured values of Th in lung, skeleton and liver in autopsy tissues from members of the public, and those predicted by the HRTM assuming Type S, and the ICRP *Publication 69* systemic model for Th (ICRP 1994b; 1995a).

(816) These results indicate that environmental thorium is inhaled mainly in insoluble forms.

Decay products of thorium formed in the lungs

(817) The general approach to treatment of decay products formed in the respiratory tract is described in Part 1, Section 3.2.3. In summary, it is expected that generally the rate at which a particle dissociates is determined by its matrix, and hence the physico-chemical form of the inhaled material. It is recognised that for decay products formed within particles by alpha emission, recoil of the daughter nucleus from the alpha emission expels some of the decay product from the particle. In the case of decay chains, this will result in successively lower activities of members compared to the parent retained in relatively insoluble particles. Experimental evidence relating to this is described below in the section on relatively insoluble forms of thorium. However, it was considered impractical to implement loss of decay products by alpha recoil in the calculation of dose coefficients and bioassay functions in this series of documents. (For further information see Part 1, Section 3.2.3.) Nevertheless, this phenomenon should be borne in mind, especially when using decay products to monitor intakes and doses of the parent. This is of particular importance in the case of thorium.

(818) Exceptions are made for noble gases formed as decay products, which are assumed to escape from the body directly, in addition to other routes of removal. For calculation purposes it is assumed that radon formed as a decay product within the respiratory tract escapes from the body at a rate of 100 d^{-1}, in addition to other routes of removal. For further information see the section below on relatively insoluble forms of thorium.

(819) The decay schemes of thorium isotopes in the natural decay series: ^{227}Th, ^{228}Th, ^{230}Th, ^{231}Th, ^{232}Th and ^{234}Th are shown in Part 1, Figures 3.9, 3.10, 3.11. The ^{232}Th decay series is also shown here and the ^{238}U and ^{235}U decay series are shown in the uranium inhalation section.

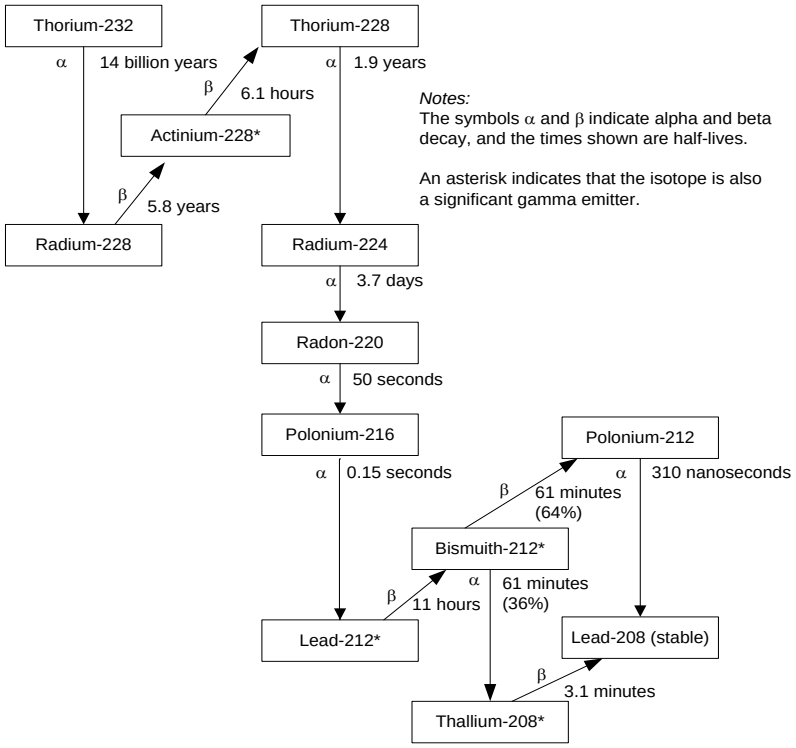

Figure 14-1. Natural decay series: Thorium-232

(820) It is expected that the behaviour of soluble (e.g. Type F) material in the respiratory tract would depend on its elemental form, i.e. that of the decay product. Nevertheless, for simplicity, in this series of documents the absorption parameter values of the parent are, by default, applied to all members of the decay chain formed in the respiratory tract.

(821) The behaviour of decay products of thorium can be of particular importance in this context, because there is generally significant long-term retention of thorium in the lungs following its deposition in water-soluble form (see above). Conversely, soluble forms of important decay products of thorium, notably radium and lead, are relatively readily absorbed from the respiratory tract into the systemic circulation. Studies specifically comparing the behaviour of thorium with that of its decay products are summarised below, although it should be noted that the decay products were administered with the thorium as well as being formed from decay of thorium (and its daughters) in the respiratory tract. For more information, see also the sections on radium, lead, polonium, bismuth and uranium, relating to the behaviour of their decay products formed in the respiratory tract.

(822) As noted above, measurements have been made of the tissue distributions of ^{212}Pb, ^{212}Bi and ^{208}Tl, following administration to rats of ^{228}Th in various chemical forms (nitrate, hydroxide, fluoride, dioxide), in equilibrium with its decay products. (Radon-220 is a precursor of ^{212}Pb, but it is unlikely that a significant amount was lost from solution before deposition in the lungs, because of its short half life of 56 seconds. Its average half-distance of diffusion in water was estimated to be 50 µm by Ballou and Hursh, 1972.) The behaviour of ^{212}Pb is compared with that of ^{228}Th for each chemical form below. (For further information see the lead inhalation section.) In all these studies the distributions of ^{212}Bi and ^{208}Tl were similar to each other and those of the parent ^{212}Pb. Because their physical half-lives are so short (61 minutes and 3 minutes respectively) measurements made at 6 hours onwards would be mainly of activity formed from decay of ^{212}Pb within the body, rather than

from intake of ^{212}Bi or ^{208}Tl. The similar distributions of ^{212}Bi and ^{208}Tl to those of ^{212}Pb might suggest that there was not rapid movement of ^{212}Bi from the site (e.g. the lungs) in which it was formed by decay of ^{212}Pb. However, ^{212}Bi (and ^{208}Tl) would have grown in rapidly between dissection of the animals and measurements of activities in tissues. Thus the activities of ^{212}Bi (and ^{208}Tl) present *in vivo*, may have been significantly lower than those measured and without detailed information (which is not available) about the time which elapsed between dissection of the animals and measurements, it is not possible to correct for this ingrowth and hence estimate the absorption rate from the respiratory tract of the bismuth formed as a decay product of lead, nor that of the thallium formed as a decay product of bismuth. However, since the half-life of ^{208}Tl is so short (as is that of ^{207}Tl present in the ^{235}U decay series, 5 minutes), the absorption rate would have to be very high to influence dose assessments.

Relatively soluble (Type M) forms

(823) Ballou et al. (1986) measured the tissue distributions of ^{232}U, ^{228}Th, ^{224}Ra, ^{212}Pb, ^{212}Bi and ^{208}Tl at 24 hours after intratracheal instillation into rats of ^{232}U nitrate with its decay products. (For further information see the uranium inhalation section.) Measurements of ^{228}Th, ^{224}Ra, and perhaps ^{212}Pb, were mainly of material administered with the parent ^{232}U, rather than formed from its decay in the lungs. The physical half-lives of ^{212}Bi and ^{208}Tl are so short, 61 minutes and 3 minutes respectively, that measurements made at 24 hours would mainly be of activity formed *in situ*. Lung retention was 7.9% ILD for ^{232}U, 52% ILD for ^{228}Th, and about 2-3% ILD for the other decay products measured, reflecting the high lung retention of thorium, and relatively rapid lung clearance of radium and lead observed in other studies in which soluble forms were administered. Similarly, the distribution between liver, skeleton and kidneys of ^{232}U, ^{228}Th, ^{224}Ra and ^{212}Pb reflected the elemental forms. The distributions of ^{212}Bi and ^{208}Tl were similar to those of ^{212}Pb, presumably because of their short physical half-lives: whatever their distribution *in vivo*, they would tend to equilibrium between dissection and measurement.

(824) Lipsztein et al. (1989) made *in vivo* measurements of ^{228}Ac and ^{208}Tl in the lungs of two workers involved in the chemical treatment of monazite sand. They considered that the exposures were to “Class W” (moderately soluble i.e. Type M) forms of thorium. The mean ratio of ^{228}Ac to ^{208}Tl was 1.5, suggesting that some members of the decay series cleared faster than the ^{228}Ac, but the differences were not great.

(825) Moody et al. (1994a; Moody and Stradling, 1992) measured the tissue distributions of ^{228}Th, ^{212}Pb, ^{212}Bi and ^{208}Tl, at times from 6 hours to 7 days after intratracheal instillation into rats of a solution of ^{228}Th nitrate in equilibrium with its decay products. For ^{228}Th, on average 48% ILD was measured in the lungs at 6 hours and 40% ILD at 1 day (see above). For ^{212}Pb, clearance was much faster, with 8.4% ILD at 6 hours and 1.2% ILD at 1 day (correcting for the physical decay of ^{212}Pb, 12.5% and 5.6% ILD respectively). Later measurements of ^{212}Pb could have included significant ingrowth of ^{212}Pb from decay of higher members of the chain in the lungs. Nevertheless the concentration of ^{212}Pb remained much lower than that of the ^{228}Th parent, (presented as a high ^{228}Th:^{212}Pb ratio).

(826) Stradling et al. (2005b; Moody et al., 1994b) measured the tissue distributions of ^{228}Th, ^{212}Pb, ^{212}Bi and ^{208}Tl, at times from 1 to 168 days after intratracheal instillation into rats of a suspension of ^{228}Th or $^{228+232}$Th fluoride in equilibrium with the decay products of ^{228}Th. For thorium (see above), on average 65% ILD was measured in the lungs at 1 day when administered with a low mass (60 pg) of thorium, and 72% ILD when administered with a high mass (6.5 µg) of thorium. For ^{212}Pb, the corresponding amounts were 6.0% and

18% ILD. Correcting for the physical decay of ^{212}Pb gives retention of 28% and 84% ILD at 1 day. Thus, at the low mass, clearance was much faster than that of the parent ^{228}Th, but not at the high mass. From the results for low mass it was assessed here that s_r was at least 1 d^{-1} (half-time ~8 hours). Later measurements of ^{212}Pb could have included significant ingrowth of ^{212}Pb from decay of higher members of the chain in the lungs. Nevertheless, as for the nitrate, the concentration of ^{212}Pb remained lower than that of the ^{228}Th parent, (presented as a high ^{228}Th:^{212}Pb ratio).

(827) Stradling et al. (2005b; Moody et al., 1994b) measured the tissue distributions of ^{228}Th, ^{212}Pb, ^{212}Bi and ^{208}Tl, at times from 1 to 168 days after intratracheal instillation into rats of a suspension of ^{228}Th or $^{228+232}$Th hydroxide in equilibrium with the decay products of ^{228}Th. For thorium (see above), on average 59% ILD was measured in the lungs at 1 day when administered with a low mass (60 pg) of thorium, and 75% ILD when administered with a high mass (6.5 µg) of thorium. For ^{212}Pb, the corresponding amounts were 2.7% and 5.3% ILD. Correcting for the physical decay of ^{212}Pb gives retention of 13% and 25% ILD at 1 day. At both mass levels clearance of ^{212}Pb was much faster than that of the parent ^{228}Th. Later measurements of ^{212}Pb could have included significant ingrowth of ^{212}Pb from decay of higher members of the chain in the lungs.

(828) In the studies by Moody et al. (1994a; 1994b), Moody and Stradling, (1992) and Stradling et al. (2005b) the concentration of ^{212}Pb remained much lower than that of the ^{228}Th parent, despite ingrowth (presented as a high ^{228}Th:^{212}Pb ratio). This might be partly due to loss of intermediate decay products by alpha recoil and diffusion of radon, but partly also due to more rapid dissolution (leaching) of the decay products, including ^{212}Pb, from the particle matrix. Stradling et al. (2004) proposed that since the decay products (radium and lead) are rapidly absorbed, as expected for radium and lead nitrates, they should be assigned to Type F.

(829) For the other moderately soluble forms the situation is less clear: retention of lead is less than that of thorium, but greater than that of lead nitrate. The decay products are therefore also assigned to Type M.

Relatively insoluble (Type S) forms

(830) As noted above (section on Uranium ore dust), Duport et al. (1991) measured the dissolution in simulated lung fluid of long lived radionuclides in uranium ore. For high grade ore, measurements were made for up to 60 days, on particles in size ranges that included respirable particles. Results were presented as undissolved fractions as functions of time, and showed two components, which were expressed as Class D (rapid) and Class Y (slow) fractions. For ^{238}U, ^{230}Th, ^{226}Ra, and ^{210}Pb, the rapidly dissolved fractions were 0.25, 0.15, 0.12 and 0.28 respectively. Marsh et al., 2011, fitted two-component exponential functions to the data (un-dissolved fractions) and obtained the following HRTM parameter values:

Nuclide	f_r	s_r (d^{-1})	s_s (d^{-1})
^{230}Th	0.14	4.6	0.0007
^{226}Ra	0.11	7.3	0.0004
^{210}Pb	0.26	3.9	0.001

(831) For these radionuclides, no effects of size were observed in total dissolution over 40 days for particles in size ranges 7–10, 3–7, 1–3 and <1 µm. For low grade and medium grade ores, measurements were made for 12 days, but only on samples of relatively coarse dust, the smallest fraction being <37 µm. For ^{238}U, rapidly dissolved fractions were higher (0.33 and 0.5 for low and medium grade ores) than those measured in the high grade ores. However, for

other radionuclides the fractions were lower: 0.07 for ^{226}Ra, and <0.01 for ^{210}Pb. Measurements were also made for ^{210}Po in low and medium grade ores, and low fractions obtained, 0.00 and 0.005 respectively. Consistent differences in dissolution between uranium, thorium and their decay products were not apparent.

Emanation of radon: recoil and diffusion

(832) Griffiths et al. (1980) developed a model to describe the retention of ^{232}U and its decay products, which include ^{228}Th, in the lungs following inhalation in ThO_2 or UO_2 particles. In addition to chemical dissolution, they considered recoil emanation of daughter product nuclei by alpha-particle decay, and diffusion emanation of ^{220}Rn from particles. They presented equations to calculate fractional losses by recoil and diffusion as functions of particle size (but only for spherical particles). They calculated recoil ranges of about 0.05 µm for the decay products, assuming a particle density of 10 g cm^{-3}, and fractional losses by recoil emanation in the range 0.3 – 0.1, for aerosols with AMAD in the range 1 – 10 µm. The calculated loss of ^{220}Rn from particles by diffusion emanation was difficult to predict, ranging from 0.03 to 0.7 depending on the assumed diffusion coefficient (10^{-15} - 10^{-11} cm^2 s^{-1}).

(833) Coombs and Cuddihy (1983) measured the fraction of ^{228}Th escaping by recoil and the fraction of ^{220}Rn escaping by diffusion from size-fractionated samples of ThO_2 and uranium oxide (mixture of $UO_{2.2}$ and U_3O_8) containing 1% ^{232}U. The fraction of ^{228}Th escaping increased from ~0.07 for particles with AMAD 2.5 µm (count median diameter, CMD ~1 µm) to ~0.3 for particles with AMAD 0.65 µm (CMD ~0.1 µm). This was in reasonable agreement with the model of Griffiths et al. (1980). Calculated recoil range was expressed in terms of recoil range times density, with values of ~20 µg cm^{-2}. The fraction of ^{220}Rn escaping by diffusion increased from ~0.07 for particles with AMAD 2.5 µm, to ~0.35 for particles with AMAD 0.65 µm, and gave a diffusion coefficient of ~3x10^{-14} cm^2 s^{-1}. This was similar to the fraction of ^{228}Th escaping by recoil, and therefore presumably similar to the fraction of ^{220}Rn escaping by recoil, since the recoil ranges of ^{220}Rn and ^{228}Th are similar (Griffiths et al., 1980).

(834) Johnson and Peterman (1984) developed a model to describe the emanation of ^{220}Rn from ThO_2 particles by alpha-particle recoil, and its exhalation from the lungs. They calculated that the fraction of ^{220}Rn atoms produced that escaped from particles (density 10 g cm^{-3}) by recoil decreased from ~1.0 at 1 nm to ~0.5 at 10 nm and ~0.1 at 0.5 µm diameter. The average fraction for an aerosol of AMAD 1 µm was calculated to be 0.2, which seems to be consistent with the results derived by Griffiths et al. (1980).

(835) Ballou and Hursh (1972) measured thoron (^{220}Rn) in the breath of dogs at times up to 150 days after inhalation of ThO_2 (see above) and, for comparison, after intravenous injection of ThO_2. (After intravenous injection, about 75% of the ThO_2 was retained in the lung vasculature.) Lung retention of ^{228}Th was also followed by *in vivo* measurements of ^{208}Tl gamma emissions over the thorax, and *post mortem* measurements of ^{228}Th in the lungs. At 14 days, the activity of the ^{224}Ra daughter was about 70% of that of the ^{228}Th, suggesting some differential loss of ^{224}Ra. The ratio of thoron in the lung space to ^{228}Th in the whole body was lower (0.065) immediately after inhalation than after intravenous injection (0.11), but increased to about 0.1 by 14 days. By this time most of the ^{228}Th was in the lungs, and the ratio of thoron in the lung space to ^{228}Th in the lungs remained fairly constant thereafter. The lower initial value was attributed to the particles' being embedded in mucus in the upper respiratory tract.

(836) Measurements of thorium decay products in the chest (^{212}Bi, and in some cases ^{228}Ac) and exhaled air (thoron, ^{220}Rn) of nearly 200 former thorium refinery workers, were

made three or more years after the end of exposure to a range of compounds from monazite ore to thorium nitrate (Stehney et al., 1980; Rundo et al., 1981; Toohey et al., 1985). Measurements of exhaled thoron were expressed as the activity of freely emanating ^{224}Ra (the parent of ^{220}Rn) at the mouth of the subject. They found an average value of 0.101 for the ratio of freely emanating ^{224}Ra to retained ^{212}Bi, from which they deduced an average exhalation of 9.2% of the thoron produced. Stebbings (1985) reported a positive correlation between this ratio and the thorium body content, which could lead to serious underestimation if it were applied to estimate the thorium body content from exhaled thoron at population exposure levels.

(837) Rundo and Toohey (1986) reported that measurements of ^{212}Bi in the thorax and of exhaled thoron made on an employee of a ceramics firm showed no change over a period of 7 years. Mean values reported gave a value of 0.07 for the ratio of freely emanating ^{224}Ra to retained ^{212}Bi, similar to that reported by Rundo et al. (1981) for former thorium refinery workers.

(838) Terry and Hewson (1993, 1995) measured thoron in the breath of 62 workers exposed to monazite dust in the mineral sands industry. For 6 of them, *in vivo* measurements were also made of ^{228}Ac, ^{212}Pb and ^{208}Tl in the lungs. The authors estimated that on average 4.7% of the thoron produced in the lungs was exhaled. They also reported that (excluding data for the two workers with the lowest lung burdens) the mean ratio of the 911 keV ^{228}Ac peak to the 2,615 keV ^{208}Tl peak was 1.42. They inferred that the ^{232}Th decay series is not in secular equilibrium, but that up to 30% of the decay products formed from ^{228}Ac to ^{208}Tl had translocated from the lungs.

(839) Hodgson et al. (2000, 2003) measured the tissue distributions of ^{228}Th, ^{212}Pb, ^{212}Bi and ^{208}Tl, at times from 1 to 168 days after intratracheal instillation into rats of suspensions of ^{232}Th dioxide enriched with ^{228}Th in equilibrium with its decay products, with geometric diameters of about 0.4 and 2 µm. There was little absorption of the thorium itself, consistent with assignment to Type S (see thorium dioxide section above). The activity of ^{212}Pb in the lungs was about 50% and 80% of that of the thorium at 1 day for the 0.4 and 2 µm particles respectively, and 25% and 70% at later times. The lower concentrations of ^{212}Pb were attributed to diffusion of ^{220}Rn (thoron) and recoil of the progeny from alpha particle decay, and the authors suggested that the concentration of ^{212}Pb relative to that of ^{228}Th would be even lower following deposition of ultrafine particles. These inferences are consistent with the conclusions of Coombs and Cuddihy, 1983 (see above), although some more rapid dissolution of lead (and/or its precursors) than of thorium cannot be completely excluded.

(840) Thus, consideration of the recoil range of decay product nuclei formed by alpha emission and measurements of emanation of such decay products indicate that an important fraction is transferred from particles to the surrounding medium. Measurements of decay product ratios to thorium seem broadly consistent with this model. The fraction decreases with increasing particle size and density, but is of the order of 10% for aerosols likely to be encountered in the workplace. However, as noted above, it was considered impractical to implement loss of decay products by alpha recoil in the calculation of dose coefficients and bioassay functions in this series of documents. (For further information see Part 1, Section 3.2.3.) Nevertheless, this phenomenon should be borne in mind, especially when using decay products to monitor intakes and doses of thorium.

(841) For calculation purposes it is assumed that radon formed as a decay product within the respiratory tract escapes from the body at a rate of 100 d^{-1}, in addition to other routes of removal (ICRP, 1995b). This rate was set as a convenient, arbitrary, rapid rate. The underlying assumption is that loss of radon is a continuous process such as diffusion. The

three radon isotopes in the natural decay series: ^{222}Rn (radon), ^{220}Rn (thoron), and ^{219}Rn (actinon) have half-lives of about 3.8 days, 56 seconds and 4 seconds, and therefore decay rates of about 0.18, 1100 and 15,000 d^{-1}, respectively. Hence the assumption of a rate of loss of 100 d^{-1} implies that nearly all ^{222}Rn escapes from the particles before it decays, about 10% of ^{220}Rn escapes, and nearly all ^{219}Rn decays within the particles.

(842) The predicted transfer to lung air of ~10% of ^{220}Rn formed is broadly consistent with observations that ~10% of the thoron produced in particles in the lungs is exhaled (see above). It was assessed here that most of the ^{220}Rn entering lung air is exhaled[3]. However, the prediction that all of the ^{222}Rn escapes from the particles is not supported by measurements of radon emanation coefficients (the fraction of radon atoms that escape from the particles in which they were formed) made on dust samples. Duport and Edwardson (1984) reported values between 0 and 0.5 for micron sized samples of uranium ore dust. Kalkwarf et al. (1985) measured radon emanation coefficients in the range 0.001 to 0.1 for coal fly ash particles in sized fractions from <0.5 µm to 11-15 µm. They recognized that since the particles in their experiments were closely packed, some recoiling radon would be injected into adjacent particles, and emanation would be somewhat greater in the lungs. Strong and Levins (1982) measured the effect of moisture content on emanation of radon from uranium mine tailings. The radon flux from a column of powder was higher when it was moist than when it was dry: this was attributed to recoiling radon atoms being stopped in the water between particles (from which it subsequently diffused) rather than becoming trapped in other particles. The discussion assumed that the main mechanism of radon loss from particles was recoil following decay of the parent ^{226}Ra. Thus the assumption of a rate of transfer of radon from particles of 100 d^{-1} appears to be pragmatic: it is simply to apply and seems to predict exhalation of ^{220}Rn (thoron) in broad agreement with observations, but probably overestimates loss of ^{222}Rn from particles in the lungs.

Rapid dissolution rate for thorium

(843) In the various studies of the biokinetics following deposition in the lungs of water soluble forms of thorium it was observed that only a fraction of the ILD, usually less than 50%, was absorbed into blood, and that most of the absorption had taken place by the time of the first measurement of tissue distribution. The earliest measurements of distribution were made <1 hour after inhalation of thorium chloride or citrate by rats, which indicated that the absorption rate corresponds to a time constant of less than an hour, i.e. that s_r was more than 20 d^{-1}. However, it was not very much greater, because it appeared that clearance from the upper respiratory tract was mainly to the alimentary tract. Values of f_r estimated here from the results of three experiments were 20, 70 and 90 d^{-1}. A central value of 50 d^{-1} is adopted here, and applied to all Type F forms of thorium. However, as noted in the introduction above, the results of studies of water-soluble forms of thorium (chloride, citrate, nitrate, sulphate) deposited in the lungs, indicate that there are no commonly encountered Type F

[3] According to Stehney et al. (1980) the average breathing rate during measurements of thoron in breath was 7.5 litres per minute. An adult male at rest takes about 12 breaths per minute (ICRP 1994c, page 194): hence the tidal volume was ~0.6 litres and each breath took ~5 seconds. The volume of air in the lungs at the start of a breath is ~3.9 litres (Functional Residual Capacity, 3.3 litres (ICRP 1994c, page 189) plus tidal volume 0.6 litres). Hence ~15% of the air in the lungs is exhaled, and it is assumed here that a similar proportion of the thoron is exhaled. During the 5 seconds of a breathing cycle, ~6% of the thoron present decays, and hence any thoron atom is ~2.5 times more likely to be exhaled than to decay during this breath, or any other. This is in broad agreement with Johnson and Peterman (1984), who calculated that the proportion of ^{220}Rn atoms entering lung air that was exhaled increased from ~60% in airway generations >20 to ~80% in airway generations <16.

forms of thorium.

Extent of binding of thorium to the respiratory tract

(844) As noted above, in the various studies of the biokinetics following deposition in the lungs of water soluble forms of thorium it was observed that only a fraction of the ILD, usually less than 50%, was absorbed into blood. Clearance from the lungs continued, with excretion mainly to faeces, indicating that the clearance was predominantly by particle transport, and that the thorium was retained in the lungs in particulate form, rather than in the bound state. Adequate fits to data were obtained here on that assumption. It is therefore assumed that for thorium the bound state can be neglected, i.e. $f_b = 0.0$.

Table 14-2. Absorption parameter values for inhaled and ingested thorium

	Absorption parameter values[a]			Absorption from the alimentary tract, f_A[b]
Inhaled particulate materials	f_r	s_r (d^{-1})	s_s (d^{-1})	
Specific parameter values[c]				
Water soluble forms, including thorium chloride, citrate, nitrate and sulphate; thorium fluoride[d]	0.1	50	0.005	5×10^{-5}
Default parameter values[e]				
Absorption Type / Assigned forms				
F — NB: Type F should not be assumed without evidence	1	50	-	5×10^{-4}
M[f] Thorium hydroxide	0.2	3	0.005	1×10^{-4}
S[f] Oxide, all unspecified forms[g]	0.01	3	1×10^{-4}	5×10^{-6}
Ingested material				
All forms				5×10^{-4}

[a] It is assumed that for thorium the bound state can be neglected, i.e. $f_b = 0.0$. The value of s_r for Type F forms of thorium (50 d^{-1}) is element-specific. The values for Types M and S (3 d^{-1}) are the general default values.

[b] For inhaled material deposited in the respiratory tract and subsequent cleared by particle transport to the alimentary tract, the default f_A values for inhaled materials are applied: i.e. the (rounded) product of f_A for the absorption Type (or specific value where given) and the f_A value for ingested soluble forms of thorium (5×10^{-4}).

[c] See text for summary of information on which parameter values are based, and on ranges of parameter values observed for individual materials. For water soluble forms of thorium specific parameter values are used for dissolution in the lungs, but the default value of f_A.

[d] Decay products assigned to Type F.

[e] Materials (e.g. thorium hydroxide) are listed here where there is sufficient information to assign to a default absorption Type, but not to give specific parameter values (see text).

[f] Decay products assigned to Type M.

[g] Default Type S is recommended for use in the absence of specific information, i.e. if the form is unknown, or if the form is known but there is no information available on the absorption of that form from the respiratory tract.

14.2.2. Ingestion

(845) Maletskos et al. (1969) measured the absorption of ^{234}Th ingested as the sulphate in a mock "dial" paint by six elderly humans. The values obtained were in the range 10^{-4} to 6.10^{-4} with a mean of 2.10^{-4}. Estimates of Th absorption have also been derived by Johnson and Lamothe (1989) from human data on skeletal content, dietary intake, estimated inhalation rates and excretion data, giving values of less than 10^{-3} to 10^{-2}. However, these estimates of absorption are uncertain because they are based on balance studies involving disparate data sources. Dang and Sunta (1992) questioned the higher uptake values reported by Johnson and Lamothe (1989) and reinterpreted the data used by them to suggest absorption values of about 10^{-3} - $2x10^{-3}$. Their own data for Th concentrations in tissues, body fluids, and daily diet for urban Indian populations suggested values lower than 10^{-3}. Roth et al. (2005) measured urinary excretion of ^{232}Th in 11 adults who were not occupationally exposed. Comparison with reference intake values suggested that absorption was around 5×10^{-3}.

(846) There have been several reports of Th absorption in rats and mice, with values of 5.10^{-5} to 6.10^{-3} for rats (Traikovich, 1970; Pavlovskaya et al, 1971; Sullivan, 1980), about 6.10^{-4} for mice (Sullivan, 1980; Sullivan et al., 1983) and 1.10^{-3} for fasted mice (Larsen et al., 1984).

(847) In *Publication 30* (ICRP, 1979), an absorption value of $2x10^{-4}$ was recommended on the basis of the study of Maletskos et al. (1969). In *Publication 67* (1993) and 69 (1994a), because similar values have been obtained in more recent human studies on the absorption of Pu, Am, Np and Cm, a general absorption value of $5x10^{-4}$ was adopted for dietary intake by adults for all actinides other than uranium. In *Publication 68* (1994b), a value of $2x10^{-4}$ was applied to oxides and hydroxides, with $5x10^{-4}$ for all other chemical forms. An f_A of $5x10^{-4}$ is adopted here for all chemical forms.

14.2.3. Systemic distribution, Retention and Excretion

14.2.3.1. Summary of the database

Human subjects

(848) Maletskos et al. (1966, 1969) examined the clearance of thorium from blood and its retention and excretion after intravenous injection of ^{234}Th citrate into normal human subjects of age 63-83 y. Detailed measurements were reported for 3 male and 2 female subjects (Maletskos et al., 1966). During the first day, thorium disappeared from blood with a half-time of a few hours. As an average, about 10% of the injected amount remained in blood after 1 d, 3% after 2 d, 1.5% after 3 d, and 0.3% after 10 d. As indicated by whole-body counting and analysis of excreta, whole-body retention was greater than 90% of the injected amount at 3 wk after injection. Cumulative urinary excretion represented 4.5-6.1% of the injected amount over the first 5 d after injection and an additional 2-3% over the next 19 d. Little activity was lost in faeces during the first five days. The ratio of urinary to faecal excretion over the first five days averaged about 12 for the male subjects and 25 for the female subjects. External measurements indicated virtually no biological removal from the body during the period from 3-16 wk after injection. There appeared to be no disproportionate accumulation of thorium in the liver compared with other soft tissues.

(849) Long-term measurements of ^{227}Th or ^{228}Th in the bodies and excreta of accidentally exposed workers suggest a minimum biological half-time of 10-15 y for the total-body content (Rundo, 1964; Newton et al., 1981). Similar measurements on workers chronically exposed to thorium over 1-3 decades (Dang et al., 1992) suggest that the rate of removal of the systemic burden to urine was less than 1% y^{-1}.

(850) Stehney and Lucas (2000) reported concentrations of ^{232}Th and activity ratios of ^{228}Th to ^{232}Th and ^{230}Th to ^{232}Th in autopsy samples from five subjects who had worked for 3-24 y at a thorium refinery. Times from the end of work to death ranged from 6 to 31 y. The subjects presumably were exposed primarily by inhalation. For three workers for whom analyses were available for both bone and liver, the ^{232}Th content of total bone averaged roughly 20 times that of the liver based on reference organs masses. For two workers for whom analyses were available for both liver and kidney, the ^{232}Th content of the liver averaged roughly 30 times that of the kidneys. In most samples the activity ratios ^{228}Th:^{232}Th and ^{230}Th:^{232}Th were in the ranges 0.2-0.4 and 0.1-0.2, respectively.

(851) Measurements of thorium isotopes in autopsy samples from non-occupationally exposed subjects (Wrenn et al., 1981; Singh et al., 1983; Ibrahim et al., 1983) indicate that the skeleton typically contains more than three-fourths of the systemic burden during or after chronic exposure to thorium. The reported contents of the liver and kidneys are variable but typically represent about 2-4% and 0.3-1%, respectively, of the systemic burden. These estimates are based on the assumption that muscle, fat, and skin do not accumulate more than 20% of the systemic content, as suggested by data on laboratory animals (Stover et al., 1960; Thomas et al., 1963; Boecker et al., 1963; Traikovich, 1970; Larsen et al., 1984).

(852) Glover et al. (2001) reported detailed measurements of ^{232}Th in tissues of a whole body donor to the United States Transuranium and Uranium Registries. The subject had no known occupational exposure to thorium but had occupational intakes of plutonium and americium and had been chelated with DTPA following an incident 19 years before his death. The authors estimated that the skeleton, liver, kidneys, and other soft tissues contained about 56%, 0.36%, 0.19%, and 43% of systemic ^{232}Th. The ratio 156 of skeletal ^{232}Th to liver ^{232}Th estimated for this subject is substantially greater than values typically determined for human subjects with or without occupational exposure to ^{232}Th.

Laboratory animals

(853) Stover et al. (1960) studied the biological behavior of ^{228}Th in adult beagle dogs over a 1300-d period following its intravenous administration. Biological retention was about 88% of the injected amount at 3 wk, 80-85% at 3 mo, and 65-70% at 2.5 y (Fig. 5). The urinary excretion rate was about 4 times the faecal excretion rate in the first few weeks, but the urinary-to-faecal excretion ratio gradually decreased and was close to 1 at 2.5 y after injection. About 70%, 5%, and 3% of injected thorium deposited in the skeleton, liver, and kidneys, respectively. At times greater than 100 d after administration, about 80% of retained thorium was in the skeleton and about 20% was widely distributed in soft tissues, with relatively high concentrations in the liver and kidneys. There was little if any decline in the thorium content of compact bone over 1300 d or in trabecular bone over 800 d, but there was a noticeable decline in activity in trabecular bone over 800-1300 d after administration. The thorium content of the liver and kidneys declined considerably in the first several months after injection but showed little or no decrease thereafter. Retention of thorium in the kidneys and its rate of urinary excretion at times remote from injection may have been affected by radiation damage at high dosage levels (Stover et al., 1960).

(854) Comparison of the organ distributions of thorium isotopes in humans and beagles exposed only to environmental levels indicate broad similarities in the long-term distributions of systemic thorium in the two species (Singh et al., 1988). There are also broad similarities in the patterns of distribution and excretion of injected thorium in human subjects (Maletskos et al., 1966, 1969) and beagles (Stover et al., 1960) at early times after administration.

(855) The biokinetics of systemic thorium has been studied in various small mammals

including rats, mice, guinea pigs, and rabbits (Scott et al., 1952; Thomas et al., 1963; Boecker et al., 1963; Traikovich, 1970; Larsen et al., 1984). In many cases, the administration of high concentrations of thorium apparently resulted in colloid formation and high deposition in the reticuloendothelial system or in the tissue into which thorium was introduced (e.g. lung with intratracheal injection, or muscle with intramuscular injection). The results of such high-dose studies do not appear to be useful for determining the biokinetics of thorium after intake at levels likely to be encountered in the environment or in most occupational situations.

(856) For tracer levels of thorium administered as the citrate to rats, deposition was considerably greater in bone than other systemic tissues (Thomas et al., 1963). Muscle and pelt accounted for about 20% of the systemic activity at 7-54 d post injection.

(857) Boecker et al. (1963) found that the level of absorption of thorium to blood and its subsequent pattern of distribution and excretion following acute inhalation by rats did not depend on the initial lung content of inhaled thorium. The absorbed activity was deposited mainly in the skeleton. The liver content at 0-40 d was about 15-20% of the skeletal content, and the kidney content during that time was about 3% of the skeletal content. The content of pelt and muscle plus connective tissue was about the same as liver. The urinary to faecal excretion ratio increased gradually to a value of about 0.6-0.7 at 40-50 d post inhalation.

(858) At 3 d after injection of thorium into mice, about 90% of the systemic burden was found in the skeleton, 6% in liver, 4% in kidneys, and 0.1% in reproductive organs (Larsen et al., 1984). A urinary to faecal excretion ratio of 16 was observed. The systemic distribution of thorium was essentially the same after gastrointestinal absorption as after intravenous injection.

14.2.3.2. Biokinetic model for systemic thorium

(859) The biokinetic model for systemic thorium used in this report is the model applied to adult members of the public in ICRP *Publication 69* (1995a) and to workers in *Publication 68* (1994). The model structure (Figure 14-1) is the generic structure for bone-surface-seeking radionuclides. Parameter values for a reference worker are listed in Table 14-3. The primary parameter values such as compartment deposition fractions and biological half-times underlying the transfer coefficients given in Table 14-3 are summarized below. The conceptual basis of the model and the selection of parameter values are described by Leggett (1997).

(860) In the following summary of the model, the "removal half-time" from a compartment refers to the biological half-time that would be observed if there were no recycling to that compartment. This will generally differ from the apparent or “externally viewed” half-time observed in the presence of recycling. Transfer coefficients from blood to various compartments are based on "deposition fractions", which provide a convenient way to describe the initial distribution of activity leaving the circulation.

(861) Blood is treated as a uniformly mixed pool. Compartment ST0 is a soft-tissue pool that includes the extracellular fluids and exchanges material with blood over a period of days. Compartment ST0 is used to depict an early build-up and decline of material in soft tissues and to account for early feedback of material to blood. Compartment ST0 is viewed as an integral part of the early circulation of thorium. In the summary of parameter values below, deposition fractions for compartments other than ST0 are given in terms of activity “leaving the circulation" and refer to the division of thorium among compartments other than ST0.

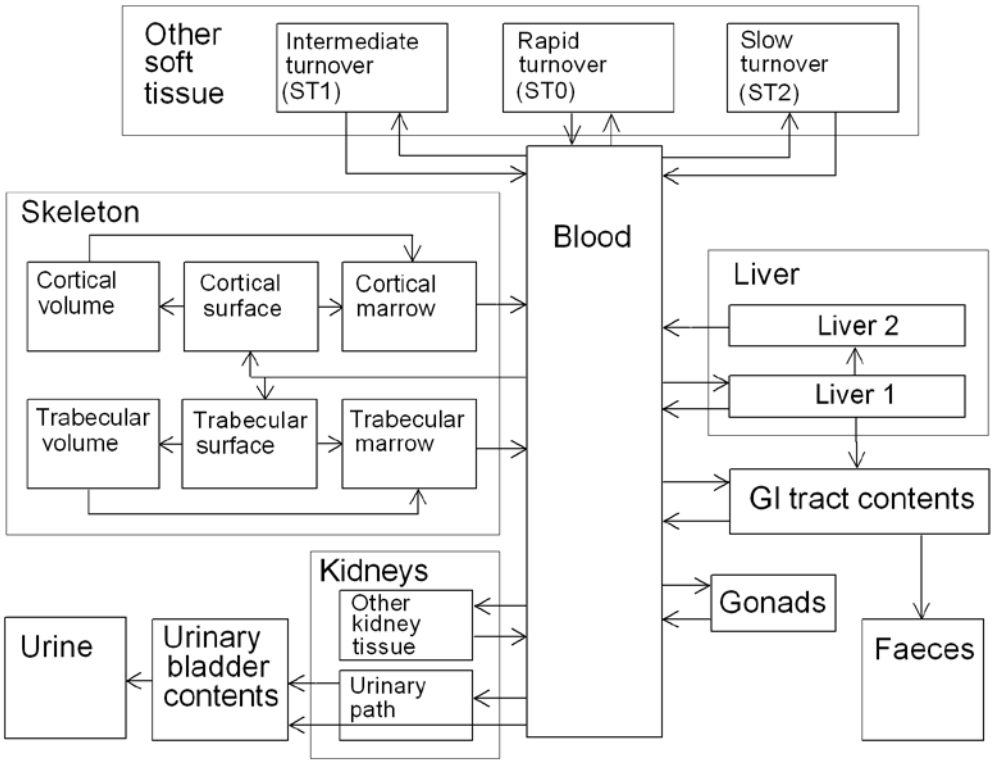

Figure 14-2. Structure of the biokinetic model for systemic thorium.

(862) The removal half-time from blood is assumed to be 0.25 d, corresponding to a total transfer coefficient (the sum of transfer coefficients to all repositories) of ln 2/0.25 d = 2.7726 d^{-1}, where ln 2 is the natural logarithm of 2. Since 30% of this goes to ST0, the transfer coefficient from blood to ST0 is 0.3 x 2.7726 d^{-1} = 0.8318 d^{-1}. Transfer coefficients from blood to other compartments are based on deposition fractions described below and the rate at which thorium leaves the circulation, which is taken to be the total transfer coefficient from blood to all compartments minus the transfer coefficient from blood to ST0: 2.7726 d^{-1} – 0.8318 d^{-1} = 1.9408 d^{-1}. For example, the transfer coefficient from blood to a compartment with a deposition fraction of 0.01 is 0.01 x 1.9408 d^{-1} = 0.019408 d^{-1}, before rounding.

(863) It is assumed that 70% of thorium leaving the circulation deposits on bone surface. One-half of the deposited amount is assigned to trabecular surface and one-half is assigned to cortical surface. The fate of thorium after its deposition on bone surface is described by the generic model for bone-surface-seeking radionuclides. That is, the rate of translocation of skeletal deposits is controlled by bone restructuring processes. The transfer coefficient from compact or trabecular bone surface or volume to the corresponding bone marrow compartment is the rate at which that type of bone surface is resorbed. The transfer coefficient from a bone surface compartment to the corresponding bone volume compartment is one-half the surface formation rate. A common rate (referred to as the “bone turnover rate”) is used for both bone formation and bone resorption and is applied both to surface and volume remodeling. Bone turnover rates used here are reference values for adults given in ICRP *Publication 89* (2002). The removal half-time from bone marrow to blood is assumed to be 0.25 y.

Table 14-3. Transfer coefficients in the biokinetic model for systemic thorium

From	To	Transfer coefficient (d^{-1})
Blood	Liver 1	0.097
Blood	Cortical bone surface	0.6793
Blood	Trabecular bone surface	0.6793
Blood	Urinary bladder contents	0.1067
Blood	Kidneys 1[a]	0.0679
Blood	Kidneys 2[b]	0.0194
Blood	Right colon contents	0.0097
Blood	Testes	0.00068
Blood	Ovaries	0.00021
Blood	ST0	0.832
Blood	ST1	0.243
Blood	ST2	0.0388
Liver 1	Blood	0.000475
Liver 1	Liver 2	0.00095
Liver 1	Small intestine contents	0.000475
Cortical bone surface	Cortical bone marrow	0.0000821
Cortical bone surface	Cortical bone volume	0.0000411
Trabecular bone surface	Red marrow	0.000493
Trabecular bone surface	Trabecular bone volume	0.000247
Kidneys 1[a]	Urinary bladder contents	0.0462
Kidneys 2[b]	Blood	0.00038
Testes	Blood	0.00019
Ovaries	Blood	0.00019
ST0	Blood	0.462
ST1	Blood	0.00095
ST2	Blood	0.000019
Liver 2	Blood	0.000211
Cortical bone marrow	Blood	0.0076
Cortical bone volume	Cortical bone marrow	0.0000821
Red marrow	Blood	0.0076
Trabecular bone volume	Red marrow	0.000493

[a] "Urinary path" in Figure 14-1

[b] "Other kidney tissue" in Figure 14-1

(864) By analogy with plutonium the liver is divided into compartments representing hepatocytes (Liver 1) and Kupffer cells (Liver 2). The deposition fraction assigned to the liver is 0.05. Thorium depositing in the liver is assigned to Liver 1. The removal half-time from Liver 1 is 1 y. Half (50%) of activity leaving Liver 1 is assigned to Liver 2, 25% is assigned to blood, and 25% is assigned to the small intestine contents (representing biliary secretion). The long-term retention compartment, Liver 2, is assumed to lose activity to blood with a biological half-time of 9 y. In addition to endogenous faecal excretion of thorium via liver bile, it is assumed that 0.5% of thorium leaving plasma is secreted into the right colon contents and subsequently excreted in faeces.

(865) The kidneys are assumed to consist of two compartments, one with relatively short retention and one with relatively long retention. These compartments are referred to as the urinary path and other kidney tissue, respectively. The urinary path receives thorium from

plasma and loses activity to the urinary bladder contents. Other kidney tissue receives thorium from blood and loses thorium to blood. It is assumed that 3.5% of outflow from plasma deposits in the urinary path and 1% deposits in other kidney tissue. The removal half-time from the urinary path to the urinary bladder contents is 15 d. The removal half-time from other kidney tissue is 5 y. It is further assumed that 5.5% of activity leaving the circulation moves instantaneously through the kidneys and deposits in urinary bladder contents. Hence, a total of 9% of thorium leaving the circulation is assumed to enter urinary excretion pathways.

(866) The model describing uptake and removal of thorium by the gonads is the default model for the actinide elements. It is assumed that deposition in the gonads, expressed as a percentage of thorium leaving the circulation, is 0.001% per gram of gonadal tissue. This yields a deposition of 0.035% of thorium leaving the circulation in the 35-g testes of the reference adult male and 0.011% in the 11-g ovaries of the reference adult female (ICRP, 2002). The removal half-time from gonads to blood is assumed to be 10 y.

(867) Other soft tissues are divided into compartments ST0, ST1, and ST2 representing fast, moderate, and slow return of thorium to blood. These compartments and associated parameter values are defined on a kinetic basis and are not physically identifiable entities. They are based mainly on observations of the time-dependent content of soft tissues other than liver and kidneys following intravenous administration of thorium to laboratory animals. As described earlier, it is assumed that 30% of outflow from blood deposits in ST0. It is assumed that 2% of activity leaving the circulation deposits in compartment ST2. The percentage left over after all other deposition fractions in the model have been chosen, amounting to ~12.5% of thorium leaving the circulation, is assigned to the intermediate-turnover soft-tissue compartment, ST1. The removal half-times from ST0, ST1, and ST2 are 1.5 d, 2 y, and 100 y, respectively.

14.2.3.3. Treatment of radioactive progeny

(868) The dosimetrically significant progeny of thorium isotopes addressed in this report are isotopes of actinium, thorium, protactinium, uranium, radium, radon, polonium, lead, bismuth, thallium, actinium, francium, or astatine.

(869) The characteristic model for thorium described above is applied to thorium isotopes produced in systemic compartments by serial decay of members of a thorium chain. Thorium produced in a compartment that is not identifiable with a compartment in the characteristic model for thorium is assumed to transfer to the central blood compartment at the rate 1000 d^{-1} if produced in a blood compartment and at the rate of bone turnover if produced in an exchangeable bone volume compartment. The model for thorium is also applied to protactinium produced in systemic compartments following intake of a thorium parent.

(870) The characteristic model for uranium is applied to uranium produced in systemic compartments following intake of a thorium parent. Uranium produced in a compartment that is not identifiable with a compartment in the characteristic model for uranium (which occurs only for certain soft-tissue compartments) is assumed to transfer to the central blood compartment at the rate 0.0347 d^{-1} (half-time of 20 d), the rate of loss from the intermediate-term compartment of Other soft tissues in the characteristic model for uranium.

(871) The models for actinium, radium, radon, polonium, lead, bismuth, thallium, actinium, francium, and astatine produced systemically by serial decay of members of a thorium chain are essentially the same as the models applied to these elements as progeny of radium (see the section on radium).

14.3. Individual monitoring

^{228}Th

(872) ^{228}Th monitoring techniques include urine and faeces bioassay. Care must be taken when interpreting intakes of ^{228}Th though measurements of the nuclide concentrations in excreta samples due to presence of natural thorium. Th-228 itself cannot be detected directly by in vivo measurement. The body content of Th-228 can be inferred from the measurement of the gamma emissions of the decay products, Pb-212 or Tl-208. Assumptions concerning the equilibrium ratio between ^{228}Th and its decay products are required. The ratios of daughters' activities to Th-228 in the source material are important. Depending on these ratios monitoring done immediately after exposure might be strongly influenced by inhaled Rn-220. The biokinetics of Pb-212 in the lung should be considered, as Pb-212 might have a faster clearing rate from the lungs than thorium.

(873) In addition, as explained in section 2.1, in the paragraphs describing *Decay products of thorium formed in the lungs*, a fraction of the daughters formed within the lung will leave the lung in a faster clearing rate, not taken into account on the bioassay functions described in this series of documents. The underestimation due to the loss of decay products by alpha recoil should be added to the uncertainty of the result.

(874) Measurement of thoron (Rn-220) in breath is a potentially useful technique for determining lung burdens of Th-228. The uncertainties in the assessment of lung burdens are difficult to quantify and may underestimate the lung burdens, as explained in section 2.1, *Emanation of radon: recoil and diffusion.*

Isotope	Monitoring Technique	Method of Measurement	Typical Detection Limit	Achievable detection limit
^{228}Th	Urine Bioassay	α spectrometry	1 mBq/L	0.1 mBq/L
^{228}Th	Faeces Bioassay	α spectrometry	2mBq/24h	0.2 mBq/24h
^{228}Th	Lung Counting	γ-ray spectrometry of ^{212}Pb	10 Bq (of Pb-212)	8 Bq (of Pb-212)

^{229}Th

(875) Urine bioassay is used to determine ^{229}Th intakes.

Isotope	Monitoring Technique	Method of Measurement	Typical Detection Limit	Achievable detection limit
^{229}Th	Urine Bioassay	α spectrometry	2 mBq/L	

^{230}Th

(876) ^{230}Th intakes are determined though urine and faeces bioassay.

Isotope	Monitoring Technique	Method of Measurement	Typical Detection Limit	Achievable detection limit
^{230}Th	Urine Bioassay	α spectrometry	1 mBq/L	0.05 mBq/L
^{230}Th	Faeces Bioassay	α spectrometry	2 mBq/24h	0.2 mBq/24h

^{232}Th

(877) Intakes of ^{232}Th are determined by in vitro bioassay of urine samples, complemented or not by analysis of faeces. In general it is necessary to use the most sensitive measurement technique to be able to detect Th-232 exposures at the investigation levels. As thorium is a nuclide naturally present in the environment and in the diet, excretion rates of natural thorium are expected and should be evaluated for the population in the region of residence of the workers. This is especially important for the interpretation of faeces sample results.

(878) Th-232 itself cannot be detected directly by in vivo measurement. In vivo lung counting is performed using the measurement of its decay products.. Assessment of Th-232 lung content by the measurement of the gamma emissions of daughter nuclides is not straightforward. It depends on equilibrium assumptions in the source material that the worker is exposed and on the biokinetics of the chain members in the lung. For sources of exposure in which Th-232 is presumed in equilibrium with the daughters, Ac-228 is in general chosen to be measured, because no assumptions about Rn-220 are needed to calculate the corresponding Th-232 activity. As explained in section 2.1, in the paragraphs describing *Decay products of thorium formed in the lungs*, Ra-228 and Ac-228 have faster clearing rates from the lungs than thorium. In addition, a fraction of the daughters formed within the lung will leave the lung in a faster clearing rate, not taken into account on the bioassay functions described in this series of documents. The underestimation due to the loss of decay products by alpha recoil should be added to the uncertainty of the result.

(879) When the source of exposure is a purified thorium source, containing only Th-232 and Th-228, in equal quantities immediately after purification, Ac-228 will not be measurable for a long time. On the other hand, in about three weeks Pb-212 will be in equilibrium with Th-228, and may be used to assign Th-232 intakes, keeping in mind the uncertainties on underestimation of thorium due to the faster clearing rate of the daughter products formed within the lung. If the Th-232 source is purified again, depending on the amount of Th-228 which is left, the measurement of Pb-212 will underestimate the Th-232, and may not be useful even for screening.

(880) Thus in order to estimate Th-232 content using lung monitoring of the daughter products, it is necessary to know the ratios of daughters activities to Th-232 in the source of exposure. In addition the biokinetics of daughter products in the lung should be carefully evaluated.

(881) Measurement of thoron (Rn-220) in breath is a potentially useful technique for determining lung burdens of Th-232. The uncertainties in the assessment of lung burdens are difficult to quantify and may underestimate the lung burdens, as explained in section 2.1, *Emanation of radon: recoil and diffusion.*

Isotope	Monitoring Technique	Method of Measurement	Typical Detection Limit	Achievable detection limit
^{232}Th	Urine Bioassay	α spectrometry	1 mBq/L	0.05 mBq/L
^{232}Th	Urine Bioassay	ICPM/S	0.3 mBq/L	0.06 mBq/L
^{232}Th	Faeces Bioassay	α spectrometry	2 mBq/24h	0.2 mBq/24h
^{232}Th	Lung Counting	γ-ray spectrometry of ^{228}Ac	20 Bq of ^{228}Ac	10 Bq of ^{228}Ac

^{234}Th

(882) ^{234}Th is a gamma emitter. Its intake may be determined through bioassay analysis of urine samples or though in vivo lung counting.

Isotope	Monitoring Technique	Method of Measurement	Typical Detection Limit	Achievable detection limit
^{234}Th	Urine Bioassay	γ-ray spectrometry	4 Bq/L	0.09 mBq/L
^{234}Th	Lung Counting	γ-ray spectrometry	50 Bq	30 Bq

References

Albert, R.E., 1966. Thorium: Its Industrial Hygiene Aspects. Academic Press, New York.

Ballou, J.E., Hursh, J.B., 1972. The measurement of thoron in the breath of dogs administered inhaled or injected ThO_2. Health Phys., 22, 155–159.

Ballou, J.E., Gies, R.A., Case, A.C., Haggard, D.L., Bushbom, R.L., Ryan, J.L., 1986. Deposition and early disposition of inhaled $^{233}UO_2(NO_3)_2$ and $^{232}UO_2(NO_3)_2$ in the rat. Health Phys. 51 755-771.

Bečková, V., Malátová, I., 2008. Dissolution behaviour of ^{238}U, ^{234}U and ^{230}Th deposited on filters from personal dosemeters. Radiat. Prot. Dosim. 129(4): 469-472, published ahead of print November 1, 2007 doi:10.1093/rpd/ncm455.

Boecker, B.B., 1963. Thorium distribution and excretion studies III. Single inhalation exposure to the citrate complex and multiple inhalation exposures to the chloride. Am. Ind. Hyg. Assoc. J. 24, 155–163.

Boecker, B.B., Thomas, R.G., Scott, J.K., 1963. Thorium distribution and excretion studies II. General patterns following inhalation and the effect of the size of the inhaled dose. Health Phys. 9, 165–176.

Chen Xing-an, Xiao Hui-juan, Cheng Yong-e, Yang Ying-je, 1995. An observation on the clearance of thorium dioxide from the lung of a miner. J. Radiol. Prot. 15, 343–346.

Chen Xing-an, Xiao Hui-juan, Dong Zhihua, Lu Hiu Min, Yang Yingjie, Wang Ji Zhong, Wang Yidien, Li Shou-Hua, Hu Ya Qin, 1988. An assessment of the estimated thorium lung burdens of 130 miners in a rare-earth and iron mine in China. In Inhaled Particles VI, Proceedings of an International Symposium and Workshop on Lung Dosimetry Organised by the British Occupational Hygiene Society in Co-operation with the Commission of the European Communities, Cambridge, 2-6 September 1985, (Eds. Dodgson, J., McCallum, R.I., Bailey, M.R., and Fisher, D.R), Pergamon Press, Oxford, United Kingdom. Ann. Occup. Hyg., 32 (Suppl. 1), 871 – 876.

Coombs, M.A., Cuddihy, R.G., 1983. Emanation of ^{232}U daughter products from submicron particles of uranium dioxide and thorium dioxide by nuclear recoil and inert gas diffusion. J Aerosol Sci. 14, 75-86.

Dang, H.S., Jaiswal, D.D., Murthy, K.B., Sharma, R.C., Nambiar, P.P., Sunta, C.M., 1992. Relevance of ICRP metabolic model of thorium in bio-assay monitoring. J. Radioanalytical Nucl. Chem. Articles 156, 55-64.

Duport, P., Edwardson, E., 1984. Characterization of radioactive long-lived dust present in uranium mines and mills atmospheres. In: Stocker, H. (Ed.), Proc. Int. Conf. on occupational radiation safety in mining, pp. 189–195. Toronto, Canadian Nuclear Association.

Duport, P., Robertson R., Ho K., Horvath F., 1991. Flow-through dissolution of uranium-thorium ore dust, uranium concentrate, uranium dioxide, and thorium alloy in simulated lung fluid. Radiat. Prot. Dosim. 38(1/3), 121-133.

Fisher, D.R. Jackson, P.O., Brodaczynski, G.G., Scherpelz, R.I., 1983. Levels of ^{238}U and ^{230}Th in excreta of uranium mill crushermen. Health Phys. 45, 617-629.

11390 Glover, S.E., Traub, R.J., Grimm, C.A., Filby, R.H., 2001. Distribution of natural thorium in the
11391 tissues of a whole body. Radiat. Prot. Dosim. 97, 153-160.
11392 Gray, S.A., Stradling G.N., Moody J.C., Pearce, M.J., Hodgson, A., Ellender, M., 1991. Biokinetics
11393 of Thorium in the Rat after Administration as Nitrate: Implications for Human Exposure.
11394 NRPB-M281, Chilton, Didcot, Oxon OX11 0RQ.
11395 Griffiths W.C., Cuddihy, R.G., Hoover, M.D. Stalnaker, N.D. 1980. Simulation of the retention and
11396 dosimetry of ^{232}U and its daughters after inhalation in ThO_2 or UO_2 particles. In: Sanders C.
11397 L., Cross F.T., Dagle G. E., Mahaffey, J.A., (Eds.), Pulmonary Toxicology of Respirable
11398 Particles. pp. 193-208. Proc. 19th Annual Hanford Life Sciences Symposium at Richland,
11399 WA, October 22-24, 1979. CONF-791002. Available from National Technical Information
11400 Service. Springfield. Virginia.
11401 Hamilton, E.I., Minsky, M.J., Cleary, J.J., 1972. The concentration and distribution of some stable
11402 elements in healthy human tissues from the United Kingdom. Sci. Total Environ., 1, 341-
11403 374.
11404 Hodge, H.C., Thomas, R.G., 1959. The questions of health hazards from the inhalation of insoluble
11405 uranium and thorium oxides. In: Marley, W.G., Morgan, K.Z. (Eds.), Progress in Nuclear
11406 Energy, Series XII, Health Physics. Pergamon Press pp. 52 – 59.
11407 Hodgson, S.A., Rance, E.R., Stradling, G.N., Hodgson, A., Fell, T.P., Youngman, M.J., Moody, J.C.,
11408 Ansoborlo, E., 2000. Biokinetics of thorium dioxide and its decay products in the rat after
11409 alveolar deposition: implications for human exposure. Chilton, NRPB-M1192.
11410 Hodgson, S.A., Stradling, G.N., Hodgson, A., Smith, T.J., Youngman, M.J., Moody, J.C., Ansoborlo, E.
11411 2003. Biokinetics and assessment of intake of thorium dioxide. Radiat. Prot. Dosim. 105,
11412 115–118.
11413 Ibrahim, S.A., Wrenn, M.E., Singh, N.P., Cohen, N., Saccomanno, G., 1983. Thorium concentration
11414 in human tissues from two U. S. populations. Health Phys. 44, Suppl. 1, 213-220.
11415 ICRP, 1979. International Commission on Radiological Protection. Limits on Intakes of
11416 Radionuclides for Workers. ICRP Publication 30, Pt.1. Pergamon Press, Oxford. Ann. ICRP
11417 2, (3/4).
11418 ICRP, 1993. International Commission on Radiological Protection. Age-dependent Doses to
11419 Members of the Public from Intake of Radionuclides. Pt.2. ICRP Publication 67. Pergamon
11420 Press, Oxford. Ann. ICRP. 23, (3/4).
11421 ICRP, 1994a. Dose Coefficients for Intakes of Radionuclides by Workers, ICRP Publication 68. Ann.
11422 ICRP 24(4). Oxford, Pergamon Press.
11423 ICRP, 1994b. International Commission on Radiological Protection. Human respiratory tract model
11424 for radiological protection. ICRP Publication 66, Ann. ICRP 24 (1-3).
11425 ICRP, 1995a. Age dependent Doses to Members of the Public from Intakes of Radionuclides: Part 3.
11426 Ingestion dose coefficients. ICRP Publication 69. Ann. ICRP 25(1). Oxford, Pergamon
11427 Press.
11428 ICRP, 1995b. Age-dependent Doses to Members of the Public from Intake of Radionuclides. Pt.4:
11429 Inhalation Dose Coefficients. ICRP Publication 71. Pergamon Press, Oxford. Ann. ICRP.
11430 25, (3 - 4).
11431 ICRP, 2002. Basic anatomical and physiological data for use in radiological protection: Reference
11432 values, ICRP Publication 89, Ann. ICRP 32(3/4). International Commission on Radiological
11433 Protection. Oxford, Pergamon Press.
11434 Jaiswal, D.D., Singh, I.S., Nair, S., Dang, H.S., Garg, S.P., Pradham, A.S., 2004. Comparison of
11435 observed lung retention and urinary excretion of thorium workers and members of the
11436 public in India with the values predicted by the ICRP biokinetic model. Radiat. Prot. Dosim.
11437 112, 237-243.
11438 Johnson, J.R., Peterman, B.F. 1984. A model to describe thoron exhalation following an inhalation
11439 exposure to thoria aerosols. In: Smith, H., Gerber, G. (Eds.) Lung Modelling for Inhalation of
11440 Radioactive Materials. EUR 9384. pp. 193 – 197 Commission of the European Communities,
11441 Luxemburg.

11442 Johnson, J.R., Lamothe, E.S., 1989. A Review of the Dietary Uptake of Th. Health Phys. 56, 165-
11443 168.
11444 Kalkwarf, D.R., Jackson, P.O., Kuti, J.C., 1985. Emanation coefficients for Rn in sized coal fly ash.
11445 Health Phys. 48, 429–436.
11446 LaMont, S.P., Filby, R.H., Glover, S.E., 2001. In vitro dissolution characteristics of aged and
11447 recrystallised high-fired $^{232}ThO_2$. Radiat. Prot. Dosim, 14, 75-86.
11448 Larsen, R.P., Oldham, R.D., Bhattacharyya, M.H., Moretti, E.S., 1984. Gastrointestinal absorption
11449 and distribution of thorium in the mouse. In: Environmental Research Division annual
11450 report, July 1982-June 1983; Argonne National Laboratory, ANL-83-100-Pt. 2; pp. 65-68.
11451 Leggett, R.W., 1997. Basis and implications of the ICRP's new biokinetic model for thorium. Health
11452 Phys. 73, 587-600.
11453 Lipsztein, J.L., Bertelli, L.N., Oliveira, C.A.N., Azeredo, A.M.G., Melo, D.R., Lourenco, M.C.,
11454 Grynspan, D., Dantas, B.M., 1989. Bioassay monitoring studies for thorium. Radiat. Prot.
11455 Dosim. 26, 57-60.
11456 Maletskos, C.J., Keane, A.T., Telles, N.C., Evans, R.D., 1966. The metabolism of intravenously
11457 administered radium and thorium in human beings and the relative absorption from the
11458 human gastrointestinal tract of radium and thorium in simulated radium dial paints. In:
11459 Radium and mesothorium poisoning and dosimetry and instrumentation techniques in
11460 applied radioactivity (MIT-952-3), Massachusetts Institute of Technology, Cambridge,
11461 Massachusetts; pp. 202-317.
11462 Maletskos, C.J., Keane, A.T., Telles, N.C., Evans, R.D., 1969. Retention and absorption of ^{224}Ra and
11463 ^{234}Th and some dosimetric considerations of ^{224}Ra in human beings. In: (Mays, C.W., Jee,
11464 W.S.S., Lloyd, R.D., Stover, B.J., Dougherty, J.H., Taylor, T.N. (Eds.), Delayed Effects of
11465 Bone-seeking Radionuclides University of Utah Press, Salt Lake City. pp. 29-49.
11466 Maniyan, C.G., Pillai, P.M., Khan, A.H., 2000. An in vivo study on clearance of thorium from the
11467 thorax. Radiat.Prot.Dosim. 90(4), 423-427.
11468 Marsh J.W., Gregoratto, D., Karcher, K., Nosske D., Bessa Y., Blanchardon E., Hofmann W.,
11469 Tomasek L., 2011. Dosimetric calculations for uranium miners for epidemiological studies.
11470 Radiat Prot Dos pp. 1-13, doi:10.1093/rpd/ncr310..
11471 Mausner, L.F., 1982. Inhalation exposures at a thorium refinery. Health Phys. 42, 231–236.
11472 Moody, J.C., Davies, C.P., Stradling, G.N., 1994b. Biokinetics of thorium and daughter radionuclides
11473 after deposition in the rat lung as fluoride and hydroxide. In: Mohr, U., Dungworth, D.L.,
11474 Mauderly, J.L., Oberdörster, G. (Eds.), Proc. Fourth International Inhalation Symposium,
11475 Hannover, March 1-5, 1993. Toxic and Carcinogenic Effects of Solid Particles in the
11476 Respiratory System, pp. 611-614.
11477 Moody, J.C., Stradling, G.N., Pearce, M.J., Gray, S.A., 1994a. Biokinetics of thorium and daughter
11478 radionuclides after deposition in the rat lung as nitrate: implications for human exposure.
11479 NRPB–M525, Chilton, UK.
11480 Moody, J.C., Stradling, G.N., 1992. Biokinetics of thorium and daughter radionuclides after
11481 deposition in the rat lung. J. Aerosol Sci. 23, Suppl. 1, S523–S526.
11482 Newton, D., Rundo, J., Eakins, J.D., 1981. Long term retention of ^{228}Th following accidental intake.
11483 Health Phys. 40, 291–298.
11484 Pavlovskaya, N.A., Provotorov, A.V., Makeeva, L.G., 1971. Absorption of thorium from the
11485 gastrointestinal tract into blood of rats and build-up in organs and tissues. Gig. Sanit. 36,
11486 47-50.
11487 Reif, R.H., 1994. Evaluation of in vitro dissolution rates of thorium in uranium mill tailings. Health
11488 Phys., 67, 545-547.
11489 Roth, P., Höllriegl, V., Li, W.B., Oeh, U., Schramel, P., 2005. Validating an important aspect of the
11490 new ICRP biokinetic model of thorium. Health Phys 88, 223-228.
11491 Rundo, J., 1964. Two cases of chronic occupational exposure to radioactive materials. In: Assessment
11492 of radioactivity in man, Vol. II (Vienna: IAEA); pp. 291-306.

11493 Rundo, J., Brewster, D.R., Essling, M.A., Sha, J.Y., 1981. Radioactivity in former workers at a
11494 thorium refinery. In: Wrenn, M.E. (Ed.), Actinides in Man and Animals, Proceedings of the
11495 Snowbird Actinide Workshop, pp. 261–267. Radiobiology Division, University of Utah,
11496 Salt Lake City, RD Press.
11497 Rundo, J., Toohey, R.E., 1986. Long-term retention of thorium in lung: Report of a case. Health
11498 Phys., 50, Suppl. 1, S24.
11499 Scott, J.K., Neuman, W.F., Bonner, J.F., 1952. The distribution and excretion of thorium sulphate. J.
11500 Pharmacol. Exp. Ther. 106, 286–290.
11501 Singh, N.P., Wrenn, M.E., Ibrahim, S.A., 1983. Plutonium concentration in human tissues:
11502 Comparison to thorium. Health Phys. 44, Suppl. 1, 469-476.
11503 Singh, N.P., Zimmerman, C.J., Taylor, G.N., Wrenn, M.E., 1988. The beagle: An appropriate
11504 experimental animal for extrapolating the organ distribution pattern of thorium in humans.
11505 Health Phys. 54, 293-299.
11506 Singh, N.P., Bennett, D.D., Wrenn, M.E., 1987. Concentrations of α-emitting isotopes of U and Th
11507 in uranium miners' and millers' tissues. Health Phys., 53, 261–265.
11508 Stebbings J.H., 1985. Personal factors affecting thoron exhalation from occupationally acquired
11509 thorium body burdens. Environmental Research Division, Center for Human Radiobiology,
11510 Annual Report June 1983 – June 1984, ANL-84-103 Part II, pp. 60 – 74. Argonne National
11511 Laboratory.
11512 Stehney, A.F., Lucas, H.F., 2000. Thorium isotopes in autopsy samples from thorium workers. Health
11513 Phys. 78, 8-14.
11514 Stehney, A.F., Polednak, A.P., Rundo, J., Brues, A.M., Lucas, H.F., Patten, B.C., Rowland, R.E.,
11515 1980, Health status and body radioactivity of former thorium workers. Argonne National
11516 Laboratory; NUREG/CR-1420 ANL-80-37.
11517 Stover, B.J., Atherton, D.R., Keller, N., Buster, D.S., 1960. Metabolism of the Th-228 decay series in
11518 adult beagle dogs. Radiat. Res. 12, 657-671.
11519 Stradling, G.N., Hodgson, A., Fell, T.P., Phipps, A.W., Etherington, G., 2004. Thorium Nitrate and
11520 Dioxide: Exposure Limits and Assessment of Intake and Dose after Inhalation NRPB–W57,
11521 Chilton, UK. Available at www.hpa.org.uk
11522 Stradling, G.N., Davies, C.P., Moody, J.C., Gray, S.A., Wilson, I., Ellender, M., 2005b. Biokinetics
11523 of thorium and daughter radionuclides after deposition as fluoride and hydroxide in the rat
11524 lung: implications for occupational exposure. NRPB-DA/05/2005, Chilton, UK.
11525 Stradling, G.N., Gray, S.A., Moody, J.C., Ellender, M., Pearce, M.J., 2005a. Biokinetics of thorium in
11526 the presence of a highly transportable form of uranium: implications for occupational
11527 exposure. NRPB-DA/04/2005, Chilton, UK.
11528 Strong, K.P., Levins, D.M., 1982. Effect of moisture content on radon emanation from uranium ore
11529 and tailings. Health Phys. 42, 27–32.
11530 Stuart, B.O., Jackson, P.O., 1975. The inhalation of uranium ores. In: Proceedings of the Conference
11531 on Occupational Health Experience with Uranium. Arlington, Virginia, April 28–30, 1975,
11532 ERDA 93 (Ed. Wrenn, M.E.). US Energy Research and Development Administration, pp.
11533 130–139. Available from National Technical Information Service, Springfield, Virginia.
11534 Stuart, B.O. Beasley, T.M., 1967, Non-equilibrium tissue distributions of uranium and thorium
11535 following inhalation of uranium ore by rats. In: Davies, C.N., (Ed.), Inhaled Particles and
11536 Vapours II. Proceedings of an International Symposium organised by the British
11537 Occupational Hygiene Society; Cambridge, UK. Oxford: Pergamon Press pp. 291-8.
11538 Sullivan, M.F., 1980. Absorption of Actinide Elements from the Gastrointestinal tract of rats, guinea
11539 pigs, pigs and dogs. Health Phys. 38, 159-171.
11540 Sullivan, M.F., Miller, B.M., Ryan, J.L., 1983. Absorption of thorium and protactinium from the
11541 gastrointestinal tract in adult mice and rats and neonatal rats. Health Phys. 44, 425-428.
11542 Sunta, C.M., Dang, H.S., Jaiswal, D.D., 1987. Thorium in man and environment, uptake and
11543 clearance. J. Radioanal. Nucl. Chem., 115, 149-158.

Terry, K.W., Hewson, G.S., 1995. Thorium lung burdens of mineral sands workers. Health Phys. 69, 233–242.

Terry, K.W.,, Hewson, G.S., 1993. Retention and excretion of thorium by mineral sands industry employees. Minerals and Energy Research Institute of Western Australia; Report No. 117.

Thomas, R.G., Lie, R., Scott, J.K., 1963. Thorium distribution and excretion studies I. Patterns following parenteral administration. Health Phys. 9, 153–163.

Toohey R.E., Rundo, J., Sha J.Y., Essling M.A., Pedersen J.C., Slane J.M. 1985. Activity ratios of thorium daughters in vivo. Environmental Research Division, Center for Human Radiobiology, Annual Report June 1983 – June 1984, ANL-84-103 Part II, pp. 53 – 59. Argonne National Laboratory.

Traikovich, M., 1970. Absorption, distribution and excretion of certain soluble compounds of natural thorium. In: Letavet, A.A., Kurlyandskaya, E.B. (Eds.), Toxicology of radioactive substances, Vol. 4: thorium-232 and uranium-238. English Translation (G.W. Dolphin, Ed.). Pergamon Press, Oxford.

Wrenn, M.E., Singh, N.P., Cohen, N., Ibrahim, S.A., Saccomanno, G., 1981. Thorium in human tissues. NUREG/CR–1277, US Nuclear Regulatory Commission. Available from National Technical Information Service, Springfield, Virginia.

Wrenn, M.E., Singh, N.P., Paschoa, A.S., Lloyd, R.D., and Saccomanno, G. (1985). Concentration of U and Th Isotopes in U Miners' and Millers' Tissues. NUREG/CR 4382, U.S. Nuclear Regulatory Commission, Washington, D.C. Available from National Technical Information Service, Springfield, Virginia.

15. URANIUM (Z = 92)

15.1. Chemical forms in the workplace

(883) Uranium is an actinide element which mainly occurs in oxidation states IV and VI. It is encountered in industry in a variety of chemical and physical forms, including oxides (UO_3, UO_4, UO_2, U_3O_8, uranates), inorganic salts (nitrates, chlorides, fluorides, carbonates, phosphates) and some organic compounds (acetylacetonate, Tri-Butyl-Phosphate). Some forms, notably the metal, carbide and oxide may be encountered as depleted uranium (~ 0.2% ^{235}U), natural (0.7% ^{235}U) or enriched (>0.7% ^{235}U) uranium. The chemical behavior of any given uranium compound will be similar irrespective of whether it is present in natural, depleted or enriched form. Depleted uranium has found use as a shielding material in aeronautics and military applications such as counterweights for aircraft control surfaces. ^{238}U, ^{235}U, and ^{234}U, are the three major isotopes and ^{235}U is typically the main fissile material for nuclear power reactors. It should be noted that intakes of the more readily absorbed uranium compounds are limited by considerations of chemical toxicity rather than radiation dose (ICRP, 1997).

Table 15-1. Isotopes of uranium addressed in this report

Isotope	Physical half-life	Decay mode
U-230	20.8 d	A
U-231	4.2 d	EC, A
U-232	68.9 y	A
U-233	1.592E+5 y	A
U-234[a]	2.455E+5 y	A
U-235[a]	7.04E+8 y	A
U-235m	26 m	IT
U-236	2.342E+7 y	A
U-237	6.75 d	B-
U-238[a]	4.468E+9 y	A,SF
U-239	23.45 m	B-
U-240	14.1 h	B-
U-242	16.8 m	B-

[a] Data for these radionuclides are given in the printed copy of this report. Data for other radionuclides are given on accompanying electronic disk.

15.2. Routes of Intake

15.2.1. Inhalation

(884) There is extensive information available on the behaviour of uranium after deposition in the respiratory tract from animal experiments (mainly in rats), *in vitro* dissolution studies, and some accidental human intakes. Much of this information has been obtained since the issue of *Publication 30* (ICRP, 1979). Absorption parameter values have been derived from the results of animal and *in vitro* studies for a wide range of compounds encountered in the nuclear fuel industry. Ansoborlo et al. (2002) and Stradling et al. (2002) compiled absorption parameter values derived from the results of a large number of *in vivo*

and *in vitro* studies carried out on materials from French and UK nuclear fuel fabrication facilities.

(885) Absorption parameter values and Types, and associated f_A values for particulate forms of uranium are given in Table 15-2.

Absorption parameter values and Types

Uranium hexafluoride (UF_6)

(886) Uranium hexafluoride exists in vapour form, but in the presence of water in the atmosphere and in the respiratory tract it is converted to uranyl fluoride (UO_2F_2) aerosol. Generally, any exposure would be to both chemical forms simultaneously, and also to HF fumes. Hence, the mixture is treated here as an aerosol rather than a vapour. In experiments with beagle dogs (Morrow et al., 1982), 80% of the initial lung deposit (ILD) of uranium was absorbed into blood within 20 minutes. The rapid urinary excretion observed after accidental inhalation exposures by humans (Boback, 1975, Beau and Chalabreysse, 1989, Fisher et al., 1991) indicates assignment to default Type F. The rapid absorption half-time was estimated by the task group to be 45 minutes (s_r = 22 d^{-1}) from the data of Fisher et al. (1991). Absorption parameter values derived here from urinary excretion data presented by Beau and Chalabreysse (1989) are f_r = 1 and s_r = 1.6 d^{-1}. Bailey and Davis (2002) derived absorption parameter values of f_r = 1 and s_r = 1.5 d^{-1} from daily urinary excretion data presented by Moore and Kathren (1985) for an accidental intake by a worker (Case G) described by Boback (1975). However, the detailed data for the first two days after exposure reported by Boback (1975) show faster absorption (s_r ~100 d^{-1}) of much of the uranium. In view of the wide range of values of s_r derived from the studies above, these data are judged to be an insufficient basis to provide specific absorption parameter values and UF_6 is therefore assigned to Type F.

Uranyl Tri-Butyl-Phosphate (U-TBP)

(887) Tri-n-Butyl-Phosphate (TBP) is used extensively as an extractant during fabrication of nuclear fuel and for the separation of uranium and plutonium during reprocessing. After administration of U-TBP to rats by intratracheal instillation, 80–90% of the U was absorbed into blood by about 1 d after exposure (Pellow et al., 1996; 1997). Absorption parameter values derived from the results by Stradling et al. (2002) were f_r = 0.97, s_r = 12 d^{-1} and s_s = 0.0021 d^{-1}. From results of a complementary gavage experiment it was estimated that fractional absorption from the alimentary tract f_A = 0.022.

(888) Specific absorption parameter values of f_r = 0.97, s_r = 12 d^{-1} and s_s = 0.002 d^{-1} (consistent with assignment to default Type F) and f_A = 0.02 are used here for U-TBP.

Uranyl nitrate ($UO_2(NO_3)_2$)

(889) Uranyl nitrate in aqueous solution is widely encountered in nuclear fuel fabrication and reprocessing. Ballou et al. (1986) followed the biokinetics of ^{232}U and ^{233}U in rats for 200 days after inhalation of aerosols of aqueous uranyl nitrate solution: 15–45% ILD was retained in the lung at 30 d, depending on particle size, supporting assignment to default Type M. Measurements made after intratracheal instillation into rat lungs are consistent with assignment to default Type F (Cooper et al., 1982, Ellender, 1987, Stradling et al., 2005). Ballou et al. (1986) reported that 1 hour after instillation of ^{232}U or ^{233}U nitrate, only 22% ILD remained in the lungs, with systemic uptake of at least 40% ILD. Hodgson et al. (2000) derived absorption parameter values of f_r = 0.93, s_r = 3 d^{-1} and s_s = 0.005 d^{-1} from the results

of the study by Ellender (1987) in which the biokinetics of uranium were followed for 30 days after intratracheal instillation of uranyl nitrate. The available human and animal data indicate that a value of 0.02 for fractional absorption in the alimentary tract is appropriate for occupational exposures to $UO_2(NO_3)_2.6H_2O$.

(890) Specific absorption parameter values of f_r = 0.9, $s_r = 3\ d^{-1}$ and s_s = 0.005 d^{-1} (consistent with assignment to default Type F) and f_A = 0.02 are used here for uranyl nitrate.

Ammonium diuranate (ADU) $(NH_4)_2U_2O_7$

(891) ADU is a basic product in the uranium fuel cycle, a component of "yellow cake" (a generic term for material which may comprise ADU, U_3O_8 or a mixture of both). Stradling et al. (1987) followed the biokinetics of uranium for 360 days after inhalation of ADU by rats. At 7 days, 11% ILD remained in the lung and 70% ILD was absorbed into blood. From these results, Hodgson et al. (2000) derived parameter values of f_r = 0.85 and $s_r = 0.78\ d^{-1}$: the value of s_s was too low to be determined and was taken to be 0.005 d^{-1}. Ansoborlo et al. (2002) derived parameter values of f_r = 0.71, s_r = 0.61 d^{-1} and s_s = 0.019 d^{-1} from the results of a study in which the biokinetics of uranium were followed for 30 days after intratracheal instillation of ADU into rats.

(892) Specific absorption parameter values of $f_r = 0.8$, s_r = 0.7 d^{-1} and s_s = 0.02 d^{-1} (consistent with assignment to default Type F) are used here for ADU.

Uranium peroxide hydrate $(UO_4.nH_2O)$

(893) Uranium peroxide hydrate is present at one stage of the enriched uranium fuel cycle. This compound, also expressed as $UO_3.H_2O_2.H_2O$, is very similar to uranium trioxide $UO_3.nH_2O$. The dissolution and biokinetic behaviour of both compounds are very sensitive to the hydration state (*n* can vary between 0 and 2.5). One main characteristic of $UO_4.nH_2O$ is that it consists of small needles with an average AMAD of about 1.1 µm. Assessments of the physico-chemical and biokinetic properties of UO_4, both *in vitro* and *in vivo*, have been carried out (Ansoborlo et al., 1998a). The biokinetics of uranium were followed for 90 days after intratracheal administration to rats. By 7 d after exposure 3–10% of uranium remained in the lungs, whereas about 65% was absorbed into blood. The calculated absorption parameter values were: f_r = 0.87, s_r = 0.93 d^{-1} and s_s = 0.024 d^{-1} (Ansoborlo et al., 1998a). Experimental data on ingestion of UO_4 by laboratory animals, reviewed by Leggett and Harrison (1995), suggest that absorption in the alimentary tract is about 0.5 times that of uranyl nitrate, which is taken here to be 0.02 (see above).

(894) Specific absorption parameter values of $f_r = 0.9$, s_r = 0.9 d^{-1} and s_s = 0.02 d^{-1} (consistent with assignment to default Type F) and f_A = 0.01 are used here for uranium peroxide hydrate.

Uranium trioxide $(UO_3.nH_2O)$

(895) In the fuel fabrication cycle, uranium trioxide is formed by heating uranyl nitrate and is then reduced to form UO_2. The biokinetic behaviour of $UO_3.nH_2O$ is very sensitive to the hydration state and its solubility depends on the value of *n*.

(896) Harris (1961) measured excretion of uranium following repeated inhalation of UO_3 by a volunteer. There was considerable clearance to urine and faeces over the first few days after each intake, indicating rapid absorption from the lower, but not from the upper, respiratory tract. The reported measurements are not straightforward to interpret, but a reasonable fit to the excretion data in the two days following the first intake was obtained here with f_r = 0.5 and s_r = 0.15 d^{-1}. Morrow et al. (1972) followed the biokinetics of uranium

for 218 days after inhalation of UO_3 by dogs. Clearance from the airways was mainly to faeces in the first day, while subsequent lung clearance was rapid, with predominantly urinary excretion. Parameter values derived here from lung retention were: $f_r = 0.82$, $s_r = 0.15$ d^{-1} and $s_s = 0.019$ d^{-1} (consistent with assignment to default Type F).

(897) Hodgson et al. (2000) derived absorption parameter values from the results of a study by Stradling et al. (1985b) in which the biokinetics of uranium were followed for 168 days after inhalation of UO_3 by rats: $f_r = 0.92$, $s_r = 1.4$ d^{-1}, $s_s = 0.0036$ d^{-1} (consistent with assignment to default Type F). Ansoborlo et al. (2002) derived absorption parameter values from the results of a study in which the biokinetics of uranium were followed for 30 days after intratracheal instillation of UO_3 into rats: $f_r = 0.71$, $s_r = 0.28$ d^{-1} and $s_s = 0.0011$ d^{-1} (consistent with assignment to default Type M). ICRP (2002), as a worked example, derived absorption parameter values from the results of a study by Moody et al. (1997) in which the biokinetics of uranium were followed for 42 days after intratracheal instillation of UO_3 into rats: $f_r = 0.77$, $s_r = 9.2$ d^{-1}, $s_s = 0.0017$ d^{-1} (consistent with assignment to default Type M). Experimental data on ingestion of UO_3 by laboratory animals, reviewed by Leggett and Harrison (1995), suggest that absorption in the alimentary tract is about 0.5 times that of uranyl nitrate, which is taken here to be 0.02 (see above).

(898) Specific absorption parameter values of $f_r = 0.8$, $s_r = 1$ d^{-1} and $s_s = 0.01$ d^{-1} (consistent with assignment to default Type M) and $f_A = 0.01$ are used here for UO_3.

Uranium tetrafluoride (UF_4)

(899) Uranium tetrafluoride is an intermediate product in the uranium fuel cycle. It can be reduced to uranium metal or oxidized by fluorine to form UF_6. The reported biokinetic behaviour of UF_4 is complex. Measurement of urinary excretion after inhalation by workers (Chalabreysse et al., 1989) and experiments in rats and baboons (Stradling et al., 1985a, André *et al.*, 1989, Ansoborlo et al., 1990) showed that a large fraction (35–40%) of the lung deposit was absorbed to the blood by 7 d after administration. However, considerable variations in behaviour were observed, with some experiments indicating assignment to default Type F and others to default Type M.

(900) Zhao and Zhao (1990) reported measurements of urinary excretion of uranium made for three years after an accidental inhalation of UF_4 powder by a worker. The excretion rate, initially very low, increased to a peak at about 2 months, and then declined. To represent this behaviour, the alternative HRTM representation of dissolution was applied here, in which material is deposited in a compartment representing “Particles in initial state”, in which it dissolves at a rate s_p, and is simultaneously transferred at a rate s_{pt} to a compartment representing “Particles in transformed state”, in which material dissolves at a rate s_t. Material specific parameter values were derived here: $s_p = 0.000002$ d^{-1}; $s_{pt} = 0.02$ d^{-1}; $s_t = 0.04$ d^{-1}; with $f_A = 0.0002$. However, it was not possible to fit a peak as sharp as that observed. The unusual behaviour may have been caused in part by the size of the intake, which was sufficient to give rise to biochemical indications of kidney dysfunction.

(901) Hodgson et al. (2000) derived absorption parameter values from the results of a study by Stradling et al. (1985a) in which the biokinetics of uranium in rats were followed for 360 days after inhalation and 168 days after intratracheal administration of two forms of UF_4: (i) $f_r = 0.51$, $s_r = 0.10$ d^{-1}, $s_s = 0.0074$ d^{-1}; (ii) $f_r = 0.52$, $s_r = 0.11$ d^{-1}, $s_s = 0.0039$ d^{-1}. Chazel et al, (2000a) derived parameter values of $f_r = 0.58$, $s_r = 0.21$ d^{-1} and $s_s = 0.026$ d^{-1} from the results of a study in which the biokinetics of uranium were followed for 30 days after intratracheal instillation of UF_4 into rats. Experimental data on ingestion of UF_4 by laboratory animals, reviewed by Leggett and Harrison (1995), suggest that absorption in the alimentary

tract is about 0.003-0.02 times that of uranyl nitrate, which is taken here to be 0.02 (see above). A central value of 0.01 times that of uranyl nitrate is applied here.

(902) Specific absorption parameter values of $f_r = 0.6$, $s_r = 0.15$ d^{-1} and $s_s = 0.005$ d^{-1} (consistent with assignment to default Type M) and $f_A = 0.0002$ are used here for UF_4.

Uranyl acetylacetonate

(903) Uranyl acetylacetonate is an organic complex of uranium with military applications. *In vitro* dissolution tests in simulated lung fluid led to the classification of 50% Class D and 50% Class W (Fisher and Briant, 1994). Absorption parameter values calculated here are $f_r = 0.52$, $s_r = 2.5$ d^{-1} and $s_s = 0.026$ d^{-1}, corresponding to default Type M. These data (*in vitro* only) are judged to be an insufficient basis to propose specific absorption parameter values and uranyl acetylacetonate is therefore assigned to Type M.

Uranium aluminide

(904) As part of an epidemiological study, Leggett et al. (2005) estimated doses for workers exposed to airborne uranium aluminide (UAl_x) during the fabrication of reactor fuel plates. Occupational monitoring data included air concentrations, urine, fecal and lung measurements with observation periods exceeding two years in several cases. In workers who were removed from exposure, the rate of urinary excretion of uranium increased for a few months, peaked, and then declined at a rate consistent with moderately soluble uranium. To represent this behaviour, the authors applied the alternative HRTM representation of dissolution, in which material is deposited in a compartment representing "Particles in initial state", in which it dissolves at a rate s_p, and is simultaneously transferred at a rate s_{pt} to a compartment representing "Particles in transformed state", in which material dissolves at a rate s_t. They derived material specific parameter values: $s_p = 0.0001$ d^{-1}, $s_{pt} = 0.004$ d^{-1}, $s_t = 0.004$ d^{-1}, with f_A taken to be 0.002. These parameter values are adopted here for uranium aluminide.

Uranium octoxide (U_3O_8)

(905) Uranium octoxide can be present in the ore concentrate ("yellow cake", see ADU above) and also occurs at later stages in the uranium fuel cycle. Human data from accidental intakes of U_3O_8 (Saxby et al., 1964, West et al., 1979, Eidson, 1990), and from monitoring data for workers in processing facilities (Barber and Forrest, 1995, Chalabreysse et al., 1989), animal studies using rats, dogs and monkeys (Métivier et al., 1992, Stradling et al., 1989), and *in vitro* studies (Eidson, 1994, Ansoborlo et al., 1998a, Chazel et al., 1998) have shown that the biokinetic behaviour of this compound depends on the particular process of manufacture. A study of the influence of specific surface area (SSA) (Chazel et al., 1998) demonstrated the importance of this parameter on dissolution characteristics. When the SSA increased from 0.7 to 16 m^2 g^{-1}, the rapidly dissolved fraction, f_r, increased from 0.01 to 0.20. At 30 d after intake by rats and baboons, lung retention and total urinary excretion were 50-90% and 2–10%, respectively, of the initial lung deposit.

(906) Ansoborlo et al. (2002) derived absorption parameter values from the results of studies in which the biokinetics of uranium were followed for 90 days after intratracheal instillation into rats of two forms of U_3O_8: (i) $f_r = 0.046$, $s_r = 2.25$ d^{-1} and $s_s = 0.0012$ d^{-1}; (ii) $f_r = 0.03$, $s_r = 2.07$ d^{-1} and $s_s = 0.00038$ d^{-1}. Hodgson et al. (2000) derived absorption parameter values from the results of a study by Stradling et al. (1987) in which the biokinetics of uranium were followed for 360 days after inhalation by rats of uranium ore concentrate (95% U_3O_8, 5% UO_2); $f_r = 0.044$, $s_r = 0.49$ d^{-1} and $s_s = 0.00035$ d^{-1}. Experimental data on

ingestion of U_3O_8 by laboratory animals, reviewed by Leggett and Harrison (1995), suggest that absorption in the alimentary tract is about 0.01 times that of uranyl nitrate, which is taken here to be 0.02 (see above).

(907) Specific absorption parameter values of $f_r = 0.04$, $s_r = 1$ d^{-1} and $s_s = 0.0006$ d^{-1} (consistent with assignment to default Type S) and $f_A = 0.0002$ are used here for U_3O_8.

Uranium dioxide (UO_2)

(908) Uranium dioxide is the final product in the manufacture of nuclear fuel pellets, and is also present as depleted uranium in mixed oxide fuel (MOX). Manufacturing processes of UO_2 differ from one industry to another. Human studies have shown that UO_2 can be very insoluble (Pomroy and Noel, 1981, Price, 1989, Schieferdecker et al., 1985). Experiments in rats, dogs, monkeys and baboons (Leach et al., 1973, Stradling et al., 1988, Métivier et al., 1992) also support the assignment of UO_2 to default Type S. At 30 d after intake by rats and baboons, the total urinary excretion was 1–4% ILD and lung retention was 60-90% ILD. The effect of SSA on dissolution has been investigated (Chazel et al., 2000b), but in contrast to U_3O_8 (see above), no clear effect was observed. For compounds with SSA varying from 1.0 to 4.4 m^2 g^{-1}, f_r values were from 0.003 to 0.004.

(909) Ansoborlo et al. (2002) derived absorption parameter values from the results of studies in which the biokinetics of uranium were followed for 75 or 90 days after intratracheal instillation into rats of three forms of UO_2: (i) $f_r = 0.03$, $s_r = 1.25$ d^{-1} and $s_s = 0.0015$ d^{-1}; (ii) $f_r = 0.01$, s_r not determined and $s_s = 0.00049$ d^{-1} (iii) $f_r = 0.01$, s_r not determined and $s_s = 0.00058$ d^{-1}. Hodgson et al. (2000) derived absorption parameter values from the results of a study by Stradling et al. (1988) in which the biokinetics of uranium were followed for 315 days after inhalation by rats of two forms of UO_2; (non-ceramic) $f_r = 0.011$, $s_r = 0.95$ d^{-1} and $s_s = 0.00061$ d^{-1}; (ceramic) $f_r = 0.008$, $s_r = 1.3$ d^{-1} and $s_s = 0.00026$ d^{-1}. All but the first of these five sets of parameter values are consistent with assignment to default Type S. Experimental data on ingestion of UO_2 by laboratory animals, reviewed by Leggett and Harrison (1995), suggest that absorption in the alimentary tract is about 0.1-0.01 times that of uranyl nitrate, which is taken here to be 0.02 (see above). Since data on U_3O_8 (which tends to dissolve somewhat more rapidly in the lungs than UO_2) suggest that absorption in the alimentary tract is about 0.01 times that of uranyl nitrate, the lower value is applied here.

(910) Specific absorption parameter values of $f_r = 0.015$, $s_r = 1$ d^{-1} and $s_s = 0.0005$ d^{-1} (consistent with assignment to default Type S) and $f_A = 0.0002$ are used here for UO_2.

Vaporised uranium metal

(911) A new method for uranium enrichment, based on laser isotopic separation, can produce three different types of aerosol identified as variable mixtures of U_{metal} + UO_2 + U_3O_8, with different particle size distributions. Ansoborlo et al. (1998b, 2002) derived absorption parameter values from the results of studies in which the biokinetics of uranium were followed for 126 or 168 days after intratracheal instillation into rats of three such materials: (i) $f_r = 0.36$, $s_r = 1.44$ d^{-1} and $s_s = 0.0046$ d^{-1}; (ii) $f_r = 0.20$, $s_r = 0.68$ d^{-1} and $s_s = 0.00094$ d^{-1} ;(iii) $f_r = 0.12$, $s_r = 1.45$ d^{-1} and $s_s = 0.0026$ d^{-1} (all consistent with assignment to default Type M).

(912) In view of the wide range of values of s_s derived in the study above, these data are judged to be an insufficient basis to propose specific absorption parameter values and vaporised uranium metal is therefore assigned to Type M.

Uranium ore dust

(913) Duport et al. (1991) measured the dissolution in simulated lung fluid of long lived radionuclides in uranium ore dust from Canadian mines (and also in samples of yellowcake and refined oxides). (For further information see the section below on decay products of uranium formed in the lungs.) Factors including ore grade (uranium content), particle size, and solution pH were investigated. For high grade ore, measurements were made for up to 60 days, on particles in size ranges that included respirable particles. Results were presented as undissolved fractions as functions of time, and showed two components, which were expressed as Class D (rapid) and Class Y (slow) fractions. For ^{238}U, the rapidly dissolved fraction was ~0.25 indicating assignment to Type M. No effect of size was observed in total dissolution over 40 days for particles in size ranges 7–10, 3–7, 1–3 and <1 µm. For low grade and medium grade ores, measurements were made for 12 days, but only on samples of relatively coarse dust, the smallest fraction being <37 µm. For ^{238}U, rapidly dissolved fractions were greater than those measured in the high grade ores; about 0.33 and 0.5 for low and medium grade ores respectively.

(914) Bečková and Malátová (2008) measured dissolution for 26 days of ^{238}U, ^{234}U and ^{230}Th in simulated serum ultrafiltrate of uranium ore dust collected on personal air filters in a mine in the Czech Republic. Retention (undissolved) was represented by a two-component exponential function, giving parameter values for ^{238}U of $f_r = 0.14$, $s_r = 0.49$ d^{-1} and $s_s = 0.004$ d^{-1} and assignment to Type M. Dissolution of ^{234}U was somewhat faster, as expected due to recoil phenomena: $f_r = 0.18$, $s_r = 0.49$ d^{-1} and $s_s = 0.006$ d^{-1}. (For further information see the section below on decay products of uranium formed in the lungs, and the thorium inhalation section.)

(915) Marsh et al. (2011) estimated the following parameter values for dissolution of uranium from ore dust, based on the results of both Duport et al. (1991) (high grade ore) and those of Bečková and Malátová (2008): $f_r = 0.2$, $s_r = 0.8$ d^{-1} and $s_s = 0.0014$ d^{-1}.

(916) For a summary of *in vivo* and autopsy studies relating to uranium ore dust see the section below on decay products of uranium formed in the lungs.

Depleted uranium (DU)

(917) Depleted uranium, a by-product of the manufacture of enriched uranium for nuclear reactor fuel, has found a number of applications resulting mainly from its high density, in particular, in anti-tank munitions, counterweights for aircraft control surfaces and radiation shielding. DU, typically alloyed with 0.75% titanium is used in 'kinetic energy penetrators', rods of the metal fired at very high speed (~1.5 km s^{-1}). On impact with a hard object such as armour plate, a significant fraction of the penetrator mass may be converted to an aerosol that could be inhaled by persons in the vicinity or downwind. *In vitro* tests have shown considerable variability in that 1–50% of the respirable material dissolves rapidly, and the rest very slowly, while X-ray analyses indicate that the uranium is present as a mixture of oxides including U_3O_7, U_3O_8, U_4O_9, and UO_2, but also combinations with other metals (Glissmeyer and Mishima, 1979, Scripsick et al.,1985a, 1985b, Chazel et al., 2003, Mitchel and Sunder, 2004). *In vitro* dissolution tests carried out by Chazel et al. (2003) gave dissolution parameter values in the following ranges: $f_r = 0.47$–0.57, $s_r = 0.06 - 0.07$ d^{-1} and $s_s = 0.00018$ to 0.00034 d^{-1}, giving assignment to Type M.

(918) In the comprehensive Capstone DU Aerosol Study, aerosols formed when DU rounds penetrated armoured vehicles were used in studies of dissolution in simulated lung fluid, making measurements over 46 days on a total of 27 samples (Parkhurst et al., 2004a, 2004b; Parkhurst and Guilmette, 2009; Guilmette and Cheng, 2009). Dissolution was fitted by two- or three-component exponential functions. Based on the two-component fits, there

was a rapidly dissolving fraction of 1-28% (geometric mean, GM, 12.5%), with an associated rapid dissolution rate of 0.1-30 d^{-1} (GM 6 d^{-1}; corresponding half-time, $t_{1/2}$ = 0.12 d). The remaining fraction dissolved at a slow rate of 0.0004-0.0095 d^{-1} (GM 0.0026 d^{-1}: $t_{1/2}$ = 268 d). Thus there was considerable variation between samples, especially in the fraction that dissolved rapidly. There appeared to be some correlation between the initial and final dissolution rates: the greater the dissolution in the first day, the faster the long term dissolution rate. Based on extrapolation of the three-component exponential function where available (two-component otherwise), 24 samples would be assigned to Type M and three to Type S. Several sets of measurements were made on different stages from the same cascade cyclone. However, there was no clear trend of dissolution with particle size and in some cases the back-up filter, with the smallest particles, showed the slowest dissolution. Two confounding factors were noted: (1) cyclone cut-offs are not sharp, so there was considerable overlap in size distribution between stages (2) scanning electron microscope examination showed great heterogeneity of particle composition, shape etc.

(919) Mitchel and Sunder (2004) followed urinary excretion of uranium for 7 days after intratracheal instillation into rats of the <50-µm fraction of dust obtained from impact of DU munitions on armour plate. Results indicate that about 10% ILD dissolved during 7 days, about half of it within 1 day. However, the large size suggests that the material was from surface deposits rather than air samples, and may not be representative of dust that might be inhaled.

(920) If large pieces of uranium metal are subjected to fire (e.g. in a burning vehicle or aircraft crash - generally depleted uranium is used in applications which require only the non-fissile properties of uranium) they will gradually oxidise and some of the oxide may be dispersed and inhaled. *In vitro* tests have shown that 0.5–10% of the respirable material dissolves rapidly, and the rest very slowly, while X-ray analyses indicate that most of the uranium is present as U_3O_8 (Mishima et al., 1985, Elder and Tinkle, 1980, Scripsick et al., 1985a, OSAGWI, 2000). Default Type M should be assumed.

(921) Overall, the available data show that the dissolution and lung absorption of particulate DU, whether formed by the impact of kinetic energy penetrators, or in fires, is very variable. It is therefore judged to be inappropriate to propose specific absorption parameter values and DU is therefore assigned to default Type M.

Irradiated fuel fragments

(922) Following an accidental release from a nuclear reactor, fission and activation products may be present in fragments of irradiated fuel, of which the matrix is predominantly uranium dioxide (Devell, 1988, Begichev et al., 1989, Toivonen et al., 1992). In studies of the *in vitro* dissolution of particles released from the Chernobyl accident, seven out of ten of which consisted mainly of uranium (Cuddihy et al., 1989), the data obtained were consistent with assignment of all the γ-emitting radionuclides to Type M.

Decay products of uranium formed in the respiratory tract

(923) Decay schemes of uranium isotopes in the natural decay series: ^{234}U, ^{238}U and ^{235}U, are described in Figure 15-1 and Figure 15-2. The ^{232}Th decay series is shown in the thorium inhalation section (Figure 14-1): it is relevant to ^{232}U, which decays to ^{228}Th, a descendent of ^{232}Th.

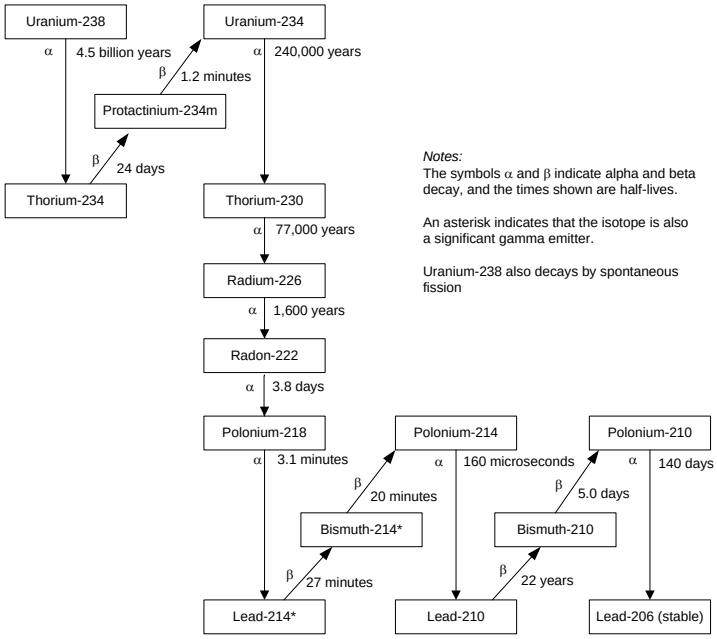

Figure 15-1. Natural decay series: Uranium-238

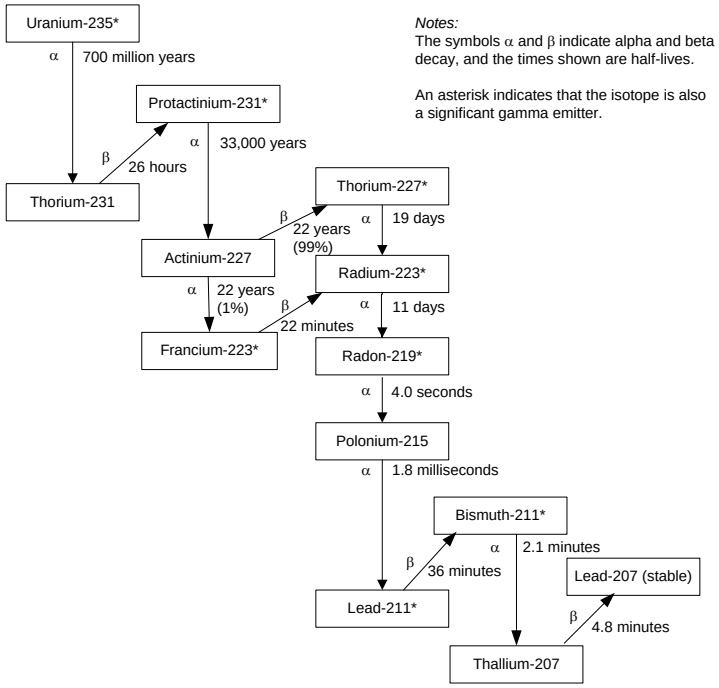

Figure 15-2. Natural decay series: Uranium-235

(924) The general approach to treatment of decay products formed in the respiratory tract is described in Part 1, Section 3.2.3. In summary, it is expected that generally the rate at which a particle dissociates is determined by its matrix, and hence the physico-chemical form of the inhaled material. It is recognised that for decay products formed within particles by alpha emission, recoil of the daughter nucleus from the alpha emission expels some of the decay product from the particle. In the case of decay chains, this will result in successively lower activities of members compared to the parent retained in relatively insoluble particles.

Experimental evidence relating to this is described in the section on relatively insoluble (Type S) forms of thorium formed in the respiratory tract. However, it was considered impractical to implement loss of decay products by alpha recoil in the calculation of dose coefficients and bioassay functions in this series of documents. (For further information see Part 1, Section 3.2.3.) Nevertheless, this phenomenon should be borne in mind, especially when using decay products to monitor intakes and doses of the parent, which can be applicable to uranium.

(925) Exceptions are made for noble gases formed as decay products, which are assumed to escape from the body directly, in addition to other routes of removal. For calculation purposes it is assumed that radon formed as a decay product within the respiratory tract escapes from the body at a rate of 100 d^{-1}, in addition to other routes of removal. For further information see the section on relatively insoluble (Type S) forms of thorium formed in the respiratory tract.

(926) It is expected that the behaviour of soluble (e.g. Type F) material in the respiratory tract would depend on its elemental form, i.e. that of the decay product. Nevertheless, for simplicity, in this series of documents the absorption parameter values of the parent are, by default, applied to all members of the decay chain formed in the respiratory tract.

(927) The formation of thorium as a decay product can be of particular importance in this context, because there can be significant long-term retention of thorium in the lungs following its deposition in soluble form (see thorium inhalation section). Conversely, important decay products of thorium, notably radium and lead, in soluble forms, are (like uranium) relatively readily absorbed from the respiratory tract into the systemic circulation. Studies specifically comparing the behaviour of uranium with that of its decay products are summarised here, although it should be noted that the thorium was mainly administered with the uranium, rather than formed from decay of uranium in the respiratory tract. For more information, see also the sections on thorium, radium, polonium, lead and bismuth, relating to the behaviour of their decay products formed in the respiratory tract.

Relatively soluble (Type F) forms

(928) As noted above, Ballou et al. (1986) studied the biokinetics of ^{232}U and ^{233}U in rats after inhalation of uranyl nitrate aerosols. For the main studies, the uranium was freshly separated from its decay products, and measurements were not made of decay products formed within the body. Uranium-233 has a long half-life (1.6×10^5 years), but that of ^{232}U is only 74 years and the authors recognised that assessment of doses from occupational exposure to ^{232}U needed to take account of the behaviour of its decay products, especially ^{228}Th. A complementary experiment was carried out in which tissue distributions of ^{232}U, ^{228}Th, ^{224}Ra, ^{212}Pb, ^{212}Bi and ^{208}Tl were measured at 24 hours after intratracheal instillation into rats of ^{232}U nitrate with its decay products. Although measurements of ^{228}Th, ^{224}Ra, and perhaps ^{212}Pb, were mainly of material administered with the parent ^{232}U, rather than formed from its decay in the lungs, it is reasonable to assume similar behaviour. (The physical half-lives of ^{212}Bi and ^{208}Tl are so short, 61 minutes and 3 minutes respectively, that measurements made at 24 hours would mainly be of activity formed *in situ*.) Lung retention was 7.9% ILD for ^{232}U, 52% ILD for ^{228}Th, and about 2-3% ILD for the other decay products measured, reflecting the high lung retention of thorium, and relatively rapid lung clearance of radium and lead observed in other studies in which soluble forms were administered. Similarly, the distribution between liver, skeleton and kidneys of ^{232}U, ^{228}Th, ^{224}Ra and ^{212}Pb reflected the elemental forms. The distributions of ^{212}Bi and ^{208}Tl were similar to those of ^{212}Pb, presumably because of their short physical half-lives: whatever their distribution *in vivo*, they would tend to equilibrium between dissection and measurement. Ballou et al. noted that the

greater retention of ^{228}Th in the lungs and deposition in skeleton than of the ^{232}U, suggested that assessments based on the assumption of shared kinetics would significantly underestimate doses.

(929) Stradling et al. (2005) followed the biokinetics of uranium and thorium for 3 months after intratracheal instillation into rats of the nitrates, given separately, or together at uranium: thorium mass ratios of $5x10^6$:1 or 50:1. Their behaviour when administered separately was as expected from other studies: by 1 day ~80% ILD of uranium but only ~30% ILD of thorium had been absorbed into blood. The behaviour of thorium was not significantly affected by the presence of uranium when they were administered together (for further information see thorium inhalation section).

Relatively insoluble (Type M or S) forms

(930) Hill (1962) noted the disequilibrium between the early long-lived members of the uranium decay series measured in a lung sample from a uranium miner, although they were probably close to equilibrium in the uranium ore to which he was exposed. The concentration of ^{230}Th was about twice, and that of ^{226}Ra about half, that of ^{238}U or ^{234}U, suggesting selective removal of radium and uranium compared to thorium.

(931) Stuart and Beasley (1967) followed the biokinetics of uranium (^{238}U + ^{234}U) and thorium (^{228}Th) for up to 4 months after repeated inhalation by rats of uranium ore dust (pitchblende, 25% U_3O_8, with uranium and thorium in secular equilibrium) over an 8-week period. Faster clearance from the lungs of uranium than thorium was observed: at 1 week after the end of exposures the thorium activity was 2 – 3 times that of ^{238}U or ^{234}U. Stuart and Jackson (1975) similarly found ^{230}Th concentrations were several times those of ^{238}U in the lungs and lymph nodes of dogs at 2 weeks or 15 months after repeated inhalation of the same uranium ore (Cross et al., 1982). They also reported that thorium concentrations in the lungs were about twice those of uranium in hamsters one year after repeated inhalation of carnotite ore dust (4% U_3O_8, with uranium and thorium in secular equilibrium), and several times higher in dogs after several years of daily inhalation exposure. Thus even though the material was relatively insoluble, and the thorium was present as a minor component by mass, its slower absorption from the lung than that of uranium could be observed.

(932) Fisher et al. (1983) measured significantly higher activity levels of ^{234}U and ^{238}U than of the daughter product ^{230}Th in both urine and fecal samples obtained from active uranium millers, indicating that uranium in the inhaled ore dust was cleared from the body with a shorter biological half-time than the daughter product ^{230}Th. Assessment of lung clearance from the results is not straightforward, especially given the chronic and continuing exposures. Higher urinary excretion of uranium than of thorium would be expected even if absorption from the lung were at similar rates, because of the higher urinary excretion of systemic uranium. For both elements fecal clearance dominated, and given the high urinary excretion of systemic uranium, this suggests greater lung clearance by particle transport than by absorption to blood. The lower fecal excretion of thorium than of uranium suggests a lower particle transport rate, and hence that there is binding of thorium released in the lungs by dissolution. However, it was recognised by the authors that other sources of fecal excretion of uranium (dietary intakes, exposure to refined uranium which is depleted in thorium) could not be excluded.

(933) In contrast, Wrenn et al. (1983) measured ^{230}Th concentrations similar to those of ^{234}U in the lungs of five uranium miners (average ^{230}Th/^{234}U ratio 1.1, range 0.54–2.6). They noted that this was surprising in view of the results of the reported disequilibrium in dogs chronically exposed to carnotite (see above). An interlaboratory comparison was conducted,

which showed that the difference was not due to differences in radiochemical methods (Singh et al., 1986a). In a later study (Singh et al., 1987) the same group found ratios of 1.5–3.5 in the lungs of three uranium miners and 1.1–1.3 in the lungs of two uranium millers: they concluded that overall, dissolution in the human lungs of uranium and thorium in uranium ore dust was similar.

(934) As noted above, Duport et al. (1991) measured the dissolution in simulated lung fluid of long lived radionuclides in uranium ore dust from Canadian mines. For high grade ore, measurements were made for up to 60 days, on particles in size ranges that included respirable particles. For ^{238}U, ^{230}Th, ^{226}Ra, and ^{210}Pb, the rapidly dissolved fractions were 0.25, 0.15, 0.12 and 0.28 respectively. Marsh et al, 2011, fitted two-component exponential functions to the data (un-dissolved fractions) and obtained the following HRTM parameter values:

Nuclide	f_r	s_r (d^{-1})	s_s (d^{-1})
^{230}Th	0.14	4.6	0.0007
^{226}Ra	0.11	7.3	0.0004
^{210}Pb	0.26	3.9	0.001

(935) For these radionuclides, no effects of size were observed in total dissolution over 40 days for particles in size ranges 7–10, 3–7, 1–3 and <1 µm. For low grade and medium grade ores, measurements were made for 12 days, but only on samples of relatively coarse dust, the smallest fraction being <37 µm. For ^{238}U, rapidly dissolved fractions were higher (0.33 and 0.5 for low and medium grade ores) than those measured in the high grade ores. However, for other radionuclides the fractions were lower: 0.07 for ^{226}Ra, and <0.01 for ^{210}Pb. Measurements were also made for ^{232}Th in low grade ore and ^{210}Po in low and medium grade ores, and much lower fractions obtained, 0.01, 0.00 and 0.005 respectively. Consistent differences in dissolution between uranium and its decay products were not apparent.

(936) As noted above, Bečková and Malátová (2008) measured dissolution for 26 days of ^{238}U, ^{234}U and ^{230}Th in simulated serum ultrafiltrate of uranium ore dust collected on personal air filters in a mine in the Czech Republic. Moderate dissolution of both uranium isotopes was observed, with f_r = 0.14 for ^{238}U and 0.18 for ^{234}U, but no dissolution of ^{230}Th was detected.

(937) Griffith et al. (1980) developed a model to describe the retention of ^{232}U and its decay products, in the lungs following inhalation in ThO_2 or UO_2 particles. In addition to chemical dissolution, they considered recoil emanation of daughter product nuclei by alpha-particle decay, and diffusion emanation of ^{220}Rn from particles. In complementary experiments, Coombs and Cuddihy (1983) measured the fraction of ^{228}Th escaping by recoil and the fraction of ^{220}Rn escaping by diffusion from size-fractionated samples of ThO_2 and uranium oxide (mixture of $UO_{2.2}$ and U_3O_8) containing 1% ^{232}U. For further information on these and other studies relating to recoil emanation of decay products and to loss of radon formed in the respiratory tract see the section on decay products of thorium formed in the respiratory tract.

Rapid dissolution rate for uranium

(938) Studies on the uranium compounds which are most rapidly absorbed from the lungs (uranium hexafluoride and uranyl tri-butyl-phosphate) give values of s_r of about 10 d^{-1}, which is applied here to all Type F forms of uranium in the absence of material-specific data.

Extent of binding of uranium to the respiratory tract

(939) Experimental evidence suggests that there is little binding of uranium to the respiratory tract. Cooper et al. (1982) and Ellender (1987) followed the behaviour of ^{233}U after instillation of uranyl nitrate and bicarbonate into the pulmonary region of the lungs of rats. Cooper et al. (1982) found that less than 2% ILD remained at 7 days. Ellender (1987) gave more information for the nitrate, for which about 8% ILD remained at 1 d and 3% at 30 d. Detailed analysis, however, indicates that clearance over this period was mainly by particle transport, and that the results did not provide evidence for binding of uranium (Hodgson, et al., 2000). It is therefore assumed that for uranium the bound state can be neglected, i.e. f_b = 0.0.

Table 15-2. Absorption parameter values for inhaled and ingested uranium

Inhaled particulate materials	Absorption parameter values[a] f_r	s_r (d^{-1})	s_s (d^{-1})	Absorption from the alimentary tract, f_A [d]
Specific parameter values[b]				
Uranyl Tri-Butyl-Phosphate (U-TBP)	0.97	12	0.002	0.02
Uranyl nitrate, $UO_2(NO_3)_2$	0.9	3	0.005	0.02
Uranium peroxide hydrate UO_4	0.9	0.9	0.02	0.01
Ammonium diuranate, ADU	0.8	0.7	0.02	0.02
Uranium trioxide UO_3	0.8	1	0.01	0.01
Uranium tetrafluoride UF_4	0.6	0.15	0.005	$2x10^{-4}$
Triuranium octoxide U_3O_8	0.04	1	$6x10^{-4}$	$2x10^{-4}$
Uranium dioxide UO_2	0.015	1	$5x10^{-4}$	$2x10^{-4}$
Uranium aluminide UAl_X	c	c	c	0.002
Default parameter values[d,e]				
Absorption Type / Assigned forms				
F — Uranium hexafluoride, UF_6	1	10	-	0.02
M — Uranyl acetylacetonate; DU aerosols from use of kinetic energy penetrators; vaporized U metal; all unspecified forms[f]	0.2	3	0.005	$4x10^{-3}$
S — —	0.01	3	$1x10^{-4}$	$2x10^{-4}$
Ingested materials				
Soluble forms (Type F)	–	–	–	0.02
Relatively insoluble forms (as assigned to Types M and S for inhalation)	–	–	–	0.002

[a] It is assumed that for uranium the bound state can be neglected, i.e. $f_b = 0.0$. The value of s_r for Type F forms of uranium (10 d^{-1}) is element-specific. The values for Types M and S (3 d–1) are the general default values.

[b] See text for summary of information on which parameter values are based, and on ranges of parameter values observed for individual materials. For uranium specific parameter values are used for dissolution in the lungs, and where information is available for absorption from the alimentary tract. For other materials, the default value of f_A is used (footnote d).

[c] See text: $s_p = 1x10^{-4}\ d^{-1}$, $s_{pt} = 4x10^{-3}\ d^{-1}$, $s_t = 4x10^{-3}\ d^{-1}$, with f_A taken to be 0.002.

[d] For inhaled material deposited in the respiratory tract and subsequent cleared by particle transport to the alimentary tract, the default f_A values for inhaled materials are applied: i.e. the (rounded) product of f_r for the absorption Type (or specific value where given) and the f_A value for ingested soluble forms of uranium (0.02).

[e] Materials (e.g. UF_6) are listed here where there is sufficient information to assign to a default absorption Type, but not to give specific parameter values (see text).

[f] Default Type M is recommended for use in the absence of specific information, i.e. if the form is unknown, or if the form is known but there is no information available on the absorption of that form from the respiratory tract.

15.2.2. Ingestion

(940) Data on the absorption of uranium have been reviewed by Wrenn et al. (1985), Harrison (1991), Leggett and Harrison (1995) and in ICRP *Publication 69* (1995).

(941) In the first controlled human study involving more than one subject, Hursh et al. (1969) administered uranyl nitrate to four hospital patients. The data obtained were taken to

suggest fractional absorption in the range 0.005 - 0.05. Leggett and Harrison (1995) have interpreted the data as suggesting absorption of 0.004, 0.01, 0.02 and 0.06, respectively, for the four subjects. Wrenn et al., (1989) estimated absorption in twelve normal healthy adult volunteers given drinking water high in uranium. On the basis that 40 - 60% of absorbed U was excreted in the urine in the first three days, rather than the author's assumption of 79%, Leggett and Harrison (1995) concluded that mean absorption was 0.01-0.015, maximum absorption was in the range 0.02-0.04, and that six subjects absorbed less than 2.5×10^{-3}. Harduin et al., (1994) reported results for the absorption of U from drinking water either administered on one day or over 15 days. The data for acute administration suggested absorption of 0.005-0.05 with an average value of 0.015-0.02. The data for 15-day administration suggested absorption of 0.003-0.02 and average absorption of 0.01-0.015. In another *in situ* study, the gastro-intestinal absorption factor was determined for 50 participants ingesting uranium at natural levels in drinking water and food. The participants, ranged in age from 13 to 87 years were selected from either a Canadian area with naturally high (2-780 $\mu g.L^{-1}$) or low (<1$\mu g.L^{-1}$) uranium levels. The distribution of f_1 values obtained was non-Gaussian with a range of 0.001 to 0.06 and a median of 0.009 (Zamora et al, 2002). These values were not gender sensitive and independent of age at the time of the study, duration of exposure and total uranium intake. Similar results have also been obtained in a number of dietary balance studies (Larsen and Orlandini, 1984; Spencer et al., 1990; Wrenn et al., 1989; Leggett and Harrison, 1995).

(942) Data from animal studies provide information on the relative uptake of U ingested in different chemical forms, showing that absorption is strongly dependent on the solubility of the compound. Measurements have been made in rats, hamsters, rabbits, dogs and baboons (reviewed by Wrenn et al., 1985; Harrison, 1991; Leggett and Harrison, 1995). Absorption appears to be greatest for U ingested as $UO_2(NO_3)_2.6H_2O$, U-TBP, UO_2F_2 or $Na_2U_2O_7$, roughly half as great for UO_4 or UO_3, and 1 - 2 orders of magnitude lower for UCl_4, U_3O_8, UO_2 and UF_4. It should be noted, however, that the solubility of some poorly soluble U compounds can vary substantially with thermal history as well as particle size (Cooke and Holt, 1974). Thus, greater absorption as UO_2 in hamsters than rats and dogs, could reflect solubility of the preparation of UO_2 rather than just species differences. A number of studies have shown that absorption is substantially greater in fasted than fed animals. For example, Bhattacharyya et al., (1989) found that uptake was increased by an order of magnitude in mice and baboons deprived of food for 24 h prior to U administration. Sullivan (1980) reported a 2 – 4 fold increase in U absorption in rats given U nitrate after a 24 hour fast.

(943) In *Publication 30* (ICRP, 1979), an f_1 of 0.05 was recommended for water soluble inorganic forms of U(VI) and a value of 0.002 for U(IV) in relatively insoluble compounds such as UF_4, UO_2 and U_3O_8. In *Publication 69* (ICRP, 1995), an f_1 of 0.02 was adopted for dietary intakes of U on the basis of human data as reviewed by Wrenn et al., (1985), Harrison (1991) and Leggett and Harrison (1995). The available human and animal data indicate that a value of 0.02 is also appropriate for occupational exposures to more soluble inorganic forms, including $UO_2(NO_3)_2.6H_2O$, UO_2F_2 and $Na_2U_2O_7$.

(944) In this report, an f_A value of 0.002 is adopted for the fractional absorption of relatively insoluble compounds (e.g. UO_2, U_3O_8) and an f_A value of 0.02 is adopted for all other more soluble chemical forms (Table 15-2).

15.3. Systemic Distribution, Retention and Excretion

15.3.1. Summary of the database

12174
12175 **Controlled studies on human subjects**

12176 (945) The systemic biokinetics of uranium has been investigated in three human injection
12177 studies known as the Boston study, the Rochester study, and the Terepka study.

12178 (946) The Boston study (Struxness et al., 1956; Bernard and Struxness, 1957; Luessenhop
12179 et al., 1958) involved 11 patients, ages 26-63 y, in the terminal phases of diseases of the
12180 central nervous system. Most of the subjects were comatose at the time of injection. Uranyl
12181 nitrate solutions enriched with ^{234}U and ^{235}U were administered to Subjects 1-6 and Subjects
12182 9-11 by intravenous injection. Subjects 7 and 8 received intravenous injections of tetravalent
12183 uranium as UCl_4. The mass of administered uranium was varied from one subject to another
12184 but ranged up to about 1 mg/kg. The mass of injected uranium is known only approximately
12185 for Subjects 2, 9, 10 and 11. In some cases, several bone biopsy samples were taken from the
12186 anterior tibia during the first day or two after injection. Extensive measurements of uranium
12187 in blood and excreta were made over the first several weeks or months after injection. Urinary
12188 uranium measurements were made over several months in some of the Boston subjects and
12189 extended to times >1 y for one subject. Autopsy samples were obtained from various bones
12190 and soft tissues of subjects dying at times from 2.5 d to 4.5 months after injection and from
12191 one subject dying 566 d after injection.

12192 (947) Selected data from the Boston study are summarised in Table 15-3. The range of
12193 values given for bone indicate the lower and upper bounds derived from different
12194 assumptions regarding the portion of the skeleton represented by samples collected at
12195 autopsy.

12196

Table 15-3. Summary of results for eight of the Boston subjects, based on data of Struxness et al. (1956) and Bernard and Struxness (1957), and logbooks from the Boston study (after Leggett, 1994).

Subject number	1	6	9	11	2	10	5	3
Time to death (d)	2.5	18	25	28	74	94	139	566
Urinary U, day 1 (%)	59	49	~80	~60	78	~80	67	84
Kidney (%)	14	6	1.7	1.6	0.6	0.8	1.0	0.3
Bone (%)	8-12	4-13	1.5-2.5	2-3	1.2-2	2.5-3	0.5-0.7	1.1-1.7
Liver (%)	1.5	1.0	0.2	0.05	0.2	0.01	0.15	0.05
Other soft tissues (%)	6	4	1	2	1.5	2.5	0.5	0.3

12197

12198 (948) The poor physical condition of the Boston subjects limits the confidence with which
12199 the data can be taken to represent the typical biokinetics of uranium. Struxness et al. (1956)
12200 pointed out that the bed-ridden condition of these subjects indicated a negative calcium
12201 balance, which might "hasten the removal of uranium from the skeleton". Also, the subjects
12202 were given relatively high masses of uranium. Animal studies indicate that administration of
12203 high masses of uranium will result in elevated uptake and retention in kidneys, among several
12204 potential effects on biokinetics (Bernard and Struxness, 1957; Leggett, 1989; 1994). A third
12205 difficulty is that the post-mortem data are not sufficiently detailed in some cases to allow a
12206 close determination of the total uranium content of some organs or tissues, particularly the
12207 skeleton.

12208 (949) The Rochester study involved two female and four male subjects, ages 24-61 y,
12209 chosen because they had reasonably good kidney function and their urine was free of protein
12210 (Bassett et al., 1948). These subjects were hospital patients but were ambulatory. Subjects 1-

6, respectively, suffered from rheumatoid arthritis, cirrhosis of the liver, chronic undernutrition, alcoholism, unresolved pneumonia, and pulmonary fibrosis plus gastric ulcer. The subjects received intravenous injections of uranyl nitrate solutions enriched with ^{234}U and ^{235}U. Administered masses ranged from 6.3 to 70.9 μg U/kg. Total urine and faecal collection was made for up to 16 d, and several blood samples were taken.

(950) Terepka and co-workers (Terepka et al., 1964; Hursh and Spoor, 1973) investigated the possibility of evaluating bone disorders based on the level of retention of intravenously injected uranium. They injected hexavalent uranium (30 μg/kg) into three control patients and seven patients with various bone disorders (Paget's disease, hyper- or hypoparathyroidism, osteomalacia, or senile osteoporosis). Some patients were investigated before and after oestrogen or parathyroid extract treatments. Urinary excretion of uranium was measured for at least 6 d in each subject. Subjects with osteomalacia and Paget's disease showed radically reduced urinary uranium compared with controls, presumably due to radically increased uptake of uranium by the skeleton. Cumulative urinary uranium over 6 d was similar in controls and subjects with osteoporosis or hyper- or hypoparathyroidism.

Occupational and environmental studies

(951) Additional information on the biological fate of uranium in humans is provided by post-mortem measurements of uranium in tissues of occupationally and environmentally exposed subjects (Donoghue et al., 1972; Campbell, 1975; Roberts et al., 1977; Igarashi et al., 1985; Fisenne and Welford, 1986; Sing et al., 1986, 1987; Kathren et al., 1989; Russell and Kathren, 2004). Such studies provide information on the long-term distribution of uranium in the human body. For example, the collective data from these studies suggest that the skeleton typically contains 15-50 (median, ~30) times as much uranium as the liver, and the kidneys typically contain 0.2-0.6 (median, ~0.5) times as much uranium as the liver at times remote from the start of exposure. Some limitations of the post-mortem data for modelling purposes are the small numbers of subjects examined in most studies; uncertainties in the exposure histories of those subjects; uncertainties in estimates of total-organ contents of the subjects based on small samples of tissue, particularly skeletal tissues; and, in some cases, unreliable techniques for determining low concentrations of uranium in tissues or fluids.

Animal studies

(952) The biokinetics of uranium has been studied in baboons, dogs, rabbits, rats, mice, monkeys, sheep, and other animal species (see reviews by Durbin, 1984; Leggett, 1994; ICRP, 1995). As indicated in the following discussion of model parameter values, data from several animal studies were used in the development of parameter values for the systemic model described below. The animal data helped to fill gaps in the human data and in selection of some parameters were given heavier weight than questionable data for human subjects. In addition to uncertainties regarding interspecies extrapolation of results, the animal data have many of the same problems that complicate the human studies. For example, most animal studies involved administration of relatively high masses of U; there was often limited sampling of tissues, particularly bone and massive soft tissues such as muscle, fat, and skin; and some studies involved small numbers of animals. When potentially significant differences in numerical results were indicated by results of different animal studies, preference was generally given to baboons or dogs over rats or other small animals, and to results involving uptake of relatively low masses of uranium.

15.3.2. Biokinetic model for systemic uranium

(953) The biokinetic model for systemic uranium used in this report is the model for adults adopted in ICRP *Publication 69* (1995) and applied in ICRP *Publication 68* (1994a) to workers. The model structure (Figure 15-3) is the generic structure for elements that follow the movement of calcium in bone. Although the chemical analogy between UO_2^{2+} and Ca^{2+} is not strong in terms of affinity constants for mineral ligands (Ansoborlo et al., 2006), the behaviour of uranium in the skeleton shows qualitative similarities to that of calcium.

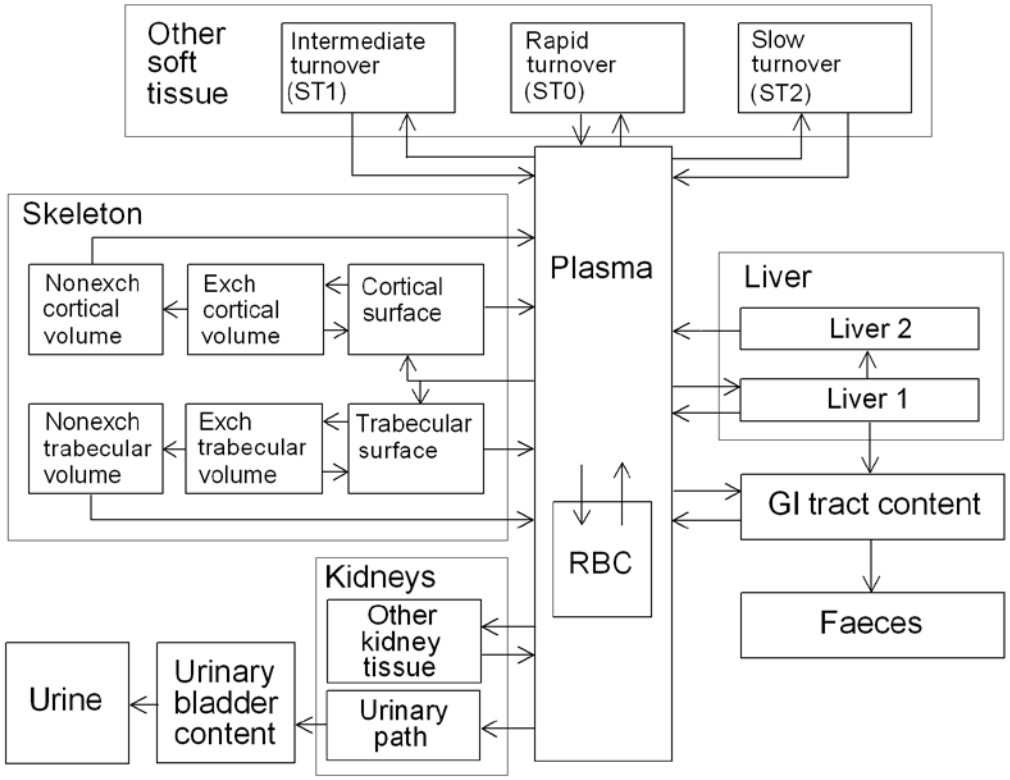

Figure 15-3. Structure of the model for systemic uranium.

(954) Parameter values for the worker are listed in Table 15-4. Primary databases and assumptions underlying parameter values are summarized below. Additional details and references can be found in an article by Leggett (1994). In that article parameter values are first discussed for a relatively detailed model with regard to the time dependent kinetics of uranium in blood and kidneys and then are adjusted to the less detailed generic model structure for calcium-like elements.

12278

Table 15-4. Transfer coefficients in the model for systemic uranium.

From	To	Transfer rate (d^{-1})
Plasma	ST0	10.5
Plasma	RBC	0.245
Plasma	Urinary bladder content	15.43
Plasma	Kidneys (Urinary path)	2.94
Plasma	Kidneys (Other kidney tissue)	0.0122
Plasma	Right colon content	0.122
Plasma	Liver 1	0.367
Plasma	ST1	1.63
Plasma	ST2	0.0735
Plasma	Trabecular bone surface	2.04
Plasma	Cortical bone surface	1.63
ST0	Plasma	8.32
RBC	Plasma	0.347
Kidneys (Urinary path)	Urinary bladder content	0.099
Kidneys (Other kidney tissue)	Plasma	0.00038
Liver 1	Plasma	0.092
Liver 1	Liver 2	0.00693
Liver 2	Plasma	0.00019
ST1	Plasma	0.0347
ST2	Plasma	0.000019
Trabecular bone surface	Plasma	0.0693
Trabecular bone surface	Exch trabecular bone volume	0.0693
Cortical bone surface	Plasma	0.0693
Cortical bone surface	Exch cortical bone volume	0.0693
Trabecular bone volume	Plasma	0.000493
Cortical bone volume	Plasma	0.0000821
Exch[a] trabecular bone volume	Trabecular bone surface	0.0173
Exch trabecular bone volume	Nonexch[b] trabecular bone volume	0.00578
Exch cortical bone volume	Cortical bone surface	0.0173
Exch cortical bone volume	Nonexch cortical bone volume	0.00578

[a] Exchangeable
[b] Non-exchangeable

12279

12280 *Blood clearance*

12281 (955) There is rapid loss of uranium from the circulation in the first few minutes after
12282 injection due to high rates of filtration by the kidneys and diffusion into extracellular fluid.
12283 The rate of disappearance declines as uranium returns from the extracellular spaces to blood
12284 and some uranium attaches to red blood cells. In human subjects given uranyl nitrate
12285 intravenously, median retention in blood was about 25% at 5 min, 10% at 2 h, 5% at 5 h, 1%
12286 at 20 h, and <0.5% at 100 h, but inter-subject variation was high (Bassett et al., 1948; Bernard
12287 and Struxness, 1957). Blood clearance rates observed in baboons (Lipsztein, 1981) and dogs
12288 (Rowland and Farnham, 1969) are similar to those determined in human subjects.

12289 (956) Limited measurements on human blood containing environmental levels of uranium
12290 indicate that a substantial portion of uranium in blood is associated with red blood cells
12291 (Leggett, 1994). Measurements of intravenously injected uranium in plasma and red blood
12292 cells of baboons showed that red blood cells contained on average about 10% of circulating

uranium after 2 hours, 25% after 6 hours, 80% after 1 day and at least 50% from 1 - 49 days (Lipsztein, 1981). These data indicate that about 0.5 – 1% of uranium from plasma attaches to red blood cells and is returned to plasma with a half-time of about 1 day (Leggett, 1994).

(957) Morrow et al. (1982) estimated that soft tissues of beagles given intravenous injections of UO_2F_2 contained about 24% of the administered amount after 24 hours and 4% after 48 hours. This presumably reflects a high rate of transfer of uranium from blood to extracellular fluids and subsequent return to the circulation over a period of hours.

(958) In the present model, plasma is taken to be a uniformly mixed pool from which uranium is removed at a rate of 35 d^{-1}, with 30% going to a soft-tissue compartment called ST0 that returns uranium to blood with a half-time of 2 h. Thus, the transfer coefficient from plasma to ST0 is 35 d^{-1} x 0.3 = 10.5 d^{-1} and from ST0 to plasma is ln(2) / 2 h = 8.32 d^{-1}. Resulting model predictions are in reasonable accord with data for blood clearance in the Boston subjects, animal data on binding of uranium to red blood cells (Lipsztein, 1981), and the early rise and fall of uranium in soft tissues of beagles (Morrow et al. (1982)).

Urinary excretion and renal retention

(959) Data from the human injection studies indicate that typically about two-thirds of intravenously injected uranium is excreted in the first 24 hours and a further 10% over the next 5 days. Similar results were obtained for baboons and beagle dogs. The human and animal data indicate that most of the remaining uranium is excreted over a period of a few months, but a few percent of the amount injected may be retained for a period of years (Bernard et al., 1957; Struxness et al., 1956; Luessenhop et al., 1958; Stevens et al., 1980; Sontag, 1984).

(960) A substantial fraction of uranium filtered by the kidneys is temporarily retained in the renal tubules before passing in the urine to the urinary bladder. Morrow et al. (1982) estimated that the kidneys of beagle dogs contained 44% of uranium reaching blood at 6 hours after inhalation of UO_2F_2 and 16% after 24 hours. At 1 – 3 days after inhalation or injection of soluble forms of uranium, the kidneys of humans, dogs and rats contained 12 – 25% of the amount entering blood (Bernard and Struxness, 1957; Muir et al., 1960; Jones, 1966; Stevens et al., 1980; Morrow et al., 1982). Durbin (1984) reviewed data on the retention of uranium in the kidneys of humans, beagles, rats and mice and concluded that 92 – 95% of the renal content at 1 day was lost with a half-time of 2 – 6 days and the remainder was lost with a half-time of 30 – 340 days. Interpretation of the data is complicated by indications that retention in the kidneys depends on the mass of uranium administered (Leggett, 1994).

(961) In the present model, urinary excretion is assumed to occur in part from direct transfer from plasma to the urinary bladder contents, accounting for 63% of uranium leaving the circulation, and in part after temporary retention in renal tubules, accounting for 12% of uranium leaving the circulation. The half-time of retention in the renal tubules is taken to be 7 days. The model also includes other kidney tissues which are assumed to receive 0.05% of uranium leaving the circulation, retained with a half-time of 5 years. These parameter values were chosen to be consistent with data on urinary excretion and renal retention of uranium, including data for the relative retention in kidneys and liver in occupationally and environmentally exposed humans. Parameter values for Kidney 2 were based to a large extent on retention data on baboons injected with tracer quantities of uranium (Neton et al., 1979, Lipsztein 1981, Bhattacharyya et al., 1989) and data on dogs administered low to moderate masses of uranium (Tannenbaum 1951, Fish and Bernard 1961). However, the model was required to remain broadly consistent with data on humans and dogs exposed to relatively

high masses of uranium.

(962) Model predictions of short-term urinary excretion of uranium are compared in Figure 15-4 with data from the human injection studies. The model was not designed to reproduce the central values of the observations for these subjects at later times due to the poor physical conditions of most of the subjects and the high variability of the data. Model predictions of daily urinary uranium are within the wide range of observations at all times but are generally higher than central values from the injection studies at times greater than a few days after injection. Essentially, predictions of urinary uranium at remote times are driven by parameter values for uptake and removal of uranium by individual tissues, particularly the skeleton, which is expected to contain most of the retained uranium by a few weeks after uptake.

Faecal excretion

(963) Faecal excretion accounted for less than 1% of total excretion in the human injection studies discussed above (Leggett, 1994; ICRP 1995a). Similar results were obtained for baboons (Lipsztein, 1981). In beagles, an estimated 2 – 5% of injected uranium was excreted in the faeces in the first 2 weeks (Stevens et al., 1980; Morrow et al., 1982). In the ICRP model, faecal excretion is included as 0.5% of uranium leaving the circulation entering the right colon.

Liver retention

(964) The assumptions for uranium retention in the liver in the ICRP model are based on the available experimental data for humans, baboons and dogs and data for chronic exposures of humans. Liver compartments called Liver 1 and Liver 2 are used to model the short-term retention of uranium shown by the experimental data and the long-term retention indicated by the environmental data. It is assumed that 1.5% of uranium leaving the circulation deposits in Liver 1 and that the retention half-time for this compartment is 7 days. Outflow from Liver 1 is divided between Liver 2 and plasma in the ration 7 : 93 The half-time of retention in Liver 2 is assumed to be 10 years.

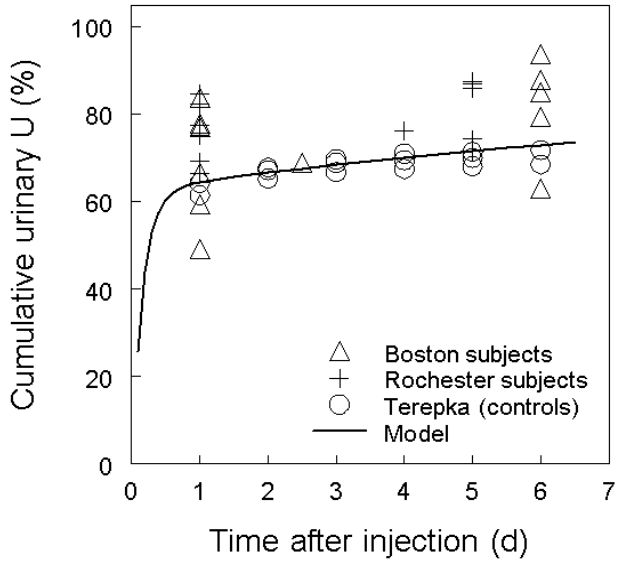

Figure 15-4. Observations and model predictions of cumulative urinary uranium in human subjects as a function of time after intravenous injection with uranium isotopes (Leggett, 1994). The three study groups indicated in the legend are described in the text.

Other soft tissues

(965) The high initial uptake of uranium by soft tissues is discussed above. This is modeled by assuming that 30% of outflow from plasma enters the soft-tissue compartment ST0. Soft-tissue compartments called ST1 and ST2 are used to model intermediate and long-term retention of uranium in soft tissues. Parameter values for these compartments were set for consistency with data for the Boston subjects and data for chronic exposure suggesting that there may be significant long-term retention of uranium in soft tissues (Igarashi et al., 1985; Fisenne et al., 1988; Gonzales and McInroy, 1991). For example, post-mortem data for two non-occupationally exposed persons indicate that muscle and skin accounted for about 25% of retained uranium, with 70% in the skeleton (Gonzales and McInroy, 1991).

(966) Compartments ST1 and ST2 are assumed to receive 6.65% and 0.3%, respectively, of uranium leaving the circulation. Removal half-times from these compartments to plasma are assumed to be 20 days and 100 years respectively. The model predicts that chronic soft tissues (ST0+ST1+ST2) contain about 20% of total body uranium in chronically exposed adults.

Retention in the skeleton

(967) There is evidence that UO_2^{++} exchanges with Ca^{++} at the surfaces of bone mineral crystals, although UO_2^{++} apparently does not participate in crystal formation or enter existing crystals. Also, the early gross distribution of uranium in the skeleton is similar to that of calcium. Like calcium, uranium is initially present on all bone surfaces but is most concentrated in areas of growth. Studies on dogs demonstrated that uranium on bone surfaces diffuses into bone volume, although at a slower rate than calcium (Rowland and Farnham, 1969; Stevens et al., 1980). Such diffusion was absent or less pronounced in rodents (Priest et al., 1982; Kisieleski et al., 1952). Autoradiographic studies of ^{233}U in mice at 1 d and 224 d after injection indicate an initial deposition of uranium on bone surfaces and subsequent

burial of lines of activity as well as some evidence of diffuse activity within bone mineral (Ellender et al., 1995). In all species for which there are data, there is evidence of similarity to calcium in that return of uranium from bone to plasma occurs at rates that are greater than could be attributed only to bone resorption.

(968) Parameter values for uptake and retention in the skeleton were based on data from the Boston study, animal data, post-mortem measurements on environmentally and occupationally exposed humans, analogy with the alkaline earth elements and considerations of bone metabolism. Each of the data sets has important limitations to their usefulness for the prediction of the skeletal kinetics of uranium in healthy humans. The Boston subjects were terminally ill, and their calcium metabolism cannot reliably be regarded as normal. Extrapolation of biokinetic data from laboratory animals to man is prone to error, particularly data for rodents. Baboon data for uranium are limited, and the dog data are subject to uncertainties resulting from the use of high masses of uranium, small number of animals and small bone samples. Some investigators have reported much higher early accumulation of uranium in the skeleton than assumed in the model. For example, Sanotskii et al. (1963, 1964) reported high initial deposition of uranium in the skeleton (25-40% of the administered amount) in dogs, rabbits and rats after subcutaneous or intratracheal administration of uranyl nitrate, although only 3-4% was retained after 6 months.

(969) It is assumed in the model that 15% of uranium leaving the circulation deposits on bone surfaces. By analogy with the alkaline earth elements (ICRP, 1993), the ratio of the amount deposited on trabecular surfaces to that deposited on cortical surfaces is assumed to be 1.25 in the mature skeleton (after 25 years of age). The value of 1.25 is derived from an average six-fold greater rate of turnover of trabecular bone divided by a four-fold greater cortical bone mass (Leggett et al., 1982; Leggett, 1992). The rate of removal of uranium from bone surfaces cannot be estimated with much certainty, but reasonable lower and upper bounds can be determined. Uranium apparently leaves bone surfaces much more slowly than calcium (Rowland and Farnham, 1969; Stevens et al., 1980), but a half-time longer than about 5 – 10 days would be difficult to reconcile with the relatively rapid loss of uranium from bone seen in human and most animal studies. The assumption made is of a removal half-time of 5 days, compared with a value of 1 day for calcium (Leggett, 1992). Because of recycling, the apparent retention time on bone surfaces will be greater than 5 days. For consistency with the available experimental data for the first few weeks after injection, it is assumed that 50% of uranium from bone surfaces returns to plasma and 50% transfers to exchangeable bone volume.

(970) The removal half-time assigned to the exchangeable bone volume is 30 days. This value was derived for radium and lead (Leggett, 1992, 1993). From exchangeable bone volume, 75% of uranium is returned to bone surfaces and 25% transfers to non-exchangeable bone volume. Removal from non-exchangeable bone volume to plasma is assumed to occur at the rate of bone turnover (reference values given in ICRP, 2002).

(971) The model predicts that the uranium content of the skeleton is about 30 times greater than that of the liver following constant chronic exposures to uranium, in reasonable agreement with most autopsy data for occupational or environmentally exposed subjects. The model predicts that the adult skeleton contains about 75% of the body content of uranium after chronic exposure, consistent with autopsy data (Gonzales and McInroy, 1991).

15.3.3. Treatment of radioactive progeny

(972) The dosimetrically significant progeny of uranium isotopes addressed in this report

are isotopes of actinium, thorium, protactinium, uranium, neptunium, plutonium, radium, radon, polonium, lead, bismuth, thallium, actinium, francium, or astatine. The models for actinium, thorium, radium, radon, polonium, lead, bismuth, thallium, actinium, francium, and astatine produced in systemic compartments by serial decay of members of a uranium chain are essentially the same as the models applied to these elements as progeny of radium (see the section on radium). Uranium produced in a systemic compartment by serial decay of members of a uranium chain is assigned the characteristic model for uranium. The characteristic models for neptunium and plutonium applied in this series of reports are applied to neptunium and plutonium, respectively, produced in systemic compartments following intake of a uranium parent. Protactinium produced in a systemic compartment following intake of a uranium parent is assigned the characteristic model for thorium. Protactinium, neptunium, or plutonium produced in a compartment that is not identifiable with a compartment in its model is assumed to transfer to the central blood compartment at the rate 1000 d^{-1} if produced in a blood compartment and at the rate of bone turnover if produced in an exchangeable bone volume compartment.

15.4. Individual monitoring

^{234}U

(973) ^{234}U intakes are determined by measuring the nuclide concentration in urine and faeces. As ^{234}U is a nuclide naturally present in the environment and in the diet, excretion rates of natural uranium are expected and should be evaluated for the population in the region of residence of the workers.

Isotope	Monitoring Technique	Method of Measurement	Typical Detection Limit	Achievable detection limit
^{234}U	Urine Bioassay	α spectrometry	0.3 mBq/L	0.05 mBq/L
^{234}U	Faeces Bioassay	α spectrometry	1 mBq/24h	0.2 mBq/24h

^{235}U

(974) Measurements of ^{235}U concentrations in urine and faeces are used to determine intakes of the nuclide. The main techniques used for urinalysis are alpha spectrometry and ICP-MS. ^{235}U may also be monitored by in vivo lung counting. Whole Body Counting might be used as a complement.

Isotope	Monitoring Technique	Method of Measurement	Typical Detection Limit	Achievable detection limit
^{235}U	Urine Bioassay	α spectrometry	0.3 mBq/L	0.05 mBq/L
^{235}U	Urine Bioassay	ICPM/S	0.001 µg/L (0.016 mBq/L)	8 E-07 Bq/L
^{235}U	Faeces Bioassay	α spectrometry	1 mBq/24h	0.2 mBq/24h
^{235}U	Lung Counting	γ-ray spectrometry	8 Bq	3 Bq
^{235}U	Whole Body Counting	γ-ray spectrometry	60 Bq	40 Bq

^{238}U

(975) Measurements of ^{238}U concentrations in urine and faeces are used to determine

intakes of the nuclide. Several techniques are used for urine bioassays, alpha spectrometry, ICP-MS, kinetic phosphorescence analysis (TrKPA) and fluorimetry. As ^{238} U is a nuclide naturally present in the environment and in the diet, excretion rates of natural uranium are expected and should be evaluated for the local population. ^{238}U may also be monitored by in vivo lung counting. ^{238} U detection is based on the 62.8 and 92.3 keV photons emitted by its decay product ^{234}Th.

Isotope	Monitoring Technique	Method of Measurement	Typical Detection Limit	Achievable detection limit
^{238}U	Urine Bioassay	α spectrometry	0.3 mBq/L	0.05 mBq/L
^{238}U	Urine Bioassay	ICPM/S	0.0015 µg/L (0.03 mBq/L)	0.002mBq/L
^{238}U	Urine Bioassay	TrKPA	0.1µg/L	0.06 µg/L
^{238}U	Urine Bioassay	Fluorimetry	1 µg/L	
^{238}U	Faeces Bioassay	α spectrometry	2 mBq/24h	0.2 mBq/24h
^{238}U	Lung Counting	γ-ray spectrometry of ^{234}Th	50 Bq of Th-234	30 Bq of Th-234

References

André, S., Métivier, H., Auget, D., Lantenois, G., Boyer, M., Masse, R., 1989. Lung dissolution of uranium tetrafluoride in rats and baboons. Comparison with dissolution by alveolar macrophages in culture and chemical dissolution. Hum. Toxicol. 8, 111-119.

Ansoborlo, E, Chalabreysse, J., Escallon, S., Hengé-Napoli, M.H., 1990. In vitro solubility of uranium tetrafluoride with oxidizing medium compared with in vivo solubility in rats. Int. J. Radiat. Biol. 58, 681-689.

Ansoborlo, E., Chazel, V., Hengé_Napoli, M.H., Pihet, P., Rannou, A., Bailey, M.R., Stradling, N., 2002. Determination of the physical and chemical properties, biokinetics, and dose coefficients of uranium compounds handled during nuclear fuel fabrication in France. Health Phys. 82(3), 279-289,

Ansoborlo, E., Chazel, V., Houpert, P., Hengé-Napoli, M.H., Paquet, F., Hodgson, A., Stradling, N., 1998a. Assessment of physico-chemical and biokinetic properties of uranium peroxide hydrate UO_4. Health Phys., 75(4), 389-397

Ansoborlo, E., Hodgson, A., Stradling, G.N., Hodgson, S., Metivier, H., Hengé-Napoli, M.H., Jarvis, N., Birchall, A., 1998b. Exposure implications for uranium aerosols formed at a new laser enrichment facility: application of the ICRP respiratory tract and systemic model. Radiat. Prot. Dosim., 79(1-4), 23-27.

Ansoborlo, E., Prat, O., Moisy, P., Denauwer, C., Guilbaud, P., Carriere, M., Gouget B.,Duffield, J., Doizi D., Vercouter, T., Moulin, C., Moulin, V., 2006. Actinide in speciation in relation to biological processes. Biochimie 88(11), 1605-18.

Bailey, M., Davis, K., 2002. Estimations of kidney uranium concentrations from published reports of uranium intakes in man where subsequent effects on kidney function were monitored. Annexe A to The Health Hazards of Depleted Uranium Munitions Part II. The Royal Society, London. www.royalsoc.ac.uk/du..

Ballou, J.E., Gies, R.A., Case, A.C., Haggard, D.L., Bushbom, R.L., Ryan, J.L., 1986. Deposition and early disposition of inhaled $^{233}UO_2(NO_3)_2$ and $^{232}UO_2(NO_3)_2$ in the rat. Health Phys. 51 755-771.

Barber, J.M. Forrest, R.D., 1995. A study of uranium lung clearance at a uranium processing plant. Health Phys. 68 661-669.

12521 Bassett, S.H., Frankel, A., Cedars, N., VanAlstine, H., Waterhouse, C., Cusson, K., 1948. The
12522 excretion of hexavalent uranium following intravenous administration.: II. Studies on
12523 human subjects. Rochester, New York, UR-37.
12524 Beau, P.G., Chalabreysse, J., 1989. Knowledge gained from bioassay data on some metabolic and
12525 toxicological features of uranium hexafluoride and its degradation products. Radiat. Prot.
12526 Dosim. 26, 107-112.
12527 Bečková, V., Malátová, I., 2008. Dissolution behaviour of ^{238}U, ^{234}U and ^{230}Th deposited on filters
12528 from personal dosemeters. Radiat. Prot. Dosim. 129(4): 469-472, published ahead of print
12529 November 1, 2007 doi:10.1093/rpd/ncm455.
12530 Begichev, S.N., Borovoj, A.A., Burlakov, E.V., Gagarinski, A., Ju Demin, V.F., Khodakovsky, I.L.,
12531 Khrulev, A.A., 1989. Radioactive releases due to the Chernobyl accident. Int. Sem. “Fission
12532 Product Transport Processes in Reactor Accidents”, May 22-26, 1989, Dubrovnik,
12533 Yugoslavia.
12534 Bernard, S.R., Struxness, E.G., 1957. A study of the distribution and excretion of uranium in man. An
12535 Interim Report. Tennessee, USA, ORNL 2304.
12536 Bernard, S.R., Muir, J.R., Royster, G.W., 1957. The distribution and excretion of uranium in man. In:
12537 Proceedings of the Health Physics Society First Annual Meeting pp. 33-48.
12538 Bhattacharyya, M.H., Larsen, R.P., Cohen, N., Ralston, L.G., Moretti, E.S., Oldham, R.D.. Ayres, L.,
12539 1989. Gastrointestinal absorption of plutonium and uranium in fed and fasted adult baboons
12540 and mice: application to humans. Radiat. Prot. Dosim. 26, 159-165.
12541 Boback, M.W., 1975. A review of uranium excretion and clinical urinalysis data in accidental
12542 exposure cases. In: Proceedings of the Conference on Occupational Health Experience with
12543 Uranium, pp. 226–243. Arlington Virginia, April 28–30, 1975, ERDA 93, US Energy
12544 Research and Development Administration.
12545 Bruenger, F.W., Atherton, D.R., Bates, D.S., Buster, D.S., Stevens, W., 1976. The early distribution
12546 and excretion of ^{233}U in the Beagle . University of Utah College of Medicine, Salt Lake
12547 City, Report No. COO-119-251, pp. 194-202.
12548 Campbell, E.E., McInroy, J.F., Schulte, H.F., 1975. Uranium in the tissue of occupationally exposed
12549 workers. Conference on Occupational Health Experience with Uranium. Arlington VA, US
12550 ERDA 93, 324-350.
12551 Chalabreysse, J., Beau, P.G., Chevalier, C., Jeanmaire, L., Bataller, G., Bérard, P., Gibert, B., 1989.
12552 French experience with uranium compounds. Radiat. Prot. Dosim. 26, 49-56.
12553 Chazel, V., Gerasimo, P., Dabouis V., Laroche, P., Paquet, F., 2003. Characterisation and dissolution
12554 of depleted uranium aerosols produced during impacts of kinetic energy penetrators against
12555 a tank. Radiat. Prot. Dosim. 105(1-4) 163-166.
12556 Chazel, V., Houpert, P., Ansoborlo, E., 1998. Effect of U3O8 specific surface area on in vitro
12557 dissolution, biokinetics, and dose coefficients. Radiat. Prot. Dosim. 79(1-4) 39-42.
12558 Chazel, V., Houpert, P., Hengé-Napoli, M.H., Paquet, F., Ansoborlo, E., 2000a. Experimental
12559 determination of the solubility of industrial UF4 particles. Radiat. Prot. Dosim. 92(4) 289-
12560 294
12561 Chazel,V., Houpert, P., Ansoborlo, E., Hengé-Napoli, M.H., Paquet, F., 2000b. Variation of
12562 solubility, biokinetics and dose coefficients of industrial uranium oxides according to
12563 specific surface area. Radiat. Prot. Dosim. 88(3) 223-231.
12564 Cooke, N., Holt, F.B., 1974. The solubility of some uranium compounds in simulated lung fluid.
12565 Health Phys. 27, 69-77.
12566 Coombs M.A., Cuddihy R.G. 1983. Emanation of 232U daughter products from submicron particles
12567 of uranium dioxide and thorium dioxide by nuclear recoil and inert gas diffusion. J. Aerosol
12568 Sci. 14, 75-86.
12569 Cooper, J.R., Stradling, G.N., Smith, H., Ham, S.E., 1982. The behaviour of uranium-233 oxide and
12570 uranyl-233 nitrate in rats. Int. J. Radiat. Biol. 41(4) 421-433.

12571 Cross, F. T., Palmer, R. F., Filipy, R. E., Dagle, G. E., Stuart, B. O., 1982, Carcinogenic effects of
12572 radon daughters, uranium ore dust and cigarette smoke in beagle dogs. Health Phys. 42(1),
12573 33-52.
12574 Cuddihy, R.G., Finch, G.L., Newton, G.J., Hahn, F.F. Mewhinney, J.A. Rothenberg, S.J., Powers,
12575 D.A., 1989. Characteristics of radioactive particles released from the Chernobyl nuclear
12576 reactor. Environ. Sci. Technol. 23, 89-95.
12577 Devell, L., 1988. Nuclide composition of Chernobyl hot particles. In: von Phillipsborn, H.,
12578 Steinhäusler F., (Eds.), Hot Particles from the Chernobyl Fallout. Proc. Int. Workshop,
12579 Theuern, October 1987, pp. 23-34. Bergbau und Industriemuseum Ostbayern, Band 16.
12580 Donoghue, J.K., Dyson, E.D., Hislop, J.S., Leach, A.M., Spoor, N.L., 1972. Human exposure to
12581 natural uranium. Brit. J. Indust. Med. 29, 81-89.
12582 Duport, P., Robertson, R., Ho, K., Horvath, F., 1991.) Flow-through dissolution of uranium-thorium
12583 ore dust, uranium concentrate, uranium dioxide, and thorium alloy in simulated lung fluid.
12584 Radiat. Prot. Dosim. 38(1/3) 121-133.
12585 Durbin, P.W., 1984. Metabolic models for uranium. In Proceedings of a colloquium: Biokinetics and
12586 analysis of uranium in man. 8-9 Aug. 1984 (Moore RH Ed). Richland, USA, United States
12587 Uranium Registry/Hanford Environmental Health Foundation. USUR-05 HEHF-47,
12588 Document No:PB86-203080, F1-F65.
12589 Eidson, A.F., 1990. Biological characterisation of radiation exposure and dose estimates for inhaled
12590 uranium mining effluents NUREG/CR-5489 TI90 012914, United States Nuclear
12591 Regulatory Commission.
12592 Eidson, A.F., 1994. The effect of solubility on inhaled uranium compound clearance: a review.
12593 Health Phys. 67, 1-14.
12594 Elder, J.C., Tinkle, M.C., 1980. Oxidation of Depleted Uranium Penetrators and Aerosol Dispersal at
12595 High Temperatures. Los Alamos National Laboratory Report LA-8610-MS. http://lib-
12596 www.lanl.gov/la-pubs/00313603.pdf
12597 Ellender, M., Haines, J.W., Harrison, J.D., 1995. The distribution and retention of plutonium,
12598 americium and uranium in CBA/H mice. Hum. Exper. Toxicol. 14, 38-48.
12599 Ellender, M., 1987. The clearance of uranium after deposition of the nitrate and bicarbonate in two
12600 regions of the rat lung. Human Toxicol. 6, 479-482.
12601 Fisenne, I.M., Welford, G.A., 1986. Natural U concentrations in soft tissues and bone of New York
12602 City residents. Health Phys. 50(6) 739-46.
12603 Fisenne, I.M., Perry, P.M., Harley, N.H., 1988. Uranium in humans. Radiat. Prot. Dosimetry 24(1/4)
12604 127-131.
12605 Fish, B.R., Bernard, S.R., 1961. Unpublished data. Sixth Conference on Industrial Hygiene and Air
12606 Pollution and summarized in Industrial Hygiene News Reports IV 1.
12607 Fisher, D.R., Jackson, P.O., Brodaczynski, G.G., Scherpelz, R.I., 1983. Levels of ^{234}U, ^{238}U and ^{230}Th
12608 in excreta of uranium mill crushermen. Health Phys. 45, 617-629.
12609 Fisher, D.R, Swint, M.J., Kathren, R.L., 1991. Modified biokinetic model for uranium from analysis
12610 of acute exposure to UF6. Health Phys. 60, 335-342.
12611 Fisher, D.R., Briant, J.K., 1994. Assessment of accidental intakes of uranyl acetylacetonate (UAA).
12612 Radiat. Prot. Dosim. 53(1-4) 263-267.
12613 Glissmeyer, J.A., Mishima, J., 1979. Characterization of Airborne Uranium from Test Firings of
12614 XM774 Ammunition. Pacific Northwest Laboratory. PNL-2944. Richland, WA.
12615 Gonzales, E.R., McInroy, J.F., 1991. Abstract WPM-A1: The distribution of uranium in two whole
12616 bodies. Health Phys. 60[Supplement 2], S51.
12617 Griffith W.C., Cuddihy R.G., Hoover M.D. Stalnaker N.D., 1980. Simulation of the retention and
12618 dosimetry of 232U and its daughters after inhalation in ThO2 or UO2 particles. In: Sanders,
12619 C.L., Cross, F.T., Dagle, G.E., Mahaffey, J.A., (Eds.), Pulmonary Toxicology of Respirable
12620 Particles. pp. 193-208 Proc. 19th Annual Hanford Life Sciences Symposium at Richland,
12621 WA. CONF-791002. Available from National Technical Information Service. Springfield.
12622 Virginia.

12623 Guilmette, R.A., Cheng, Y.S., 2009. Physicochemical characterization of Capstone depleted uranium
12624 aerosols IV: in vitro solubility analysis. Health Phys. 96, 292-305.
12625 Harduin, J.C., Royer, Ph., Piechowski, J., 1994. Uptake and urinary excretion of uranium after oral
12626 administration in man. Radiat. Prot. Dosim. 53, 245-248.
12627 Harris, W.B., 1961. Experimental clearance of uranium dust from the human body. In: Davies, C.N.,
12628 (Ed.), Inhaled Particles and Vapours. Proc. of an International Symposium organised by the
12629 British Occupational Hygiene Society. Oxford, Pergamon Press, pp. 209-220.
12630 Harrison, J.D., 1991. The gastrointestinal absorption of the actinide elements. Sci. Total Environment
12631 100, 43-60.
12632 Hill, C. R., 1962, Identification of alpha emitters in normal biological material. Health Phys. 8, 17–
12633 25.
12634 Hodgson, A., Moody, J.C., Stradling, G.N., Bailey, M.R., Birchall, A., 2000. Application of the ICRP
12635 respiratory tract model to uranium compounds produced during the manufacture of nuclear
12636 fuel. NRPB-M1156, Chilton.
12637 Hursh, J.B., Spoor, N.L., 1973. Data on Man. In: Hodge, H.C., Stannard, J.N., Hursh, J.B., (Eds.),
12638 Uranium, plutonium, transplutonic elements. Handbook of Experimental Pharmacology 36.
12639 New York. Springer-Verlag, pp. 197-239.
12640 Hursh, J.B., Neuman, W.R., Toribara, T., Wilson, H., Waterhouse, C., 1969. Oral ingestion of
12641 uranium by man. Health Phys. 17, 619-621.
12642 ICRP, 1979. Limits for Intakes of Radionuclides by Workers. ICRP Publication 30 Part 1. Ann.
12643 ICRP 2(3/4).
12644 ICRP, 1993. Age-dependent Dose to Members of the Public from Intake of Radionuclides. Part 2.
12645 ICRP Publication 67. Ann. ICRP 23(3/4).
12646 ICRP, 1994a. Dose Coefficients for Intakes of Radionuclides by Workers. ICRP Publication 68, Ann
12647 ICRP, 24(4), 12.
12648 ICRP, 1994b. Human Respiratory Tract Model for Radiological Protection. ICRP Publication 66.
12649 Ann. ICRP 24(1/3).
12650 ICRP, 1995. Age-dependent Doses to Members of the Public from Intake of Radionuclides. Pt.3.
12651 ICRP Publication 69. Ann. ICRP 25(1).
12652 ICRP, 1997. Individual monitoring for internal exposure of workers. ICRP Publication 78. Ann. ICRP
12653 27(3-4).
12654 ICRP, 2002. Guide for the Practical Application of the ICRP Human Respiratory Tract Model.
12655 Supporting Guidance 3. Ann. ICRP, 32(1-2).
12656 Igarashi, Y., Yamakawa, A., Seki, R., Ikeda, N., 1985. Determination of U in Japanese human tissues
12657 by the fission track method. Health Physics 49, 707-712.
12658 Jones, E.S., 1966. Microscopic and autoradiographic studies of distribution of uranium in the rat
12659 kidney. Health Physics 12, (10) 1437-51.
12660 Kathren, R.L., McInroy, J.F., Moore, R.H., Dietert, S.E., 1989. Uranium in the tissues of an
12661 occupationally exposed individual. Health Phys. 57, 17-21.
12662 Kisieleski, W.E., Faraghan, W.G., Norris, W.P., Arnold, J.S., 1952. The metabolism of uranium-233
12663 in mice. J. Pharm. Exper. Therapeutics 104(4) 459-67.
12664 Larsen, R.P., Orlandini, K.A., 1984. Gastrointestinal absorption of uranium in man. In:
12665 Environmental Research Division Annual Report, July 1982 - June 1983; Argonne National
12666 Laboratory, ANL-83-100-Pt.2. pp.46-50.
12667 Leach, L.J., Yuile, C.L., Hodge, H.C., Sylvester, G.E., Wilson, H.B., 1973. A five-year inhalation
12668 study with natural uranium dioxide (UO_2) dust—II. Post-exposure retention and biologic
12669 effects in the monkey, dog and rat. Health Phys. 25, 239-258.
12670 Leggett, R.W., 1989. The behavior and chemical toxicity of U in the kidney: a reassessment. Health
12671 Phys., 57(3) 365-83.
12672 Leggett, R.W., 1992. A generic age-specific biokinetic model for calcium-like elements. Radiation
12673 Protection Dosimetry 41, 183-198.
12674 Leggett, R.W., 1993. An age-specific kinetic model of lead metabolism in humans. Environmental

Health Perspectives 101(7) 598-616.
Leggett, R.W., 1994. Basis for the ICRP's age-specific biokinetic model for uranium. Health Phys. 67, 589-610.
Leggett, R.W., Pellmar, T.C., 2003. The biokinetics of uranium migrating from embedded DU fragments. J Environ. Radioact. 64(2-3) 205-25.
Leggett, R.W., Eckerman, K.F., Williams, L.R., 1982. Strontium-90 in bone: A case study in age-dependent dosimetric modelling. Health Phys. 43(3) 307-322.
Leggett, R.W., Eckermann, K.F., Boice, J.D., 2005. A respiratory model for uranium aluminide based on occupational data. J. Radiol. Prot. 25, 405–416.
Leggett, R.W., 1994. Basis for the ICRP's age-specific biokinetic model for uranium. Health Phys. 67, 589-610.
Leggett, R.W., Harrison, J.D., 1995. Fractional absorption of ingested U in humans. Health Phys. 68, 1-15.
Lipsztein, J.L., 1981. An improved model for uranium metabolism in the primate. Ph.D Dissertation, New York University.
Luessenhop, A.J., Gallimore, J.C., Sweet, W.H., Struxness, E.G., Robinson, J., 1958. The toxicity of hexavalent uranium following intravenous administration. Am J. Roentgenol. 79, 83-100.
Marsh J.W., Gregoratto, D., Karcher, K., Nosske D., Bessa Y., Blanchardon E., Hofmann W., Tomasek L., 2011. Dosimetric calculations for uranium miners for epidemiological studies. Radiat. Prot. Dos. pp. 1-13, doi:10.1093/rpd/ncr310.
Metivier, H., Poncy, J.L., Rateau, G., Stradling, G.N., Moody, J.C., Gray, S.A., 1992. Uranium behaviour in the baboon after the deposition of a ceramic forms of uranium dioxide and uranium octoxide in the lungs: Implications for human exposure. Radioprot. 27, 263-281.
Mishima, J., Parkhurst M.A., Scherpels, R.L., Hadlock, D.E., 1985. Potential Behavior of Depleted Uranium Penetrators under Shipping and Bulk Storage Accident Conditions. Pacific Northwest Laboratory. PNL-5415. Richland, WA.
Mitchell, R.E.J., Sunder, S., 2004. Depleted uranium dust from fired munitions: physical, chemical and biological properties. Health Phys. 87(1) 57–67.
Moody, J.C., Birchall, A., Stradling, G.N., Britcher, A.R., Battersby, W., 1997. Biokinetics of recycled uranium trioxide and implications for human exposure. Inhaled Particles VIII. Annals of Occupational Hygiene. 41 Suppl.1, 104-110.
Moore, R.H., Kathren, R.L., 1985. A World War II uranium hexafluoride inhalation event with pulmonary implications for today. J. Occup. Med. 27, 753–756.
Morrow, P., Gelein, R., Beiter, H., Scott, J.B., Picano, J.J., Yuile, C.L., 1982. Inhalation and intravenous studies of UF_6/UO_2F_2 in dogs. Health Phys. 43(6) 859-874.
Morrow, P.E., Gibb, F.R., Beiter, H.D., 1972. Inhalation studies of uranium trioxide. Health Phys. 23, 273-280.
Muir, J.R., Fish, B.R., Jones, E.S., Gillum, N.L., Thompson, J.L., 1960. Distribution and excretion of uranium. Oak Ridge, USA, Health Physics Division Annual Progress Report for period ending July 31, 1960. Report No. ORNL-2994.
Neton, J., Lo Sasso, T., Lipsztein, J., Wrenn, M.E., Cohen, N., 1979. Short term kinetics of uranium in the adult baboon : Preliminary data. Radioactivity studies progress report. COO-3382-18, Institute of Environmental Medicine, New York University Medical Center.
OSAGWI, 2000. (Office of the Special Assistant to the Deputy Secretary of Defense for Gulf War Illnesses. DoD) Exposure Investigation Report, Depleted Uranium in the Gulf (II), December 2000 at www.gulflink.osd.mil in the Environmental Exposure Reports Section.
Parkhurst, M.A., Szrom, F., Guilmette, R.A., Holmes, T.D., Cheng, Y.S., Kenoyer, J.L., Collins, J.W., Sanderson, T.E., Fliszar, R.W., Gold, K., Beckman, J.C., Long, J.A., 2004a. Capstone Depleted Uranium Aerosols: Generation and Characterization, Volumes 1. Main Text. Attachment 1 of Depleted Uranium Aerosol Doses and Risks: Summary of U.S. Assessments. PNNL-14168, Prepared for the U.S. Army by Pacific Northwest National Laboratory, Richland, Washington.

12727 Parkhurst, M.A., Szrom, F., Guilmette, R.A., Holmes, T.D., Cheng, Y.S., Kenoyer, J.L., Collins,
12728 J.W., Sanderson, T.E., Fliszar, R.W., Gold, K., Beckman, J.C., Long, J.A., 2004b. Capstone
12729 Depleted Uranium Aerosols: Generation and Characterization, Volume 2. Appendices.
12730 Attachment 2 of Depleted Uranium Aerosol Doses and Risks: Summary of U.S.
12731 Assessments. PNNL-14168, Prepared for the U.S. Army by Pacific Northwest National
12732 Laboratory, Richland, Washington.
12733 Parkhurst, M.A., Guilmette, R.A., 2009. Overview of the Capstone depleted uranium study of
12734 aerosols from impact with armored vehicles: Test setup and aerosol generation,
12735 characterization, and application in assessing dose and risk. Health Phys. 96, 207-220.
12736 Pellow, P.G., Stradling, G.N., Hodgson, A., Fell, T.P., Phipps, A. Ellender, M., 1996. Biokinetics of
12737 Uranium Tributyl Phosphate in the Rat : Implications for Occupational Exposure. NRPB-
12738 M682, Chilton.
12739 Pellow, P.G., Stradling, G.N., Hodgson, A., Fell, T.P., Phipps, A. and Ellender, M., 1997. Absorption
12740 kinetics of uranium tri-n-butyl phosphate in the rat: Implications for occupational exposure.
12741 Journal of Radioanalytical and Nuclear Chemistry 226, 93-98.
12742 Pomroy, C., Noel, L., 1981. Retention of uranium thorax burdens in fuel fabricators. Health Phys. 41,
12743 393-400.
12744 Price, A., 1989. Review of methods for assessment of intake of uranium by workers at BNFL
12745 Springfields. Radiat. Prot. Dosim. 26(1/4) 35-42.
12746 Priest, N.D., Howells, G.R., Green, D. Haines, J.W., 1982. Uranium in bone: metabolic and
12747 autoradiographic studies in the rat. Human Toxicol. 1, 97-114.
12748 Roberts, A.M., Coulston, D.J., Bates, T.H., 1977. Conformation of in vivo uranium-in chest survey
12749 by analysis of autopsy specimens. Health Phys., 32(5) 435-7.
12750 Rowland, R.E., Farnham, J.E., 1969. The deposition of uranium in bone. Health Phys. 17(1) 139-44.
12751 Russell, J.J., Kathren, R.L., 2004. Uranium deposition and retention in a USTUR whole body case.
12752 Health Phys. 86, 273-284.
12753 Sanotskii, V.A., Mikhailovich, S.M., Ivannikov, A.T., 1963. Abstract No. 40513: The toxic effect of
12754 uranium compounds. Nuclear Science Abstracts 17, 5450.
12755 Sanotskii, V.A., Mikhailovich, S.M., Ivannikov, A.T., 1964. The toxic effect of uranium compounds.
12756 In: Radiological Health and Safety in mining and milling of nuclear materials. Vienna,
12757 IAEA pp. 275-288.
12758 Saxby, W.N., Taylor, N.A., Garland, J., Rundo, J., and Newton, D., 1964. A Case of inhalation of
12759 enriched uranium dust. In: Assessment of Radioactivity in Man, Volume II. Vienna, IAEA,
12760 pp. 535-547.
12761 Schieferdecker, H., Dilger, H., Doerfel, H., 1985. Inhalation of U aerosols from UO2 fuel element
12762 fabrication. Health Phys. 48(1) 29-48.
12763 Scripsick, R.C., Crist, K.C., Tillery, M.I., Soderholm, S.C., Rothenberg, S.J., 1985a. Preliminary
12764 Study of Uranium Oxide Dissolution in Simulated Lung Fluid. LA-10268-MS, Los Alamos
12765 National Laboratory. http://lib-www.lanl.gov/la-pubs/00318819.pdf.
12766 Scripsick, R.C., Crist, K.C., Tillery, M.I., Soderholm, S.C., 1985b. Differences in in vitro dissolution
12767 properties of settled and airborne uranium material. In: Stocker, H., (Ed.), Occupational
12768 Radiation Safety in Mining Canadian Nuclear Association pp. 255-260. http://lib-
12769 www.lanl.gov/la-pubs/00374828.pdf.
12770 Singh, N. P., Wrenn, M. E., McInroy, J. F., Gonzales, E., Cross, F. T., Jackson, P. O. 1986a Ratios of
12771 ^{234}U, ^{238}U and ^{230}Th in dogs' lungs exposed to uranium ore dust: An interlaboratory
12772 comparison. Health Phys., 50, 292-297.
12773 Singh, N.P., Bennett, D.D., Wrenn, M.E., Saccomanno, G., 1987. Concentrations of alpha-emitting
12774 isotopes of U and Th in uranium miners' and millers' tissues. Health Phys. 53(3) 261-265.
12775 Singh, N.P., Lewis, L.L., Wrenn, M.E., 1986b. Abstract THAM-E3: Uranium in human tissues of
12776 Colorado, Pennsylvania and Utah populations. Health Phys., 50, (Supplement 1) S83.
12777 Sontag, W., 1984. Long-term behaviour of ^{239}Pu, ^{241}Am and ^{233}U in different bones of one-year-old
12778 rats: macrodistribution and macrodosimetry. Human Toxicol. 3, 469-483.

12779 Spencer, H., Osis, D., Fisenne, I.M., Perry, P.M., Harley, N.H., 1990. Measured intake and excretion
12780 patterns of naturally occurring 234U, 238U and calcium in humans. Radiat. Res. 124, 90-95.
12781 Stevens, W., Bruenger, F.W., Atherton, D.R., Smith, J.M., Taylor, G.N., 1980. The distribution and
12782 retention of hexavalent ^{233}U in the Beagle. Radiat. Res., 83, 109-126.
12783 Stradling, G.N., Stather, J.W., Gray, S.A., Moody, J.C., Ellender, M., Hodgson, A., Sedgwick D.,
12784 Cooke, N., 1987. The metabolism of uranium in the rat after inhalation of two industrial
12785 forms of ore concentrate: the implications for occupational exposure. Human Toxicol. 6,
12786 385-393.
12787 Stradling, G.N., Stather, J.W., Price, A., Cooke, N., 1989. Limits on intake and the interpretation of
12788 monitoring data for workers exposed to industrial uranium bearing dusts. Radiat. Prot.
12789 Dosim. 26(1/4). 83-87.
12790 Stradling, G.N., Stather, J.W., Strong, J.C., Sumner, S.A., Moody, J.C., Towndrow, C.G., Hodgson,
12791 A., Sedgwick, D., Cooke, N., 1988. The metabolism of ceramic and non-ceramic forms of
12792 uranium dioxide after deposition in the rat lung. Human Toxicol. 7, 133 - 139.
12793 Stradling, G.N., Stather, J.W., Strong, J.C., Sumner, S.A., Towndrow, C.G., Moody, J.C., Sedgwick,
12794 D., Cooke, N., 1985a. The metabolism of some industrial uranium tetrafluorides after
12795 deposition in the rat lung. Human Toxicol. 4, 159-168.
12796 Stradling, G.N., Stather, J.W., Ellender, M., Sumner, S.A., Moody, J.C., Towndrow, C.G., Hodgson,
12797 A., Sedgewick, D., Cooke, N., 1985b. Metabolism of an industrial uranium trioxide dust
12798 after deposition in the rat lung. Human Toxicol. 4, 563-572.
12799 Stradling, N., Hodgson, A., Ansoborlo, E., Berard, P., Etherington, G., Fell, T., Rance, E., Le Guen,
12800 B., 2002. Industrial uranium compounds: exposure limits, assessment of intake and toxicity
12801 after inhalation NRPB-W22, Chilton.
12802 Stradling, G.N., Gray, S.A., Moody, J.C., Ellender, M., Pearce, M., 2005. Biokinetics of thorium in
12803 the presence of a highly transportable form of uranium: Implications for occupational
12804 exposure. NRPB-DA/04/2005, Chilton.
12805 Struxness, E.G., Luessenhop, A.J., Bernard, S.R., Gallimore, J.C., 1956. The distribution and
12806 excretion of hexavalent uranium in man. IN Proceedings of the international conference on
12807 the peaceful uses of atomic energy 8 Aug. 1955-20 Aug. 1955 New York, United Nations,
12808 186-196.
12809 Stuart, B. O. Beasley, T. M., 1967, Non-equilibrium tissue distributions of uranium and thorium
12810 following inhalation of uranium ore by rats. In: Davies, C. N., editor. Inhaled Particles and
12811 Vapours II. Proceedings of an International Symposium organised by the British
12812 Occupational Hygiene Society; Cambridge, UK. Oxford: Pergamon Press pp. 291-8.
12813 Stuart, B.O., Jackson, P.O., 1975. The inhalation of uranium ores. In: Wrenn, M.E., (Ed.), Proc. of
12814 the Conference on Occupational Health Experience with Uranium. Arlington, Virginia,
12815 ERDA 93. US Energy Research and Development Administration, pp. 130–139. Available
12816 from National Technical Information Service, Springfield, Virginia.
12817 Sullivan, M.F., 1980. Absorption of actinide elements from the gastrointestinal tract of rats, guinea
12818 pigs and dogs. Health Phys. 38, 159-171.
12819 Tannenbaum, A., 1951. Toxicology of uranium: Survey and collected papers. New York, USA,
12820 McGraw-Hill Book Company Inc. National Nuclear Energy Series, Manhattan Project
12821 Technical Section.
12822 Terepka, A.R., Toribara, T.Y., Neuman, W.F., 1964. Abstract 22: Skeletal retention of uranium in
12823 man. In: 46th meeting of the Endocrine Society 1964, p. 33.
12824 Toivonen, H., Pöllämem, R., Leppänen, A., Klemola, S., Lathinen, J., 1992. Release from the nuclear
12825 power plant in Sosnovyy Bor in March 1992. Radiochimica Acta 57, 169-172.
12826 West, C.M., Scott, L., Schultz, N.B., 1979. Sixteen years of uranium personnel monitoring
12827 experience. In retrospect. Health Phys. 36, 665-669.
12828 Wood, S.K., Farnham, J.E., Marshall, J.H., 1970. ^{45}Ca, ^{133}Ba, and ^{226}Ra in 6- to 10-year-old Beagle
12829 dogs: a 100 day study. Argonne, Illinois, ANL-7760 Part II Biology and Medicine. July
12830 1969-June 1970, pp. 110-132.

12831 Wrenn, M.E., Singh, N. P., Saccomanno, G., 1983. Uranium and thorium isotopes and their state of
12832 equilibria in lungs from uranium miners. Health Phys. 44 Suppl. 1, 385-389.
12833 Wrenn, M.E., Durbin, P.W., Howard, B., Lipzstein, J., Rundo, J., Still, E.T., Willis, D.L., 1985.
12834 Metabolism of ingested U and Ra. Health Phys. 48, 601-603.
12835 Wrenn, M.E., Singh, N.A., Ruth, H., Rallison, M.I., Burleigh, D.P., 1989. Gastrointestinal absorption
12836 of soluble uranium from drinking water by man. Radiat. Prot. Dosim. 26, 119-122.
12837 Zamora, L., Zielinski, J.M., Meyerhof, D.P., Tracy, B.L., 2002. Gastrointestinal absorption of
12838 uranium in humans. Health Phys. 83(1) 35-45.
12839 Zhao, S.L., Zhao, F.-Y., 1990. Nephrotoxic limit and annual limit of intake for natural U. Health
12840 Phys; 58(5) 619-623.
12841